

Yasuhisa Okumoto  
Yu Takeda  
Masaki Mano  
Tetsuo Okada

# Design of Ship Hull Structures

A Practical Guide for Engineers



 Springer

# Design of Ship Hull Structures

Yasuhisa Okumoto · Yu Takeda ·  
Masaki Mano · Tetsuo Okada

# Design of Ship Hull Structures

A Practical Guide for Engineers

 Springer

Prof. Yasuhisa Okumoto  
Kinki University  
School of Engineering  
1 Takayaumenobe  
Takaya  
HIGASHI-OIROSHIMA  
739-2166 JAPAN

Dr. Masaki Mano  
Ex-Professor of Kinki University  
School of Engineering  
1 Takayaumenobe  
Takaya  
HIGASHI-OIROSHIMA  
739-2166 JAPAN

Dr. Yu Takeda  
IHI Corporation  
1 Shin-Nakahara-cho  
Isogo-ku  
YOKOHAMA  
239-8501 JAPAN

Dr. Tetsuo Okada  
IHI Marine United Inc.  
22-23 Kaigan 3-chome  
Tokyo  
108-0022 JAPAN

ISBN: 978-3-540-88444-6

e-ISBN: 978-3-540-88445-3

DOI 10.1007/978-3-540-88445-3

Library of Congress Control Number: 2008938352

© Springer-Verlag Berlin Heidelberg 2009

This work is subject to copyright. All rights are reserved, whether the whole or part of the material is concerned, specifically the rights of translation, reprinting, reuse of illustrations, recitation, broadcasting, reproduction on microfilm or in any other way, and storage in data banks. Duplication of this publication or parts thereof is permitted only under the provisions of the German Copyright Law of September 9, 1965, in its current version, and permission for use must always be obtained from Springer. Violations are liable to prosecution under the German Copyright Law.

The use of general descriptive names, registered names, trademarks, etc. in this publication does not imply, even in the absence of a specific statement, that such names are exempt from the relevant protective laws and regulations and therefore free for general use.

Printed on acid-free paper

9 8 7 6 5 4 3 2 1

springer.com



# Preface

The ship design is divided generally into four parts, hull form design, arrangement design, hull structure design, and fitting design (hull fitting and machinery fitting). The design of merchant ships starts with the owner's requirements such as kind and volume of cargo, transportation route and time generally. Sometimes the owner has a special requirement such as no bulkhead in hold.

Based on the above requirements a general arrangement plan is roughly designed and the studies are to be done from stability, strength, operation, and habitability viewpoints. Thus the general arrangement plan is finally decided with correction if necessary. Referring the lines plan, which shows the hull form, and the general arrangement plan, in the hull structure design the size, position, and materials of the structural members are decided, including the fabrication and assembly methods.

The most important duty of the hull structure design is to supply a strong enough hull structure against the internal and external loads. The text books or hand books of hull strength are helpful to the hull structure designer. However these books are generally written from the viewpoint of the strength theory and seem not to be sufficient from the design viewpoint.

The authors are hull structure designers in four generations, from the developing era of the structural design by large increase of the ship size and increase of ship production to establishing era of the design technology using computer; CAD and CAE. In this book the experiences of the authors in the above generations are condensed from the design viewpoint. Hence this book includes not only basic theory but also practical design matter. The authors are convinced that this book will be strong weapon for designers to design the hull structure as well as for students to understand the hull structure design in the world.

Takaya, Yokohama, and Tokyo  
20 August 2008

*Masaki Mano*  
*Yasuhisa Okumoto*  
*Yu Takeda*  
*Tetsuo Okada*

# Contents

## Part I Fundamentals

<b>1</b>	<b>Philosophy of Hull Structure Design</b> . . . . .	3
1.1	Importance of Hull Structure Design . . . . .	3
1.2	Design Procedure of Structures . . . . .	5
1.3	Hull Structure Design Policy . . . . .	7
1.4	Basic Idea of Hull Structure Design . . . . .	8
1.5	Studies on Loads Applied . . . . .	9
1.6	Reliable Design . . . . .	10
<b>2</b>	<b>Structural Design Loads</b> . . . . .	17
2.1	Introduction . . . . .	17
2.2	Longitudinal Strength Load . . . . .	20
2.3	Transverse Strength Load . . . . .	23
2.4	Ship Response Calculation in Waves . . . . .	27
2.4.1	Introduction . . . . .	27
2.4.2	Strip Method . . . . .	27
2.4.3	Short-Term Prediction . . . . .	28
2.4.4	Long-Term Prediction . . . . .	30
<b>3</b>	<b>Strength Evaluation</b> . . . . .	33
3.1	General . . . . .	33
3.1.1	Introduction . . . . .	33
3.1.2	Procedure of Structural Strength Evaluation . . . . .	33
3.2	Stress and Strain . . . . .	37
3.2.1	Stress Pattern . . . . .	37
3.2.2	Biaxial Stress Condition [12] . . . . .	38
3.2.3	Combination of Normal Stress and Shearing Stress [12] . . . . .	39
3.2.4	Principal Stress and Principal Shearing Stress [12] . . . . .	40
3.2.5	Equivalent Stress . . . . .	42
3.2.6	Evaluation of Stress Calculated by FEM . . . . .	43
3.3	Evaluation of Stress . . . . .	45
3.3.1	Criteria of Failure . . . . .	45
3.3.2	Allowable Stress . . . . .	47

3.4	Fatigue Strength	49
3.4.1	Introduction	49
3.4.2	S–N Curve	49
3.4.3	Fatigue Damage	52
3.5	Buckling of Ship Structure	54
3.5.1	Introduction	54
3.5.2	Column Buckling	55
3.5.3	Plate Buckling	57
3.6	Plastic Strength	60
3.6.1	Philosophy of Plastic Strength	60
3.6.2	Plastic Bending	62
3.6.3	Plastic Section Modulus	64
3.6.4	Collapse of a Beam	65
3.6.5	Collapse of a Plate	68
3.7	Vibration in Ship	69
3.7.1	Introduction	69
3.7.2	Basic Theory of Single Degree of Freedom Vibration System	70
3.7.3	Vibration Problems in Ships	74
3.7.4	Vibration Prevention Design	75
3.8	Selection of Strength Analysis Method	76
3.8.1	Introduction	76
3.8.2	Type of Analysis Method	77
3.8.3	Analysis Procedure	78
3.8.4	Evaluation of Analysis Result	79
<b>4</b>	<b>Hull Structure Design System</b>	<b>81</b>
4.1	Design Flow	81
4.2	Basic Design of Hull Structures	84
4.2.1	Role of Basic Design	84
4.2.2	Check of General Arrangement	87
4.2.3	Check of Other Drawings	87
4.2.4	Optimization Technique in Basic Design Process	88
4.3	Structural Drawings	90
4.3.1	Approval Drawings	90
4.3.2	Detail Drawings	90
4.3.3	Production Data	92
4.4	Standardization	92
4.5	Negotiation with Owner	95
<b>5</b>	<b>Progress in Ship Design</b>	<b>97</b>
5.1	Increase in Ship Dimensions of Tankers	97
5.2	Specialization of Ships	100
5.3	Change of Hull Form	104
5.4	Ship Vibration Caused by Socio-Economical Change	105
5.5	Regulations for Environmental Conservation	108
5.6	Technical Innovation	109

- 6 Materials** ..... 111
  - 6.1 Hull Steel ..... 111
  - 6.2 Grades of Steel ..... 112
  - 6.3 Higher-Strength Steel ..... 116
  - 6.4 Steel Sections ..... 116
  - 6.5 Other Materials ..... 117
  - 6.6 Scattering of Material Properties ..... 117
  - 6.7 Scattering of Physical Properties ..... 121
  - 6.8 Residual Stress [42] ..... 122
  
- 7 Finite Element Method** ..... 125
  - 7.1 Characteristics of FEM ..... 125
  - 7.2 Fundamentals of FEM ..... 126
    - 7.2.1 Stiffness Matrix [44] ..... 126
    - 7.2.2 Plane Stress [43] ..... 128
  - 7.3 Procedure of FEM ..... 130
  - 7.4 Application of FEM ..... 133
    - 7.4.1 Mesh Division ..... 133
    - 7.4.2 Loading and Supporting Condition ..... 134
    - 7.4.3 Degrees of Freedom ..... 136
  
- References** ..... 139

**Part II Theory**

- 1 Design of Beams** ..... 143
  - 1.1 Effective Breadth of Attached Plates ..... 143
    - 1.1.1 Bending in Elastic Conditions ..... 144
    - 1.1.2 Effective Width After Plate Buckling ..... 144
  - 1.2 Span Point of Beams ..... 146
  - 1.3 Design of Cross Section ..... 149
    - 1.3.1 Calculation of Section Modulus ..... 150
  - 1.4 Bending Moment ..... 152
  - 1.5 Easy Solution of Statically Indeterminate Beams ..... 154
  - 1.6 Boundary Condition ..... 156
  - 1.7 Cross-Sectional Area of Beams ..... 161
  - 1.8 Optimum Design of Beam Section ..... 162
    - 1.8.1 Elastic Design ..... 163
    - 1.8.2 Plastic Design ..... 165
    - 1.8.3 Optimal Proportion for Beams ..... 166
  - 1.9 Simply Supported Beams and Continuous Beams ..... 167
  - 1.10 Effect of Struts ..... 170
  - 1.11 Additional Bending Moment due to Forced Displacement ..... 172
  - 1.12 Lateral Movement of Beams ..... 174

<b>2</b>	<b>Design of Girders</b> .....	177
2.1	Shearing Force .....	177
2.2	Rational Design of Girders .....	181
2.3	Bottom Transverses Supported by Centerline Girder [5] .....	184
2.4	Deflection of Girders .....	187
<b>3</b>	<b>Damage of Girders</b> .....	191
3.1	Buckling Caused by Compression .....	191
3.2	Buckling Caused by Bending .....	194
3.3	Buckling Caused by Shearing .....	195
3.4	Buckling Caused by Concentrated Loads .....	199
3.5	Cracks Around Slot .....	202
3.5.1	Cracks of First Generation [8] .....	202
3.5.2	Cracks Propagating into Longitudinals .....	208
3.5.3	Cracks Around Slots due to Shear Stress on Transverses .....	210
<b>4</b>	<b>Design of Pillars</b> .....	211
4.1	Slenderness Ratio of Pillars .....	211
4.2	Sectional Shape of Pillars .....	214
4.3	Pillar Supporting Tensile Force .....	217
4.4	Connection of Pillar at Top and Bottom .....	219
4.5	Cross Ties .....	221
4.6	Radius of Gyration of Square Section .....	224
<b>5</b>	<b>Design of Plates</b> .....	227
5.1	Boundary Conditions of Plates .....	227
5.2	Strength of Plates Under Lateral Loads .....	230
5.3	Strength of Plates by In-Plane Loads .....	237
5.4	Plates Supporting Bending and Compression Simultaneously .....	242
5.5	Stress Concentration Around Openings .....	244
5.6	Material and Roll Direction .....	248
5.7	Damage of Plates .....	251
<b>6</b>	<b>Design of Stiffened Panel</b> .....	253
6.1	Grillage Structure .....	254
6.2	Optimum Space of Girders .....	257
6.3	Optimum Space of Beams .....	258
6.3.1	Design Condition Against Lateral Load like Water Pressure .....	258
6.3.2	Design Conditions from Vibration Viewpoint .....	259
6.3.3	Minimum Plate Thickness .....	260
6.3.4	Optimum Beam Space .....	260
<b>7</b>	<b>Torsion</b> .....	267
7.1	Overview of the Theory .....	267
7.2	Torsion Theory of Closed Section Bars .....	268
7.3	Torsional Rigidity of Various Sections .....	274

7.4	Torsion Theory of I-Section .....	277
7.5	Torsion Theory of Open Section Bars .....	279
<b>8</b>	<b>Deflection of Hull Structures</b> .....	<b>285</b>
8.1	Deflection of Hull Girder .....	286
8.2	Deflection of Beams with Optimum Section .....	291
8.3	Deflection of Girders and Web Frames .....	292
8.4	Additional Stress Caused by Deflection .....	293
8.5	Shearing Deflection .....	295
<b>9</b>	<b>Welding</b> .....	<b>297</b>
9.1	Butt Welding .....	298
9.2	Fillet Welding .....	302
9.3	Fillet Welding with Higher Strength Electrode .....	308
9.4	Water Stopping Welding .....	309
9.5	Scallop and Serration .....	309
9.6	Conversion of Butt Welding to Fillet Welding .....	311
9.7	Long Intermittent Welding .....	314
9.8	Shrinkage of Deposit Metal .....	315
9.9	One Side Welding .....	317
<b>10</b>	<b>Fracture Control</b> .....	<b>319</b>
10.1	Jack-Knifed Failure of Liberty Ships .....	319
10.2	Fracture Mechanics .....	321
10.2.1	Principles .....	321
10.2.2	Linear Fracture Mechanics .....	322
10.2.3	Non-Linear Fracture Mechanics .....	324
10.2.4	Fracture Toughness .....	325
10.2.5	Grade of Steel .....	325
10.3	Fatigue Strength Design .....	328
10.3.1	Crack Propagation Calculation by Paris's Equation .....	328
10.3.2	Fatigue Strength Design Taking into Account Construction Tolerances [39] .....	330
<b>11</b>	<b>Hull Structural Vibration</b> .....	<b>335</b>
11.1	Introduction .....	335
11.2	Basic Features of Hull Structure Vibration .....	336
11.3	Overview of Ship Vibration .....	338
11.4	Boundary Conditions of Hull Structure Vibration .....	341
11.5	Current Boundary Conditions of Hull Structure Vibration .....	345
	<b>References</b> .....	<b>349</b>

**Part III Applications**

- 1 Hull Structure Arrangement** ..... 353
  - 1.1 Hold Arrangement ..... 353
  - 1.2 Criteria of Design of Hull Structure Arrangement ..... 355
    - 1.2.1 Wing Tanks of Tankers ..... 355
    - 1.2.2 Bulkhead Arrangement of Bulk Carriers ..... 358
  - 1.3 Bulkhead Arrangement Beyond Cargo Hold ..... 359
    - 1.3.1 Bow Construction Without Extended Longitudinal Bulkheads ..... 360
    - 1.3.2 Engine Room Construction Without Extended Longitudinal Bulkheads ..... 360
- 2 Longitudinal Strength of Hull Girder** ..... 363
  - 2.1 Allowable Stress for Longitudinal Strength ..... 363
  - 2.2 Position of Maximum Longitudinal Bending Moment ..... 367
  - 2.3 Calculation of Section Modulus of Hull Girder ..... 369
  - 2.4 Longitudinal Strength and Hull Steel Weight ..... 370
  - 2.5 Application of High Tensile Steel ..... 372
  - 2.6 Longitudinal Strength Analysis in Waves ..... 374
  - 2.7 Arrangement of Longitudinal Strength Members ..... 379
  - 2.8 Stress Concentration on Longitudinal Strength Members ..... 381
  - 2.9 Additional Bending of Local Members Due to Hull Girder Bending ..... 383
  - 2.10 Longitudinal Bending Stress in Fore & Aft Parts of Ship ..... 385
  - 2.11 Hull Steel Weight Reduce to Ultimate Strength ..... 386
- 3 Transverse Strength of Ship** ..... 387
  - 3.1 Allowable Stress for Transverse Strength ..... 388
  - 3.2 Long Taper & Snake Head ..... 391
  - 3.3 Shape of Bottom Transverse in Center Tank ..... 392
  - 3.4 Shape of Bottom Transverse in Wing Tank ..... 393
  - 3.5 Transverse Strength of Tanker ..... 394
    - 3.5.1 Cross Ties ..... 394
    - 3.5.2 Load Applied on Transverse Strength Members ..... 397
    - 3.5.3 Inside Pressure in Wide Tanks ..... 399
    - 3.5.4 Connection Between Transverse Ring and Side Shell ..... 400
    - 3.5.5 Buckling on Web of Transverse Rings ..... 401
    - 3.5.6 Straight Type and Circular Type Construction ..... 403
    - 3.5.7 Transverse Rings at Fore & Aft Parts of Tank ..... 405
  - 3.6 Transverse Strength of Ore Carrier ..... 405
  - 3.7 Transverse Strength of Bulk Carrier ..... 410
  - 3.8 Transverse Strength of Container Ships ..... 415

<b>4</b>	<b>Torsional Strength</b> .....	417
4.1	Structural Damage Due to Torsion (Example No. 1) .....	418
4.2	Structural Damage Due to Torsion (Example No. 2) .....	420
<b>5</b>	<b>Shell Structure</b> .....	423
5.1	Thickness of Shell Plates .....	423
5.2	Shell at Bottom Forward .....	425
5.3	Shell at Bow Flare .....	426
5.4	Bilge Shell .....	428
5.5	Shell near Stern Frame .....	428
5.6	Shell Damage .....	429
<b>6</b>	<b>Bulkheads</b> .....	431
6.1	Strength of Bulkhead Plates .....	431
6.2	Horizontal Girders on Transverse Bulkheads (in Center Tank) .....	433
6.3	Horizontal Girder Arrangement on Bulkheads .....	436
6.4	Vertical Stiffeners on Transverse Bulkheads .....	439
6.5	Swash Bulkheads .....	440
6.6	Horizontal Stiffeners on Transverse Bulkheads .....	443
6.7	Minimum Thickness of Longitudinal Bulkhead Plates .....	447
6.8	Sharing Ratio of Shearing Force .....	449
6.9	Corrugated Bulkheads .....	451
6.10	Horizontal Girders on Corrugated Bulkheads .....	454
6.11	Stiffness of Corrugated Bulkheads Against In-Plane Loads .....	456
<b>7</b>	<b>Deck Structure</b> .....	461
7.1	Stress Concentration at Hatch Corners .....	461
7.1.1	General .....	461
7.1.2	Contour Shape Optimization of Container Ship Hatch Corners .....	464
7.2	Deck Strength for Locally Distributed Loads .....	467
7.3	Deck Sustaining Upward Loads .....	471
7.4	Damage to Deck Structure .....	472
<b>8</b>	<b>Double Hull Structure</b> .....	475
8.1	Structural System of Double Hull Structure .....	475
8.2	Double Hull Structure and Single Hull Structure .....	477
8.3	Examples of Double Hull Structures .....	478
8.3.1	Cargo Ships .....	478
8.3.2	Tankers .....	479
8.3.3	Container Ships .....	480
8.3.4	Nuclear Ships .....	480
8.3.5	Large Bulk Carriers .....	481



<b>9</b>	<b>Fore Construction</b> .....	483
9.1	Structural Arrangement .....	483
9.2	Structure of Shell Construction .....	485
9.3	Vertical Acceleration Depending on Pitching.....	486
9.4	Deck Structure .....	487
9.5	Structural Continuity.....	488
9.6	Large Damage in Fore Construction .....	488
<b>10</b>	<b>Engine Room Construction</b> .....	491
10.1	Engine and Pump Rooms Arrangement .....	492
10.2	Rigidity Criteria in Engine Room Structure Design .....	494
10.2.1	Double Bottom in Engine Room.....	495
10.2.2	Panel, Web, Stiffener Etc. ....	496
10.3	Design of Structural Members in Engine Room .....	497
10.4	Girders and Floors in Engine Room Double Bottom.....	499
10.5	Problems Caused by Deflection of Engine Room Double Bottom... ..	501
10.6	Deflection of Engine Room Double Bottom.....	503
10.6.1	Bending and Shearing Deflection of Hull Girder in the Vicinity of Engine Room .....	503
10.6.2	Deformation of Web Frame Which Supports Engine Room Double Bottom .....	505
10.6.3	Bending and Shearing Deflections of Engine Room Double Bottom Itself .....	505
10.7	Allowable Limit of Deflection of Engine Room Double Bottom... ..	506
10.8	Control of Deflection of Engine Room Double Bottom .....	509
10.9	Sea Chest in Engine Room Double Bottom .....	511
<b>11</b>	<b>Stern Construction and Stern Frame</b> .....	513
11.1	Aft Peak Tank Construction .....	514
11.2	Vibration of Stern Structure .....	515
11.2.1	Vibration of Stern Overhang .....	515
11.2.2	Transverse Vibration of Stern Bossing of a Single Screw Vessel .....	518
11.2.3	Vertical Vibration of Twin Bossing in Twin Screw Vessel ... ..	518
11.3	Stern Frame .....	521
<b>12</b>	<b>Vibration Prevention</b> .....	527
12.1	Exciting Forces .....	528
12.1.1	Magnitude of Propeller Excitation .....	529
12.1.2	Magnitude of Diesel Engine Excitation .....	532
12.1.3	Magnification of Exciting Force by Resonator .....	534
12.1.4	Cancellation of Exciting Force .....	541
12.1.5	Reduction of Main Engine Exciting Force by Elastic Mounting .....	543

- 12.2 Prevention of Ship Vibration ..... 545
  - 12.2.1 Flexural Vibration of Hull Girder ..... 546
  - 12.2.2 Vibration of Superstructure ..... 548
  - 12.2.3 Active Mass Damper for Superstructure Vibration ..... 550
  - 12.2.4 Vibration of In-Tank Structures ..... 552
  - 12.2.5 Calculation Methods of Natural Frequency of In-Tank Structures ..... 552
- 13 Superstructure** ..... 559
  - 13.1 Example of Damage to Long Superstructures ..... 559
  - 13.2 Interaction of Superstructures and Main Hull ..... 559
  - 13.3 Magnitude of Longitudinal Bending Stress ..... 561
  - 13.4 Prevention of Structural Failures ..... 564
    - 13.4.1 Structural Discontinuity ..... 564
    - 13.4.2 Round Shape of Side Wall Opening Corner ..... 565
    - 13.4.3 Buckling ..... 568
    - 13.4.4 Expansion Joints ..... 570
- References** ..... 571
- Index** ..... 573

# About the Authors

**Yasuhisa Okumoto, Dr. Eng.**

1965–1991: Ishikawajima-Harima Heavy Industries Co., Ltd.(IHI)  
Shipbuilding & Offshore Division and Research institute  
1992–: Kinki University, School of Engineering  
Professor

**Yu Takeda, Dr. Eng.**

1981–1997: Ishikawajima-Harima Heavy Industries Co., Ltd.(IHI)  
Shipbuilding & Offshore Division  
1997–: Ishikawajima-Harima Heavy industries Co., Ltd.(IHI)  
Research institute  
Manager

**Masaki Mano, Dr. Eng. FRINA**

1952–1986: Ishikawajima-Harima Heavy Industries Co., Ltd.(IHI)  
Shipbuilding & Offshore Division and Research institute  
1987–1999: Professor of Kinki University, Faculty of Engineering  
Consulting Naval architect

**Tetsuo Okada, Dr. Eng.**

1986–2002: Ishikawajima-Harima Heavy Industries Co., Ltd. (IHI)  
Shipbuilding and Offshore Division  
2002–: IHI Marine United Inc.  
Manager

**Part I**  
**Fundamentals**

# Chapter 1

## Philosophy of Hull Structure Design

### 1.1 Importance of Hull Structure Design

Hull structure design has recently become more and more important. Ship hull structure design has always been considered, technically as well as economically, to be a very important part of the shipyard management, since the strength of a ship is concern and the cost of the hull steel is about 20% of total ship's cost. Therefore, a good executive needs many talented designers to assist especially in hull structure design.

Between 1950 and 1970, due to economical demand, ship dimensions had to increase, ship speed had to be higher, and the specialization of ships was promoted. Worldwide economies developed quickly, due to the consumption of cheap fuel oil, and a mass consumption era commenced. Consequently cargo movement increased. In order to satisfy this social requirement, large, high speed and specialized ships were designed and constructed. In Fig. 1.1.1 worldwide sea born cargo movement is shown.

The hull structure designers played a major role in this era. They produced reliable ships and simultaneously increased the size of the ships step by step, based on past experience and immediate feeding back of performance results of newly completed ships. In Fig. 1.1.2 the transition of scaling-up of ships is shown. It goes without saying that the ship dimensions increased step by step. The largest ship actually constructed was the 565,000 DWT (dead weight tons) tanker the *Seawise Giant*. However, a preliminary design of a 1,000,000 DWT tanker (Million tonner) was carried out also, and building docks, to make the construction of that ship possible, were actually constructed. However, after the oil crisis, no bigger tanker than the *Seawise Giant* was built.

The main engine output increased in order to obtain higher vessel speeds, and vibration problems became apparent due to a rigid propeller shaft in a flexible hull structure of the increasing in vessel dimensions. However these problems were solved by the joint efforts of hull structure designers.

The specialization of ships occurred in response to the need for effective transportation. In addition to the tankers previously in service, ore and bulk carriers, container ships, designated car carriers etc. appeared. In these specialized ships many special requirements of hull structure, that were not necessary before, had

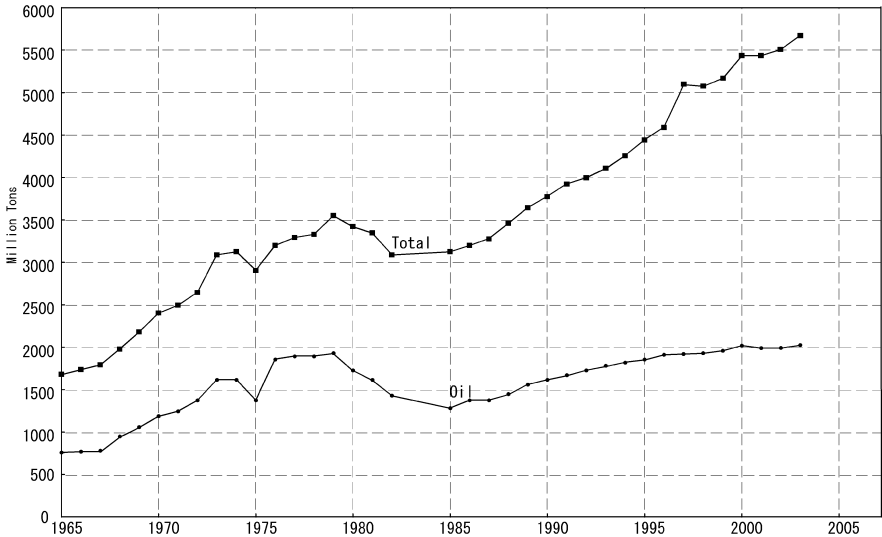


Fig. 1.1.1 World seaborne trade

to be incorporated in order to increase transportation efficiency. Hull structure designers overcame these problems due to these special requirements when designing these ships.

The oil crises of 1973 and 1979 halted the size increase of ships and further development of higher vessel speeds. At the same time worldwide shipbuilding and shipping recessions started. As the price of crude oil increased from U.S. \$1.6 to

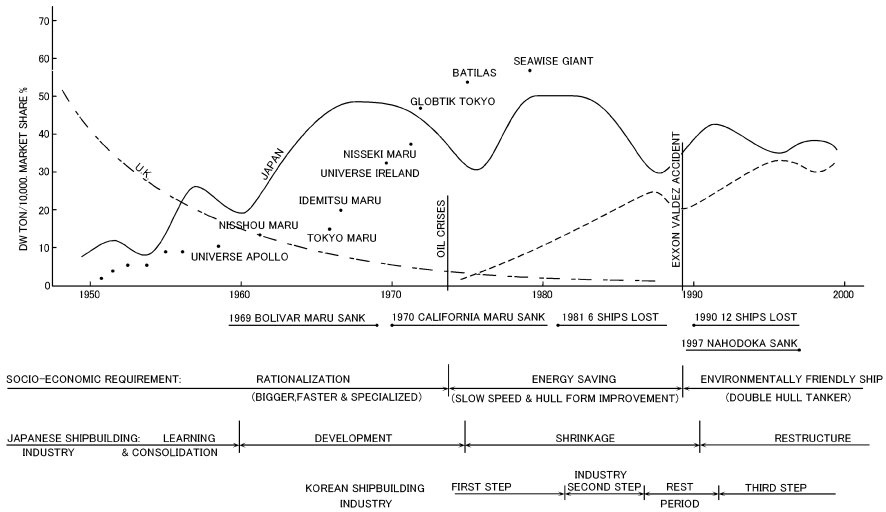


Fig. 1.1.2 Environments and ship's large sizing

U.S. \$12 and then sky-rocketing to U.S. \$34, energy saving trends spread all over the world. The earlier increase in cargo movement reversed and gradually decreased. The surplus of shipbuilding industry facilities and the over-tonnage of ships accelerated the recession.

The most important topic in the energy saving era was to reduce fuel consumption. So the utmost was done on hull form improvement, propulsion (propeller) efficiency, main engine fuel consumption and efficiency of the propulsion plant. The main actors in this period were hull form designers, machinery designers, and main engine builders.

Regarding energy saving, hull structure designers could not contribute a great deal. They could only reduce hull steel weight to have smaller ships which have less resistance.

Shipbuilding was depressed to 1990, and hull structure designers have been the main players once again in the recovering period after that.

Due to competition among ship owners themselves and also among shipyards it was hard to survive in such depressed times. Under these circumstances the specialization of ships was promoted to achieve a more profitable cargo transportation unit. Consequently the demands on the hull structure were greater and greater, and some of them seemed to be impossible to carry out.

Whether a new structure can be realized or not, depends on what the boundary conditions are, and this is up to the hull structure designer to decide. It has been said for a long time that shipbuilding is “experience engineering” and ships are to be designed and built, based on past experience. However, the situation has changed as the hull structure designer has to design new and unusual structures which have never been built before, so there is not much experience available. Survival of the shipyard will depend on the success of the hull structure design team.

## 1.2 Design Procedure of Structures

Not only the hull structure design but also general structural design is carried out in accordance with the procedure shown in Fig. 1.2.1. It is a well known fact in the shipbuilding field that design starts with the requirements of the type and volume of cargoes, routes of transportation, speed (from where to where in how many days), or for new types of ship, e.g. the million tonner, whether it will be available or not.

Then a preliminary general arrangement is to be prepared based on these requirements. The purpose of a ship is to carry cargo so that the size, shape and the arrangement of cargo holds are decided in the first stage. The results of hull structure research are important in the decision-making process regarding the shape and arrangement of cargo holds.

The estimation of the forces applied to the structures shown in Fig. 1.2.1 means the establishment of static loads such as buoyancy, weight of ship, cargo weight and the estimation of dynamic loads such as wave load and exciting force. The wave load is a kind of natural phenomenon and is to be estimated based on accumulated observed data.

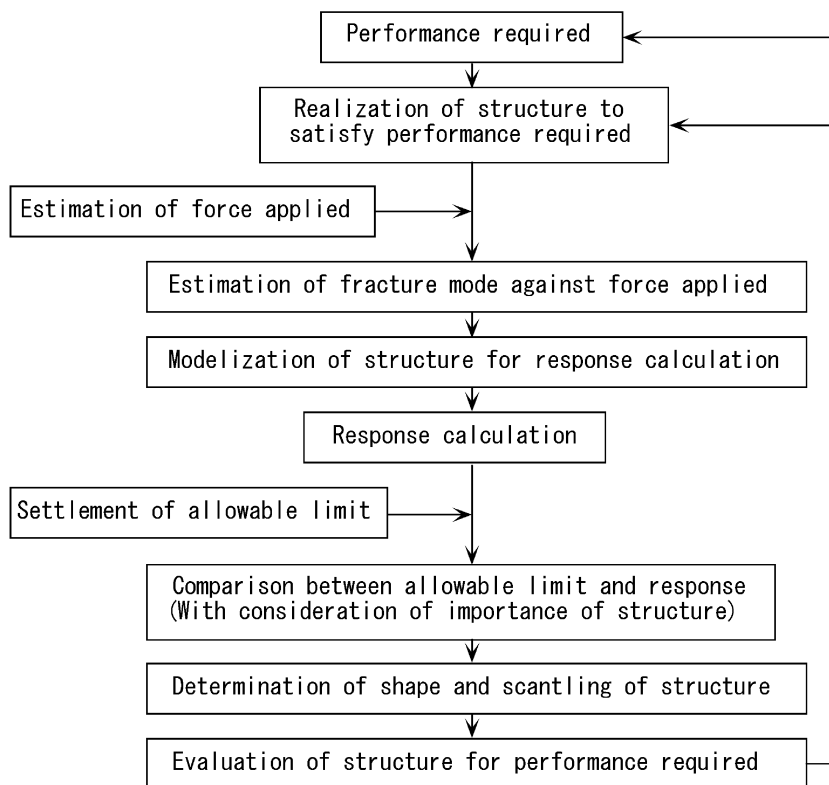


**Fig. 1.2.1** Sequence of structure design

In Fig. 1.2.1 the design flow, shown in vertical arrows, is decided by the structural designer, and the horizontal arrows show the items to be based on social standards and research results. These concepts are supplied to the designers by outsiders. Because the setting of the forces applied to the hull structure affects the design very much, hull structure designers should always pay attention to research in this subject.

The estimation of structural failure mode due to such forces is important for a reliable design. Not only theoretical knowledge but also observations experienced on actual failures are necessary in estimating the failure modes correctly. In the modelization of strength response calculations the correct failure mode should be applied.

Around 1965 many buckling and cracks occurred on the web plates of big girders in newly built large ships because designers designed the girder based on bending moment without considering shear force, which is important for big girders.

It is easy to understand the phenomena after solving the problem when it happened for the first time, but it is difficult to visualize and predict it beforehand. And even if it can be predicted, it is very hard for designers to apply countermeasures in



advance, which require time, money and labor. With the correct estimation of failure mode and the effective response calculation, hull structure designers can design satisfactory structures.

The next step is to calculate responses calculation for the forces applied. In the old style response calculation, each structural member is assumed to be a simple beam fixed at both ends. Recently, with the help of a computer whole structures can be modeled and analyzed for the estimated forces. However, for the reliable design, considering statistical distribution of forces and deterioration of materials, more research will be required.

Recently in the design of land structures and building, the probabilistic finite element analysis is used to obtain damage probability when we input the statistical force data and scantling data [1]. This method can be also applied to the hull structure design.

For the allowable limit, there are allowable stress, allowable deformation, allowable amplitudes of vibration and allowable reliability. These limits are usually stipulated by external and social requirements such as the classification society's rules. The hull structure designer has no decisive right but should pay special attention to them. And here there are very important items, which include: load estimations, response calculations and allowable limit. They should be investigated together and simultaneously. Any changes in the method of load estimation must be followed by modifying the allowable limit.

The importance of the structural members is based on the damage caused by the failure of the member. It is reasonable to apply a different safety factor, corresponding to the importance of the member.

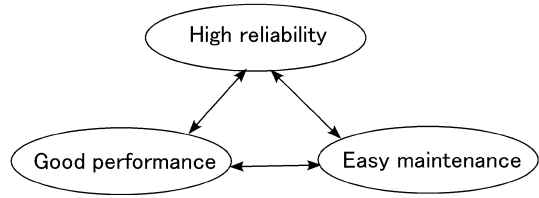
Where the calculated response is within the allowable limit, the shape and the scantling of the member are to be accepted and decided upon, provided that the values are moderate. If these values are not moderate, further options must be considered. For example, with the existing material and facilities, the million tonner can not be built and the maximum available tanker will be one of 700,000 DWT. Additionally a 5-hold arrangement gives problems, while a 6-holds one would be preferable from a structural viewpoint.

In Fig. 1.2.1 there is no description of the material, which is one of the most important items in the structural design, because mild steel, which has been a major shipbuilding material, has splendid properties, tough, strong, high weldability and low price. The hull structure designer can use it without any special attention. However, nowadays high tensile steel is becoming more common as a shipbuilding material. When the high tensile steel and other special materials are used as shipbuilding material, the hull structure designer must pay careful attention to these materials.

### 1.3 Hull Structure Design Policy

Prior to designing a ship, a design policy must be established and confirmed. The principle of hull structure design is illustrated in Fig. 1.3.1; high reliability, good

**Fig. 1.3.1** Optimun reliability



performance, and easy maintenance, same as in any other design process. These three elements are to be established from the user's point of view, who operates ships and contributes to worldwide economy.

High reliability can be achieved by reliable design stated after. Good performance means a well-balanced structure which can carry out the given duty during the given period. Good performance can be obtained by rationalization. Reliability concerns the safety of ship, crew member, and cargo, so as to prevent any failures which could jeopardize the ship's safety. Easy maintenance means less repair cost and good accessibility for inspection.

To realize a good balance in the above policy; high reliability, good performance, and easy maintenance, a rational design system must be established, based on the theoretical approach and plentiful experience.

## 1.4 Basic Idea of Hull Structure Design

The basic idea of hull structure design is: "A ship will break when the load applied is bigger than the ship's strength". It is a simple but grim reality. Once the ship is broken the safety of the ship will be in jeopardy, then the crew's lives and the owner's property (ship and cargo) are at stake.

Even today when science and technology have progressed remarkably, there still exists an unknown part in the forces applied on the ship and the strength of the ship's structure. The hull structure designer should design the structure very careful, based on the updated knowledge.

Actually hull structures are designed using the classification society's rules; however, the rules are not 100% perfect. The designer must do his/her utmost in the design.

When a failure such as a crack, buckling, collapse, etc. arises in a ship, it is regarded as a good chance to gain engineering knowledge, though the damage is not pleasing in itself;

1. to go to the spot on board
2. to see the appearance of the failure
3. to consider the phenomenon at that locality

It is important to observe carefully the detail such as figure, size, direction, etc., and to estimate the magnitude, direction, source, and transmitting route of the forces,

by seeing the actual damage to the structure. If possible, learn of the operating conditions at the time of the event from the crew concerned.

After that, experiments are also carried out if necessary. Next, the cause of the damage and failures are predicted by analysis, and countermeasures are determined in accordance with the calculation. The worst case is to calculate using a complex model such as the FEM program without seeing the actual damage. Recently, this tendency is increasing due to the rise in computer simulations. Structural designers tend to rely on the result of FEM calculations without considering the principle of strength.

## 1.5 Studies on Loads Applied

Before 1960, the wave bending moment was calculated by assuming that the wave had the same length as the ship and the height was 1/20 of this length. After intense and numerous observations, research of ocean waves, and research on ship motion in waves, the wave bending moment can be estimated rather accurately nowadays. In Fig. 1.5.1 the reduction of the midship section modulus required by Nippon Kaiji Kyokai (NK) is shown. In the figure the level of 1.0 shows the guidelines for the 1930 load line regulations [2, 3].

Figure 1.5.1 shows that the required section modulus has reduced year by year especially for larger ships. These are the fruits of the above research. Due to this research, large ships can be satisfactorily constructed.

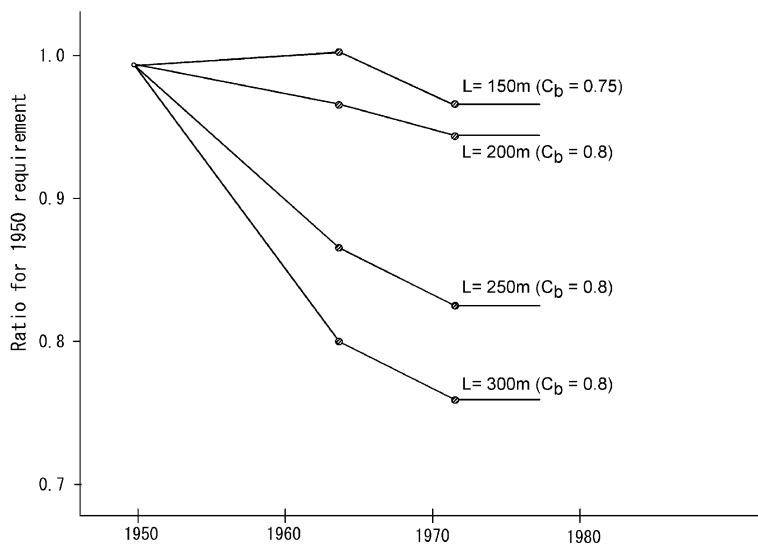


Fig. 1.5.1 Reduction of section modulus required (tanker)

Also before 1960, the tank length of a tanker was limited to 15 m. It was too limiting in order to build large tankers economically from the hull steel weight, fitting weight and cargo operation viewpoints. However, the designer did not have any reason to increase the tank length over 15 m.

Much research was carried out on cargo oil movement in tanks caused by ship motion and sloshing pressure by the cargo oil motion. And as a result tank length was extended up to a value of 20% of the total ship length. According to the old regulation, a 250,000 DWT VLCC tanker must have 40 or 50 tanks of 20 m breadth, 35 m depth and 15 m length which is uneconomical and inconvenient for operation.

As the above examples show, rationalization can be achieved by research, thus discarding the obsolete traditional ways and methods.

## 1.6 Reliable Design

It is stressed in Sect. 1.4 that the structural design is based on the forces applied and the strength of the ship. In this chapter how to maintain the ship's safety and reliability, for the applied forces and the strength of the ship itself, is introduced [4].

There are three important procedures in the hull structure design:

1. The forces applied are to be estimated
2. The structural response is calculated applying by these forces on the hull structure
3. The obtained responses are assessed against allowable values.

To maintain safety and reliability it is important to have good accuracy in these three values. In the design of ship structures the force applied is divided into two, static loads which are the difference between weight and buoyancy, and dynamic loads such as fluctuating forces and impact forces from waves. The former can be calculated with sufficient accuracy, but the latter is difficult to estimate because it has many variations depending on the geographical area and the season.

Response calculations can now be done with sufficient accuracy by means of a framework or Finite Element Method thanks to the development of computers. The calculated results coincide well with the results of model tests and full-scale tests.

The allowable limits can be decided, in the case of ordinary ships for which past experience has accumulated, by comparing results of response calculations for estimated applied forces with damage data of the ship in service. This is an empirical reliable design.

For new types of ship and for special ships which have no damage history, the empirical method can not be applied. In this case response calculations will be done with applied forces which are estimated as accurately as possible. And the allowable limit is to be decided based on the property of materials to be used and the theory of fracture mechanics. This is a theoretical reliable design.

A flowchart of a reliable design is shown in Fig. 1.6.1 in which "theoretical failure probability flow" corresponds to the above theoretical reliable design and "empirical failure probability flow" corresponds to the empirical reliable design.

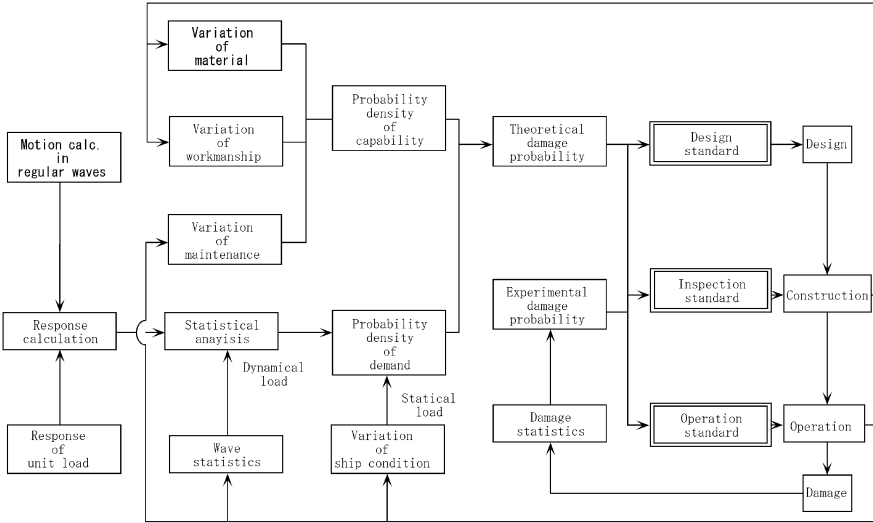


Fig. 1.6.1 Flow diagram of reliable design

The values in Fig. 1.6.1 are variable and statistical. In that many parameters in ship design are not definite but take statistical values which have a distribution around representative values. For example, concerning the forces applied and the strength of the structure, the former changes depending on loading and wave conditions, and the latter changes depending on tolerance of materials, accuracy of manufacturing, and design standards.

Theoretical reliable design aims to keep reliability by gathering data on statistical parameters and calculating failure probabilities theoretically for many kinds of failure modes.

The failure probability can be obtained by considering the distribution patterns of the forces applied and the strength of the structure [5]. As shown in Fig. 1.6.2, if probability density functions of forces applied  $D$  (hereafter forces applied is to be called demand) and strength of structure  $C$  (hereafter strength of structure is to be called capacity) are given with the horizontal axis indicating stress  $X$ , the failure probability is given by the following equation:

$$P_f = \int_0^{\infty} Q_d\{X\}P_c\{X\}dX = \int_0^{\infty} (1 - Q_c\{X\})Pd\{X\}dX \quad (1.6.1)$$

where

- $P_d\{X\}$ : probability density function of demand
- $P_c\{X\}$ : probability density function of capacity
- $Q_d\{X\}$ : probability of demand exceeding certain value
- $Q_c\{X\}$ : probability of capacity exceeding certain value

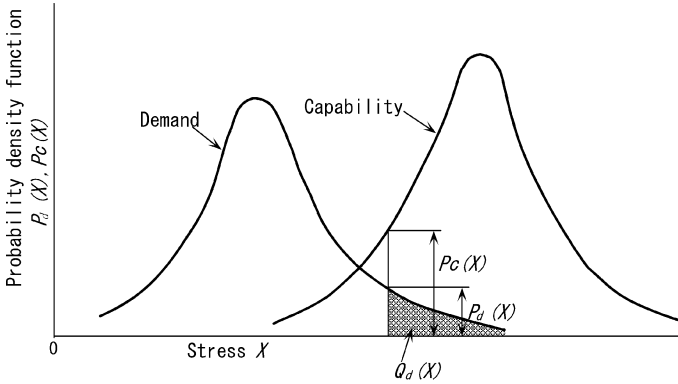


**Fig. 1.6.2** Probability of fracture

$P_f$  can be estimated approximately by the overlapped area of  $P_d \{X\}$  and  $P_c \{X\}$  in Fig. 1.6.2. A ship's failure is divided into plastic collapse, buckling, fatigue fracture and brittle fracture. For plastic collapse and buckling the maximum demand is most important. And the maximum demand caused by the biggest wave once per  $10^8$  cycles is applied for plastic collapse and buckling analysis. Assuming the wave period is about 7 s and there are 320 sailing days in a year, a ship encounters  $10^8$  waves in 25 years of her life. And for fatigue fracture analysis a concept of cumulative damage intensity is applied using distributions of demand in these  $10^8$  cycles of waves. Brittle fracture can be avoided by selecting a grade of materials and welding condition to meet the ship's service environment.

To reduce the probability of failure, it is effective to reduce the overlapping area of curve D (demand) and curve C (capacity) in Fig. 1.6.2. For that there are two ways, one is to have a bigger ratio between the mean values of C and D which is called safety factor, and the other is to make both curves more sharp which means more accurate estimation of demand and more accurate control of capacity. Treating this matter theoretically, Fig. 1.6.3 is obtained [6]. Here, the distributions of demand and capacity are assumed to be normal.

In Fig. 1.6.3 the horizontal axis is the mean safety factor  $N$  which is the ratio  $\bar{C}/\bar{D}$  of the mean value of the demand  $\bar{D}$  and mean value of the capacity  $\bar{C}$ . And the failure probability is plotted for various combinations of the variation factor  $V$  (standard deviation/mean value) of demand and capacity. From Fig. 1.6.3 it can be seen that the failure probability changes remarkably with the factor  $V$ , and in the case of smaller factor  $V$ , failure probability can be reduced considerably by a small increase in the safety factor. In the case of a bigger  $V$  factor, failure probability can be reduced a little by increasing safety factor.

To achieve reliable design it is important first to determine the variation in the necessary parameters. Standardization and systematization will reduce these variables and the probability of failure. Design standards, inspection standards, and operation standards play very important roles in keeping a ship's reliability by limiting the variation in every parameter which affects a ship's safety over her life.

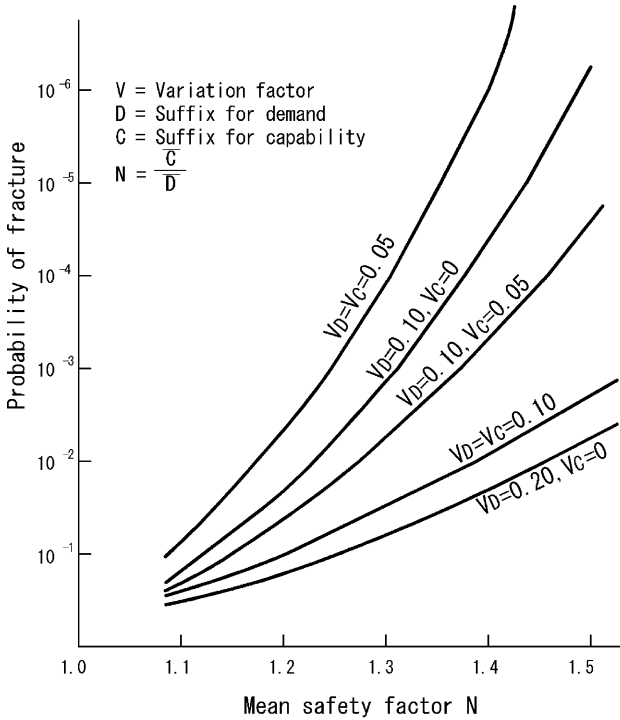


Fig. 1.6.3 Probability of fracture and mean safety factor

On the other hand, reliable design based on the theoretical failure probabilities as stated above can be gained by using empirical failure probability. In the case of ordinary ships which have accumulated past experiences, allowable limits are to be decided based on the past experiences. And ships built with similar design, material, and workmanship, and operated with similar operation standards will have similar reliability as the previous ship.

For new types and special ships never built before, reliable design with theoretical failure probability is the surest way at this moment. However for ordinary ships which have previous experience reliable design using empirical failure probability is most applicable.

In addition to the above it is important for the designer to keep in mind that the reliability, rationalization, and economy have to be well balanced.

Apart from the above explanation for new buildings, the failure probability of ships in service changes year by year depending on the maintenance. This is shown in Fig. 1.6.4 [1]. Hatched part shows failure probability after aging.

Given the distributions of demand and capacity, failure probability can be calculated according to a text book [7]. The important point in reliable design is how much failure probability is to be applied.

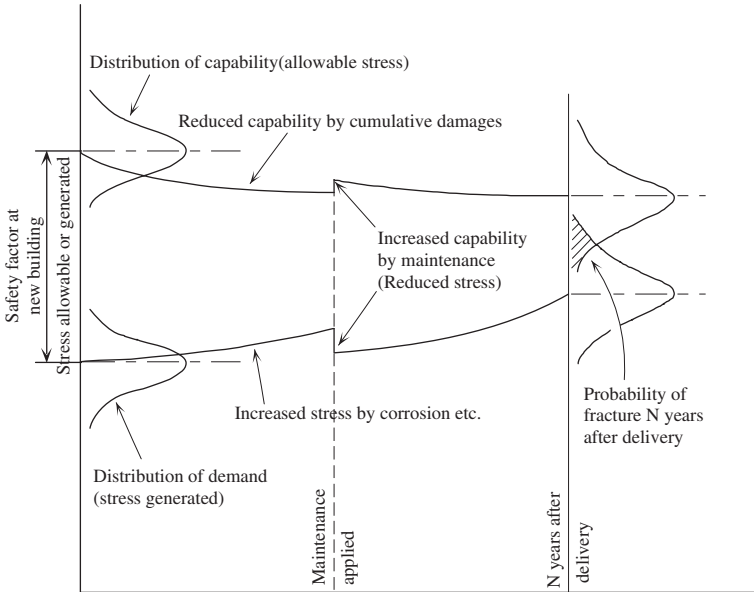


**Fig. 1.6.4** Probability of fracture with consideration of reduced strength and increased stress by aging

There are many kinds of structural members, for example longitudinal strength members, transverse strength members, and local strength members, in the hull structure. How much reliability to be given to each member is to be decided by the designer according to his/her design policy.

In this procedure the degree of importance stated in Fig. 1.2.1 can be applied. The degree of importance will be proportional to the damage suffered from the failure of the member, and a bigger degree of importance corresponds to bigger damage. A smaller degree of importance is for a member which has failure before damage can be repaired. There are three kinds of damage suffered as follows:

- (1) how dangerous and how extensive
- (2) how much will social matters be affected
- (3) how big the economical loss

In the case of land structures with hazardous materials such as a nuclear power stations, chemical plants, etc. where people live who have no direct connection with these companies, the failure probability should not be decided only by the designer but should be decided with social agreement, because once failure happens the local inhabitants will suffer from the damage. In the case of a ship it is decided usually without any social agreement.

Transportation is also a part of social welfare and a ship will be one of the life-lines where there is no alternative transportation, for example supplying electricity, gas and water.



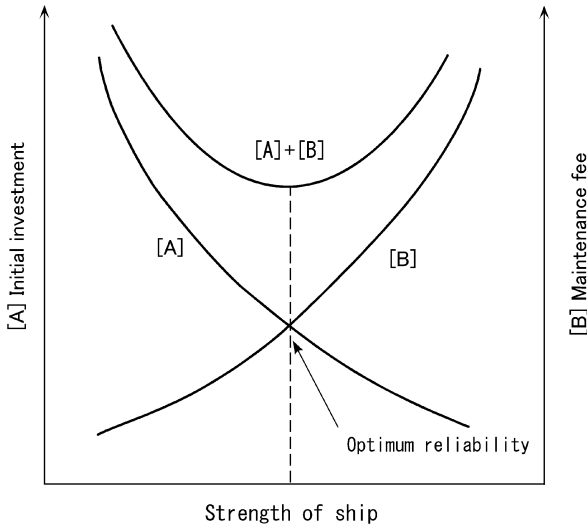


**Fig. 1.6.5** How to decide optimum reliability

The optimum criterion of reliability is shown in Fig. 1.6.5. The horizontal axis is ship's total reliability in which each member of the hull structure is evaluated by the reliable design rational. The curve [A] is initial investment which increases with the improvement of the ship's total reliability. The curve [B] is the maintenance cost including repair cost due to the damage suffered, which decreases with the improvement of the reliability. The optimum point will be the minimum point of the curve [A] + [B].

# Chapter 2

## Structural Design Loads

### 2.1 Introduction

When a ship is sailing at sea, it is subjected to various load patterns with many magnitudes which cause deformation of its structure, as well as stresses. The structural designer needs to know the hull structure load features, as accurately as possible: direction of the working load, frequency of occurrence, distribution pattern on the hull structure and behavior in the time domain, etc. The first design step is to assume exact loads acting on the structure concerned, in order to estimate the structural strength in a reasonable way and consequently to develop the design.

In this chapter, the classification of loads being applied to a hull structure will be explained, then the features of typical load components will be described, and finally the method of estimating wave loads will be discussed.

When considering the load features where the load is transmitted gradually and continuously from a local structural member to an adjacent bigger supporting member, the best way to categorize loads on the hull structure is as follows:

- Longitudinal strength loads
- Transverse strength loads
- Local strength loads

(1) *Longitudinal Strength Load*: Longitudinal strength load means the load concerning the overall strength of the ship's hull, such as the bending moment, shear force and torsional moment acting on a hull girder. Since a ship has a slender shape, it will behave like a beam from the point view of global deformation. Now let's assume a ship is moving diagonally across a regular wave as shown in Fig. 2.1.1. The wave generates not only a bending moment deforming the vessel in a longitudinal vertical plane but also a bending moment working in the horizontal plane, because of the horizontal forces acting on side shell. In addition, the wave causes a torsional moment due to the variation of the wave surface at different sections along the ship's length. If the above longitudinal strength loads exceed the upper limit of longitudinal strength for the hull, the hull will be bent or twisted. Therefore the longitudinal strength load is one of the most important loads when calculating the overall strength of a hull structure.

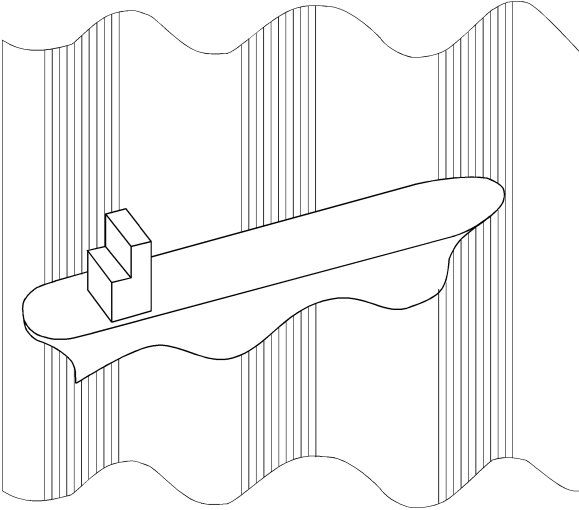


**Fig. 2.1.1** Ship in oblique waves

(2) *Transverse Strength Loads*: The transverse strength loads represent the loads which act on transverse members and cause structural distortion of a cross section. Transverse strength loads include hydrostatic pressure on the outer shell, weight of cargo load working on the bottom structure, ballast water pressure inducing the deformation of the ballast tank, etc. For instance, let's imagine a transverse section of a ship floating in still water as illustrated in Fig. 2.1.2. This section is subjected to: (a) hydrostatic pressure due to surrounding water, (b) internal loading due to self weight and cargo weight. These loads are not always equal to each other at every point, consequently loads working on transverse members will produce transverse distortion as shown by the broken line in Fig. 2.1.2. When we consider transverse loads and longitudinal loads, the following characteristic is significant from the strength analysis point of view: The distortion due to longitudinal loads does not

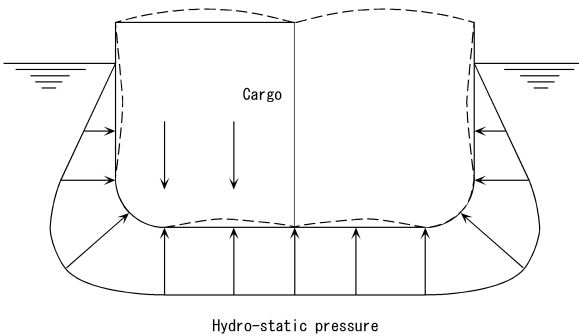


**Fig. 2.1.2** Example of deformation due to transverse strength loads

affect the deformation of the transverse section. For example, the longitudinal bending moment or shear force can never have an influence on the distortion of the cross section. It is therefore necessary to recognize the transverse deformation of the ship structure due to the transverse load, independently from the deformation induced by a longitudinal load. Transverse strength loads are commonly used in cases where we investigate the strength of primary members, such as transverse rings, transverse web frames, etc.

(3) *Local Strength Loads*: The local strength loads include loads which affect the local strength members such as shell panels, stiffeners and connecting constructions between stiffeners.

The above load categories are so convenient that they are extensively used for practical design purposes. A load acting on the structure can be treated independently by considering the load transferring from a local structure to a bigger structure. For example, let's consider the case where the designer commences the design of a bottom structure as shown in Fig. 2.1.3. Firstly, the strength of bottom shell panels must be determined regarding lateral water pressure, secondly, the strength of longitudinal stiffeners, which support the subject panels, must be evaluated, thirdly, the strength of transverse webs holding stiffeners at their ends must be estimated and finally, the global strength of the bottom structure must be discussed. Investigations can be done separately for each member by only considering the magnitudes of the loads which are transmitted by each member.

This is a convenient concept, however, time-dependent relations between those simplified loads have been intentionally omitted. Therefore careful attention must be paid, particularly when analyzing the simultaneous response of the entire structure

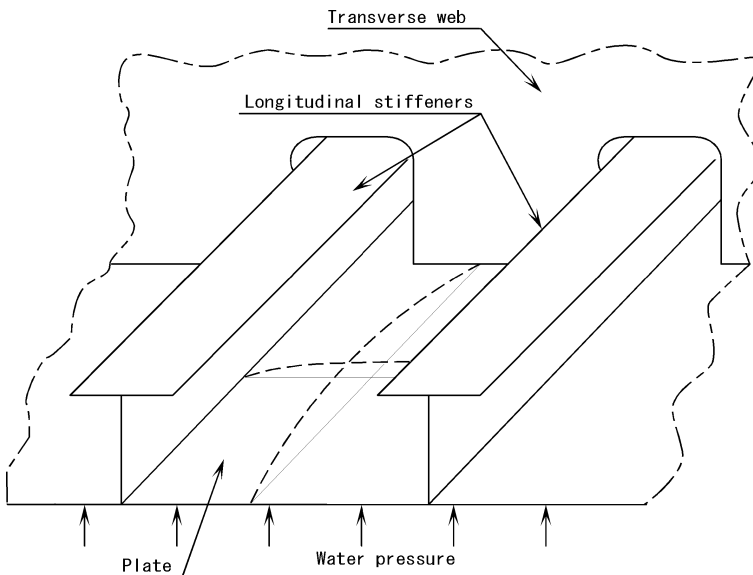


Fig. 2.1.3 Bottom structure under water pressure

to combined loads, because the phase of the loads plays an important roll when calculating the overall response.

## 2.2 Longitudinal Strength Load

Longitudinal strength loads are loads which affect the overall strength of a ship's hull girder, in which the ship is regarded as a beam or girder, because of it's slender profile. They are represented in terms of longitudinal bending moment, shear force and torsional moment. The longitudinal strength loads may be divided into two categories: static longitudinal loads and dynamic longitudinal loads.

Static longitudinal loads are induced by the local inequalities of weight and buoyancy in the still water condition. For instance, differences between weight and buoyancy in longitudinal direction cause a static bending moment and a static shear force, and asymmetrical cargo loading causes in a static torsional moment.

Dynamic longitudinal loads are induced by waves. When the ship is on top of a wave crest in head sea condition, it causes a "hogging" bending moment and a shear force. When in a wave trough a "sagging" bending moment and shear force are experienced, as indicated in Fig. 2.2.1. These loads act alternately on the hull girder as the wave progresses along the ship. In cases where the ship encounters oblique seas a dynamic torsional moment is produced.

The magnitude of the dynamic longitudinal load used in strength calculations of wave bending moment and wave shear force used to vary with each Classification Society. However, the rules were standardized by the IACS (International

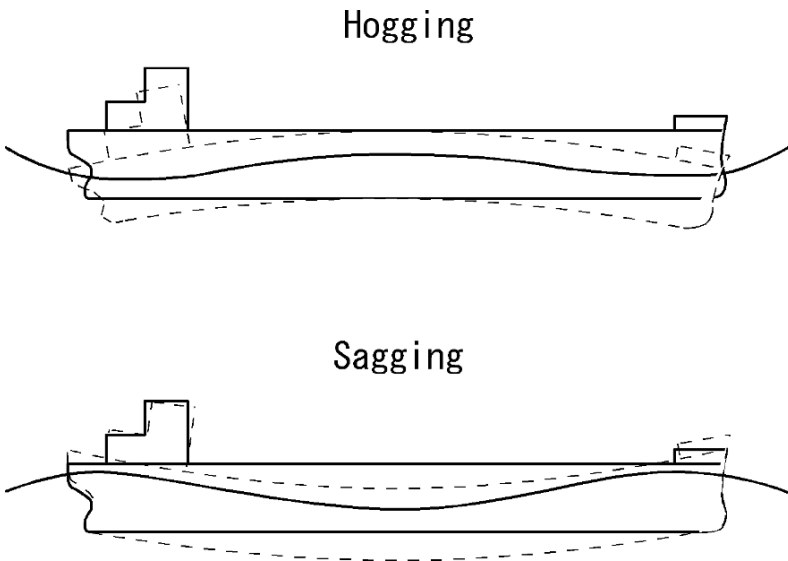


Fig. 2.2.1 Vertical bending due to waves

Association of Classification Societies) in the Unified Rule Requirement in 1989 and were accepted by all Classification Societies. For example, IACS specifies the wave bending moments with the following equations, which are common equations used by the major Classification Societies that belong to IACS:

$$Mw(+) = +0.19C_1C_2L_1^2BC'_b \quad (\text{kN-m}) \quad (2.2.1)$$

$$Mw(-) = -0.11C_1C_2L_1^2B(C'_b + 0.7) \quad (\text{kN-m}) \quad (2.2.2)$$

where

$Mw(+)$ : the wave bending moment of hogging

$Mw(-)$ : the wave bending moment of sagging

$C_1$ : the parameter determined by ship length

$$C_1 = \begin{cases} 10.75 - \left(\frac{300 - L_1}{100}\right)^{1.5} & L_1 \leq 300\text{m} \\ 10.75 & 300\text{m} \leq L_1 \leq 350\text{m} \\ 10.75 - \left(\frac{L_1 - 350}{100}\right)^{1.5} & 350\text{m} \leq L_1 \end{cases} \quad (2.2.3)$$

$C_2$ : distribution factor along ship length as specified in Fig. 2.2.2

$L_1$ : ship length (m)

$B$ : ship breadth (m)

$C'_b$ : block coefficient

The above dynamic longitudinal loads can be obtained by the long-term prediction method on the basis of ship motion calculations by strip theory. The details will be discussed in Sect. 2.4. The long-term prediction method means a method to predict a response statistically over a rather long period, e.g. the 20 years life cycle of a ship. So, instead of using the Classification Societies' Rules formulae to calculate the dynamic loads in the conventional way, the direct calculation method for practical design purpose has become more popular for its convenience and accuracy. The wave induced bending moment of IACS is determined in such a way that the magnitude of the bending moment is expected to be approximately equal to the maximum

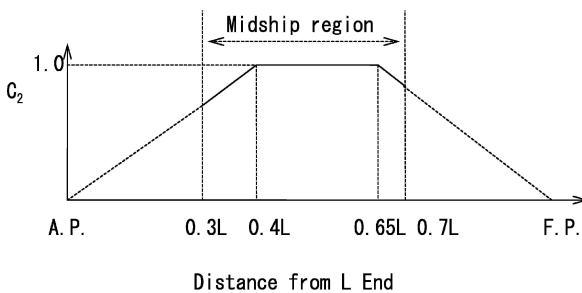
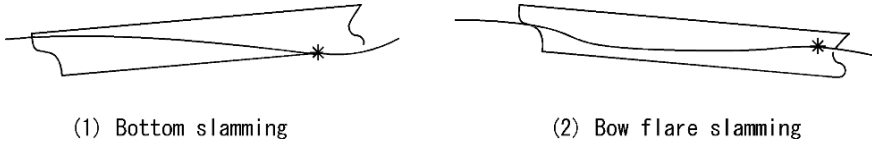


Fig. 2.2.2 Coefficient  $C_2$  : distribution factor



**Fig. 2.2.3** Types of slamming impact of a ship

value once in 20 years, i.e. the expected probability of occurrence is:  $Q = 1 \times 10^{-8}$ . The IACS formulae were found to be reasonable with the aid of the above mentioned long-term prediction method carried out by several classification societies.

In the case of moderate seas the above prediction method, based on linear strip theory, is reliable enough to estimate the wave loads accurately. However, with



**Fig. 2.2.4** Wave impact at sea

rough sea conditions this linear theory cannot be applied, since the calculated results of ship motion and dynamic loads are influenced by the wave impact force and/or by the non-linear effect of the vertical change of ship breadth at each cross section. These impact loads can contribute to the increase of longitudinal loads, for they may generate both an additional bending moment and shear force in the hull girder.

Wave impact loads can be divided into two loads: (a) impact force induced by slamming and (b) impact force of green seas on the deck.

Slamming occurs when the hull hits the water surface hard, when ship movement is severe, particularly in heave and pitching conditions. When the bottom emerges from the wave surface, “bottom slamming” is induced on the ship’s bottom plating, as shown in Fig. 2.2.3. In the case of slamming on bow flare, it is called “bow flare slamming”. Figure 2.2.4 shows also a container vessel subjected to wave impact in rough seas at the bow area.

If a ship’s bow is pushed into the water in a severe downward pitch, the wave crest may come down on the forecastle deck, which may cause damage to the ship structure and deck machinery. This is called “deck wetness by green water.”

## 2.3 Transverse Strength Load

Transverse strength loads denote the loads which cause distortion of transverse members due to unbalance of external and internal loads, including structural and cargo weights. These loads can be regarded as being independent of longitudinal strength loads, for the longitudinal loads only cause a ship to behave as a beam and they do not cause distortion of the transverse section. These loads are categorized as follows:

- Structural weight, ballast water weight and cargo weight
- Hydrostatic and hydrodynamic loads
- Inertia force of cargo or ballast due to ship motion
- Impact loads

(1) *Structural weight, ballast water weight and cargo weight*: These loads are dead loads, which mean constant loads that are time independent, induced by gravity at the centers of gravity of the members.

(2) *Hydrostatic and hydrodynamic loads*: The hydrostatic load is the static pressure from the water surrounding a transverse section, which acts on the hull structure as an external load. Another external load is the hydrodynamic load induced by the interaction between waves and the ship motion and subjects the outer shell of the ship to fluctuating water pressure. It is superimposed on the hydrostatic load and creates the total water pressure.

Each classification society gives the empirical formula for calculating the fluctuating external pressure by waves in a different way. For example, NK specifies the calculation form of the external water pressure by including the fluctuating pressure as shown in Fig. 2.3.1. In the figure,  $H_0$ ,  $H_1$ ,  $H_2$  are the symbols representing the magnitude of fluctuating pressure distribution at the wave trough position below the static draft, at the wave crest position above the static draft and at the bottom base line respectively.



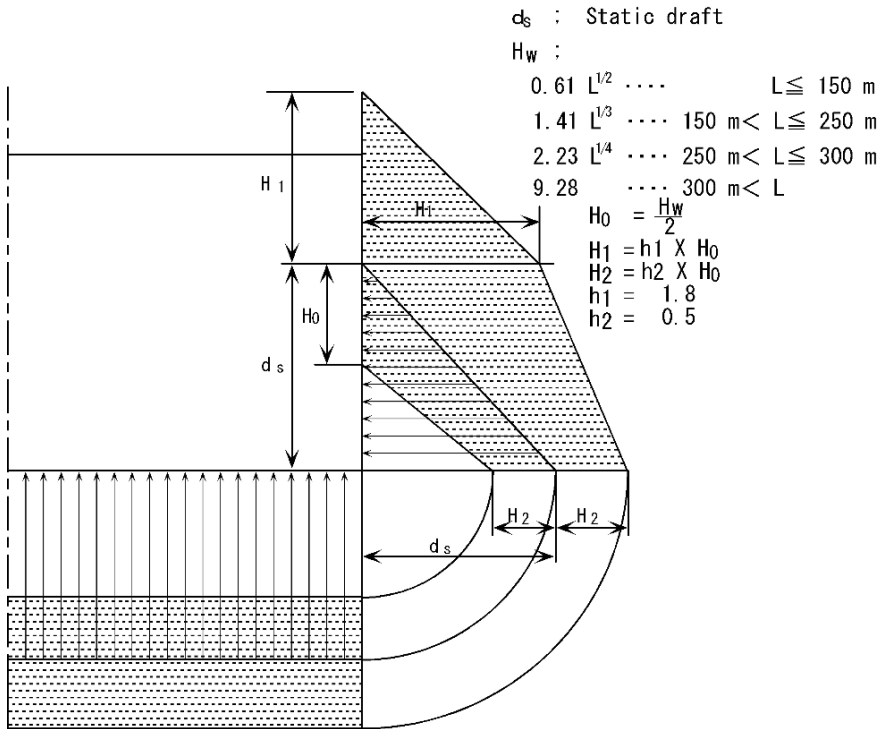


Fig. 2.3.1 Transverse strength calculation loads by NK

An alternative way to estimate the wave fluctuating pressure is to calculate it with the aid of the long-term prediction method which is also the case when calculating the longitudinal strength load which will be described hereafter. For practical purposes this method is accurate enough to be used in structural design.

(3) *Inertia force of cargo or ballast due to ship motion:* The inertia force is induced by the reaction force of self weight, cargo weight or ballast weight due to the acceleration of the ship motion. Assume that a tanker is rolling among waves in a fully loaded condition, then the cargo oil in the hold has a cyclic movement in the transverse direction. This must result in a fluctuating pressure of the hull structure of the tank due to the inertia force of the cargo oil movement. In addition, internal pressure is introduced not only by rolling but also by the ship's other motions, such as heaving, pitching, etc. A similar phenomenon can be observed when a cargo oil tank is partially filled.

The same long-term prediction method is applicable in the prediction of the internal pressure, since it gives an accurate prediction of the acceleration.

(4) *Impact loads:* There are two impact loads classified as transverse strength loads: slamming and sloshing.

Slamming may be categorized as a transverse strength load, as well as a longitudinal strength load. It means the impact force as the shell plating hits the water surface severely. Therefore, it generates not only a longitudinal load but also a load

affecting the transverse strength simultaneously. Many ships are damaged by slamming, resulting in denting of shell plating, in particular the bottom forward shell plating. Wave impact pressure is an item for which the pure theoretical approach is very difficult, so experiments are necessary to estimate the impact pressure with reliable accuracy. Figure 2.3.2 denotes one of the test results from a dropping test of an inclined 2 dimensional bow structure model.

Sloshing is a phenomenon where the fluid movement in the tank gets into resonance with the ship motion and creates an impact force between the moving free surface of the fluid and the tank structure. Sloshing is caused by the movement of the fluid's free surface, therefore, if the tank is fully filled with fluid, sloshing will never happen since the free movement of the liquid's surface is restricted. When the level of the liquid reaches to a certain portion of the tank, the liquid resonates with the movement of the tank and then sloshing occurs.

The natural frequency of sloshing is determined by the tank dimensions and the level of the liquid. Figure 2.3.3 shows one of the experimental results of a sloshing

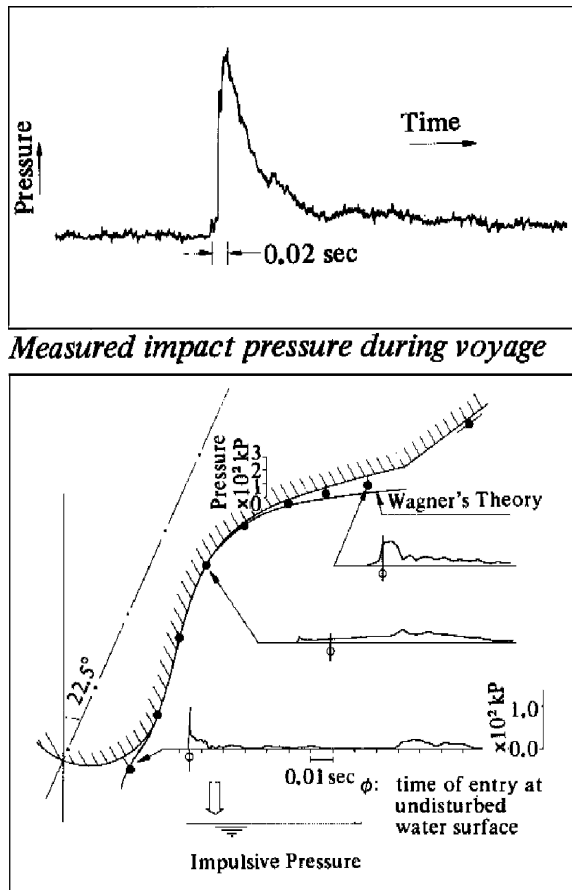


Fig. 2.3.2 Drop test results of inclined 2- dim. model

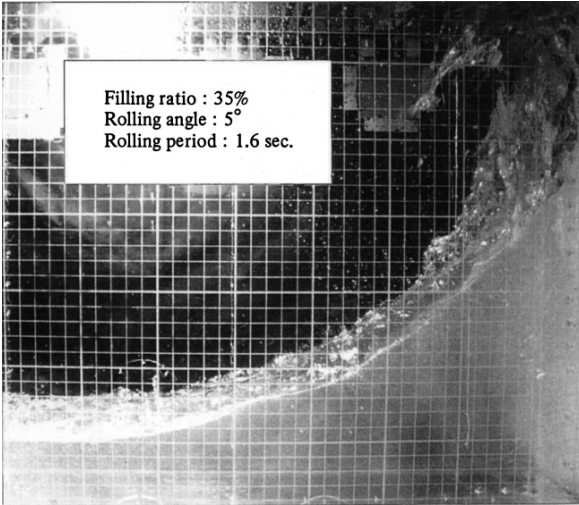


Fig. 2.3.3 Sloshing test of a rectangular tank

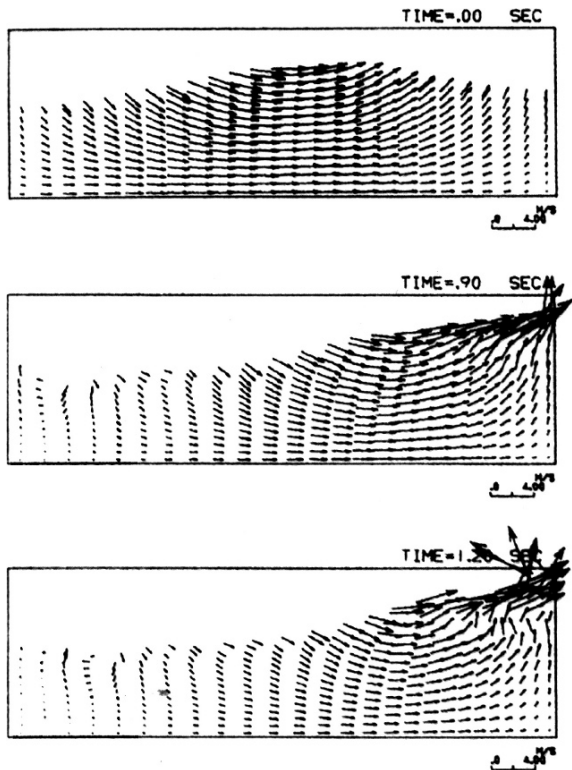


Fig. 2.3.4 Computer simulation of liquid sloshing in a tank

test of a rectangular tank model and Fig. 2.3.4 indicates the result of a computer simulation program utilizing the finite difference technique.

## 2.4 Ship Response Calculation in Waves

### 2.4.1 Introduction

In order to obtain an accurate estimation of wave induced loads, the designer has to know an exact wave load calculation method. In this article the evaluation procedure of wave loads is briefly introduced; for a more detailed discussion the reader is referred to [8–10]. A prediction method of wave loads and ship responses has been developed on the basis of the strip method, and it was found that the calculated result can be used for the practical design of conventional vessels. The ordinary evaluation procedure follows the calculation steps as below:

- Calculation of ship responses among regular waves by the strip method
- Short-term prediction method for ship responses among irregular waves
- Long-term prediction method for ship responses among irregular waves

### 2.4.2 Strip Method

A ship has a long and slender hull shape in comparison with its breadth and depth. Taking advantage of the above assumption, fluid motion around hull surface due to ship motion can be regarded as if it moves in cross sectional plane. In other words, the fluid force can be obtained by integrating the force acting on transverse strips delivered as shown in Fig. 2.4.1; consequently the interaction force between

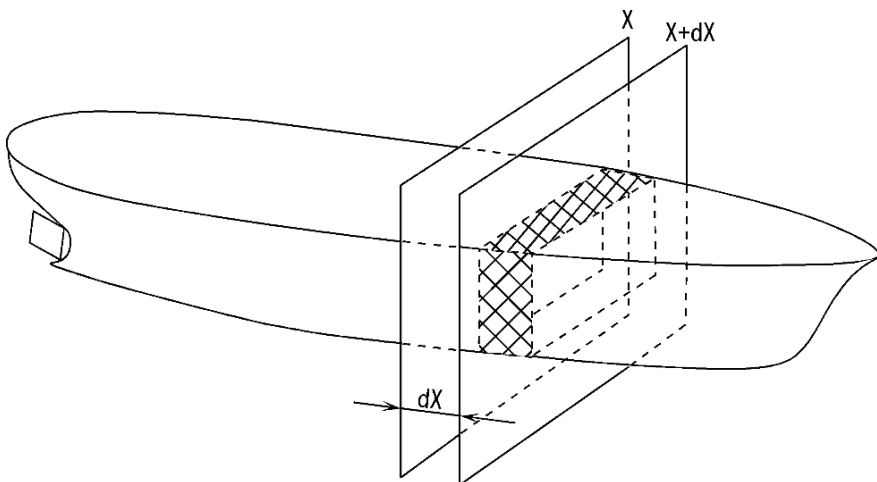


Fig. 2.4.1 Definition of ship's strip

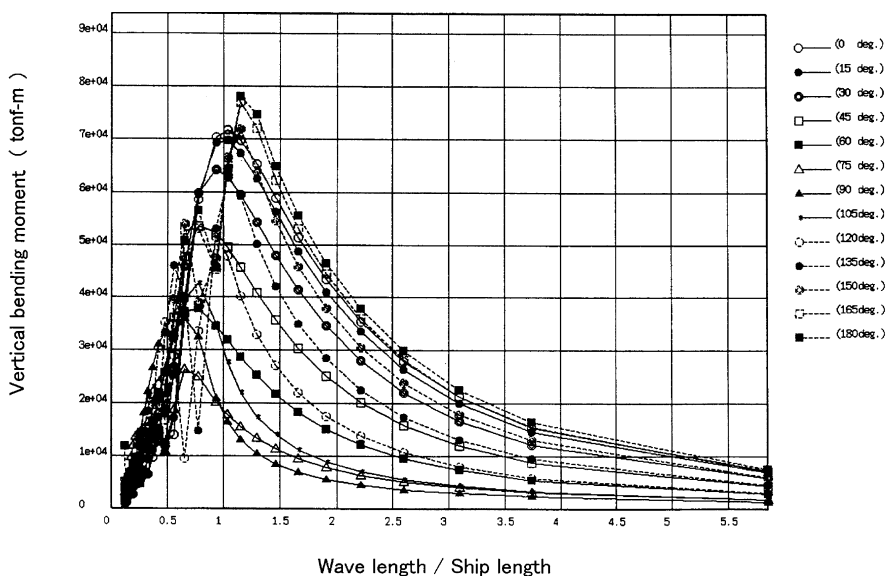


Fig. 2.4.2 Response function of vertical wave bending moment (150,000 DWT tanker)

each strip is neglected. The strip method is utilized to calculate ship motion, wave induced longitudinal strength loads and wave pressure distribution around the hull in regular waves. An example of the calculation results is presented in Fig. 2.4.2 and it shows the response functions due to a vertical bending moment at midship of double hull tanker of 150,000 DWT in regular waves [11]. According to the figure, it can be seen that the maximum bending moment occurs in the head sea condition, where the wave length is almost same as ship length, i.e. wave length/ship length = 1.0.

### 2.4.3 Short-Term Prediction

A short-term prediction method is useful to evaluate the ship's response in irregular waves by the statistical prediction theory. Short-term means a short period, say 30 min or so, where the significant wave height and the average wave period are considered to be constant. This prediction method is used for calculating the ship's response over a relatively short period of time in terms of ship accelerations, relative wave height, deck wetness, slamming, etc.

Although the waves at sea are not regular waves, these waves can be dealt with by a combination of regular waves having various frequencies and various heights. If the relationship between wave height and frequency of irregular waves is given in spectrum form and the response function of the ship in regular waves is known, then the spectrum of the ship response against irregular waves can be predicted with the following equation:

$$S'(\omega, \gamma) = S'_w(\omega, \gamma) \cdot |A(\omega, \mu)|^2 \quad (2.4.1)$$

where

$S'(\omega, \gamma)$ : power spectra of ship response,

$S'_w(\omega, \gamma)$ : power spectra of component wave in the  $\gamma$ -direction,

$A(\omega, \mu)$ : ship's response function in regular wave to component wave in the  $\mu$ -direction,

$\delta$ : angle between ship's course direction and average wave direction of irregular waves as defined in Fig. 2.4.3

$\gamma$ : angle between average wave direction and component wave direction of irregular waves

$\mu = \delta + \gamma$ : angle between ship's course direction and component wave direction of irregular waves

$\omega$ : circular frequency

The standard deviation  $R$  of the ship's response in the  $\delta$ -direction among irregular waves can be obtained by integrating Eq. (2.4.1) for all frequencies  $\omega$  and for all heading angles  $\gamma$  as in the form:

$$R(\delta)^2 = \int_{-\pi}^{\pi} \int_0^{\infty} S_w^{\eta}(\omega, \gamma) \cdot |A(\omega, \delta + \gamma)|^2 d\omega \cdot d\gamma \quad (2.4.2)$$

Although several types of spectrum functions  $S'_w(\omega)$  of irregular waves are proposed, the Modified Pierson-Moskowitz wave spectrum, which was proposed in the second ISSC (International Ship Structure Committee) held in 1964, is usually applied for practical design purposes to express the long crested wave. These are determined by only two parameters, the average wave period and the significant wave height. The ISSC's wave spectrum is in the following form:

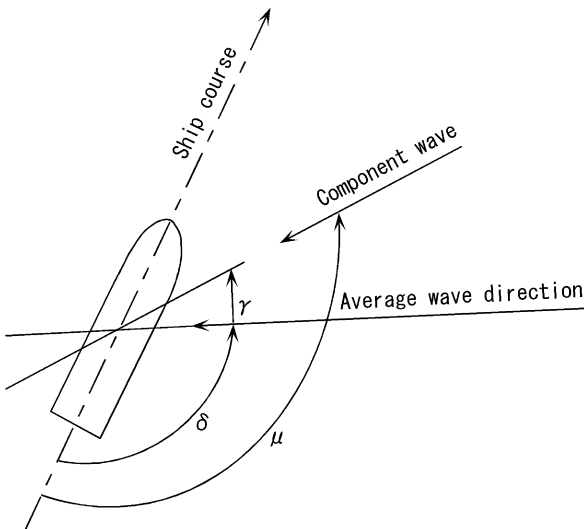


Fig. 2.4.3 Definition of ship's course and wave incident direction

$$S'_w(\omega)/H^2 = 0.11\omega_1^{-1}(\omega/\omega_1)^{-5} \cdot \exp[-0.44(\omega/\omega_1)^{-4}] \tag{2.4.3}$$

where

$H$ : significant wave height

$\omega_1 = 2\pi/T$

$T$ : average wave period

This spectrum looks as illustrated in Fig. 2.4.4. When the effect of short crested waves must be taken into account, it is often assumed that the density of wave power is given by a  $\cos^2 \gamma$  distribution, where the heading direction of the average wave varies from  $-\pi/2$  to  $+\pi/2$ .

Once the Standard Deviation  $R$  of the ship's response is obtained, a short-term prediction can be made by assuming that the probability distribution of the extreme response will follow Rayleigh's Distribution, that is:

$$\begin{aligned} \text{Average} &= 1.25R \\ \text{Average of 1/3 max.} &= 2.00R \\ \text{Average of 1/10 max.} &= 2.55R \\ \text{Expect of 1/100 max.} &= 3.22R \\ \text{Expect of 1/1000 max.} &= 3.87R \end{aligned} \tag{2.4.4}$$

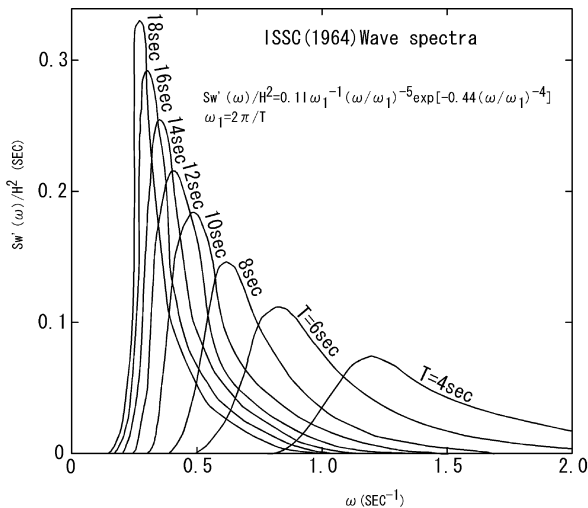


Fig. 2.4.4 Modified Pierson-Moskowitz wave spectra (ISSC spectra)

### 2.4.4 Long-Term Prediction

The long-term prediction is a method to predict statistically the ship's response in irregular waves over a rather long period of time, such as 20 years of the life cycle

of a ship. This method can be applied to cases such as the prediction of the maximum bending moment in 20 years, or of the fatigue damage life, etc. The prediction procedure is explained in Fig. 2.4.5. Once the Standard Deviation  $R(\delta)$  of the ship response is obtained by the short-term prediction, it is possible to calculate the excess probability  $Q(r_1, \delta)$  by providing the ship's wave data over the specified life time in the following equation:

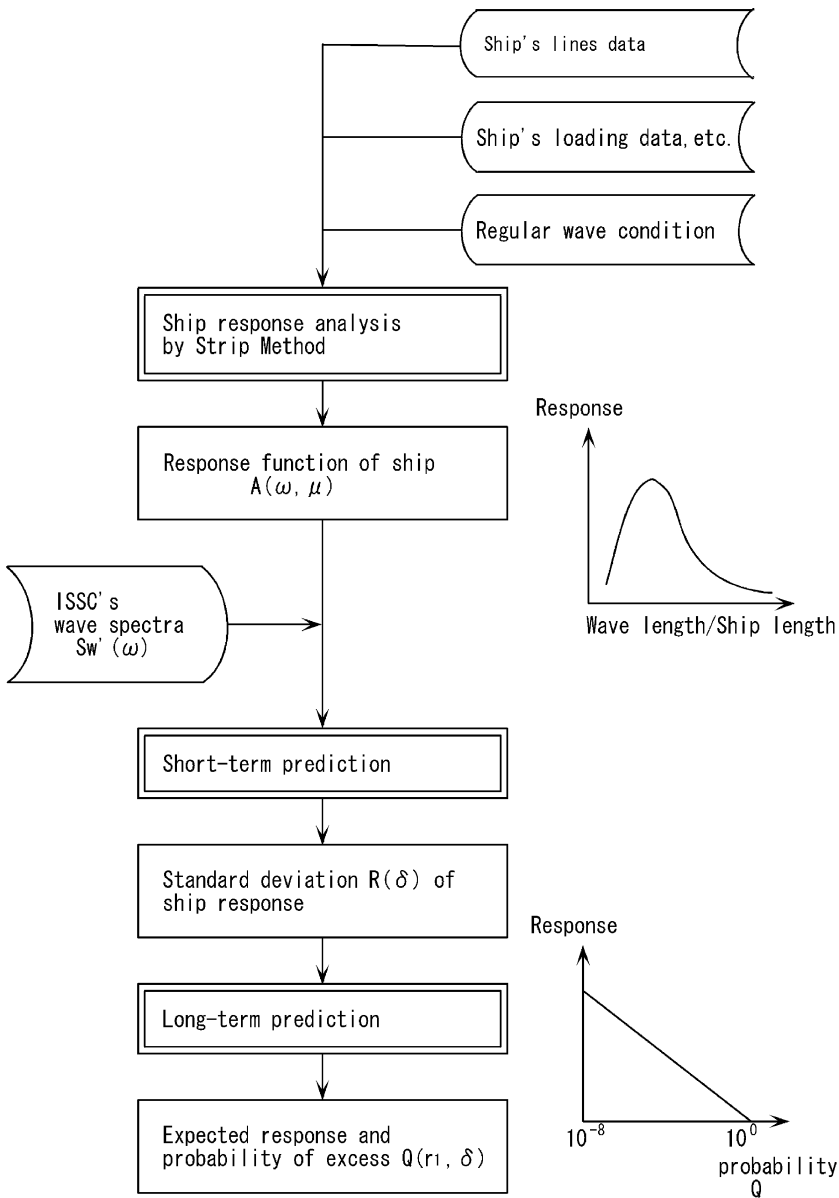


Fig. 2.4.5 Procedure of long-term prediction



$$Q(r_1, \delta) = \int_0^\infty \int_0^\infty \exp \left\{ -\frac{r_1^2}{2R^2(H_w, T_w, \delta)} \right\} \cdot p(H_w, T_w) dH_w \cdot dT_w \quad (2.4.5)$$

where

- $H_w$ : significant wave height
- $T_w$ : average wave period
- $p(H_w, T_w)$ : probability of wave occurrence in the specified sea area

It is therefore possible to obtain the probability of the occurrence that an extreme response may exceed the specified value  $r_1$ :

$$Q(r_1) = \int_0^{2\pi} Q(r_1, \delta) \cdot p^* d\delta \quad (2.4.6)$$

where

- $Q(r_1)$ : probability of occurrence
- $p^*(\delta)$ : probability density function of the ship's course direction

Figure 2.4.6 shows an example of a long-term prediction with regard to a vertical bending moment at midship of 150,000 DWT, for a double hull tanker sailing all over the world.

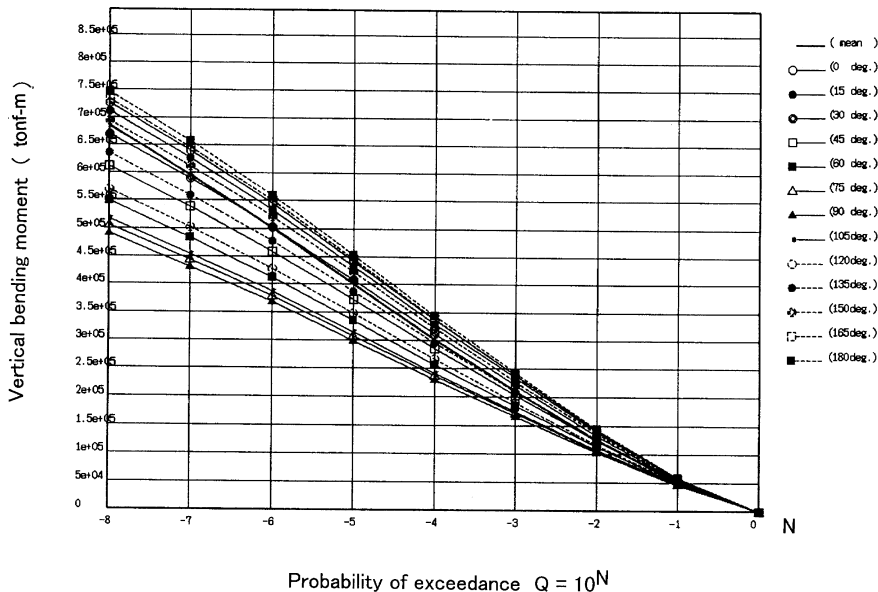


Fig. 2.4.6 Long-term prediction of vertical wave bending moment (150,000 DWT tanker)

# Chapter 3

## Strength Evaluation

### 3.1 General

#### 3.1.1 Introduction

If structural damage to a ship occurs, it means that the load acting on the structure must have exceeded the maximum limit of structural strength. The hull structure has been planned originally by the designer in such a way that the structure can effectively resist the presumed maximum load, which is estimated from previous experience of failure modes of damage. Therefore, once damage occurs in the structure, it indicates the following facts:

- The magnitude of the load causing the failure is greater than that expected. and/or
- The actual failure takes place in a different mode from the presumed one.

By using that damage experience for planning the next structure, the designer is able to improve the accuracy of the load estimation and to accumulate knowledge relating to various modes of failure, and consequently the designer can achieve a design where there would be no future damage to the structure.

When the designer starts a hull structure design, the very first step is to establish the magnitude, direction, probability of occurrence of the load, and also the structural failure modes experienced in the past.

The behavior of the load was discussed in Chap. 2, and in this chapter several failure modes, such as yielding, buckling, fatigue and vibration are explained.

#### 3.1.2 Procedure of Structural Strength Evaluation

We have already explained the summary of structural design procedure in Chap. 1 Sect. 1.2, but in order to consider particularly the evaluation of structural strength, we will repeat again the following design procedure:

1. *Determine an initial system of structural members*
2. *Presume a magnitude, direction, and probability of load*

3. *Assume a failure mode of structure due to the load:* Various kinds of loads act on a hull structure during a voyage and these may cause damage to the structure when the load reaches a certain critical level.

Although there may be several failure modes, the following modes are significant for structural designers:

- yielding
- buckling
- fatigue

**Yielding:** Now let's assume that a tensile load is gradually applied to a structure, then some elongation might be induced and be proportional to the load increment as long as the load is small. Once the load exceeds a certain critical value, then elongation would increase rapidly. That failure mode is called yielding. The designer usually takes care to maintain the strength of the structure so as not to exceed the yield point.

**Buckling:** In the case of a structure under compression load, the structure may suddenly be deflected when the load reaches a critical value. Such a failure mode is called buckling. Once a large deflection takes place, the structure may not recover its original shape even when the load is removed.

**Fatigue:** The structure may be fractured by small loads when the loads are provided repeatedly to the structure. That failure mode is called fatigue. Fatigue is very dangerous, because it may result even from substantially lower loads than yielding strength, especially where the number of cycles is very large. That type of fracture is sometimes caused by vibration, because its frequency is very high.

(4) *Select an appropriate analysis method:* Since a hull structure is mainly composed of several types of stiffened plate, the load on the hull is at first transmitted from panels to stiffeners, then from stiffeners to primary member such as transverse rings or longitudinal girders, and finally from primary members to shell plating.

For instance, Fig. 3.1.1 illustrates the structure of the bottom of a cargo tank, which is composed of shell plating sustained by longitudinal stiffeners and bottom transverses. The working load may be induced by the difference of external pressure  $p_1$  and internal pressure  $p_2$ , therefore, a panel is subjected to the lateral load of  $(p_1 - p_2)sl$  where  $s$ ,  $l$  are the spacing and span of longitudinal stiffeners, respectively. The panel is supported mainly by the adjacent two longitudinal stiffeners and the lateral load of  $(p_1 - p_2)sl$  indicated by the hatched area of plate, is transmitted from the panel to each stiffener. Each stiffener is connected to transverse webs, then finally the lateral load of  $(p_1 - p_2)sl$  is transmitted to these transverse webs.

As shown in the above example, we can deal with the strength of structural members individually according to their components. Thus we often investigate the strength of a panel by thin shell theory, and as for stiffeners and primary members,

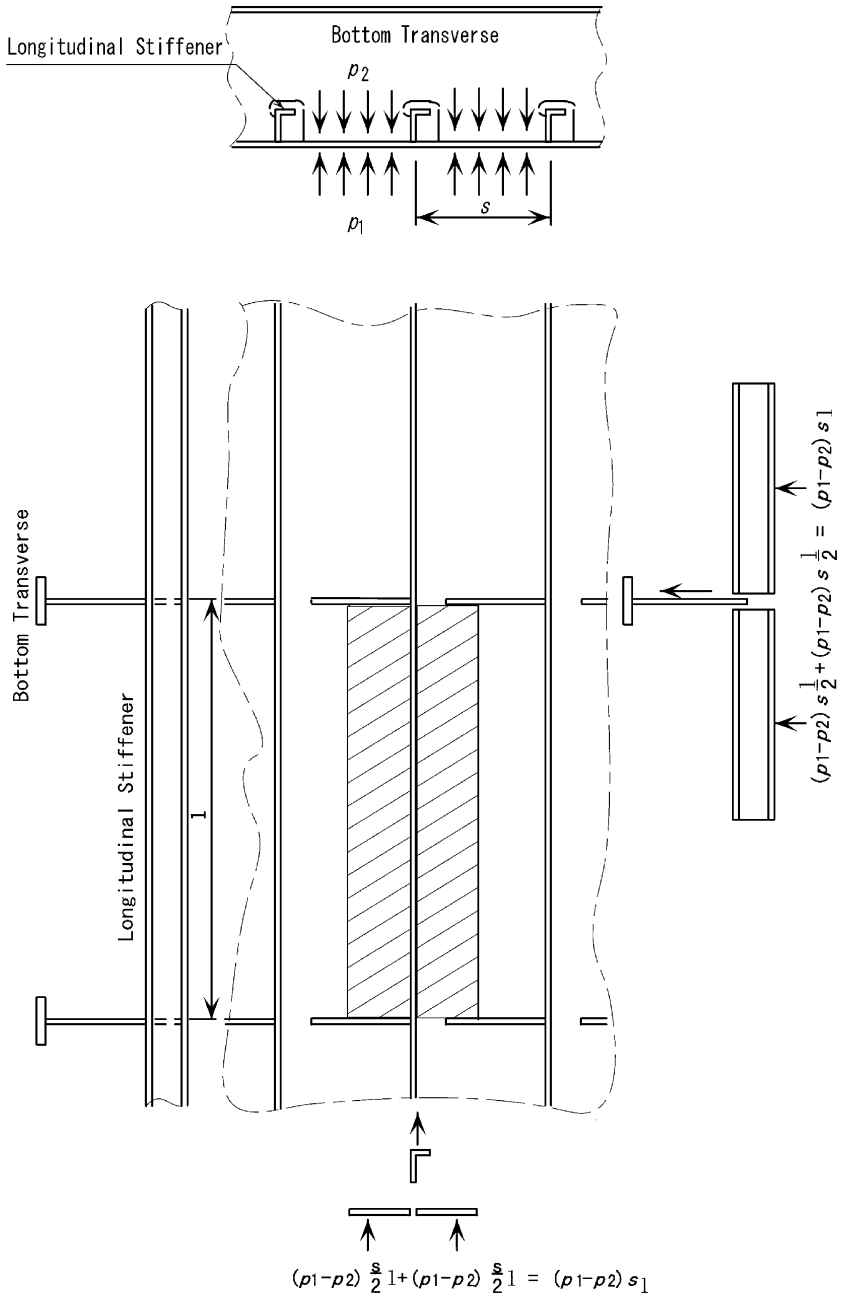


Fig. 3.1.1 Bottom structure under inner and outer pressure

simple beam theory is usually applied. If we are obliged to study the stress concentration problem in association with fatigue strength, the above analysis method is no longer helpful, therefore, more sophisticated analysis such as finite element analysis must be adopted.

Anyhow, it is important to select an adequate analysis method to be able to evaluate the strength efficiently.

(5) *Choice of an acceptable strength criteria for a particular failure mode:* In starting a structural design, the designer is required to establish acceptable strength criteria of each member depending on the assumed failure mode. Although these strength criteria conform to the rules requirement for Classification Society, they are not always explicitly expressed in the rule formulas. Thus the designer should bear in mind the background of the rule on the basis of strength criteria which exist behind the rule formulas. Strength criteria are usually established in the following steps and they are included in the rule formulae in the form of safety factors:

- Step 1:** Long-term statistic analysis of waves is carried out by analyzing the waves in the whole life-cycle of the ship and the maximum load is settled as design load.
- Step 2:** The response of the structure against the design load is calculated to obtain the maximum response.
- Step 3:** Safety factors are established by considering the above maximum stress or force by considering the critical strength for each failure mode.

As mentioned in the above steps, the strength criteria are strongly associated with the load, so they cannot be dealt with separately. In other words, acceptable strength criteria are not always unchangeable i.e. they may vary where the prediction method of load is altered, or where the analysis method is improved.

(6) *Analysis of structural response:* In order to maintain the strength performance at a satisfactory level in the design of a ship structure, it is necessary to analyze the behavior of the structure under the subjected loads and to recognize the stress distribution over the structure. Therefore, we have to undertake some kind of experiments to simulate the behavior and the stress level. We used to carry out model tests, where a structural model of small size is utilized and the stress on the structural members is measured with the aid of strain gauges or photoelastic Moire experiment.

Nowadays, however, in parallel with the rapid progress of computers, we often execute numerical simulation successfully for the purpose of strength analysis by computer instead of the above mentioned structural model test.

(7) *Evaluation of the response for given criteria:* The calculated result is compared with the chosen strength criteria and the strength of the structure evaluated. If it is acceptable, the design is completed but if not acceptable, the design must be revised and the calculation must be done again.

By following the above design steps, the designer ensures the integrity of the structure and proceeds along a so-called “Design Spiral” as shown in Fig. 3.1.2 until the strength of the structure complies with the required strength. In the figure, a ○ mark shows that the process must be carried out but ● mark indicates the process is to be omitted usually in the second step or beyond.

- : Item to be performed
- : Item to be omitted

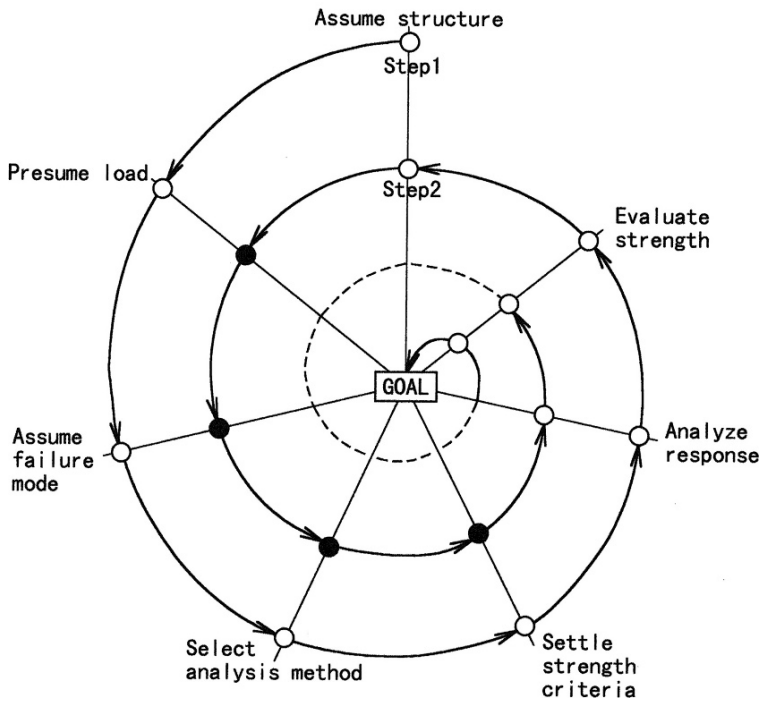


Fig. 3.1.2 Procedure of FEM structure analysis

## 3.2 Stress and Strain

### 3.2.1 Stress Pattern

Stresses acting on an element of a structure are thought to be a combination of stress patterns as shown in Fig. 3.2.1(a)–(e) [12]:

1. simple stress condition
2. biaxial stress condition (x–y plane)
3. triaxial stress condition
4. simple shearing stress condition (x–y plane)
5. simple shearing stress condition (x–z plane)

In this coordinate system, when the stress in the z-direction is zero and the deformation in the z-direction is free, it is called a plane stress condition, and when the deformation in the z-direction is zero and the stress in the z-direction is acting, it is

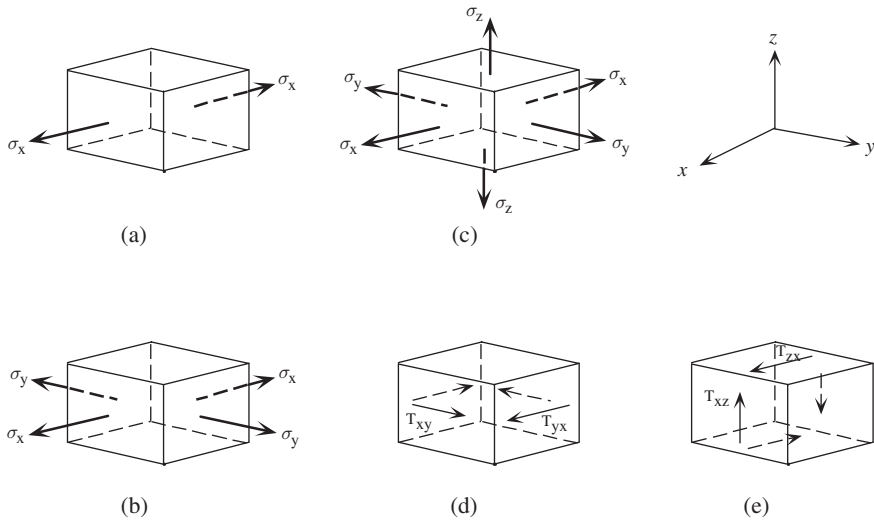


**Fig. 3.2.1** stress pattern

called a plane strain condition. Since a hull is mainly composed of thin plates, most of them are treated as being in the plane stress condition.

In the case where shearing stresses do not act – normal stress only acts – as shown in Fig. 3.2.1(a)–(c), the normal stress at each condition is called the principal stress, and the corresponding plane is the principal plane, while the corresponding stress axis is the principal axis.

### 3.2.2 Biaxial Stress Condition [12]

Figure 3.2.2 shows a biaxial stress condition in the x–y plane, same as Fig. 3.2.1(b);  $\sigma_x$  acts in the x direction and  $\sigma_y$  acts in the y-direction. Considering a section m–n, where its normal is at  $\varphi$  degrees to the x-axis, the stress along this normal and the shearing stress along m–n line are given by the following equation, in case that only  $\sigma_x$  acts.

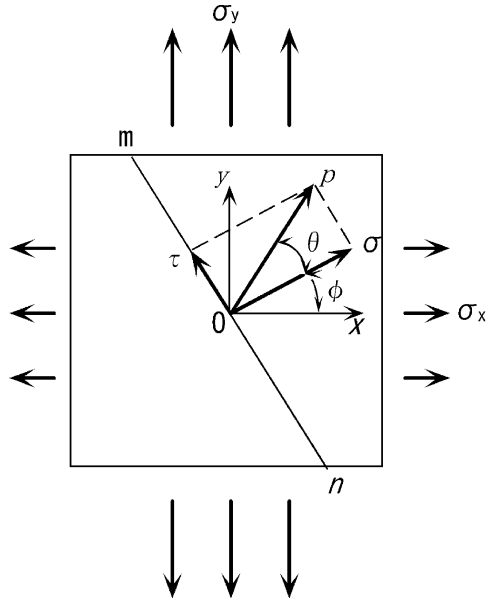
$$\begin{aligned} \sigma &= \sigma_x \cos^2 \varphi \\ \tau &= -(\sigma_x/2) \sin 2\varphi \end{aligned} \tag{3.2.1}$$

Where  $\tau$  is defined as positive in the counter clockwise direction.

In the case that  $\sigma_y$  acts:

$$\begin{aligned} \sigma &= \sigma_y \sin^2 \varphi \\ \tau &= (\sigma_y/2) \sin 2\varphi \end{aligned} \tag{3.2.2}$$

**Fig. 3.2.2** Biaxial stress condition



Therefore, if both  $\sigma_x$  and  $\sigma_y$  act,

$$\begin{aligned} \sigma &= \sigma_x \cos^2 \varphi + \sigma_y \sin^2 \varphi \\ &= \frac{1}{2}(\sigma_x + \sigma_y) + \frac{1}{2}(\sigma_x - \sigma_y) \cos 2\varphi \end{aligned} \tag{3.2.3}$$

$$\tau = \frac{1}{2}(\sigma_y - \sigma_x) \sin 2\varphi \tag{3.2.4}$$

If  $\sigma_x = \sigma_y$ ,  $\tau$  is zero irrespective of the angle  $\varphi$ .

### 3.2.3 Combination of Normal Stress and Shearing Stress [12]

Figure 3.2.3 shows stress distribution acting on a small element  $dx \times dy$  (thickness = 1) in the case of a combination of normal stress and shearing stress. Considering an equilibrium in triangle m-k-n along the x-axis:

$$\sigma ds \cos \varphi - \tau ds \sin \varphi - \sigma_x dy - \tau_z dx = 0$$

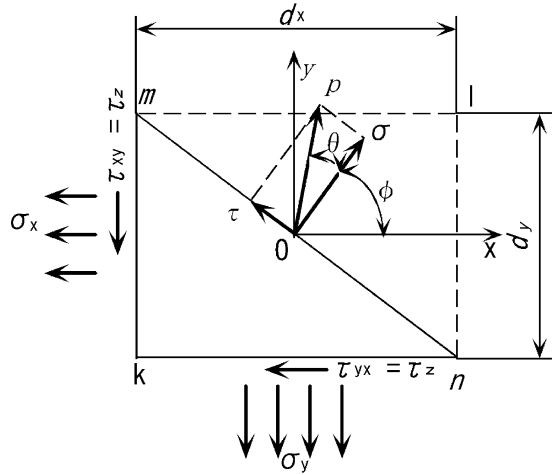
Where  $ds$  is the distance of m-n.

Being divided by  $ds$ ,

$$\sigma \cos \varphi - \tau \sin \varphi - \sigma_x \cos \varphi - \tau_z \sin \varphi = 0 \tag{3.2.5}$$



**Fig. 3.2.3** Biaxial and shearing stress



For the y-axis

$$\sigma ds \sin \varphi + \tau ds \cos \varphi - \tau_z dy - \sigma_y dx = 0$$

Being divided by  $ds$ ,

$$\sigma \sin \varphi + \tau \cos \varphi - \tau_z \cos \varphi - \sigma_y \sin \varphi = 0 \quad (3.2.6)$$

From (3.2.5)  $\times \cos \varphi$  + (3.2.6)  $\times \sin \varphi$ ,

$$\begin{aligned} \sigma &= \sigma_x \cos^2 \varphi + \sigma_y \sin^2 \varphi + \tau_z \sin 2\varphi \\ &= \frac{1}{2}(\sigma_x + \sigma_y) + \frac{1}{2}(\sigma_x - \sigma_y) \cos 2\varphi + \tau_z \sin 2\varphi \end{aligned} \quad (3.2.7)$$

From (3.2.6)  $\times \cos \varphi$  - (3.2.5)  $\times \sin \varphi$

$$\tau = \frac{1}{2}(\sigma_y - \sigma_x) \sin 2\varphi + \tau_z \cos 2\varphi \quad (3.2.8)$$

The combined stress and angle to the normal line are

$$p = \sqrt{\sigma^2 + \tau^2} \quad (3.2.9)$$

$$\tan \theta = \tau / \sigma \quad (3.2.10)$$

### 3.2.4 Principal Stress and Principal Shearing Stress [12]

Principal stress and principal shearing stress are used for evaluation of hull strength. Principal stress is the normal stress to a plane, on which the stress becomes maximum or minimum. It can be derived by applying  $d\sigma/d\varphi = 0$  at Eq. (3.2.7).

$$(\sigma_y - \sigma_x) \sin 2\varphi + 2\tau_z \cos 2\varphi = 0 \quad (3.2.11)$$

We represent  $\varphi_n$  for  $\varphi$  obtained from Eq. (3.2.11)

$$\therefore \tan 2\varphi_n = \frac{2\tau_z}{\sigma_x - \sigma_y} \quad (3.2.12)$$

If we substitute  $\varphi_n^m$  which satisfies Eq. (3.2.12),  $\varphi_n^m$  is

$$\begin{aligned} \varphi_n^m &= \frac{1}{2} \tan^{-1} \frac{2\tau_z}{\sigma_x - \sigma_y} \pm \frac{\pi}{2} m \\ m &= 1, 2, 3, \end{aligned}$$

Hence the value of  $\varphi_n$  satisfying above equation is infinite, however a pair of  $\varphi_n^m$  and  $\varphi_n^{m+1}$  is always orthogonal. This means that there are two principal stresses in  $2\pi$  and both (maximum principal stress and minimum principal stress) appear orthogonally.

Since this formula satisfies for  $\varphi_n \pm (\pi/2)$ , the principal stresses are orthogonal. And the shearing stress  $\tau$  is zero at the principal plane from Eqs. (3.2.11) and (3.2.8). The principal stress can be obtained from Eqs. (3.2.12) and (3.2.7):

$$\begin{aligned} \cos 2\varphi_n &= \frac{1}{\pm \sqrt{1 + \tan^2 2\varphi_n}} = \frac{\sigma_y - \sigma_x}{\pm \sqrt{(\sigma_x - \sigma_y)^2 + 4\tau_z^2}} \\ \sin 2\varphi_n &= \frac{\tan 2\varphi_n}{\pm \sqrt{1 + \tan^2 2\varphi_n}} = \frac{2\tau_z}{\pm \sqrt{(\sigma_x - \sigma_y)^2 + 4\tau_z^2}} \end{aligned}$$

Representing maximum principal stress as  $\sigma_1$ , and minimum principal stress as  $\sigma_2$ ,

$$\begin{aligned} \sigma_1 &= \frac{1}{2}(\sigma_x + \sigma_y) + \frac{1}{2}\sqrt{(\sigma_x - \sigma_y)^2 + 4\tau_z^2} \\ \sigma_2 &= \frac{1}{2}(\sigma_x + \sigma_y) - \frac{1}{2}\sqrt{(\sigma_x - \sigma_y)^2 + 4\tau_z^2} \end{aligned} \quad (3.2.13)$$

On the other hand, if we consider shearing stress, from  $d\tau/d\varphi = 0$  in Eq. (3.2.8)

$$\begin{aligned} (\sigma_y - \sigma_x) \cos 2\varphi - 2\tau_z \sin 2\varphi &= 0 \\ \therefore \tan 2\varphi_t &= \frac{\sigma_y - \sigma_x}{2\tau_z} \end{aligned} \quad (3.2.14)$$

Since  $\varphi_t \pm \pi/2$  also satisfies (3.2.14), the maximum shearing stress and minimum shearing stresses are also orthogonal with each other.

From

$$\tan 2\varphi_n \tan 2\varphi_t = \frac{2\tau_z}{\sigma_x - \sigma_y} \frac{\sigma_y - \sigma_x}{2\tau_z} = -1 \quad (3.2.15)$$

$\varphi_t = \varphi_n \pm (\pi/4)$  is obtained, i.e. the plane, at which maximum or minimum shearing stress acts, is at  $45^\circ$  to the principal plane. If we get  $\cos 2\varphi_t$  and  $\sin 2\varphi_t$  from Eq. (3.2.14), and substitute it into Eq. (3.2.8),

$$\tau_1, \tau_2 = \pm \frac{1}{2} \sqrt{(\sigma_x - \sigma_y)^2 + 4\tau_z^2} = \pm \frac{1}{2}(\sigma_1 - \sigma_2) \quad (3.2.16)$$

These values are called principal shearing stress.

### 3.2.5 Equivalent Stress

We denote principal stresses by  $\sigma_1, \sigma_2, \sigma_3$  and principal shearing stresses by  $\tau_1, \tau_2, \tau_3$ . Strain energy per unit volume is

$$\bar{U} = \frac{1}{2}(\sigma_1 \varepsilon_1 + \sigma_2 \varepsilon_2 + \sigma_3 \varepsilon_3) \quad (3.2.17)$$

Substituting  $\tau_1, \tau_2, \tau_3$  for  $\sigma_1, \sigma_2, \sigma_3$  in Eq. (3.2.17), applying the relationship between stress and strain,

$$\begin{aligned} \bar{U} &= \frac{1}{2E} [\sigma_1 \{\sigma_1 - \nu(\sigma_2 + \sigma_3)\} + \sigma_2 \{\sigma_2 - \nu(\sigma_3 + \sigma_1)\} + \sigma_3 \{\sigma_3 - \nu(\sigma_1 + \sigma_2)\}] \\ &= \frac{1-2\nu}{6E} (\sigma_1 + \sigma_2 + \sigma_3)^2 + \frac{1+\nu}{6E} \{(\sigma_1 - \sigma_2)^2 + (\sigma_2 - \sigma_3)^2 + (\sigma_3 - \sigma_1)^2\} \\ &\equiv \bar{U}_1 + \bar{U}_2 \end{aligned} \quad (3.2.18)$$

Where

$$\bar{U}_1 = \frac{1-2\nu}{6E} (\sigma_1 + \sigma_2 + \sigma_3)^2 \quad (3.2.19)$$

$$\bar{U}_2 = \frac{1+\nu}{6E} \{(\sigma_1 - \sigma_2)^2 + (\sigma_2 - \sigma_3)^2 + (\sigma_3 - \sigma_1)^2\} \quad (3.2.20)$$

$E$ : modulus of elasticity

$\nu$ : Poisson's ratio

$\bar{U}_1$  is dilatational strain energy by uniform tensile stress  $\sigma_m$ ;

$$\sigma_m = \frac{1}{3}(\sigma_1 + \sigma_2 + \sigma_3) \quad (3.2.21)$$

and  $\bar{U}_2$  is shearing strain energy without volume change.

In the case of simple tension,  $\sigma_1 = \sigma_e, \sigma_2 = \sigma_3 = 0$ , Shearing strain energy is

$$\bar{U}_{2e} = \frac{1+\nu}{6E} (2\sigma_e^2) \quad (3.2.22)$$

In accordance with Mises yield stress criterion, the failure will occur when the shearing strain energy reaches that corresponding to the yield stress under simple tension, that is  $\bar{U}_2 = \bar{U}_{2e}$ . From Eqs. (3.2.20) and (3.2.22),

$$\sigma_e^2 = \frac{1}{2} \{ (\sigma_1 - \sigma_2)^2 + (\sigma_2 - \sigma_3)^2 + (\sigma_3 - \sigma_1)^2 \} \quad (3.2.23)$$

For arbitrary stresses  $\sigma_1, \sigma_2, \sigma_3$ , if taking  $\sigma_0 = \sigma_e$

$$\sigma_0 = \sqrt{\frac{1}{2} \{ (\sigma_1 - \sigma_2)^2 + (\sigma_2 - \sigma_3)^2 + (\sigma_3 - \sigma_1)^2 \}} \quad (3.2.24)$$

$\sigma_0$  is termed equivalent stress. In case the plane stress condition,  $\sigma_3 = 0$

$$\sigma_0 = \sqrt{\sigma_1^2 + \sigma_2^2 - \sigma_1 \sigma_2} \quad (3.2.25)$$

$$\text{or } \sigma_0 = \sqrt{\sigma_x^2 + \sigma_y^2 - \sigma_x \sigma_y + 3\tau_{xy}^2} \quad (3.2.26)$$

In the case of simple tension,

$$\sigma_0 = \sqrt{\sigma_x^2 + 3\tau_{xy}^2} \quad (3.2.27)$$

Figure 3.2.4 shows the relation, where the length of the tangential line represents the equivalent stress; if the normal stress only acts the failure will occur at  $\sigma_x = \sigma_y$  (yield stress) and if shearing stress only acts the failure occurs at  $\tau_{xy} = \sigma_y / \sqrt{3}$ .

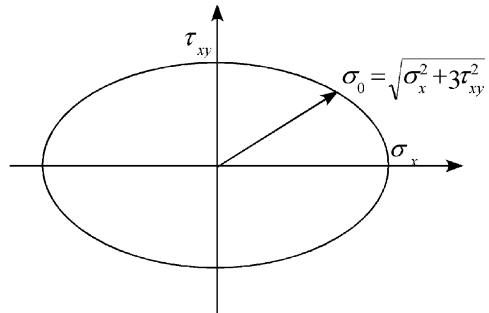


Fig. 3.2.4 Equivalent stress

### 3.2.6 Evaluation of Stress Calculated by FEM

In general, the FEM calculation produces several kinds of stresses. In the case of a 2-dimensional shell model, the following stresses are calculated:

- Stresses at nodes or at the center of an element
- Stresses on upper surfaces, lower surfaces, or in the middle
- Normal stress or shearing stress
- Maximum principal stress, minimum principal stress, or equivalent stress

Structure designers should recognize what kind of stress is output as a result of the FEM calculation, and should select them in accordance with each strength evaluation.

In general,

1. Principal stress is used as failure criterion for brittle materials, and equivalent stress for ductile materials such as mild steel.
2. Maximum principal stress is used for crack propagation analysis (Fig. 3.2.5).

Fig. 3.2.5 Crack propagation

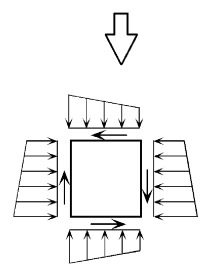
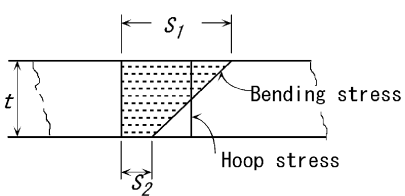
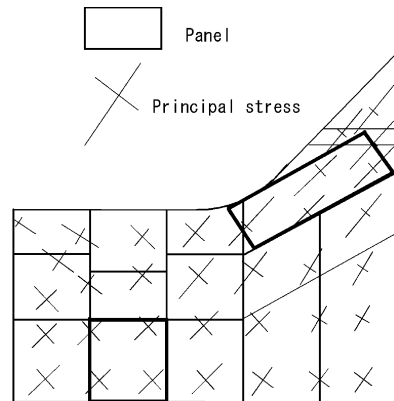
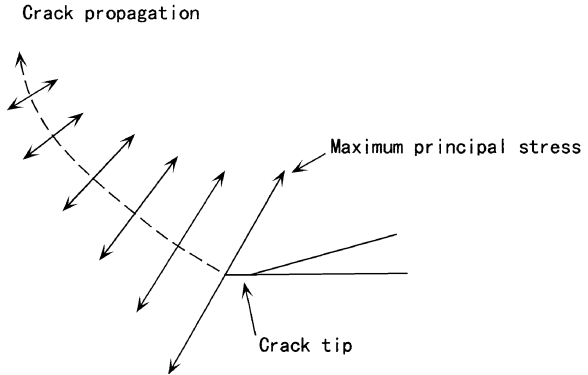


Fig. 3.2.6 Buckling check of a panel

3. The mean stress between upper and lower surfaces is used for plate buckling analysis, which is adjusted for the boundary stress of a panel. Figure 3.2.6 shows the procedure of panel buckling analysis of a bottom transverse web in a cargo tank [13].

### 3.3 Evaluation of Stress

#### 3.3.1 Criteria of Failure

Ductile materials, such as mild steel and higher-strength steel used in ship hull structure, deform when the load exceeds the yield stress. Under such plastic deformation, materials reach finally failure. On the other hand, the failure of brittle materials such as cast iron may happen without such plastic deformation. Hence the strength of materials is based on the yield stress or the tensile stress for ductile materials, and the fracture stress for brittle materials.

The stress distribution in an actual structure is very complex because both the loading and the structure are complex. Although the strength criteria in such conditions are not known, some criteria have been proposed. Typical theories used for hull structure are introduced later, where principal stresses are denoted by  $\sigma_1, \sigma_2, \sigma_3$  ( $\sigma_1 \geq \sigma_2 \geq \sigma_3$ ), and stresses corresponding to failure in simple stress condition are  $\sigma_t, \sigma_c, \tau_s$  for tension, compression, and shear respectively.

(1) *Maximum principal stress theory*: Rankine proposed this theory, which shows that materials fail when the maximum value of  $\sigma_1, \sigma_2, \sigma_3$  reaches  $\sigma_t$  or  $\sigma_c$ .

$$\begin{aligned} \sigma_1 &= \sigma_t & \sigma_1 \geq |\sigma_3| \geq 0 \\ \sigma_3 &= \sigma_c & -\sigma_3 \geq |\sigma_1| \geq 0 \end{aligned} \quad (3.3.1)$$

According to this theory, the following premise must hold:

$$\tau_s / \sigma_t = 1$$

However, since measurement results for ductile materials show

$$\tau_s / \sigma_t = 0.5 \sim 0.6$$

This theory can not be applied for ductile materials, but is applied widely for brittle materials.

(2) *Maximum shearing stress theory*: Guest or Tresca proposed this theory, which shows that materials fail when maximum shearing stress  $\tau_{\max}$  reaches maximum shearing stress  $\tau_s$  corresponding to the yield stress of simple tension.

$$\begin{aligned} \tau_{max} &= \tau_s \\ \tau_{max} &= \frac{|\sigma_1 - \sigma_3|}{2} \\ \tau_s &= \frac{\sigma_t}{2} \end{aligned} \tag{3.3.2}$$

This theory means  $\tau_s/\sigma_t = 0.5$ , and this agrees with experiments for ductile materials. And also this shows that failure occurs along the plane of maximum shearing stress ( $45^\circ$  to maximum principal stress). This also agrees with experiments on the material. Hence this theory is widely used for ductile materials.

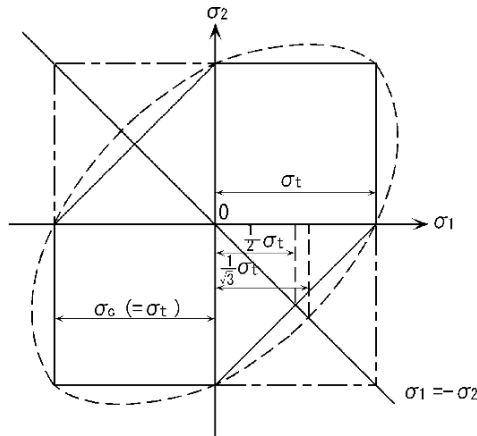
(3) *Shearing strain energy theory*: This theory is called Mises-Hencky theory. As shown in Eq. (3.2.21), this theory denotes that failure occurs when the shearing strain energy in the material reaches that corresponding to the yield stress from simple tension. In this case  $\tau_s/\sigma_t = 1/\sqrt{3} = 0.577$ , which agrees with experiments of ductile materials such as mild steel. Accordingly this theory is widely used to evaluate ship hull strength.

Figure 3.3.1 compares the above mentioned theories for a 2-dimensional model [14]. Large differences between these theories appear especially in pure shearing conditions, that is

$$\sigma_1 = -\sigma_2 \geq 0 \text{ or } \sigma_2 = -\sigma_1 \geq 0$$

For example, when  $\sigma_1 = -\sigma_2 \geq 0$

- $\sigma_1 = \sigma_t$  for maximum principal stress theory
- $\sigma_1 = \sigma_t/2$  for maximum shearing stress theory
- $\sigma_1 = \sigma_t/\sqrt{3}$  for shearing strain energy theory



- : Maximum principal stress theory
- : Maximum shearing stress theory
- : Shearing strain energy theory

Fig. 3.3.1 Criteria of failure

### 3.3.2 Allowable Stress

This paragraph states the allowable stress and the required scantling for the hull structures based on the rule of Nippon Kaiji Kyokai.

(1) *Plate*: A steel plate is assumed as a rectangular sheet with all edges clamped, on which axial stress and uniform lateral pressure are loaded as shown in Fig. 3.3.2. The plastic moment is expressed as follows, when the aspect ratio of a plate is larger than 2 [15]:

$$M_p = \frac{\sigma_y}{4} t^2 \left\{ 1 - \left( \frac{\sigma_{ax}}{\sigma_y} \right)^2 \right\} \text{ for a transverse system} \tag{3.3.3}$$

$\sigma_{ax}$ : axial stress  
 $\sigma_y$ : yield stress  
 $t$ : plate thickness

$$M_p = \frac{\sigma_y}{4} t^2 \cdot 2 \left\{ 1 - \left( \frac{\sigma_{ax}}{\sigma_y} \right) \right\} \text{ When } \frac{\sigma_{ax}}{\sigma_y} < \frac{1}{2}, \quad \frac{\sigma_{ax}}{\sigma_y} = \frac{1}{2} \text{ for a longitudinal system} \tag{3.3.4}$$

system

On the other hand,

$$M_p = \frac{C_p h S^2}{16} \tag{3.3.5}$$

$C_p$ : safety factor  
 $h$ : lateral pressure  
 $S$ : space

From the Eqs. (3.3.3), (3.3.4) and (3.3.5), required plate thickness is

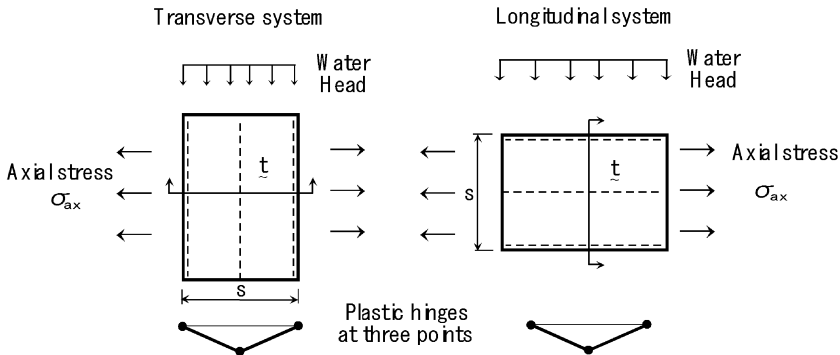


Fig. 3.3.2 Plate model



$$t = \sqrt{\frac{C_p h}{4\sigma_y}} \cdot \frac{S}{\sqrt{1 - \left(\frac{\sigma_{ax}}{\sigma_y}\right)^2}} \text{ for a transverse system} \quad (3.3.6)$$

$$t = \sqrt{\frac{C_p h}{4\sigma_y}} \cdot \frac{S}{\sqrt{2 \left\{ 1 - \left(\frac{\sigma_{ax}}{\sigma_y}\right) \right\}}} \text{ for a longitudinal system} \quad (3.3.7)$$

For example, the required plate thickness of bulkheads in oil tankers is expressed as follows:

$$t = C_1 C_2 S \sqrt{h} + 3.5 \text{ (mm)} \quad (3.3.8)$$

$S$ : spacing of stiffeners (m)

$h$ : water head (m)

$C_1$ : coefficients for ship length

$$C_1 = 1.0 \text{ for } L \leq 230 \text{ m} \quad C_1 = 1.70 \text{ for } L \geq 400 \text{ m}$$

$C_1$  is interpolated between them

$C_2$ : coefficients

$$C_2 = 3.6\sqrt{K}$$

$K$ : material factor

$$K = 1.0 \text{ for MS, } K = 0.78 \text{ for HT32, } K = 0.77 \text{ for Ht36}$$

where 3.5 is the corrosion margin.

In this rule,  $C_p$  of Eq. (3.3.5) is taken as 1.44 and  $\sigma_y$  is  $27.7/K$  (kgf/mm<sup>2</sup>) (272/K) (N/mm<sup>2</sup>).

(2) *Stiffener*: The maximum bending stress of a beam clamped at both ends and loaded uniformly is

$$\sigma = \frac{Shl^2}{12 \cdot Z} \quad (3.3.9)$$

$S$ : stiffener space

$h$ : lateral pressure

$l$ : span

$Z$ : section modulus

Considering the effect of axial forces,

$$Z = C_s \frac{Shl^2}{12(\sigma_y - \sigma_{ax})} \quad (3.3.10)$$

$\sigma_y$ : yield stress

$\sigma_{ax}$ : axial stress

$C_s$ : safety factor

For example, the required section modulus of longitudinal frames of oil tankers is expressed as follows;

$$Z = 100C_1C_2Shl^2 \quad (\text{cm}^3) \quad (3.3.11)$$

$C_2$  : effect of axial stress

$$C_2 = \frac{K}{\sigma_y - \sigma_{ax}K}$$

$C_1, K$  : stated before

In this rule,  $C_s$  of Eq. (3.3.10) is taken as 1.2,  $\sigma_y$  is  $24/K(\text{kgf}/\text{mm}^2) = 235/K$  ( $\text{N}/\text{mm}^2$ ) and  $\sigma_{ax}$  is  $15.5\text{kgf}/\text{mm}^2 = 152$  ( $\text{N}/\text{mm}^2$ )

## 3.4 Fatigue Strength

### 3.4.1 Introduction

Ship structures are subjected to cyclically fluctuating loads as well as to static loads. Figure 3.4.1 shows the time history of the longitudinal stress on the upper deck of a container ship during a voyage [16]. In such cases, they may sometimes fracture due to a large number of repeating loads, even when the magnitude of the cyclic load is much smaller than the strength against static load. It is a phenomenon called “fatigue failure” and the number of cycles causing fatigue failure is called “fatigue life”. Fatigue is an important problem in the design of structural members exposed to cyclic loads, because cyclic loads due to wave are always present in almost all structural members of the ship during the voyage. The vibration is also regarded as a repeated load.

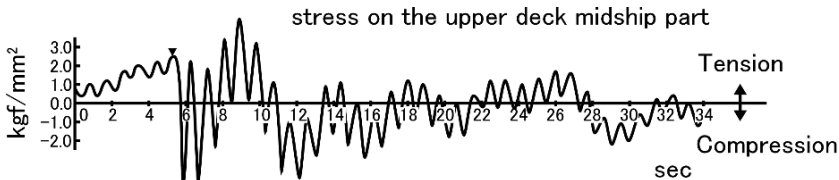


Fig. 3.4.1 Typical time history of stress

### 3.4.2 $S-N$ Curve

Though the time history of stress is very complex as shown in Fig. 3.4.1, the pattern induced by cyclically repeating loads is simply illustrated in Fig. 3.4.2.

where

$\sigma_{\max}$  : maximum stress

$\sigma_{\min}$  : minimum stress

$\sigma_m = (\sigma_{\max} + \sigma_{\min})/2$  : mean stress

$\sigma_a = (\sigma_{\max} - \sigma_{\min})/2$  : stress amplitude

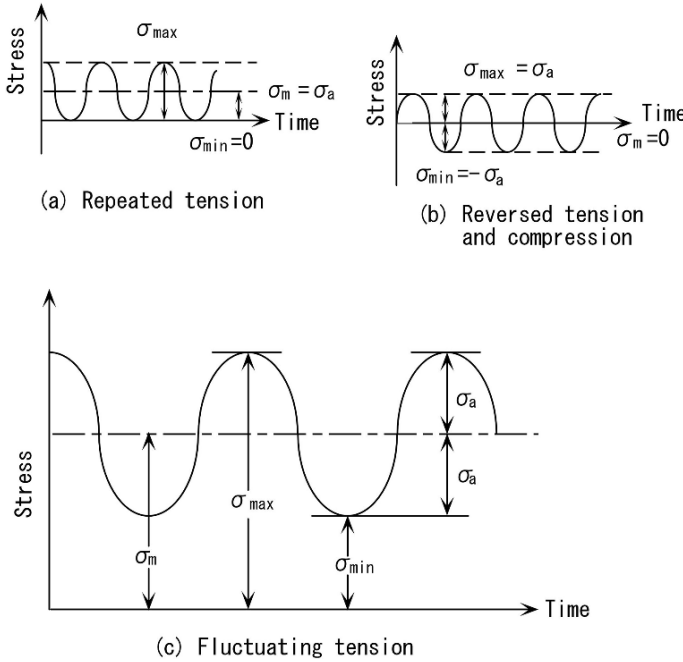


Fig. 3.4.2 Simplified time history of stress

Even in the case of the same material, the cycle number for fatigue life may differ depending on the magnitude or type of applied loads as shown in Fig. 3.4.2. Figure 3.4.2(a)–(c) show stress behavior corresponding to the test cases of repeated tension ( $\sigma_{\max} = 2\sigma_a$ ,  $\sigma_{\min} = 0$ ), reversed tension and compression ( $\sigma_m = 0$ ), and fluctuating tension, respectively. The relation between stress amplitude  $S$  and fatigue life  $N$  can be obtained by a fatigue test as shown in Fig. 3.4.3, where the axis of abscissas is represented by a logarithmic scale and the axis of ordinates is a normal or logarithmic coordinate. The figure is simply called an “S–N curve”.

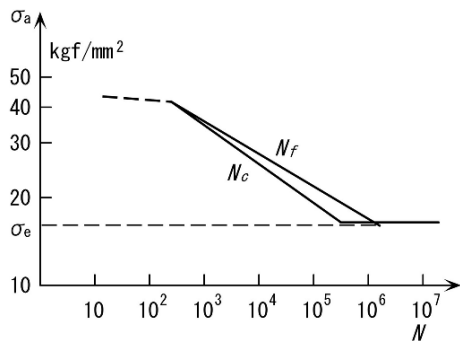


Fig. 3.4.3 S-N curve

In the figure,  $N_c$  represents the number of cycles in which a crack was initiated in the test specimen, i.e. crack initiation life, and  $N_f$  means the number of cycles when the specimen fractures, i.e. failure life.

If the stress amplitude becomes small, the fatigue life will increase. However, failure never occurs where the stress amplitude is lower than a certain stress level as indicated by a flat line in the figure. That critical stress which never induces fatigue failure is called the “fatigue limit” or “endurance limit”. From a practical point of view, the fatigue limit can often be specified as the stress at  $N = 10^6$ , when the test specimen doesn't cause failure. The fatigue limit, in general, is much lower than the ultimate strength of the material due to static stress.

When the fatigue life is lower than  $N = 10^5$ , it is conveniently called “low cycle fatigue” and when higher than  $N = 10^5$ , it is “high cycle fatigue”. In the case of low cycle fatigue, the stress amplitude may reach yield stress, because low cycle fatigue tends to take place in the area of high stress concentration. Therefore, in the low cycle fatigue test, the strain amplitude should be taken instead of the stress amplitude, then the fatigue strength is formulated as follows;

$$S = CN^{-k}, \varepsilon = CN^{-k} \quad (3.4.1)$$

$S$ : stress amplitude  
 $\varepsilon$ : strain amplitude  
 $N$ : repetition number for crack initiation or failure  
 $C, k$ : coefficient

$$\text{or } S = a - b \log N, \varepsilon = a - b \log N \quad (3.4.2)$$

Table 3.4.1 shows the fatigue life for the base metal and welding joints of mild steel [17], which were tested under repeated tension. The fatigue life of welding joints is generally reduced because of the stress concentration around the beads, compared with the base metal.

In high cycle fatigue, the fatigue limit must be discussed. The fatigue limit depends not only on the stress amplitude but also on the mean stress. If we plot the mean stress and stress amplitude corresponding to the fatigue limit, we can obtain the line ABD in Fig. 3.4.4. Point A represents the fatigue limit of  $\sigma_m = 0$ , i.e. reversed tension and compression, and Point B means the case of  $\sigma_m = \sigma_a$ , i.e. repeated tension ( $\sigma_{\max} = 2\sigma_a$ ,  $\sigma_{\min} = 0$ ). Fatigue failure never occurs in the case where the stress amplitude and mean stress are within the area below the line ABD. In addition, if we add another line YY' representing critical yield stress ( $\sigma_m + \sigma_a = \sigma_y$ ,  $\sigma_y$ : yield stress), the area below the line ABEY indicates the safe area where failure will never be induced by fatigue or by yielding.

Cyclic loads in a marine environment result in the reduction of fatigue life due to corrosive conditions rather than in air. Corrosive conditions reduce fatigue life to a much greater extent in high cycle fatigue than in low cycle fatigue. In addition, fatigue tests in sea water do not show a clear fatigue limit.

Table 3.4.1 Fatigue strength of welding joints

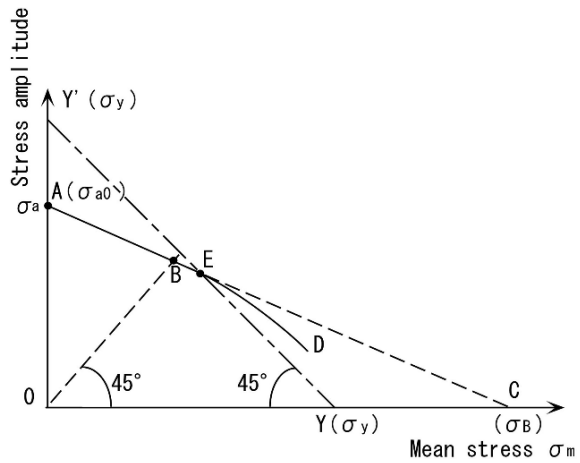
Joints	Mean line		90% reliability	
	Formula	$N = 2 \times 10^4$	$N = 10^4$	$N = 2 \times 10^4$
Mild steel, as rolled	$\log S = \log 40.15$ $-0.075 \log(N/10^4)$	26.8	29.0~40.0	23.0~32.0
"    , grinding	$\log S = \log 36.02$ $-0.0611 \log(N/10^4)$	26.1	28.2~34.8	23.4~28.9
"    , scouring	$\log S = \log 38.18$ $-0.0493 \log(N/10^4)$	29.7	30.6~38.2	25.2~32.6
Butt joint, transverse	$\log S = \log 39.66$ $-0.184 \log(N/10^4)$	14.9	20.5~33.0	11.7~18.8
"    , "    , finishing	$\log S = \log 32.12$ $-0.054 \log(N/10^4)$	24.0	21.2~38.0	17.9~32.8
Butt joint, longitudinal	$\log S = \log 38.22$ $-0.1408 \log(N/10^4)$	18.2	25.0~30.8	16.4~20.2
"    , "    , finishing	$\log S = \log 42.59$ $-0.1148 \log(N/10^4)$	23.3	30.7~35.2	21.6~24.7
Front fillet weld	$\log S = \log 23.41$ $-0.1557 \log(N/10^4)$	10.3	11.0~25.3	6.6~15.9
"    , compression	$\log S = \log 30.81$ $-0.1053 \log(N/10^4)$	17.5	19.4~30.8	14.0~22.3
Side fillet weld, throat	$\log S = \log 24.47$ $-0.1218 \log(N/10^4)$	13.5	16.7~22.5	11.6~15.7
"    , base metal	$\log S = \log 12.53$ $-0.0503 \log(N/10^4)$	9.6	7.0~17.7	6.0~15.3
Front and side fillet, throat	$\log S = \log 10.02$ $-0.0751 \log(N/10^4)$	6.7	6.0~11.7	4.8~9.4
"    , base metal	$\log S = \log 15.60$ $-0.3387 \log(N/10^4)$	4.6	7.0~12.3	3.5~6.1
T-fillet, throat	$\log S = \log 25.93$ $-0.2011 \log(N/10^4)$	13.6	—	11.4~16.6
Bead welding, longitudinal	$\log S = \log 42.54$ $-0.1651 \log(N/10^4)$	17.7	24.4~34.5	14.7~21.0
"    , transverse	$\log S = \log 33.34$ $-0.1713 \log(N/10^4)$	13.4	—	12.2~14.4

### 3.4.3 Fatigue Damage

Loads acting on a ship's structure are not constant loads but random loads. On the other hand, S-N curves are generally obtained by fatigue tests with constant loads, therefore fatigue strength life is normally calculated based on the following linear assumption, which is called as Miner-Palmgren approach.

Assume that all stress cycles can be divided into the several stress blocks, i.e. the structure is subjected to a stress cycle  $n_1$  with constant stress amplitude  $\sigma_1$ ,  $n_2$  with  $\sigma_2$  and so on as shown in Fig. 3.4.5. The damage factor of the  $i$ -th stress block is defined by the ratio of number of encountered stress cycles  $n_i$  and failure life  $N_i$  at the stress amplitude of  $\sigma_i$ , and the total damage factor can be obtained by summing each damage factor by the following equation:

**Fig. 3.4.4** Mean stress versus stress amplitude



$$C_w = \sum_{i=1}^k \frac{n_i}{N_i} = \frac{n_1}{N_1} + \frac{n_2}{N_2} + \dots + \frac{n_k}{N_k} \tag{3.4.3}$$

where

$k$ : number of stress blocks

$n_i$ : number of stress cycles in  $i$ -th stress block with constant stress range  $\sigma_i$

$N_i$ : number of cycles to failure at constant stress range  $\sigma_i$

$C_w$  is called the “cumulative fatigue damage factor” and fatigue failure would happen if  $C_w$  exceeded a certain critical value. According to the experiments, the

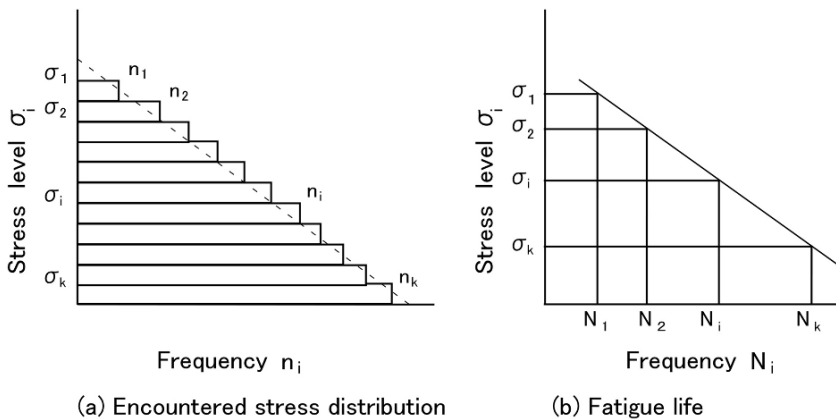


**Fig. 3.4.5** Fatigue life in random fluctuation

critical value which gives fatigue failure varies from 0.1 to 10. In spite of that,  $C_w = 1.0$  is often applied as a guideline for fatigue life assessment.

## 3.5 Buckling of Ship Structure

### 3.5.1 Introduction

Now let's consider the behavior of structures subjected to compressive loads. Under such circumstances the structure behaves in a quite different way to that under tensile loads. The structure under tensile stress may cause cracks, while compressive stress will result in buckling. Nearly all the parts of a structure of a ship consisting of plates and beams are sometimes loaded with compressive loads, and it is therefore important to consider the buckling problems.

Before starting the derivation of the buckling equation based on the references [18, 19], it is necessary to clarify the notation of buckling behavior. Figure 3.5.1 shows a simple compression rod subjected to an axial load  $P$ . The straight form of the rod would be maintained under small loads (stable condition). If the axial load increases and reaches to a certain amount, lateral deflection would suddenly take place (neutral condition) and the rod could no longer sustain loads exceeding  $P_{cr}$  (unstable condition). Lateral deflection would occur even where the load is applied in a uniform manner to the cross section of the column. This is due to imperfections in the rod's straightness, non-homogeneous material, or non-uniformity on the cross-section of the rod.

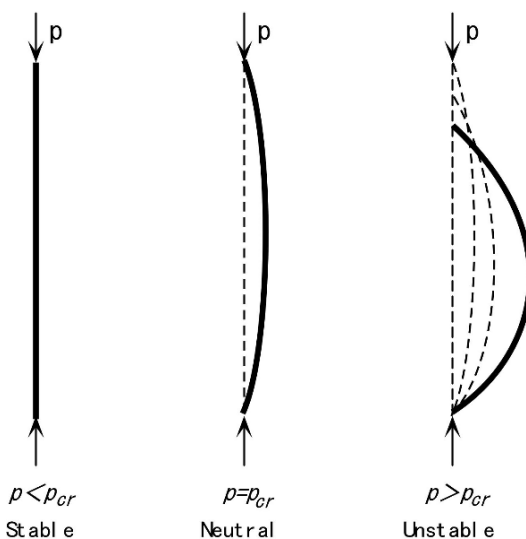


**Fig. 3.5.1** Behavior of a rod subjected to an axial compression load

The phenomenon where lateral deflection may arise in the athwart direction against the axial working load is called “buckling”. In addition, the load  $P_{cr}$  which buckles the member is called the “buckling load” or “critical load”.

### 3.5.2 Column Buckling

Figure 3.5.2 shows a hinged-ended column to which the critical load  $P_{cr}$  is applied. The column is slightly curved by that axial load. The bending moment created by the axial load due to the horizontal distance  $y$  between the load and the deflection of the column must be sustained by the bending moment of the column. It follows that

$$\begin{aligned} -EI \frac{d^2y}{dx^2} &= P_{cr} \cdot y \\ \frac{d^2y}{dx^2} + \frac{P_{cr}}{EI} y &= 0 \end{aligned} \quad (3.5.1)$$

where  $I$  is the moment of inertia of the column section.

By assuming the following harmonic function, the solution of Eq. (3.5.1) can be obtained;

$$y = A \cos \sqrt{\frac{P_{cr}}{EI}} x + B \sin \sqrt{\frac{P_{cr}}{EI}} x \quad (3.5.2)$$

where  $A$ ,  $B$  are arbitrary constants determined by boundary conditions.

For the hinged-edge boundary condition, we substitute  $y = 0$  at  $x = 0$  and  $y = 0$  at  $x = l$  into Eq. (3.5.2) and the following equations can be derived:

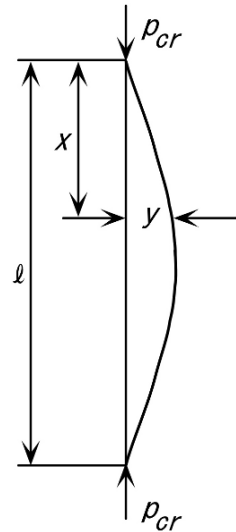


**Fig. 3.5.2** A column under critical load with hinged supports



$$A = 0$$

$$B \sin \sqrt{\frac{Pcr}{EI}} l = 0 \quad (3.5.3)$$

In order to obtain a meaningful solution, the following relation must be satisfied from Eq. (3.5.3):

$$\sqrt{\frac{Pcr}{EI}} l = n\pi \quad (3.5.4)$$

where  $n$  is an arbitrary integer number. Equation (3.5.4) can be formed into

$$Pcr = \frac{n^2 \pi^2 EI}{l^2} \quad (3.5.5)$$

The above equation means that the stable condition can be achieved only in the case where the load  $Pcr$  reaches to the amount expressed by Eq. (3.5.5). For design purposes, the smallest value of the critical load is significant, therefore, we put  $n = 1$  and the result is

$$Pcr = \frac{\pi^2 EI}{l^2} \quad (3.5.6)$$

Thus the above formula provides the critical load for a uniform hinged-ended column.

Corresponding buckling form for  $n = 1$  can be expressed as in the form

$$y = B \sin \frac{\pi x}{l} \quad (3.5.7)$$

The formula (3.5.6) was originally developed by L. Euler, in the eighteen century, and is usually called ‘‘Euler’s buckling’’. It gives the load at which a compression member will transform from a stable form of straight shape and becomes another stable form in curved shape.

A critical buckling stress is often used instead of a buckling load and it can be derived by dividing  $Pcr$  by  $A$ , the cross sectional area of the column

$$\begin{aligned} \sigma_{cr} &= \pi^2 E \frac{I}{A} \frac{1}{l^2} \\ &= \pi^2 E \left( \frac{k}{l} \right)^2 \end{aligned} \quad (3.5.8)$$

where  $k$  ( $k^2 = I/A$ ) is the radius of gyration of the section of the column. The ratio  $l/k$ , often called the slenderness ratio, is the main factor which governs the critical stress. When we plot  $\sigma_{cr}$  against  $l/k$ , the relation between them is as shown in Fig. 3.5.3. For large value of  $l/k$  the critical stress tends toward zero, and at small values of  $l/k$  it tends to infinity. In Euler’s formula, the buckling stress may become infinite for a small value of  $l/k$ , however, buckling stress never goes up above the yield stress of the material in actual conditions, because the material would fail if the stress exceeded the yield stress. Therefore, by theoretical consideration, a horizontal

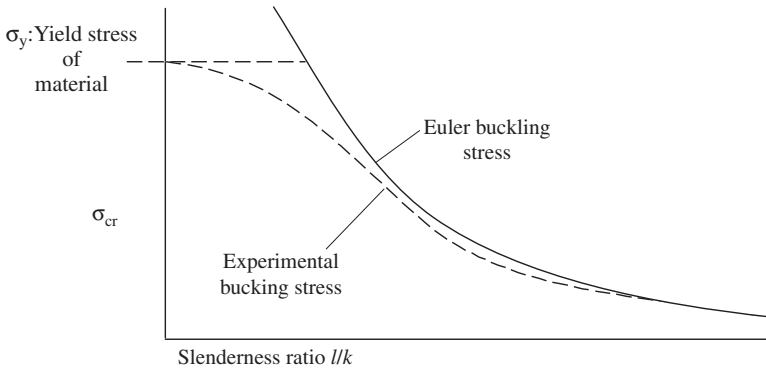


**Fig. 3.5.3** Curves of buckling stress

line of yield stress connected to Euler buckling stress is specified as an upper limit of Euler's buckling curve.

The above mentioned theory is obtained by analytical approaches, on the other hand, several buckling curves are proposed on the basis of experiments as follows:

$$\sigma_{cr} = a - b \left( \frac{l}{k} \right) \quad \text{Tetmayer's formula} \quad (3.5.9)$$

$$\sigma_{cr} = a - b \left( \frac{l}{k} \right)^2 \quad \text{Johnson's formula} \quad (3.5.10)$$

$$\sigma_{cr} = \frac{a}{1 + b(l/k)^2} \quad \text{Rankine's formula} \quad (3.5.11)$$

For example, one of the Classification Societies, ABS (American Bureau of Shipping) specifies the permissible load of a pillar or strut of mild steel material in the following equation:

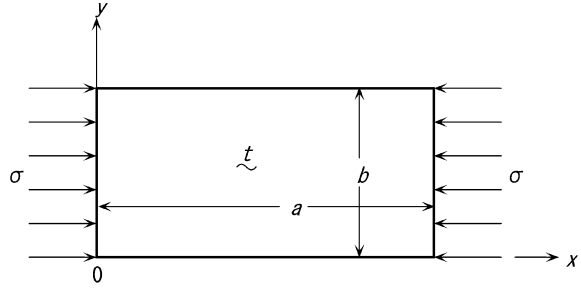
$$\sigma_{cr} = 1.232 - 0.00452 \left( \frac{l}{k} \right) \quad \text{tonf/cm}^2 \quad (3.5.12)$$

From the above equation, we can see that the ABS formula is theoretically based on Tetmayer's experimental result.

### 3.5.3 Plate Buckling

A ship hull is a stiffened-plate structure, the plating supported by a system of transverse or longitudinal stiffeners. The character of the support at the panel edges depends upon the rigidity of the supporting members. For practical design purposes,

**Fig. 3.5.4** Rectangular plate under uni-axial compression



it is often assumed that the panel is simply supported at the all edges, since it gives the least critical stress and is on the safe side.

Now let's consider the rectangular plate with only supported edges as shown in Fig. 3.5.4. The equation of elastic buckling stress of the above panel under uni-axial compressive stress  $\sigma$  can be derived by referring to the textbooks [18,19] as follows:

$$D \left( \frac{\partial^4 w}{\partial x^4} + 2 \frac{\partial^4 w}{\partial x^2 \partial y^2} + \frac{\partial^4 w}{\partial y^4} \right) + \sigma t \frac{\partial^2 w}{\partial x^2} = 0 \quad (3.5.13)$$

$$\text{where } D = \frac{Et^3}{12(1-\nu^2)} \quad (3.5.14)$$

The boundary condition where all four edges are simply supported, can be expressed in the form:

$$w = 0 \quad \frac{\partial^2 w}{\partial x^2} + \nu \frac{\partial^2 w}{\partial y^2} = 0 \quad \text{at } x = 0 \text{ and } a \quad (3.5.15)$$

$$w = 0 \quad \frac{\partial^2 w}{\partial y^2} + \nu \frac{\partial^2 w}{\partial x^2} = 0 \quad \text{at } y = 0 \text{ and } b \quad (3.5.16)$$

Let's assume the following formula for the deflection of a panel and substitute it in Eq. (3.5.13)

$$w = f \sin \frac{m\pi x}{a} \sin \frac{n\pi y}{b} \quad (3.5.17)$$

where  $m, n$  are integers presenting the number of half-wave of buckles.

Then we will obtain the elastic buckling stress

$$\sigma = \frac{\pi^2 D}{b^2 t} \left( \frac{m}{\alpha} + n^2 \frac{\alpha}{m} \right)^2 \quad (3.5.18)$$

where  $\alpha = a/b$

Elastic buckling stress is a minimum critical stress, therefore, we put  $n = 1$  in Eq. (3.5.18) then

$$\sigma_e = \frac{\pi^2 E}{12(1-\nu^2)} \left( \frac{t}{b} \right)^2 K \quad (3.5.19)$$

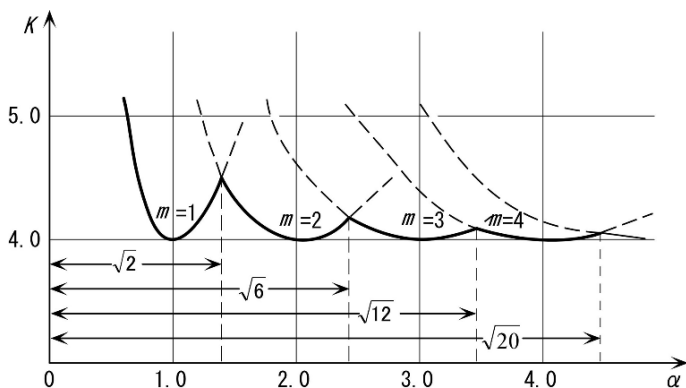


Fig. 3.5.5 Relation between aspect ratio  $\alpha$  and  $K$  value

$K =$  minimum value of  $k$

$$k = \left( \frac{m}{\alpha} + \frac{\alpha}{m} \right)^2 \tag{3.5.20}$$

If we plot the relation between  $\alpha$  and  $K$  in Fig. 3.5.5, it can be seen that the least value of  $K$  is 4 at the point where  $\alpha$  becomes  $m$ . An example is shown in Fig. 3.5.6, where  $a = 3b$ , i.e.  $\alpha = 3$ . In this example, three half wave buckles forming in same square panels may arise, as  $K$  values reach a minimum of 4 when the wave number  $m$  becomes 3. That is, in other words, a long panel of plating tends to buckle into a number of square panels. This will only be true if  $a$  is an exact multiple of  $b$  and, if it is not so, the panel will buckle into the nearest round number of half waves which will make the critical stress a minimum. In practical designing,  $K=4$  is usually applied for a panel of  $\alpha \geq 1$ , because  $K = 4$  gives minimum buckling stress.

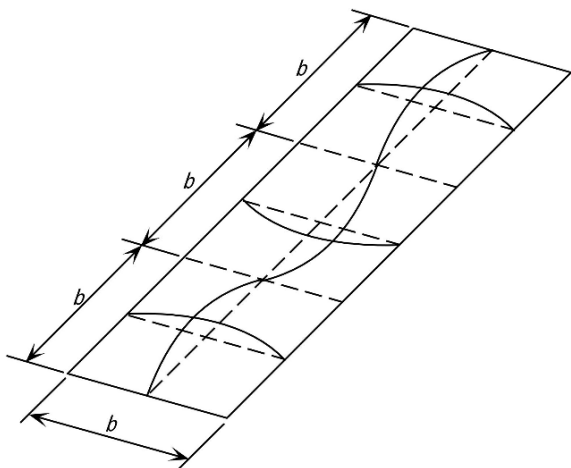


Fig. 3.5.6 Example of buckling form in case of 3 half buckling waves ( $\alpha = 3$ )

For the small  $b/t$ , i.e. small  $b$  in comparison with  $t$ , the elastic buckling stress indicated by Eq. (3.5.19) becomes more than the yield stress of the plate material, however, this is obviously impractical. Therefore, a similar modification is used as in the case of column buckling. For this purpose, it is usual to use Johnson's modification factor  $\eta$  and the critical buckling stress  $\sigma_{cr}$  for the full range of value of  $t/b$  as follows:

$$\sigma_{cr} = \frac{\pi^2 E}{12(1-\nu^2)} \left(\frac{t}{b}\right)^2 K \eta \quad (3.5.21)$$

$$\text{where } \eta = \begin{cases} 1 & \sigma_e \leq \sigma_y/2 \\ \frac{\sigma_y}{\sigma_e} - \frac{1}{4} \left(\frac{\sigma_y}{\sigma_e}\right)^2 & \sigma_e \geq \sigma_y/2 \end{cases} \quad (3.5.22)$$

## 3.6 Plastic Strength

### 3.6.1 Philosophy of Plastic Strength

In general, the strength criterion of a hull structure is where the elastic stress calculated for the design load does not exceed the allowable stress:

$$\sigma_{\max} \leq \sigma_{all} = \frac{\sigma_u}{\alpha} \text{ or } \frac{\sigma_y}{\alpha'} \quad (3.6.1)$$

$\sigma_{\max}$  : maximum design stress

$\sigma_{all}$  : allowable stress

$\alpha, \alpha'$  : safety factor

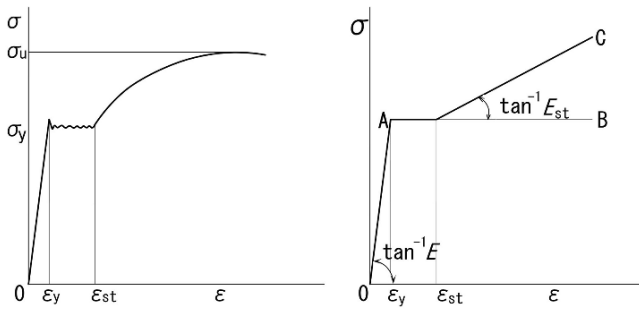
$\sigma_u$  : tensile strength

$\sigma_y$  : yield stress

However, even if maximum design stress exceeds yield stress locally in some actual structure, fracture does not always occur because of redistribution of stress. Therefore, it is desirable to estimate the collapse load of a structure and to apply the safety factor for it. Plastic design is based on conditions where plastic regions develop in structural members leading to collapse, and defines the safety factor as the ultimate load divided by the design load.

Plastic design was introduced in ship structure design in the mid-1960s and now it is applied to the following design areas:

- bow structure loading by wave impact
- deck structure loading by local force such as wheel load
- bulkhead structure loading by water pressure
- tank boundary structure loaded by sloshing impact

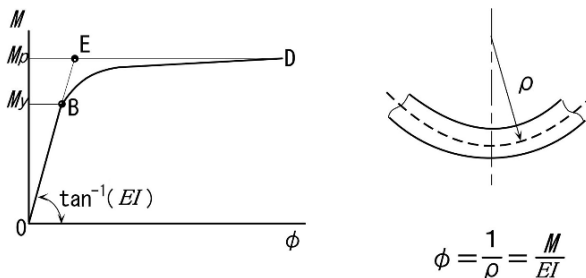


(a) Actual stress-strain curve (b) Idealized stress-strain curve

Fig. 3.6.1 Stress-strain curve

As a result of the tensile tests on mild steel used in ship structures, the stress-strain curve shown in Fig. 3.6.1(a) has been derived, and this curve is idealized as Fig. 3.6.1(b), in which Young’s modulus is  $E = 2.1 \times 10^5$  MPa and the tangent modulus in the plastic zone is  $E_{st} = 4000 \sim 7000$ MPa. If  $E_{st} = 0$ , the stress-strain curve is simply O–A–B, which is termed elastic-perfectly plastic body, neglecting strain-hardening.

Considering bending of a beam, the relation between the bending moment and curvature is shown in Fig. 3.6.2 for an elastic-perfectly plastic body, where the stress distributions in the rectangular sections are as illustrated in Fig. 3.6.3 in accordance with increasing bending moment. In Fig. 3.6.3(a), the stress in the section is proportional to the distance from the neutral axis in O–A in Fig. 3.6.2, and the maximum stress reaches yield stress  $\sigma_y$  at A in Fig. 3.6.2. From this point, the stress does not exceed  $\sigma_y$  and it spreads inside the section. Finally the stress becomes  $\pm\sigma_y$  wholly in the section at B in Fig. 3.6.2, at which the bending moment is called the plastic moment. The neutral axis changes from (a) to (d) in Fig. 3.6.3, and it become the axis passing the centroid in fully plastic conditions (d).



$$\phi = \frac{1}{\rho} = \frac{M}{EI}$$

Fig. 3.6.2 Moment-curvature curve

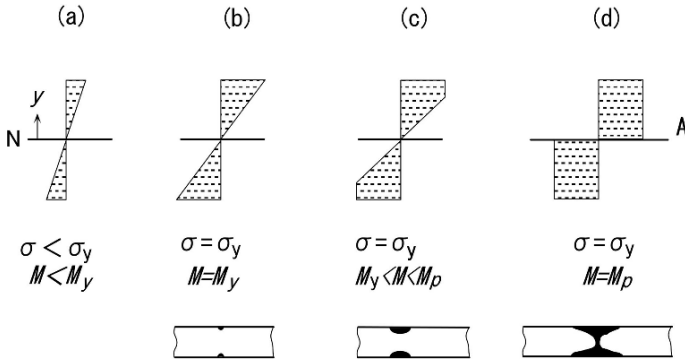


Fig. 3.6.3 Stress distribution along plate thickness

### 3.6.2 Plastic Bending

As shown in Fig. 3.6.4, the stress is  $+\sigma_y$  and  $-\sigma_y$  at the upper and lower areas of the axis X-X when the plastic moment  $M_p$  occurs. If the distance from the axis to the centroid of the upper area is denoted as  $y_U$  and of lower is  $y_L$ , then:

$$\begin{aligned}
 M_p &= y_U \times \frac{A}{2} \sigma_y + y_L \times \frac{A}{2} \sigma_y \\
 &= \frac{A}{2} \sigma_y (y_L + y_U)
 \end{aligned}
 \tag{3.6.2}$$

A : sectional area

If we define plastic modulus as  $\frac{A}{2}(y_L + y_U) = Z_p$ ,

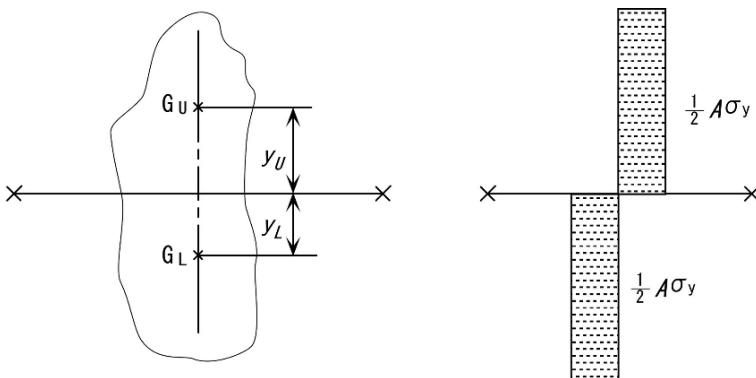


Fig. 3.6.4 Stress distribution in plastic condition

$$M_p = Z_p \times \sigma_y$$

$Z_p$  : plastic modulus

(3.6.3)

Since  $M_y = Z_e \times \sigma_y$  at yield point ( $Z_e$ : section modulus),

$$f = \frac{M_p}{M_y} = \frac{Z_p}{Z_e}$$
(3.6.4)

f: shape factor

The safety factor of plastic design is denoted as:

$$\text{S.F.} = \frac{M_p}{M} = \frac{M_p M_y}{M_y M} = \frac{M_p Z_e \sigma_y}{M_y Z_e \sigma_{all}} = f \times \frac{\sigma_y}{\sigma_{all}}$$

$\sigma_{all}$  : allowable stress of elastic design

(3.6.5)

i.e. multiplying shape factor by the safety factor of elastic design.

In the case of a square section shown in Fig. 3.6.5,

$$Z_p = \frac{1}{2} A (y_u + y_L) = \frac{bh^2}{4}$$
(3.6.6)

On the other hand,

$$Z_e = \frac{bh^2}{6}$$
(3.6.7)

Therefore,

$$f = \frac{Z_p}{Z_e} = 1.5$$
(3.6.8)

In general, if the safety factor is the same as in the elastic design, the allowable stress of a plastic design may be greater than that of an elastic design.

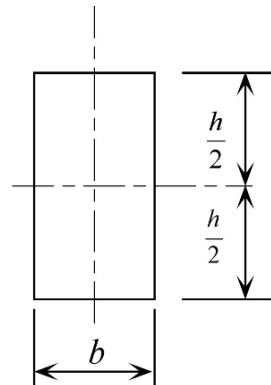


Fig. 3.6.5 Box shape section



### 3.6.3 Plastic Section Modulus

Let us consider bending of a beam, having a section shown in Fig. 3.6.6. Since the total axial force at any section is zero in the elastic condition,

$$0 = \int_A \sigma dA = \int_A E \varepsilon dA = \int_A E \frac{y}{\rho} dA = \frac{E}{\rho} \int_A y dA \quad (3.6.9)$$

$$\therefore \int_A y dA = 0 \quad (3.6.10)$$

Therefore, the neutral axis is taken in the elastic design that the 1st moment around the axis is zero (Fig. 3.6.7(a)).

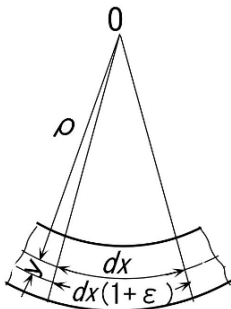
On the other hand, in the plastic design

$$0 = \int_A \sigma_y dA = \int_{A_u} \sigma_y dA_u - \int_{A_L} \sigma_y dA_L \quad (3.6.11)$$

$A_u$ : area of the upper part

$A_L$ : area of the lower part

$$A_u = A_L \quad (3.6.12)$$



$$\frac{dx(1+\varepsilon)}{dx} = \frac{\rho + y}{\rho}$$

$$\therefore \varepsilon = \frac{y}{\rho}$$

Fig. 3.6.6 Bending of beam

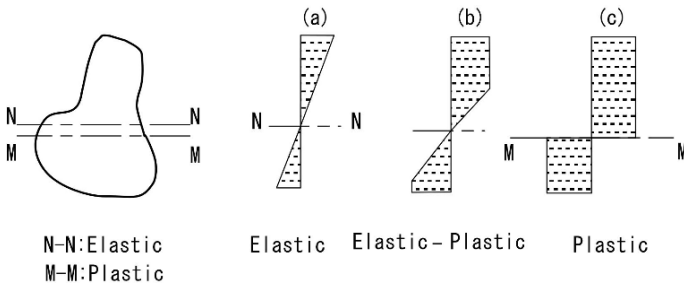
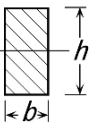
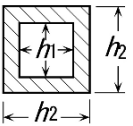
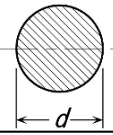
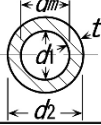


Fig. 3.6.7 Neutral axis

**Table 3.6.1** Section properties

A: Sectional area, I: Moment of inertia, Z: Section modulus, Z<sub>p</sub>: Plastic section modulus

	A	I	Z	Z <sub>p</sub>
	$bh$	$\frac{1}{12}bh^3$	$\frac{1}{6}bh^2$	$\frac{1}{4}bh^2$
	$h_2^2 - h_1^2$	$\frac{1}{12}(h_2^4 - h_1^4)$	$\frac{1}{6} \frac{(h_2^4 - h_1^4)}{h_2}$	$\frac{1}{4}(h_2^3 - h_1^3)$
	$\frac{1}{4}\pi d^2$	$\frac{1}{64}\pi d^4$	$\frac{1}{32}\pi d^3$	$\frac{1}{6}d^3$
	$\frac{1}{4}\pi (d_2^2 - d_1^2)$	$\frac{1}{64}\pi (d_2^4 - d_1^4)$	$\frac{\pi}{32} \frac{(d_2^4 - d_1^4)}{d_2}$	$\frac{1}{6}\pi (d_2^3 - d_1^3)$

Hence, if the cross section is symmetric vertically, the neutral axis in the plastic condition is the same as the elastic one, while it is not the same for non-symmetric sections.

The plastic section modulus thus can be obtained as the sum of the area moment of upper and lower, distance from the line of mid-area to each area center multiplied by the half area. Some examples are shown in Table 3.6.1 [20] for simple figure of a section, while Fig. 3.6.8 is a complex section.

### 3.6.4 Collapse of a Beam

Let us consider a beam clamped at the both ends, and loaded by a lateral concentrated force  $P$  as shown in Fig. 3.6.9(a). Within the elastic range the curvature of the beam is linearly proportional to the bending moment. If the load  $P$  is increased, the nearest support point (point A), will reach the yield stress, and then plasticity will spread throughout the depth of the beam until the section becomes fully plastic, known as the plastic moment  $M_p$ , as shown in Fig. 3.6.9(b). Even if the load increases further, the beam can absorb no further bending moment in this section. It is as if a hinge has been inserted in the beam at this section, and hence this condition in a beam is termed plastic hinge. Thereafter with an increase of the load, the mo-

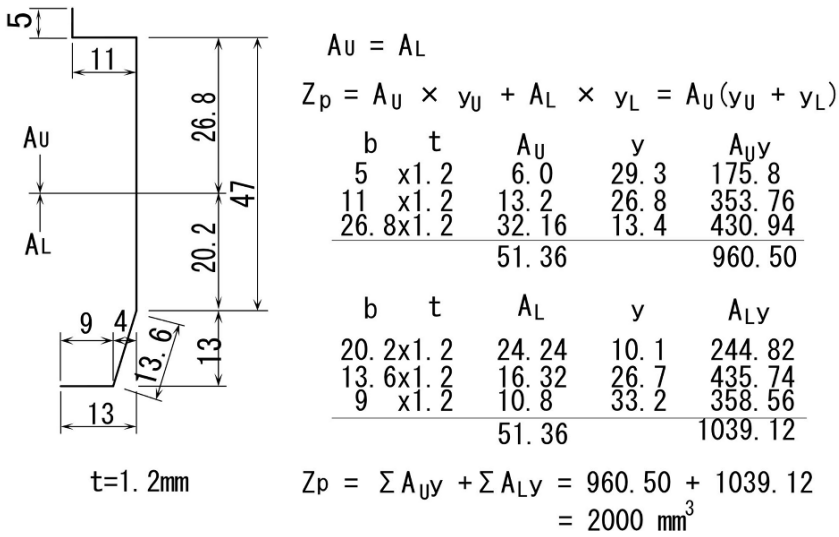


Fig. 3.6.8 Calculation of plastic section modulus

ment at point B becomes  $M_p$  and the plastic hinge occurs again, and finally at point C. The occurrence of such conditions makes the structure incapable of carrying any further load and it is called a collapse by mechanism, and the final load is called the collapse or ultimate load.

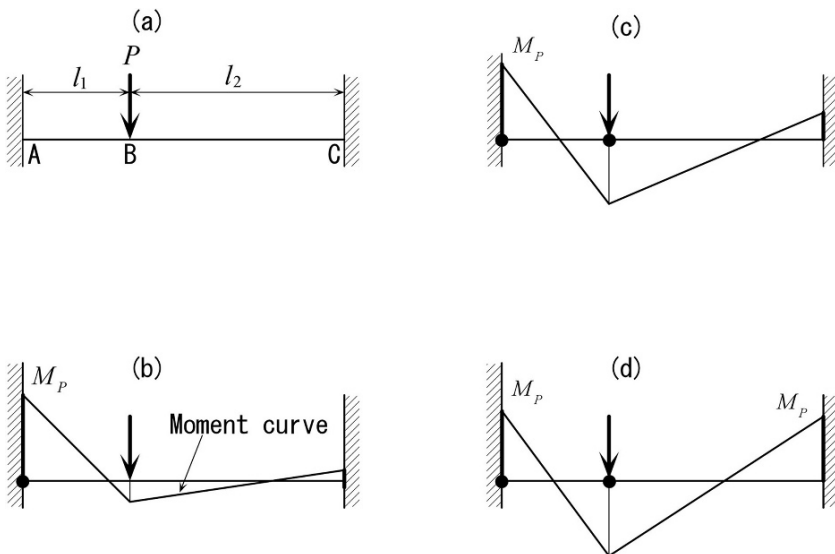


Fig. 3.6.9 Collapse of a beam

A typical method to estimate the ultimate load is the mechanism method, which applies the principle of virtual work, that is, the work done by an external load equals the work done at plastic hinges.

$$\sum Pu = \sum Mp\theta \tag{3.6.13}$$

- $P$  : external force
- $u$  : displacement
- $Mp$  : plastic moment
- $\theta$  : rotation angle
- $w$  : uniform load

Let us take a simple example of a clamped beam which carries uniformly distributed loads, as shown in Fig. 3.6.10. The work done by the external load is

$$We = \int_0^l wydx = 2w \int_0^{l/2} \theta x dx = wl \cdot \frac{l\theta}{2} \cdot \frac{1}{2} = \frac{wl^2}{4} \theta \tag{3.6.14}$$

On the other hand, the work done by hinges is

$$Wi = Mp\theta(1 + 2 + 1) = 4Mp\theta \tag{3.6.15}$$

Therefore, as  $We=Wi$ ,

$$Mp = \frac{wl^2}{16} \tag{3.6.16}$$

From  $P=wl$ ,

$$P = \frac{16}{l} Mp \tag{3.6.17}$$

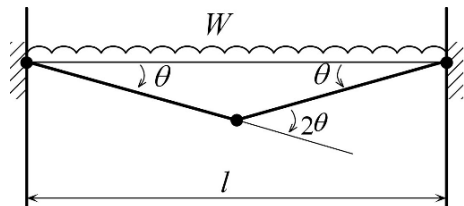
This  $P$  is the collapse load. Table 3.6.2 [20] shows some examples of the calculation formulae for collapse loads.

In actual design of a beam, the procedure is:

1. calculate plastic section modulus,  $Zp$  (see Table 3.6.1, Fig. 3.6.8)
2. obtain plastic moment, by multiplying plastic section modulus by the yield stress,

$$Mp = Zp \times \sigma_y$$

3. obtain the ultimate load, by multiplying  $Mp$  by a coefficient depending the loading condition (see Table 3.6.2)
4. calculate the safety factor, from ultimate load/working load.

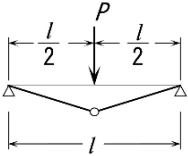
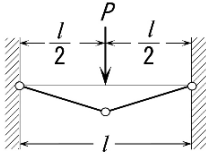
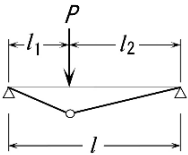
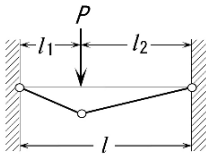
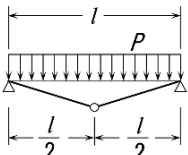
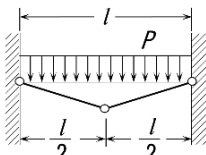


**Fig. 3.6.10** Collapse of clamped beam

**Table 3.6.2** Ultimate load

$P_c$  : Ultimate load

$M_p$  : plastic moment

 $P_c = \frac{4}{l} M_p$	 $P_c = \frac{8}{l} M_p$
 $P_c = \frac{l}{l_1 l_2} M_p$	 $P_c = \frac{2l}{l_1 l_2} M_p$
 $P_c = \frac{8}{l} M_p$	 $P_c = \frac{16}{l} M_p$

### 3.6.5 Collapse of a Plate

Let us consider a square plate clamped on the four boundaries, which carry a uniform distributed lateral load, as shown in Fig. 3.6.11. If the load increases, plastic zones occur and spread in the mid-part of the four boundaries, as shown in (a) and (b) of the figure. Then these pass through the plate thickness and spread along the supporting lines (plastic hinge lines) and also plastic areas occur in the center as shown in (c) of the figure. Such ultimate load is also obtained using the principle of virtual work.

In the case of a rectangular plate simply supported around the entire boundary as shown in Fig. 3.6.12, the uniformly distributed collapse pressure is [21].

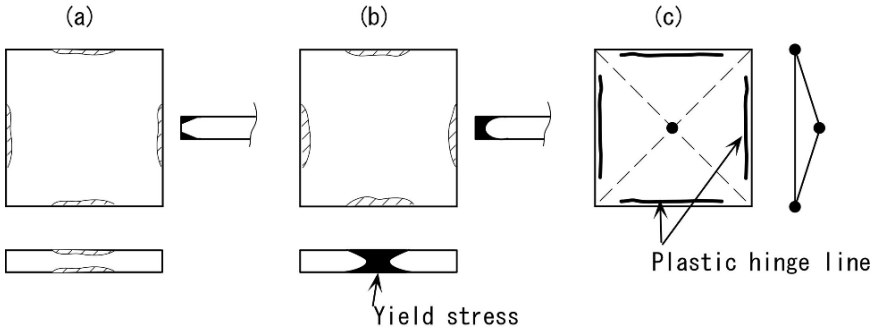


Fig. 3.6.11 Collapse of plate

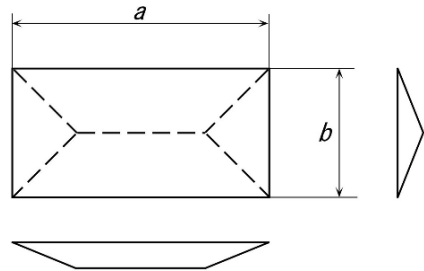


Fig. 3.6.12 Collapse of rectangular plate

$$p_c = \frac{24Mp}{b^2(\sqrt{3 + \beta^2} - \beta)^2} \tag{3.6.18}$$

$Mp$ : plastic collapse moment per unit length =  $\sigma_y h^2 / 4$

$h$ : plate thickness

$\beta = b/a$

In the case where the boundary around a rectangular plate is fully clamped, the uniformly distributed collapse pressure is [21]

$$p_c = \frac{48Mp}{b^2(\sqrt{3 + \beta^2} - \beta)^2} \tag{3.6.19}$$

These formulas are used for the design of plates which are loaded by water pressure.

### 3.7 Vibration in Ship

#### 3.7.1 Introduction

While buckling and yielding are mainly induced by static loading, in contrast, dynamic loading may cause vibrations in structures. It is important for the structural

engineer to prevent vibration problems, because, cyclic forces due to the propeller or main engine may produce heavy vibrations in accommodation spaces, or they may result in failures of structural members due to vibration.

Thus, in order not to suffer from vibration problems, it is a very important to obtain vibration characteristics of structures with high accuracy, especially in the initial stage of design.

### 3.7.2 Basic Theory of Single Degree of Freedom Vibration System

Regarding vibration phenomena, two important concepts “natural frequency” and “resonance” are explained hereafter. There are several well known textbooks [22,23] on vibration and further details should be obtained by reference to these books, since the theory of vibration is a well established field.

(1) *Free Vibration:* Now let's consider the simple spring-mass system illustrated in Fig. 3.7.1, where  $m$  is the mass of weight and  $k$  is the spring stiffness. Suppose that the mass is forced downward an additional distance  $x$  and then suddenly released. The mass would vibrate vertically up and down around the equilibrium position. Let's assume that vertical displacement  $x$  is only allowed and horizontal movement is restricted, such systems are called one degree of freedom systems. The configuration will be determined completely by the vertical displacement  $x$  of the weight.

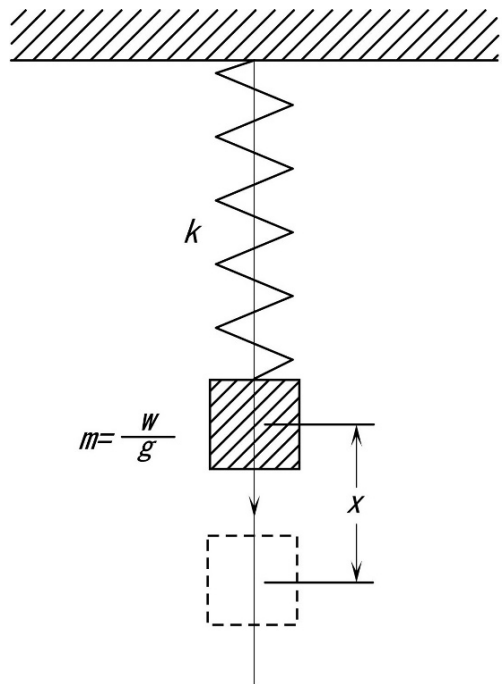


**Fig. 3.7.1** Free vibration of a single degree of freedom

If the weight is pulled to the downward position  $x$  below the equilibrium state, an elastic force is produced on the weight by the spring. According to Newton's principle, the product of the mass and its acceleration is equal to the spring force acting in the reverse direction of acceleration. Thus a differential equation of motion is obtained in the following formula:

$$m\ddot{x} = -kx \quad (3.7.1)$$

where  $\ddot{x} = d^2x/dt^2$

Introducing the notation

$$k/m = v^2 \quad (3.7.2)$$

Equation (3.7.1) can be represented in the following form:

$$\ddot{x} + v^2x = 0 \quad (3.7.3)$$

This equation will be satisfied if we assume the following general solution:

$$x = A \cos vt + B \sin vt \quad (3.7.4)$$

where  $A$  and  $B$  are arbitrary constants, which are determined by initial conditions.

From the above equation, we find that the vertical motion of the weight has a vibrating characteristic, and such a vibration without external force or damping is called free vibration. And from Eq. (3.7.2), the frequency of a vibrating system is:

$$v = \sqrt{\frac{k}{m}} \quad (3.7.5)$$

$$f = \frac{1}{2\pi} \sqrt{\frac{k}{m}}$$

In the Eq. (3.7.5), the frequency of the system is determined only by the magnitude of mass and spring, and is independent of the magnitude of the oscillations, therefore, the above frequency is called the "natural frequency".

(2) *Forced Vibration*: Now let's consider a mass-spring system without damping subjected to periodical external force  $P \cos pt$  as shown in Fig. 3.7.2. The equation of motion of this system is expressed in the form:

$$m\ddot{x} + kx = P \cos pt \quad (3.7.6)$$

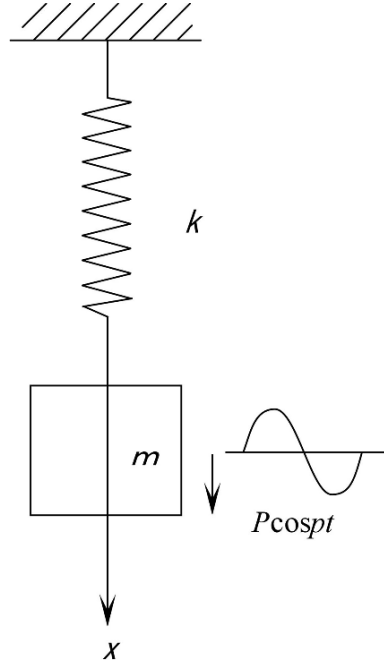
Or it is transformed into

$$\ddot{x} + v^2x = \frac{P}{m} \cos pt \quad (3.7.7)$$

The solution of Eq. (3.7.7) is a combination of (1) a general solution, which was already given in the form of free vibration, and (2) a particular solution to Eq. (3.7.7). To obtain the particular solution, substituting  $x = C \cos pt$  into Eq. (3.7.7), we find:



**Fig. 3.7.2** Forced vibration of a single degree of freedom



$$C = \frac{P/m}{\nu^2 - p^2} \quad (3.7.8)$$

Then the particular solution is given in the form:

$$x = \frac{P/m}{\nu^2 - p^2} \cos pt \quad (3.7.9)$$

Finally the solution of Eq. (3.7.7) can be expressed as follows:

$$x = A \cos \nu t + B \sin \nu t + \frac{P/m}{\nu^2 - p^2} \cos pt \quad (3.7.10)$$

In Eq. (3.7.10), the first two terms indicate free vibration and the last one forced vibration. Therefore, the motion of the mass is the combination of free vibration whose frequency is  $\nu$  and forced vibration with frequency  $p$  of external force.

In practical cases, however, there may be some damping forces which decrease free vibration, the first two terms decrease with time, and the last forced vibration term only remains in a steady condition. Now let's consider the steady condition where free vibration has completely diminished, then the amplitude of a mass in forced vibration is given by Eq. (3.7.10) and can be derived as follows:

$$\begin{aligned}
 a &= \frac{P/m}{v^2 - p^2} \\
 &= \frac{P/mv^2}{1 - p^2/v^2} \\
 &= \frac{P/k}{1 - p^2/v^2}
 \end{aligned}
 \tag{3.7.11}$$

where  $P/k$  means a static displacement of the mass and Eq. (3.7.11) can be modified in the following form by using the notation of static displacement  $x_{st}$ :

$$\frac{a}{x_{st}} = \frac{1}{1 - p^2/v^2}
 \tag{3.7.12}$$

The ratio  $a/x_{st}$  gives the magnification factor of dynamic amplitude in comparison with the static deformation. If we plot the magnification factor against  $p/v$ , we obtain the figure in Fig. 3.7.3. Figure 3.7.3 states that if  $p/v$  is near to zero, i.e. exciting frequency is much lower than the natural frequency of the system, the amplitude of forced vibration is close to the static deflection. On the contrary, as the exciting frequency increases vibration amplitude becomes large and grows infinite when  $p/v = 1$ . Also when the exciting frequency exceeds  $p/v = 1$ , then the amplitude is reduced and converges to zero eventually. In actual situations, we know that an infinite oscillation never happens because of the presence of damping which restricts movement of the mass.

Nevertheless, it is an important fact that the amplitude reaches a very large magnitude when the exciting frequency becomes very close to the natural frequency of the system, i.e.  $p = v$ . That phenomenon is called “resonance”.

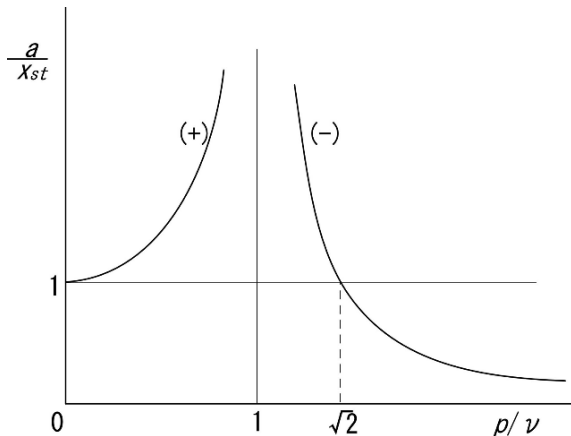


**Fig. 3.7.3** Resonance curve of a single degree of freedom

### 3.7.3 *Vibration Problems in Ships*

Although there are several exciting sources, such as propellers, main engines, auxiliary machines and wave force, which induce ship hull vibration and local structure vibration, serious vibration problems are caused mainly by propeller and by the main engine. As illustrated in Fig. 3.7.4, some part of the propeller exciting force occurs experienced as a fluctuating pressure acting on the outer shell plating of the after-body above the propeller and is called the surface force. Another part is transmitted to the engine room double bottom structure through propeller shafting, and resulting in bearing forces and thrust forces. Those exciting forces induced by the propeller cause hull girder vibration, superstructure vibration, as well as local structure vibration. Hull girder vibration means a hull flexural vibration as shown in Fig. 3.7.5.

The exciting forces of the main engine, which take the form of unbalanced moments, guide forces, guide moments and thrust fluctuation of the line shafting, are transferred from the main engine bed or from the thrust block to the engine room double bottom and may finally induce hull girder vibration or superstructure vibration.

The above vibrations due to propeller or the main engine are steady vibrations, while another type of vibration, such as whipping and springing of hull girders, may be induced transiently by wave forces. A whipping vibration represents a transient hull girder response created by the impact force of slamming. A springing vibration is a constant hull girder vibration in a rather calm sea, which is induced by the resonance between hull girder natural frequency and higher-order frequencies of the ocean waves.

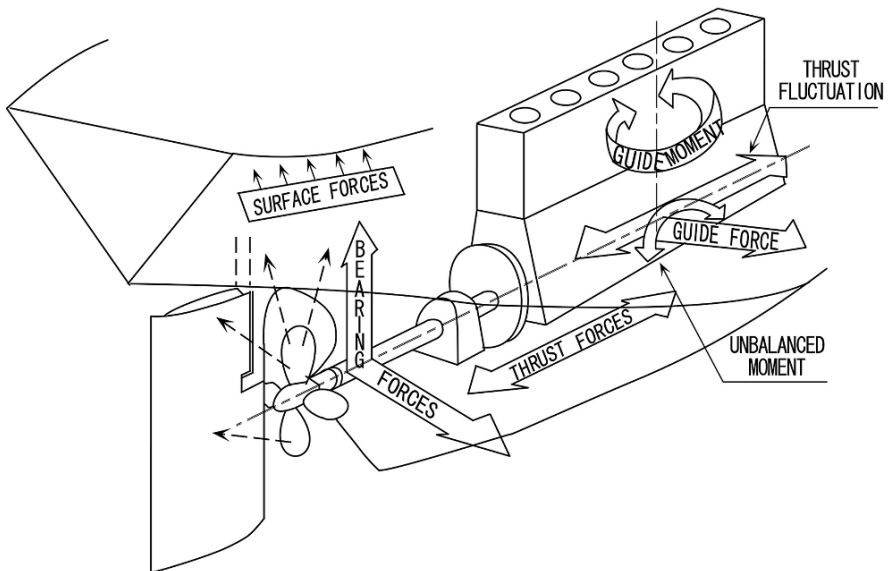


Fig. 3.7.4 Overview of ship vibration

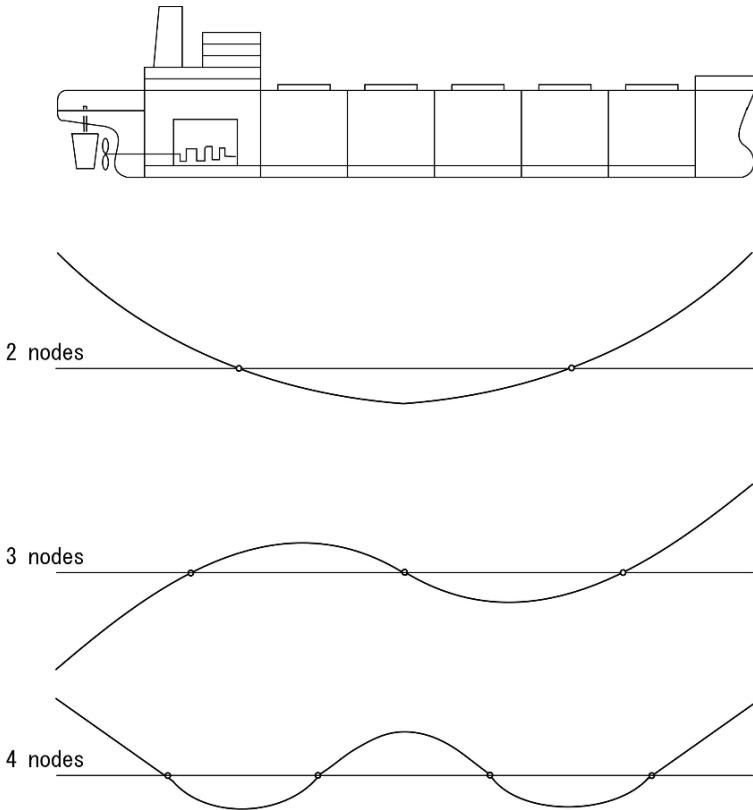


Fig. 3.7.5 Hull girder flexural vibration

### 3.7.4 Vibration Prevention Design

To prevent vibration in a ship, we have to design structures in such a way as to avoid resonance or to restrain the vibration amplitude of the structure to below the allowable limit. This is done by estimating the vibration magnitude in the resonance condition in the case where resonance in the designed structure cannot be avoided.

(1) *Avoiding Resonance:* In the case where the natural frequency of a structure coincides with the exciting frequency of the external force, the structure will experience severe vibration in resonance. Therefore, to prevent a vibration problem, the structure should be design so as to avoid resonance.

The design concept for avoiding resonance is achieved by the following procedure:

**(1) Establish the resonance frequency ranges for the exciting source:** For instance, with a propeller of 6 blades rotating at 100 rpm (revolution per minute), the principal order of resonance frequency is:

$$6 \times 100 = 600 \text{ cpm}$$

where cpm indicates a unit of cycle per minute.

Using a safety factor of 1.2, the target range of avoiding resonance is:

$$600/1.2 \sim 1.2 \times 600 = 500 \sim 720 \text{ cpm}$$

**(2) Design a structure whose natural frequency is less or greater than the resonance range:** It is seldom that the natural frequency of the designed structure is lower than the range, since such a design brings excessive flexibility to the structure due to low rigidity, even if the structure doesn't resonate from any exciting forces. Hence, in general, a higher natural frequency of the structure, than the range should be aimed for.

The "avoiding resonance design" method is so convenient that it is often used in actual design stages, since we have only to examine the natural frequency of the structure once the exciting frequency is determined. This design method can be used under the following conditions:

The exciting frequency or order of force is clearly known.

The resonance peak of the structure is sharp and steep.

The natural frequency of the structure can be accurately estimated.

*(2) Vibration Response Estimation:* If resonance between the structure and the exciting frequency cannot be avoided, a different design method is alternatively adopted, in which the structural response to the exciting force is estimated. In this design process, firstly the vibration amplitude or vibration stress of the structure resulting from the force is calculated by a suitable method, secondly this value is examined to check whether it satisfies the allowable limit or not. The design of the structure is then accepted when the estimated response is satisfactory.

Judgment on whether the design is valid or not is very dependent on the accuracy of vibration calculation, because the response estimation method is available only where;

Mass, stiffness and damping of the structure are properly evaluated.

Magnitude of the exciting force is accurately calculated.

Consequently, both highly advanced analysis techniques and much practical ship-building experience is necessary when applies the above sophisticated estimation method to actual designs.

## 3.8 Selection of Strength Analysis Method

### 3.8.1 Introduction

In this article, several analysis methods utilized in ship structure design are explained, because strength analysis is essential for the integrity of a designed structure. In or-

der to maintain the strength performance to a satisfactory level, it is necessary to analyze the behavior of the structure under the subjected loads and to investigate the stress distribution over the structure. Therefore, we have to make some kind of experiment to simulate the behavior and the stress level. We used to carry out a model test, where a structural model of small size was used and the stress in the members was measured with the aid of strain gauges or photoelastic Moire experiment.

Nowadays, however, in parallel to the rapid progress of electric computers, we often execute numerical simulation successfully for the purpose of strength analysis by computer instead of the above structural model test.

### 3.8.2 *Type of Analysis Method*

A ship structure is, in general, so huge and statically indeterminate that 3-D analysis is not easy. For example, Fig. 3.8.1 indicates an example of a global 3 dimensional model of a container vessel. This model was specially utilized for the strength analysis of local structures around the hatch opening corners with regard to torsional strength analysis; however, such a huge structural model is not always essential in the design of every kind of vessel. In a practical design case, the designers strategically regard the whole structure as a collection of independent components, such as pillars, beams, plates, and shell etc., according to their mechanical characteristics and they select an appropriate analysis method for each component.

Those strength analysis methods are categorized as:

- Analysis using simple beam theory:
- Analysis of frame structure: Slope deflection method
  - Transfer matrix method,
  - Finite element method, etc.
- Analysis of 3 dimensional structure: Finite element method

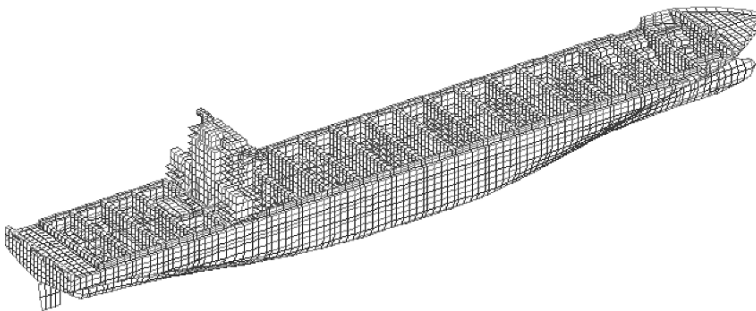


**Fig. 3.8.1** Global FEM model of container vessel

**Table 3.8.1** Comparison table of multi-purpose structure analysis programs

Program name Analysis function		MARC	ANSYS	NASTRAN	ABAQUS
		Kind of analysis	Stress analysis	○	○
Dynamic analysis	EV · RS · RT		EV · RS · RT	EV · RS · RT	EV · RS · RT
Creep analysis	○		○	○	○
Elasto-plastic analysis	○		○	○	○
Large deflection analysis	○		○	○	○
Contact problem	○		○	×	○
Buckling analysis	○		×	○	○

※1 EV : Eigen value Eigen vector  
 RS : Steady vibration response  
 RT : Transient vibration response analysis

Boundary element method, etc.

Recently we have many numerical analysis programs and Table 3.8.1 shows the typical computer programs extensively utilized for strength analysis. These programs are all based on the finite element method, therefore they have the following advantages:

1. They can deal with any shape of structure.
2. They can solve the structure with various types of boundary conditions.
3. They can calculate the structural response for any arbitrary patterns of loads.
4. They can take account of non-linear effects due to physical property changes in the materials, or geometric changes in the structure.

In choosing a suitable analysis program, the designers have to take into account the following:

1. A program which has capable functions to solve the particular problem.
2. A program which is able to calculate with sufficient accuracy.
3. A program which performs the analysis with reasonable cost and time.

### 3.8.3 Analysis Procedure

Figure 3.8.2 illustrates the typical process of structural analysis or vibration analysis using the finite element method program. For the first step, an appropriate analysis program must be chosen for the specified problem, then the modeling is done by determining the appropriate size of the structure. It may be possible to reduce the size of the model by choosing suitable boundary conditions and loading conditions. The next step is to prepare the geometrical data of the finite elements

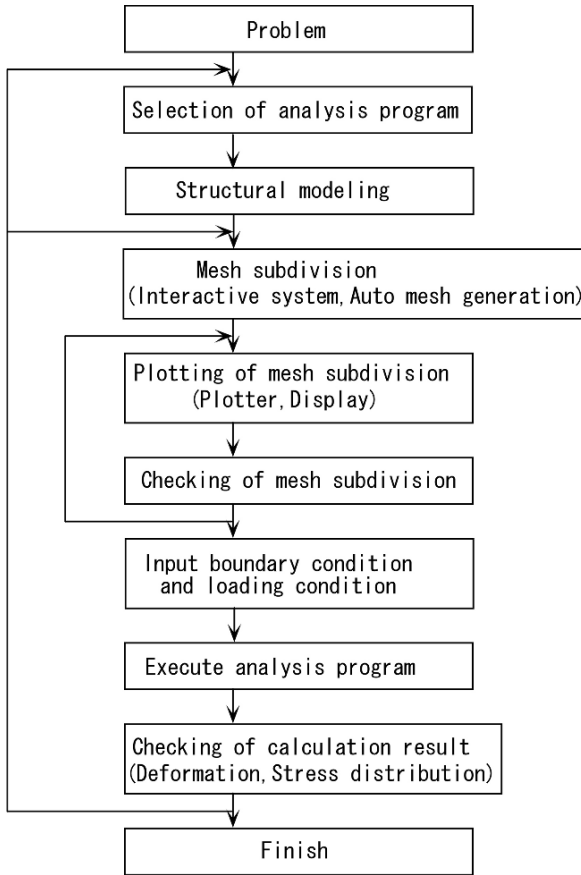


Fig. 3.8.2 Procedure of FEM structure analysis

with visual checking of the validity of the input data through the computer display. The loading data as well as the boundary conditions of the structure are then added.

After executing the analysis program, the calculated result must be assessed to check whether there could be some error in the input data in view of the calculated deformation, stress, etc. If there was a mistake in the input or misunderstanding of the problem, the procedure should be repeated from the beginning.

### 3.8.4 Evaluation of Analysis Result

A most important point of strength analysis using a finite element program is to make a reasonable evaluation of the system. If you evaluate the output of the



program in a wrong way, or if you fail to read the necessary information from the output, all the calculation efforts become useless for the structural design.

Since the finite element program is able to produce the analyzed result in numerical form, it is helpful to specify the stress or deformation at the point of concern. On the other hand, it is dangerous to believe in the output value without checking the total output data from the global point of view. Therefore, before making a final judgment, we must examine carefully the output data in total and obtain a better understanding of the behavior of the analyzed structure to the applied loads and to the boundary conditions.

It is recommended to use the following procedure in order that you can perform an exact calculation and obtain a reasonable evaluation efficiently:

(1) *Make preparations prior to calculation:* A prediction of the deformed shape of a structure and the stress distribution are needed to evaluate quickly the calculated output. Before starting a calculation, the magnitude of deformation and stress levels is roughly estimated. The analysis of a similar structure in the past is also to be studied.

(2) *Make an equivalent model of the behavior:* It is necessary to create an equivalent model which can give accurate structural response to the loads and which is also can evaluate the strength of the designed structure. In addition, the cost and time of computer modeling encourage an economical approach.

(3) *Investigate the calculated result:* We should check whether the calculated results, such as the deformation mode, stress distribution, and eigen-value, resemble the predicted ones. If they differ largely, we had better be suspicious of the input data and consider the reasons why it is different. We should check whether the deformation mode is reasonable considering the direction of applied loads and the constrained degrees of freedom of the boundary condition. We should check whether the total value of input loads coincides with the total value of reaction forces in the output.

By checking the above items, we can judge both qualitatively and quantitatively the validity of the input data, i.e. the structural modeling, boundary conditions and loading conditions, consequently we can be assured of the reliability of the calculated analysis.

# Chapter 4

## Hull Structure Design System

### 4.1 Design Flow

The design of a hull structure is generally carried out in three stages: basic design, detail design, and production design.

(1) *Basic design*: Following the determination of a preliminary structural arrangement in the planning step, the midship section drawings are prepared, followed by the rule-based scantling calculations, strength and vibration calculations, and hull steel weight estimation.

(2) *Detail design*: Following the completion of the detailed midship section drawings, which also include the production method; the bow, stern, engine room, and superstructure are designed in detail. These designs take into account the fitting arrangement and hull block assembly process.

(3) *Production design*: To the above detailed design further information for structure manufacturing is added.

Finally the configuration of individual components is determined to provide supplementary information required for the fabrication process, and data is generated to feed the numerically-controlled (NC) machine tools.

Figure 4.1.1 illustrates the procedure of how to generate the components in each structural design stage, taking a floor plate in the double bottom as an example:

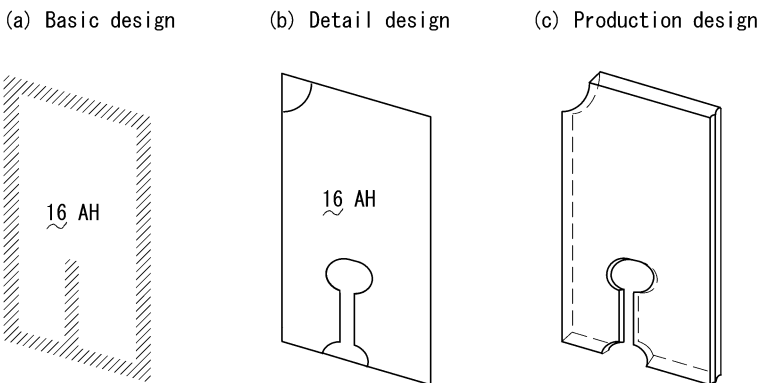


Fig. 4.1.1 Generation of parts in accordance with design stage

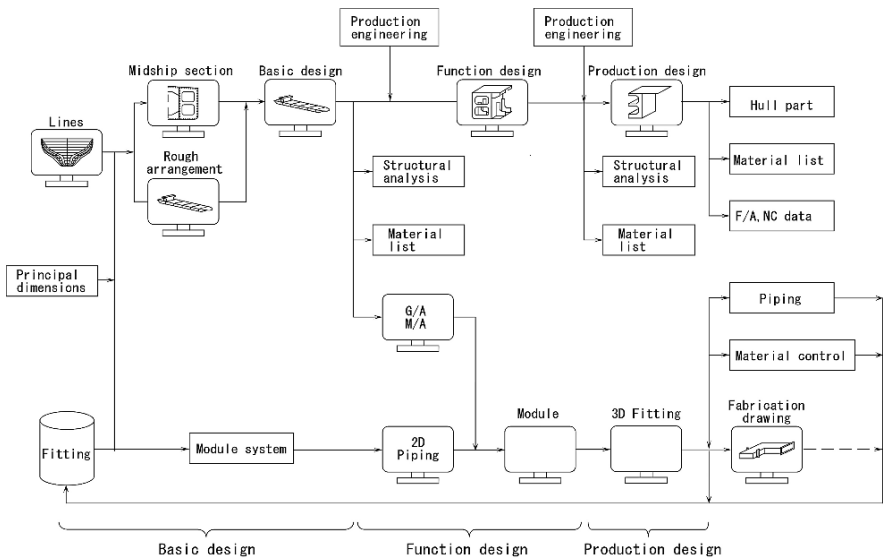
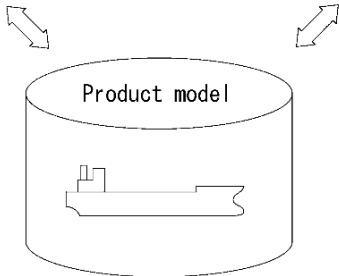
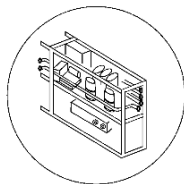
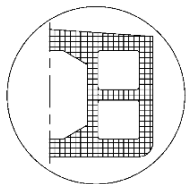


Fig. 4.1.2 CAD/CAM system

Structural analysis

Hull fitting



Production system

Material list

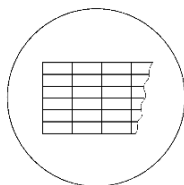
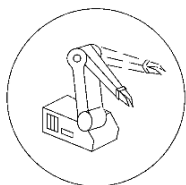


Fig. 4.1.3 Concurrent engineering using product model

Month (Before keel lay)	K-9	K-8	K-7	K-6	K-5	K-4	K-3	K-2	K-1	
Stage	Basic design		Function design		Detail design		Parts design			
Drawings	Lines → General arrangement → Midship section → Machinery arrangement →	Shell landing → Shell expansion → Construction profile (panel) → Construction profile (section) →	do. Purchase of steel materials Study of production procedure	Study of production procedure Definition of detail shape Naming of parts code Material list	Piece table → Parts list →					
	<ul style="list-style-type: none"> <li>◦ Negotiation to owner, classification society</li> <li>◦ Functional design</li> <li>◦ Strength analysis, vibration analysis</li> </ul>									

Fig. 4.1.4 Design procedure of hull structure

- (1) *Basic design*: rough shape of boundaries, plate thickness, materials, outline of slots, arrangement of web stiffeners, etc.
- (2) *Detail design*: determination of the 2-dimensional shape which is defined by the mould line, shapes of slots and scallops, as a result of consideration of the cutting, welding, and block assembly method.
- (3) *Production design*: the 3-dimensional shape is developed taking into consideration of elongation to compensate for welding shrinkage, the preparation of plate edges. This is referred to the accuracy control and detail work practice.

In recent design systems, design data is linked to a production system like CAD/CAM, as shown in Fig. 4.1.2 [24] and will be integrated in the near future by using a product model like a CIM system. The design data of the old systems was input manually for the production system. By using the product model, so-called concurrent engineering will be successfully applied as shown in Fig. 4.1.3, and the design time will be shortened.

The organization of the design department and the design schedule depends on the shipyard and the type of ship to be designed, however an example is shown in Fig. 4.1.4, in which hull structure design is carried out in four stages: (a) basic design, (b) function design, (c) detail design, and (d) part design.

## 4.2 Basic Design of Hull Structures

### 4.2.1 Role of Basic Design

Design work generally takes the form of the so-called design spiral – where a higher precision is progressively achieved at each cycle. The basic design of a ship is as shown in Fig. 4.2.1 [25]. This sequence starts with the determination of the principal dimensions, followed by the ship's speed and engine horsepower, as well as the type of engine, and continues with the determination of preliminary lines, arrangement of compartments, structural arrangement, fittings, engine room arrangement, etc. until a final setting of the list of materials, specifications, and ship price. Thus, starting from a blank sheet, basic ship design consists of making a series of decisions on alternative choices to obtain the outline of a ship possessing, the required characteristics, and performance in the shortest possible time.

The hull structure element in Step 1 consists of roughly determining the structural arrangement, while in Step 2 the same elements will be examined in more detail to consider strength and vibration. In Step 3, the scantlings are determined for the principal members forming the midship structure, and approval drawings are prepared, from which strength and vibration calculations are performed. The resulting data serve to estimate hull steel weight more accurately.

Figure 4.2.2 shows a hull structure basic design system COSMOS as an example [25], which includes four modules:

- (1) Rule-based scantling calculations
- (2) Strength calculations

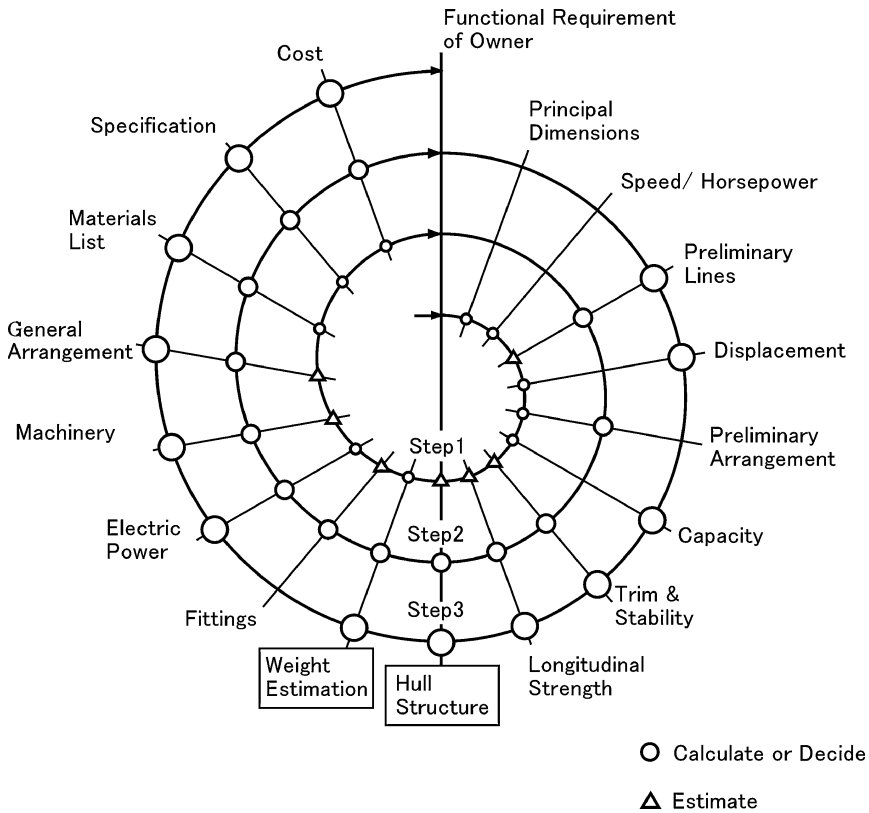


Fig. 4.2.1 Design spiral of basic design

- estimation of loads using hull motion calculations
- direct stress calculations using FEM analysis
- evaluation of stress, fatigue strength, and buckling strength

- (3) Vibration analysis
- (4) Hull steel weight estimation

An important requirement of hull basic design is to rapidly respond to inquiries from the ship owner or from another basic design section, as well as ensuring safety and performance concerning structural strength. To meet such demands, a procedure is needed for estimating the total hull steel weight quickly and accurately using simple formulas, charts from experience of sister ships, or trial-and-error method. A data base system, including a feed back system, is essential.

The drawing to be studied first is the “rough midship section”, considering classification rules, design standards, production methods, etc. The important thing is that it satisfies not only the requirements of the classification society, but also experience from past ships including damage history of cracks and buckling. In addition, since the allowable value (or safety factor) depends on the method and accuracy of

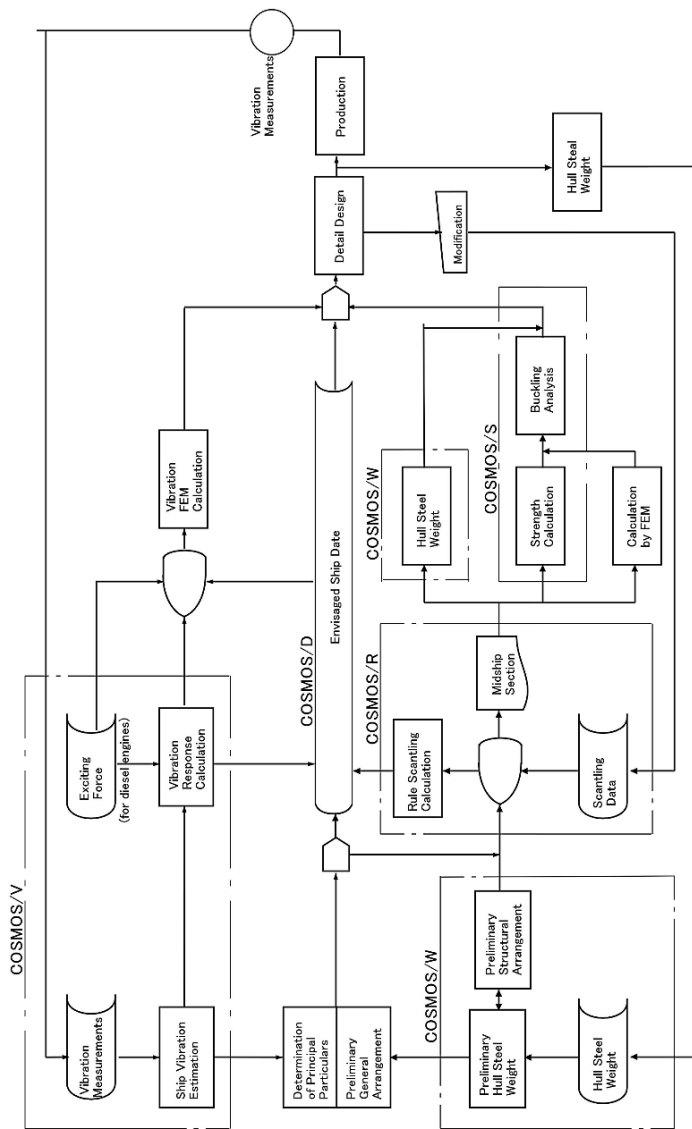


Fig. 4.2.2 System flow of COSMOS

external load calculations and FEM structural analysis, the structural arrangement should be revised in accordance with any improvement in calculation methods.

In the arrangement of primary and secondary structural members and in their scantling calculations, optimum design technique should be applied to reduce hull steel weight and also working man-hours in cooperation with the design section in charge of the general arrangement. Hull steel weight directly influences ship cost and dead weight, therefore, it should be checked often during progress in the design.

Hull vibration affects not only comfort in living quarters on board, but also occurrence of cracks in hull structure and troubles with instruments. In hull girder vibration, possible resonance with unbalance forces or moments due to the diesel main engine, is checked. If resonance is expected, countermeasures to avoid resonance are considered, or ways of reducing the external force or moment are studied. An electric balancer is often provided in steering gear room to reduce the vibration amplitude.

In addition propeller exciting forces affect vibration in the superstructure, therefore the number of blades and propeller aperture should be carefully studied. Local vibration should be checked in structural members in the engine room, in the aft construction, and in tanks in the hold part.

### ***4.2.2 Check of General Arrangement***

Since the general arrangement also affects strength of the ship's hull, the hull structure designer should watch it carefully and give suggestions from a strength point of view. The main items are as follows:

- (1) *Ratio of ship length and depth (L/D)*: If L/D is larger, deflection becomes larger, and hull weight becomes larger because of the difficulty to keep the midship section modulus.
- (2) The arrangement of longitudinal and transverse bulkheads, double bottom, hatch openings in hold space – considerations for the structural continuity and global strength are needed
- (3) Midship section shape – double bottom height, side tank shape including bilge and top side tank
- (4) Type of bulkhead in cargo hold – plane, corrugated, or double plated
- (5) Transverse (frame) space and longitudinal space, considering minimum steel weight
- (6) Position of superstructure, deck house, deck machinery
- (7) Arrangement of steel walls in superstructure, considering vibration

### ***4.2.3 Check of Other Drawings***

Engine particulars and machinery arrangement should be checked by the structure designer from strength and vibration points of view.

- (1) Main engine particulars such as type and revolution number, regarding vibration



- (2) Arrangement of the double bottom, flat, and bulkhead in the engine room, regarding engine room rigidity from engine vibration

Propeller particulars and rough lines should be also checked by the structural designer from strength and vibration points of view.

- (1) Propeller blade number, regarding vibration
- (2) Bow shape, considering wave impact
- (3) Propeller aperture, considering transmission of the propeller exciting force to the ship's hull
- (4) Shape of body in way of propeller bossing, regarding vibration

#### ***4.2.4 Optimization Technique in Basic Design Process***

As described in Sect. 4.2.1, the conventional practice in ship hull design is to follow what is known as the “design spiral”, whereby the design parameters are first assumed on the basis of past experiences, and which are then sought to be amended through the repeated cycles of modifications by trial and error, spreading over various different design sections. This is quite time consuming, and as a result, varieties of simulated design parameters are limited to a certain extent, and the design needs to satisfy design constraints and progress by step-by-step improvement rather than optimization.

From hull structure designers' point of view, for example, shorter ship in length will result in lighter hull steel weight, but it will be necessary to increase ship's depth and breadth to keep tank volume. This small  $L/B$  or  $L/D$  will make propulsive and maneuverability performance worse. To compensate this, if  $C_b$  is designed smaller, the extent of the curved shell will increase, resulting in increased construction cost. Regarding spacing of stiffeners and frames, smaller spacing will make the steel weight lighter, but also increase the number of pieces and welding length, leading to increased construction cost.

These are only a few examples. Actual investigation and decision making conducted in the basic design stage from various standpoint in each design section are very widely ranged. They are considered under various design conditions and constraints, such as international conventions, regulations, classification rules, internal design standards, constraints from operational aspects, constraints from construction aspects, etc.

Because of the complexity and variety of the problems, it has been difficult to apply a direct optimization approach to hull basic design. In the early times, the sequential unconstrained minimization technique was successfully applied to optimization problems of primary and secondary structural member arrangement [26]. However, to achieve true global optimum design, we must simultaneously deal with principal dimensions, hull form, and other general arrangement parameters. To deal with such complex problems, new optimization approaches such as the genetic algorithm have been developed, and are being successfully applied to each type of ship [27–29]. Figure 4.2.3 shows the conceptual flow chart of optimum structure design applying the genetic algorithm.

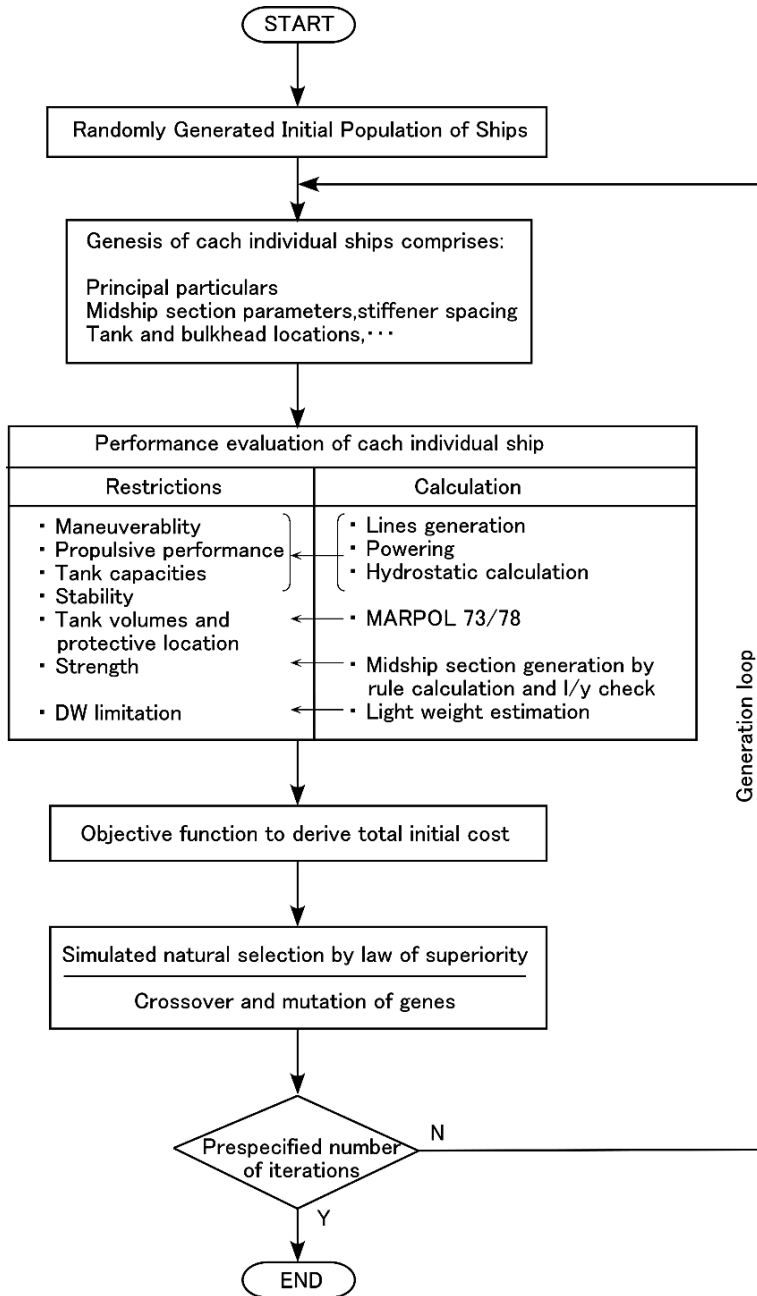


Fig. 4.2.3 Concept of optimum structure design applying genetic algorithm

### 4.3 Structural Drawings

Each hull structural member is developed with regard to detail in accordance with each design stage, and is modeled on a computer recently. Therefore drawings are now the only output of design by computer. The aim of a presentation by drawings is to get approval from the ship owner and classification society, and to inform production engineering.

#### 4.3.1 Approval Drawings

Approval drawings are prepared to get approval from the ship owner and classification society, which are called the “key plan”. The structural strength of each member and the ship as a whole, including vibration, should be included in the drawings. Since these drawings are also used to provide information to other design sections and the production engineering section, they should be submitted as soon as possible in order to shorten the design time.

After midship section drawings are completed, shell landing is firstly planned using lines, and panels representing decks, bulkheads, flats, etc. are successively designed. In these steps, the location of seams and butts of plates, and the position of longitudinals are decided, and these scantlings are calculated.

During the next step, transverse members are designed on cut sections of the above mentioned panels. Both longitudinal and transverse members are now designed and calculated using computer.

The timing of the orders for the required materials is important in order to shorten the building period. Since steel sections such as angle and bulb plate need much time to procure, their scantlings and quantity should be decided as soon as possible, on discussion with the production engineering side.

#### 4.3.2 Detail Drawings

Detail drawings are also called the “yard plan”, which adds the following information in the key plan:

- detail information of the assembling method such as detail of joints
- welding scheme
- detail information of fitting design, such as piping holes, supports, reinforcements, etc.
- *piece codes*: The drawing is usually developed by editing and adding to the key plan. These data give information to the next stages shown in the following:
- *piece drawing*: In general, a piece drawing is generated from CAD data representing contour shapes, markings, edge preparation data, etc. These data are

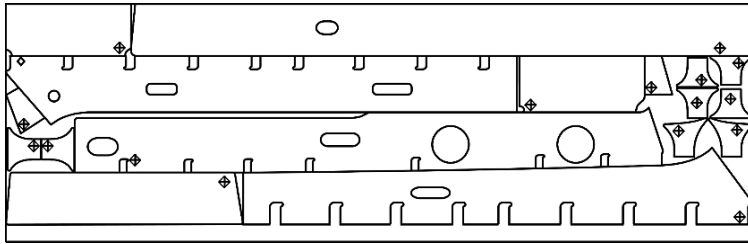


Fig. 4.3.1 Nesting of plates

called CL data (cutter location data). An example of this type of piece drawing is shown in Fig. 4.3.1. On the other hand, long strip material such as shape steels, face plates, flat bar, built-up longitudinals, etc. are shown using table format which includes rough sketches, sizes, and piece codes. These data generate dimensional piece drawings of strip, and are called IL data (item list data), whose example is as shown in Fig. 4.3.2.

- rough cutting plan and detailed cutting plan (nesting): Nesting is the process where many complicated hull structure shapes are cut from the rectangular steel plate. There are two stages of nesting: one is nesting to produce a rough cutting plan, which is used to decide the dimensions and quantity of steel plates to be purchased. The other is nesting to produce a detailed cutting plan, where final piece data are arranged on rectangular plates and are directly transformed to NC cutting data.

Automation of the nesting process has been studied for many years, and in recent years some practical systems are in actual service. One example is the FINEST automatic nesting system [30,31], which reduces the man-hours and the ratio of scrap. Figure 4.3.3 is an example of output from the FINEST system. It is observed that the pieces are not regularly arranged, yet the scrap ratio is excellent. In this system, narrow flat bars are required to be arranged in the longitudinal direction.

- the ordering of the steel
- welding length (for work management)
- fitting design
- working plan for each stage
- quality control

1	-99- F19A (Y) P(S)	P	C	S		X= 0.0 EL= 5386
		SHOWN				
		P- DN				
2	-100- F2 (Y) P(S)	P	C	S		X= 0.0 EL= 2946
		SHOWN				
		P- DN				

Fig. 4.3.2 Piece drawing

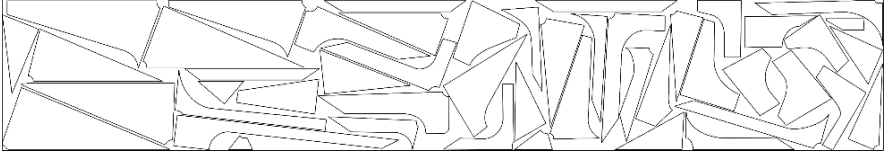


**Fig. 4.3.3** Output from FINEST automatic nesting system

### **4.3.3 Production Data**

Production data includes cutter path for nesting data, and piece table data.

(1) *Cutter path data*: Cutter path data gives torch movement for NC cutting of the web plates, brackets, floor plates, girders, etc., which are nested on a steel plate. The geometric piece data includes:

- elongation to compensate welding shrinkage
- details of the groove to weld
- details of the shape of the slots, scallops, holes, etc.

(2) *Piece table*: Piece table includes:

- code name
- information for plate bending
- information for primer coating on steel surface
- place or stage to deliver
- number
- weight
- surface area etc.

## **4.4 Standardization**

Standardization is essential in design, which contributes to design efficiency because the procedures are already defined, and it makes high quality design possible because it includes past experience. A feed back system of experiences in service is shown in Fig. 4.4.1.

On the other hand, standardization has some demerits:

- It is costly, because it is often necessary to review or renew.
- Creative attitude to new ideas may decrease gradually.

Standardization includes that of shape, arrangement, and design procedure. At early stages of design, a standard of arrangement is useful, while shape standards are applicable in the detail design stage. In these cases, a parametric design method may offer a more flexible approach. Standardization of the design procedure is needed

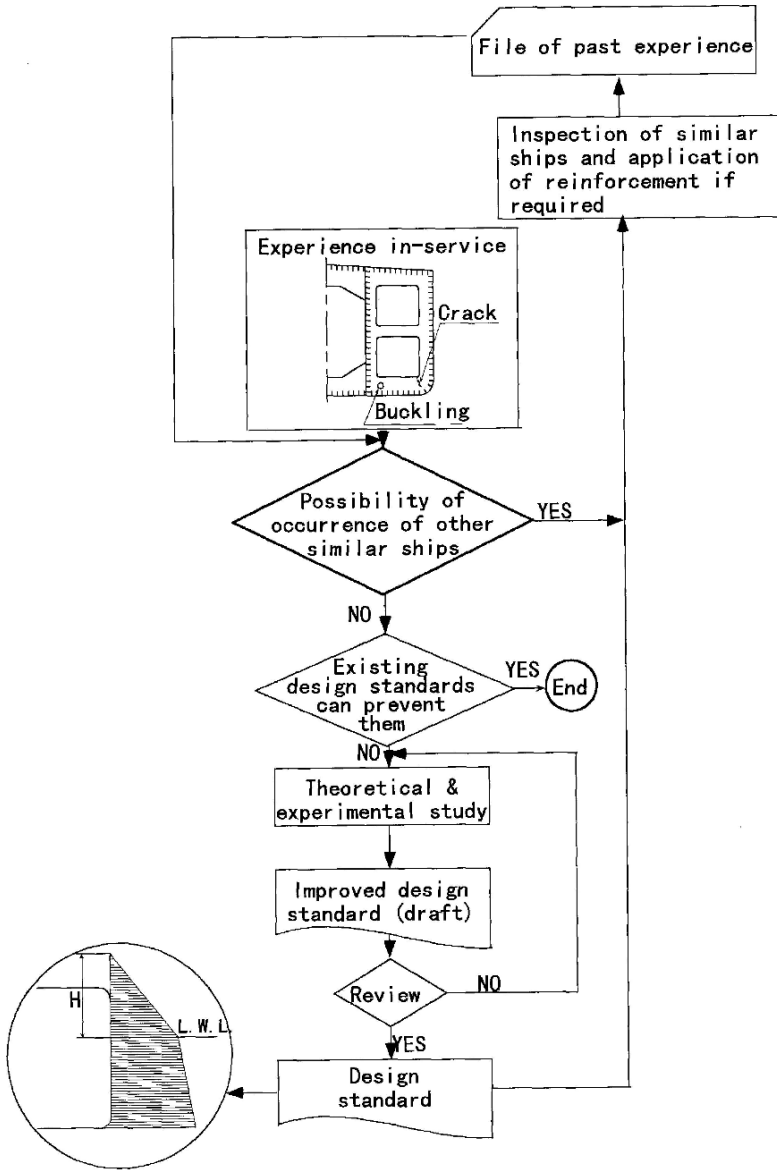


Fig. 4.4.1 Feedback system of experiences in service

for important structures from a strength point of view in order to improve safety and reliability.

Key points of standardization are as follows:

- (1) Standardization of the superficial or external appearance is not effective, but a systematic combination of the various elements is useful by analysis of the function of each. Combination design or module design may be applicable. As

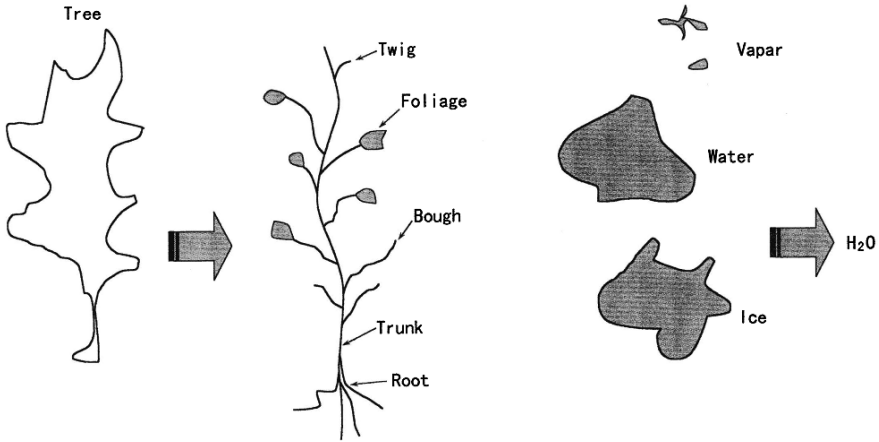


Fig. 4.4.2 Combination of functional elements

shown in Fig. 4.4.2, standardization of each component is useful, but not for the shape as a whole.

- (2) Having flexible standards is essential, to allow changes of ship type, design method, and production procedure. If the standard is too rigid, the applications become narrow. The economic factor and applicability related to flexibility are illustrated in Fig. 4.4.3, and the optimum zone should be investigated to ensure suitability of purpose. Thanks to factory automation and computer techniques, the shape of material or pieces can be cut and fabricated with a degree of flexibility.
- (3) A global and long-term view is necessary for standardization, hence patience is required. Even if it is not profitable for one ship, an accumulation of applications yields a profit. A shortsighted view reduces the impact of standardization.

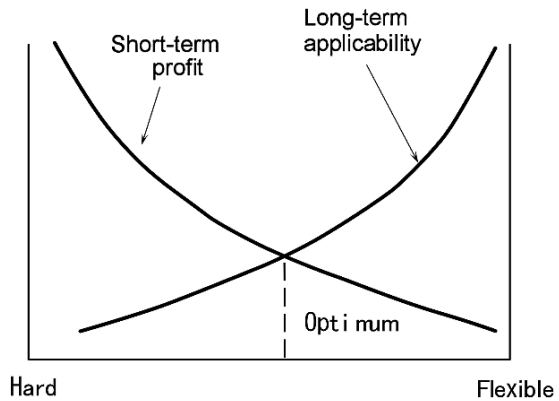


Fig. 4.4.3 Optimum degree of standard

- (4) *Top-down management*: In order to instigate the “standard based design system”, top-down management is necessary. A manager should enforce the application of standards by designers and also always make effort to improve them.

## 4.5 Negotiation with Owner

Hull structure designers usually have little chance for discussion with the ship owner, compared with fitting designers. However it is very important to have good communication with the owner in order to avoid unnecessary troubles, and to get a satisfactory outcome.

Discussions with them are noted on “specification” and approval drawings. In the specifications the following items should be included:

- application of hull steel materials, especially for higher-strength steel, or other special materials
- loading conditions including specific gravity of cargo load
- structural detail of stern frame, rudder, and rudder carrier

The ship owner is usually interested in the rudder system because of the necessity of periodical inspection and maintenance.

- type of chain locker, sea chest, etc.
- vibration, especially allowable levels in living quarters, referring to ISO 6954 guidelines.

As to working practice,

- welding scheme
- hull construction standards
- accuracy standards, referring to JSQS (Japan Shipbuilding Quality Standards)



# Chapter 5

## Progress in Ship Design

### 5.1 Increase in Ship Dimensions of Tankers

The increase of ship dimensions (from VLCC to ULCC), started around 1950 and came to a stand-still in 1980 after the oil crisis. Here the dimension increase is reviewed from the hull structure design viewpoint.

From 1950 onwards it started with the standard tanker of 18,000 DWT or 20,000 DWT; the super tankers of 28,000 DWT (the *Yuhou-Marū* & *Kohou-Marū* of Iino Shipping Co. Ltd.), 35,000 DWT, and 45,000 DWT (the *Gohou-Marū* of Iino Shipping Co. Ltd.) were built one after the other. The mammoth tanker of 100,000 DWT (Universe Apollo) was also built at the end of the 1950s by NBC (National Bulk Carriers) Kure Shipyard.

These ships had common structural characteristics, i.e., 3 m of transverse space, 9 m of tank length for the standard tanker and 12 m for the super tanker and above. The tank arrangement was in general: three tanks next to each other, divided by 2 longitudinal bulkheads.

Even with the Universe Apollo, the length of the center tank was 12 m, divided by three longitudinal bulkheads; so there were 32 center tanks in 2 rows with the following dimensions: 12 m length, 21 m breadth and 21 m depth, just like a deep well. The length of the wing tanks was 24 m.

The main policy of the scaling up of ship size in the 1950s was to apply already established technology. Then in the 1960s this policy changed into rationalization of which the original idea was: “sardines and tuna have the same number of bones”. It is natural that big fish have big bones which are arranged with more space in between and small fish have their smaller bones arranged more closely. Therefore the number of bones is equal. Subsequently it would be natural to design a big ship with wider frame spacings and longer tank lengths.

Before the tank length could be increased, a lot of research was carried out on cargo oil movement in tanks. And from this, the effectiveness of the swash bulkhead was confirmed. The 50 m long cargo oil tank with a swash bulkhead was designed. And the transverse space was increased to about 6 m, thus breaking through the 3 m limit. In Fig. 5.1.1 tank arrangements are shown for a 12 m tank and a longer tank.

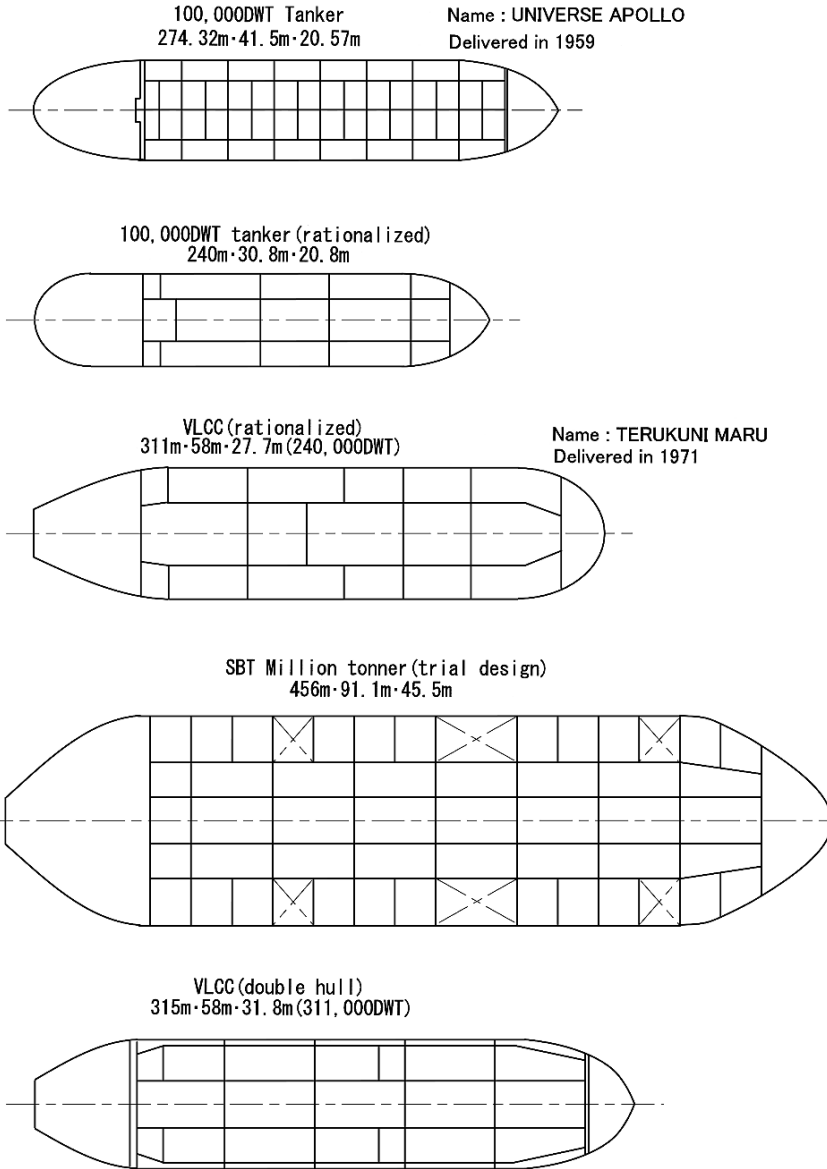


**Fig. 5.1.1** Tank arrangement of each era

One important item which contributed to the scaling up of ships was the rationalization of longitudinal strength, shown in Fig. 1.5.1. A ship is subjected to hogging and sagging moments in waves. The magnitudes of these moments have been calculated by assuming that the wave length is equal to the ship length and the wave height is 1/20 of the length. For a large ship this assumption cannot be applied. For example the wave height of a 300 m long wave is 15 m, which is not realistic. The

research results proved that the actual wave height for a long wave is smaller than expected, and therefore the required longitudinal strength could be reduced. Consequently a large ship can be constructed without riveted doubling plates on deck and bottom.

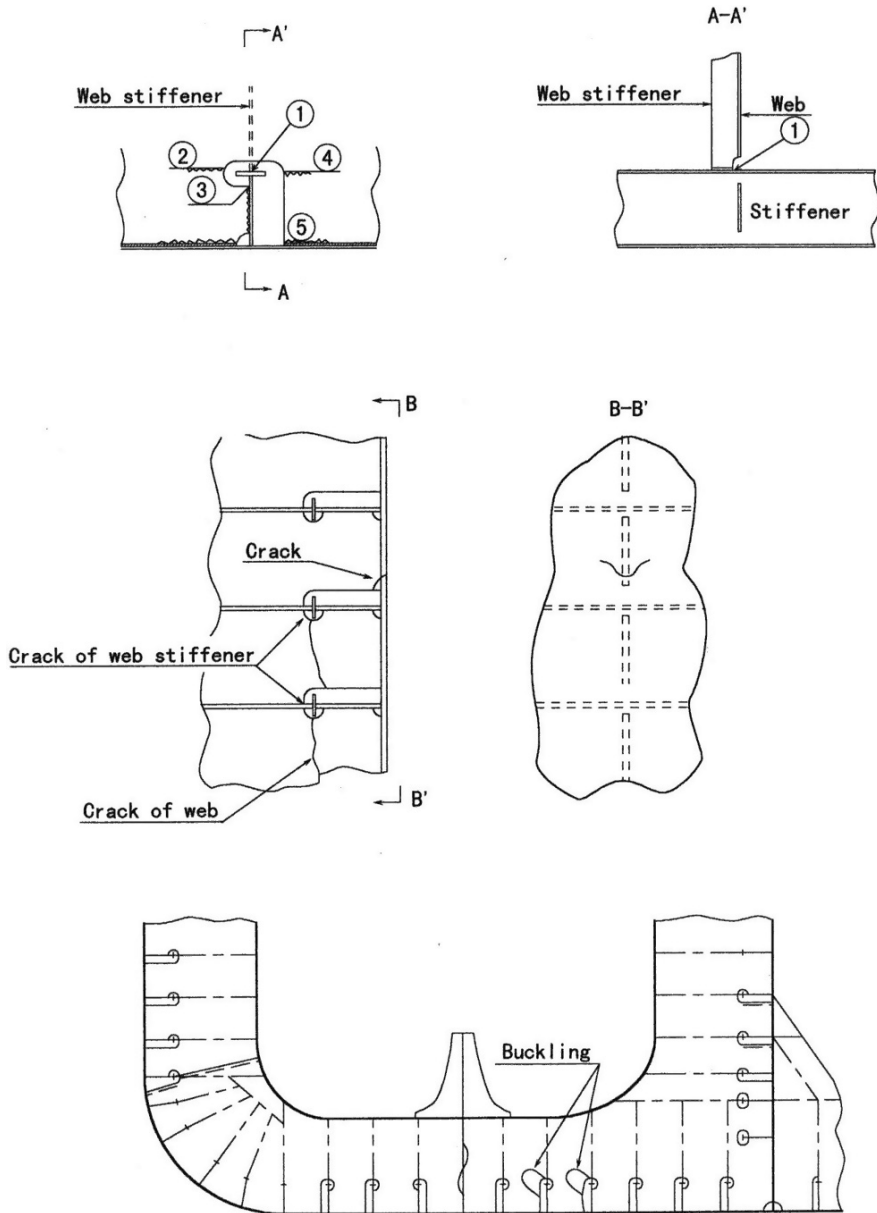


Fig. 5.1.2 Examples of damage around slot

By these three technical innovations, longer tanks, wider spacing and reduced longitudinal strength, the scaling up of ships was achieved smoothly. Many large ships, designed and constructed with reduced longitudinal strength now have terminated their service lives without any serious failures. This means that the reduced longitudinal strength has still some margin.

On the other hand many failures were caused by the longer tank and wider spacing in the transverse strength members of large ships built in 1960s. Cracking and buckling occurred at the cross points of frames and webs, the so called slot parts, where the load supported by the frame is transmitted onto the web. Wrong design was the main reason for these failures, that is by not applying a thicker plate to the web which supports the increased load (about two times) from wider spacing. Moreover, the longer tank had a relative displacement between the longitudinal bulkhead and the side shell which nullified the fixed condition on both ends (design condition) of the bottom transverse. This accelerated the failures. Examples of failures are shown in Fig. 5.1.2.

The main loads applied to a hull structure are weight and buoyancy, which act in the vertical direction. Against these vertical loads, vertical members, such as the side shell, longitudinal and transverse bulkheads, form the framework of the hull structure. For small ships the framework is rigid enough to keep both ends in the fixed boundary condition of the primary supporting members. For a large ship, which has longer tanks, the framework is not rigid enough and causes many failures.

In the hull structure this framework is most important and should be defined before longitudinal, transverse and local strength. The strength of this framework is called “basic strength” hereafter. In Table 5.1.1 the technical conditions, which led to the scaling up of ships, are shown.

In 1973 “The International Regulations for the Prevention of Pollution at Sea by Ships” was accepted, thus limiting tank size and tank arrangement. In addition to the minimally required structures for carrying cargo oil, a ship was to have extra structures to prevent sea pollution. This regulation constrained the scaling up of ships. The prevention of sea pollution regulation had a drastic effect on the rationalization which continued for a long time after World War II.

## 5.2 Specialization of Ships

To achieve more efficiency in transportation, specialization of ships was promoted simultaneously with scaling up. In addition to tankers and general cargo ships previously operated, the ore carrier, bulk carrier, container ship, designated car carrier, liquefied gas carrier, car ferry, twin hull ship and the Techno-Super-Liner appeared. And other special purpose ships have been built. These specialized ships introduced new problems in structural design, which have been investigated and solved by hull structure designers. The in-service experiences with these special ships were fed back and applied in the next ship designs. Sections of such specialized ships are shown in Fig. 5.2.1.

**Table 5.1.1** Technical environments to realize ship's large sizing

Research items	Results	Problems	Countermeasures
Brittle fracture	Thicker plate & higher tensile steel can be applied	Higher material cost	Improved material (TMCP) (See Part I Chap. 6.3)
Welded construction	Lighter & bigger ship Block building method	Reduced buckling strength due to initial deformation	Improved structural system Allowable limit of deform
Sloshing pressure of liquid	Longer cargo oil tank	Relative displacement between side shell and longl. bhd.	Total strength design Rigid swash bhd
Estimation of wave load	Reduced longl. bending moment	Lack of trans. & local strength Unordinary casualty	Reinforcement Operation manual
Finite element analysis	Reliable design based on reduced piece number with wider spacing	Structural arrangement exceeding past experiences	Development of accurate direct calculation method
Shorter & wider hull form	Reduced longl bending moment	Higher resistance	Smaller Cb
Plastic design	Rationalized trans. member	Poor maneuverability	Bigger rudder area
Anti-corrosion	Electrical & chemical methods	Lack of fatigue strength Unti-corrosion in ballast tank	Fracture control design Painting

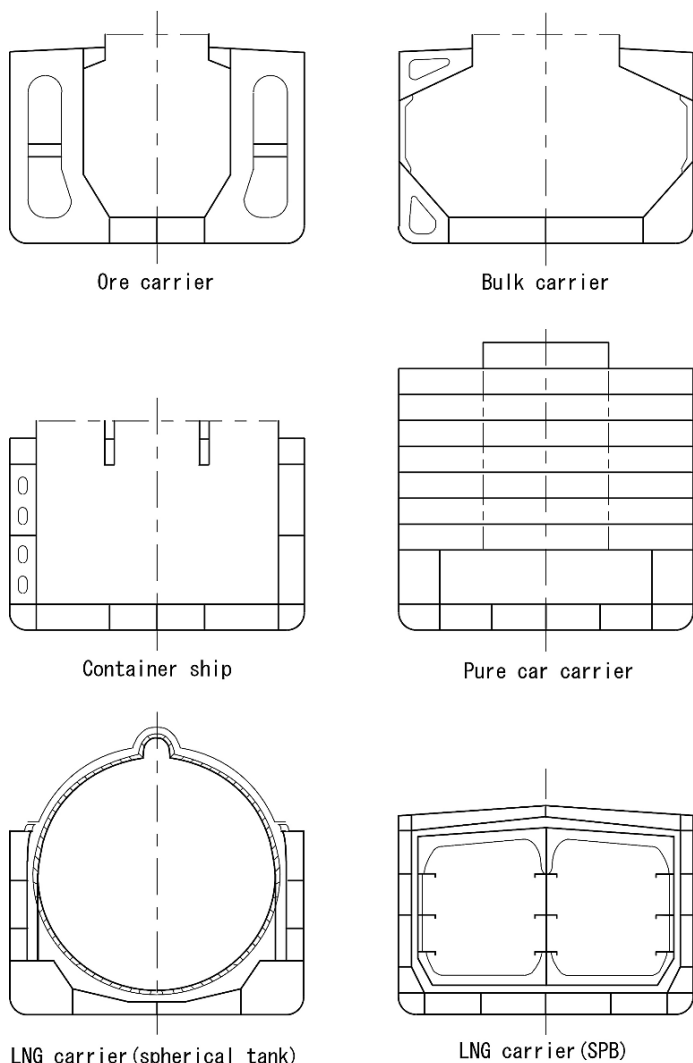


**Fig. 5.2.1** Specialized ships

The ore carrier has a long and big ore hold in the middle of ship which is sandwiched by ballast tanks. To achieve a more efficient handling of ore, no transverse bulkhead is provided in the cargo hold and the hatch opening is bigger than on an ordinary cargo ship. The transverse bulkhead is an important member to maintain the strength of the transverse section of a ship, and special care must be taken when designing a hull structure without transverse bulkheads. In this case the double bottom and decks between hatches play a major role of maintaining the strength of the transverse section of a ship.

In the case of a bulk carrier, the hold volume has priority, for which a lower double bottom and holds without structures are a prerequisite. There are hopper tanks on both sides of the double bottom for good cargo handling and shoulder tanks below the upper deck, thus avoiding cargo movement and creating room for ballast water. The transverse strength of the double bottom and the side frame are retained by the torsional rigidity of hopper and shoulder tanks, supported by transverse bulkheads. The torsional rigidity depends on the distance between transverse bulkheads, namely the hold length. Then for the bulk carrier, hold length is a very important factor. For this reason it once was common sense for ship designers that 7 holds for a 50,000 DWT, and 9 holds for a 100,000 DWT ship should be the norm. A cargo hold without a structure in it, means an extra difficulty to maintain the long spans of the upper deck and double bottom. However, the torsional rigidity of hopper and shoulder tanks make it possible. It is appropriate to say that this was a rather clever design. The hopper and shoulder tanks are connected by an ordinary frame which is another clever design.

A container ship has very big hatch openings and a small upper deck area. This is a problem for the longitudinal and torsional strength, but transverse bulkheads are suitably arranged to maintain the strength in the transverse section.

The most difficult point for designated car carriers is that no transverse bulkheads are provided in the car hold, in order to maintain good accessibility. Moreover no pillars, shallow girders and web frames are allowed from the operational viewpoint.

A transverse bulkhead is like a node of bamboo and the total strength can be obtained from the transverse section of the node.

Most popular liquefied gas carriers are LPG and LNG ships. Typical midship sections of different kind of liquefied gas carriers are shown in Fig. 5.2.2. In the 1960s, for the first time a self-standing tank type LPG ship was constructed. During the 1970s many spherical type LNG ships were built. The spherical tank is made of aluminum, supported by a skirt at the equator. This is a patent of a Norwegian company. Two self-standing tank type LNG ships were built in the 1990s. There are some extra difficulties with the construction of aluminum tanks, because the shape of the fillet welds of frame and girder is strictly to be adhered to. On the other hand the construction of a spherical tank is not difficult at all, because there are no frame

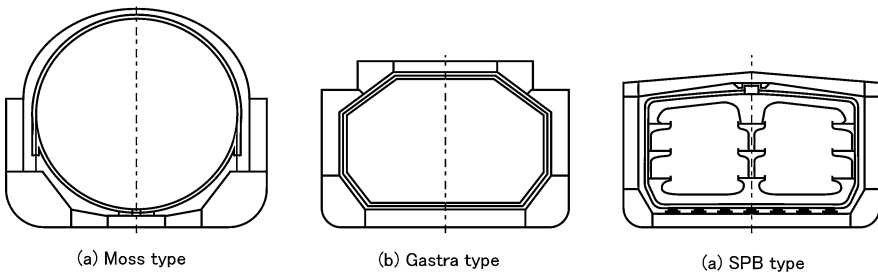


Fig. 5.2.2 Typical midship section of liquefied gas carriers

members and girders in a spherical tank. However, in spite of that advantage of construction, it may cause sloshing problem in spherical tank structure, since there is no obstacle members for liquid movement inside of the tank.

### 5.3 Change of Hull Form

In the 1960s there appeared new hull forms with the scaling up of ships, thus obtaining higher speeds. They had a wider and shortened hull form with a bulbous bow. The so-called “Shinto hull form” was developed to reduce a ship’s cost with greater breadth, limited length and smaller block-coefficient. The resistance increase caused by greater breadth and limited length was avoided by applying a smaller block-coefficient. Limited length gave a smaller longitudinal bending moment. With a smaller bending moment and greater breadth, the longitudinal strength can be maintained without doubling plates on deck and bottom.

With the bulbous bow many structural problems were encountered. With high speed ships it is not a bulb any more, but a cylinder of which the top part is connected to the main hull structure by a thin plate, as shown in Fig. 5.3.1.

Container ships and ferry boats have big flares to improve sea worthiness and protect containers on deck from green sea. Very big wave impact forces are exerted on flare part, exceeding  $45^\circ$ .

The traditional hull form had small radii, say 50 R or 70 R, in front of the stem. It was said that: the smaller the radius, the better the performance would be, and therefore the smallest possible radius was applied. It is an old story that 100 R could not guarantee the speed but 50 R was OK. And the radius of curvature, in the vicinity of the fashion plate above the water line, is not so big that countermeasures against wave impact are necessary.

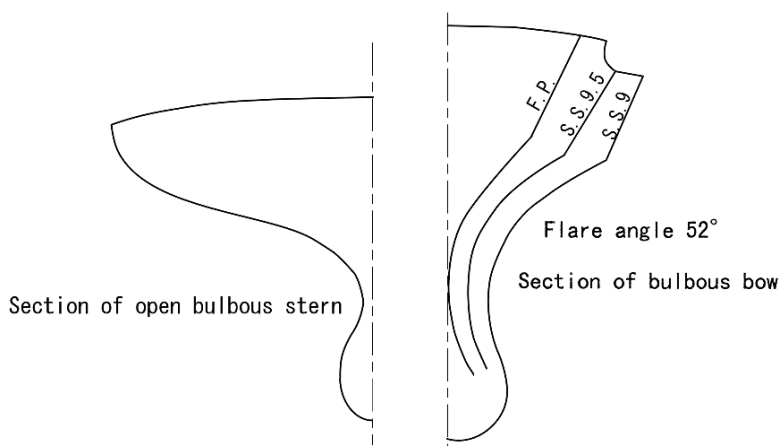


Fig. 5.3.1 Special hull form



With the bulbous bow and the large radius of curvature on the stem, large flare was applied to protect the bulbous bow against damage from the anchors and cables. Due to the changed circumstances and hull forms, much bow flare damage occurred because the traditional design was still applied in spite of the increased wave impact pressure. The cylindrical bow was developed instead of the bulbous bow, which reduced bow damage because it had a big radius of curvature at the stem water line but no flare.

High-speed ships with a smaller block coefficient have no parallel part and the longitudinal strength can not be maintained in the region of 0.4L midship with midship scantling of deck and bottom, because the deck breadth reduces rapidly away from the midship.

Actually around 1970 the forward part of a 10,000 DWT cargo ship had broken downwards at the section 1/4 L from F.P., as if a jack knife was used. On this occasion, because of the damage, the traditional design standard of maintaining midship scantlings was improved in order to maintain the midship section modulus in the vicinity of 0.4 L midship.

The open bulbous stern, which appeared in the energy saving era, had a very narrow stern construction and buckling occurred in the double bottom top plate in the aft part of the engine room because of a reduced section modulus in this section.

The hull structure designer did not anticipate this phenomena well enough, which was caused by a change in hull form, but suitable countermeasures were designed and applied in time, based on lessons learned from the damage.

## 5.4 Ship Vibration Caused by Socio-Economical Change

It is said that ship vibrations are a problem that will never be solved by the ship designer because, as soon as one ship vibration problem is solved, a new one will appear. This is not due to the inability of the ship designer, but by the change of the boundary conditions around ship vibrations.

Before the 1950s a three islander, with the engine at midship, was the typical arrangement and ship vibrations were often caused by lateral vibrations of the long propelling shaft. In the 1960s, with the arrangement of the engine and the bridge on the aft end of the ship, vibrations appeared in the fore and aft direction of the aft bridge. Higher aft bridges vibrate in the fore and aft direction corresponding to vertical hull girder vibrations.

A high-speed turbine container ship, which has a 6-blade propeller with 130 rpm shaft revolutions, is under investigation. The propeller exciting blade frequency is  $130 \times 6 = 780$  cpm instead of the traditional  $90 \times 5 = 450$  cpm for a turbine ship or  $110 \times 5 = 550$  cpm for a diesel ship. By changing the propeller exciting frequency from 450 cpm  $\sim$  550 cpm to 780 cpm (40%  $\sim$  70% increase) the fittings in the accommodation quarters started to vibrate heavily. The lesson learned from this case was: it is most important to consider the exciting frequency closely.

The bigger structures of VLCC or ULCC tankers have lower natural frequencies than smaller tankers and there is possibility that the natural frequency will coincide

**Table 5.4.1** Environment and ship vibration problem

	Socioeconomic conditions	Technical conditions	Phenomena	Solution
1950-		Midship engine } Midship bridge }	Shaft lateral vib.	Rational alignment
1960-	Rationalization High power for economy	Aft engine } Aft bridge } 6RD90 (unbalanced MT) 10RD90 (crank shaft axial vib.)	Hull girder vibration Super structure fore & aft vib.	Balancer Damper
1970-	Specialize for economy	ULCC High speed container ship (50,000 HP 25 kt) Bigger ship with high power engine	Vibration of structure in tank Higher blade freq. (130 rpm x 6 = 780 opm) Stern and local vibration	Avoid resonance by reinforcement Reinforcement Integral design system
1980-	Energy saving due to oil crisis	Less-cylinder engine Hull form improvement	Vibration caused by engine	Engine
1990-	Leisure era Mega competition	Cruise ship Large containership Double hull tanker	Local vibration Long. vibration of superstructure	Elastic mounting of main engine Active mass damper
2000	Less impact to environment	Low revolution engine Increased engine power	Tank structure vibration in engine room	Prediction method of tank vibration

with the exciting frequency of the propeller or main engine. This will cause resonance and heavy vibrations. Consequently it became necessary to estimate the natural frequency of the structures of the tanks of VLCC and ULCC tankers. Generally the natural frequency of a structure is calculated by the formula below. And in principal it can be estimated accurately.

$$f = c\sqrt{k/m} \tag{5.4.1}$$

where  $c$  is a constant,  $k$  is rigidity and  $m$  is mass

An error in  $k$  or  $m$  of 1% causes a 0.5% error in  $f$ .

After the oil crises in 1973 and 1979, energy saving was most importance. All efforts were made to reduce the ship’s resistance, increase the propulsion and machinery plant efficiency. Great success was achieved.

Uniform wake, thanks to hull form improvement, reduced propeller revolutions, and allowed higher propulsion efficiency, which resulted in a reduction in power. This resulted in smaller propeller excitation forces. On the other hand, 4 and 5 cylinder diesel main-engines were developed to reduce fuel consumption while requiring less maintenance. The 4 and 5 cylinder engines with a longer stroke have bigger exciting forces of the 4th or 5th order. In the energy saving era, propeller excitation was not the main concern but engine excitation affected the ship vibrations very much.

The change in boundary conditions of ship vibrations is shown in Table 5.4.1 and the existing boundary conditions caused by energy saving are shown in Fig. 5.4.1 [32].

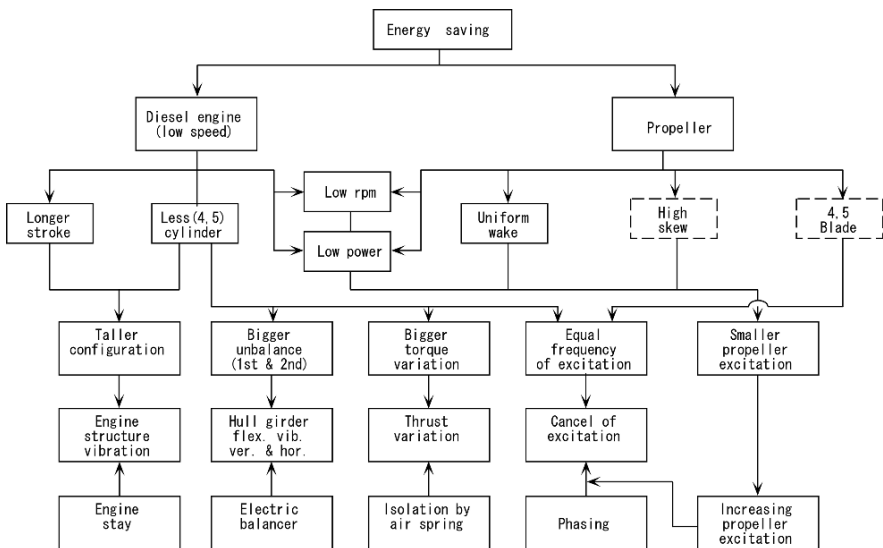


Fig. 5.4.1 Energy saving and ship vibration

## 5.5 Regulations for Environmental Conservation

After 1970, from the viewpoint of the Prevention of Pollution at Sea, tank volumes in tankers were limited. The IMO (International Maritime Organization) issued the SBT (Segregated Ballast Tank) rule, which restricts the volume of oil outflow when damage occurs, and regulates the volume of exclusive ballast tanks to maintain the necessary draft, by estimating the damaged area by grounding.

By applying this SBT rule, 700,000 and 1,000,000 DWT tankers were designed. For a 700,000 DWT tanker, the trial designs were carried out with combinations of the ratio  $L/B = 5.0$  &  $5.5$  and with three & four longitudinal bulkhead anticipate arrangements. Also 1,000,000 DWT tankers were designed, with a ratio  $L/B = 5.0$  and four longitudinal bulkheads with horizontal and vertical main structures. It was possible to build these ships by stress, deflection, and vibration analyses [33]. The tank arrangement of a 1,000,000 DWT tanker is shown in Fig. 5.1.1 together with other ships. She has many wing tanks with a breadth of 18.55 m, a length of 23.2 m and a depth of 45.5 m and she also has three transverses in a tank just like the “Universe Apollo”, built before the rationalization using computer technology.

The trial designs of these big ships were carried out but actually such big ships were never built from the economic point of view and because of the big damage risk.

After the SBT rule was issued, which limits tank volume, a VLCC grounded in May 1989 off the coast of Alaska and the out-flow of oil caused great damage to the sea and the seashore. After that the double hull arrangement was required for tankers, which increased the hull weight by approximately 20% in comparison with the single hull construction. The best efforts of hull structure designers, to reduce by 1% or 0.5% the steel weight by rationalization, were wasted.

In the 1960s, the collision proof double hull construction for nuclear ships was investigated. Based on that knowledge modern research has been carried out by means of newly developed computer and measuring techniques.

The conventional VLCC with single hull construction has cross ties in the wing tanks, which connect vertical webs onto the side shell and longitudinal bulkhead. As the double hull side shell construction has enough strength by itself without cross ties, a new type of construction, which has cross ties in the center tank, was designed.

Double hull construction has been applied in the double bottom of general cargo ships and bulk carriers, and the bottom and side construction of container ships. However, in these cases the load on the double hull is not as high as for tankers. The rigidity of the double hull is proportional to the depth squared, when it works as a beam, but when the two panels work separately, the rigidity is just twice the amount of one panel, and independent of the depth. A suitable girder arrangement for double hull construction, to work as a beam, was investigated and the optimum design method was carried-out [33].

### 5.6 Technical Innovation

Technical innovation is a field that has a big effect on ship design. From the construction viewpoint, welding was the most important technical innovation in this century, and recently steel mill technology has also developed remarkably. One example is the wider plate. Usually the width of steel plate for shipbuilding was maximum 2400 mm (8'). Newly developed high power rolling mills could produce wider plates of 5000 mm which reduced welding seams in the deck, shell and bulkheads.

Another example is TMCP high tensile steel which can be welded in the same way as mild steel and the price is not much higher, therefore it has been widely applied in hull structures. TMCP steel is explained in Sect. 6.3 of Part I, in detail.

Referring to advanced steel mill technology, tapered thickness plate and changing thickness plate can be rolled as shown in Fig. 5.6.1 [34]. Tapered thickness plate is used in bulkhead plate; changing thickness plate is used on decks and for the shell.

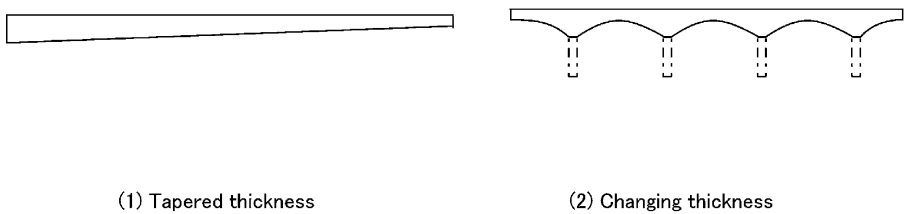


Fig. 5.6.1 Special section of plate

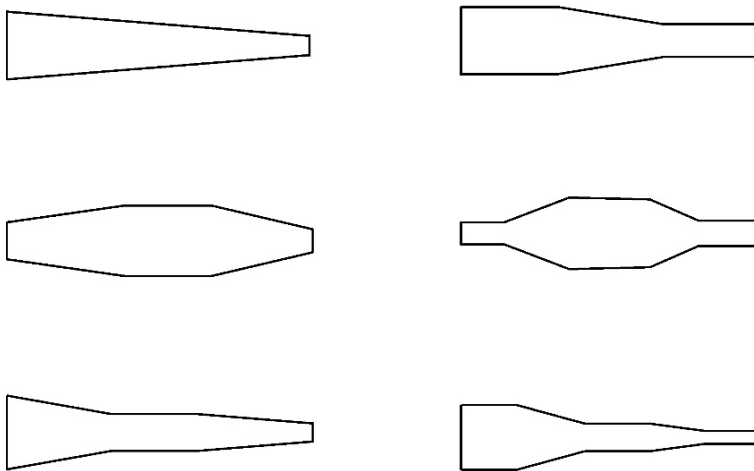


Fig. 5.6.2 Longitudinally profiled steel plate

Tapered thickness plate is effective in reducing the hull steel weight. Another way to decrease the steel weight is to apply longitudinally profiled steel plate as shown in Fig. 5.6.2.

Moreover, recently SUF steel (Surface layer of Ultra Fine grain microstructure) has been developed, which has advantages in preventing buckling and plastic collapse [35].

# Chapter 6

## Materials

Selection of materials is very important in structure design, because it directly affects ship cost and strength. Hence, the structure designer should know well the characteristics of materials, especially newly developed ones.

### 6.1 Hull Steel

Mild steel and higher-strength steel are used for hull structure because of their excellence such as high strength, sufficient ductility, and low price.

Fundamental strength evaluations of the steel are done by a tension test, which is illustrated in Fig. 6.1.1 as a stress–strain curve. The line from O to A is called the elastic zone, in which the stress is proportional to the strain, while B to E is called plastic zone. B and C are called the upper yield point and lower yield point respectively, and the latter is the nominal yield stress, which is 235–280 MPa for mild steel in shipbuilding structures. Some materials have no dominant peak on yield point, in this case the stress corresponding to 0.2% strain is assumed as the yield stress. As shown in the figure, the elongation becomes much larger after yield, and the stress reaches a maximum value at D, which is termed the tensile strength, of 400–500 MPa for mild steel. After that, the strain becomes large and finally the steel fractures at E or E'; D–E is for nominal stress using the original cross-sectional area and D–E' is for actual stress using actual cross-sectional area considering its reduction.

If it is unloaded in the plastic zone, it goes from F to G in the figure, parallel to O–A, and residual strain O–G remains, while in the elastic condition this value is zero. If it is loaded again after the plastic deformation, the stress increases again along G–F, hence, the yield stress is greater than B. This is termed work hardening.

When a compressive load is applied, the stress–strain curve is symmetric around point O of Fig. 6.1.1.

In the case of mild steel, strain at the beginning of yielding is 0.01–0.001, and at failure is 0.3–0.4, therefore it retains some strength after yielding and before failure. Hence it is assumed that mild steel is a superior material.

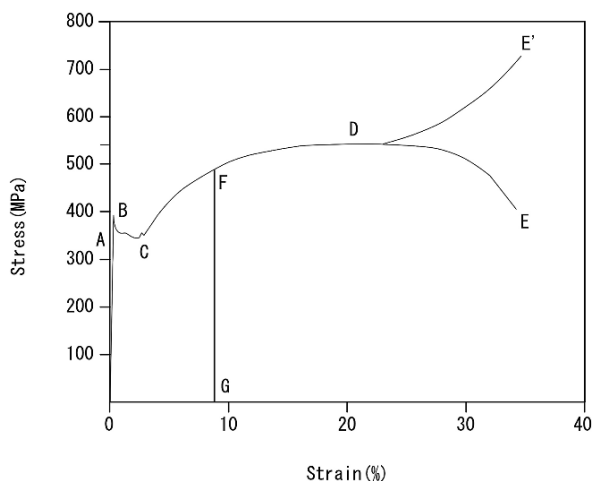


**Fig. 6.1.1** Stress-strain curve

Many structural engineers often make the mistake that structural steel always start with a zero stress condition at the beginning of a life of structures and the stress goes along line O–A–B– in Fig. 6.1.1 during external loading. However, actual structure has residual stress initially as described in Sect. 6.8. Hence we have to know stress and strain conditions at the initial state.

## 6.2 Grades of Steel

Since rivets were used to join plates and stiffeners in old steel ships before world war II, cracks often stopped at a rivet hole. However, if a crack occurs in a more recently built recent welded ship, it can propagate a long distance and it may cause disaster. Hence, quality to arrest the crack propagation as well as weldability are required for hull steel. Welded structure ships newly built in USA during World War II sometimes broke in two under sail in winter with a loud bang. Almost all of the failure section of the steel were crystalloid on the surface, therefore it was concluded after the investigations that the failure was brittle fracture. Hence IACS regulated the application of ship hull steel, categorized as A, B, C, D, and E in accordance with the notch toughness.

Grade A steel is widely used. Rimmed steel is allowed to be used up to and including 12.5 mm in thickness, otherwise killed or semi-killed steels should be used. There is no requirement for the impact test of a specimen.

Grade B steel is killed or semi-killed steel. It has higher notch toughness than A steel. Grade C is no longer used.

Grade D steel has much toughness as defined by impact tests. The value of absorbed energy is specified by whether cracks were arrested or not in previously



**Table 6.2.1** Mechanical properties of hull steel

Grade	Heat treatment	Tensile strength			Impact test			
		Yield stress (N/mm <sup>2</sup> )	Tensile strength (N/mm <sup>2</sup> )	Elongation (%)	Temperature (°C)	Absorbed energy (J)		
						L	T	
KA	-	235-	400~490	22-	-	-	-	
KB					0			
KD					Normalizing	-10	27-	20-
KE					Normalizing	-40		
KA32	Normalizing	315-	470~590	22-	0	31-	22-	
KD32					-20			
KE32					Normalizing			-40
KA36	Normalizing	355-	490~620	21-	0	34-	24-	
KD36					-20			
KE36					Normalizing			-40
KA46	Quenched and tempered	450-	590~700	16-	0	47-	34-	
KD46					-20			
KE46					-40			

built ships. D steel is also killed or semi-killed steel up to and including 25 mm in thickness.

Grade E steel is used as a crack arrester, hence it is highest grade. It is killed steel.

Examples of mechanical properties and chemical composition from the NK rule are shown in Tables 6.2.1 and 6.2.2 respectively. Impact tests are defined for both the

**Table 6.2.2** Chemical properties

Kind	Grade	Deoxidation	C	Si	Mn	P	S	Cu	Cr	Ni	Mo	A <sub>g</sub>	Nb	V									
Mild steel	KA	Rimmed	-0.23	-0.35	2.5×C-	-0.040	-0.040	C <sub>eq</sub> ≤ 0.4															
	KB	Semi-killed	-0.21	-0.35	0.80-	-0.040	-0.040																
	KD	Semi-killed	-0.21	-0.35	0.60-	-0.040	-0.040																
	KE	Killed	-0.18	0.10~0.35	0.70-	-0.040	-0.040							0.015-	—								
Higher-strength steel	KA32	Killed	-0.18	0.10~0.50	0.90~1.60	-0.040	-0.040	-0.35	-0.20	-0.40	-0.08	0.015-											
	KD32											(8) (9)											
	KA36											0.015-	-0.05	-0.10									
	KD36											(8) (9)											
	KE36											0.015-	0.02~0.05	0.05~0.10									
	KA46											Killed	-0.18	-0.55	0.90~1.60	-0.040	-0.040	C <sub>eq</sub> ≤ 0.45					
	KD46																						
KE46																							

roll direction and the normal direction at each test temperature, because absorbed energy by the impact test depends on the direction of the specimen and temperature as shown in Fig. 6.2.1 [36]. Chemical compositions are defined by the percentage of C, Si, Mn, P, S, etc. The larger the percent of carbon, the stronger it becomes, but the ductility, toughness, and weldability become worse. Hence, the percentage of carbon is restricted to within about 0.2%, and Si and Mn are added in lieu of it. P and S are also limited within 0.04% each. In order to prevent welding cracks, the carbon equivalent is defined by the following equation:

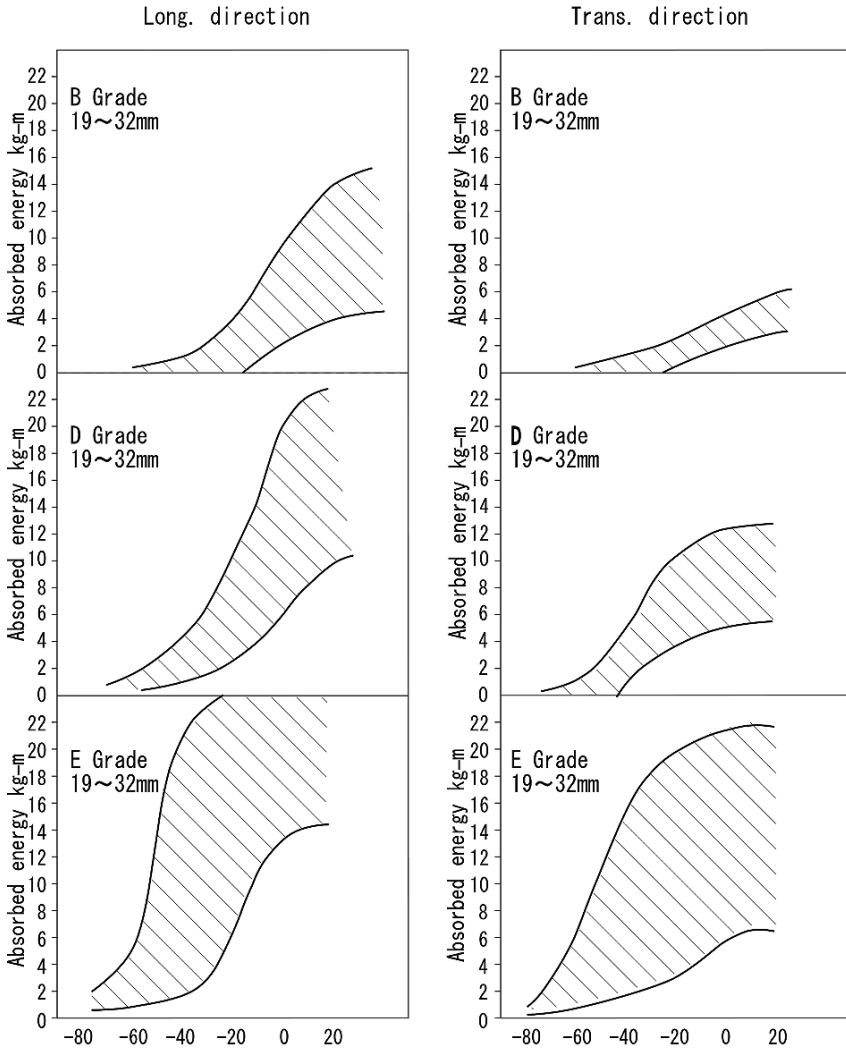
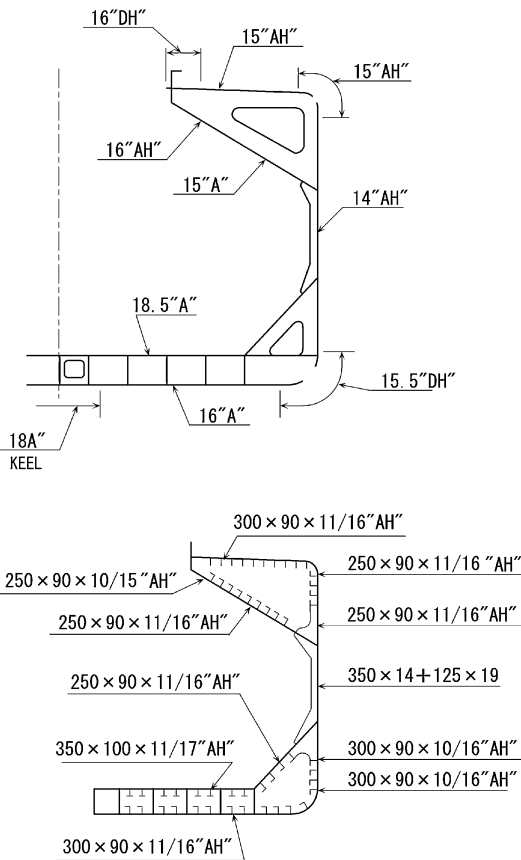


Fig. 6.2.1 Absorbed energy of mild steel

$$K \text{ or } K32 : Ceq = C + \frac{Mn}{6} \quad (\%) \quad (6.2.1)$$

$$K46 : Ceq = C + \frac{Mn}{6} + \frac{Cr + Mo + V}{5} + \frac{Ni + Cu}{15} \quad (\%) \quad (6.2.2)$$

Application of the steel grade depends on the region of the of hull and plate thickness. An example of a 60,000 DWT bulk carrier is shown in Fig. 6.2.2 [37], in which high grade steels are used for the bilge strake, round gunnel, and hatch side plate on the upper deck.



"AH" indicates higher tensile steel of grade "A"  
 "DH" indicates higher tensile steel of grade "D"

Fig. 6.2.2 Application of steel grade

### 6.3 Higher-Strength Steel

Higher-strength steel is recently widely used in main hull structures, because of decreasing material costs and hull steel weight, resulting in increased dead weight and ship speed. At first, it was expensive and the welding procedure for it was difficult and complicated, however it is now not so expensive and is easy to weld thanks to improvements in the steel making process. Hence its application has expanded the extent that 60–70% of total hull steel uses it in recent merchant ships.

The newly developed higher-strength steel is termed CR (Controlled Rolling) or TMCP (Thermo Mechanical Controlled Process) steel, which improves notch toughness and weldability by the treatment of rapid water cooling using control cooling technology during steel making. The plate has a finer grain size than that of conventional higher-strength steel, and hence increases strength.

Classification societies regulate scantling reduction formulas for higher-strength steel by using a coefficient  $k$  based on yield stress criterion. Coefficient  $k$  is a ratio of yield stresses such as 0.78 for K32, 0.72 for K36 as examples of the NK rule. In general, the plate thickness is multiplied by the square root of  $k$  and the section modulus of stiffener multiplied by  $k$ . For example,

$$\text{Bulkhead plate in deep tank : } t_h = \sqrt{k}(t_{ms} - 3.5) + 3.5 \quad (6.3.3)$$

$t_{ms}$ : thickness for mild steel

3.5 mm means corrosion margin

$$\text{Stiffener in deep tank : } Z_h = kZ_{ms} \quad (6.3.4)$$

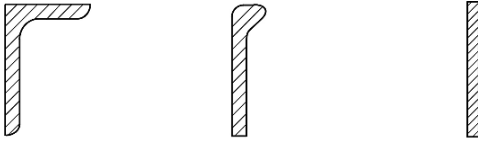
$Z_{ms}$ : section modulus for mild steel

On the other hand, the fatigue strength of higher-strength steel does not increase proportionally with yield strength, therefore it is necessary to take care of design details and working procedures, especially stress concentrations around the welding. In addition, consideration of deflection and buckling strength are necessary, because plate scantlings decrease relative to the yield stress.

### 6.4 Steel Sections

There are steel sections as well as steel plates in hull steel materials, having several shapes as shown in Fig. 6.4.1; angle, bulb plate, and flat bar. Angle steel is widely used for longitudinals, of 100–350 mm depth. Sectional geometry of the angle is standardized in steps. Therefore welded built-up sections, using combinations of web plate and face plate, are applied for large sized sections.

Usually the steel sections have higher toughness and strength compared with the built-up section, and are easy to work with because of less assembly welding.



(a) Angle

(b) Bulb plate

(c) Flat bar

**Fig. 6.4.1** Steel sections of stiffener

## 6.5 Other Materials

Cast steel is used in a part of the stern frame, rudder, propeller bossing, hawse pipe, etc., where the shape is complex and strength is needed. Compared with cast iron, its ductility, strength, and weldability are excellent. It is necessary to pay attention to avoiding high residual stress due to the welding of connecting parts to the steel plate. If needed, annealing or other stress relief process will be carried out. The stern frame was once made by the cast steel wholly, but now a combination of built-up steel is used.

Forged steel is used for rudder stock, rudder pintle, etc., where the shape is simple and strength is needed.

Aluminium alloy is used in high-speed boats and tank structures for liquefied gas, because of the advantage of light weight, excellent corrosion resistant, and its strength regarding brittleness toughness in the cold. The specific gravity of the aluminium alloy is one third of mild steel, and the yield strength is two thirds, therefore it is favorable in saving ship weight. However, special tools or facilities are necessary for the fabrication and assembly of it.

## 6.6 Scattering of Material Properties

It is very important to know well the characteristics of hull steel in order to evaluate the structural strength. Even for mild steels the values of yield stress and tensile strength vary widely in accordance with their grade, specification, size, temperature, steel making company, rolling conditions, and even part in one plate. Higher-strength steel also has a scattering in its strength. Table 6.2.1 only shows the lower limit or range of the strength and the actual value is not always the same. Figure 6.6.1 is an example of a mill sheet, which is the inspection certificate of each steel plate, describing actual mechanical properties and chemical compositions. The specified yield point of this plate is 235 MPa, but it is observed that actual yield point of this plate is 309 MPa.

Figure 6.6.2 shows the scattering of the yield stress and the tensile strength of mild steel, obtained from the mill sheet on delivery to the shipyard, in which the stress varies over a range of 100 MPa. These histograms seem approximately to have a normal distribution, shown as the curve in the figure. The standard deviation is 15–20 MPa



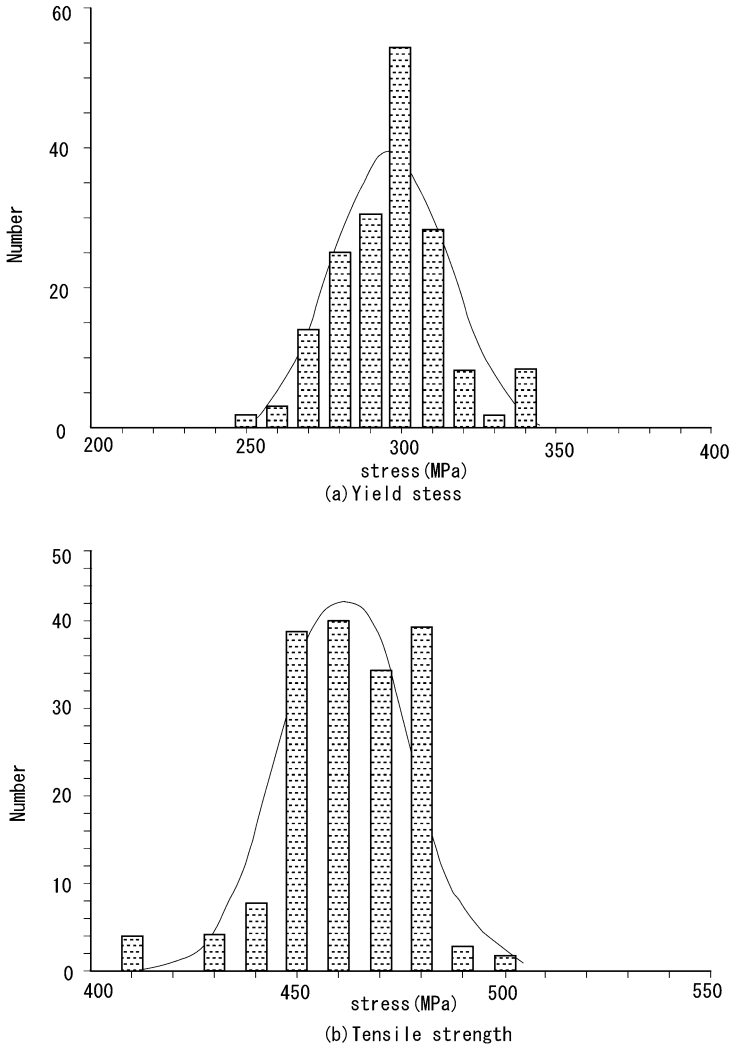


**Fig. 6.6.2** Scattering of strength of mild steel

Strength differs also with the roll direction (L) and the normal direction (T), usually that of the L direction is higher than that of the T direction. The difference in the tensile strengths of L and T is now not so large, but that of toughness is larger. Hence, plates of longitudinal strength members must be arranged longitudinally along the L direction. The strength of a plate in the thickness direction (Z) is less than that in the in-plane direction. Therefore, if the tension force along the Z-direction is loaded through a rib or stiffener, tearing inside the plate may occur, which is termed lamellar tearing (Fig. 6.6.3).

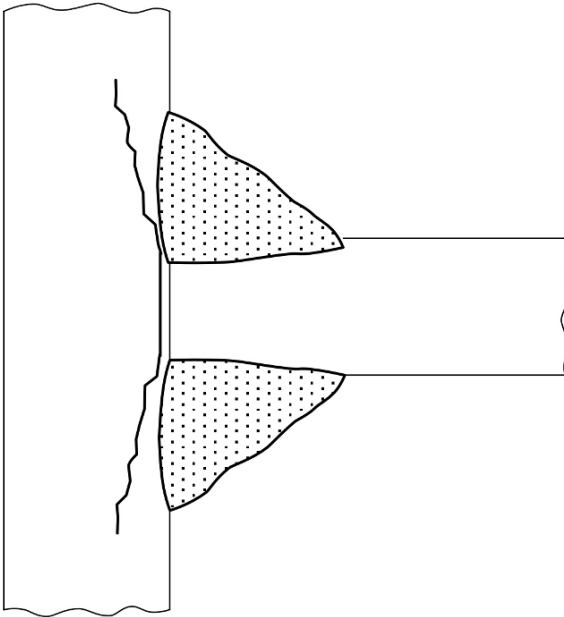


**Fig. 6.6.3** Examples of lamellar tears

Material properties depend on temperature, and Fig. 6.6.4 shows temperature-dependent characteristics of Young’s modulus, yield stress, and coefficient of linear expansion [38]. Steel reduces in strength beyond 400°C and loses it at about 700°C, and the coefficient of linear expansion increases gradually in accordance with the

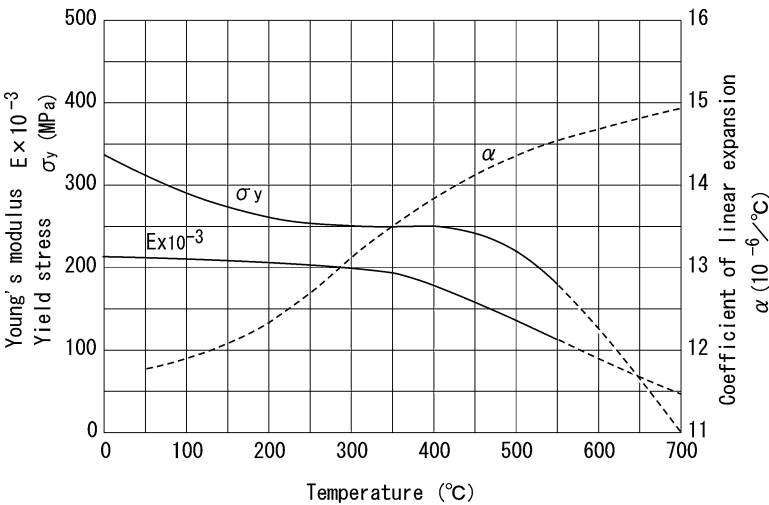


**Fig. 6.6.4** Temperature dependency of material properties



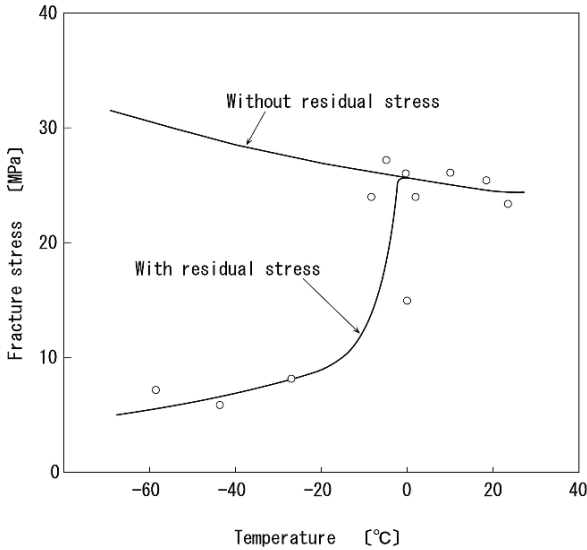


Fig. 6.6.5 Fracture stress in lower temperature

temperature. On the other hand, for temperatures below 0°C the strength increases with temperature decrease; however, it decreases sharply when materials have defects or residual stresses caused by welding as shown in Fig. 6.6.5 [39]. These cause brittle fracture at low temperature.

## 6.7 Scattering of Physical Properties

Plate thickness also varies depending on the roll condition in accordance with the steel maker, material properties, nominal thickness, etc., and the classification societies regulate the minus tolerance in plate thickness being 0.3 mm. The plus error will be no problem, but we should pay attention to the minus error, because it causes a reduction in strength. Figure 6.7.1 shows measurements of actual thickness before fabrication in a shipyard [40]. It is known that the error spreads over a wide range. The plate thickness may be reduced due to the press bending with sharp angle.

Reduction of the plate thickness by corrosion is well known; it also causes cracks or buckling. Figure 6.7.2 shows a statistical analysis of the plate thickness reduction for both deep tank and water tight bulkheads as an example [41]. It is necessary to know the actual plate thickness in the case of damage analysis.

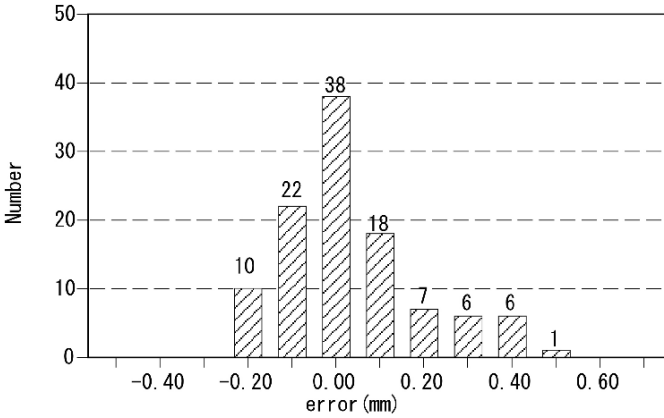
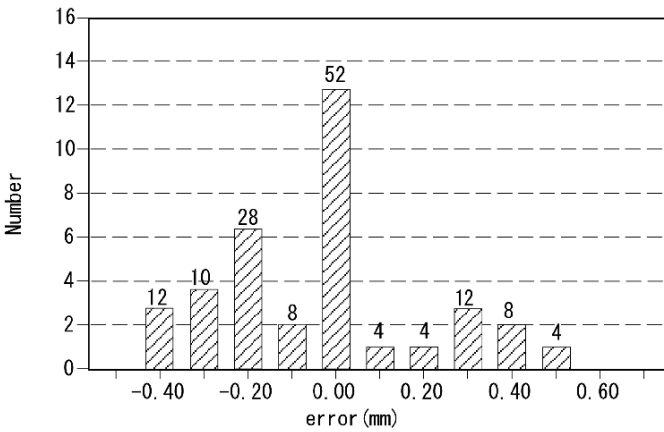
(a)  $t=6\sim 15\text{mm}$ (b)  $t=20\sim 25\text{mm}$ 

Fig. 6.7.1 Scattering of plate thickness

## 6.8 Residual Stress [42]

In accordance with the recent prevalence of computer hardware and software due to lower price and easy operation, hull structure design has become more reliable and accurate by applying direct calculation methods. This is especially true when structural analysis becomes more precise by using FEM analysis. If the structural FEM model is more large and fine, the stress will be calculated more precisely.

On the other hand, it is well known that structural materials have some residual stresses from the heat process of steel making and assemble processes (cutting, bending, welding, straightening, etc.), and these affect the ship hull strength. It is necessary to consider the residual stresses in structure design in order to evaluate

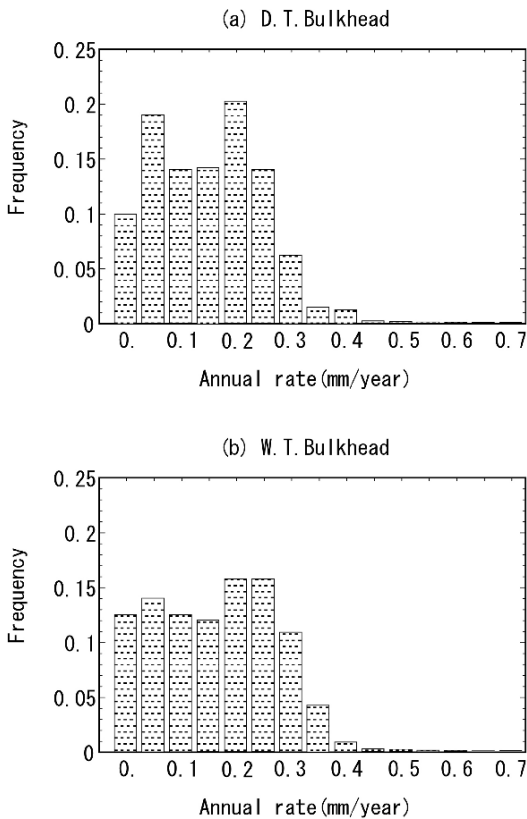


Fig. 6.7.2 Frequency distributions of annual corrosion rates

the strength more precisely, while these are usually not considered in FEM calculations so far because the stresses are not exactly known.

Higher-strength steel such as TMCP (Thermo-Mechanical Control Process) steel, in conjunction with controlled rolling and controlled cooling, has been widely adopted recently in hull structure. It is said that the TMCP steel plate as rolled has greater residual stress around the plate edges, and also the stresses is distributed intricately inside the plate.

When constructing a ship's hull, residual stresses occur during surface preparation such as shot blasting, and also occur at various stages. The plastic deformation results after the heat treatment such as welding, cutting, straightening, and line heating. Residual stress occurs due to mechanical processing such as press bending, and the self weight and outside forces.

The residual stresses are thought to affect the hull strength as follows;

- buckling in the skin plate
- fatigue cracks from welding beads
- brittle fractures in the vicinity of butt welding

# Chapter 7

## Finite Element Method

### 7.1 Characteristics of FEM

Nowadays the finite element method (FEM) is an essential and powerful tool for solving structural problems not only in the field of shipbuilding but also in the design of most industrial products and even in non-structural fields. FEM can be used for a wide variety of problems in linear and nonlinear solid mechanics, dynamics, and ships' structural stability problems, in accordance with the development of computer technology and its popularization.

The conventional method in solving stress and deformation problems is an analytical one using theories of beams, columns and plates, etc. Hence its application is restricted to most simple structures and loads. On the other hand FEM:

- (1) divides a structure into small elements
- (2) assumes each element to be a mathematical model
- (3) assembles the elements and solves the overall

as shown in Fig. 7.1.1 [43].

The element shown in Fig. 7.1.2 as a typical example is termed a finite element.

Characteristics of FEM are as follows:

It does not give an exact solution but solves approximately, because structures are modeled as a combination of simple elements and/or loads.

- It is a kind of numerical experiment without experimental devices, models, or instruments. Hence it is economical and time-saving.
- It can solve actual structural problems by using some models, although their shapes and loads are complex. It is even used for non-structural problems.
- It is used for a wide variety of steel, nonferrous materials and complex materials.
- It relies on computer technology for both hardware and software.
- It is applicable as “a black box tool”, even engineers do not have to know the theory, because there are many general purpose FEM programs which are easy to operate.

Hence FEM has merits and demerits.

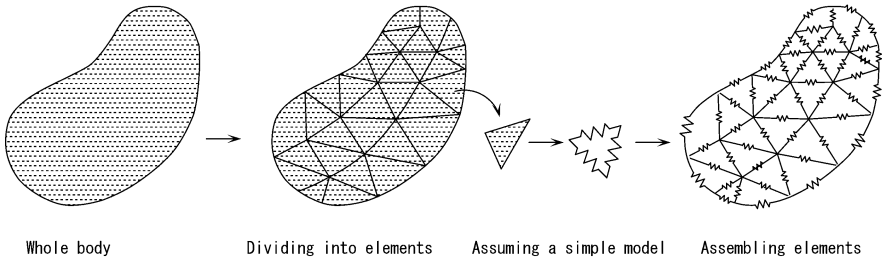


Fig. 7.1.1 Basic concept of FEM

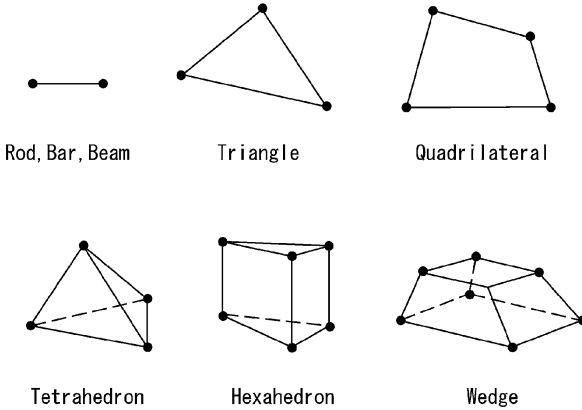


Fig. 7.1.2 Elements of FEM

## 7.2 Fundamentals of FEM

### 7.2.1 Stiffness Matrix [44]

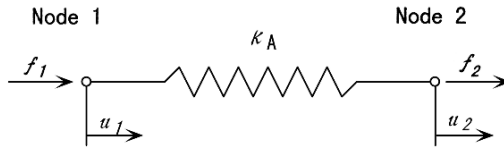
As a simple example, let's take a spring element and a combination of it, as shown in Fig. 7.2.1. When displacements of node 1 and 2 are  $u_1$  and  $u_2$  respectively and the spring constant is  $k_A$  as shown in the figure (a), the elongation of the spring is  $u_2 - u_1$ . Hence

$$\begin{aligned} f_1 &= -k_A(u_2 - u_1) \\ f_2 &= k_A(u_2 - u_1) \end{aligned} \tag{7.2.1}$$

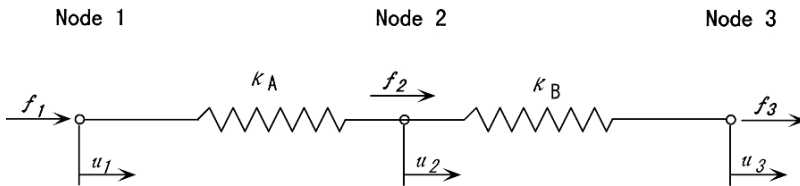
Denoted in matrix form,

$$\begin{Bmatrix} f_1 \\ f_2 \end{Bmatrix} = \begin{bmatrix} k_A & -k_A \\ -k_A & k_A \end{bmatrix} \begin{Bmatrix} u_1 \\ u_2 \end{Bmatrix} \tag{7.2.2}$$

If two springs are connected as shown in Fig. 7.2.1(b), the elongations of spring A and B are  $u_2 - u_1$  and  $u_3 - u_2$  respectively. Hence,



(a) Spring element



(b) Combination of two springs

Fig. 7.2.1 Spring structure

$$\begin{aligned}
 f_1 &= -k_A(u_2 - u_1) \\
 f_2 &= k_A(u_2 - u_1) - k_B(u_3 - u_2) \\
 f_3 &= k_B(u_3 - u_2)
 \end{aligned}
 \tag{7.2.3}$$

Then,

$$\begin{Bmatrix} f_1 \\ f_2 \\ f_3 \end{Bmatrix} = \begin{bmatrix} k_A & -k_A & 0 \\ -k_A & k_A + k_B & -k_B \\ 0 & -k_B & k_B \end{bmatrix} \begin{Bmatrix} u_1 \\ u_2 \\ u_3 \end{Bmatrix}
 \tag{7.2.4}$$

This equation, the load-displacement relation, can be expressed as follows:

$$\{f\} = [K]\{u\}
 \tag{7.2.5}$$

in which  $\{f\}$  and  $\{u\}$  are vectors of nodal loads and nodal displacements respectively and  $[K]$  is termed the “stiffness matrix” of the structure. Equation (7.2.5) is also termed “stiffness equation”.

When comparing (7.2.2) and (7.2.4) it is clear that the combined stiffness matrix is the sum of each stiffness matrix, considering the order of the nodal points. This is the same principle as with other elements, i.e., the overall stiffness matrix can be obtained only by the sum of each element.

When the structure is supported at node 1 and a force  $P$  acts at node 3, as in Fig. 7.2.1(b),  $u_1 = 0$ ,  $f_3 = P$ ,  $f_1 = -P$ . The unknown values are then  $f_2$ ,  $u_2$ ,  $u_3$ . Hence they can be solved by Eq. (7.2.4). Therefore FEM will first assemble the whole stiffness matrix from the elements and then solve the simultaneous equations with respect to the given loads and displacements at the nodes.

## 7.2.2 Plane Stress [43]

A ship's structure consists mainly of thin plate structures and it is assumed to be flat locally, although there are curved shell plates. Therefore we now examine the in-plane deformation of a plate element in the case of linear stress analysis in plane stress condition. A triangular element of constant thickness  $t$  is used for its versatility or simplicity, as shown in Fig. 7.2.2. The displacements and forces are represented by three nodes, as shown in the figure:

$$\{f\} = \begin{Bmatrix} f_{x1} \\ f_{y1} \\ f_{x2} \\ f_{y2} \\ f_{x3} \\ f_{y3} \end{Bmatrix} \quad \{u\} = \begin{Bmatrix} u_1 \\ v_1 \\ u_2 \\ v_2 \\ u_3 \\ v_3 \end{Bmatrix} \quad (7.2.6)$$

We choose a polynomial to describe the internal displacements in the triangle, and represent each of these displacement components by a linear polynomial in the  $x$ - and  $y$ -direction. This means that the strain in the element is constant in  $x$  and  $y$ .

$$\begin{aligned} u &= c_1 + c_2x + c_3y \\ v &= c_4 + c_5x + c_6y \end{aligned} \quad (7.2.7)$$

Since there are 6 degrees of freedom as shown in Fig. 7.2.2, the coefficients  $c_1 \sim c_6$  can be represented by  $u_1, v_1, u_2, v_2, u_3, v_3$ .

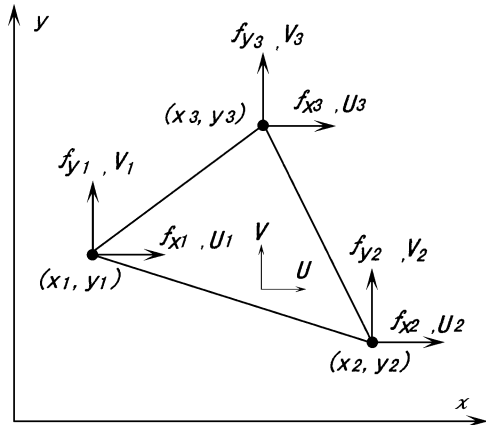


Fig. 7.2.2 Linear triangle element

$$\{u\} = \begin{bmatrix} 1 & x_1 & y_1 & 0 & 0 & 0 \\ 0 & 0 & 0 & 1 & x_1 & y_1 \\ 1 & x_2 & y_2 & 0 & 0 & 0 \\ 0 & 0 & 0 & 1 & x_2 & y_2 \\ 1 & x_3 & y_3 & 0 & 0 & 0 \\ 0 & 0 & 0 & 1 & x_3 & y_3 \end{bmatrix} \begin{Bmatrix} c_1 \\ c_2 \\ c_3 \\ c_4 \\ c_5 \\ c_6 \end{Bmatrix} \equiv [F]\{c\} \tag{7.2.8}$$

On the other hand

$$\epsilon_x = \frac{\partial u}{\partial x}, \quad \epsilon_y = \frac{\partial v}{\partial y}, \quad \gamma_{xy} = \frac{\partial u}{\partial y} + \frac{\partial v}{\partial x} \tag{7.2.9}$$

Then, strain vector  $\{\epsilon\}$  is

$$\begin{Bmatrix} \epsilon_x \\ \epsilon_y \\ \gamma_{xy} \end{Bmatrix} = \begin{bmatrix} 0 & 1 & 0 & 0 & 0 & 0 \\ 0 & 0 & 0 & 0 & 0 & 1 \\ 0 & 0 & 1 & 0 & 1 & 0 \end{bmatrix} \begin{Bmatrix} c_1 \\ c_2 \\ c_3 \\ c_4 \\ c_5 \\ c_6 \end{Bmatrix} \equiv [S]\{c\} \tag{7.2.10}$$

Therefore

$$\{\epsilon\} = [S]\{c\} = [S][F^{-1}]\{u\} \equiv [B]\{u\} \tag{7.2.11}$$

Matrix  $[B]$  can be calculated in the following equation;

$$[B] = \frac{1}{2A} \begin{bmatrix} y_2 - y_3 & 0 & y_3 - y_1 & 0 & y_1 - y_2 & 0 \\ 0 & x_3 - x_2 & 0 & x_1 - x_3 & 0 & x_2 - x_1 \\ x_3 - x_2 & y_2 - y_3 & x_1 - x_3 & y_3 - y_1 & x_2 - x_1 & y_1 - y_2 \end{bmatrix} \tag{7.2.12}$$

$[B]$ : strain coefficient matrix  
 A: area of a triangular element

$[B]$  is defined only by geometric characters of the element.

On the other hand, the stress–strain relationship is shown in the following equation for the plane stress condition.

$$\{\sigma\} = [D]\{\epsilon\}$$

$$[D] = \frac{E}{1 - \nu^2} \begin{bmatrix} 1 & \nu & 0 \\ \nu & 1 & 0 \\ 0 & 0 & (1 - \nu)/2 \end{bmatrix} \tag{7.2.13}$$

$[D]$ : elasticity matrix  
 E: Young’s modulus  
 ν: Poisson’s ratio  
 $\{\sigma\}$ : stress vector

Matrix  $[D]$  is defined only by material properties of the element.



Next, let's consider the equilibrium of energy in an element. The external work for an element is the sum of the displacement multiplied by the force at each node;

$$E_e = \{u\}^T \{f\} \quad (7.2.14)$$

The internal work for an element is the sum of the strain multiplied by the stress in an element. Using Eqs. (7.2.11) and (7.2.13),

$$U_i = \int \{\varepsilon\}^T \{\sigma\} dV = \int \int \{\varepsilon\}^T \{\sigma\} t dx dy = \int \int ([B]\{u\})^T [D][B]\{u\} t dx dy \quad (7.2.15)$$

$V$ : Volume of an element

$t$ : plate thickness of an element

Using the principle of the virtual work, i.e. the external work equals the internal work in the element, i.e.  $U_e = U_i$ ,

$$\{u\}^T \{f\} = \int \int ([B]\{u\})^T [D][B]\{u\} t dx dy \quad (7.2.16)$$

Then, the stiffness equation for the triangular element is

$$\{f\} = t [B]^T [D][B]\{u\} \int \int dx dy = At [B]^T [D][B]\{u\} \equiv [K]\{u\} \quad (7.2.17)$$

$[K]$ : stiffness matrix

$$= At [B]^T [D][B] \quad (7.2.18)$$

$[B]^T$ : transposed matrix of  $[B]$

When combining many elements, we assemble the overall stiffness matrix from each element and solve the stiffness equation with the given loads and displacements at the nodes. We then can get the displacement of each node, the strain of each grid from Eq. (7.2.11), and the stress from Eq. (7.2.13), one by one.

### 7.3 Procedure of FEM

The procedure of displacement and stress calculations by computer, in the case of requiring linear solutions, is generally as follows:

- (1) calculate  $[B]$  matrix using the geometry of an element, and to calculate  $[D]$  matrix using material properties.
- (2) calculate matrix  $[K]$  of an element
  - (1) and (2) are repeated for all elements.
- (3) assemble the overall stiffness matrix

- (4) calculate displacements of each node from load and support conditions by solving the stiffness Eq. (7.2.17).
- (5) calculate the strains of each element by (7.2.11)
- (6) calculate the stresses of each element by (7.2.13)
- (7) calculate principal stresses, equivalent stresses, etc.

Figure 7.3.1 shows the process from (1) to (4) and Fig. 7.3.2 shows the program flow of FEM [43].

Figure 7.3.3 also shows the procedure of the FEM analysis. General purpose FEM program MSC/NASTRAN is widely used for linear structural problems and dynamic response. MARC, ANSYS, ABAQUS, etc. are also used, especially for nonlinear fields such as in geometric or material problems. User interfaces like pre-processor or post-processor have become more “user friendly.” I-DEAS, PATRAN, etc. are useful to create and evaluate large-scale 3-dimensional models.

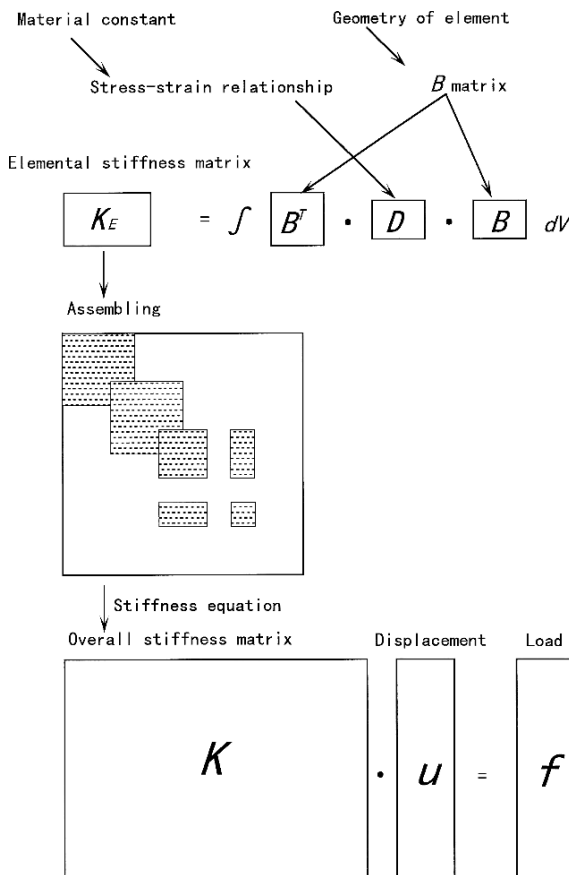


Fig. 7.3.1 Procedure to get stiffness equation

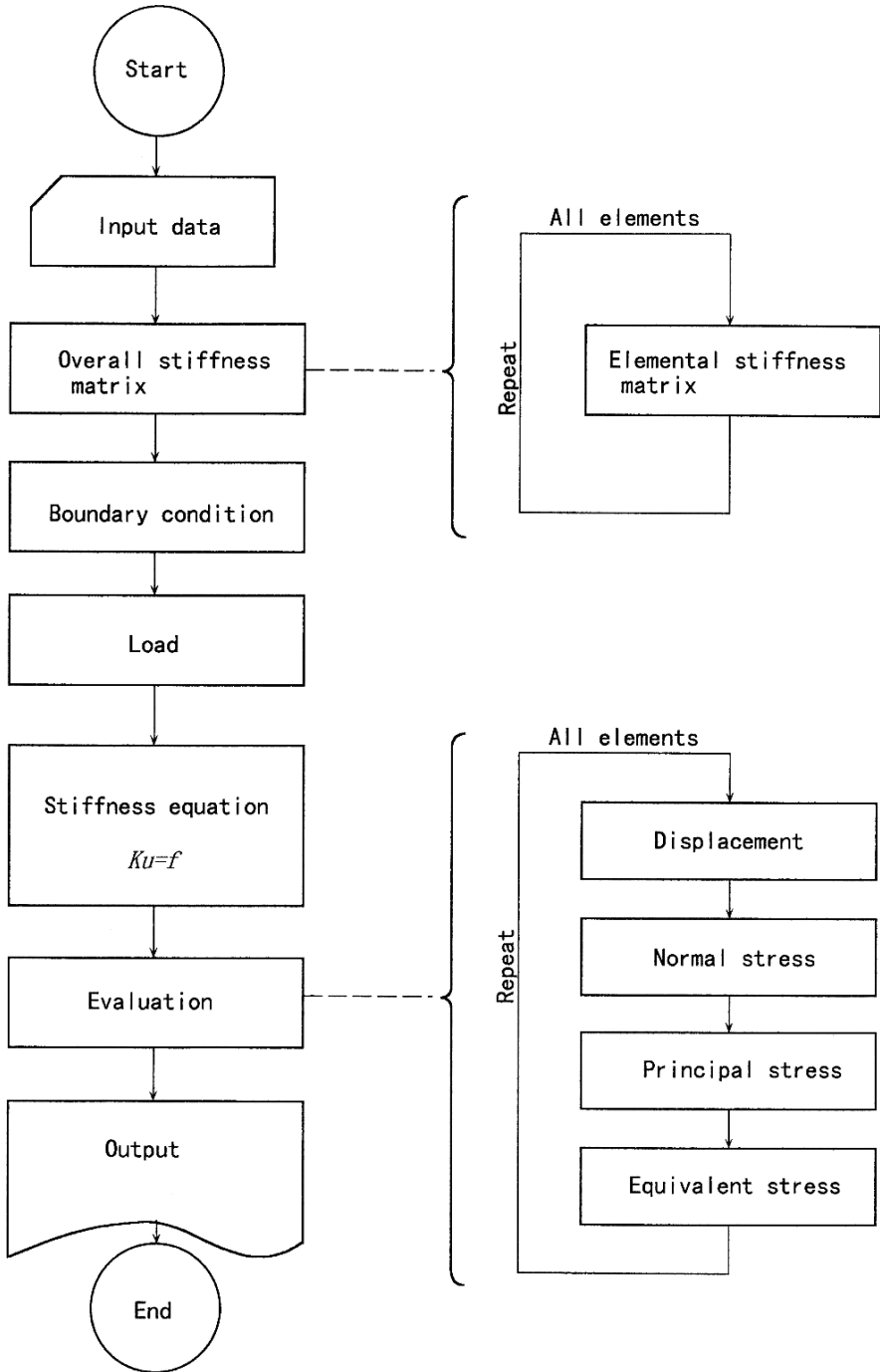
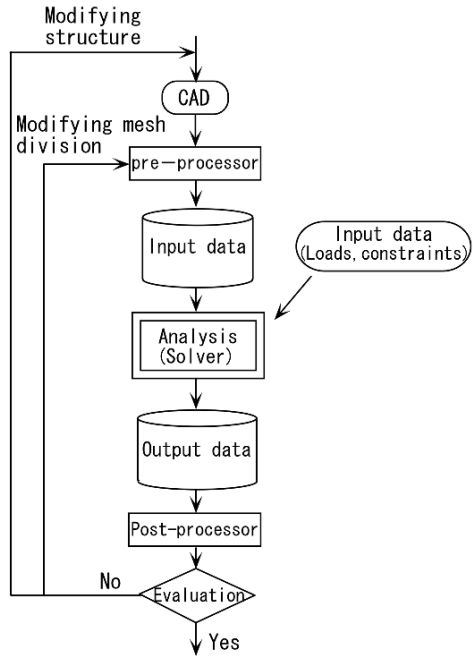


Fig. 7.3.2 Sequence of FEM Calculation

**Fig. 7.3.3** Procedure of FEM analysis

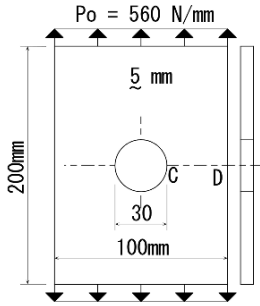


## 7.4 Application of FEM

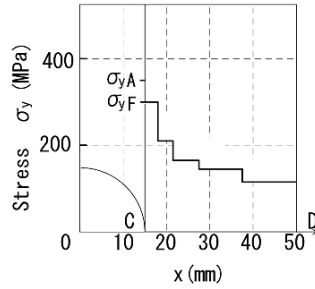
As mentioned earlier, FEM analysis is a numerical approximation method, hence some errors will inevitably be included. We have to reduce these to an acceptable level by making the model intrinsically adequate, in accordance with the theory of material strength.

### 7.4.1 Mesh Division

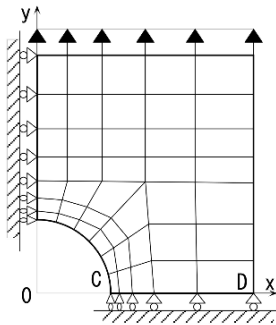
As shown by the basic theory, the stress and strain in an element are constant, hence the mesh size has to be sufficiently small, where the stress distribution is increasing sharply. Figure 7.4.1(a) shows an example of stress concentration around a hole for which the exact solution is given by the theory of elasticity, and this will allow us to assess the accuracy. Figure 7.4.1(b) is an FEM model using the MSC/NASTRAN linear program, and (c) is the calculation result [45]. The maximum theoretical nominal stress in this case is  $\sigma_{yA} = 378 \text{ MPa}$ , however, the FEM calculation result was  $\sigma_{yF} = 294 \text{ MPa}$ , which includes a 22% error, hence a finer mesh is desirable near the hole. Even better is to provide a bar element around the circular edge as a dummy element to evaluate the stress.



(a) Plate includes a hole



(c) Calculation results



(b) FEM model

**Fig. 7.4.1** Stress distribution around a hole

The aspect ratio of a rectangular element and the shape of a triangular element are important. An unusual slender form is not desirable.

In addition it is important to avoid

- a connection with great differences in rigidity
- a connection of a plate element and a beam, bar or rigid element
- a connection of a large element and a very small element

### 7.4.2 Loading and Supporting Condition

The loading condition should be carefully determined to correspond with the aim of the analysis, FEM model, and evaluation method. The balance of the accuracy between input load and output stress should be considered; usually the load is quite rough and the mesh division is more detailed. It is also necessary to know the characteristics of the applied load – static, dynamic, repeated, or random.

The use of symmetrical conditions allow us to reduce computer calculation time, as shown in Fig. 7.4.1(b), which models only 1/4 of the whole model, considering appropriate support conditions.

In the case where we apply symmetrical boundary conditions, it is very important to keep in mind that boundary conditions should be determined based on the assumed deformation mode. Static stress analysis is quite simple, but we sometimes encounter careless mistakes in eigenvalue analysis such as buckling and vibration analysis.

Figure 7.4.2 is an example of buckling analysis of a simply supported panel with aspect ratio of 1:2. The resulting buckling mode must be of two half waves as shown in the figure. In the figure, the solid line circle means buckling deformation toward the fore side perpendicular to the panel, and the dotted line circle means buckling deformation toward the opposite (aft) side.

If we model this problem with a 1/4 model taking into account symmetry, and apply symmetrical conditions at the boundary, the resulting buckling mode becomes three half waves as shown in Fig. 7.4.3. That is, the calculated buckling stress is mistakenly higher than the actual buckling stress. This example tells us that we must set boundary conditions taking into account the deformation mode carefully.

In zooming calculations, the range of the FEM model and the loading method should be carefully considered.

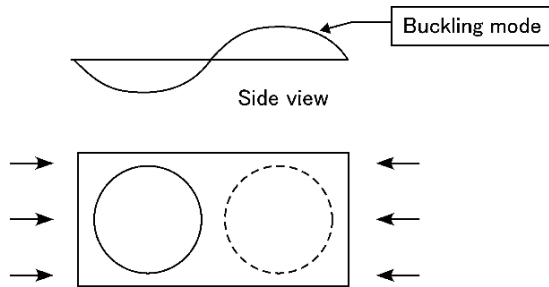


Fig. 7.4.2 Buckling mode of a panel of aspect ratio 1:2

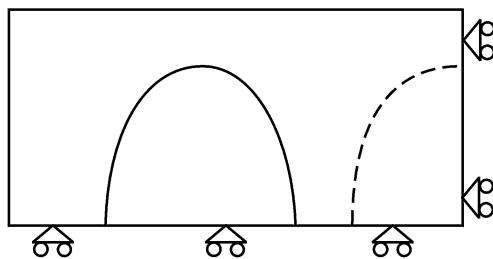


Fig. 7.4.3 Mistaken boundary conditions in buckling analysis

### 7.4.3 Degrees of Freedom

In actual application of finite element analysis, it is important to be conscious of degrees of freedom of each element.

- a. plane stress (membrane) element, plane strain element      2       $u, v$
- b. plate bending element      3       $w, \theta_x, \theta_y$
- c. shell element (combination of a and b)      5       $u, v, w, \theta_x, \theta_y$
- d. rod element (bar element)      1       $u$
- e. beam element      6       $u, v, w, \theta_x, \theta_y, \theta_z$
- f. solid element      3       $u, v, w$

When membrane elements are assembled into three dimensional object, each joint acquires 3 degrees of freedom ( $u, v, w$ ). In this case, there is no rigidity in the out-of-plane direction, and the calculation becomes unstable. Therefore, the analysis system usually adds temporary support to the unstable direction automatically. Similarly, shell elements have 6 degrees of freedom when three-dimensionally assembled.

This knowledge of degrees of freedom helps us to avoid mistakes in connections between different kinds of elements. Figure 7.4.4(a) is a mistake. Since membrane or shell elements do not have degrees of freedom of rotation around the z-axis, the

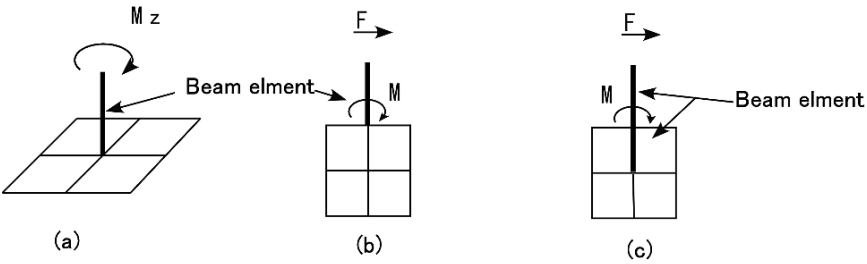


Fig. 7.4.4 Load transfer between beam and membrane elements

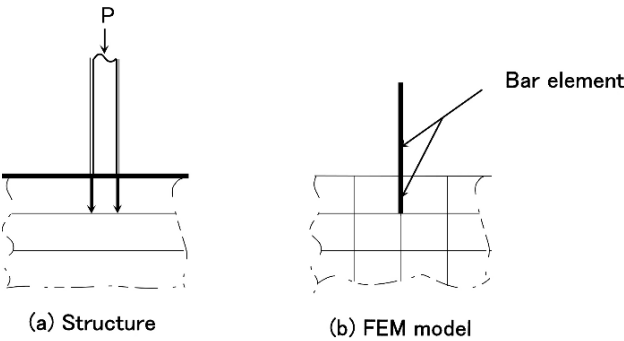


Fig. 7.4.5 FEM modeling of heel of pillar

torsional moment of the beam element cannot be transferred to the plate elements. Figure 7.4.4(b) is also a mistake. In this case, if we want to transfer the load to the plate elements, we should insert the beam elements into the plate elements as shown in Fig. 7.4.4(c).

It is appropriate to model typical pillars in engine room construction by bar elements. In this case, to avoid extraordinary high stress at the connection between the pillar and the base structure, we should insert the pillar bar elements into the base structure as shown in Fig. 7.4.5. Such insertion of beam or bar elements is quite a simplified method in the computer model, but as long as we do not evaluate the stress just at this location, it is a useful solution to transfer load correctly.



# **Part II**

## **Theory**

# Chapter 1

## Design of Beams

### 1.1 Effective Breadth of Attached Plates

Main hull structures such as decks, shells, and bulkheads are composed of stiffened panels, which include plates and stiffeners, and these structures endure the lateral forces such as water pressure as well as in-plane loads. When the forces are imposed, the stress distribution in the plates and the stiffeners is complex as shown in Fig. 1.1.1. The longitudinal stress in the attached plate will be a maximum at the connection line to the stiffener and become smaller gradually beyond this line. Considering the strength, the stiffened panel will be assumed to be a collection of beams which include some parts of the attached plate. The breadth of this plate is called the effective breadth or effective width; the former is normally used with reference to the effective area of the attached plate of a stiffener under a bending moment, and the latter is that for a stiffener under axial load.

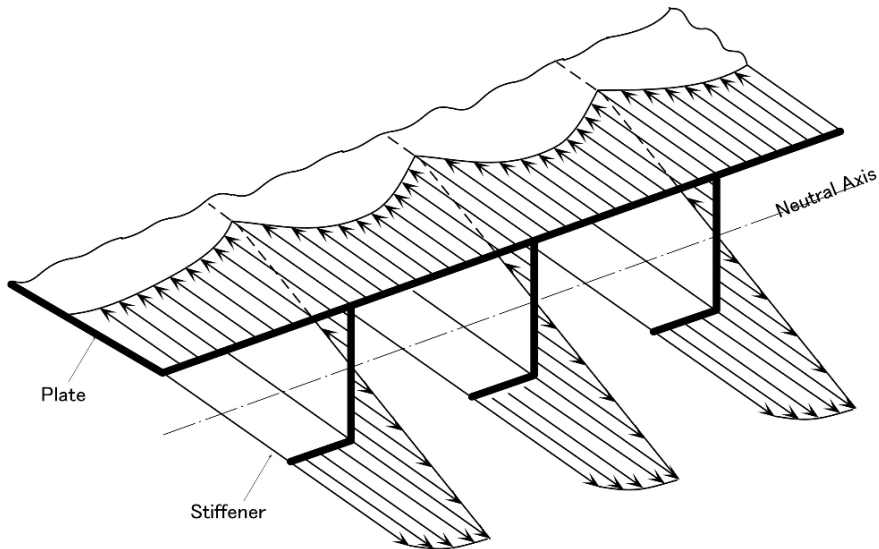


Fig. 1.1.1 Bending stress distribution of stiffened panel

### 1.1.1 Bending in Elastic Conditions

The effective breadth is represented as follows:

$$B_e = \frac{2}{\sigma_{\max}} \int_0^{B/2} \sigma_x dy \tag{1.1.1}$$

- $B_e$ : effective breadth
- $\sigma_{\max}$ : maximum stress at connection line of a stiffener
- $B$ : distance between stiffeners
- $\sigma_x$ : stress of longitudinal direction along with  $B$

Though this value depends on loading conditions, structural dimensions, and end connections, it is related mainly to the ratio  $l$  (length between two points where the bending moment is zero) and  $B$ . If it is uniformly loaded,  $B_e/B$  is given in Fig. 1.1.2 [1]. If  $l/B$  becomes large,  $B_e/B$  becomes 1, i.e. full width, and if  $l/B$  becomes small,  $B_e/B$  becomes smaller than 1. NK rules simply state the effective breadth as follow:

$$\begin{aligned} B_e &= 0.2 \times (\text{stiffener span}) \\ B_e &= B \end{aligned} \tag{1.1.2}$$

whichever is lesser

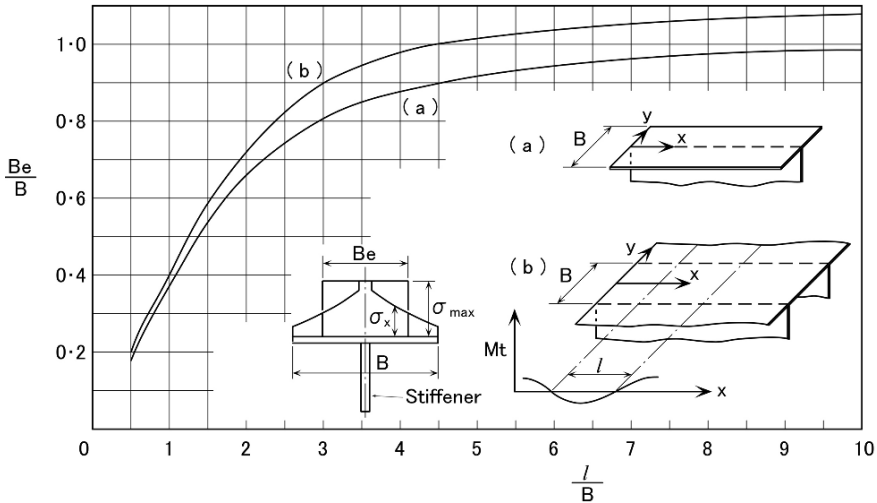


Fig. 1.1.2 Effective breadth of stiffened plate

### 1.1.2 Effective Width After Plate Buckling

If the stiffened panel buckles by axial forces, the middle part between the stiffeners will deform and the resistance to lateral loads will decrease. Considering the

ultimate strength of the stiffener with effective width of the attached plate, the decrease of effective width should be investigated.

After the buckling, the plate near the stiffeners still offers some resistance as shown in Fig. 1.1.3 and the effective width after buckling  $b_e$  is defined in the figure. Faulkner shows the ultimate strength of a simply supported panel as follows [2]:

$$\frac{\sigma_u}{\sigma_y} = \frac{2}{\beta} - \frac{1}{\beta^2} \tag{1.1.3}$$

$\sigma_u$ : ultimate strength

$\sigma_y$ : yield stress

$$\beta = \frac{b}{t} \sqrt{\frac{\sigma_y}{E}}$$

$t$ : plate thickness

$b$ : plate breadth

$E$ : Young's modulus

Then,

$$\frac{b_e}{b} = \frac{\sigma_u}{\sigma_y} \tag{1.1.4}$$

After buckling

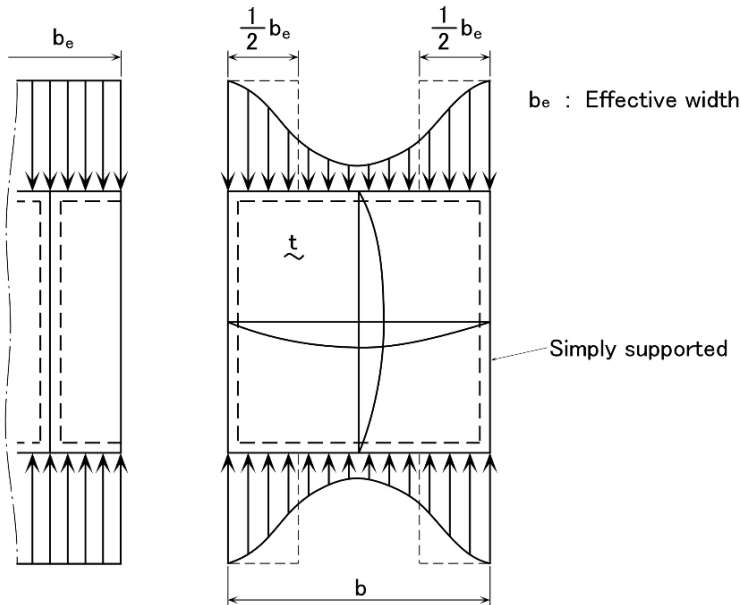


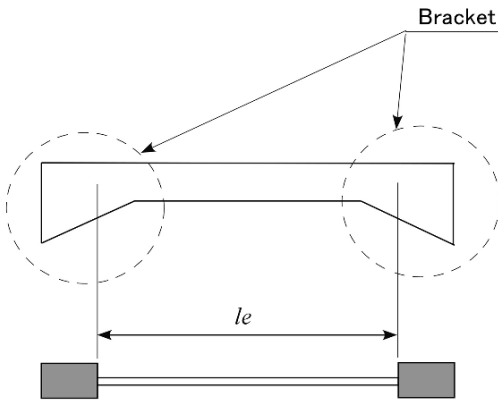
Fig. 1.1.3 Effective width after buckling

## 1.2 Span Point of Beams

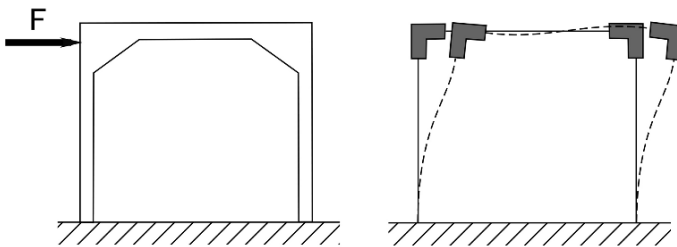
Both ends of a beam are usually connected with brackets or other structures. Hence beam theory is not always applicable even if the cross section of middle part has uniform shape. It is convenient to assume a member to be a uniform section beam, having an equivalent length between two span points, and to assume the outside structures of the span points to be rigid bodies as illustrated in Fig. 1.2.1. The span point depends on structural details and loading conditions.

LR defines simply as follows [3]:

- (1) *For secondary stiffening members such as frames, beams, and stiffeners:* The span point is taken as the point where the depth of the end bracket, measured from the face of the secondary stiffening member, is equal to the depth of the member.
- (2) *For primary support members such as web frames, girders, and stringers:* The distance of span point from the end of the member is taken as,



(a) Definition of span point



(b) Larmen structure with bracket

Fig. 1.2.1 Span point of beam

$$b_e = b_b \left( 1 - \frac{d_w}{d_b} \right) \tag{1.2.1}$$

Figure 1.2.2 illustrates these.

On the other hand, Yamaguchi proposed a formula for bending which was obtained theoretically and experimentally [4] as shown in Fig. 1.2.3.

For straight type end connections

$$\frac{S^b}{b} = \frac{h_0}{h_A} \tag{1.2.2}$$

This equation is the same as Eq. (1.2.1) of LR rule.

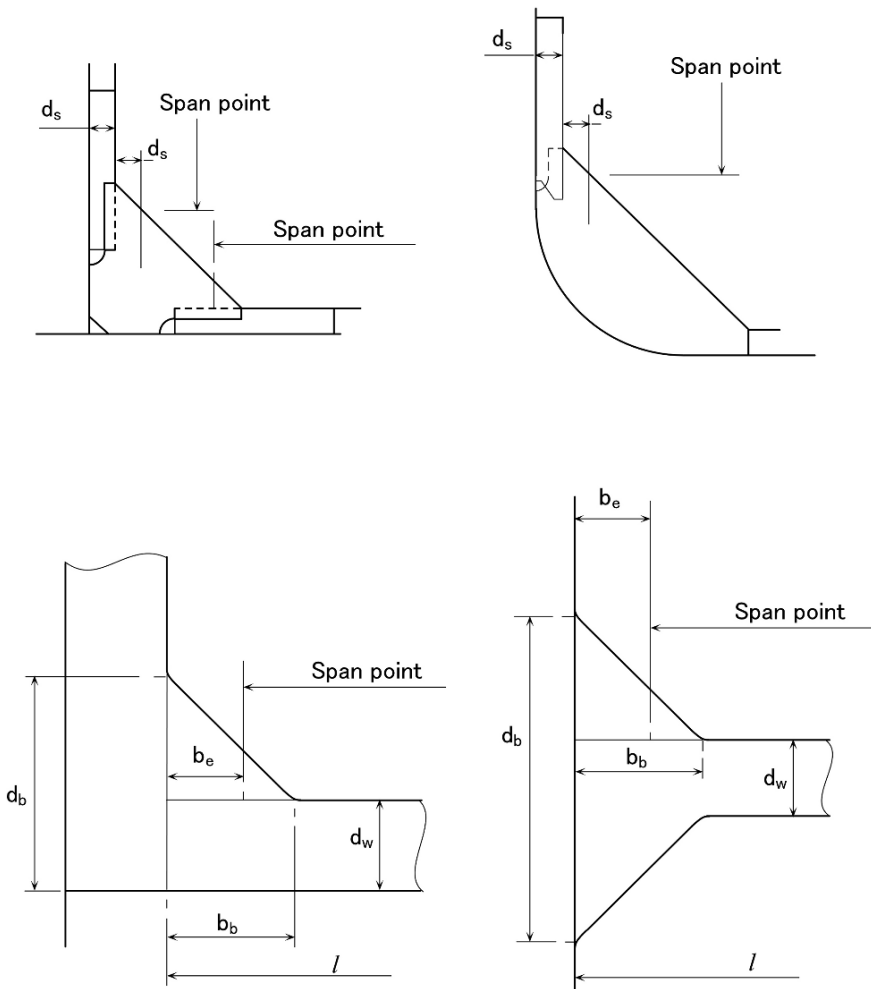


Fig. 1.2.2 Span points

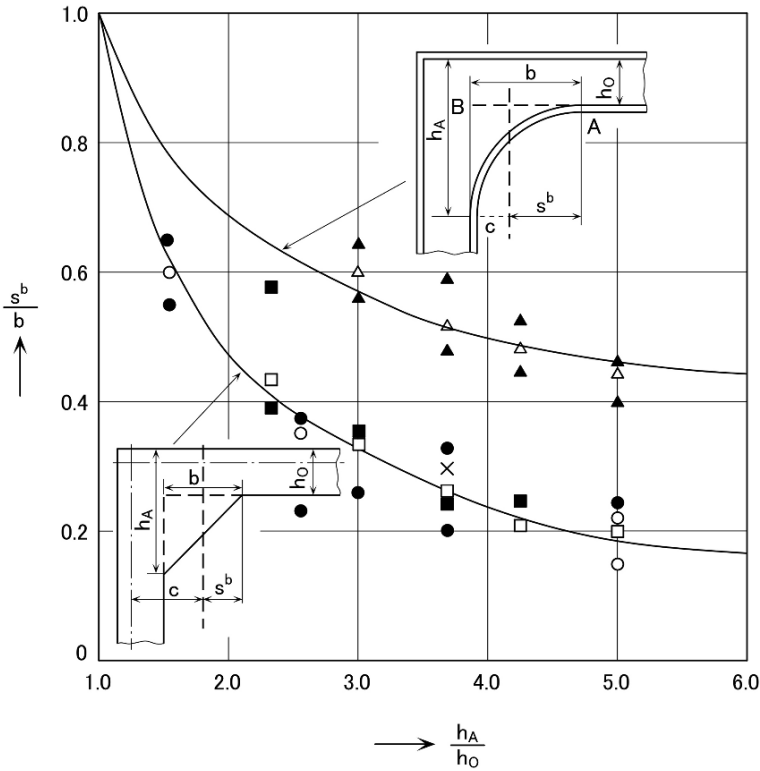


Fig. 1.2.3 Comparison of span point experiment vs. calculation

For arc type end connections

$$\frac{s^b}{b} = 0.276 + \frac{0.724h_0}{0.724h_A + 0.276h_0} \tag{1.2.3}$$

Figure 1.2.4 shows the span point for the load of shearing forces [4].

For straight type end connections

$$\frac{s^b}{b} = \frac{h_0}{h_A} \log \left( 1 + \frac{h_a}{h_0} \right) \tag{1.2.4}$$

For arc type end connections

$$\frac{s^b}{b} = \frac{2h_0/h_a(h_0/h_a + 1)}{\sqrt{(h_0/h_a)^2 + 2h_0/h_a}} \tan^{-1} \sqrt{1 + 2h_0/h_a} - \frac{\pi}{2} \frac{h_0}{h_a} \tag{1.2.5}$$

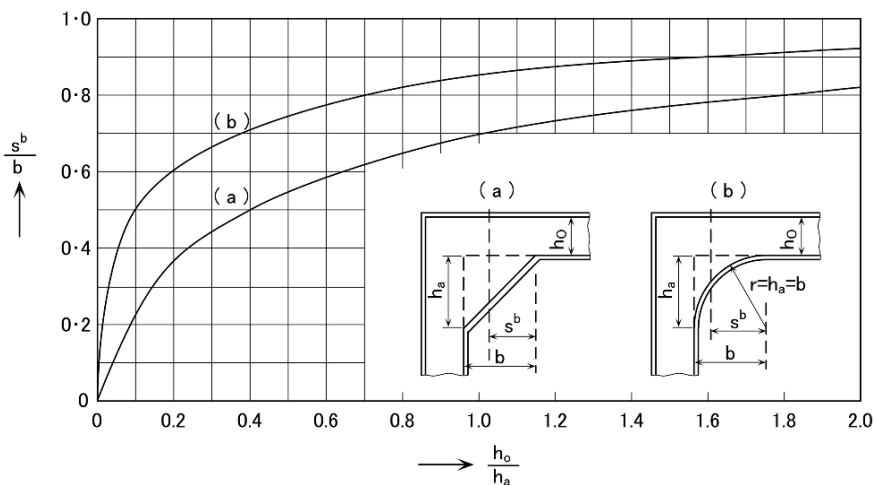


Fig. 1.2.4 Span points for shearing deformation

### 1.3 Design of Cross Section

The shape of cross section of a beam is generally designed as follows:

- 1) decide the beam span between span points, derive the bending moment curve from the loading condition, and decide maximum bending moment  $M_{max}$
- 2) estimate cross sectional shape, and calculate the section modulus  $Z$

$$Z = I/y \tag{1.3.1}$$

$I$ : sectional moment of inertia

$y$ : distance from neutral axis to the extreme tip of a beam

$Z$  has two values of top and bottom.

- 3) calculate the maximum stress

$$\sigma_{max} = \frac{M_{max}}{Z} \tag{1.3.2}$$

- 4) compare  $\sigma_{max}$  with allowable stress  $\sigma_{all}$  or compare required section modulus  $Z_{req}$  to actual section modulus  $Z$

$$Z_{req} = \frac{M_{max}}{\sigma_{all}} \tag{1.3.3}$$

- 5) adjust the sectional shape so as to be  $\sigma_{max} < \sigma_{all}$  or  $Z_{req} < Z$



### 1.3.1 Calculation of Section Modulus

(1) *Balanced section*: A beam having two flanges, which have the same sectional area, is called a balanced girder (Fig. 1.3.1). In this case, if the thickness of the flanges is thinner comparatively, the sectional moment of inertia  $I$  and the section modulus  $Z$  are:

$$\begin{aligned} I &= 2A_f \left( \frac{d}{2} \right)^2 + \frac{td^3}{12} \\ &= \frac{d^2}{2} \left( A_f + \frac{A_w}{6} \right) \end{aligned} \quad (1.3.4)$$

$A_f$ : area of flange  
 $A_w$ : area of web  
 $d$ : depth of web  
 $t$ : thickness of web

$$\begin{aligned} Z &= \frac{I}{d/2} \\ &= d \left( A_f + \frac{A_w}{6} \right) \end{aligned} \quad (1.3.5)$$

$$\text{Hence } A_f = \frac{Z}{d} - \frac{A_w}{6} \quad (1.3.6)$$

Equation (1.3.6) is often represented in classification societies' rules.

(2) *Beam with plate*: Usually a beam has an attached plate and a face plate as shown in Fig. 1.3.2. In this case:

$$e = \left( A_f d + A_w \frac{d}{2} \right) / A = \frac{d}{A} \left( A_f + \frac{A_w}{2} \right) \quad (1.3.7)$$

$e$ : distance from attached plate to neutral axis

$$I_m = A_f d^2 + A_w \left( \frac{d}{2} \right)^2 + \frac{A_w}{12} d^2 = d^2 \left( A_f + \frac{A_w}{3} \right) \quad (1.3.8)$$

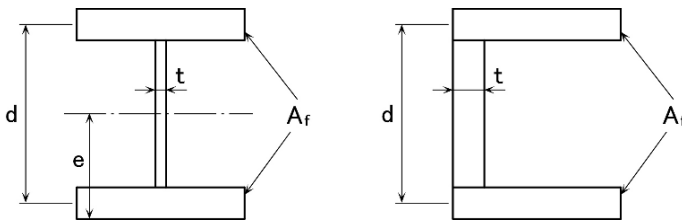
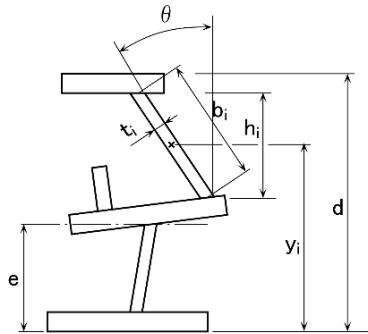
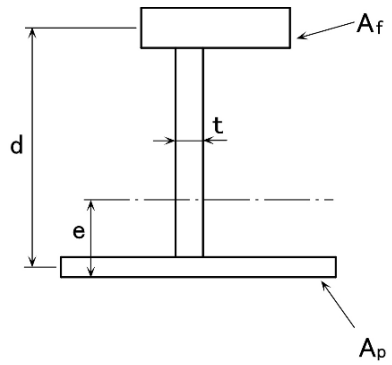


Fig. 1.3.1 Balanced girder

Fig. 1.3.2 T section



Member	Thickness	Breadth	Area	Lever	1st moment	I(e=0)	I <sub>o</sub>
Plate i	t <sub>i</sub>	b <sub>i</sub>	A <sub>i</sub> =t <sub>i</sub> b <sub>i</sub>	y <sub>i</sub>	A <sub>i</sub> y <sub>i</sub>	I <sub>i</sub> =A <sub>i</sub> y <sub>i</sub> <sup>2</sup>	I <sub>o</sub> = $\frac{t_i h_i^3}{12} \cos \theta$
			$\Sigma A_i$		$\Sigma A_i y_i$	$\Sigma I_i$	$\Sigma I_{o_i}$

$$e = \frac{\Sigma A_i y_i}{\Sigma A_i} = e^2 \Sigma A_i$$

$$I = (\Sigma I_i + \Sigma I_{o_i}) - e \Sigma A_i y_i$$

$$\left. \begin{aligned} Z_1 &= I/e \\ Z_2 &= I/(d-e) \end{aligned} \right\}$$

d : Depth

Fig. 1.3.3 Built-up section

$I_m$ : sectional moment of inertia around the axis of  $e = 0$

Hence

$$I = I_m - e^2 A = d^2 \left\{ A_f + \frac{A_w}{3} - \frac{(A_w + 2A_f)^2}{4A} \right\} \quad (1.3.9)$$

$A$ : total sectional area

If the area of an attached plate is comparatively greater than that of face plate and web plate,  $e = 0$ . Then

$$I = d^2 \left( A_f + \frac{A_w}{3} \right) \quad (1.3.10)$$

$$Z_f = d \left( A_f + \frac{A_w}{3} \right) \quad (1.3.11)$$

$Z_f$ : section modulus on face plate

(3) *built-up section*: The section modulus of a beam built up by some plates is calculated as in Fig. 1.3.3.

## 1.4 Bending Moment

In designing a hull structure, many structural members can be regarded as beams, which are mainly subjected to lateral load. For instance, an entire hull structure is often considered as a beam, since it is deflected by the action of the vertical forces due to buoyancy and gravity. Another example of a beam is the shell plate. This may seem curious, but when a shell plate is sliced into plates of unit width, then these narrow band plates can be regarded as a group of beams under lateral pressure.

The strength of a structural member is usually investigated by modeling it as a beam, with fixed ends, subjected to a uniform load as shown in Fig. 1.4.1. Consequently, the maximum bending moment of the beam occurs at both ends and its magnitude can be calculated as follows:

$$M = \frac{wl^2}{12} = \frac{Wl}{12} \quad (1.4.1)$$

where

$M$ : maximum bending moment

$w$ : uniform load per unit length

$W$ : total load  $W = wl$

$l$ : beam span

On the other hand, if a concentrated load  $W$  is applied to a beam having both ends fixed as illustrated in Fig. 1.4.2, the maximum bending moment is generated at a fixed end and it is

**Fig. 1.4.1** Fixed beam subjected to uniform load

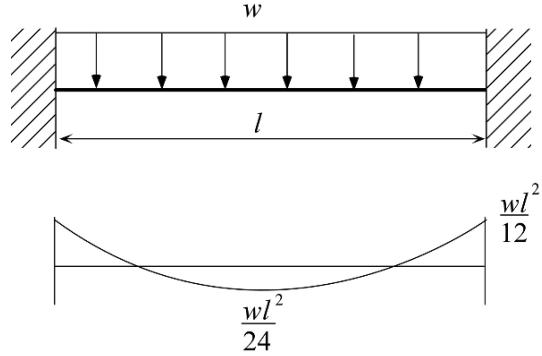
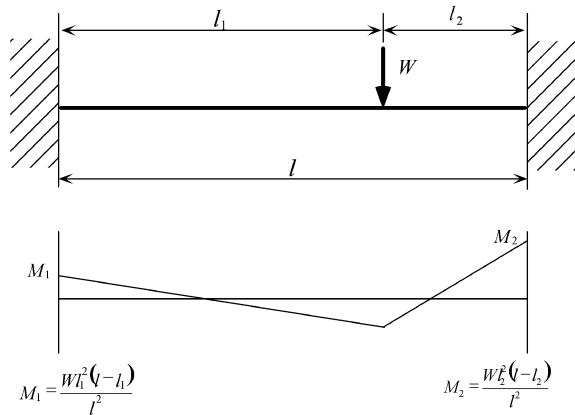


**Fig. 1.4.2** Fixed beam subjected to concentrated load



$$M = \frac{Wl_1^2(l-l_1)}{l^2} \tag{1.4.2}$$

where  $l_1$ : greater distance between loaded position and beam end

Since the maximum bending moment varies according to the position of the concentrated load applied, we have to fully understand the position where it creates the ultimate maximum bending moment. In order to investigate this position of load giving the maximum value, the first derivative of Eq. (1.4.2) is taken and then the following equation is obtained:

$$\frac{dM}{dl_1} = \frac{W}{l^2} (2ll_1 - 3l_1^2) = 0$$

$$\therefore l_1 = 0 \text{ or } \frac{2}{3}l \tag{1.4.3}$$

$$M_{ultimate} = \frac{4}{27}Wl \tag{1.4.4}$$

Therefore, the maximum moment is produced where the load is applied to the position of  $l_1 = 2l/3$ . This load creates a maximum bending moment of  $4Wl/27$ , which is about  $4/27 \times 8 = 1.18$  times larger than when the load is applied to the center

of the span. We are likely to misunderstand that the maximum bending moment be induced by a load applied to the mid-point of the beam span. But the above calculation shows this understanding is not correct. In addition, comparing this value with Eq. (1.4.1), the maximum bending moment of a concentrated load is about  $4/27 \times 12 = 1.8$  times greater than that of uniform load.

In contrast to the above discussion, the tendency is sometimes opposite when the strength of beam is considered from the view point of plastic design. In the case of a beam rigidly fixed at both ends subjected to a concentrated load at the center of span, the load causing the collapse is calculated as  $8M_p/l$ , where  $M_p$  is the plastic moment of the cross section of a beam. On the contrary, the beam will collapse from a load of  $9M_p/l$ , when the load acts at a position  $l/3$  from an end. That means the beam can carry greater load in the latter case. This example shows that the bending moment will differ due to a difference in the design philosophy applied.

## 1.5 Easy Solution of Statically Indeterminate Beams

A straight beam structure, which consists of at least 2 beam elements supported by more than 3 points, is usually called as “continuous beam”. A structure as shown in Fig. 1.5.1 is an example of a continuous beam. The bending moment and shearing force distributions of continuous beams cannot be determined generally but only by the equation of static equilibrium.

For example, in the case of Fig. 1.5.1, the number of equations at equilibrium is two, although the number of unknown reaction forces is four ( $R_1, R_2, R_3, M$ ) as shown below. Therefore, the reaction forces cannot be determined, since the number of reactions exceeds the number of equations.

$$R_1 + R_2 + R_3 = P \quad (1.5.1)$$

$$R_2 \cdot l - P \cdot \frac{3}{2}l + R_3 \cdot 2l = M \quad (1.5.2)$$

If the unknown reactions cannot be determined simply by the equations of static equilibrium, the reactions of the beam are said to be statically indeterminate. In order to determine the unknown reaction forces, not only the static equilibrium but also the continuity of deflection and slope of the beam must be taken into account. Several kinds of solutions are proposed, however the method explained below is the most simple and practical. In this method, a continuous beam is regarded as a set of

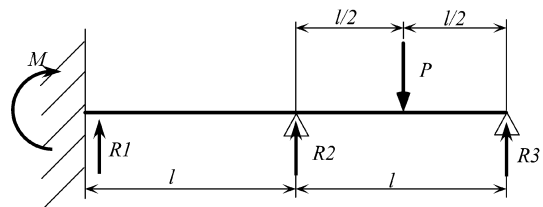


Fig. 1.5.1 Sample of continuous beam

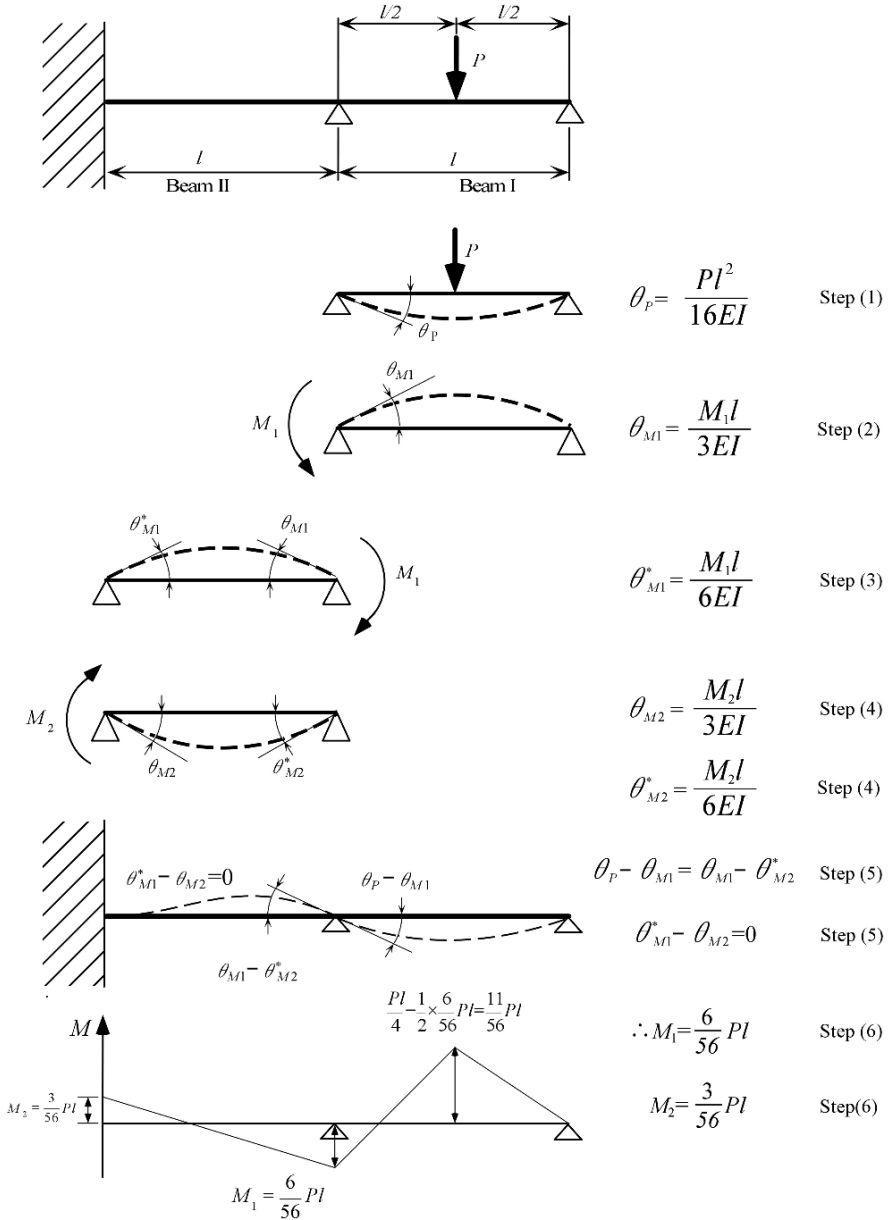


Fig. 1.5.2 Simplified method to solve continuous beam

simply supported beam elements. Let's make use of the example in Fig. 1.5.2 and divide the continuous beam into two simply supported beams (Beam I and Beam II) as shown in the upper figure in Fig. 1.5.2. The solution procedure follows the Steps (1)–(7):

- (1) Force  $P$  causes a deflection of its slope  $\theta_p$  in Beam I in the place of its connection to Beam II.
- (2) Neglecting Beam II generates the connecting moment  $M_1$  at the end of Beam I and it creates slope  $\theta_{M1}$  at the left end of Beam I.
- (3) The same connecting moment  $M_1$  creates deflection in Beam II and its slope is  $\theta_{M1}$  at the right end and  $\theta_{M1}^*$  at the left end.
- (4) Neglecting fixed end of Beam II results in the end moment  $M_2$  at the left end and the moment  $M_2$  causes deflection with a slope  $\theta_{M2}$  at the left end and slope  $\theta_{M2}^*$  at right end.
- (5) Considering that the slope must be continuous at the connection of Beam I and Beam II, and that the slope must be zero at the left end of Beam II, then we obtain the equations of Step (5) as shown in the figure.
- (6) By solving the above equations, the unknown moments  $M_1, M_2$  can be expressed in the form of Step (6).
- (7) Consequently, the distribution of bending moment in Beam I and II can be illustrated in the lowest figure in Fig. 1.5.2.

## 1.6 Boundary Condition

In the design of hull structures, beams used to be designed to support uniform load, fixed at both ends. This is practical and correct in many cases but some times this assumption is not adequate during detailed analysis.

One example is the longitudinal stiffener on longitudinal bulkheads [5]. It experiences not only the bending moment caused by lateral water pressure but also axial tensile or compressive forces due to hull girder bending.

However, except in case which are near the top and bottom of the longitudinal bulkhead where the axial force is large, the axial force can be neglected and the longitudinal stiffener on longitudinal bulkhead can be designed considering only the bending moment caused by lateral water pressure.

The longitudinal stiffener on a longitudinal bulkhead is supported by transverse webs of equal span and can be assumed to be a continuous beam with equal spans and uniform load. In this case as shown in Fig. 1.6.1 it can be replaced by one of beam member with uniform load and both ends fixed. However at the transverse bulkhead, the water pressure comes not always from one side so the assumption of one span with uniform load and of both-ends fixed can not be applied. In this case it is reasonable to assume both ends fixed with a support at the center. The load depends on the tank condition on both sides of the transverse bulkhead as shown in Fig. 1.6.2. The bending moments and the reactions at the supporting points are given by the following equations.

$$M_1 = -\frac{(5w_1 - w_2)}{48}l^2 \equiv -K_1 \frac{w_1 l^2}{12} \quad (1.6.1)$$

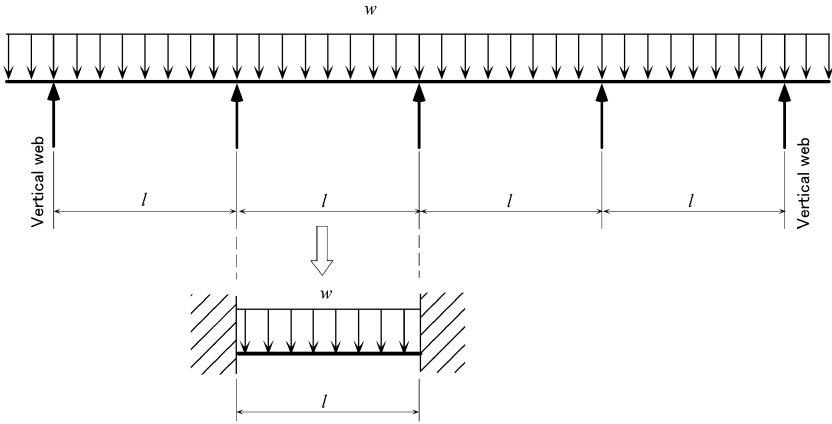


Fig. 1.6.1 Continuous beam with uniform load

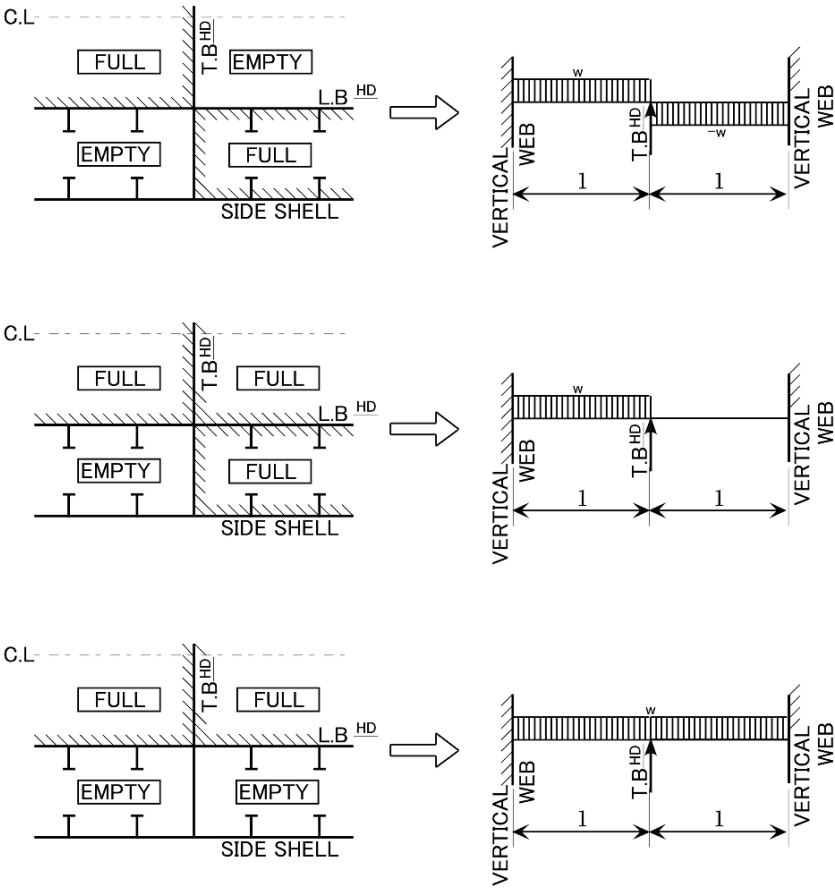


Fig. 1.6.2 Change of load by loading in tanks



$$M_2 = -\frac{(w_1 + w_2)}{24}l^2 \equiv -K_2 \frac{w_1 l^2}{12} \quad (1.6.2)$$

$$M_3 = \frac{(w_1 - 5w_2)}{48}l^2 \equiv K_3 \frac{w_1 l^2}{12} \quad (1.6.3)$$

$$R_1 = \frac{(9w_1 - w_2)}{16}l \equiv k_1 \frac{w_1 l}{2} \quad (1.6.4)$$

$$R_2 = \frac{(w_1 - w_2)}{2}l \equiv k_2 w_1 l \quad (1.6.5)$$

$$R_3 = \frac{(9w_1 - w_2)}{16}l \equiv k_3 \frac{w_1 l}{2} \quad (1.6.6)$$

With the change of  $w_2/w_1$  from  $-1$  to  $+1$ ,  $K_1, K_2, K_3, k_1, k_2$  and  $k_3$  will change as shown in Fig. 1.6.3.  $|K_2|$  is always less than 1.0.  $|K_1|$  and  $|K_3|$  are bigger than 1.0 in some cases. They reach 1.5 in the case where  $w_2/w_1$  is  $-1$ .

From the above consideration it is clear that the bending moment on the longitudinal stiffener on the longitudinal bulkhead at the transverse bulkhead position is always less than  $w_1 l^2/12$  but reaches 1.5 times at the transverse webs adjacent to the transverse bulkhead.

In addition to the bending moment, the reaction at the transverse webs adjacent to the transverse bulkhead reaches values greater than expected.  $|k_2|$  is always less than 1.0 but  $|k_1|$  and  $|k_3|$  are 1.25 when  $w_2/w_1 = -1$ . Accordingly the transverse webs adjacent to the transverse bulkhead have to support  $1.125 w_1 l$  of load from the longitudinal stiffener on the longitudinal bulkhead. The load, bending moment and shearing force in the above case are shown in Fig. 1.6.4.

From the above consideration we can learn that in the case of staggered loading the force on the transverse web adjacent to the transverse bulkhead is 1.125 times that of other transverse web and the bending moment on the longitudinal stiffener on longitudinal bulkhead is 1.5 times of point at the ordinary transverse web.

This is an example that hull structure designers should carefully check, not only structural arrangement but also the loading pattern to assume appropriate boundary conditions. For design improvement such practical and detailed boundary conditions are to be considered.

However, we can design the structural to reasonably reduce such additional bending moments and reaction forces. In the case of staggered loading, the transverse bulkhead also supports staggered loading from the cargo oil. If the longitudinal stiffener on the longitudinal bulkhead is designed so as to be rigidly connected to the adjacent vertical stiffener on the transverse bulkhead as shown in Fig. 1.6.5, rotation is restricted and boundary condition at the transverse bulkhead can again be assumed to be fixed.

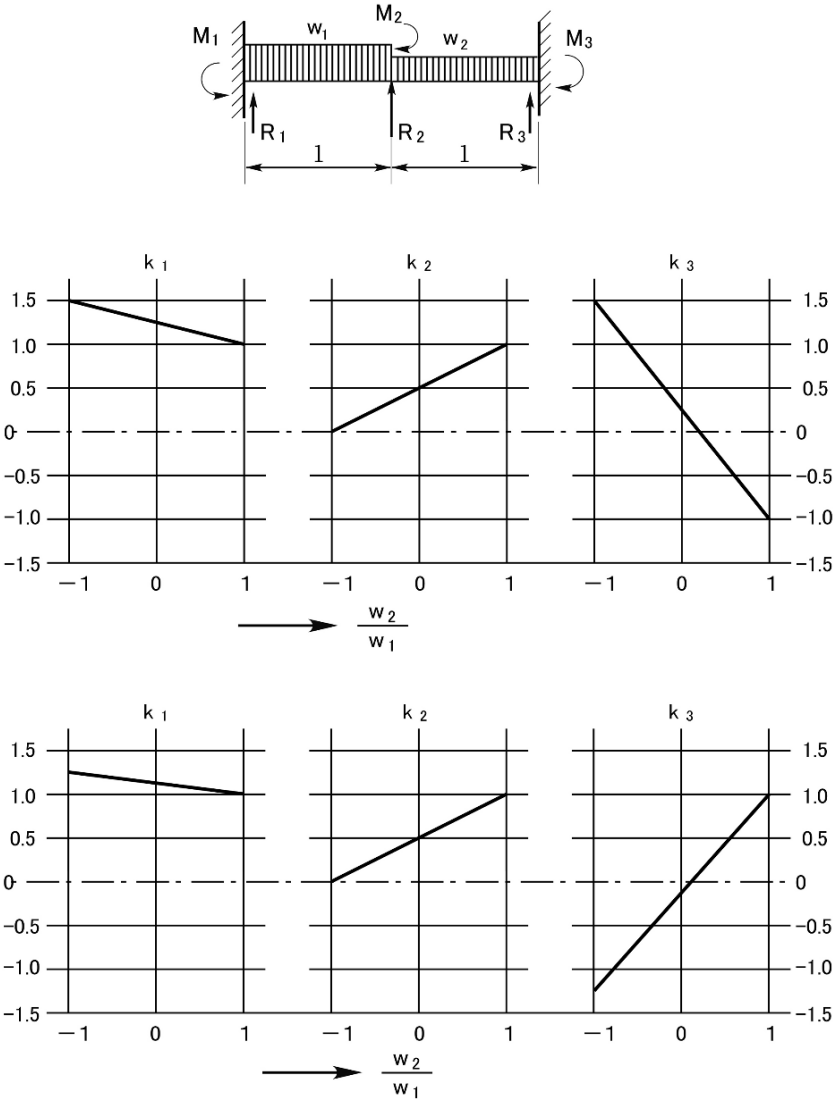


Fig. 1.6.3 Change of bending moment and shearing force by loading

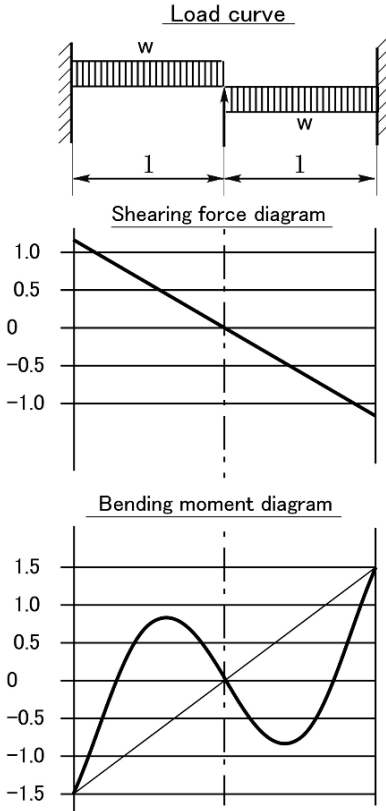
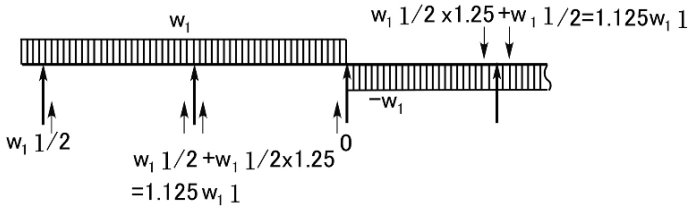


Fig. 1.6.4 Load on web adjacent to Bhd. and BMD & SFD on longitudinal

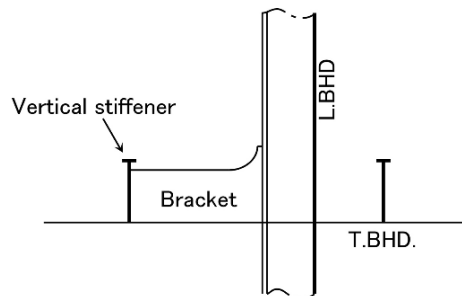


Fig. 1.6.5 Bracket connection between longitudinal and vertical stiffener

### 1.7 Cross-Sectional Area of Beams

Sizes of web plate and face plate of a beam are to be calculated so as to have the given section modulus  $I/y$ . As an example a simple calculation method is explained for the hull girder midship section modulus to meet the required value hereunder [6].

For the hull girder midship section modulus to meet the required value, it is usual to adjust upper deck plate thickness after deciding the sizes of other members to have enough local strength. It can be achieved usually by a trial and error method because in this case by adjusting the upper deck plate thickness the position of the neutral axis moves accordingly. The method explained here is not a trial and error method but a direct method obtained by a simple approach.

Figure 1.7.1 shows a midship section of a tanker. For this midship section, section modulus  $Z_1$ , sectional area  $A_1$ , sectional moment of inertia  $I_1$  and the distance between neutral axis and upper deck at side  $y_1$  are to be calculated using the minimum scantling of each member to satisfy local strength.

Then the sectional area of  $A_2$  is added on the upper deck to meet the required section modulus  $Z$ . The following relations will be obtained.  $y_2$  is the distance between the neutral axis and the added area  $A_2$ .

The neutral axis moves by a distance of  $d$  by adding  $A_2$  on the upper deck.

$$d = \frac{A_2 y_2}{A_1 + A_2} \tag{1.7.1}$$

The increment of the sectional moment of inertia is  $\Delta I$ .

$$\Delta I = A_1 d^2 + A_2 \left( \frac{A_1 y_2}{A_1 + A_2} \right)^2 = \frac{A_1 A_2 y_2^2}{A_1 + A_2} \tag{1.7.2}$$

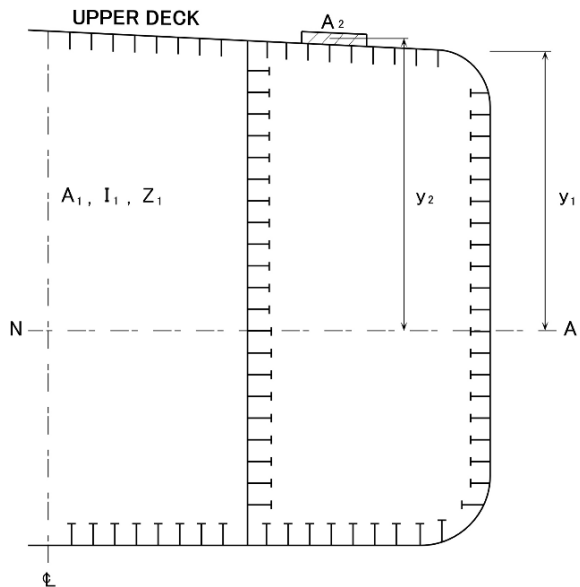


Fig. 1.7.1 Midship section of tanker

The distance between the upper deck at the side and the neutral axis decreases by  $\Delta y_1$ .

$$\Delta y_1 = d = \frac{A_2 y_2}{A_1 + A_2} \quad (1.7.3)$$

From the above relations, the section modulus  $Z$  after adding additional area  $A_2$  on the upper deck is expressed by the following equations.

$$\begin{aligned} Z &= \frac{I_1 + \frac{A_1 A_2 y_2^2}{A_1 + A_2}}{y_1 - \frac{A_2 y_2}{A_1 + A_2}} \\ &= \frac{I_1}{y_1} + \frac{\frac{A_1 A_2 y_2^2}{A_1 + A_2} + \frac{A_2 y_2}{A_1 + A_2} \cdot \frac{I_1}{y_1}}{y_1 - \frac{A_2 y_2}{A_1 + A_2}} \\ &= Z_1 + \frac{A_2 y_2 (A_1 y_2 + Z_1)}{(A_1 + A_2) y_1 - A_2 y_2} \end{aligned} \quad (1.7.4)$$

When  $y_1$  is nearly equal to  $y_2$ , the following simple relation is obtained:

$$Z = Z_1 + \frac{A_2 (A_1 y_2 + Z_1)}{A_1} \quad (1.7.5)$$

$$\therefore A_2 = \frac{A_1 (Z - Z_1)}{A_1 y_2 + Z_1} \quad (1.7.6)$$

Applying the above Eq. (1.7.6), the necessary additional area on the upper deck can be calculated directly instead of by the traditional trial and error method.

In the Eq. (1.7.4)  $Z$  is always bigger than  $Z_1$  in the case where  $y_2$  is positive for  $y_2$  and  $y_1$  on the same side of the neutral axis. That is, by adding  $A_2$  the section modulus can be increased.

Attention should be paid to the case where  $y_2$  is negative where  $y_2$  and  $y_1$  are on the opposite side of the neutral axis. That is, by adding  $A_2$  the section modulus may not always be increased. In the case where  $(A_1 y_2 + Z_1)$  is positive, that is,  $|y_2| < Z_1/A_1$ , the section modulus is reduced by adding  $A_2$ . On the contrary, the section modulus can be increased by taking off  $A_2$  in the region where  $|y_2| < Z_1/A_1$ . This phenomenon is caused by the bigger effect of moving the neutral axis than the increase in sectional moment of inertia.

## 1.8 Optimum Design of Beam Section

In the design of a beam, the designer should firstly pay attention to having least weight for the required strength, because a light and strong ship can carry more cargo more safely. By deciding the boundary conditions, loading conditions, and

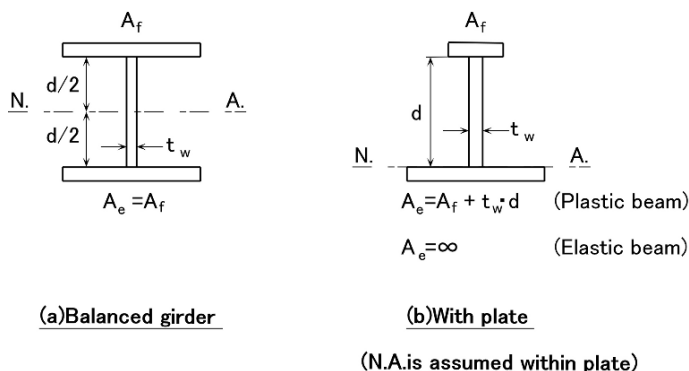


Fig. 1.8.1 Section of beam

allowable stress of the beam, the required section modulus is given. Here some considerations for lighter section of beams for a required section modulus are explained.

Usually a beam section consists of three parts, plate, web and face plate, as shown in Fig. 1.8.1. The plate supports the lateral force such as water pressure and the face plate supports the bending moment because of its greater distance from the neutral axis where bending stress is the maximum. And the web supports the shearing force keeping the distance between plate and face plate.

In the case where the area of the plate is equal to that of the face plate, the neutral axis comes at the mid depth of the web as shown in Fig. 1.8.1(a) which is called “balanced girder”. And in the case where the area of the plate is far bigger than that of the face plate, the neutral axis lies on the plate as shown in Fig. 1.8.1(b) which is called “girder with plate”.

Since a beam or girder has an attached plate which area is same as that of the face plate, they are treated as a “balanced girder”. On the other hand a big girder such as a bottom transverses or a transverse rings of a tanker has a big plate compared with the face plate and this is treated as a “girder with plate” which has the neutral axis on the plate.

In the Sect. 1.4, an elastic design and a plastic design are explained and it is stressed that a different design philosophy will bring a different result. For the optimum section of a beam an elastic design and a plastic design will also have different results. The optimum sections by an elastic design and by a plastic design are explained hereunder.

### 1.8.1 Elastic Design

(1) *Balanced girder*: In the case of a balanced girder, as explained in Sect. 1.3.1(1), the area of the face plate  $A_f$  to meet the required section modulus  $Z$  is obtained by following equation.

$$A_f = \frac{Z}{d} - \frac{t_w d}{6} \quad (1.8.1)$$

The sectional area  $A$  of the beam is the sum of the web area and face plate area.

$$A = A_f + t_w d \quad (1.8.2)$$

Keeping the web thickness constant the optimum depth of the web is obtained.

$$\frac{dA}{dd} = -\frac{Z}{d^2} + \frac{5}{6}t_w = 0 \quad (1.8.3)$$

$$\therefore d = \sqrt{\frac{6Z}{5t_w}} = 1.10\sqrt{\frac{Z}{t_w}}$$

In the above case the area of the face plate is obtained as follows.

$$A_f = \left( \sqrt{\frac{5}{6}} - \frac{1}{6}\sqrt{\frac{6}{5}} \right) \sqrt{Zt_w} = 0.73\sqrt{Zt_w} \quad (1.8.4)$$

(2) *Girder with plate:* As explained in Sect. 1.3.1(2), a big girder such as a bottom transverse or transverse ring of a tanker has a big plate compared with the face plate and it is treated as a “girder with plate” which has the neutral axis on the plate. In this case the sectional area of the face plate is shown by the following equation.

$$A_f = \frac{Z}{d} - \frac{t_w d}{3} \quad (1.8.5)$$

Keeping the web thickness constant the optimum depth of the web is obtained.

$$\frac{dA}{dd} = -\frac{Z}{d^2} + \frac{2}{3}t_w = 0 \quad (1.8.6)$$

$$\therefore d = \sqrt{\frac{3Z}{2t_w}} = 1.23\sqrt{\frac{Z}{t_w}}$$

In the above case the area of the face plate is obtained as follows.

$$A_f = \left( \sqrt{\frac{2}{3}} - \frac{1}{3}\sqrt{\frac{3}{2}} \right) \sqrt{Zt_w} = 0.41\sqrt{Zt_w} \quad (1.8.7)$$

Comparing Eq. (1.8.3) with (1.8.6) and (1.8.4) with (1.8.7) it is observed that the “girder with plate” is optimal with a deeper web and smaller face plate. On the other hand the “balanced girder” is optimal with a shallow web and bigger face plate.

In Table 1.8.1(a), the optimum sections of the elastic beams are shown for a “balanced girder” including “flat bar” which has no face plate, “girder with plate”, and the intermediate shape between two. In addition to the web depth and the face plate area, sectional moment of inertia  $I$  and weight per unit length  $w$  are shown in the table.

**Table 1.8.1** Optimum section of beam

(a) Elastic design				(b) Plastic design				
With face plate	Shape				Shape			
	d (cm)	$1.10\sqrt{Z/t_w}$	$1.16\sqrt{Z/t_w}$	$1.23\sqrt{Z/t_w}$	d (cm)	$1.15\sqrt{Z_p/t_w}$	$1.28\sqrt{Z_p/t_w}$	$1.41\sqrt{Z_p/t_w}$
	Af (cm <sup>2</sup> )	$0.73\sqrt{Z/t_w}$	$0.58\sqrt{Z/t_w}$	$0.41\sqrt{Z/t_w}$	Af (cm <sup>2</sup> )	$0.58\sqrt{Z_p/t_w}$	$0.29\sqrt{Z_p/t_w}$	0
	I (cm <sup>4</sup> )	$0.55Z\sqrt{Z/t_w}$	$0.89Z\sqrt{Z/t_w}$	$1.23Z\sqrt{Z/t_w}$	I (cm <sup>4</sup> )	$0.51Z_p\sqrt{Z_p/t_w}$	$0.72Z_p\sqrt{Z_p/t_w}$	$0.93Z_p\sqrt{Z_p/t_w}$
	w (kg/m)	$1.43\sqrt{Z/t_w}$	$1.36\sqrt{Z/t_w}$	$1.28\sqrt{Z/t_w}$	w (kg/m)	$1.36\sqrt{Z_p/t_w}$	$1.23\sqrt{Z_p/t_w}$	$1.11\sqrt{Z_p/t_w}$
Without face plate	Shape				Shape			
	d (cm)	$2.45\sqrt{Z/t_w}$	$2.12\sqrt{Z/t_w}$	$1.73\sqrt{Z/t_w}$	d (cm)	$2.00\sqrt{Z_p/t_w}$	$1.71\sqrt{Z_p/t_w}$	$1.41\sqrt{Z_p/t_w}$
	Af (cm <sup>2</sup> )	$2.45\sqrt{Z/t_w}$	$2.12\sqrt{Z/t_w}$	$1.73\sqrt{Z/t_w}$	Af (cm <sup>2</sup> )	$2.00\sqrt{Z_p/t_w}$	$1.71\sqrt{Z_p/t_w}$	$1.41\sqrt{Z_p/t_w}$
	I (cm <sup>4</sup> )	$1.22Z\sqrt{Z/t_w}$	$1.48Z\sqrt{Z/t_w}$	$1.73Z\sqrt{Z/t_w}$	I (cm <sup>4</sup> )	$0.67Z_p\sqrt{Z_p/t_w}$	$0.80Z_p\sqrt{Z_p/t_w}$	$0.93Z_p\sqrt{Z_p/t_w}$
	w (kg/m)	$1.92\sqrt{Z/t_w}$	$1.67\sqrt{Z/t_w}$	$1.36\sqrt{Z/t_w}$	w (kg/m)	$1.57\sqrt{Z_p/t_w}$	$1.34\sqrt{Z_p/t_w}$	$1.11\sqrt{Z_p/t_w}$

In designing a beam with the required section modulus  $Z$ , the derived section, sectional moment of inertia and weight per unit length depend on the designer's intention and are not unified. As shown in Table 1.8.1 under the optimal conditions, these values are unified independent of the designer's intention. By optimization, the differences in design by each designer's intention are unified, and accordingly the reliability and the accuracy of the design can be improved.

### 1.8.2 Plastic Design

In a plastic beam the neutral axis divides the sectional area equally into two, above and below the neutral axis. Also the neutral axis lies nearer the plate than the center of gravity for an elastic beam.

(1) *Balanced girder*: Expressing the plastic section modulus by  $Z_p$  the area of the face plate  $A_f$  will be given by the following.

$$A_f = \frac{Z_p}{d} - \frac{t_w d}{4} \tag{1.8.8}$$

$$\frac{dA}{dd} = -\frac{Z_p}{d^2} + \frac{3}{4}t_w = 0 \tag{1.8.9}$$

$$\therefore d = \sqrt{\frac{4Z_p}{3t_w}} = 1.15\sqrt{\frac{Z_p}{t_w}}$$



$$A_f = \sqrt{\frac{Z_P t_w}{3}} = 0.58 \sqrt{Z_P t_w} \quad (1.8.10)$$

(2) *Girder with plate:* The plastic neutral axis is assumed to be in the plate.

$$A_f = \frac{Z_P}{d} - \frac{t_w d}{2} \quad (1.8.11)$$

$$\frac{dA}{dd} = -\frac{Z_P}{d^2} + \frac{1}{2} t_w = 0 \quad (1.8.12)$$

$$\therefore d = \sqrt{\frac{2Z_P}{t_w}} = 1.41 \sqrt{\frac{Z_P}{t_w}}$$

$$A_f = \sqrt{\frac{Z_P t_w}{2}} - \sqrt{\frac{Z_P t_w}{2}} = 0 \quad (1.8.13)$$

In Table 1.8.1(b) the optimum sections of the plastic beams for plastic section modulus  $Z_P$  are shown. It can be found that in the plastic beam the web is more effective than the face plate while on the other hand in the elastic beam the face plate is more effective than the web.

### 1.8.3 Optimal Proportion for Beams

In Table 1.8.1, an intermediate shape is shown between a balanced girder and a girder with plate. The values for the intermediate shape are the mean values between balanced girder and girder with plate. Strictly speaking these are not correct but practically it can be accepted. In hull structure design such approximations bring very good and fruitful results.

Figure 1.8.2 shows the optimum depth and weight of an elastic beam for a required section modulus compared with those values for a standard angle. It can be said that the standard angle is very close to that for the optimum intermediate shape.

In Table 1.8.1(a), if we tabulate the ratio of web area to face plate area ( $d_{tw}/A_f$ ), we can obtain a value of 1.5 for a balanced girder, 2.0 for an intermediate beam, and 3.0 for beams with a neutral axis on the skin plate. That is, we can say that the optimal proportion for ordinary beams is such that the web area is approximately twice the face plate area. This is a very simple and useful guidance. Designers should take note if they find built-up beam proportions very different from the above value.

However, everything has exceptions. Designers must not apply such guidance blindly. From the derivation described through Sects. 1.8.1 and 1.8.2, we find that the optimum proportion was obtained postulating that the web thickness is constant. Some longitudinal stiffeners such as bottom longitudinals are under large axial compression, and thus, web thickness has to be increased as the beam depth increases due to the web buckling criterion. Under these conditions, deep beams become inefficient, and the optimum proportion shifts to the side of smaller  $A_w/A_f$  (web

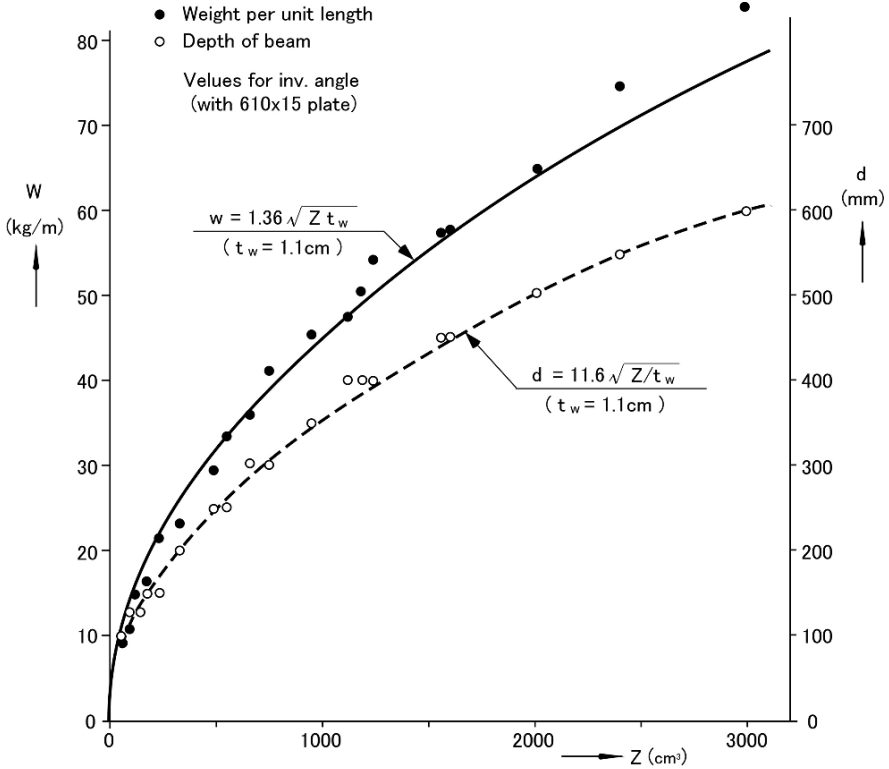


Fig. 1.8.2 Optimum section and standard section

area/face plate area) ratio. In the case where a very large axial compression acts, such as in higher tensile steel application, this ratio may become down to around 1.0.

Another exception is beams under forced displacement, where deeper beams are also inefficient. This will be detailed in Sect. 1.11.

### 1.9 Simply Supported Beams and Continuous Beams

In the case where a partial load is applied to a beam as shown in Figs. 1.9.1(a) and 1.9.2(a), the beam is to be designed as a continuous beam which takes more time, labour and expense. Approximately the beam may be designed as a simply supported beam. Here the difference between them will be examined.

In Fig. 1.9.1 assuming beam A is a simply supported beam then maximum bending moment  $M$  at the midspan is obtained by the following equation.

$$M = \frac{Pl}{4} \left( 1 - \frac{b}{2l} \right) \tag{1.9.1}$$

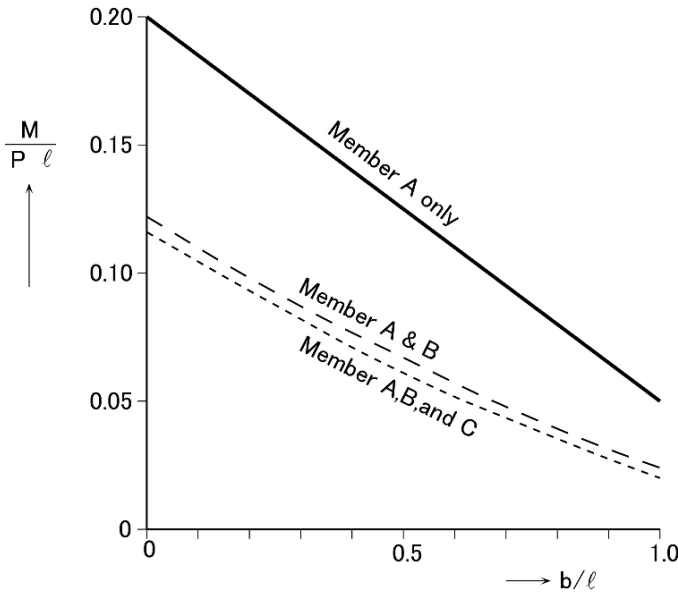
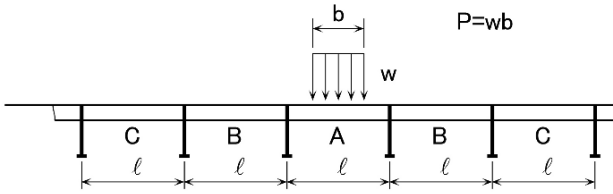


**Fig. 1.9.1** Effect of load range in continuous beam

where

$P$ : concentrated load.

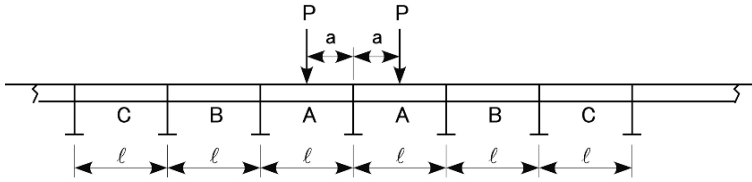
$l$ : span of beam.

Including adjacent span B the maximum bending moment  $M$  at the midspan is as follows:

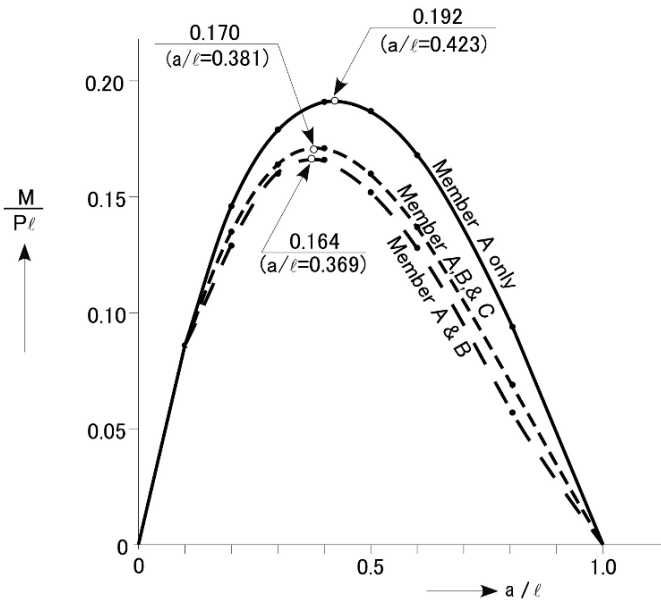
$$M = \frac{Pl}{4} \left\{ \frac{7}{10} - \frac{b}{2l} + \frac{1}{10} \left( \frac{b}{l} \right)^2 \right\} \tag{1.9.2}$$

Including adjacent span B and C the maximum bending moment  $M$  at the midspan is as follows:

$$M = \frac{Pl}{4} \left\{ \frac{13}{19} - \frac{b}{2l} + \frac{2}{19} \left( \frac{b}{l} \right)^2 \right\} \tag{1.9.3}$$



(a) Wheel load on continuous beam



(b) Change of bending moment at centre

Fig. 1.9.2 Bending moment of beam due to wheel load

The above relations are shown in Fig. 1.9.1(b). The result of the simply supported assumption gives about 20% higher value than that of the continuous beam. This is enough to take into account the adjacent span B. In Fig. 1.9.1(b) the effect of the width of the load is also shown, that is, the wider load reduces the bending moment very much.

In the case where the load is applied separately on the adjacent two spans of beam as shown in Fig. 1.9.2(b) following equations are obtained.

Considering the span A in Fig. 1.9.2(a) only, the maximum bending moment  $M$  is as follows:

$$M = Pl \left\{ \frac{a}{l} - \frac{3}{2} \left( \frac{a}{l} \right)^2 + \frac{1}{2} \left( \frac{a}{l} \right)^3 \right\} \quad (1.9.4)$$

where  $a$  is the distance between the load and the support at the midpoint.

Considering the span A and B in Fig. 1.9.2(a), the maximum bending moment  $M$  is as follows:

$$M = Pl \left\{ \frac{a}{l} - \frac{43}{24} \left( \frac{a}{l} \right)^2 + \frac{19}{24} \left( \frac{a}{l} \right)^3 \right\} \quad (1.9.5)$$

Then considering the span A, B and C in Fig. 1.9.2(a), the maximum bending moment  $M$  is as follows:

$$M = Pl \left\{ \frac{a}{l} - \frac{45}{26} \left( \frac{a}{l} \right)^2 + \frac{19}{26} \left( \frac{a}{l} \right)^3 \right\} \quad (1.9.6)$$

The above relations are shown in Fig. 1.9.2(b). The result for span A is only about 15% higher than that for the continuous beam.

## 1.10 Effect of Struts

In the case that two parallel beams are connected by a strut at their midspan as shown in Fig. 1.10.1(a), the applied force on the beam deforms the whole structure and causes a reaction distribution which depends on the rigidity ratio of each member. One example is the longitudinal framing of a cargo ship double bottom where the inner bottom and the bottom longitudinals are connected by a strut.

In this case the bending moments on the beams and the axial force in the strut are expressed by the following equations:

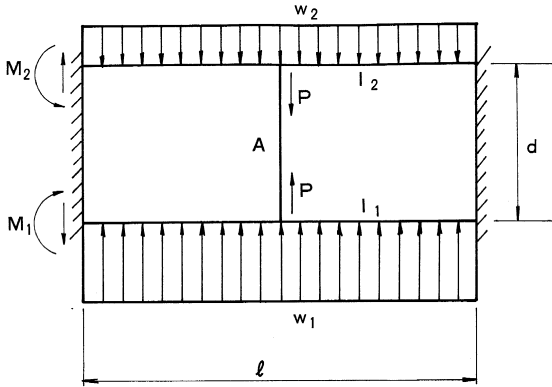
$$P = K \frac{w_1 l}{2} \quad (1.10.1)$$

$$M_1 = \left( 1 - \frac{3}{4} K \right) \frac{w_1 l^2}{12} \quad (1.10.2)$$

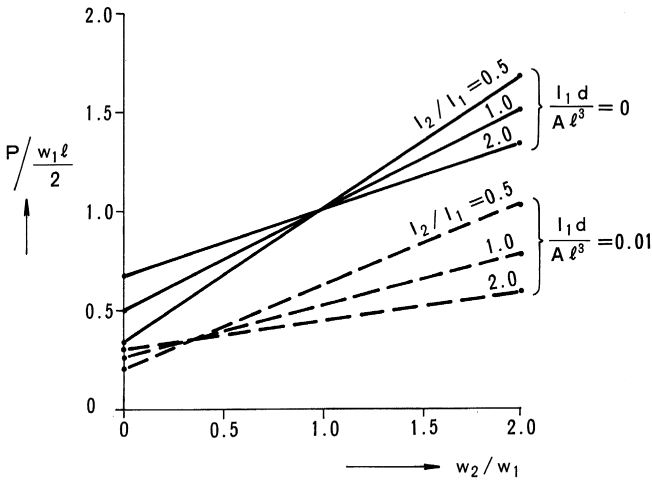
$$\text{where } K = \frac{1 + \frac{w_2}{w_1} \cdot \frac{I_1}{I_2}}{1 + \frac{I_1}{I_2} + \frac{192 I_1 d}{A l^3}}$$

- $w_2, w_1$ : loads on top and bottom beams respectively
- $I_2, I_1$ : sectional moment of inertias of top and bottom beams respectively
- $A, d$ : sectional area and the length of the strut
- $P$ : axial compressive force in the strut
- $M_1$ : bending moment at the fixed end of the bottom beam

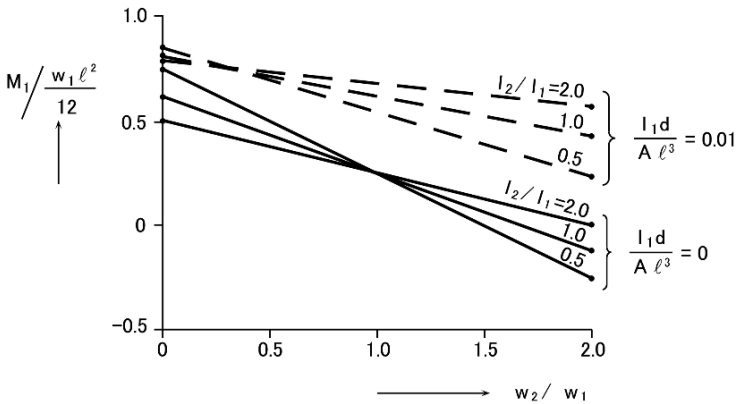
Figure 1.10.1(b) shows that the axial compressive force in the strut is the mean value of the loads applied on the top and the bottom beams where the strut is rigid



(a) Strut in double bottom and load



(b) Compression in strut



(c) Decrement of bending moment due to strut

Fig. 1.10.1 Effect of strut in double beams

and the rigidities of the top and the bottom beams are equal. In the case of an equal load on the top and the bottom beams, the rigidity of the beam has no affect at all. The axial compressive force in the strut is increased by increasing the rigidity of the beam on which the smaller load is applied. Assuming elasticity in the strut, the axial compressive force in the strut is reduced. The bigger axial compressive force in the strut causes a smaller bending moment at the fixed ends. A bigger load on the top beam reduces the bending moment of the bottom beam at its fixed ends. Where the load on the bottom beam is bigger than that on the top beam, increasing the rigidity of the top beam is effective. Having a more rigid strut gives a better design.

### 1.11 Additional Bending Moment due to Forced Displacement

A secondary member such as a beam supported by a primary member as a girder, is usually designed assuming that the primary member has no deflection. However primary members are not 100% rigid and an additional bending moment is generated in the secondary member by the deflection of the primary members. One example is the additional bending moment at the bottom bracket of the vertical stiffener on a transverse bulkhead which is caused by deflection of the horizontal girders on the transverse bulkhead.

To overcome this additional bending moment due to forced displacement, increasing only the sectional moment of inertia and section modulus of the beam is not sufficient.

As shown in Fig. 1.11.1 the additional bending moment  $M_\delta$  due to the forced displacement and the additional bending moment  $M_\theta$  due to forced rotation are expressed by the following equations.

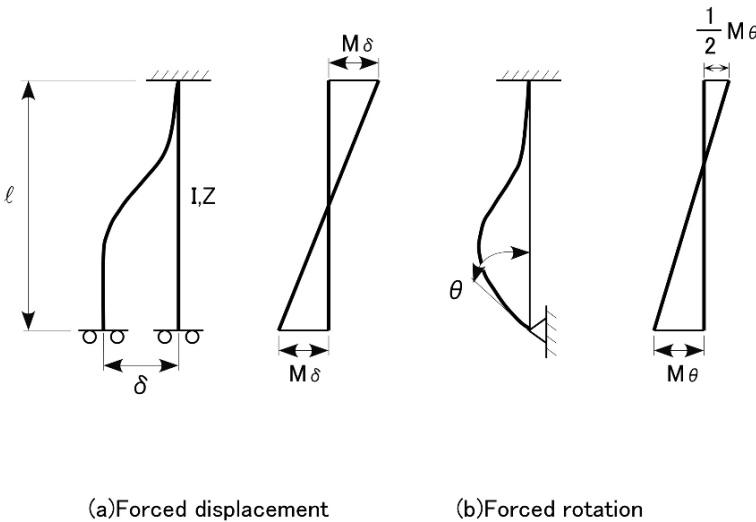


Fig. 1.11.1 Bending moment of beam due to forced displacement

$$M_{\delta} = \frac{6EI}{l^2} \delta \quad (1.11.1)$$

$$M_{\theta} = \frac{4EI}{l} \theta \quad (1.11.2)$$

The allowable stress for this additional moment is  $\sigma_a$ .

$$\begin{aligned} \sigma_a &\geq \frac{M_{\delta}}{Z} \text{ or } \frac{M_{\theta}}{Z} \\ \therefore \frac{I}{Z} &\geq \frac{\sigma_a l^2}{6E\delta} \text{ or } \frac{\sigma_a l}{4E\theta} \end{aligned} \quad (1.11.3)$$

$Z = I/y$  then  $I/Z = y$  which is the distance between the neutral axis and the extreme fiber. In the case of a balanced girder  $y = d/2$  then the following equation is obtained.

$$\begin{aligned} \frac{I}{Z} &= \frac{d}{2} \leq \frac{\sigma_a l^2}{6E\delta} \\ \therefore \frac{l}{d} &\geq \frac{3E}{\sigma_a} \cdot \frac{\delta}{l} \end{aligned} \quad (1.11.4)$$

From the above result the slenderness ratio of the beam should be increased proportionally to the amount of the forced displacement to keep the additional stress within the allowable limit. From these discussions, it is important for a designer to find and feel in his bones the fact that the bending stress due to forced displacement depends on (or is proportional to) the distance from the neutral axis only, and is independent from other sectional properties such as  $I$  or  $Z$ . Based on this fact, in case of ordinary beam with skin plate under forced displacement, we can easily understand intuitively and qualitatively that to make the beam shallower is extremely effective, on the other hand to make the face plate thicker is less effective because it makes the distance from the neutral axis closer only slightly.

A flexible (smaller Young's modulus) and slender beam is good for the forced displacement. "A willow twig will never be broken by strong wind." However a weak and slender beam will not support ordinary loads. The correct solution in this case is to reduce the deflection of the primary member itself or the relative displacement of the adjacent primary members. However, if such relative displacement is inevitable, it is necessary to make the combined stress due to lateral loads and forced displacement less than allowable value. As discussed above, the stress due to forced displacement depends only on  $y$  (the distance from the neutral axis), and the stress due to lateral loads depends only on  $Z$  (section modulus). Therefore, when we design beam under lateral loads and forced displacement, we must first decide the appropriate depth of the beam, and then control the section modulus by adjusting the scantling of the face plate, roughly imaging the amount of each stress component.

In Sect. 1.8, we discussed optimal design of beam section and found that the best proportion of ordinary beams is that the area of web is about 2 times of the area of



face plate. In case of beams under simultaneous forced displacement, the optimal proportion shift to the side of shallower beam and bigger face plate, sometimes resulting in the ratio of web area to face plate area to be about 1.0.

### 1.12 Lateral Movement of Beams

The face plate of a beam lies at the distance  $y$  from the neutral axis and the assumption that the bending stress in the face plate is uniform is usually applied in beam design. However as shown in Fig. 1.12.1 it is not uniform but is maximum at the attachment point to the web and minimum at the free edge. The concept of the effective breadth  $b_e$  is such that the force in the face plate is equal to the product

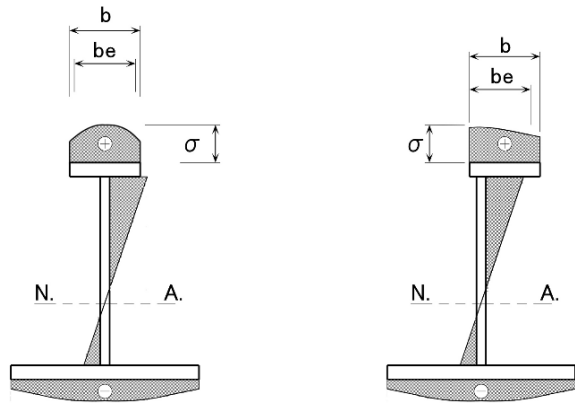
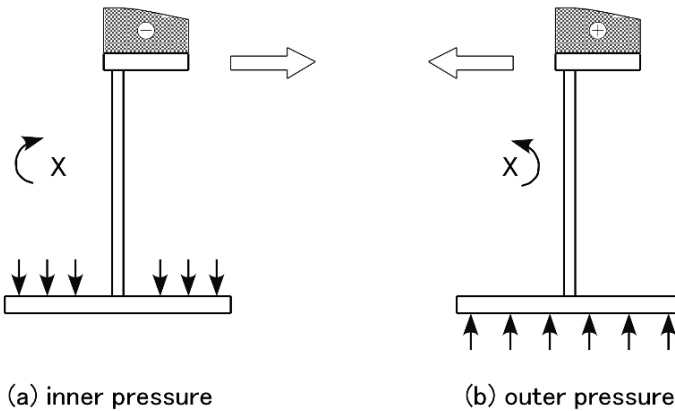


Fig. 1.12.1 Bending stress distribution in beam section

X : Shear center



(a) inner pressure

(b) outer pressure

Fig. 1.12.2 Lateral movement of beam due to torsional moment induced by pressure

of the maximum bending stress and the face plate area, which assume an effective breadth  $b_e$ .

In the case where a beam is subjected to bending, the beam deforms in a vertical direction and it may move in lateral direction simultaneously according to the shape of its cross-section. For example, an L section beam will move in a lateral direction due to bending, while a beam with a symmetric cross-section never causes lateral movement.

As shown in Fig. 1.12.2 in the case of a tensile stress in the face plate due to outer pressure, the beam wants to move in left direction, whereas for a compressive stress in the face plate due to inner pressure, the beam wants to move in right direction. This phenomenon is explained by noting that the beam has a torsional axis called a “shear center” as described in Sect. 7.5. When a torsional moment is applied to the beam, the beam twists around the shear center. The position of this shear center depends only on the shape of the cross section of the beam and it lies on the opposite side of the flange in the case of an L section beam, as illustrated in Fig. 1.12.2. Hence, as presented in Fig. 1.12.2(a), a beam subjected to inner pressure will move to the right side due to a clockwise torsional moment around the shear center induced by the pressure. On the contrary, in the case of a beam of a symmetric cross-section, lateral movement of the beam never occurs, because the shear center of this beam is in the middle of the web plate and no torsional moment is created.

# Chapter 2

## Design of Girders

In Chap. 1, it was explained that beams resist the bending moment caused by lateral forces and that the section modulus is important in resisting this bending moment. In the design of mammoth tankers, 40,000–50,000 DWT, built around 1960, girders were designed based only on bending theory. For the bigger ships built after that era, shearing theory has been also applied.

A girder is a structural member which supports lateral forces imposed by beams. Beams, stiffeners, frames, longitudinals, etc. are called secondary members. Girders, web frames, transverse webs, etc. are called primary members for which the shearing force has to be taken into consideration during design. Simply speaking, a beam is designed against bending and a girder is designed against bending and shearing.

### 2.1 Shearing Force

In a book of strength of materials, shearing force and shearing stress are explained in detail based on the equilibrium of forces. However for the design of a girder, the information shown in Fig. 2.1.1 will simply illustrate. Complicated theory will not help to understand this phenomenon.

In Fig. 2.1.1 a cantilever girder with a concentrated load  $F$  at the free end is shown. Taking out a small part  $\Delta x$  from the girder, the mean shearing stress  $\tau$  in this part is  $F/A$ , where  $F$  is the shearing force and  $A$  is the sectional area of the web. The shearing strain  $\gamma$  is shown by the following equation:

$$\gamma = \frac{F}{AG} \tag{2.1.1}$$

where  $G$  is the shear modulus.

Then the shearing deflection  $\Delta y$  in the vicinity of  $\Delta x$  is expressed as follows:

$$\begin{aligned} \Delta y &= \gamma \Delta x \\ &= \frac{F \Delta x}{AG} \end{aligned} \tag{2.1.2}$$

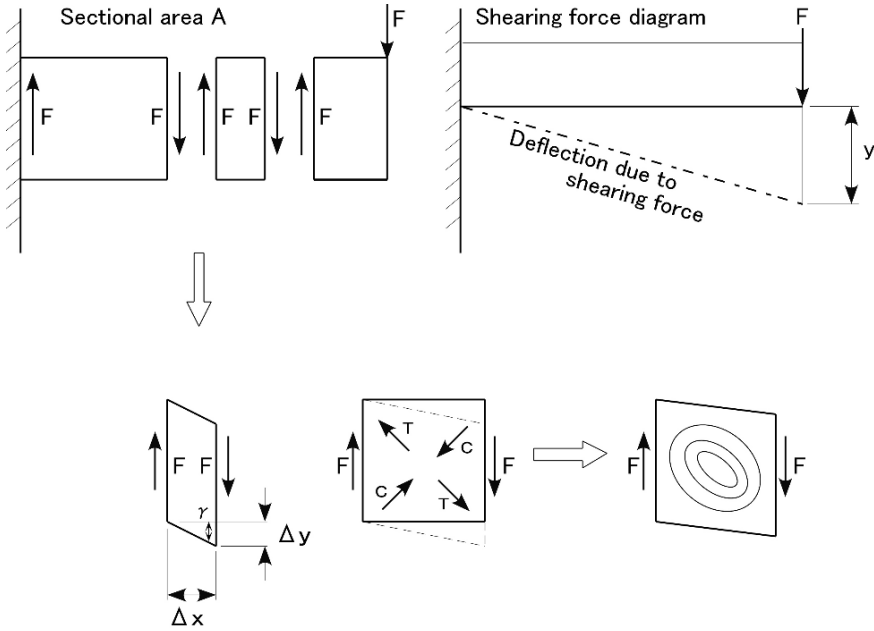


Fig. 2.1.1 Shearing force

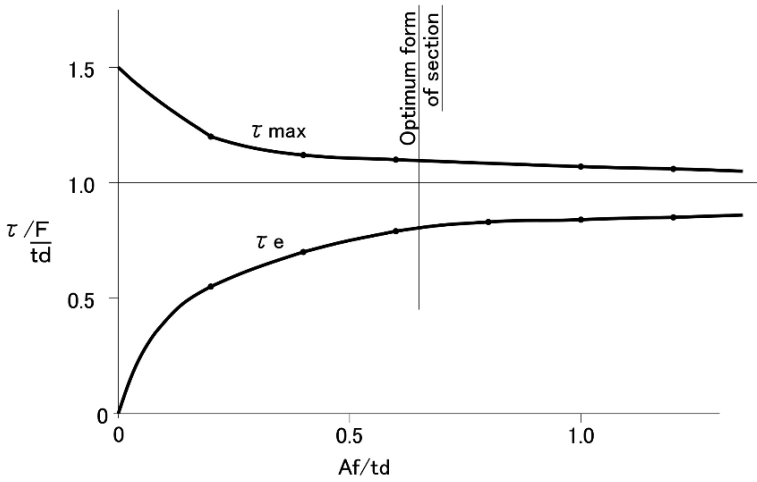
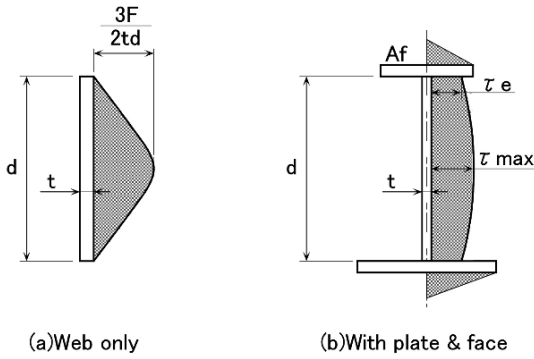
$$\therefore y = \int_0^x \frac{F}{AG} dx \tag{2.1.3}$$

Equation (2.1.3) shows that the shearing deflection  $y$  is proportional to  $x$  where  $F$  is constant, therefore the shearing deflection is a straight line as shown in Fig. 2.1.1.

Under the action of the shearing force, the part of the girder, which has a rectangular shape, initially deforms just like a squashed match box, and consequently a tensile force  $T$  in a diagonal direction and a compressive force  $C$  in the other diagonal direction, are generated. The tensile force  $T$  sometimes causes cracks and the compressive force  $C$  causes buckling in the web plate. This is the reason why shearing buckling occurs in a diagonal direction.

A girder consists of a web plate and a face plate similar to a beam, and the web plate supports shearing force. The behaviors can be easily understood from Fig. 2.1.1. The face plate has only its thickness in the shearing force direction and can be easily deformed without resisting the shearing force applied.

The distributions of the shearing stresses are shown in Fig. 2.1.2(a) and (b) in the cases of web plates and built-up sections respectively. The shearing stress is 0 at the free edge, and in the case of a web plate, the maximum shearing stress is 1.5 times of the mean value. In the case of a built-up section the shearing stress distribution in the web plate is more even and its maximum stress is considered to be nearly equal to the mean value, which is obtained by dividing the shearing force by the sectional area of the web plate.



(c) Area of face plate and shearing force in web

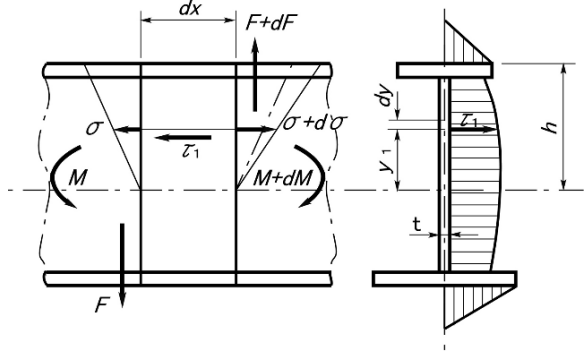
Fig. 2.1.2 Shearing stress distribution

Plates connected at the top and bottom of the web plate do not support the shearing force very much, but they even out the distribution of shearing stress in the web plate.

The shearing stress  $\tau_1$  in the section parallel to and at the distance  $y_1$  from the neutral axis is obtained as shown in Fig. 2.1.3.

$$\tau_1 t dx = \int_{y_1}^h d\sigma t dy \tag{2.1.4}$$

**Fig. 2.1.3** How to obtain shearing stress distribution



$$\sigma = \frac{M}{I}y \quad (2.1.5)$$

$$\therefore d\sigma = \frac{y}{I}Fdx \quad (2.1.6)$$

From Eqs. (2.1.4) and (2.1.6) the following is derived.

$$\begin{aligned} \tau_1 &= \frac{F}{It} \int_{y_1}^h ytdy \\ &= \frac{Fm_1}{It} \end{aligned} \quad (2.1.7)$$

where

$M$ : bending moment

$F$ : shearing force

$t$ : thickness of web plate

$I$ : sectional moment of inertia

$m_1$ : moment of the part farther than distance  $y_1$  from the neutral axis

In the case of a balanced girder, the shearing stress in the web plate is calculated as below. The area of the face plate is  $A_f$  and the depth and the thickness of the web plate are  $d$  and  $t$  respectively. The maximum shearing stress  $\tau_{\max}$  at the neutral axis can be calculated as follows.

$$I = \frac{A_f d^2}{2} + \frac{td^3}{12} \quad (2.1.8)$$

$$m = \frac{A_f d}{2} + \frac{td^2}{8} \quad (2.1.9)$$

$$\therefore \frac{m}{I} = \frac{\frac{A_f}{2} + \frac{td}{8}}{d \left( \frac{A_f}{2} + \frac{td}{12} \right)} \quad (2.1.10)$$

here putting  $A_f = ktd$

$$\frac{m}{I} = \frac{12k+3}{d(12k+2)} \quad (2.1.11)$$

$$\begin{aligned} \therefore \tau_{\max} &= \frac{Fm}{It} \\ &= \frac{F(12k+3)}{td(12k+2)} \end{aligned} \quad (2.1.12)$$

The shearing stress of web at top and bottom  $\tau_e$  is obtained as follows.

$$m = \frac{A_f d}{2} \quad (2.1.13)$$

$$\begin{aligned} \therefore \frac{m}{I} &= \frac{A_f}{2} \cdot \frac{1}{d \left( \frac{A_f}{2} + \frac{td}{12} \right)} \\ &= \frac{6k}{d(6k+1)} \end{aligned} \quad (2.1.14)$$

$$\tau_e = \frac{6Fk}{td(6k+1)} \quad (2.1.15)$$

The relationship of Eq. (2.1.12) with (2.1.15) is shown in Fig. 2.1.2(c). The origin,  $A_f/td$  corresponds to the section without face plates.

$F/td$ , the value of the shearing force divided by the sectional area of web plate (assuming the plate and the face plate do not support the shearing force), is the mean shearing stress. It can be said that the shearing stress distribution in a web plate is nearly uniform and its value is nearly equal to the mean shearing stress expressed by  $F/td$  where the sectional area of the face plate is sufficient.

## 2.2 Rational Design of Girders

The rational design of girders is explained below for the bottom transverse in a center tank of a tanker under the assumption that the web plate supports the shearing force and the face plate supports the bending moment.

As shown in Fig. 2.2.1 the bottom transverse in the center tank of a tanker can be assumed to be a girder with both ends fixed and with uniform load. Accordingly the shearing force diagram is a straight line passing through the 0 point at the midspan. The thickness of the web plate  $t$  and the depth of the girder at the ends  $h$  are to be expressed as follows:

$$h = \frac{wl}{2t\tau_a} \quad (2.2.1)$$

where  $\tau_a$ : allowable shearing stress

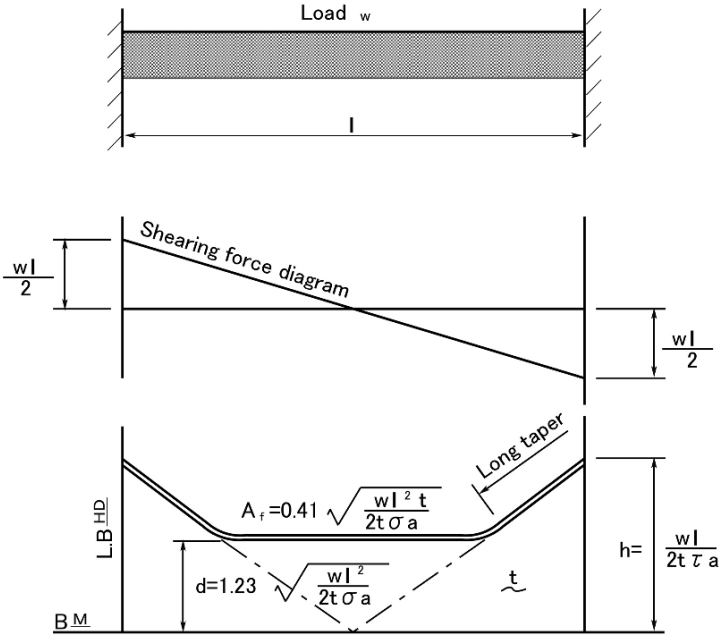


Fig. 2.2.1 Rational girder design

The bending moment at midpoint in the span is  $M = wl^2/24$ , and for an allowable bending stress given by  $\sigma_a$  the required section modulus  $Z$  is as follows:

$$Z = \frac{wl^2}{24\sigma_a}$$

Using an optimal section shown in Sect. 1.8, the depth  $d$  and the sectional area of the face plate  $A_f$  of the girder are obtained as follows.

$$d = 1.23 \sqrt{\frac{wl^2}{24t\sigma_a}} \tag{2.2.2}$$

$$A_f = 0.41 \sqrt{\frac{wl^2 t}{24\sigma_a}} \tag{2.2.3}$$

From Eqs. (2.2.1) and (2.2.3) the ratio of  $h$  and  $d$  can be obtained.

$$\begin{aligned} \frac{h}{d} &= \frac{wl\sqrt{24t\sigma_a}}{2t\tau_a \times 1.23\sqrt{wl^2}} \\ &= \frac{\sqrt{6\sigma_a w}}{1.23\tau_a\sqrt{t}} \end{aligned} \tag{2.2.4}$$



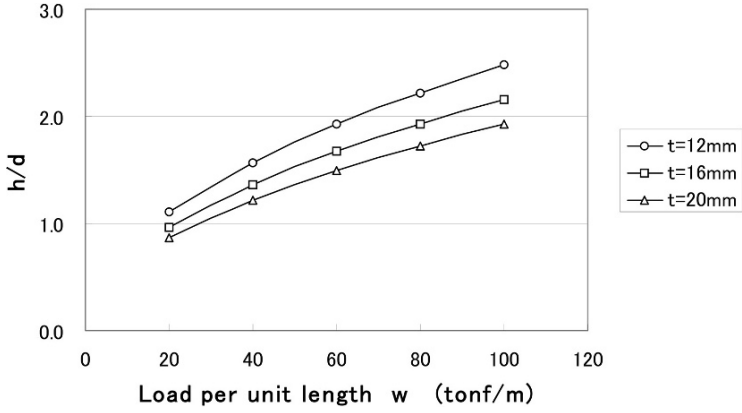


Fig. 2.2.2 Ratio of depth at end and center of rationally designed girder

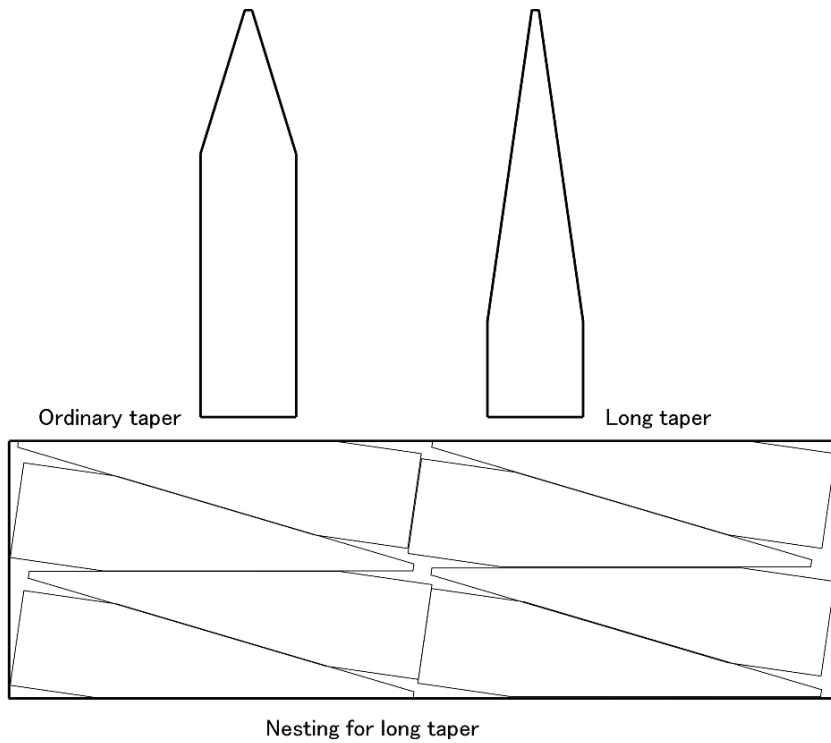


Fig. 2.2.3 Long tapered face plate end

Assuming that the allowable bending stress and the shearing stress are  $\sigma_a = 120$  MPa and  $\tau_a = 80$  MPa respectively,  $h/d$  is obtained as shown in Fig. 2.2.2.

Judging from the appearance of the girder,  $h/d$  will be around  $1.5 \sim 2.5$ . By using Fig. 2.2.2 the thickness of the web plate  $t$  for a given load  $w$  can be derived for the design  $h/d$ . After that the area of the face plate  $A_f$  is derived using Eq. (2.2.3).

The sectional area of the face plate  $A_f$  is to be maintained in the vicinity of the parallel part of the girder. However in the vicinity of the end bracket where the depth of the girder is deeper than the parallel part, the required section modulus can be obtained even with a reduced sectional area of the face plate. In this consideration the long taper of the face plate is developed as shown in Fig. 2.2.3 [5]. The long tapered face plate brings not only a weight saving but also a decrease in the scrap percentage thus killing two birds with one stone.

### 2.3 Bottom Transverses Supported by Centerline Girder [5]

In Sect. 1.11 the increase of the bending moment due to forced displacement is explained. In this section the additional bending moment and shearing force in the bottom transverse due to the displacement of the bottom centerline girder are explained.

The bottom transverse shown in Fig. 2.3.1 used to be designed assuming that it is a girder fixed at the longitudinal bulkhead and the centerline girder. However the centerline girder has less rigidity than the longitudinal bulkhead and a relative displacement between the longitudinal bulkhead and the centerline girder will be generated. Therefore it will be more practical to assume that the bottom transverse is fixed at the longitudinal bulkheads and is elastically supported by the centerline girder. With the reaction force at the centerline girder  $W$  and the deflection at the centerline  $\delta$ , the following equation is obtained:

$$\delta = \frac{wl^4}{384EI} - \frac{Wl^3}{192EI} \quad (2.3.1)$$

where

$l$ : span of bottom transverse (distance between longitudinal bulkheads)

$E$ : Young's modulus

$I$ : sectional moment of inertia of bottom transverse

$w$ : uniform load per unit length

Expressing the shearing force and the bending moment at fixed ends by  $F$  and  $M$  respectively, following equation can be obtained:

$$F = \frac{wl}{2} - \frac{W}{2} \quad (2.3.2)$$

$$M = \frac{wl^2}{12} - \frac{Wl}{8} \quad (2.3.3)$$

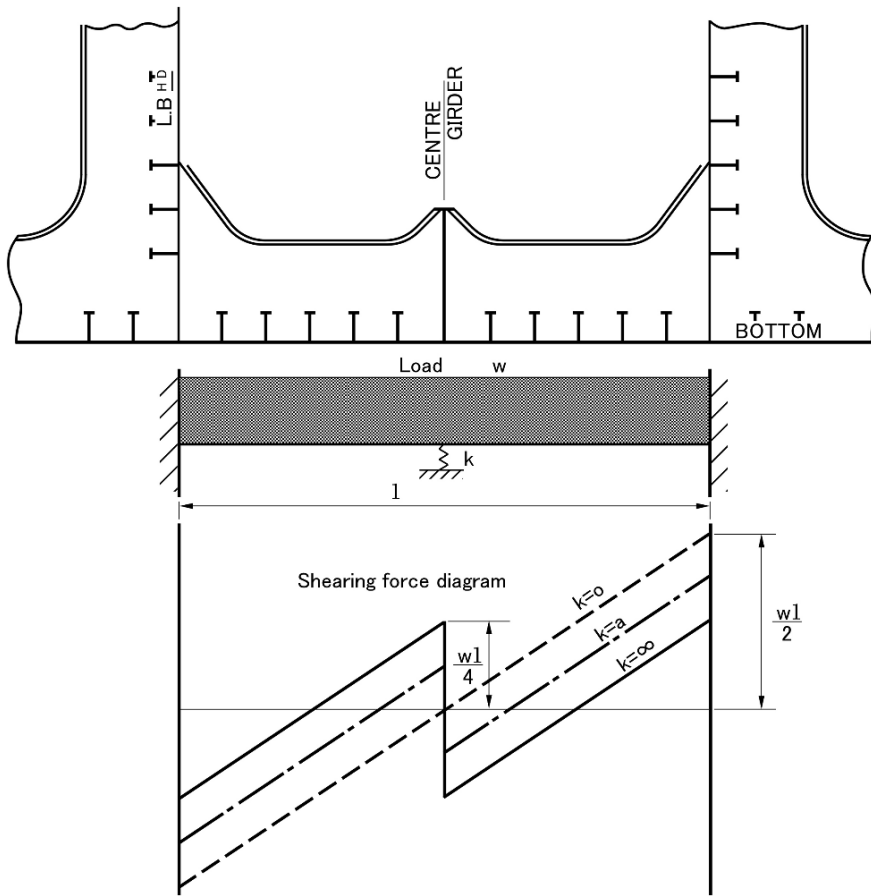


Fig. 2.3.1 Bottom transverse supported by center line girder

Eliminating  $W$  from Eqs. (2.3.1), (2.3.2) and (2.3.3), the relation between  $\delta$ ,  $F$  and  $M$  can be derived as follows:

$$F = \frac{96EI}{l^3} \delta + \frac{wl}{4} \tag{2.3.4}$$

$$M = \frac{24EI}{l^2} \delta + \frac{wl^2}{48} \tag{2.3.5}$$

$F$  and  $M$  where  $\delta = 0$  are expressed by  $F_0$  and  $M_0$  respectively, then  $F_0$  and  $M_0$  will be as follows:

$$F_0 = \frac{wl}{4} \tag{2.3.6}$$

$$M_0 = \frac{wl^2}{48} \tag{2.3.7}$$

$F_0$  and  $M_0$  are the shearing force and the bending moment at the fixed ends when the bottom transverse is designed as a girder fixed at the longitudinal bulkhead and the centerline girder. Accordingly the rate of increase in the shearing force  $F/F_0$  and the bending moment  $M/M_0$  of the bottom transverses, where the displacement at the centerline girder occurs, is as follows:

$$\frac{F}{F_0} = \frac{384EI}{wl^4} \delta + 1 \quad (2.3.8)$$

$$\frac{M}{M_0} = \frac{1152EI}{wl^4} \delta + 1 \quad (2.3.9)$$

From the above equations it can be seen that the rate of increase of the bending moment is bigger than that of the shearing force.

In reality the rate of increase can be calculated, assuming that the allowable bending stress  $\sigma_a$  in the case of no displacement at the centerline is 120 MPa, and the ratio between span and depth of the bottom transverse is 4.0.

$$M_0 = \frac{I}{y} \sigma_a \quad (2.3.10)$$

$$\therefore \frac{wl^2}{48} = 12 \frac{I}{y}$$

$$\frac{l}{y} = 4 \quad (2.3.11)$$

where  $y$  is the distance between the neutral axis and face plate of bottom transverse (assuming neutral axis lies in plate, and  $y$  equals to the depth of bottom transverse).

From Eqs. (2.3.8) and (2.3.9) the following values are obtained.

$$\frac{F}{F_0} = 3,500 \frac{\delta}{l} + 1$$

$$\frac{M}{M_0} = 10,500 \frac{\delta}{l} + 1$$

The above results are shown in Fig. 2.3.2. With 1 mm displacement in the 10 m span of a bottom transverse at the mid-span, the shearing force and the bending moment increase by 1.35 times and 2.05 times respectively.

As shown above the shearing force at both ends increases, but the shearing force at the centerline reduces by the same value as the increase at the fixed ends. In the case where the centerline girder is not effective, the shearing force at the center is zero.

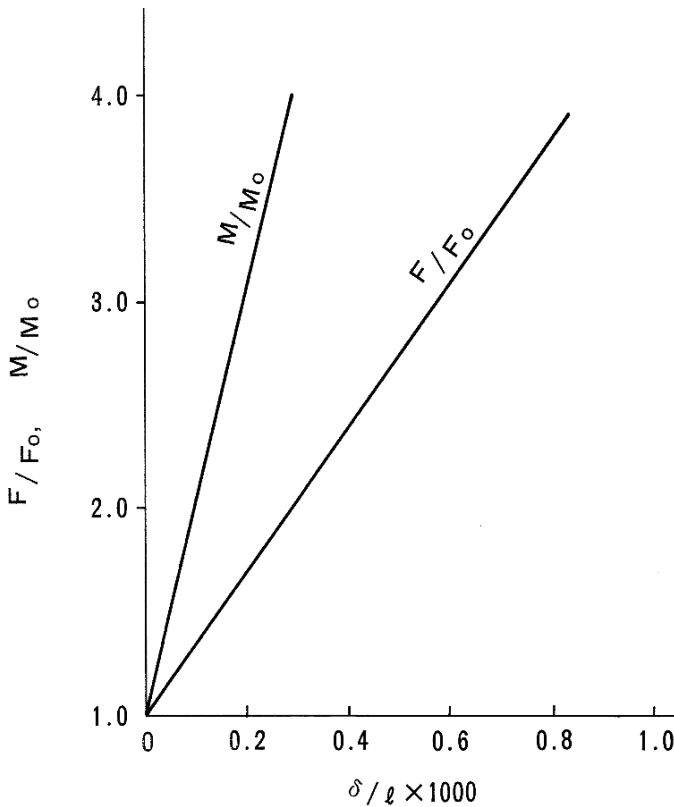


Fig. 2.3.2 Increments of SF & BM in bottom transverse due to displacement of center line girder

## 2.4 Deflection of Girders

In Fig. 2.1.1 the shearing deflection mode of a cantilever beam with a concentrated load at the free end is shown. The mode seems strange for those who are familiar with the bending deflection mode.

In Fig. 2.4.1 several shearing deflection modes are shown. Figure 2.4.1(a) shows the deflection mode of a cantilever beam with a concentrated load at the mid-point. The end part far from the load has no shearing force, consequently no shearing deflection appears. Figure 2.4.1(b) shows the deflection mode of a cantilever beam with a uniform load. The part near the fixed end has a higher shearing force then bigger shearing deformation with bigger curvature. At the free end the shearing force is zero and the deflection curve is tangential to the horizontal.

Figure 2.4.1(c) and (d) show beams with a concentrated load at the midspan, with c simply supported at both ends and d fixed at both ends. In these cases the end conditions do not make any difference.

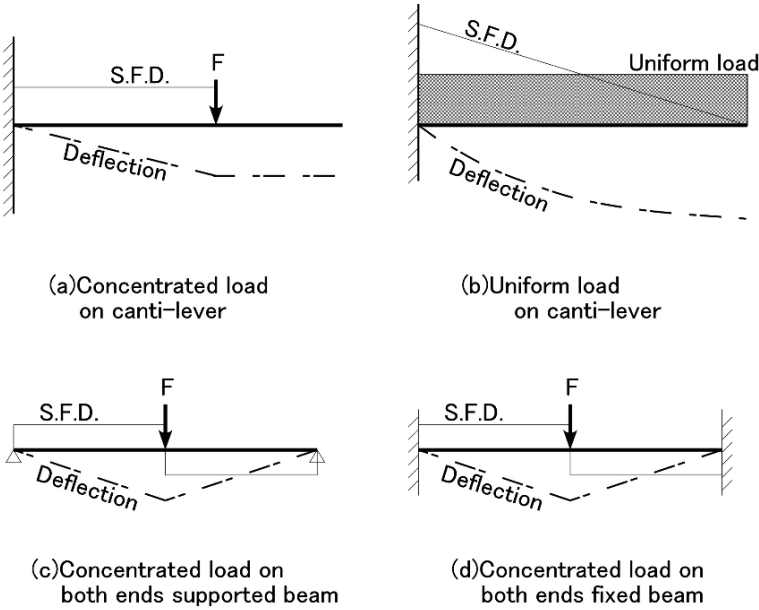


Fig. 2.4.1 Shearing deflection mode of girder

In a deep girder the shearing deflection is dominant and with a shallow girder the bending deflection is dominant. Below, the relationship between the slenderness of a girder and the ratio of the bending and the shearing deflections is investigated. The maximum bending deflection  $\delta_b$  of a girder with both ends fixed for uniform load is expressed by the following equation:

$$\delta_b = \frac{wl^4}{384EI} \tag{2.4.1}$$

The maximum shearing deflection  $\delta_s$  is obtained as follows:

$$\begin{aligned} \delta_s &= \int_0^{\frac{l}{2}} \frac{1}{AG} \left( \frac{wl}{2} - wx \right) dx \\ &= \frac{wl^2}{8AG} \end{aligned} \tag{2.4.2}$$

From Eqs. (2.4.1) and (2.4.2) the following equation is delivered:

$$\frac{\delta_s}{\delta_b} = \frac{48EI}{AGl^2} \tag{2.4.3}$$

$I$  and  $A$  can be expressed by allowable bending and shearing stresses respectively.

$$I = \frac{wl^2}{12\sigma_a} y \quad (2.4.4)$$

$$A = \frac{wl}{2\tau_a} \quad (2.4.5)$$

$$\therefore \frac{I}{A} = \frac{ly\tau_a}{6\sigma_a}$$

Putting Eqs. (2.4.4) and (2.4.5) into Eq. (2.4.3) the following equation can be obtained.

$$\frac{\delta_s}{\delta_b} = \frac{8E\tau_a}{G\sigma_a} \times \frac{y}{l} \quad (2.4.6)$$

where

$E$ : Young's modulus (206,000 MPa)

$G$ : shear modulus (78,000 MPa)

$\sigma_a$ : allowable bending stress (assumed to be 120 MPa)

$\tau_a$ : allowable shearing stress (assumed to be 80 MPa)

$y$ : distance between neutral axis and face plate

(in the case of a section with a plate,  $y$  equals the depth of girder)

$l$ : span of girder

Putting the above figures into Eq. (2.4.6) the following simple relation is delivered.

$$\frac{\delta_s}{\delta_b} = 14 \frac{d}{l} \quad (2.4.7)$$

Equation (2.4.7) means that in the case of an ordinary girder design ( $\sigma_a$  is 120 MPa and  $\tau_a$  is 80 MPa) the bending and shearing deflections are comparable at a slenderness ratio of 14. Usually the span of a girder is 4–8 times the depth and therefore the shearing deflection will be 2–3 times that of the bending deflection.

## Chapter 3

# Damage of Girders

With the large increase in the size of ships since 1965, many kinds of damage on the transverse strength members, especially on the transverse rings of tankers, appeared. Initially the web plate of the transverse ring buckled under water pressure tests. Then cracks appeared at slots where the load is transmitted to the girder's web plate from the longitudinal frames.

The main reason for these damages was the lack of a thicker web plate in spite of the increased load which was brought on by the deeper depth and the wider longitudinal and transverse frame spaces. The local buckling or the cracking developed sometimes up to the extensive damage which is shown in Fig. 3.1 [7].

For a reliable design it is important that the hull structure design is based on a design standard which is revised according to feed back from ships in service. Damage is the most important feed back obtained from ships in service.

For the large-increase in the size of ships which started around 1955 the classification society's rules were not suitably revised until 1970, and the hull structure designer had to design bigger ships based on his own experience as well as the classification society's rules.

This chapter explains how the hull structure designer established his/her own design standard for new designs based on the damage experienced by girders in previous ships in service. In Fig. 3.2 a feed back system of damage is shown.

### 3.1 Buckling Caused by Compression

Figure 3.1.1 shows buckling damage in a wide panel (4000 mm × 800 mm) at the connection between a horizontal stringer and a strut in a fore peak tank. Here the buckling happened first which then caused the crack later.

In this case the load was the water pressure from the outside. Assuming the water head of  $1.35 d$  ( $d$  is full load draft) above base line the actual water head at the horizontal stringer level is 5 m. If the side shell area supported by the strut is 10 m (breadth) × 5.2 m (depth) = 52 m<sup>2</sup>, then the load supported by the buckled part is 52 m<sup>2</sup> × 5 tf/m<sup>2</sup> = 260 tf = 2.55 × 10<sup>6</sup> N. And the sectional area at the buckled part



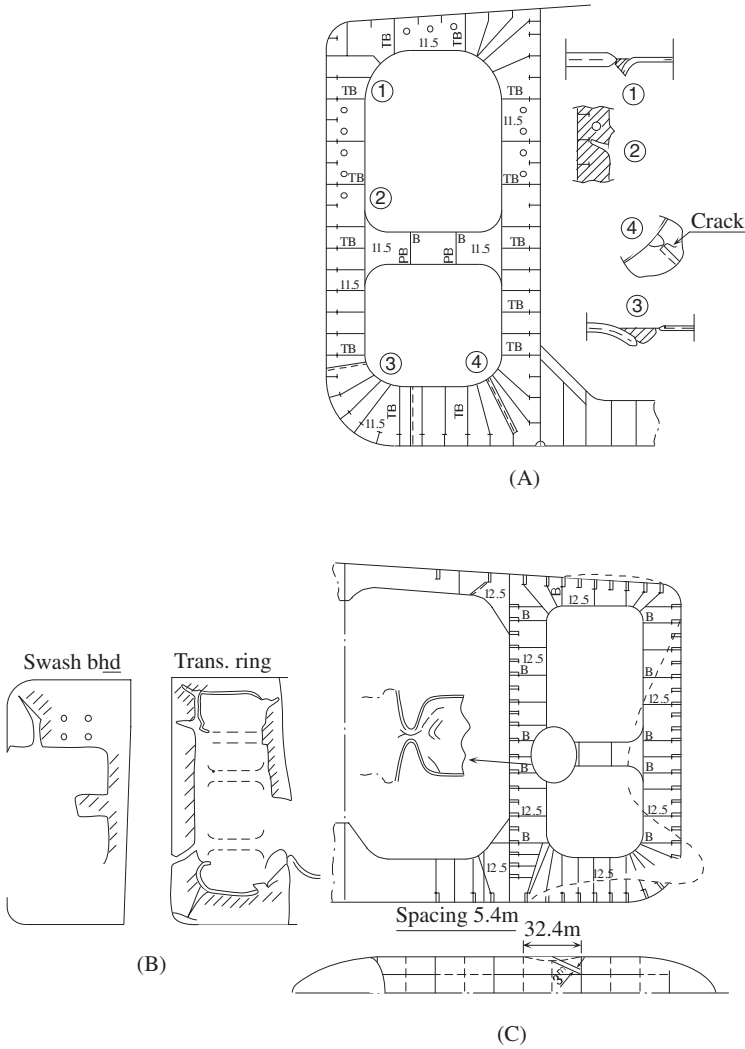


Fig. 3.1 Examples of damages on transverse members

is  $224\text{cm}^2$  (face plates) +  $230\text{cm}^2$  (web plate) =  $454\text{cm}^2$ . Accordingly the compressive stress at the buckled section  $\sigma_w$  is  $2.55 \times 10^6 \text{N} / 454\text{cm}^2 = 56 \text{MPa}$ .

On the other hand the critical buckling stress of this panel  $\sigma_{cr}$  is calculated as follows with the assumption that the rectangular plate is simply supported at all edges.

$$\sigma_{cr} = K \frac{\pi^2 E}{12(1 - \nu^2)} \left(\frac{t}{b}\right)^2 = 39 \tag{3.1.1}$$

$$\therefore \sigma_{cr} \leq \sigma_w$$

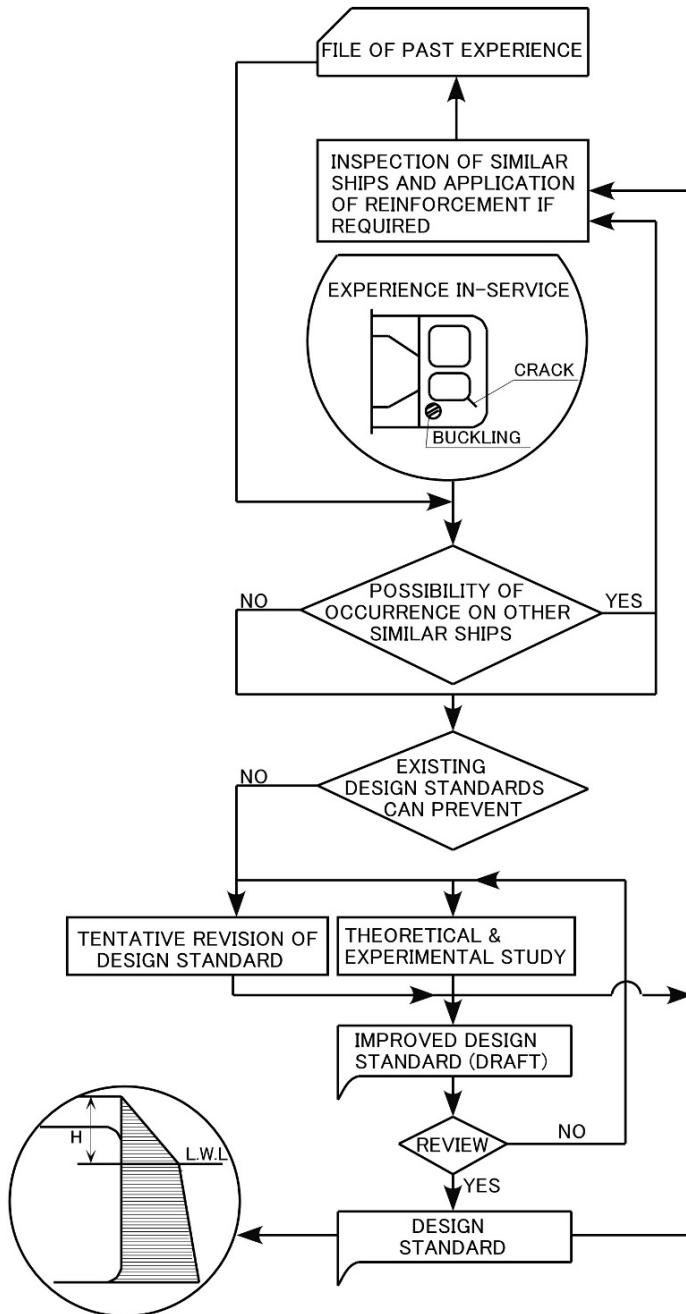


Fig. 3.2 Feedback of experiences in service

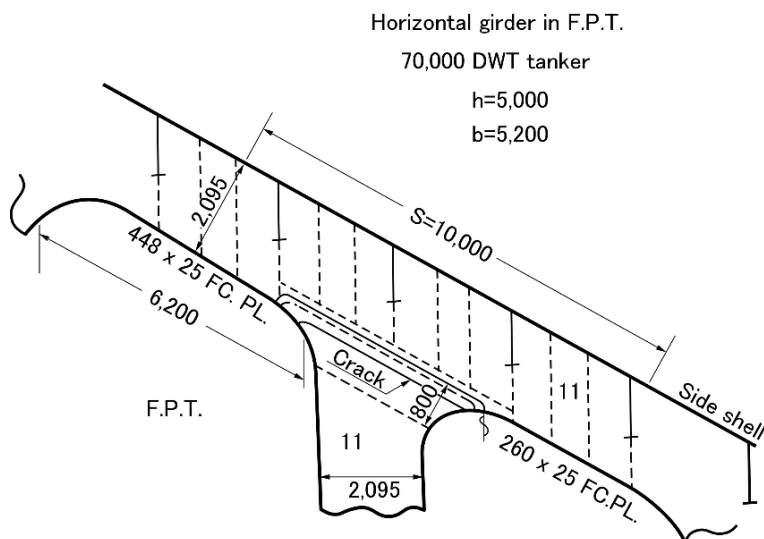


Fig. 3.1.1 Buckling due to compression

It is clear that the possibility of buckling existed.

Based on this buckling damage the design standard of  $\sigma_{cr}/\sigma_w \geq 2.0$  was established. Similar parts to which attention should be paid are the “ends of cross tie”, “the lower parts of vertical web on longitudinal bulkheads in wing tanks” and “the upper deck between the hatches of ore carriers”.

In applying this design standard special attention should be paid to the following two points:

- (1) The load is to be calculated with a water head of 1.35  $d$ .
- (2) The critical buckling stress is to be calculated assuming that the rectangular plate is simply supported at all edges.

The design standard of  $\sigma_{cr}/\sigma_w \geq 2.0$  is only valid with a unified load and unified calculation method.

When similar buckling happens after applying this design standard, the safety factor of 2.0 is to be increased.

## 3.2 Buckling Caused by Bending

The buckling shown in Fig. 3.2.1 is caused by the compression due to the bending of the horizontal girder on the transverse bulkhead.

Assuming that the water head at the water pressure test is 2.45 m above the upper deck, the bending stress of this part is about 100 MPa. On the other hand  $\sigma_{cr}$  is 75 MPa. In this case also  $\sigma_{cr} \leq \sigma_w$  and there exists the possibility of buckling.

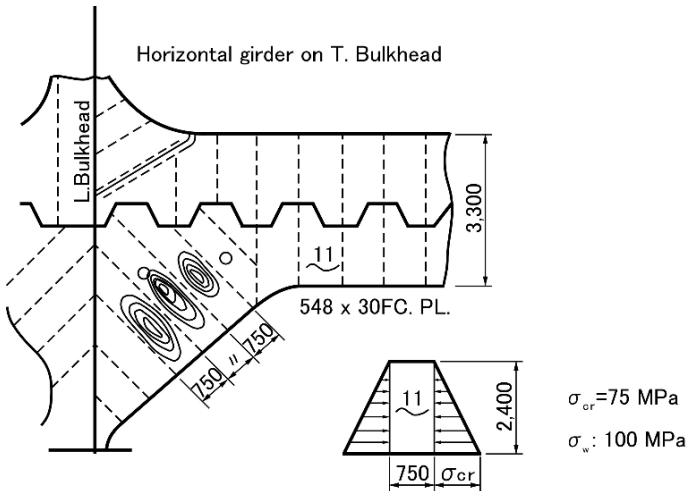


Fig. 3.2.1 Buckling due to bending

The horizontal girder on the transverse bulkhead is designed to sustain a bending stress of about 100 MPa, and the design standard of  $\sigma_{cr} \geq 150 \text{ MPa}$  was established.

The safety factor is 1.5 which is smaller than 2.0 mentioned in Sect. 3.1 because the water pressure on the transverse bulkhead can be estimated more accurately than the water pressure on the side shell plate.

Parts in which similar attention should be paid are “bracket parts of horizontal girders in the fore peak tank”, “the corner of the bottom transverse at the lower part of the vertical web of longitudinal bulkhead in the wing tank”, etc.

### 3.3 Buckling Caused by Shearing

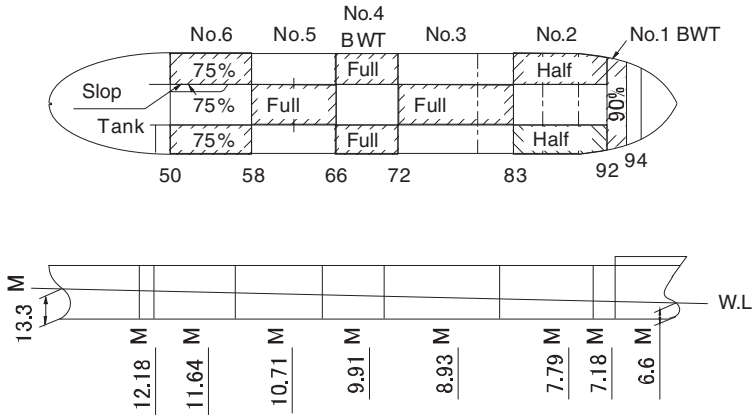
Figure 3.3.1 shows buckling on the bottom transverse of a tanker. The buckling pattern takes a diagonal direction in a rectangular plate and indicates that the buckling is caused by the shearing force as explained in Sect. 2.1. In this case the free edge of a slot buckled first.

The critical buckling stress of a plate with a slot is not clear theoretically and an experiment was carried out on a 3/10 scale model of the bottom transverse of 100,000 DWT tanker as shown in Fig. 3.3.2 [5]. Two models were tested, one had the original depth of the slot and the other had a 1.5 times deeper slot than that of the original.

The buckling started at the corner of the free edge of the slot in both cases. Actually the buckling was generated not in the vicinity of the slot but in the full depth of the web, so the shearing stress was calculated by dividing the shearing force by the full depth of the web.

108,600DWT tanker

a) Test condition



b) Bucklings (No. 3 & No. 5 wing tanks)

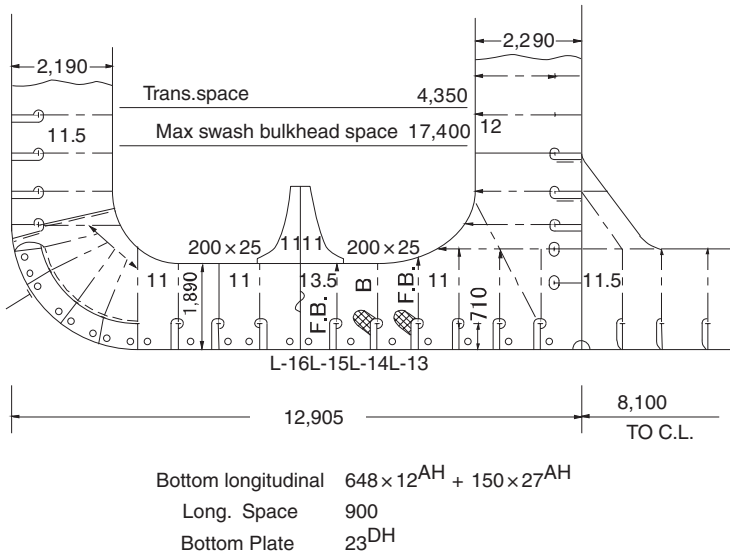


Fig. 3.3.1 Example of buckling on bottom transverse

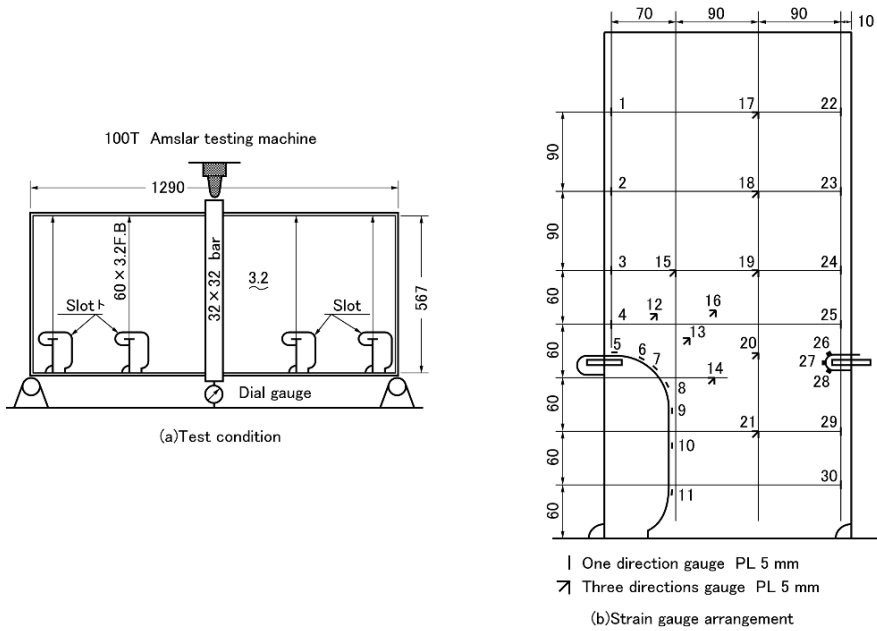


Fig. 3.3.2 Buckling tests of panels with slots

The above results are shown in Fig. 3.3.3 with the ratio of the slot depth to the web depth on the horizontal axis and the lower ratio of the critical buckling stress on the vertical axis. The shearing critical buckling stress of a plate without a slot is calculated with the assumption of the boundary in a simply-supported condition.

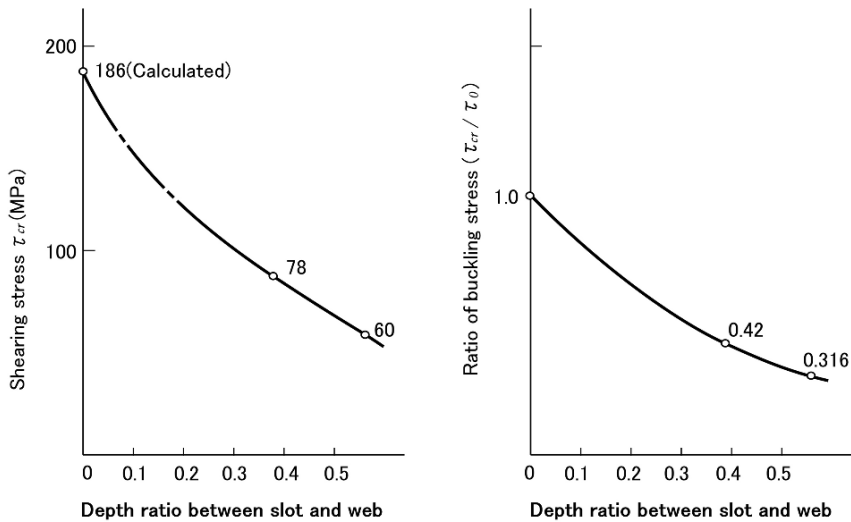


Fig. 3.3.3 Buckling stress of web plate and size of slot

Figure 3.3.3 shows that in the range where the ratio of slot depth and web depth is 0.3–0.5, the value of the shearing critical buckling stress decreases in a straight line with an increase in this ratio.

In the model shown in Fig. 3.3.2 the orientation of the slot is not symmetrical for the centre bar and the buckling happened only at right side slots. This is a simple but very important finding. The buckling is caused only by compression not by tension. The free edge of the slot in the left side of the center bar has tensile stress and has no buckling in this case. In designing a slot, the designer should pay attention to the direction of the shearing force and decide the direction of the slot which does not cause any compression at the free edge. The direction of the slot does not affect the fabrication cost and a clever designer can design a sound slot without any extra expense.

By means of Fig. 3.3.3 the shearing critical buckling stress  $\tau_{cr}$  can be obtained for a rectangular plate with a slot. The actual working shearing stress  $\tau_w$  is calculated with the following assumptions:

- (1) Water pressure is supported by the bottom transverse.
- (2) The bottom transverse in a wing tank is fixed at both ends, the longitudinal bulkhead and the side shell.
- (3) The relative displacement between the longitudinal bulkhead and the side shell is the same value as the shearing deflection of the side shell.

Applying the above method, the calculations for several ships were carried out and the results are shown in Fig. 3.3.4 in which a proposed design standard is shown by the full line. The design standard without a slot is as follows:

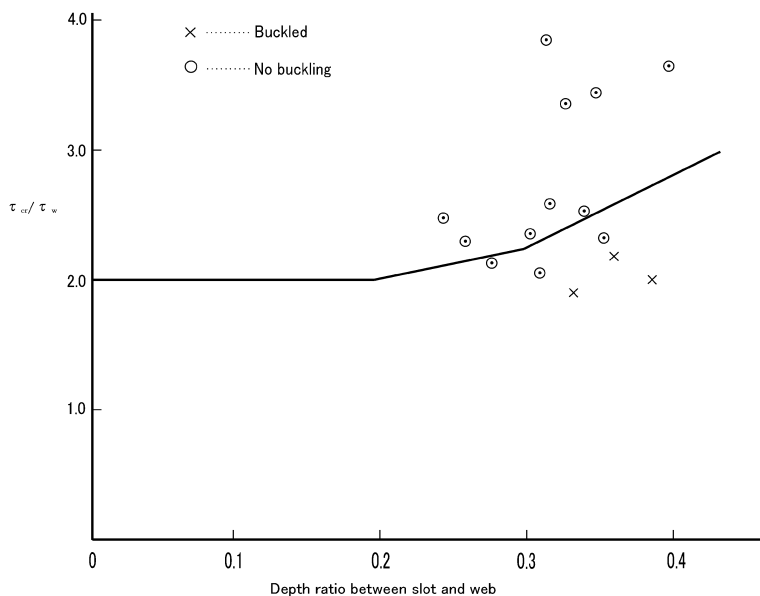


Fig. 3.3.4  $\tau_{CR}/\tau_w$  on bottom transverse web

$$\frac{\tau_{cr}}{\tau_w} \geq 2.0 \quad (3.3.1)$$

where there is a slot the standard is divided into two parts as follows:

$$\frac{\tau_{cr}}{\tau_w} \geq \frac{20}{9}\lambda + \frac{14}{9} \quad \text{for } 0.2 \leq \lambda \leq 0.3 \quad (3.3.2)$$

$$\frac{\tau_{cr}}{\tau_w} \geq \frac{400}{63}\lambda + \frac{20}{63} \quad \text{for } 0.3 \leq \lambda \leq 0.4 \quad (3.3.3)$$

where  $\lambda$  is the ratio of slot depth to web depth.

It is clear from Fig. 3.3.4 that the design standards shown by Eqs. (3.3.1), (3.3.2) and (3.3.3) can avoid the buckling due to the shear forces, shear buckling, in the web plate.

### 3.4 Buckling Caused by Concentrated Loads

Figure 3.4.1 shows buckling of a web plate of a vertical web on a longitudinal bulkhead. In this case no web stiffener was fitted where the buckling occurred.

In smaller ships, a web stiffener is provided alternately or on every third longitudinal stiffener. Smaller ship practices are no longer effective for larger ships. The load transmitted from the longitudinal stiffener is big enough to cause buckling of the web where no web stiffener is fitted.

With the water head at the water pressure test (2.45 m above upper deck) the load transmitted from the longitudinal stiffener to the web plate is calculated and shown in Fig. 3.4.1. From this, it can be said that in cases of 11 mm or 11.5 mm thickness of the web plate the following values of the loads can cause buckling:

- (1) alternately arranged web stiffener — 441 kN
- (2) every third arranged web stiffener — 294 kN

The critical buckling stress by compression  $\sigma_{cr}$  is expressed as follows.

$$\begin{aligned} \sigma_{cr} &= K \left( \frac{t}{b} \right)^2 \\ \therefore K &= \sigma_{cr} \left( \frac{b}{t} \right)^2 = \frac{F}{bt} \left( \frac{b}{t} \right)^2 = \frac{Fb}{t^3} \end{aligned} \quad (3.4.1)$$

where

$t$ : thickness of web plate

$b$ : breadth of edge on which load is applied

In case (1) for the alternately arranged web stiffener,  $F = 441$  kN,  $t = 11$  mm and assuming  $b = 0.8$  m  $K$  is calculated as follows.



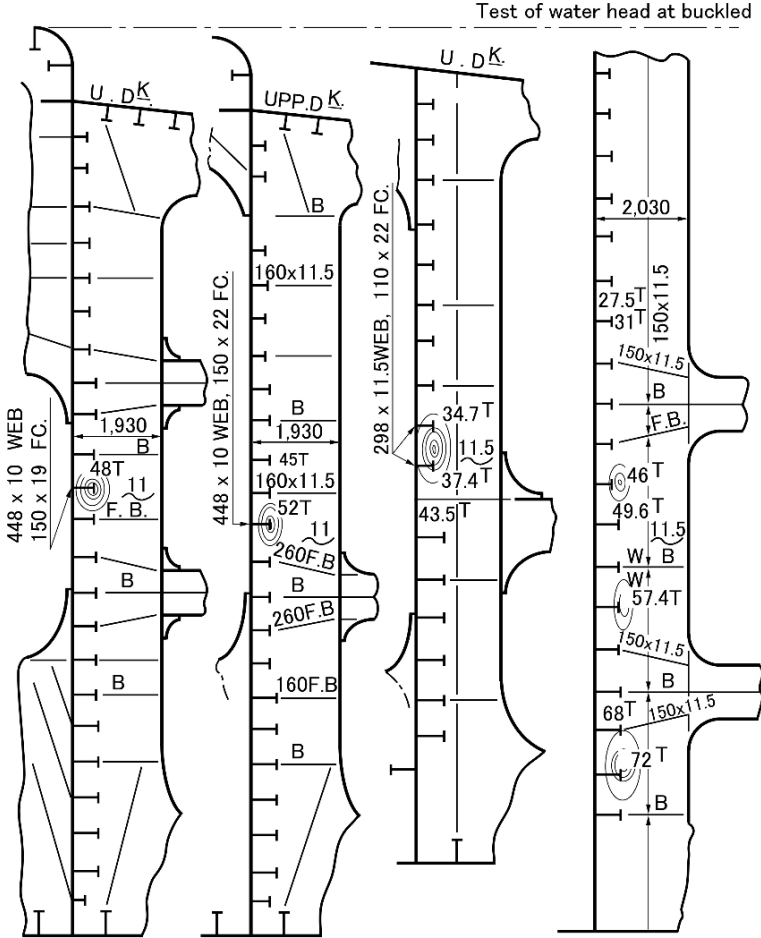


Fig. 3.4.1 Buckling of web due to concentrated load

$$K = \frac{441 \text{ kN} \times 0.8 \text{ m}}{(11 \text{ mm})^3} = 265 \text{ kN/mm}^2$$

$$\therefore \sigma_{cr} = 265 \left(\frac{t}{b}\right)^2 \text{ kN/mm}^2 \tag{3.4.2}$$

where

- t*: thickness of web plate
- b*: space of longitudinal stiffeners

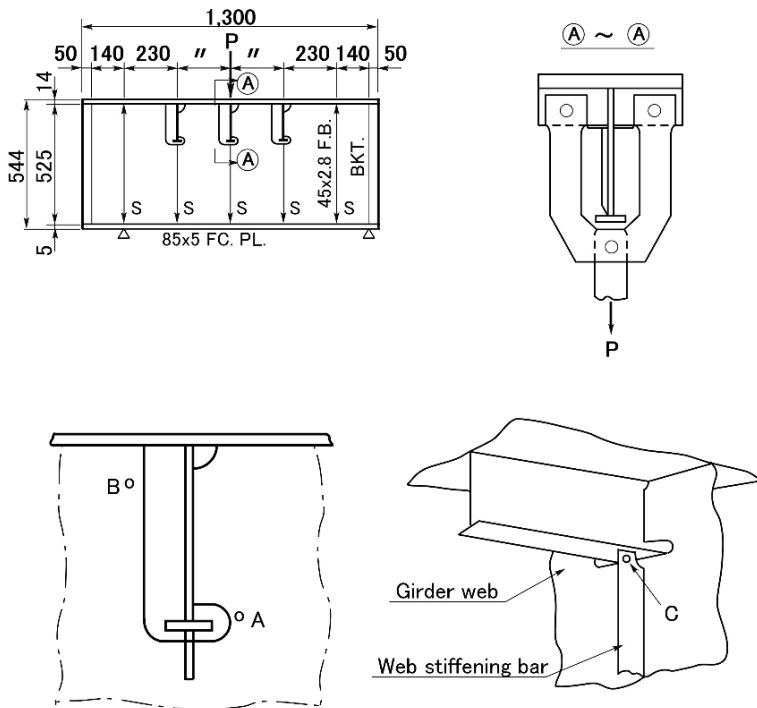
In case (2) for web stiffeners on every third longitudinals,  $F = 294 \text{ kN}$ ,  $t = 11.5 \text{ mm}$  and assuming  $b = 0.8 \text{ m}$   $K$  is calculated as follows:

$$K = \frac{294 \text{ kN} \times 0.8 \text{ m}}{(11.5 \text{ mm})^3} = 155 \text{ kN/mm}^2$$

$$\therefore \sigma_{cr} = 155 \left(\frac{t}{b}\right)^2 \text{ kN/mm}^2 \tag{3.4.3}$$

$\sigma_{cr}/\sigma_w \geq 1.5$  will be the design criteria then the necessary web plate thickness is obtained from Eqs. (3.4.2) and (3.4.3).

Hull structure designers often apply the equation of critical buckling stress of uniform loading to the buckling caused by a concentrated load. This is not a correct way because the buckling pattern caused by a uniform load and a concentrated load is quite different. Only in cases where the buckling pattern is similar is it correct



Buckling load			Ultimate load
A	B	C	
15 T.000	16 T.600	10 T.000	18 T.500

Fig. 3.4.2 Buckling test on web stiffening bar

to apply this equation. It is very important for hull structure designers to keep in mind that a critical buckling stress corresponds to each buckling mode in the same way as a natural frequency corresponds to each vibration mode. In the above cases where the buckling pattern seems to be similar to that due to a uniform load, Equations (3.4.1) was applied.

Bigger loads from a longitudinal stiffener sometimes cause buckling at the root of web stiffener. To establish the maximum load which can be supported by a web stiffener, an experimental test was carried out using a 1/4 scale model of the structure as shown in Fig. 3.4.2. In the model test the web stiffener started to buckle at point C at the load of 98 kN which corresponds to 1570 kN ( $98 \text{ kN} \times 4^2$ ) in the actual structure.

### 3.5 Cracks Around Slot

#### 3.5.1 Cracks of First Generation [8]

Buckling is caused by compression and a crack is caused by tension. In a discussion of the strength of a structure it is very important to make clear the magnitude and the direction of the force to be applied on the structure. Most of the cracks which occur in a web plate were around a slot, which is a cutout in the web plate to allow the passage of a longitudinal stiffener at the intersection of it and the web plate, as shown in Fig. 3.5.1. The load, from the water pressure, is supported firstly by the longitudinal stiffener then transmitted to the web plate through the welded connection between the longitudinal stiffener and the web plate. Many cracks happened around the welded connection between the longitudinal stiffener and the web plate where there is a neck in the load transmission. In addition to the above the slot deforms and generates additional stress at the root of the web stiffener from shearing force.

The points where cracks occur are shown in Fig. 3.5.1 as No. 1, No. 2, No. 3, No. 4 and No. 5. No. 1 crack, which happened at the root of the web stiffener, is the most common and sometimes is accompanied by other cracks. It is considered that the No. 1 crack happens first then other cracks follow.

As a result of leaving these cracks they grow and become extensive, for example No. 2 and No. 4 cracks cause the loss of the connection between web plate and the side shell plate as shown in Fig. 3.5.2. And No. 5 crack goes into the side shell plate which causes oil leakage in the vicinity of a tank. The pattern of this crack on side shell plate looks like a flying bird spreading her wings which is why it is called the flying bird crack as shown in Fig. 3.5.2.

As it will take a while for these cracks to grow to dangerous ones, sound inspection and early repair can prevent major damage. However from the maintenance viewpoint it is important to prevent such cracks.

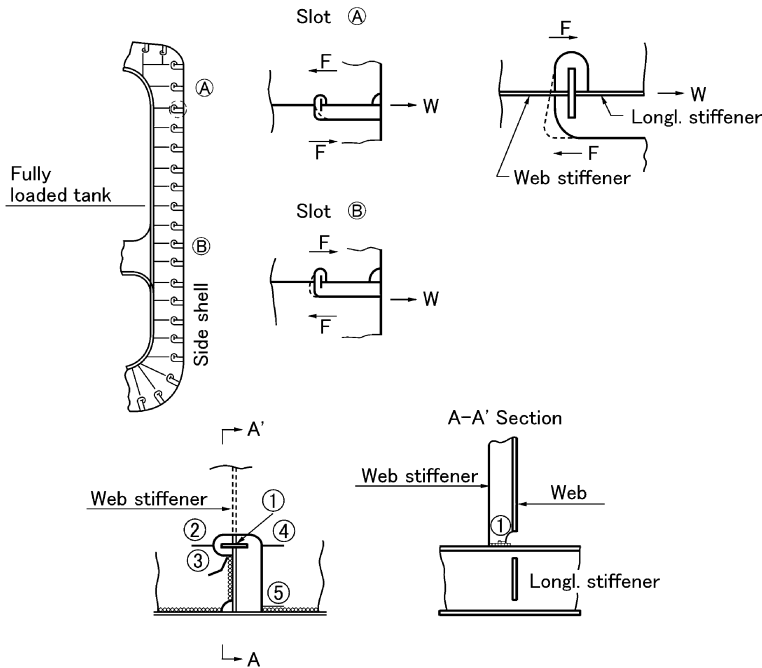


Fig. 3.5.1 Detail of slot and example of crack around slot

To prevent cracking around a slot it is most important to prevent crack No. 1 which happens at the connection between a web stiffener and a longitudinal frame. For the prevention of crack No. 1 a stress calculation method and the allowable stress are decided as follows.

The water head of the inside pressure is  $D + 2.45$  m where  $D$  is the ship's depth, and the outside pressure is  $0.32d_f$  where  $d_f$  is full draft. For the longitudinal and the transverse bulkheads the water head is  $D + 2.45$  m assuming the adjacent tank is empty.

Then the load  $W$  transmitted from the longitudinal stiffener to the web plate is expressed by the following equation:

$$W = \rho \times S \times l \times h_i \tag{3.5.1}$$

where

- $\rho$ : specific gravity of the liquid
- $S, l$ : spaces of longitudinal and web frame
- $h_i$ : water head at the longitudinal stiffener

The shearing force is to be calculated as a both ends fixed girder. The stress  $\sigma_{AP}$  at the bottom of the web stiffener caused by the load  $W$  is given by the following equation:

Side shell vertical web

F. 58, 59, 60, 61, 62, 63

Tank arrangement

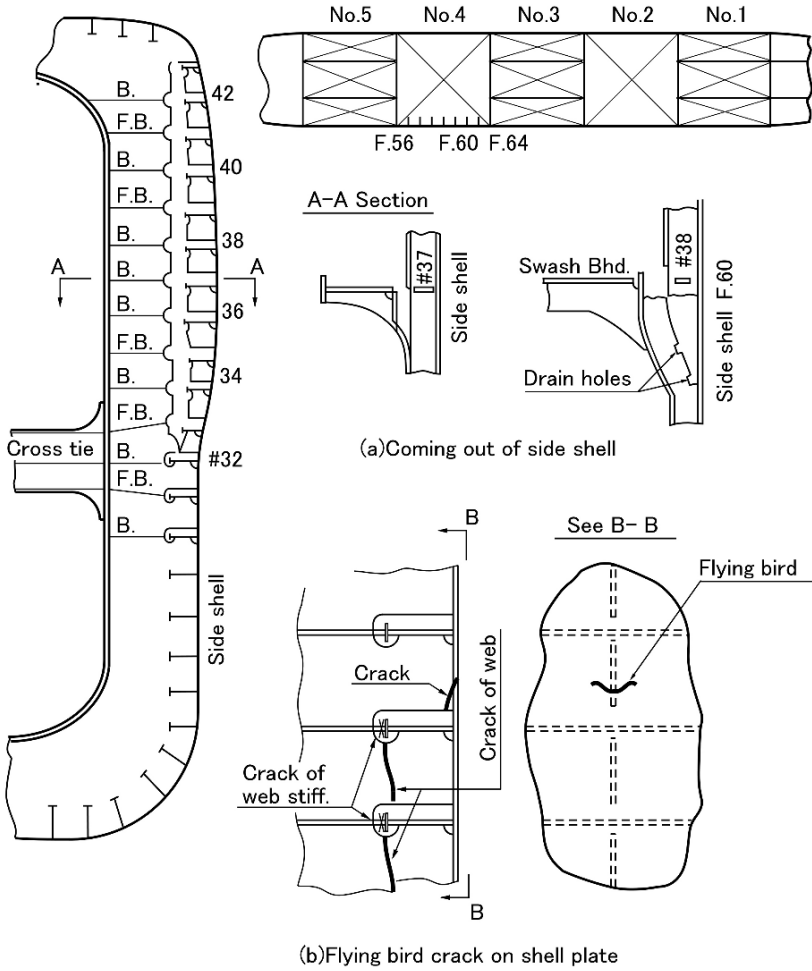


Fig. 3.5.2 Example of cracks developed around slot

$$\sigma_{AP} = \frac{W}{A_1} \tag{3.5.2}$$

where

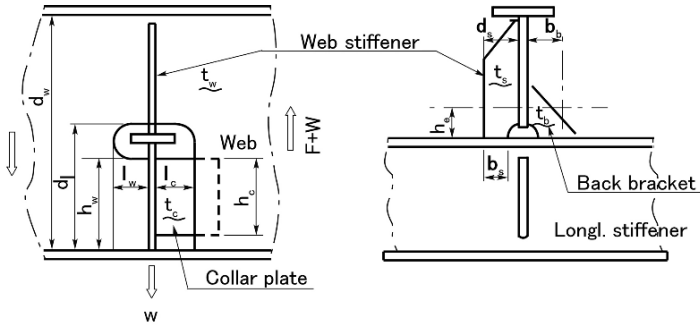
$$A_1 = Ct_s b_s + \alpha t_w h_w + \beta t_c h_c$$

$t_s, b_s, t_w, h_w, t_c, h_c, h_e, l_w$  and  $l_c$  are shown in Fig. 3.5.3.

$$\alpha = \frac{Gh_e}{El_w}, \beta = \frac{Gh_e}{El_c}$$

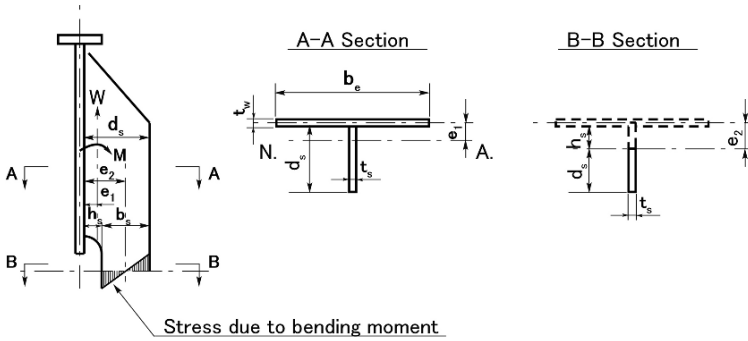
$C = 2$  where bracket is fitted.

$C = 1$  where no bracket is fitted.



$b_0$  ... Effective breadth of back bracket  
 $h_e$  ... Effective length of back bracket and web stiff.

(a) Structural detail around slot



(b) Detail of web stiffener

Fig. 3.5.3 Detail of structure around slot

The stress  $\sigma_{AF}$  at the bottom of the web stiffener caused by the shearing force  $F$  is given by the following equation:

$$\sigma_{AF} = \frac{F}{A_2} \cdot \frac{t_w h_w - t_c h_c}{A_1} \quad (3.5.3)$$

where

$$A_2 = (d_w - d_l)t_w + t_c h_c$$

$d_w$  and  $d_l$  are shown in Fig. 3.5.3.

By putting  $W$  and  $F$  into Eqs. (3.5.2) and (3.5.3),  $\sigma_{AP}$  and  $\sigma_{AF}$  can be obtained simplifying  $\alpha$  and  $\beta$  as follows.

$h_e$  is the effective height where the axial force is supported by the web stiffener and is assumed to be at least equal to the breadth  $b_s$  of the web stiffener at the bottom. Then

$\alpha = \frac{Gb_s}{El_w}$  is obtained. For actual stiffeners  $\alpha$  is calculated and the results are as follows:

For a T section stiffener  $\alpha$  is  $0.39 \sim 0.7$ , say 0.5.

For a L section stiffener  $\alpha$  is  $0.77 \sim 1.9$ , say 1.0 because of smaller  $l_w$  than that of the T section. In the case of a slot closed by a collar plate  $\alpha$  is to be 1.0 because of continuous web plate and added rigidity of the shell plate. And  $\beta$  is also simplified to be 1.0 for the same considerations.

Applying the above simplified method on the slots of ships in service,  $\sigma_{AP}$  and  $\sigma_{AF}$  are plotted in Fig. 3.5.4 from which the following results are observed.

In the case of a web stiffener only, the border line of no crack is  $\sigma_{AP} + \sigma_{AF} \leq 70$  MPa, which is the mean stress at the bottom of the web stiffener, and the maximum stress including bending effect and stress concentration will be 210 MPa.

In the case of a web stiffener and back bracket, the border line of no crack is  $\sigma_{AP} + \sigma_{AF} \leq 185$  MPa.

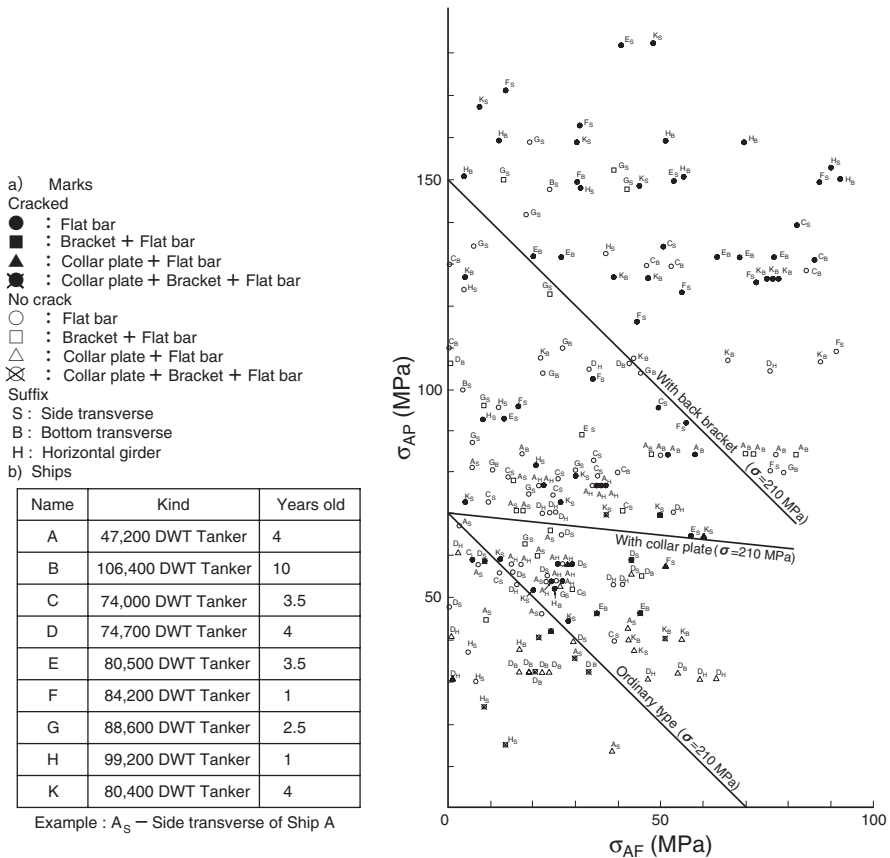


Fig. 3.5.4 How to decide allowable stress for web stiffening bar

In the case where a collar plate is fitted  $\sigma_{AF}$  is small, less than 10 MPa, which means the shearing force can have very little affect.

First the calculation method of the stress of the web stiffener at the bottom is established and by applying this method to the slots of many ships in service, some of which cracked and others did not, Fig. 3.5.4 was prepared. The empirical reliable design is established as the above, that is, firstly an analytical method is decided then by analyzing many data an allowable limit is decided. By applying the empirical reliable design method, a similar level of reliability can be kept for similar conditions.

From Fig. 3.5.4 the allowable limit, in this case it is the design standard, is as follows.

(a) web stiffener only:

$$\sigma_{AP} + \sigma_{AF} \leq 70 \text{ MPa}, \quad \text{maximum stress 210 MPa} \\ \text{(stress concentration factor 3.0)}$$

(b) web stiffener and back bracket:

$$\sigma_{AP} + \sigma_{AF} \leq 150 \text{ MPa}, \quad \text{maximum stress 210 MPa} \\ \text{(stress concentration factor 1.5)}$$

Figure 3.5.4 shows the allowable limit will be 185 MPa, but to have similar maximum stress as in case of (a) 150 MPa is adopted as a design standard.

(c) web stiffener and collar plate:

$$\sigma_{AP} + \sigma_{AF} \leq 70 \text{ MPa}, \quad \text{maximum stress 210 MPa} \\ \text{(stress concentration factor 3.0)}$$

In this case  $\sigma_{AF} = 0$  and  $\sigma_{AP}$  plays a main role.

In the above the design standard where  $\sigma_{AP}$  and  $\sigma_{AF}$  have the same sign the effect is superposed, however as shown in Fig. 3.5.1 there is a possibility for  $\sigma_{AP}$  and  $\sigma_{AF}$  to have opposite signs. In this case  $\sigma_{AP}$  and  $\sigma_{AF}$  will cancel each other and the resultant will be smaller than  $\sigma_{AP}$ . This is a simple but important phenomena and by deciding the slot direction that  $\sigma_{AP}$  and  $\sigma_{AF}$  have opposite signs, the stress of the web stiffener at the bottom can be reduced.

However the direction of the shearing force is changed by loading conditions, outside wave load etc. and the accuracy of the shearing force calculation is poorer than that for a direct load  $W$ , then the design standard is decided as follows.

$$\sigma_{AP} + \sigma_{AF} \leq 30 \text{ MPa} \quad \text{where } \sigma_{AF} \leq -40 \text{ MPa}, \\ \sigma_{AP} \leq 70 \text{ MPa} \quad \text{where } -40 \text{ MPa} < \sigma_{AF} < 0$$

In the actual design, first  $\sigma_{AP} + \sigma_{AF}$  is calculated for the case of a web stiffener only for a given load condition. If the value of  $\sigma_{AP} + \sigma_{AF}$  exceeds the allowable value a collar plate is to be fitted. Then  $\sigma_{AP} + \sigma_{AF}$  is calculated again with a collar plate



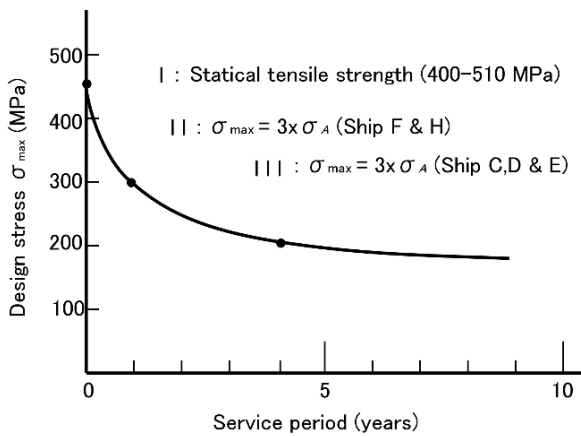


Fig. 3.5.5 Relation between service period and allowable stress

and if  $\sigma_{AP} + \sigma_{AF}$  still exceeds the allowable value a back bracket is fitted. Where  $\sigma_{AP} + \sigma_{AF}$  exceeds the allowable value for the case where a web stiffener only is fitted, then to fit a back bracket or to increase the scantling of the web stiffener is also a correct alternative, but to provide a collar plate is better because it is effective not only in reducing  $\sigma_{AP} + \sigma_{AF}$  but also in reinforcing the free edge of the slot.

The mechanism of crack generation in Fig. 3.5.1 shows that where  $\sigma_{AF}$  is negative the stress on the free edge of the slot is positive, that is tension and good for reducing buckling. The direction of the slot which reduces the stress of the web stiffener at the bottom is best in avoiding buckling. The designer should apply the best direction of the slot to prevent cracking and buckling.

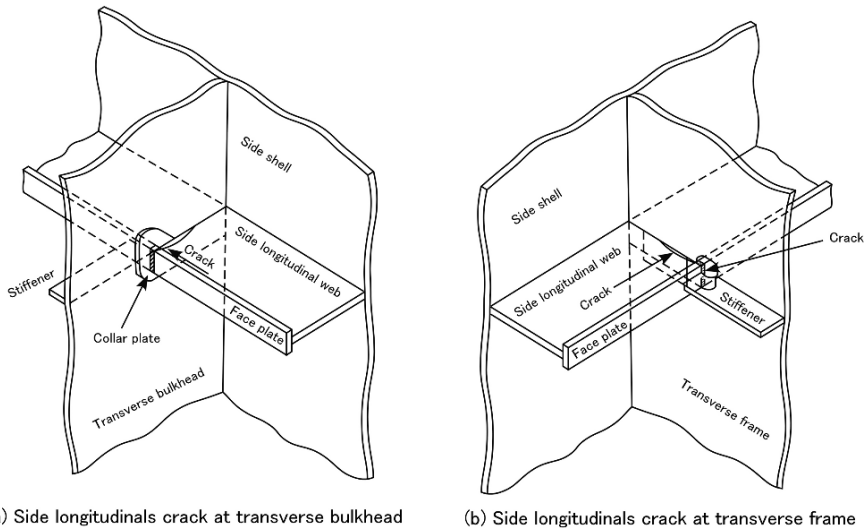
The crack at the bottom of the web stiffener is caused by fatigue. A longer service period causes more fatigue cracks. In Fig. 3.5.5 the relationship between the service period and the allowable stress is shown which is obtained from ships of different service periods. Figure 3.5.5 shows that a ship with a service period 3.5–4.0 years has no crack where  $\sigma_{AP} + \sigma_{AF} \leq 70$  MPa (maximum stress 210 MPa) and the ship with a service period of 1.0 year has no crack where  $\sigma_{AP} + \sigma_{AF} \leq 100$  MPa (maximum stress 300 MPa).

The crack at the bottom of a web stiffener is generated generally in base metal not in deposited metal.

### 3.5.2 Cracks Propagating into Longitudinals

After the 1990s, new type of cracks began to be observed around slot cutouts. These new type of cracks are characterized by propagation into the longitudinals, as shown in Fig. 3.5.6 [9].

Many of the new VLCC's in service for 2–5 years suffered these cracks, and comprehensive study was carried out [10]. The facts found were as follows:



(a) Side longitudinals crack at transverse bulkhead

(b) Side longitudinals crack at transverse frame

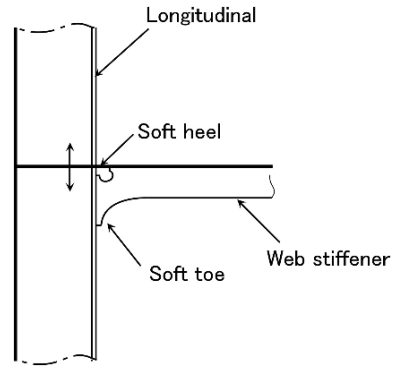
**Fig. 3.5.6** Fatigue crack propagating into longitudinals

Higher tensile steel of higher specified yield stress such as  $355 \text{ N/mm}^2$  to  $390 \text{ N/mm}^2$  was widely applied to the side longitudinals. The scantling of the longitudinals was determined by the rule formulae of the classification societies, taking into account only static stresses. The application of higher tensile steel resulted in smaller scantling and increase in exerted stress of the longitudinals, with regard to both static and fluctuating stress. Wave variable pressure is relatively large near the waterline level, and become smaller toward the bottom. On the other hand, static pressure is larger at the bottom, leading to larger scantling toward the bottom. The result was the cracks of the side longitudinals, caused by the excessive fluctuating stress near the waterline level.

Another factor, which caused these cracks, was the L type section usually applied to side longitudinals. In cargo oil tanks, accumulated sludge on the side longitudinals is a problem, and L-shaped side longitudinals were considered to be beneficial in this regard, and were widely used. However, additional longitudinal stress is exerted in the case of an L section, as explained in Sect. 1.12. This phenomenon is considered to have accelerated the crack damage.

Countermeasures were soon taken. Each classification society also studied this problem, and established new rules, which took into account not only the static stress but also the fluctuating stress caused by the waves. Moreover, further countermeasures to enhance fatigue strength were applied, such as the application of a T section to side longitudinals, soft heel and toe of the web stiffeners at the connection to the side longitudinals as shown in Fig. 3.5.7, etc. Thanks to these countermeasures, cracks of this type have been seldom observed in recent years.

**Fig. 3.5.7** Soft heel and toe of web stiffener



### 3.5.3 Cracks Around Slots due to Shear Stress on Transverses

According to Sect. 3.5.1, a collar plate is a very effective member to enhance fatigue strength, because shear stress on the transverse web is canceled from both sides of the longitudinal, and does not cause additional stress in the web stiffener. Moreover, the collar plate supports some portion of the load transmitted and reduces stress on the web stiffener.

However, if the transverse web itself was designed using higher tensile steel, and the wave variable pressure was large, high stress is exerted at the connection between the collar plate and the transverse web, i.e. near the end of the transverse web where the shear stress is large.

As countermeasures for this type of cracks, softly shaped collar plate as shown in Fig. 3.5.8, and the collar plate attached skin plate, is effective.

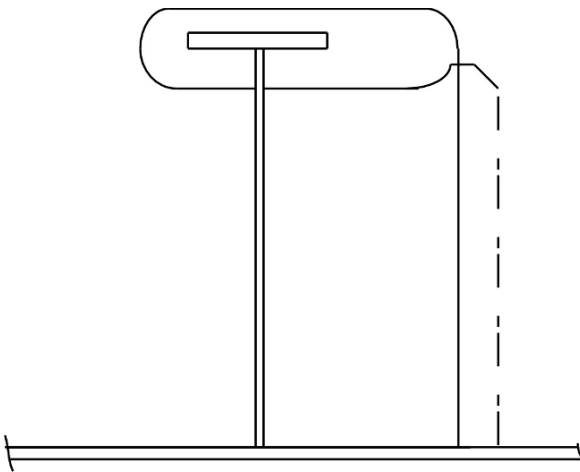


**Fig. 3.5.8** Softly shaped collar plate

# Chapter 4

## Design of Pillars

A pillar supports the axial force and generally supports the axial compression but sometimes it supports the axial tension. For axial tension, the pillar is a very effective structural member, for example 40 cm<sup>2</sup> sectional area of mild steel can support 1000 kN force ( $\sigma = 250$  MPa). Considering that the pillar sometimes supports tension, attention should be paid to the connection at both ends of the pillar.

For axial compression, buckling phenomena are important. A slender pillar can buckle at a relatively low compressive stress. As the buckling happens in the weakest direction of the pillar, the section of the pillar should be designed so as to have homogeneous strength in all directions. From this view point square or circular pillars (solid or hollow) are desirable.

The end connections of the pillar affect very much the buckling strength. Brackets are fitted usually at the end connection of a built up pillar but rarely for a circular pillar.

The cross tie in a wing tank of a tanker is this kind of the pillar. Section of the cross ties are also studied in this chapter.

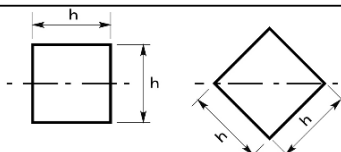
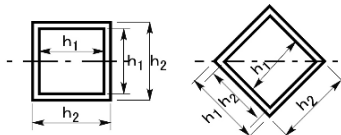
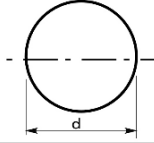
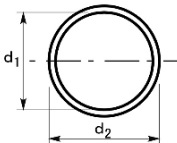
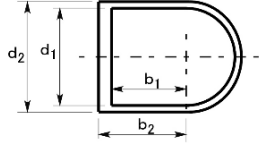
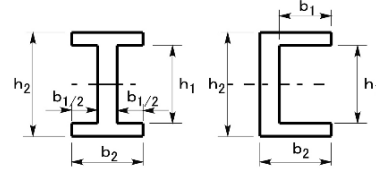
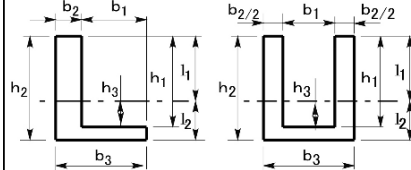
### 4.1 Slenderness Ratio of Pillars

A slender pillar under a compressive load will break by bending when the load exceeds some limit which is called buckling. The stress at buckling is decided by the slenderness ratio of the pillar. The slenderness ratio is given by  $l/k$  where  $l$  is length of the pillar and  $k$  is the radius of gyration. The radius of gyration  $k = \sqrt{I/A}$  where  $I$  is sectional moment of inertia and  $A$  is sectional area.

$k$  values for several sections are shown in Table 4.1.1 [11]. It is important to note that comparing a solid pillar with a hollow pillar of the same diameter it has smaller  $k$  than that of the hollow pillar. However the solid pillar has a bigger sectional area and can support a bigger load accordingly.

Comparing a solid circular pillar with a solid square pillar,  $k$  for the former is  $0.25 d$  ( $d$  is diameter of the pillar) and  $k$  for the latter is  $0.289 h$  ( $h$  is length of an edge) which is bigger than  $k$  for the solid circular pillar. This is reasonable because the solid square pillar has a bigger sectional area than the solid circular pillar. Then

**Table 4.1.1** I. A and k for each section

Sectional form	I	A , k
	$\frac{1}{12} h^4$	$A = h^2$ $k = 0.289h$
	$\frac{1}{12} (h_1^4 - h_2^4)$	$A = h_2^2 - h_1^2$ $k^2 = \frac{1}{12} (h_2^2 - h_1^2)$
	$\frac{\pi}{64} d^4$	$A = \frac{\pi}{4} d^2$ $k = 0.25d$
	$\frac{\pi}{64} (d_2^4 - d_1^4)$	$A = \frac{\pi}{4} (d_2^2 - d_1^2)$ $k = 0.25 \sqrt{d_2^2 + d_1^2}$
	$\frac{\pi}{128} (d_2^4 + d_1^4)$ $+ \frac{1}{12} (b_2 d_2^3 - b_1 d_1^3)$	$A = \frac{\pi}{8} (d_2^2 - d_1^2)$ $+ (b_2 d_2 - b_1 d_1)$
	$\frac{1}{12} (b_2 h_2^3 - b_1 h_1^3)$	$A = b_2 h_2 - b_1 h_1$ $k^2 = \frac{1}{12} \frac{b_2 h_2^3 - b_1 h_1^3}{b_2 h_2 - b_1 h_1}$
	$\frac{b_3 l_2^3 - b_1 h_3^3 + b_2 l_1^3}{3}$	$A = b_2 h_2 - b_1 h_1$

with the condition that the sectional area is the same, both of them are compared as follows:

$$\frac{\pi}{4} d^2 = h^2$$

$$\therefore \frac{\sqrt{\pi}}{2} d = h$$

The radius of gyration of a solid circular pillar of diameter  $d$  is  $0.25 d$ , whereas the radius of gyration of a solid square pillar with the same sectional area as the solid circular pillar is  $0.289 \times \sqrt{\pi}d/2 = 0.256d$ . From the above comparison it can be said that a solid square pillar is better than a solid circular pillar. The value of the radius of gyration for square sections is homogeneous for all axes passing through the center of gravity just as in circular sections (this is proved in Sect. 4.6).

In Fig. 4.1.1 the relation between critical buckling stress and the slenderness ratio  $\lambda (= l/k)$  is shown [11]. Here, as for the critical buckling stress for slender pillars of mild steel with both ends hinged, Euler's theoretical formula, Rankine's and Tetmajer's experimental formula, and the Tetmajer's experimental results are summarized. The required sectional area  $A$  for an I-section pillar, according to by Nippon Kaiji Kyokai (NK) is given by the following equation, and is also shown in Fig. 4.1.1.

$$A = \frac{1.52W}{2.76 - \frac{l}{k}} \tag{4.1.1}$$

If the size of a hollow circular pillar under the forecastle deck, for example, is  $l = 3\text{--}4$  m and the diameter = 200–300 mm, the slenderness ratio  $\lambda$  is 33–67. If the size of a solid circular pillar in the accommodation space, for example, is  $l = 2.5 \sim 3$  m and the diameter = 50–70 mm, the slenderness ratio  $\lambda$  is 140 ~ 240. The solid pillar is more slender than the hollow one.

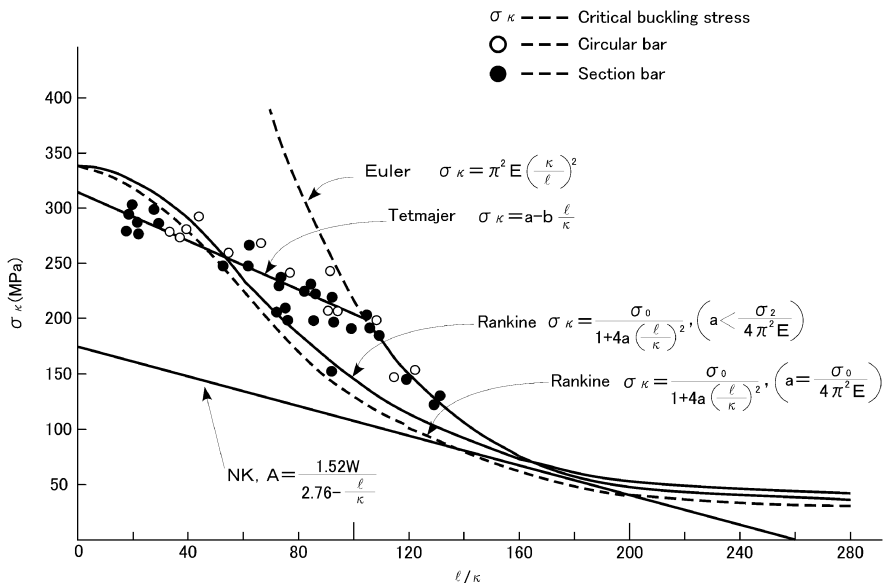


Fig. 4.1.1 Slenderness and buckling critical stress of pillar

### 4.2 Sectional Shape of Pillars

Here characteristics of hollow and built up pillars are explained. The applicable sectional shapes are shown in Table 4.1.1; D shape pillars support hatch end coaming at the hold center of a cargo ship. The circular part faces the hatch opening and on the flat part a ladder is fitted.

A pillar will buckle in its weakest direction and therefore it should have a homogeneous strength in all directions (homogeneous  $k$  for each axis through the center of gravity). A circular and a square section satisfy this requirement.

The above condition for an I-section is studied as follows. Assuming the thickness of web and flange plates is equal,  $I_x$  and  $I_y$  in Fig. 4.2.1 are given by the following equation:

$$I_x = 2at \left( \frac{d}{2} \right)^2 + \frac{td^3}{12} \tag{4.2.1}$$

$$I_y = 2 \times \frac{ta^3}{12} \tag{4.2.2}$$

Putting Eq. (4.2.1) = (4.2.2)

$$\frac{atd^2}{2} + \frac{td^3}{12} = \frac{ta^3}{6} \tag{4.2.3}$$

$$\therefore d^3 + 6ad^2 - 2a^3 = 0$$

Then  $d \approx 0.55a$  is derived. This is an I-section with wide flanges and narrow web. The sectional moment of inertia  $I_\theta$  for axis  $\theta$ - $\theta$  in Fig. 4.2.1(b) is calculated as follows. Here  $d$  is the depth of web,  $a$  is the breadth of flange and  $t$  and  $t'$  are the

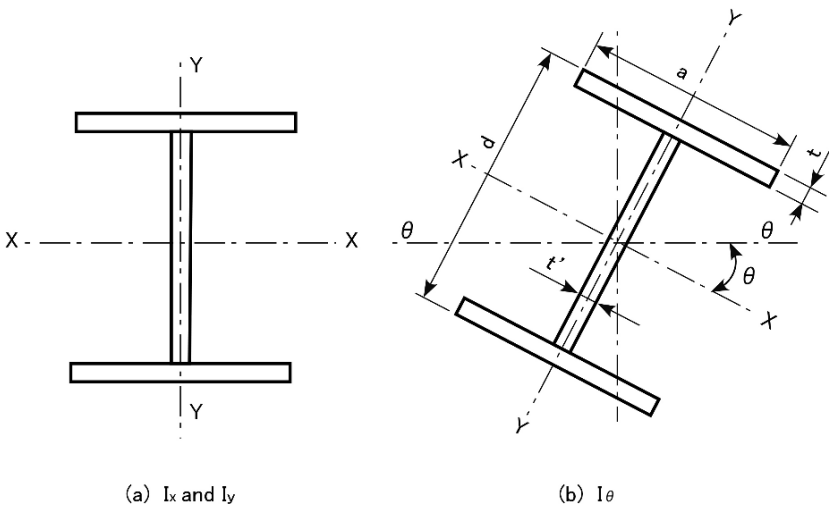


Fig. 4.2.1 Sectional moment of inertia of I shaped section

thickness of the web and flange plates respectively.

$$\begin{aligned}
 I_{\theta} &= \frac{t'd(d \cdot \cos \theta)^2}{12} + 2 \left\{ \frac{at \cdot (a \cdot \sin \theta)^2}{12} + at \left( \frac{d}{2} \cdot \cos \theta \right)^2 \right\} \\
 &= \frac{ta^3}{6} \cdot \sin^2 \theta + \left( \frac{tad^2}{2} + \frac{t'd^3}{12} \right) \cos^2 \theta
 \end{aligned} \tag{4.2.4}$$

Putting  $d \equiv \alpha a$  and  $t' = \beta t$ , the following relation can be obtained.

$$I_{\theta} = \frac{ta^3}{12} \{2 \sin^2 \theta + (6\alpha^2 + \alpha^3 \beta) \cos^2 \theta\} \tag{4.2.5}$$

From Eq. (4.2.5) it can be clear that in the condition of  $6\alpha^2 + \alpha^3 \beta = 2$ ,  $I_{\theta}$  has a constant value of  $ta^3/6$  without regard to  $\theta$ . This corresponds to the case  $\beta = 1$  and  $\alpha = 0.55$ . In conditions other than the above,  $I_{\theta}$  will change depending on  $\theta$  as shown below. Taking the differential of  $I_{\theta}$  by  $\theta$  the following equation can be obtained.

$$\begin{aligned}
 \frac{dI_{\theta}}{d\theta} &= \frac{ta^3}{12} \{4 \sin \theta \cdot \cos \theta + 2(6\alpha^2 + \alpha^3 \beta) \cos \theta \cdot \sin \theta\} \\
 &= \frac{ta^3}{12} \{2 + (6\alpha^2 + \alpha^3 \beta)\} \sin 2\theta
 \end{aligned} \tag{4.2.6}$$

From Eq. (4.2.6) it can be said that where  $\{2 + (6\alpha^2 + \alpha^3 \beta)\} < 0$ , that is  $I_x > I_y$ ,  $I_{\theta}$  has a maximum value at  $\theta = 0^\circ$  and a minimum value at  $\theta = 90^\circ$ . On the contrary where  $\{2 + (6\alpha^2 + \alpha^3 \beta)\} > 0$ , that is  $I_x < I_y$ ,  $I_{\theta}$  has a minimum value at  $\theta = 0^\circ$  and a maximum value at  $\theta = 90^\circ$ . As  $I_x$  is usually bigger than  $I_y$ , from Eq. (4.2.5)  $I_x/I_y$  is calculated as shown below.

$$\begin{aligned}
 \frac{I_x}{I_y} &= \frac{2 \sin^2 0 + (6\alpha^2 + \alpha^3 \beta) \cos^2 0}{2 \sin^2 90 + (6\alpha^2 + \alpha^3 \beta) \cos^2 90} \\
 &= \frac{6\alpha^2 + \alpha^3 \beta}{2}
 \end{aligned} \tag{4.2.7}$$

The relation obtained by (4.2.7) is shown in Fig. 4.2.2. For I-section pillar's  $I_x/I_y$  has been little affected by  $\beta$ , which is the ratio of web and flange plate thickness, but mainly affected by  $\alpha$ , which is the ratio of web depth and flange breadth. In an ordinary I-section pillar  $\alpha$  will be nearly 1.0 and  $I_x/I_y$  will be more than 3.0.

For a  $\Pi$  shape section a similar equation is derived as follows:

$$I_{\theta} = \frac{ta^3}{12} \left\{ (6\alpha^2 + \alpha^3 \beta) \cos^2 \theta + \frac{4(2\alpha\beta + 1)}{(\alpha\beta + 2)} \sin^2 \theta \right\} \tag{4.2.8}$$

Furthermore, under the condition of  $(6\alpha^2 + \alpha^3 \beta)(\alpha\beta + 2) = 4(2\alpha\beta + 1)$ ,  $I_{\theta}$  has a constant value of  $\frac{ta^3}{12}(6\alpha^2 + \alpha^3 \beta)$  without regard to  $\theta$ . This corresponds to the case  $\beta = 1$  and  $\alpha = 0.76$  which is bigger than  $\alpha = 0.55$  for an I-shape section.



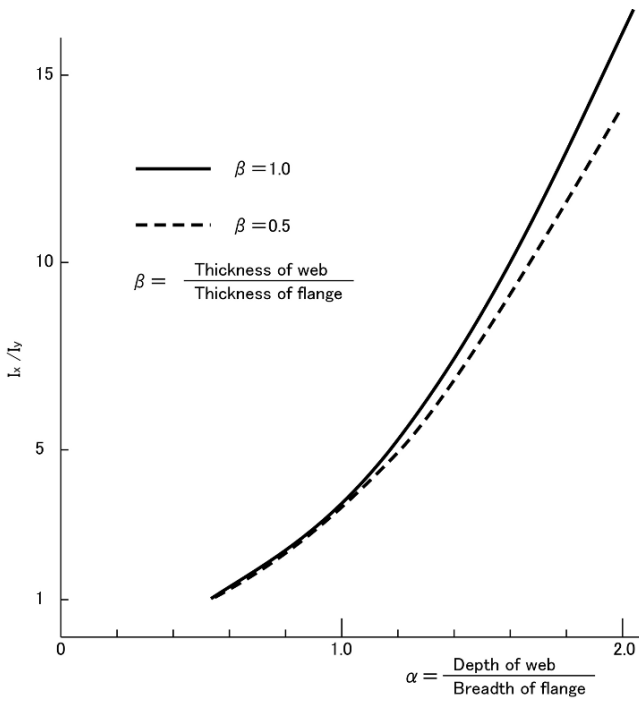


Fig. 4.2.2  $\alpha$  and  $I_x/I_y$  of I shaped section

In the case of  $\alpha > 0.76$ , in a similar way to that of an I-shape section,  $I_x$  will be a maximum and  $I_y$  will be the minimum and the ratio  $I_x/I_y$  is expressed by the following equation:

$$\frac{I_x}{I_y} = \frac{\alpha^2(\alpha\beta + 6)(\alpha\beta + 2)}{4(2\alpha\beta + 1)} \tag{4.2.9}$$

The relation of Eq. (4.2.9) is shown in Fig. 4.2.3.

Comparing Fig. 4.2.2 with Fig. 4.2.3 from the viewpoint of the  $I_x/I_y$  ratio, the  $\Pi$  shape section is better than the I-shape section. For example in the case of  $\beta = 1$  and  $\alpha = 1$ ,  $I_x/I_y = 3.5$  for the I-shape section and 1.75 for the  $\Pi$  shape section. In this case  $I_x$  is the same value for both sections therefore  $I_y$  of the  $\Pi$  shape section is twice that for the ‘‘I’’ shape section.

For equal flanges of an angle section it should be kept in the designer’s mind that in some cases of  $\theta$ ,  $I_\theta$  is smaller than  $I_x$  or  $I_y$ . Assuming the length of a flange is  $a$  and the thickness is  $t$ ,  $I_\theta$  is obtained as follows.

$$I_\theta = \frac{ta^3}{12} + \frac{ta^3}{8}(1 + \sin 2\theta) \tag{4.2.10}$$

In the case of  $\theta = 0$ ,  $I_\theta \equiv I_x$  or  $I_y$  and its value is as follows:

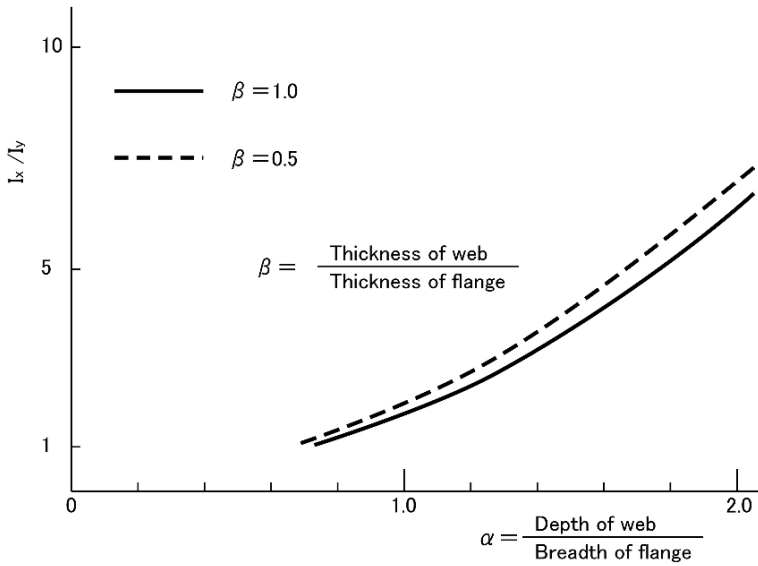


Fig. 4.2.3  $\alpha$  and  $I_x/I_y$  of  $\Pi$  shaped section

$$I_x = I_y = \frac{ta^3}{12} + \frac{ta^3}{8} = \frac{5}{24}ta^3 = 0.208ta^3$$

$I_\theta$  becomes maximum at  $\theta = 45^\circ$  and minimum at  $\theta = -45^\circ$  for which the values are as follows:

$$I_{\max} = \frac{ta^3}{12} + \frac{ta^3}{4} = \frac{1}{3}ta^3 = 0.33ta^3$$

$$I_{\min} = \frac{ta^3}{12} = 0.083ta^3$$

The minimum value is 40% of  $I_x$  and the maximum value is four times that of the minimum value.

### 4.3 Pillar Supporting Tensile Force

A pillar in a tank sometimes supports a tensile force. The tank top plate supports an upwards load when it is filled up to the overflow pipe. In this case a pillar connecting the top plate and the bottom of the tank has a tensile load.

A long superstructure of a ship deforms in the opposite direction to the main hull girder at hogging and sagging condition. In the case of hogging the upper deck has tensile strain longitudinally and the bottom of the long superstructure also has tensile strain longitudinally which means the long superstructure will bend in a sagging form. The hogging of the main hull girder and the sagging of a long superstructure causes tensile forces at the both ends of the long superstructure in the vertical

direction. In this case pillars below the upper deck at both ends of the long superstructure will suffer from tensile forces.

A pillar is stronger against tension than against compression because there is no buckling phenomenon. However attention should be paid to the connection at the top and bottom. In the case of compression the connection at the top and bottom is not so important. But in the case of tension the welded sectional area should be equivalent to the sectional area of the pillar. The doubling plate at the connection of the top and bottom of a pillar is effective in distributing the compressive load but it is weak for

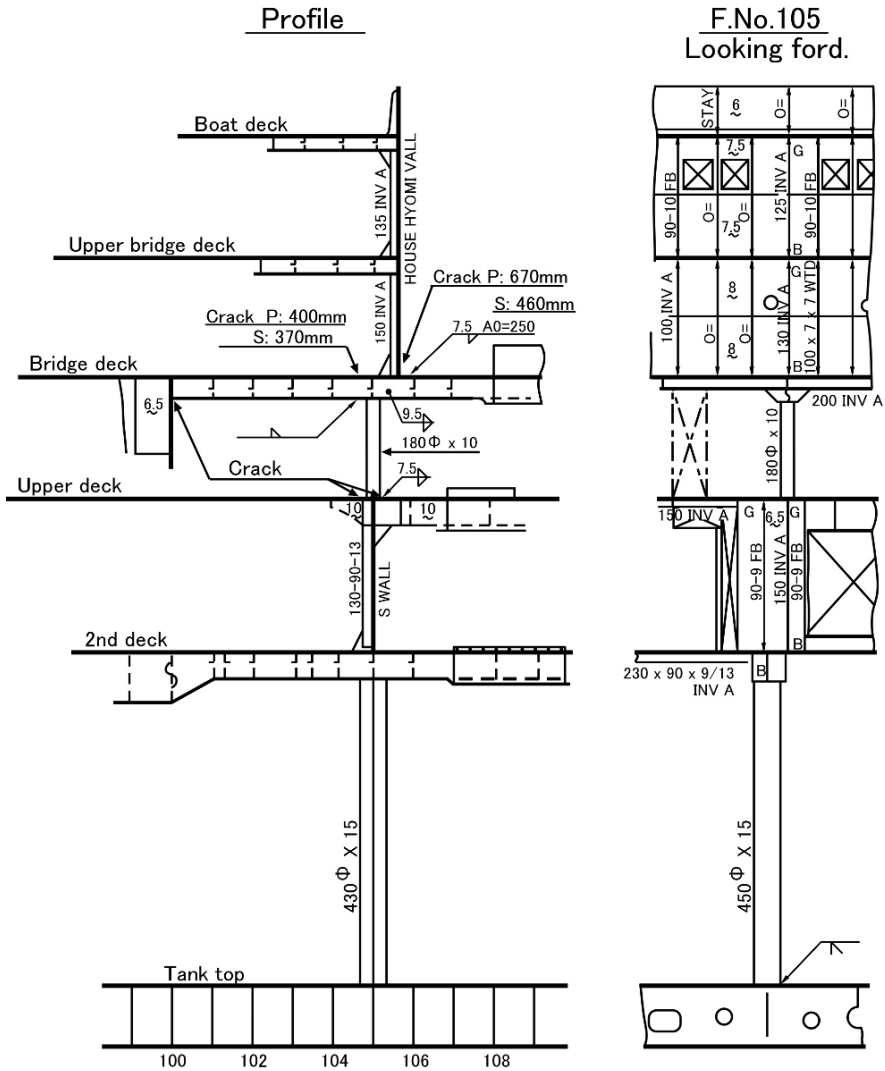


Fig. 4.3.1 Crack at fixed end of circular pillar due to tension

the tensile load. In the case of a tensile load the doubling plate should be omitted or a thick and narrow doubling plate should be fitted. The examples of cracks at the connections of the top and bottom of a pillar are shown in Fig. 4.3.1 [12].

### 4.4 Connection of Pillar at Top and Bottom

In Fig. 4.1.1 the critical buckling stress of a pillar is shown against the slenderness ratio  $\lambda (= l/k)$  in the case of hinged ends. In the case of fixed ends the critical buckling stress is higher than that of hinged ends.

In Fig. 4.4.1 the buckling modes of hinged and fixed-ended pillars are shown. The midpart  $l/2$  ( $l$  is the length of the pillar) of a fixed-end pillar has the same buckling mode as that of a hinged-ended pillar. Accordingly the critical buckling stress of the fixed-end pillar will be the same as that for the hinged-ended pillar of half length ( $l/2$ ).

As far as Euler's theoretical formula  $\sigma_k = \pi^2 E \left(\frac{k}{l}\right)^2$  can be applied,  $\sigma_k$  is inversely proportional to  $l^2$ , and the critical buckling stress of a fixed-ended pillar is four times of that for hinged-ended pillar.

The above consideration can be applied not only to a pillar but also to a beam. The deflection curve of a beam supported at both ends (length is  $2 \times l$ ) with a concentrated load  $W$  at midspan is equivalent to that of cantilever (length is  $l$ ) with a

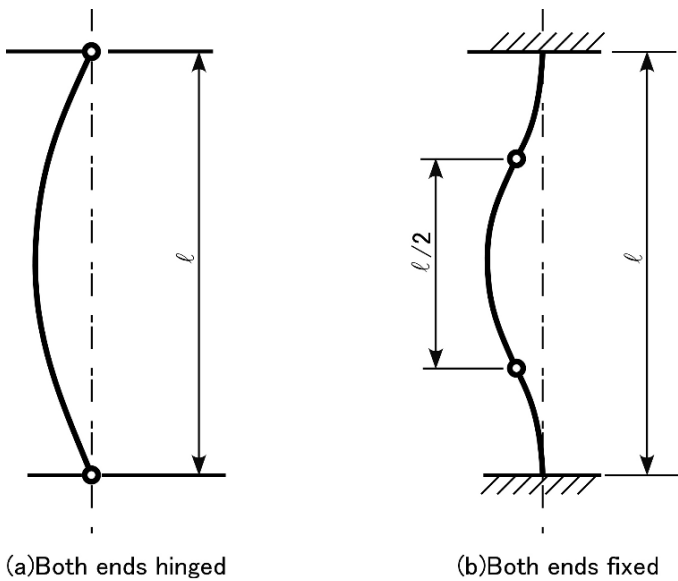


Fig. 4.4.1 Buckling mode of pillar

concentrated load  $W/2$  at the free end. The maximum bending moment in each case is  $W l/2$ .

The critical buckling stress depends on the buckling mode, and the equation for critical buckling stress for one mode cannot be applied to a different buckling mode. On the other hand, as explained above the critical buckling stress can be easily found for each buckling mode by comparing with the other mode.

In Sect. 4.2 it is explained that the circular and square sections have homogeneous sectional moment of inertia in every axis through the center of gravity, whereas I,  $\Pi$  and L sections are not homogeneous in all axes. And the ratio of maximum and minimum sectional moment of inertia is usually about 3. In practice the actual condition of the end connections of a pillar will be between hinged and fixed. By increasing the rigidity of the end connections in the weak direction, the above unbalance can be reduced.

Considering the above, bracket arrangements at the top and bottom of a pillar are proposed as shown in Fig. 4.4.2. The dotted lines in the figure mean snapped flanges because no structural member lies underneath.

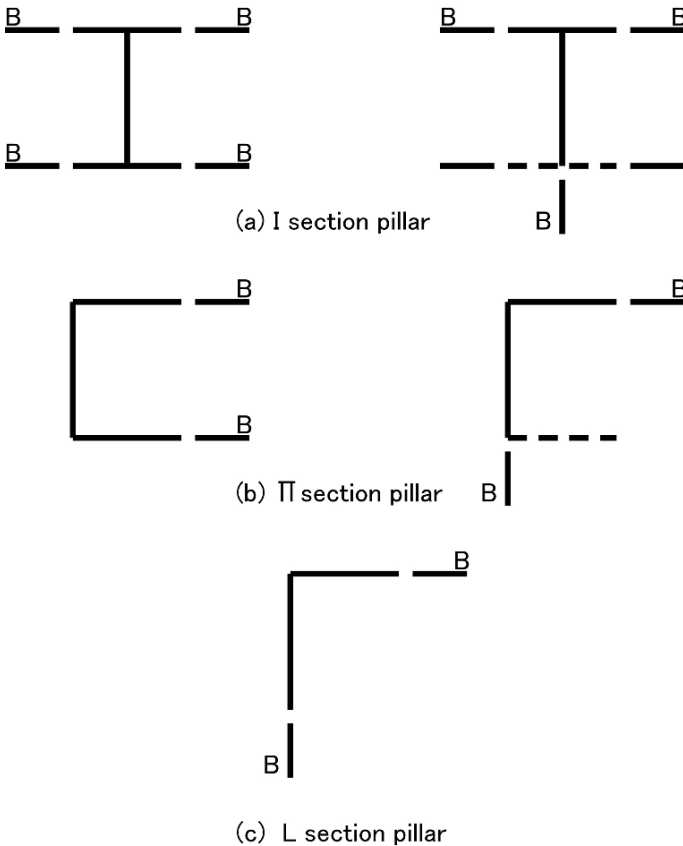


Fig. 4.4.2 Brackets at both ends of pillar

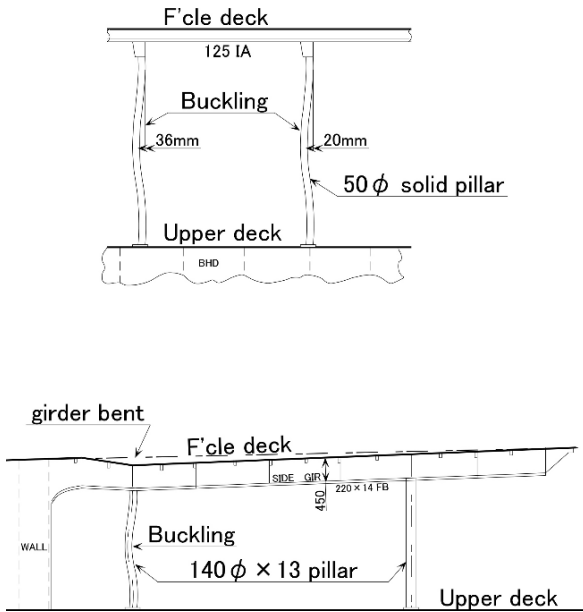


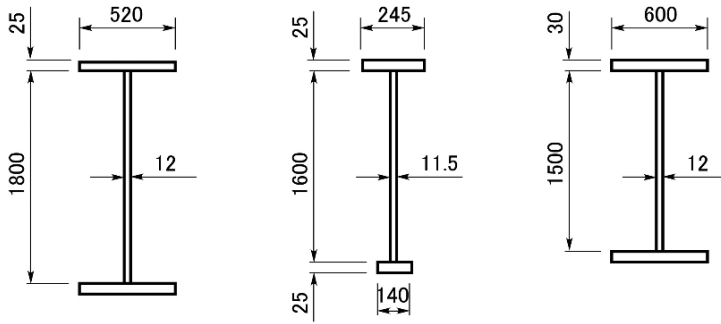
Fig. 4.4.3 Buckling of circular pillar

It is reasonable not to fit brackets on circular and square pillars. This is especially the case of brackets on a hollow circular pillar which will not work well because they are connected only to the outside of the thin plate of the pillar. In Fig. 4.4.3 examples of buckled pillars are shown [12]. From the figure it can be said that without brackets the top and bottom connections of a circular pillar have a nearly fixed condition. Therefore, a damage plan or sketch is very useful to show the actual condition, and the buckling mode and crack pattern should be shown correctly on the drawings.

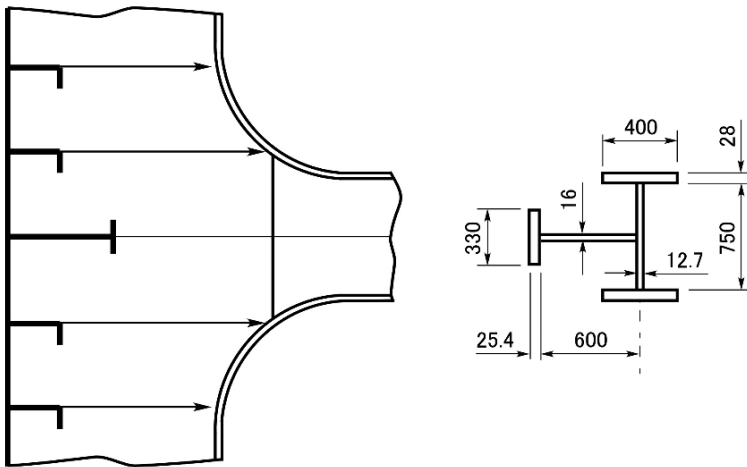
## 4.5 Cross Ties

The cross tie in a wing tank of a tanker is a kind of pillar. It supports not only compression and tension as a pillar but also as part of the transverse ring it supports bending and shearing. As explained in Sect. 4.2 a pillar should preferably have homogeneous strength for each axis through its center of gravity, however the cross tie has a deep web and narrow flanges and consequently  $I_x/I_y$  is very big as shown in Fig. 4.5.1(a), because such cross ties used to be designed as part of a transverse ring to maintain transverse strength.

However the cross ties are too weak to maintain the transverse strength and deeper cross ties will suffer from the effect of forced deformation caused by the relative displacement between the side shell and longitudinal bulkhead. To reduce the additional bending stress due to the relative displacement between side shell



(a) Section of cross tie



(b) Well balanced cross tie  
(Increased fixity in  $I_y$  by side stringer on L. Bhd)

Fig. 4.5.1 Sectional shape of cross tie

and longitudinal bulkhead, a cross tie with shallow depth is proposed and applied as shown in Fig. 4.5.1(b). To reduce the relative displacement between the side shell and the longitudinal bulkhead, a partial bulkhead at midpoint of the tank is the best way.

In the shallow web cross tie the balance between  $I_x$  and  $I_y$  is improved. Furthermore, by providing a side stringer on the longitudinal bulkhead and extending the

horizontal web plate of the cross tie, the connection at the end in the horizontal plane can be improved. These horizontal members are useful for access in a tank, killing two birds with one stone.

In Fig. 4.5.2 examples of damage to cross ties are shown, one caused by compression and another by tension. There are two kinds of construction for the connection between a cross tie and the vertical web on the side shell or longitudinal bulkhead. One is a straight face plate type with brackets and another is a curved face plate type (It is called R type.). The latter is usually applied because of good continuity of face plate and its light weight.

In the case of an R type, tension and compression are generated between the web and the face plate in the vicinity of the R part, by the tension and the compression in the cross tie as shown in Fig. 4.5.3. In the design of land structures attention is paid to this tension and compression between web and face plate in the vicinity of the R part, but hull structure designers pay very little attention to it.

Figure 4.5.3 shows the mechanism of generating tension and compression.  $P$  is the force in the flange and the normal component  $N$  to the flange is  $Pd\theta/2$ . The normal component acting on the  $ds$  part is  $2N = Pd\theta$ . If the thickness of the web plate is  $t$ , the area to support the force of  $2N$  is  $tds$ . Then the stress is

$$\frac{2N}{tds} = \frac{Pd\theta}{tds} = \frac{Pd\theta}{trd\theta} = \frac{P}{tr}$$

Putting the sectional area of the flange into  $A$  and the stress in the flange into  $\sigma$ , the relation of  $P = A\sigma$  is obtained. Finally the stress  $\sigma_w$  in the web perpendicular to the flange is expressed by the following equation:

$$\sigma_w = \frac{A\sigma}{tr} \quad (4.5.1)$$

From Eq. (4.5.1) it can be deduced that a bigger sectional area in the flange and a smaller radius results in a bigger  $\sigma_w$ . One example is calculated below.

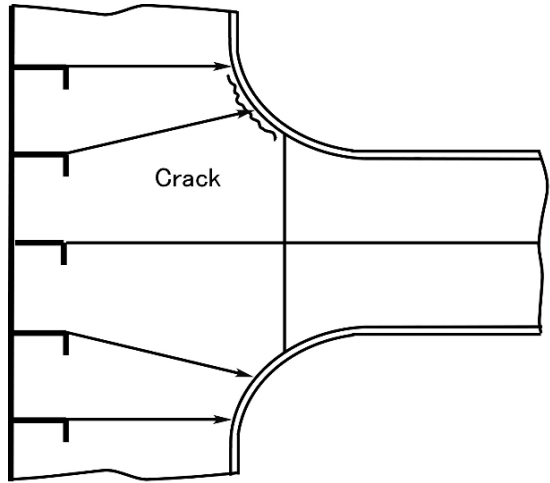
$$\begin{aligned} A &= 500 \text{ mm} \times 30 \text{ mm} \\ t &= 12 \text{ mm} \\ r &= 600 \text{ mm} \\ \sigma &= 150 \text{ MPa} \end{aligned}$$

$$\sigma_w = \frac{500 \text{ mm} \times 30 \text{ mm} \times 150 \text{ MPa}}{12 \text{ mm} \times 600 \text{ mm}} = 312 \text{ MPa}$$

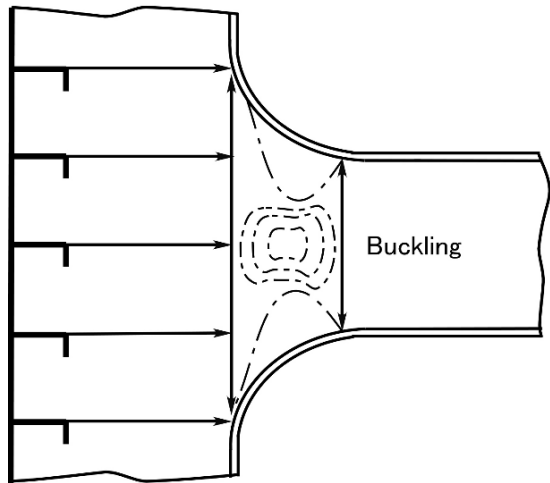
In this case  $\sigma_w$  is about twice that of  $\sigma$ . In designing R-type cross tie ends attention should be paid to the above  $\sigma_w$  and the thickness of the web  $t$  and the radius of R should be chosen to make  $\sigma_w$  equivalent to  $\sigma$ .



**Fig. 4.5.2** Buckling at end of cross tie



(a) Crack due to tension

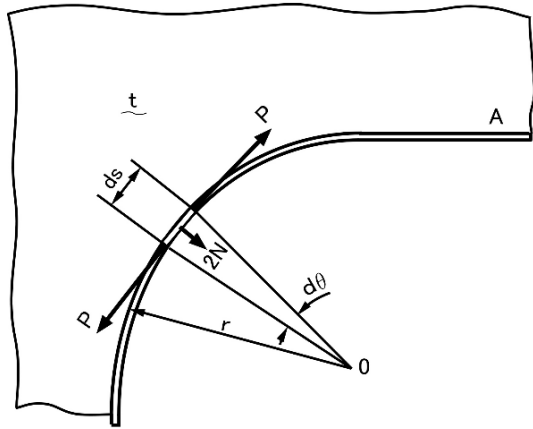


(b) Buckling due to compression

### 4.6 Radius of Gyration of Square Section

In a square section the radius of gyration is homogeneous for each axis passing through the center of gravity. This is easily understood as being based on a very important principle on the sectional moment of inertia "In a plane, the sum of the

**Fig. 4.5.3** Secondary stress at curved face plate



sectional moment of inertia for the axes crossing perpendicularly to each other is equal to the sectional moment of inertia for the axis perpendicular to the plane and passing through the cross point of the axes in the plane.”

Keeping the sectional area of the square section constant, discussion on the radius of gyration is the same as that for the sectional moment of inertia. Assuming  $I_\theta$  is the sectional moment of inertia for an axis passing through the center of gravity,  $I_{\theta+90}$  is the sectional moment of inertia for the axis crossing perpendicularly the above axis at the center of gravity, and  $I_0$  is the sectional moment of inertia for the axis perpendicular to the plane passing through the center of gravity of the square section, the following relations are obtained.

$$I_\theta = I_{\theta+90}$$

$$I_\theta + I_{\theta+90} = I_0$$

From the above relations it can be said that  $I_\theta$  is constant.

# Chapter 5

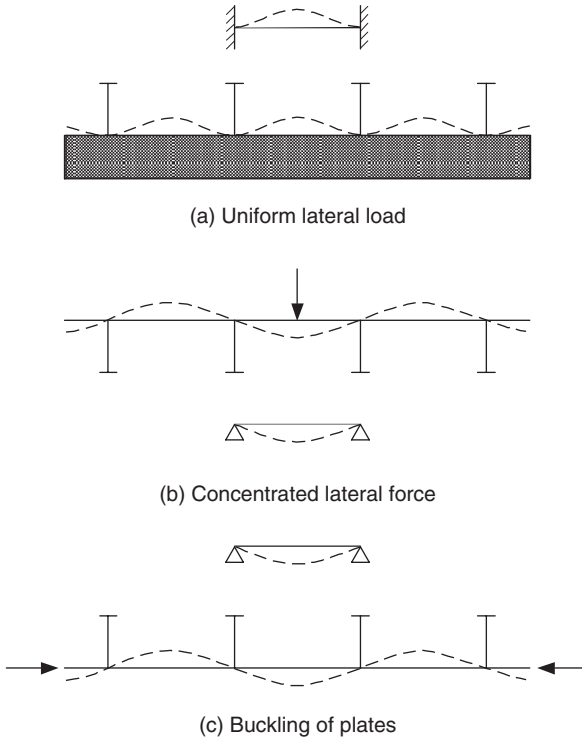
## Design of Plates

### 5.1 Boundary Conditions of Plates

Plates make up the main hull structure such as shells, decks and bulkheads, in conjunction with secondary supporting members such as stiffeners and primary supporting members such as girders. The strength of such plates is most important since many kinds of load act directly on the plates, especially water pressure and longitudinal bending. The strength of plates is usually taken as a plane rectangular plate having uniform thickness. The boundaries, i.e. the four sides of a plate, are considered as fixed, simply supported, or elastically supported, in accordance with the kind of loads. Decisions relating to the boundary supporting conditions are very important because the calculated deformation and stress depend on these conditions.

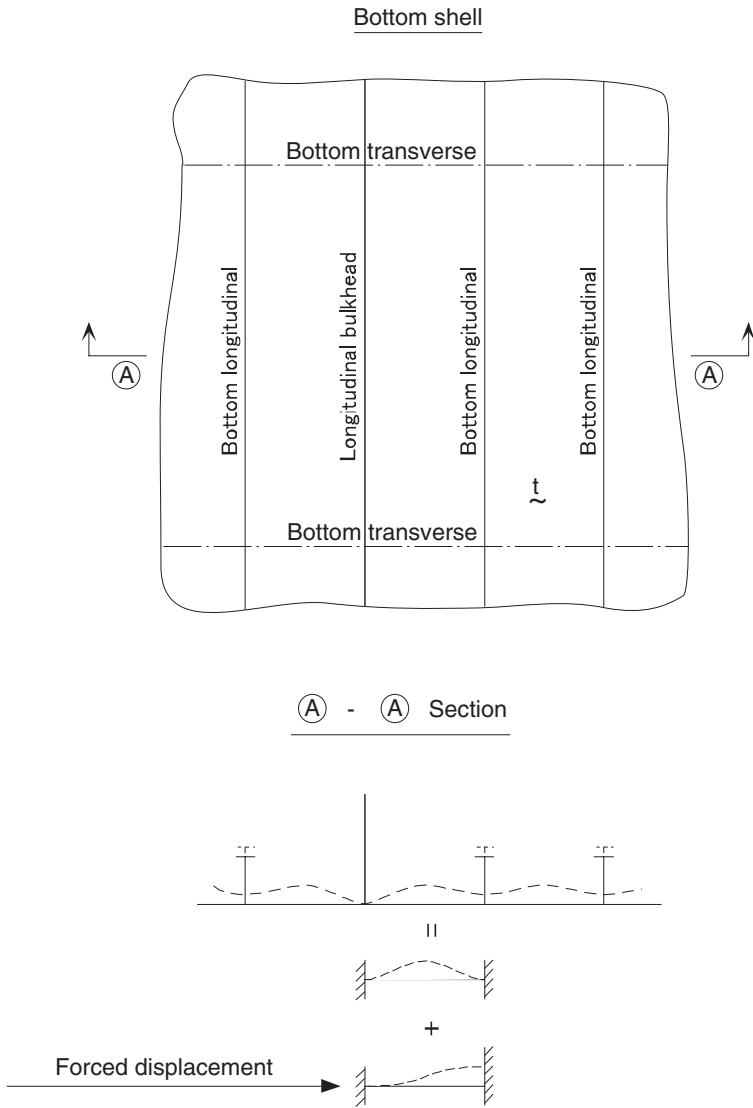
Usually it is assumed as fixed when uniformly distributed pressure is acting on a plate, while as simply supported when concentrated lateral loads and in-plane loads are acting; the latter is also assumed for vibration analysis of a plate. The reason can be understood if we consider their deformations.

Figure 5.1.1 illustrates this concept. Figure 5.1.1(a) shows uniformly distributed pressure on a continuous plate having equal stiffener spacing. In this case the plate is assumed to have fixed boundaries, the same as for a continuous beam, because slope of the stiffeners is zero due to symmetrical conditions around the stiffeners. Figure 5.1.1(b) shows a concentrated load in the mid-region of a plate. In this case simply supported boundaries are assumed, because the slope at the stiffeners is not zero. Figure 5.1.1(c) is a case of plate buckling by in-plane forces. Since the fundamental buckling mode of a continuous plate is convex–concave figure alternately, their boundaries are considered to be simply supported, as shown in case (b).



**Fig. 5.1.1** Deformation of plates

If the stiffeners, which support a plate, deform vertically, the boundary condition is considered to be elastically supported. When the deflection of the adjacent stiffeners is same, these effects are neglected and both ends are assumed as not to move. If the deflection of two adjacent stiffeners differs, additional stress occurs as shown in Fig. 5.1.2, which is an example in the vicinity of a bulkhead; the shell plate is fixed along the longitudinal bulkhead and the bottom longitudinal is deformed by water pressure. Here the deformation is the sum of that due to water pressure as both ends fixed and of the forced displacement. This additional stress by forced displacement often causes some defects such as cracking.



**Fig. 5.1.2** Additional stress due to forced displacement

## 5.2 Strength of Plates Under Lateral Loads

Plates such as shells, decks, and bulkheads are mostly loaded by uniform lateral pressure. The strength of the plate is based on a rectangular plate with fixed edges as shown in Fig. 5.2.1.

(1) *Elastic design*: The deflection and stress of a plate having constant thickness is [13]

$$w = \alpha \frac{qa^4}{D} \quad (5.2.1)$$

where

- $w$ : deflection at plate center
- $\alpha$ : coefficient (See Fig. 5.2.2(a))
- $q$ : intensity of uniformly distributed load
- $a$ : length of shorter edge of plate
- $b$ : length of longer edge of plate
- $D$ : flexural rigidity of a plate

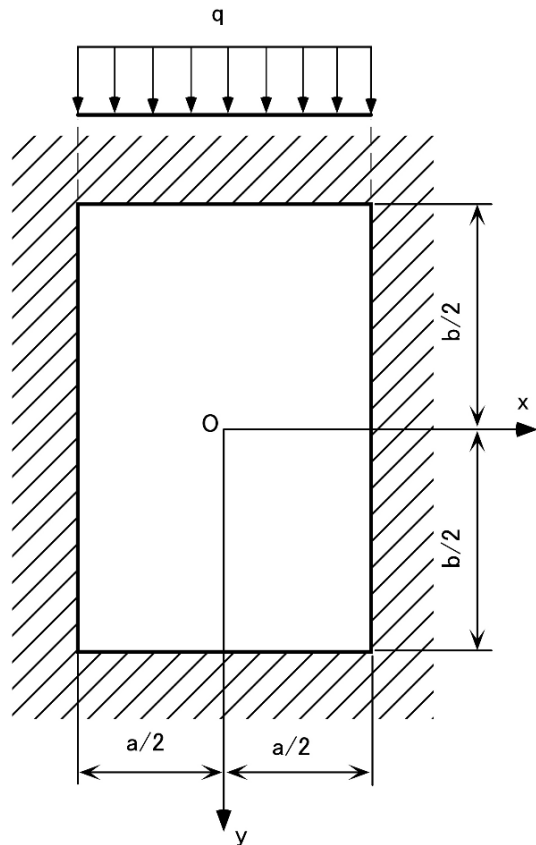
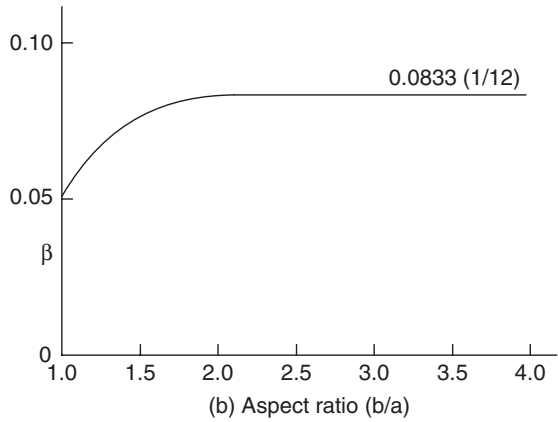
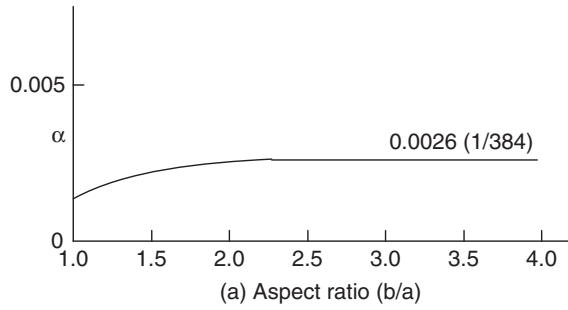


**Fig. 5.2.1** Rectangular plate with all edges built in

Fig. 5.2.2 Coefficient  $\alpha, \beta$



$$D = \frac{Et^3}{12(1-\nu^2)} \tag{5.2.2}$$

- $E$ : Young's modulus
- $\nu$ : Poisson's ratio
- $t$ : plate thickness

$$M = \beta qa^2 \tag{5.2.3}$$

where

- $M$ : bending moment at  $x = a/2, y = 0$
- $\beta$ : coefficient (See Fig. 5.2.2(b))

$$\sigma = \frac{M}{Z} = M \Big/ \frac{t^2}{6} \tag{5.2.4}$$

If the aspect ratio of a plate  $b/a$  exceeds 2.0, the maximum deflection  $w$  and maximum stress  $\sigma$  become constant from Fig. 5.2.2.

$$w = 0.0026 \frac{qa^4}{D} = \frac{0.0026qa^4}{Et^3/12(1-\nu^2)}$$

$$\sigma = \frac{0.0833qa^2}{t^2/6} \quad (5.2.5)$$

On the other hand, the maximum deflection and maximum stress of a strip having unit breadth and span of  $a$  is

$$w = \frac{qa^4}{384EI} = \frac{qa^4}{384E(t^3/12)} = \frac{0.0026qa^4}{Et^3/12}$$

$$\sigma = \frac{qa^2}{12} \bigg/ Z = \frac{0.0833qa^2}{t^2/6} \quad (5.2.6)$$

For steel  $\nu = 0.3$ , and Eq. (5.2.6) is approximately the same as Eq. (5.2.5). Hence deflection and stress of a plate can be approximately calculated by a beam of unit breadth if its aspect ratio is greater than 2, which is usual in ship hull structures.

(2) *Plastic design*: There are two equations for the collapse load in accordance with the upper and lower bound theorem. When uniformly distributed pressure acts on a rectangular plate, the collapse load is given [14]:

$$p_u = \gamma_u \frac{M_p}{a^2}$$

$$p_l = \gamma_l \frac{M_p}{a^2} \quad (5.2.7)$$

where

- $p_u$  : upper collapse load per unit area
- $p_l$  : lower collapse load per unit area
- $\gamma_u, \gamma_l$  : coefficient
- $M_p$  : plastic collapse moment per unit length

$$M_p = \frac{t^2 \sigma_y}{4} \quad (5.2.8)$$

- $\sigma_y$  : yield stress
- $t$  : plate thickness
- $a$  : length of shorter edge of plate
- $b$  : length of longer edge of plate

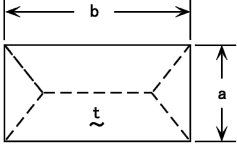
Coefficients  $\gamma_u, \gamma_l$  are given in Table 5.2.1 and Fig. 5.2.3. If the aspect ratio  $\beta = b/a$  becomes large, the coefficients converge gradually to a constant value.

As shown in (1), Elastic design, we consider a strip having unit breadth:

$$P = \frac{16}{a} M_p \quad (5.2.9)$$



**Table 5.2.1** Coefficient  $\gamma_u, \gamma_l$

Boundary condition		Upper bound ( $\gamma_u$ )	Lower bound ( $\gamma_l$ )
 --- Plastic hinge	Simply supported	$\frac{24 k^2}{(1 - \sqrt{1+3 k^2})^2}$	$8 \left( 1 + \frac{1}{k} + \frac{1}{k^2} \right)$
	Fixed	$\frac{48 k^2}{(1 - \sqrt{1+3 k^2})^2}$	$1b \left( 1 + \frac{1}{k^2} \right)$

$$k = \frac{b}{a} \text{ (Aspect ratio)}$$

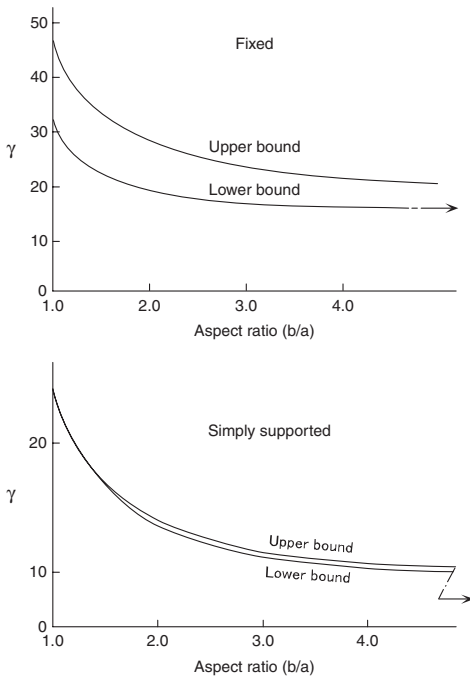


**Fig. 5.2.3** Coefficient  $\gamma_u, \gamma_l$

(3) *Plate thickness required by the Classification Society:* Table 5.2.2 indicates the calculation formula for plate thickness required by the Classification Society. The requirement for a deep tank bulkhead consists of two terms: the first term is proportional to the product of the panel length  $a$  of shorter edge and the square root of water head pressure  $h$ , and the second term is a corrosion margin.

**Table 5.2.2** Required thickness of bulkhead plate (mild steel)

	NK (1977)	AB S(1982)	LR S(1982)
Watertight bulkhead	$3.2 s \sqrt{h} + 2.5$	$\frac{h+6.1}{1.83} s + 3.05, h \leq 18$	$4 s f \sqrt{h}$
Deep tank bulkhead	$3.6 s \sqrt{h} + 3.5$	$\frac{1000}{254} s \sqrt{h} + 2.54$	$4 s f \sqrt{h} + 2.5$

- 1) s : Stiffener space-
- 2) h : Water head.
- 3) f : Coefficient.

On the basis of elastic design, the plate stress can be obtained from Eq. (5.2.4) by assuming  $q$  is the uniform load per unit area:

$$\sigma = \frac{a^2 q}{2t^2}$$

$$\therefore t = a \sqrt{\frac{q}{2\sigma}} \tag{5.2.10}$$

We find that this theoretical formula is similar to the above rule requirement, since the formula gives the plate thickness which equals the product of shorter edge length  $a$  and the square root of uniform load per unit length  $q$ , the latter being proportional to water head pressure  $h$ .

From another point of view, plastic design, the requirement of the Classification Society is also rational. The collapse load  $P$  for plate per unit length is provided by Eq. (5.2.9) in the following form:

$$\left. \begin{aligned} P &= \frac{16\sigma_y t^2}{4a} \\ P &= qa \end{aligned} \right\}$$

$$\therefore t = \sqrt{\frac{q}{4\sigma_y}} a \tag{5.2.11}$$

This plate thickness based on plastic design takes a similar form to that in the rule requirement as well.

Let us compare the rule requirements and the theoretical formulae by substituting realistic values as follows:

$$\begin{aligned} a &= 800 \text{ mm} \\ b &= 4,800 \text{ mm} \\ h &= 20 \text{ m} \end{aligned}$$

In this case, the water head  $h$  is taken from the lowest panel of a deep tank bulkhead of a 100,000 DWT tanker.

According to NK's formula, the plate thickness is specified as

$$\begin{aligned} t &= 3.6s\sqrt{h} + 3.5 \\ &= 3.6 \times 0.8\sqrt{20} + 3.5 \\ &= 16.5 \text{ mm} \end{aligned}$$

From the equation of elastic design, the pressure of 20 m water head corresponds to a load of  $20 \text{ tonf/m}^2$ , therefore, the maximum plate stress appears at the midpoint of the longer edge and is calculated as

$$\sigma = \frac{a^2 q}{2t^2} = \frac{800^2 \times 20}{2 \times 16.5^2} = 23,400 \text{ tonf/m}^2 = 23.4 \text{ kgf/mm}^2$$

This result underestimates the stress, since the stress is obtained on the assumption that all the plate thickness including the corrosion margin is effective. Neglecting the corrosion margin, the stress of the plate can be modified to be  $38 \text{ kgf/mm}^2$ .

In the case of a plastic design, the collapse load  $P$  for unit length is given in the form:

$$P = \frac{16\sigma_y}{4a} t^2 = \frac{16 \times 24}{4 \times 800} \times 16.5^2 = 32.7 \text{ kgf/mm}$$

The applied load to this plate having unit length is  $qa = 0.02 \times 800 = 16 \text{ kgf/mm}$ , therefore, the safety factor becomes  $32.7/16 = 2.0$ . If the corrosion margin is taken from the plate thickness, the safety factor decreases to

$$32.7 \times (16.5 - 3.5)^2 / 16 = 20.3 / 16 = 1.3$$

In the above two theoretical ways, we find that the maximum panel stress induced in the existing vessels is quite high in the vicinity of the deep tank bulkheads.

(4) *Stress at various points in the panel:* In the previous discussion, panel strength is investigated in association with bending stress at the mid-point of the longer edge of a panel, because the maximum stress occurs at this point. Let us consider the stress level at other main points.

According to Fig. 5.2.4, we find that the stress at the middle of shorter edge is 60–70% of the maximum and that the stress at the panel center in both directions is lower than that of the shorter edge: i.e. stress direction is parallel to the longer edge and shorter edge.

(5) *Panel strength considering membrane stress [15]:* In actual ships, the stress in a bulkhead panel, of which thickness is specified by the Classification Society's rule, exceeds the yield stress, and the safety factor for collapse load in plastic design is not so high. Nevertheless, strictly speaking, the real strength of a panel under water pressure is much higher than the calculated strength based on simple elastic

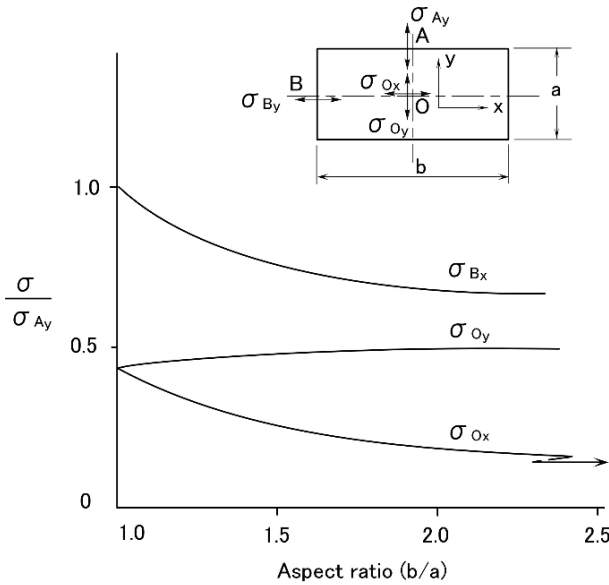


Fig. 5.2.4 Aspect ratio of plate vs. stress at each point

design or plastic design, because the membrane stress increases the strength of the panel and it is not taken into account in the above.

Experimental results are shown in Fig. 5.2.5, which shows the effect of the membrane stress on increasing the collapse load of the panel. This experiment was carried out on a mild steel plate specimen, breadth  $b = 30.05$  cm, length  $l = 90$  cm, thickness  $h = 0.634$  cm, which is loaded by gradually increasing the water pressure. The vertical and horizontal axes denote applied water pressure and deflection measured at the panel center, respectively. In Fig. 5.2.5,  $q_p = 6.78 \text{ kgf/cm}^2$  indicates the collapse load of a panel  $4(h/b)^2\sigma_y$  without considering the effect of membrane stress. This figure represents the panel deflection against the change of water pressure through three inflection points. First, both ends of a panel become plastic hinges, then, a plastic hinge appears at the panel center. It must be noted that the panel neither collapses nor produces a rapid increase in deflection, even when the plastic hinges occur in the panel edges and panel center. This phenomenon is explained by the fact that the water pressure increase does not create an increase in bending stress but the increase in membrane stress. Finally, the area reaching the yield stress covers the whole plate and the plate becomes a plastic membrane. Then the deflection of the plate increases approximately proportionally to the increment of water pressure. Therefore, the plate can bear loads well exceeding the collapse load.

Once the whole plate becomes a plastic membrane, failure of the plate may be caused by some defect in welding or in the material, and thus it is reasonable for the designer to take the plastic membrane condition as the design limit.

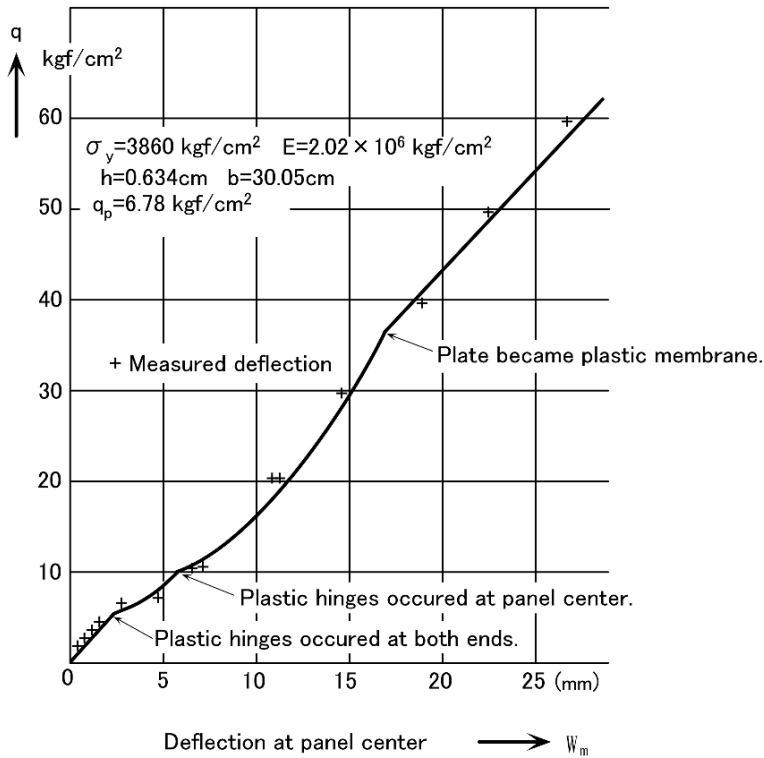


Fig. 5.2.5 Plastic design of plate affected by membrane force

Figure 5.2.6 shows the panel ratio  $b/h$ , in terms of panel breadth and thickness on the horizontal axis and water pressure  $q$  in the vertical axis. In this figure, collapse pressure is plotted according to various assumptions: i.e. NK rule pressure on deep tank bulkheads, critical pressure without membrane stress, pressure causing plastic hinges at plate ends, NK rule pressure for ordinary bulkheads, pressure causing the plastic hinge at the plate center, and pressure causing the plastic membrane.

The NK rule requirements for a deep tank bulkhead have a considerably large safety factor as long as the panel can be loaded up to the ultimate condition where whole panel becomes a plastic membrane.

### 5.3 Strength of Plates by In-Plane Loads

The upper deck plates and bottom plates are subjected to in-plane loads, for they act as face plates of the hull girder against longitudinal bending. The in-plane load has two nominal components; tension and compression. The former may cause

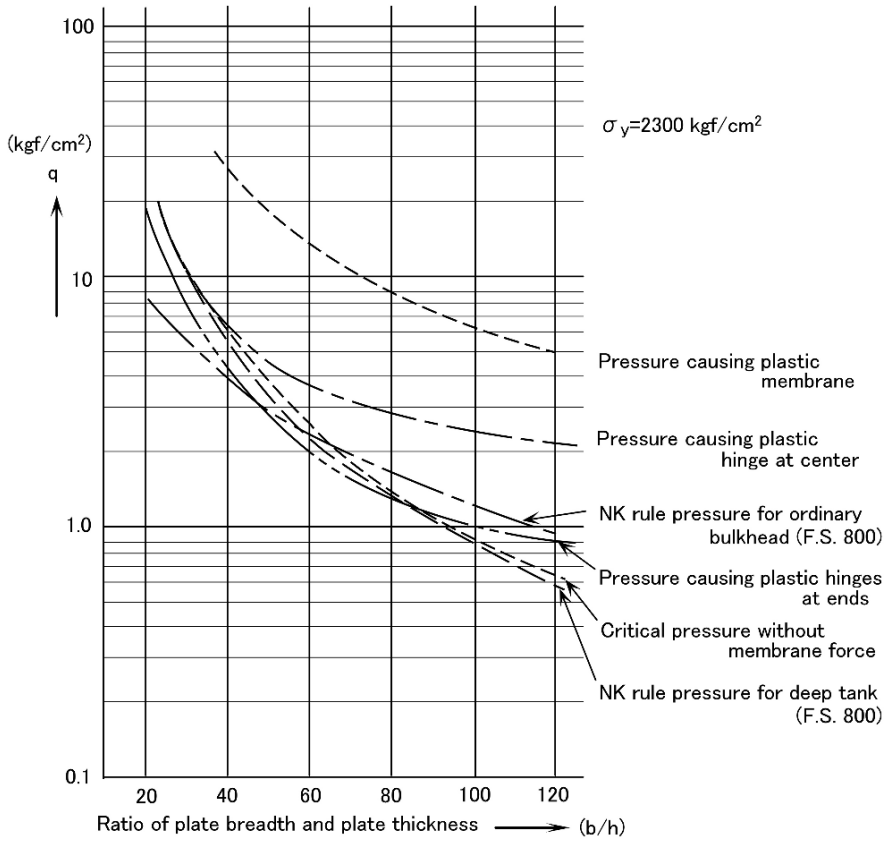


Fig. 5.2.6 Comparison of critical pressure based on different assumptions

cracking, which will be discussed in Sect. 5.4. Let us now consider the latter, which may cause buckling of a plate in the same manner as for a pillar.

Let us investigate the buckling stress according to stiffening arrangement: i.e. longitudinally-stiffened system and transversely-stiffened system. The critical buckling stress can be obtained as follows by referring to Eq. (3.5.21) in Part I.

$$\sigma_{cr} = \frac{\pi^2 E}{12(1 - \nu^2)} \left(\frac{t}{b}\right)^2 K \eta \tag{5.3.1}$$

$K$  = minimum value of  $k$

$$k = \left(\frac{m}{\alpha} + \frac{\alpha}{m}\right)^2 \quad (\text{See Fig. 5.3.1})$$

$$\alpha = a/b$$

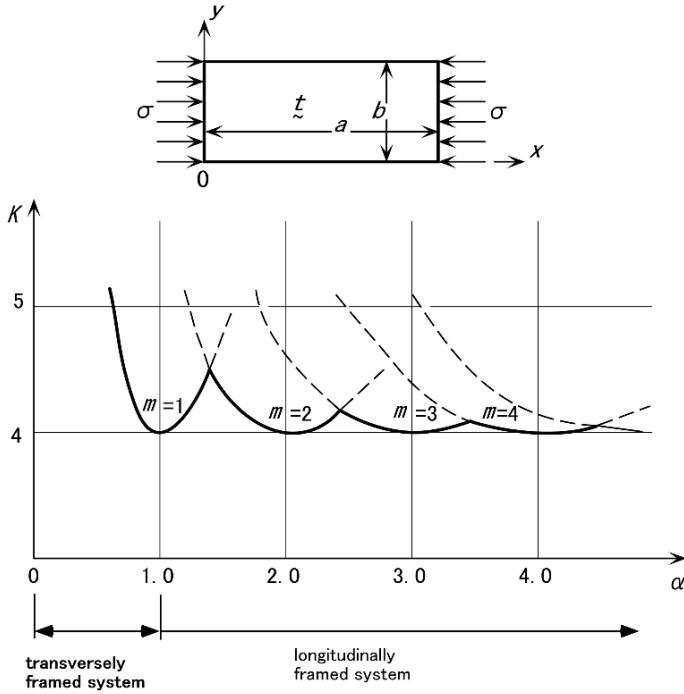
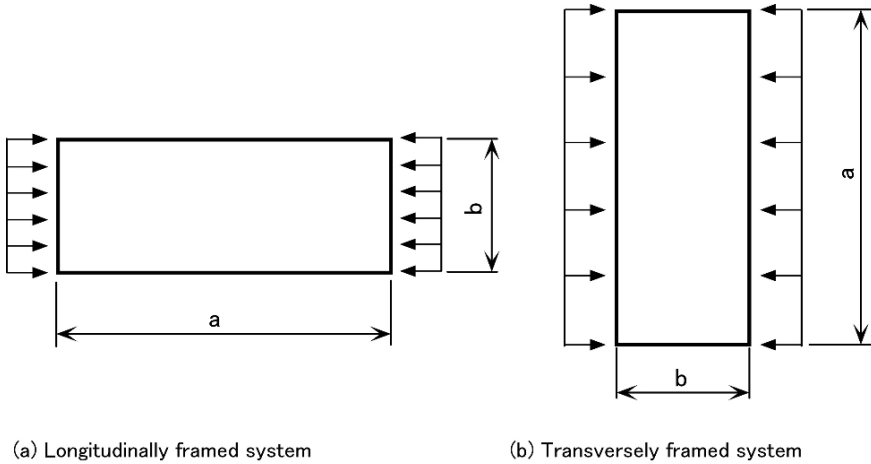


Fig. 5.3.1 Buckling coefficient  $K$  against aspect ratio  $\alpha$

Regarding the longitudinal-stiffened system as illustrated in Fig. 5.3.2(a), the aspect ratio  $\alpha$  of the panel is much greater than 1.0, because the length of the unloaded edge  $a$  is larger than that of the load carrying edge  $b$  in this system. Thus buckling coefficient  $K$  can be taken approximately as 4.0 from Fig. 5.3.1. Hence the critical buckling stress of the longitudinally-framed panel  $\sigma_{cr}^l$  is expressed in the following form:

$$\sigma_{cr}^l = \frac{4\pi^2 E}{12(1-\nu^2)} \left(\frac{t}{b}\right)^2 \eta \tag{5.3.2}$$

Next, let us imagine a transversely-stiffened panel where the length of the unloaded edge is  $b$  and the length of the load carrying edge is  $a$ . In this case, the length of the load carrying edge is  $a$  instead of  $b$  in Eq. (5.3.1), and the critical buckling stress of transversely-framed panel  $\sigma_{cr}^t$  is given as in the form:



**Fig. 5.3.2** Comparison of buckling strength according to framing system

$$\begin{aligned}
 \sigma_{cr}^t &= \frac{\pi^2 E}{12(1-\nu^2)} \left(\frac{t}{a}\right)^2 K \eta \\
 &= \frac{\pi^2 E}{12(1-\nu^2)} \left(\frac{t}{\alpha b}\right)^2 K \eta \\
 &= \frac{K}{\alpha^2} \frac{\pi^2 E}{12(1-\nu^2)} \left(\frac{t}{b}\right)^2 \eta
 \end{aligned} \tag{5.3.3}$$

By taking the ratio  $\sigma_{cr}^t$  and  $\sigma_{cr}^l$ , we find the following relation:

$$\frac{\sigma_{cr}^t}{\sigma_{cr}^l} = \frac{K}{4\alpha^2} \tag{5.3.4}$$

In the case of a transversely-framed system,  $K$  takes a minimum value by putting  $m = 1$  within the range where the aspect ratio is less than 1.0, therefore, the following relationship can be derived:

$$\begin{aligned}
 K &= \left(\alpha + \frac{1}{\alpha}\right)^2 \\
 \therefore \frac{\sigma_{cr}^t}{\sigma_{cr}^l} &= \frac{1}{4} \left(1 + \frac{1}{\alpha^2}\right)^2
 \end{aligned} \tag{5.3.5}$$

When the aspect ratio  $1/\alpha$  of this panel is close to zero, this buckling stress ratio converges to  $1/4$ . Consequently, roughly speaking, the buckling strength of a transversely-framed panel is one-fourth of that of a longitudinally-framed panel.

Figure 5.3.3 illustrates one example of buckling damage observed in transversely-framed upper deck plates of a cargo vessel. The measurement of the buckle was taken as 1.250 mm from the hatch side on the starboard side, and 1.500 mm on the port side.



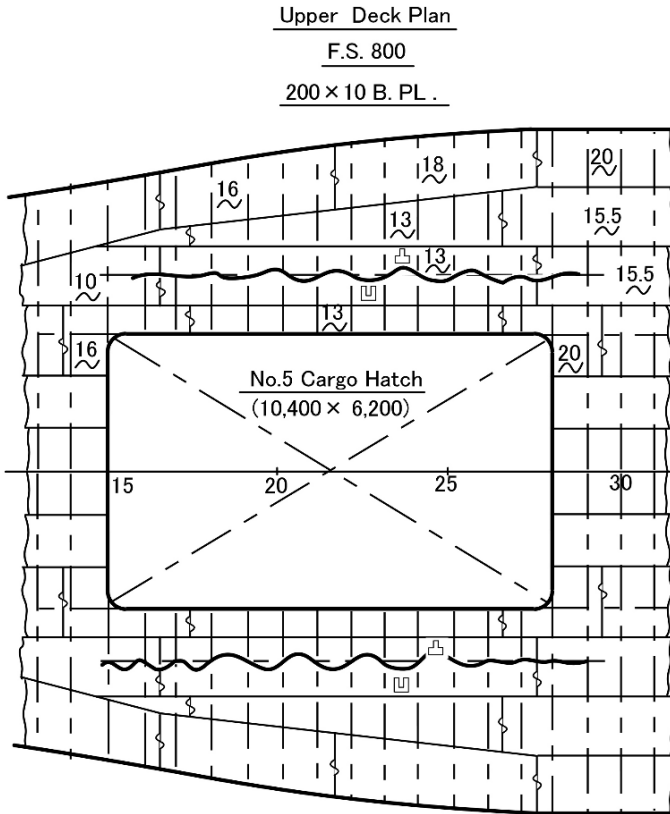


**Fig. 5.3.3** Example of buckling on transversely framed upper deck (maximum deflection 17 cm)

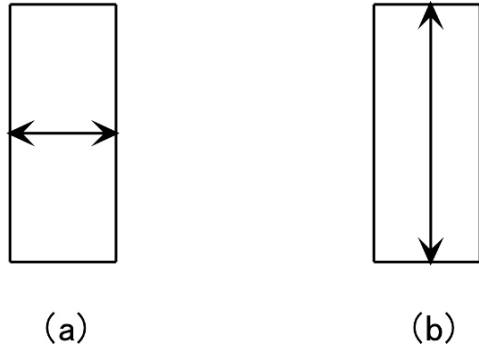
Unlike longitudinally framed vessels, transversely-framed vessels sometime suffer from such buckling damage.

However, it is sometimes inevitable to arrange framing in the weaker direction. In such a case, we must be carefully to maintain buckling strength by increasing the thickness of the plate or by fitting additional stiffeners.

Now, let us consider a quiz. Suppose you must reinforce a panel shown in Fig. 5.3.2(b) by adding only one piece of carling, how would you arrange the carling to achieve the maximum increase in buckling strength? You may have a fixed idea that it is better to arrange stiffeners parallel to the direction of stress, and consider adding a small piece of carling parallel to the stress as shown in Fig. 5.3.4(a). However, the actual carling arrangement shown in Fig. 5.3.4(b) is much stronger. It is very important and useful for designers to have a quantitative sense of the efficiency of each arrangement of additional carling, and the readers are expected to calculate buckling strength by themselves and feel it in his bones once in his technical career.

Regarding the web stiffeners and carlings fitted to divide panels to ensure sufficient buckling strength, how should we determine scantlings? There are many

**Fig. 5.3.4** Two way of buckling reinforcement



criteria to consider such as vibration, etc., but fundamental idea is that the overall buckling should not precede the buckling of each divided plate. To achieve this, the stiffeners should have minimum flexural rigidity, and usually designers apply an appropriate depth/length ratio (such as 0.08) to flat bar stiffeners to keep this minimum flexural rigidity. The thickness of a flat bar stiffener is determined from the viewpoint of torsional buckling. If the stiffener is under axial compression, the depth/thickness ratio should be less than 15, but otherwise it can be about 18 or 20. “Know-why” is more important than “know-how.” The theoretical background of these values can be learned from many other textbooks available, and practical designers should realize why such values are required in order to correctly apply them to actual design.

## 5.4 Plates Supporting Bending and Compression Simultaneously

Let us suppose that a rectangular panel is subjected to bending due to water pressure and compression due to longitudinal bending of the hull girder simultaneously. In this case, the compressive stress is assumed to be uni-axial, because compressive stress is caused by hull girder bending. There are two configurations for a rectangular plate which supports compressive stress: compression is loaded on the longer edge of the plate (transversely-framed system) and on shorter edge (longitudinally framed system), as previously shown in Fig. 5.3.2.

The plastic moment  $M_p$  of the panel supporting bending and compression simultaneously is given in the following form according to the direction of compressive stress [16]:

- (a) In the case where the compression loads are on the longer edge (transversely-framed system)

$$M_p = \frac{\sigma_y t^2}{4} \left\{ 1 - \left( \frac{\sigma_x}{\sigma_y} \right)^2 \right\} \quad (5.4.1)$$

- (b) In the case where the compression loads are on the shorter edge (longitudinally-framed system)

$$M_p = \frac{\sigma_y t^2}{4} \cdot 2 \left\{ 1 - \frac{\sigma_x}{\sigma_y} \right\} \quad (5.4.2)$$

where

$$\frac{\sigma_x}{\sigma_y} = 0.5 \text{ if } \sigma_x \leq \frac{\sigma_y}{2}$$

$\sigma_y$ : yield stress of material

$t$ : plate thickness

$\sigma_x$ : compressive stress

Comparing the plastic moment of a panel supporting only bending as shown in Eq. (5.2.8) with the above Equations, these plastic moments are reduced due to compressive stress. It is, in another word, necessary to increase the plate thickness in cases where the plate is subjected to bending and compression simultaneously rather than just bending alone. This increment of plate thickness can be calculated in the case of a transversely-framed system by letting the plate thickness be  $t^*$  in Eq. (5.2.8) and the plate thickness  $t$  in Eq. (5.4.1) as follows:

$$M_p = \frac{\sigma_y t^2}{4} \left\{ 1 - \left( \frac{\sigma_x}{\sigma_y} \right)^2 \right\} \quad (5.4.3)$$

$$M_p = \frac{\sigma_y t^{*2}}{4} \quad (5.4.4)$$

If the plastic moment is equalized in the above two equations, the increase  $\alpha_T$  of the plate thickness in a transversely-framed system is obtained:

$$\alpha_T = \frac{t}{t^*} = \frac{1}{\sqrt{1 - \left( \frac{\sigma_x}{\sigma_y} \right)^2}} \quad (5.4.5)$$

In the same manner, the increase  $\alpha_L$  of plate thickness in longitudinally-framed system is evaluated

$$\alpha_L = \begin{cases} 1 & \text{when } \sigma_x \leq \frac{\sigma_y}{2} \\ \frac{1}{\sqrt{2 \left\{ 1 - \frac{\sigma_x}{\sigma_y} \right\}}} & \text{when } \frac{\sigma_y}{2} < \sigma_x \end{cases} \quad (5.4.6)$$

Figure 5.4.1 represents  $\alpha_T$  and  $\alpha_L$  against the longitudinal compression. According to this figure, we find both  $\alpha_T$  and  $\alpha_L$  are not so large within the area where the compression is half of the yield stress. Whereas they rapidly increase, if compression exceeds 80% of yield stress.

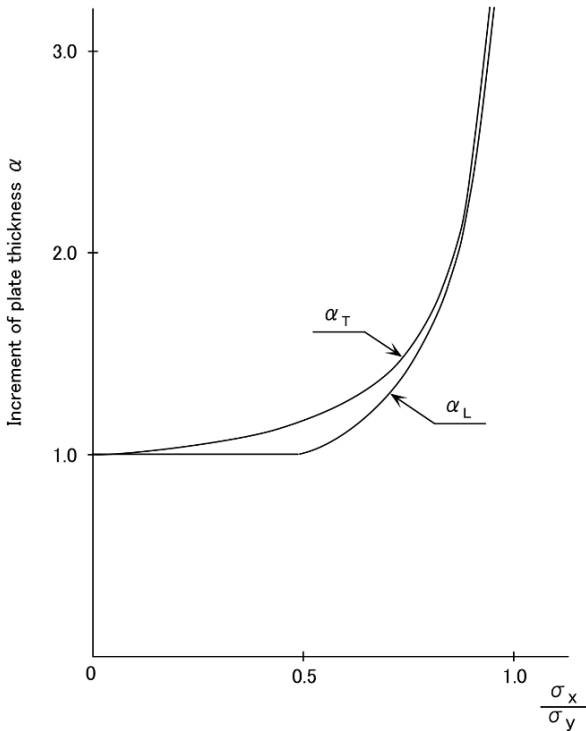


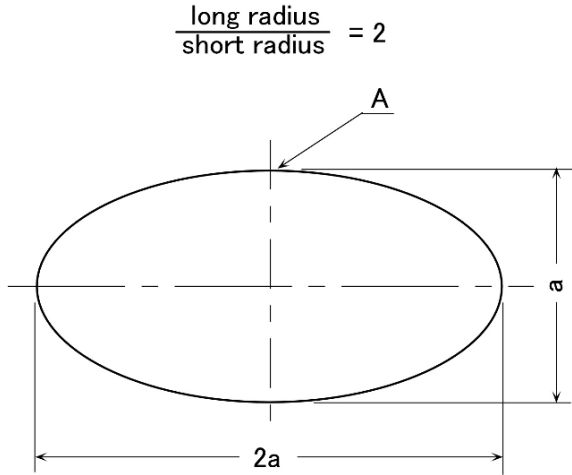
Fig. 5.4.1 Increase of plate thickness due to axial compression  $\alpha_x$

## 5.5 Stress Concentration Around Openings

If an in-plane load acts on a plate having an opening such as the upper deck plate or bottom plate, the opening induces a stress concentration around its free edge. It is a well known fact that the stress concentration factor around a circle in an infinitely wide plate subjected to a uniform tensile stress is 3.0 maximum. On the other hand, the stress concentration factor of an ellipse is 2.0, in the case where the elliptic opening, of which length ratio of the longer axis and shorter axis is 2:1, is subjected to uniform tension along the longer axis. The ellipse in Fig. 5.5.1 is normally applied in hull structure design. The maximum stress occurs at Point A of the ellipse. In providing this shape of ellipse to an upper deck opening, the free edge of the opening is not reinforced as long as the size of opening is not so big compared with the breadth of upper deck. We will discuss this point later.

Although the ellipse, with length ratio 2:1, has the advantage of reducing the stress concentration around the opening, it has an economical disadvantage because of the size of the associated manhole cover plate or hatch coaming. To solve this problem, a smart shape of opening, which has smaller length ratio between longer and shorter axis than the ordinary ellipse, was developed by the authors [17] as

Fig. 5.5.1 Elliptic opening



shown in Fig. 5.5.2. This shape of opening was discovered in 1965 from the results of photo-elastic experiments. The length ratio of the longer axis against the shorter axis of this opening is 1.4 and it is called a “semi-elliptic opening”.

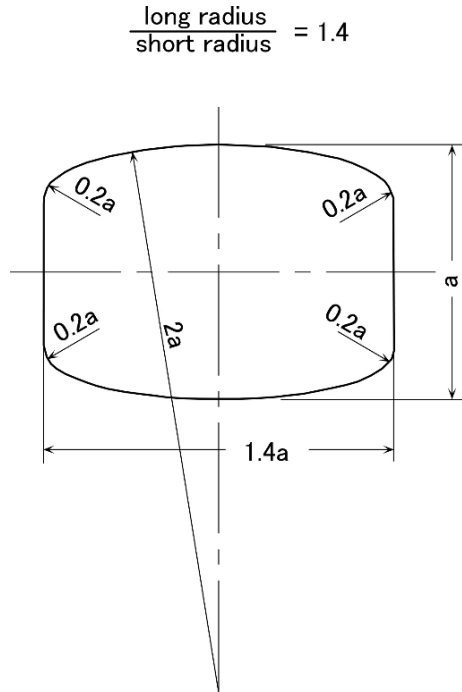
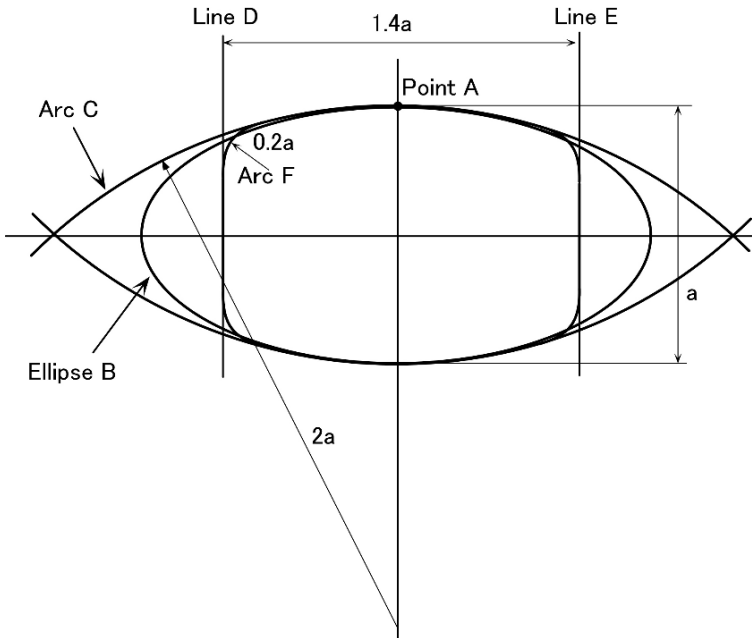


Fig. 5.5.2 Semi-elliptic opening



**Fig. 5.5.3** Concept of semi-elliptic opening

This semi-ellipse is developed on the basis of the following idea as shown in Fig. 5.5.3:

- (1) A large arc C touching the ellipse B at point A can be drawn in such a way that the curvature of the arc ought to be about the same as that of the ellipse. The stress concentration is approximately proportional to the curvature, therefore the stress concentration factor of this large arc becomes around 2.0, similar to that of the ellipse at point A. In this case, we found the radius of the large arc should be  $2a$ .
- (2) Both ends of a large arc are cut off by line D and line E, in order to decrease the length along the longer axis. Here we took the length of  $1.4a$ .
- (3) To avoid a stress concentration due to abrupt cutting of the large arc by line D, arc C and line D should be connected with a small arc F. The stress concentration in arc F can be less than 2.0, if the radius of arc F is  $0.2a$ .

In this manner, we obtained a suitable shape called a semi-elliptic opening in Fig. 5.5.2. Figure 5.5.4 represents the stress distribution around the semi-elliptic opening under uni-axial tension, which indicates that the stress in the small arc is lower than in the center of the large arc.

By further investigations, the stress concentration in the elliptic opening and semi-elliptic opening were measured for the case where the longer axis of both openings was slightly inclined against the tensile direction. This measurement was aimed at confirming the increase of the stress concentration around the openings due to a small inclination, because the actual opening in the vessel has a certain fabrication tolerance and because the direction of the longitudinal stress due to bending

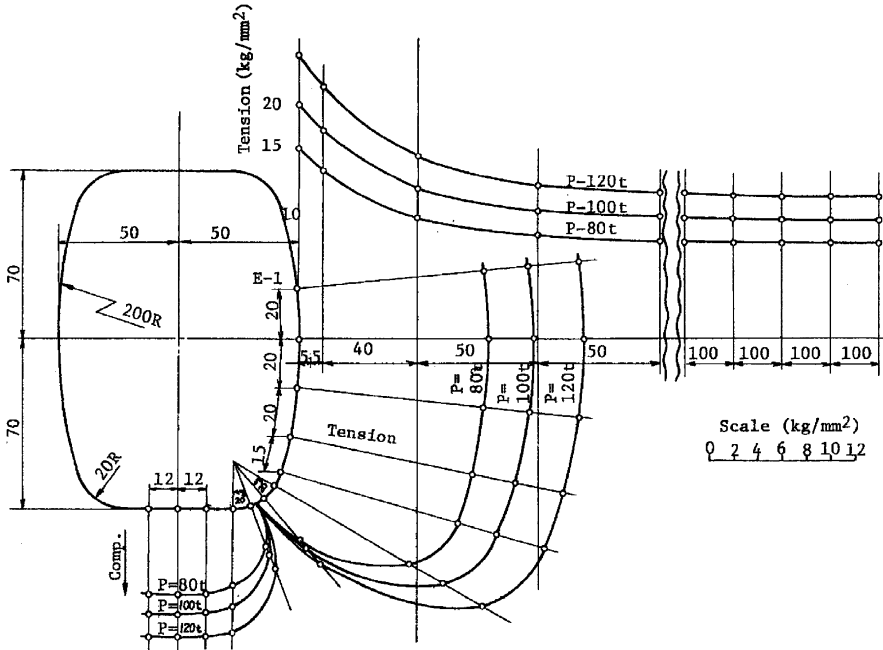


Fig. 5.5.4 Improved shape of opening and stress distribution

is distorted in oblique waves. From this additional measurement, the stress concentration around the opening increased by the increment of inclination angle both in the case of the elliptic opening and the semi-elliptic opening. Comparing these two openings, the stress concentration of a semi-elliptic opening is more affected by the inclination angle than the elliptic opening.

Indeed the above discussion is true, as long as the opening exists in a plate with infinite breadth. But the situation is different if the opening is made in a plate of finite width such as an upper deck plate, since the stress around the opening varies according to the opening size. When the opening size is sufficiently large compared with the breadth of the upper deck plate, the remaining plate area around the opening becomes so small that the nominal stress increases at the opening section. In addition to this increased nominal stress, the stress around the opening becomes large due to the stress concentration of the opening itself. To prevent such large stresses, a reinforcement is necessary to compensate for the reduced plate area.

In order to clarify the upper limit of the opening size allowable without reinforcement, a calculation of the stress distribution around a semi-elliptic opening was performed using the Finite Element Method for changes in the opening size in a plate with constant breadth. Figure 5.5.5 represents the results [18]. According to Fig. 5.5.5, we find the stress concentration at the free edge of the opening is about 2.0 where  $a/b$  is less than 10%. And this concentration is almost the same as that of a semi-elliptic opening in a plate with infinite breadth.

Keeping such a situation in mind, let us consider the critical limit of opening without reinforcement specified by the Classification Societies' rules. NK allows

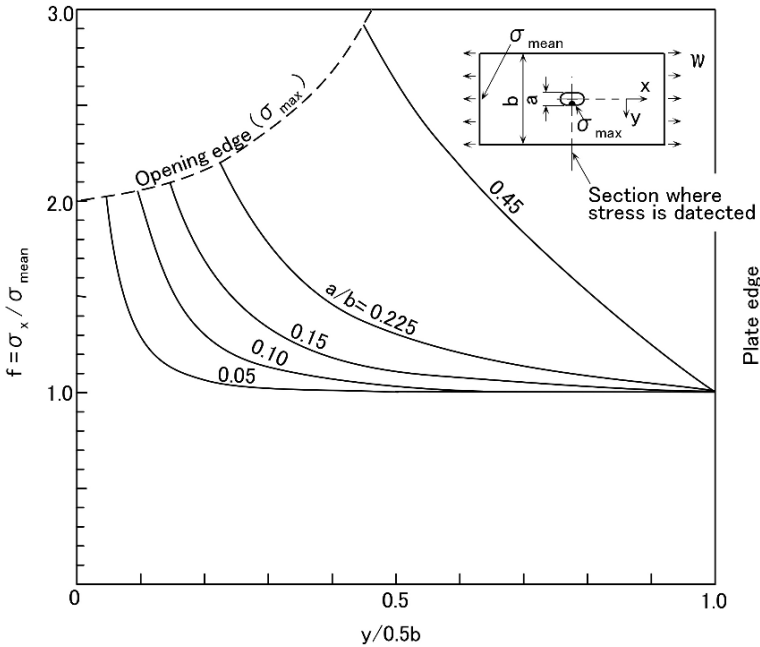


Fig. 5.5.5 Relation between opening size and stress concentration

an opening without reinforcement when its breadth is within 6% of the upper deck breadth, and LRS allows an opening within 10%. These requirements seem to be quite reasonable considering the above calculation results.

### 5.6 Material and Roll Direction

Steel plate material is very important in designing a hull structure, since there is nothing the designer could do other than replace the steel plate by another good plate once the different grade of plate had been misapplied. It is not such a serious problem to have a thinner thickness of plate or stiffener scantlings by mistake, because the former can be compensated by adding stiffeners to the plate and the latter can be solved by providing suitable reinforcement such as additional face plate. A mistake in the selection of grade of steel sometimes occurs in refrigerated cargos vessel constructed with low temperature steel plates. Such steel plates are usually covered by insulation material, therefore, replacing this steel caused by a design mistake causes serious problems at the ship construction stage. Thus, the designer has to pay careful attention not to use improper steel material.

With regard to steel material, let us discuss the strength of steel plate which is different in different axes of the plate; i.e. roll direction (L), the athwart direction to the roll (T) and the plate thickness direction (Z). In general, the strength of normal steel plate in the L direction is higher than that of in T or in Z. Hence, plates of



**Table 5.6.1** Deviation of steel strength due to difference of rolled direction

Steel	Direction	Yield stress (kgf/mm <sup>2</sup> )	Breaking stress (kgf/mm <sup>2</sup> )	Elongation (%)
A	L	40.4	53.6	29.2
	T	41.8	54.3	25.8
	Z	39.3	54.7	68.2
B	L	36.9	50.3	29.9
	T	37.9	51.0	26.8
	Z	37.0	51.8	61.7

Note : A and B steel are higher tensile strength steel of 36kgf/mm<sup>2</sup> with grade E.

longitudinal strength members such as upper deck plates and bottom shell plates must not be arranged along the T direction but along L direction.

Nevertheless, these strengths have a scatter in the L, T, and Z direction depending on the method used to produce the steel plate. For instance, steel plate produced by the controlled rolling method (CR steel) has a similar strength both in the L direction and in the T direction as described in Table 5.6.1. If such steel is adopted, the T

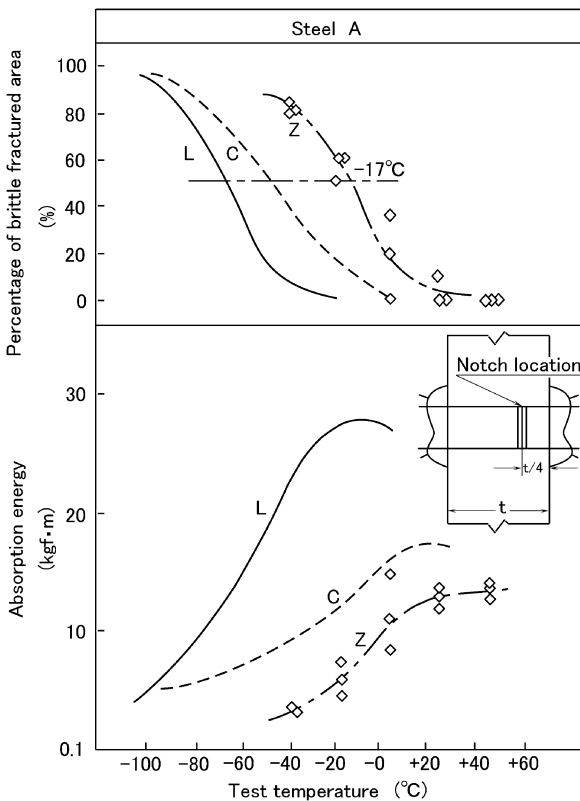


**Fig. 5.6.1** Charpy V-notch impact test according to specimen's roll direction

direction can be applied even as the longitudinal direction of a longitudinal strength member. This type of steel is beneficial for easy construction.

An example of CR steel is given in Table 5.6.1 and Fig. 5.6.1 which shows the strength deviation according to roll direction [19]. From Table 5.6.1, we find that both yield stress and ultimate stress in the T direction exceed those in the L direction and that the strength in the Z direction is approximately the same as that in the L and T directions. Nevertheless, regarding absorption energy given by the V-notch Charpy test, the absorption energy in the T direction is less than that of the L direction. Furthermore the energy in the Z direction is much lower.

A steel plate formed by the cold bending process such as bilge shell plate or gunwale can absorb less energy than a plate without form bending, and the reduction of absorption energy depends on the amount of bending strain. Figure 5.6.2 represents the results of V-notch Charpy impact tests of strain-aging steel plate of two types of E grade steel; i.e. Steel A and Steel B. The absorption energy of strain aged steel is considerably less than that of as rolled steel. A bilge shell plate or gunwale, if constructed by cold bending, may have less absorption energy which might threaten structural damage. However, we can say no problem would arise because the direction of bending strain of the plate is perpendicular to the longitudinal stress due to hull girder bending.

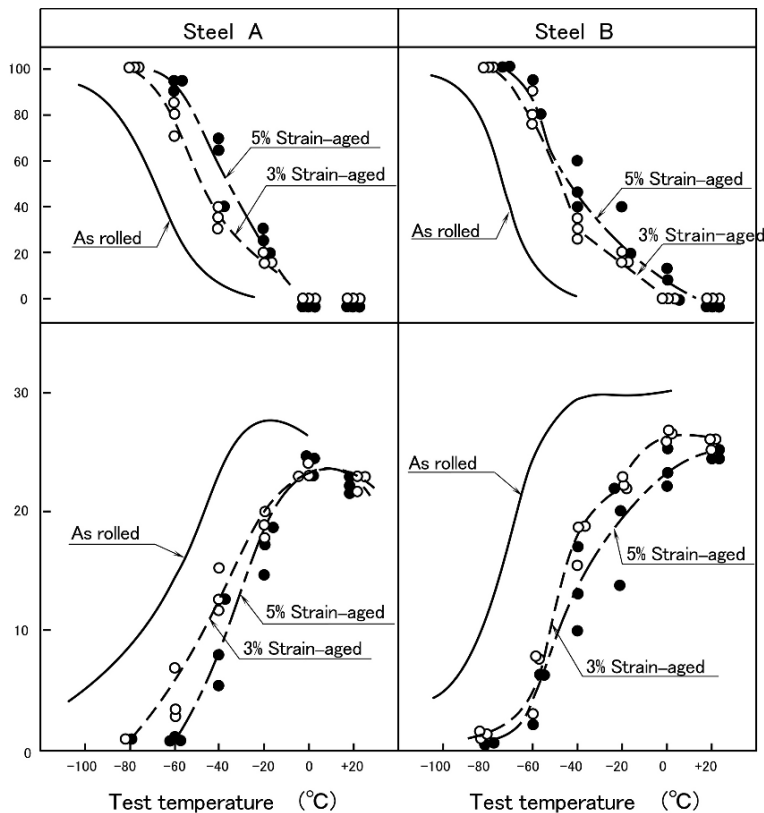
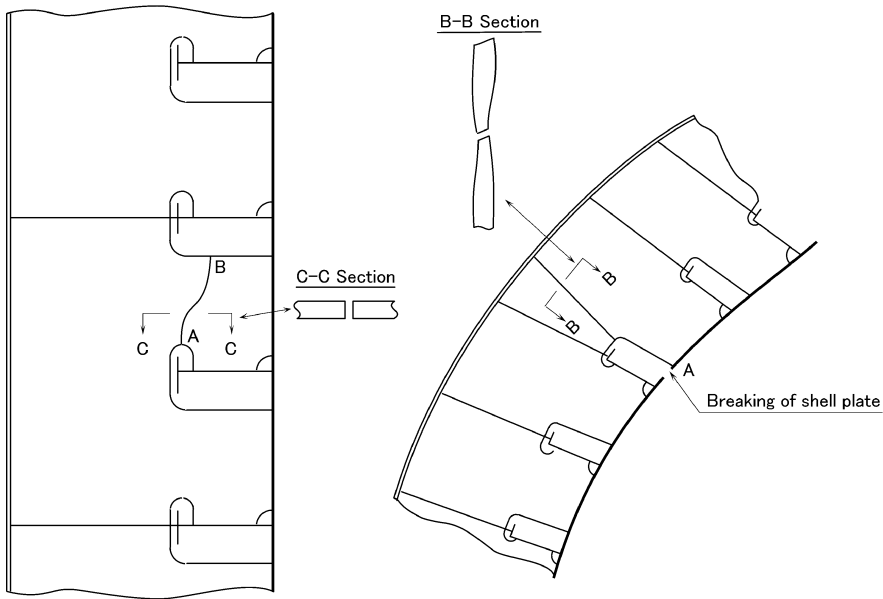


Fig. 5.6.2 Impact test result of strain-aged steel

### 5.7 Damage of Plates

In the tensile test of a rod specimen, constriction begins at some part of the specimen and finally it breaks at this narrow part. In such tests the fractured surface is not normal to the tensile direction but is inclined at about 45°. This is a typical ductile fracture, whereas, a plate fracture observed in an actual vessel often shows a different way of breaking. The breaking rarely happens by a thinning of part of the plate and no narrow part exists in the plate. In addition, the fractured surface is usually approximately normal to the plate surface. This fact suggests that the breaking damage in a plate is brought about by lower stress in the actual vessel compared to the breaking stress measured in experiments.

According to this actual damage of vessels, we consider it is not reasonable to apply the design concept based on tensile strength  $\sigma_B$  to practical design. Figure 5.7.1 illustrates the example of plate fractures in damaged vessels. Figure 5.7.1(a) indicates that the damage is caused by fatigue cracking. This crack firstly initiates from Point A, the highest stress part around the slot opening, and secondly it propagates to Point B tracing the high stress path in the web plate. There is neither narrowing of plate thickness nor an inclination of the broken surface. Figure 5.7.1(b) shows the structural damage of the outer shell plating and transverse web plate. This damage is caused by wave impact force; i.e. the breaking of the shell plate is initiated by tensile stress due to wave impact acting on the curved shell plate at Point A. There



a) Failure of side transverse web

b) Failure of shell plating and side transverse web

**Fig. 5.7.1** Examples of plate failure

is no plate thinning and the fractured surface is normal to the shell plate. On the contrary, the broken surface of the web plate at B–B section shows the same tendency as experimental results; namely the web plate is constricted at the broken line and the fractured surface is not normal. The crack in the above outer shell plate is called a rapid fracture due to wave impact force and shows the Chevron pattern. And after the breaking of the shell plate a very big force was applied on the web plate which showed a ductile fracture.

In the case of the damage on transverse members shown in Fig. 3.1(B), the side shell vertical web was damaged by the breaking down of the cross tie, then the side shell was broken. On the other hand in the case of the damage shown in Fig. 3.1(C) the side shell was dented in about 3 m and the bottom shell about 1 m. The bilge plate deformed very much. In such a situation the shell plate kept water tightness.

As for the stranding damage of the bottom shell plate, one example indicated that the bottom shell was dented about 30 cm, which created the failure of the internal member but didn't cause the breaking of the shell plate.

From the above examples of plate damage, we can say that plate has sufficient toughness that in most situations it rarely fails. However, the plate might fracture under an unlucky case as in Fig. 5.7.1(b).

## Chapter 6

# Design of Stiffened Panel

The hull structure consists of stiffened panels; bottom construction, side shell construction, upper deck construction, bulkhead, etc. Usually stiffened panels consist of plates, beams (small member, secondary member) and girders (big member, primary member). The plate receives loads such as water pressure, the beam supports the loads from the plate and the girder supports the loads from the beam.

In Sect. 1.8 Optimum Design of Beam Section and Sect. 2.2 Rational Design of Girders, the investigation was carried out based on the concept that optimum means minimum weight. The concept stands on the understanding that for a single structural member, the lighter member maintaining the same strength is preferable.

With a stiffened panel many beams and girders are arranged in longitudinal and transverse directions. In designing a definite area of the stiffened panel, spacing between each member is very important not only for saving weight but also saving construction labour costs. The weight and the labour are important parameters to manage in a shipyard.

Under the above considerations “minimum building cost” depends on the design philosophy for the stiffened panels. However, construction methods are being improved year by year and the construction cost is getting smaller, therefore mainly minimum weight viewpoint discussions will be presented below.

In this chapter firstly a rational grillage structure which has girders crossing each other (mutually-supported structure) is explained, then secondly the optimum spacing of girders which are arranged only in one direction is discussed, and finally optimum beam space is introduced.

The girder arrangement of the grillage structure and the space of girders are studied from a strength viewpoint, and the beam arrangement is studied not only from a strength viewpoint but also from a vibration viewpoint especially to the stern and engine room construction where vibration problems are generated so often.

In the case of a simple lateral load, the results in this section can be applied as they are, but in the design of a stiffened panel for an upper deck, the longitudinal strength of the hull girder is to be considered where another criteria, the minimum cost of the hull girder including upper deck structure, will be applicable.

### 6.1 Grillage Structure

Figure 6.1.1 shows a stiffened panel with length of longer edge  $a$ , shorter edge  $b$  and uniform load  $p$ . It is common sense for the girders to be arranged in the direction of the shorter span as the girders in the longer span are not so effective. Here common sense is proved quantitatively.

As the results for fixed-boundary conditions and for simply supported conditions are similar hereafter, the simply-supported boundary condition is to be applied [1].

The maximum stress  $\sigma_y$  is generated at the midpoint  $O$  in Fig. 6.1.1 and the stress  $\sigma_y$  and the deflection  $\delta$  are as follows:

$$\begin{aligned} \sigma_y &= \frac{\pi^2 \delta E e_y}{b^2} \\ \delta &= \frac{abp}{\frac{\pi^6 E}{16} \left\{ \frac{I_x(m+1)}{a^3} + \frac{I_y(n+1)}{b^3} \right\}} \end{aligned} \tag{6.1.1}$$

where  $\delta$ : deflection at point  $O$ .

Applying the following notations, maximum stress  $\sigma_y$  is described below.

$I_x$  and  $I_y$  are sectional moment of inertia with effective breadths

$m$  and  $n$  are numbers of girders

$e_x$  and  $e_y$  are distances from center of gravity of section to face plates

spaces of girders  $l_x = b/(m+1)$  and  $l_y = a/(n+1)$

rigidity ratio per unit breadth  $i_x = I_x/l_x$  and  $i_y = I_y/l_y$

rigidity ratio in longer and shorter edge directions (mutually-supporting ratio)

$\alpha = i_x/i_y$

$$\sigma_y = \frac{16b^2 p l_y}{\pi^4 \frac{I_y}{e_y} \left( 1 + \alpha \frac{b^4}{a^4} \right)} \tag{6.1.2}$$

Considering  $\sigma_y$  as the allowable stress, the required section modulus  $Z_y$  is given by the following equations.

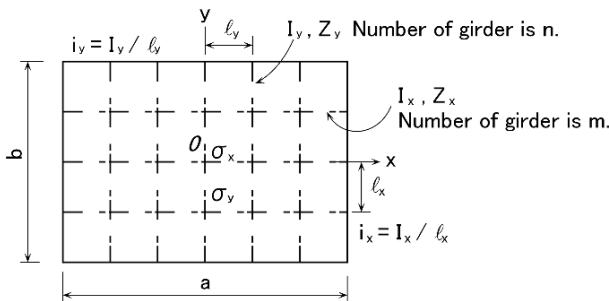


Fig. 6.1.1 Grillage structure

$$\begin{aligned}
 Z_y &= \frac{I_y}{e_y} \\
 &= \frac{16b^2pl_y}{\pi^4\sigma_y\left(1 + \alpha\frac{b^4}{a^4}\right)} \quad (6.1.3)
 \end{aligned}$$

Putting weight per unit area of grillage structure as  $W_1$ , and weights per unit length of girders in longer and shorter directions as  $W_x$  and  $W_y$  respectively, the following relation is obtained.

$$W_1 = \frac{W_x}{l_x} + \frac{W_y}{l_y} \quad (6.1.4)$$

Usually the same scantling girders are to be applied for  $X$  and  $Y$  directions in a mutually-supported grillage structure. Applying this principle the following results are obtained.

$$I_x = I_y \quad Z_x = Z_y \quad W_x = W_y \quad (6.1.5)$$

$$\alpha = \frac{i_x}{i_y} = \frac{I_x l_y}{l_x I_y} = \frac{l_y}{l_x} \quad (6.1.6)$$

In Sect. 1.8, Optimum Design of Beam Section, the relation between the section modulus of a beam and its weight per unit length is explained. This principle can be applied to girders assuming the web thickness is 12 mm. The result is shown in Eq. (6.1.7).

$$W_y = 1.5\sqrt{Z_y} \quad (6.1.7)$$

where

$W_y$  : weight per unit length of girder in kgf/m

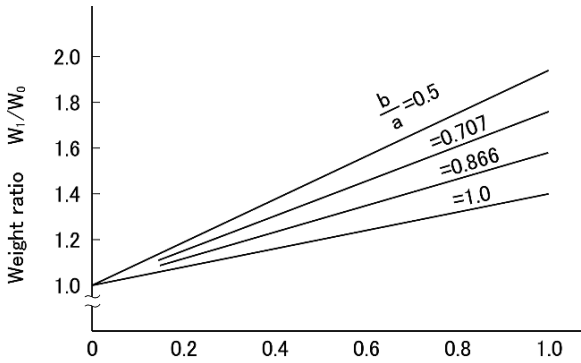
$Z_y$  : section modulus of girder in  $\text{cm}^3$

Putting Eqs. (6.1.7) and (6.1.3) into (6.1.4) and with the conditions described by (6.1.5) and (6.1.6), the weight per unit area  $W_1$  of girders is given by the following equation.

$$W_1 = \frac{1.5}{l_y} \sqrt{\frac{16b^2pl_y}{\pi^4\sigma_y}} \cdot \frac{1 + \alpha}{\sqrt{1 + \alpha\frac{b^4}{a^4}}} \quad (6.1.8)$$

Where a grillage (mutually-supported) arrangement is not applied, a girder arrangement in one direction is usually applied. In this case the weight per unit area  $W_0$  is obtained by putting  $\alpha = 0$  in Eq. (6.1.8). The weight ratio  $W_1/W_0$  of the mutually-supported and the one-direction girder arrangement is given as follows:

$$\frac{W_1}{W_0} = \frac{1 + \alpha}{\sqrt{1 + \alpha\frac{b^4}{a^4}}} \quad (6.1.9)$$



$$\alpha = \frac{i_x}{i_y} = \frac{I_x I_y}{I_x I_y} = \frac{I_y}{I_x}$$

Fig. 6.1.2 Weight increase due to mutually-supported arrangement

The relation of Eq. (6.1.9) is shown in Fig. 6.1.2 with  $\alpha$  along the horizontal axis and  $b/a$  as a parameter. It can be seen that the smaller  $b/a$ , which means a slender rectangular, and bigger  $\alpha$ , mutually-supporting ratio, will bring a bigger weight difference. It is important to note that the ratio  $W_1/W_0$  is always bigger than 1.0 which means the mutually-supported arrangement is always heavier than the one-direction girder arrangement. This result is in agreement with the designer’s common sense.

The stress  $\sigma_y$  at the point  $O$  in Fig. 6.1.1 in the shorter edge direction is expressed by Eq. (6.1.1) and the stress  $\sigma_x$  at the same point  $O$  in the longer edge direction is expressed by the following equations:

$$\sigma_x = \frac{\pi^2 \delta E e_x}{a^2}$$

$$\frac{\sigma_x}{\sigma_y} = \frac{b^2 e_x}{a^2 e_y}$$

$\sigma_x/\sigma_y$  is proportional to the square of  $b/a$  which means for a slender panel,  $\sigma_x$  is very much smaller than  $\sigma_y$  and the mutually-supported condition will disappear. Even in the case of a square panel the one-direction arrangement is better than the mutually-supported arrangement because the weight ratio between two girders with section modulus  $Z_y$  and one girder with section modulus  $2Z_y$  is:

$$2 \times 1.5\sqrt{Z_y}/1.5\sqrt{2Z_y} = 1.41.$$

And in Fig. 6.1.2,  $W_1/W_0 = 1.41$  for  $b/a = 1.0$  and  $\alpha = 1.0$  is the same story.

Regarding the minimum weight of grillage structure, Yagi and Yasukawa’s study is famous [20], and Kitamura’s study as a non-linear programming method is also useful [21].



### 6.2 Optimum Space of Girders

As shown in Fig. 6.2.1 it is usual for a panel to be stiffened by beams parallel to the longer edge which are supported by girders parallel to the shorter edge. Assuming that the girders are fixed at both ends, the maximum stress in the girder  $\sigma_y$  is expressed as follows.

$$\sigma_y = \frac{M}{Z_y} = \frac{plb^2}{12Z_y} \tag{6.2.1}$$

The maximum stress in the beam  $\sigma_s$  is as follows:

$$\sigma_s = \frac{M}{Z_s} = \frac{psl^2}{12Z_s} \tag{6.2.2}$$

where  $Z_y$  and  $Z_s$ : section modulus with effective breadth

$p$ : uniform load

Considering  $\sigma_y$  and  $\sigma_s$  as allowable stresses, the required section modulus  $Z_y$  and  $Z_s$  are given by the following equations:

$$Z_y = \frac{plb^2}{12\sigma_y} \tag{6.2.3}$$

$$Z_s = \frac{psl^2}{12\sigma_s} \tag{6.2.4}$$

Applying Eq. (6.1.7) to the girder and beam then the weight per unit area of beam and girder  $W_2$  is derived as follows:

$$\begin{aligned} W_2 &= \frac{W_s}{s} + \frac{W_y}{l} \\ &= \frac{1.5}{s} \sqrt{\frac{psl^2}{12\sigma_s}} + \frac{1.5}{l} \sqrt{\frac{plb^2}{12\sigma_y}} \end{aligned} \tag{6.2.5}$$

where  $W_s$  and  $W_y$ : weight per unit length of beam and girder respectively

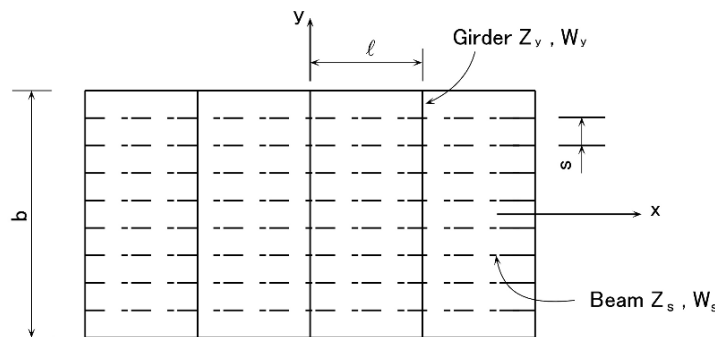


Fig. 6.2.1 One direction girder arrangement

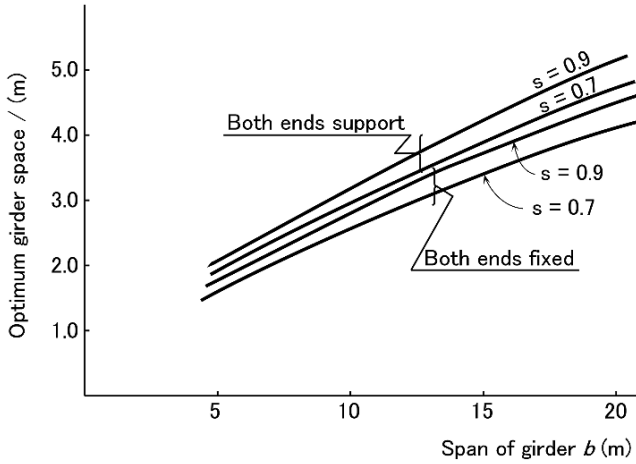


Fig. 6.2.2 Optimum girder space

Assuming the allowable stresses for the girder and beam are equal, the optimum girder space  $l$  is obtained as below putting  $dW_2/dl = 0$ .

$$l = 2^{-\frac{2}{3}} \cdot s^{\frac{1}{3}} \cdot b^{\frac{2}{3}} = 0.63s^{\frac{1}{3}} \cdot b^{\frac{2}{3}} \tag{6.2.6}$$

In the case of a girder with both ends supported, the following relation is obtained because  $\sigma_y = plb^2/8Z_y$ .

$$l = \frac{3^{\frac{1}{3}}}{2} s^{\frac{1}{3}} \cdot b^{\frac{2}{3}} = 0.72s^{\frac{1}{3}} \cdot b^{\frac{2}{3}} \tag{6.2.7}$$

The optimum girder spaces obtained by Eqs. (6.2.6) and (6.2.7) are shown in Fig. 6.2.2. It shows that for a girder with a longer span, a wider space is preferable. It is recommended to study the weight changing ratio using Eq. (6.2.5) together with Fig. 6.2.2 because in the case where the weight changing ratio at the optimum point is small a wider space than optimum point will be decided.

### 6.3 Optimum Space of Beams

Stiffened plates around the stern and machinery room are to be designed not only from the strength viewpoint but also from the vibration viewpoint. Accordingly the presentation below will be done from both viewpoints.

#### 6.3.1 Design Condition Against Lateral Load like Water Pressure

As shown in Fig. 6.2.1 in a one-direction girder arrangement, the plate thickness and the section modulus of the beams are given by Nippon Kaiji Kyokai (NK) rules for water tight bulkheads as follows:

$$t = 3.6s\sqrt{h} + 3.5 \quad (\text{mm}) \quad (6.3.1)$$

$$Z = 7shl^2 \quad (\text{cm}^3) \quad (6.3.2)$$

where

$s$ : beam space

$l$ : span of beam

$h$ : water pressure head on beam and plate

### 6.3.2 Design Conditions from Vibration Viewpoint

(1) *Plate thickness*: The stiffened plate vibrates heavily usually in the case of contact with water. The natural frequency of the panel of size  $l \times s$  and thickness  $t$ , as shown in Fig. 6.2.1 with the boundary supported condition, is as follows:

$$N_p = \alpha \cdot 1.46 \times 10^2 \frac{t}{s^2} \left\{ 1 + \left( \frac{s}{l} \right)^2 \right\} \quad (\text{cpm})$$

where

$t$  : plate thickness in mm

$l$  : span of beam in m

$s$  : space of beam in m

$\alpha$  is the coefficient of frequency reduction by contact with water and usually it is about 0.3–0.5 for hull structures. Here it is assumed that  $\alpha = 0.3$  to be on the safety side, and  $(s/l)^2$  is negligibly small in comparison with 1.0, because usually  $s/l$  is about 1/4. Then the following simplified relation can be obtained.

$$N_p = 0.3 \times 1.46 \times 10^2 \times \frac{t}{s^2} \quad (\text{cpm})$$

On the other hand the frequency of the exciting force on the stiffened panel is usually lower than 1000 cpm, therefore to avoid resonance with the exciting frequency  $N_p \geq 1000$  condition will be applied. Accordingly the following relation is obtained:

$$t = \frac{1,000}{43.8} s^2 = 22.8s^2 \quad (6.3.3)$$

(2) *Scantling of beams*: Considering a stiffened plate  $l \times b$  surrounded by girders and boundaries in a boundary supported condition, the natural frequency of the stiffened panel is nearly equal to the natural frequency  $N_s$  of a beam being cut out from the stiffened panel. This is expressed by the following equation:

$$N_s = \frac{4,830}{l^2} \sqrt{\frac{I_S}{A}} \quad (\text{cpm})$$

where

$$A = A_S + A_P + A_W$$

$A_S$  : sectional area of beam in  $\text{cm}^2$

$A_P$  : sectional area of plate; i.e.  $10ts$  ( $t$  in mm and  $s$  in m)

$A_W$  : equivalent sectional area due to added mass of water i.e.  $400ls$  ( $l$  and  $s$  in m)

$I_S$  : sectional moment of inertia including effective breadth in  $\text{cm}^4$

Neglecting  $A_S$  and  $A_P$ , because in usual hull structure they are negligibly small in comparison with,  $A_W$  the following relation can be obtained:

$$N_s = \frac{4830}{l^2} \sqrt{\frac{I_S}{4000ls}} \quad (\text{cpm})$$

Similar to the case of plate thickness where  $N_s \geq 1000$ , the following simple relation is obtained:

$$I_S = 17.1 sl^5 \quad (6.3.4)$$

where  $s$  and  $l$  are in m, and  $I_S$  in  $\text{cm}^4$ .

### 6.3.3 Minimum Plate Thickness

In addition to the strength and vibration viewpoints explained in Sect. 6.3.1 and 6.3.2, consideration should be given also to construction methodology with regard to the minimum plate thickness. And the classification societies give the minimum plate thickness in their rules. Here considering welding distortion during fabrication, the following is proposed:

$$t_{\min} \geq 8 \quad (\text{mm}) \quad (6.3.5)$$

### 6.3.4 Optimum Beam Space

The weight  $W_3$  per unit area, which consists of plate and beams, is expressed by the following equations:

$$W_3 = W_P + W_S = \gamma t + \frac{W_S}{s} \quad \text{or} \quad W_3 = W_P + W_S = \gamma t + \frac{\gamma A_S}{10s} \quad (6.3.6)$$

where

$W_P$  : weight of plate per unit area in  $\text{kgf/m}^2$

$\gamma$  : weight of plate per unit volume, that is,  $7.85 \text{ kgf/m}^2 \text{ mm}$

$s$  : beam space in m

$W_S$  : weight of stiffened panel per unit length in  $\text{kgf/m}$

$A_S$  : sectional area of beams in  $\text{cm}^2$

In Fig. 6.3.1 the relation between sectional area  $A_S$  and sectional moment of inertia  $I$  is shown, which is derived from following formula:

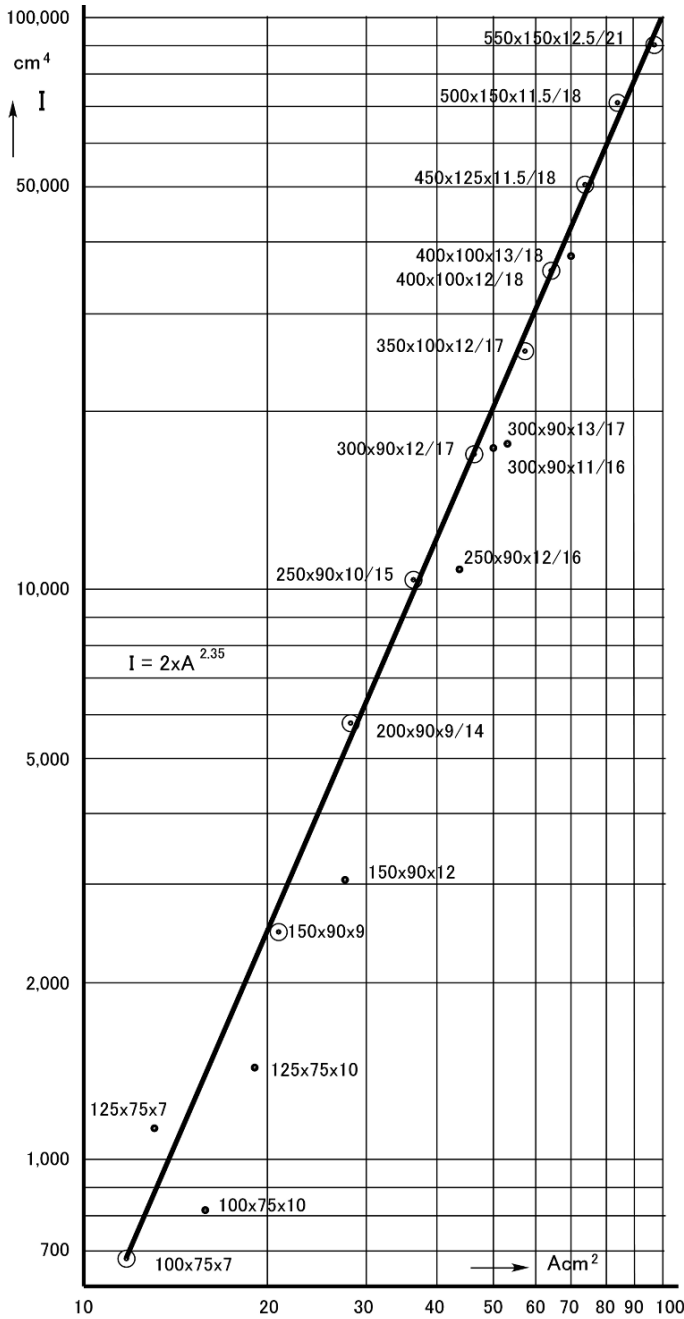


Fig. 6.3.1 Sectional area and sectional moment of inertia of beam

$$A_s = \left(\frac{I}{2}\right)^{\frac{1}{2.35}} \tag{6.3.7}$$

(1) *Case 1: Plate and beams are designed from a strength viewpoint:* Putting Eqs. (6.1.7), (6.3.1) and (6.3.2) into (6.3.6) the following relationship can be obtained.

$$W_3 = 7.85 \times (3.6s\sqrt{h} + 3.5) + \frac{1.5}{s} \sqrt{7shl^2} \tag{6.3.8}$$

By the condition of  $dW_3/ds = 0$  the optimum beam space  $s$  is as follows:

$$s = 0.17l^{\frac{2}{3}} \tag{6.3.9}$$

In Table 6.3.1 the optimum beam spaces for different span  $l$  are shown. The results in Table 6.3.1 coincide well with the results of Nagasawa and Honma’s study [22] relating to minimum weight analysis, including plastic deformation. However they are considerably smaller in comparison with 0.6 ~ 0.9 m which are usually applied in practice because the condition of the minimum plate thickness for fabrication is not included.

Figure 6.3.2 shows the weight difference caused by the change of beam space  $s$  based on Eq. (6.3.8). In Fig. 6.3.2 the weight difference using the condition of the minimum thickness of Eq. (6.3.5), is also shown. With this condition the optimum beam space becomes bigger than that shown in Table 6.3.1. Figure 6.3.2 shows the weight difference when the change of beam space is small, and a wider space can be applied from the construction viewpoint with very small weight increase.

(2) *Case 2: Plate and beams are designed from vibration viewpoint:* Putting Eqs. (6.3.3), (6.3.4) and (6.3.7) into (6.3.6) the following relationship can be obtained:

$$W_3 = 7.85 \times 22.8s^2 + \frac{0.785}{s} \left\{ \frac{17.1}{2} sl^5 \right\}^{\frac{1}{2.35}} \tag{6.3.10}$$

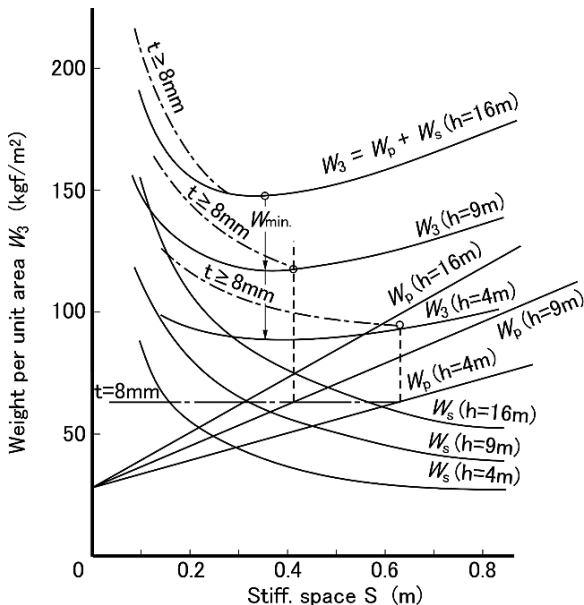
With the condition of  $dW_3/ds = 0$  the optimum beam space  $s$  is as follows:

$$s = 0.107l^{0.826} \tag{6.3.11}$$

**Table 6.3.1** Optimum beam space (without account of  $t_{min}$ .)

Span of stiff.	Case 1	Case 2	Case 3		Case 4	
			h = 9 m	h = 16 m	h = 9 m	h = 16 m
2 m	0.288 m	0.190	0.244	0.273	0.164	0.137
3	0.354	0.265	0.287	0.321	0.284	0.237
4	0.429	0.336	0.322	0.361	0.419	0.350
5	0.497	0.405	0.352	0.394	0.566	0.473

**Fig. 6.3.2** Weight per unit area (strength design for plate and beam)



In Table 6.3.1 Case 2, the optimum beam spaces for different spans  $l$  are shown. Assuming the beam span is  $l = 3.0$  m, the weight difference due to the change of space is shown in Fig. 6.3.3. The optimum space shown in Table 6.3.1 is narrow, however by considering the minimum thickness it comes up to the space usually applied. The weight difference due to a change of space is considerably bigger in the case of the design from a vibration viewpoint, relative to that in the case of the strength design viewpoint shown in (1) Case 1.

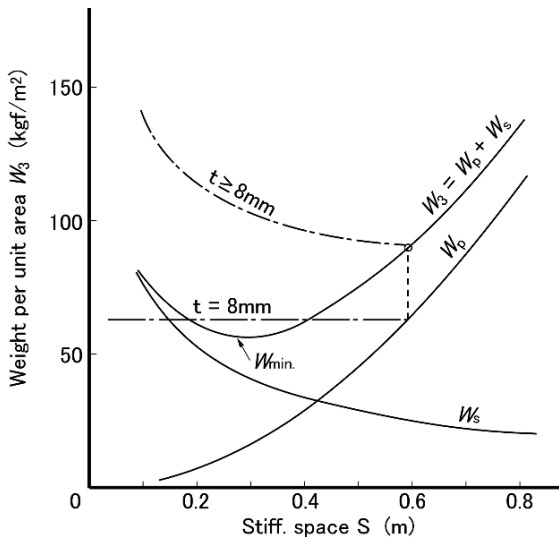


**Fig. 6.3.3** Weight per unit area (vibration design for plate and beam)

(3) Case 3: Plate is designed from a vibration viewpoint and the beam is designed from strength viewpoint: Putting Eqs. (6.1.7), (6.3.2) and (6.3.3) into (6.3.6) the following relation can be obtained:

$$W_3 = 7.85 \times 22.8s^2 + \frac{1.5}{s} \sqrt{7shl^2} \tag{6.3.12}$$

By the condition of  $dW_3/ds = 0$  the optimum beam space  $s$  is as follows:

$$s = \left\{ 4.9 \times 10^{-3} \sqrt{h} \right\}^{\frac{2}{5}} \cdot l^{\frac{2}{5}} \tag{6.3.13}$$

In Table 6.3.1 Case 3, the optimal beam spaces for different spans of  $l$  and different water head  $h$  are shown. And the weight difference due to the change of space is shown in Fig. 6.3.4.

(4) Case 4: The plate is designed from a strength viewpoint and the beam is designed from a vibration viewpoint: Putting Eqs. (6.3.1), (6.3.4) and (6.3.7) into (6.3.6) the following relation can be obtained:

$$W_3 = 7.85 \times (3.6s\sqrt{h} + 3.5) + \frac{0.785}{s} \left\{ \frac{17.1}{2} sl^5 \right\}^{\frac{1}{2.35}} \tag{6.3.14}$$

With the condition of  $dW_3/ds = 0$  the optimum beam space  $s$  is as follows:

$$s = \left\{ 3.95 \times 10^{-2} \frac{1}{\sqrt{h}} \right\}^{\frac{5}{3.7}} \cdot l^{\frac{5}{3.7}} \tag{6.3.15}$$

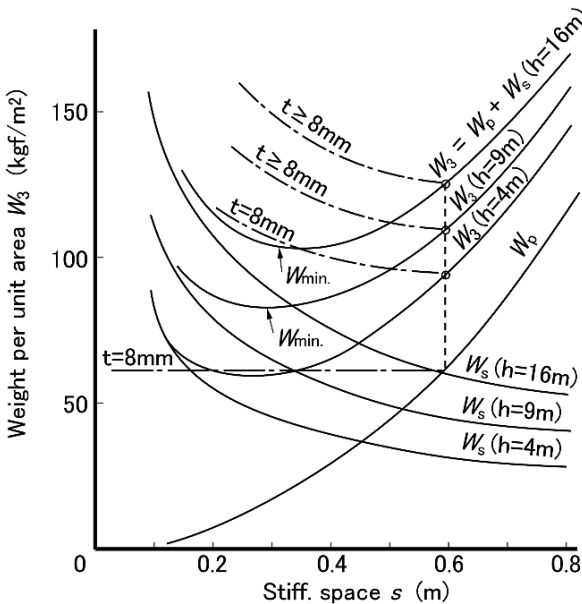


Fig. 6.3.4 Weight per unit area (vibration for plate and strength for beam)



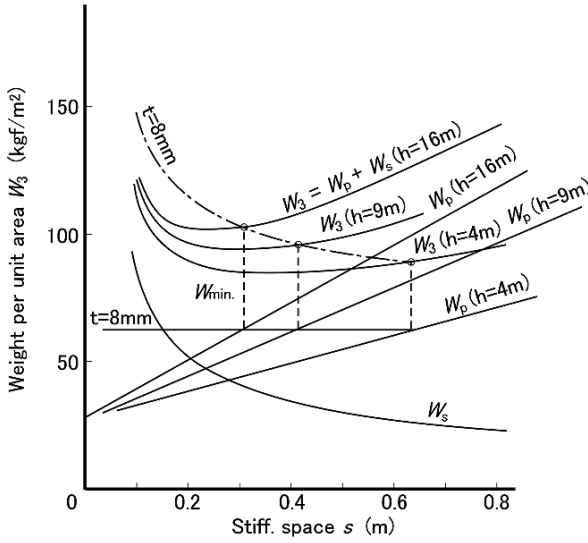


Fig. 6.3.5 Weight per unit area (strength for plate and vibration for beam)

In Table 6.3.1 Case 4 the optimum beam space  $s$  for different spans of  $l$  is shown. Figure 6.3.5 shows the weight difference based on Eq. (6.3.14).

Table 6.3.1, Figs. 6.3.2, 6.3.3, 6.3.4 and 6.3.5 show considerably smaller optimum beam spaces than usually applied, they are, 0.6 ~ 0.9 m.

However, it is recommended that by applying the minimum thickness condition they come up close to the practical values, and the effect of beam space on weight is not so large that a little wider space than the optimum can be applied.

# Chapter 7

## Torsion

### 7.1 Overview of the Theory

Let us discuss the torsion of a bar. The discussion will be proceeded on the basis of the following assumptions:

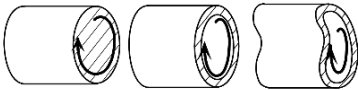
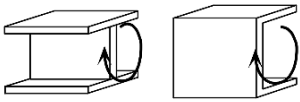
**Assumptions**

- (A) A bar is straight.
- (B) A bar is twisted uniformly.
- (C) A bar has the same cross sectional shape at any point.

The theory of a bar subjected to torsion can be roughly categorized by the following two groups according to the cross sectional shape of the bar as listed in Table 7.1.1:

- solid cylindrical section or closed section composed of thin plate elements
- open section made up of thin plate elements such as I-shape section, U channel section, etc.

**Table 7.1.1** Category of torsional theory

Category	Pure torsion	Torsion with warping
Typical section		
Feature	<ul style="list-style-type: none"> <li>• Solid section</li> <li>• Closed section</li> <li>• No deformation of cross section due to torsion</li> </ul>	<ul style="list-style-type: none"> <li>• Open section</li> <li>• Deformation of cross section causing additional stress</li> </ul>
Theory	Saint-Venant	Wagner
Equation	$T = C \theta$ <p>or</p> $T = C \frac{d\phi}{dz}$	$T = C \frac{d\phi}{dz} + \left( -\Gamma \frac{d^2\phi}{dz^2} \right)$

In this Chapter, the following items are explained.

Section 7.2 will go on to explain the torsion theory of a cylindrical solid section bar. The simple case of a twisted bar, and then describes “pure torsion” theory established by Saint-Venant [23]. That is a general theory applicable to a twisted bar with a closed section. This theory is derived on the basis of the assumption that the plane of a cross section of a twisted bar still remains in the original plane. That is the reason why the theory is called pure torsion. And then, the analogy of a membrane under lateral pressure is introduced, since the analogy can explain the behavior of the twisted bar.

In Sect. 7.3, several examples are shown to calculate the torsional rigidity of various cross sections. The membrane analogy is fully utilized in calculating the torsional rigidity.

In Sect. 7.4, the torsion of an I-section is investigated, since this section behaves in a different way from the above closed section bar. An I-section bar is a simple case of a twisted bar which has an open cross section. In that case, the assumption of Saint-Venant’s theory is not applicable, because the cross section is distorted and the plane of the cross section deforms. The flanges of an I-section generate additional shearing stress due to bending of the flange induced by twisting. The deformation of the plane is called “warping” [24].

In Sect. 7.5, the general theory of torsion with warping is presented. Torsion with warping occurs usually in the case of twisting of an open section bar; the problem of torsion with warping was theoretically analyzed by Wagner. The theory assumes that the cross section of a twisted bar causes deformation of the section and it results in a normal stress along the bar’s length. Wagner’s theory is usually called “torsion with warping”, in contrast with “pure torsion” by Saint-Venant. Table 7.5.1 provides a list of torsional rigidity and warping rigidity for various sections.

## 7.2 Torsion Theory of Closed Section Bars

Before discussing the general case of a twisted bar with a closed section, let us consider a cylindrical solid bar subjected to twisting because this is the most simple and important case. Let us assume a circular bar fixed at one end is subjected to twisting at another end. This creates shearing stress  $\tau$  due to the twisting angle  $\phi$  as shown in Fig. 7.2.1, and the shearing deformation  $\gamma$  occurs

$$\gamma dz = rd\phi \quad (7.2.1)$$

Corresponding to this deformation, we have shearing stress as in the form;

$$\tau = G\gamma \quad (7.2.2)$$

Substituting Eq. (7.2.2) in Eq. (7.2.1), we find

$$\tau = Gr \frac{d\phi}{dz} \quad (7.2.3)$$

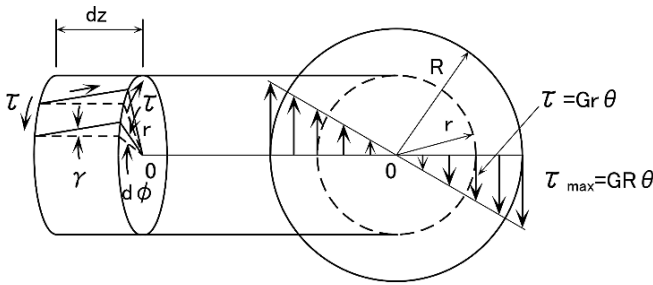


Fig. 7.2.1 Shearing stress distribution in circular cylinder section

Let us introduce the twisting ratio  $\theta$  as the twisting angle per unit length i.e.  $\theta = d\phi/dz$ , then Eq. (7.2.3) can be rewritten

$$\tau = Gr\theta \tag{7.2.4}$$

Since  $\theta$  is a constant value at any point in a cross section because of the assumption (B), the shearing stress increases in proportion to the radius of the circular bar. Consequently maximum shearing stress occurs at the outermost surface of the cylinder. If we sum the shearing stress around the z-axis in the area of a cross section, this balances the twisting moment  $T$  applied to the bar and  $T$  becomes:

$$T = \int_0^R \mathbf{T} \cdot (2\pi r \cdot dr) \cdot r = C\theta \tag{7.2.5}$$

where  $C = \frac{1}{2}G\pi R^4$

or

$$T = C \frac{d\phi}{dz} \tag{7.2.6}$$

In Eqs. (7.2.5) and (7.2.6), the constant  $C$  is called “torsional rigidity”.

The generalized theory of a closed section is established by Saint-Venant and that is usually called “pure torsion” as indicated in Table 7.1.1. The reason for this naming is because the theory is based on the following assumption:

**Assumption**

- (D) The cross section of a twisted bar never distorts, it only rotates perpendicularly around the torsional axis. Even after twisting, the plane of a cross section still remains in a plane. This, in other words, means that there is no normal stress along the bar’s length due to twisting.

Figure 7.2.2(a) illustrates a cylindrical bar twisted by a torsional moment  $T$  around the z-axis. The stress condition of a small portion of the bar is expressed as in Fig. 7.2.2(d), where the normal stress in the z-direction is neglected on the above assumption (D) and only the shearing stresses  $\tau_{xz}$ ,  $\tau_{yz}$  are taken into account. The equation for the shearing force equilibrium in the z-direction can be obtained as follows:

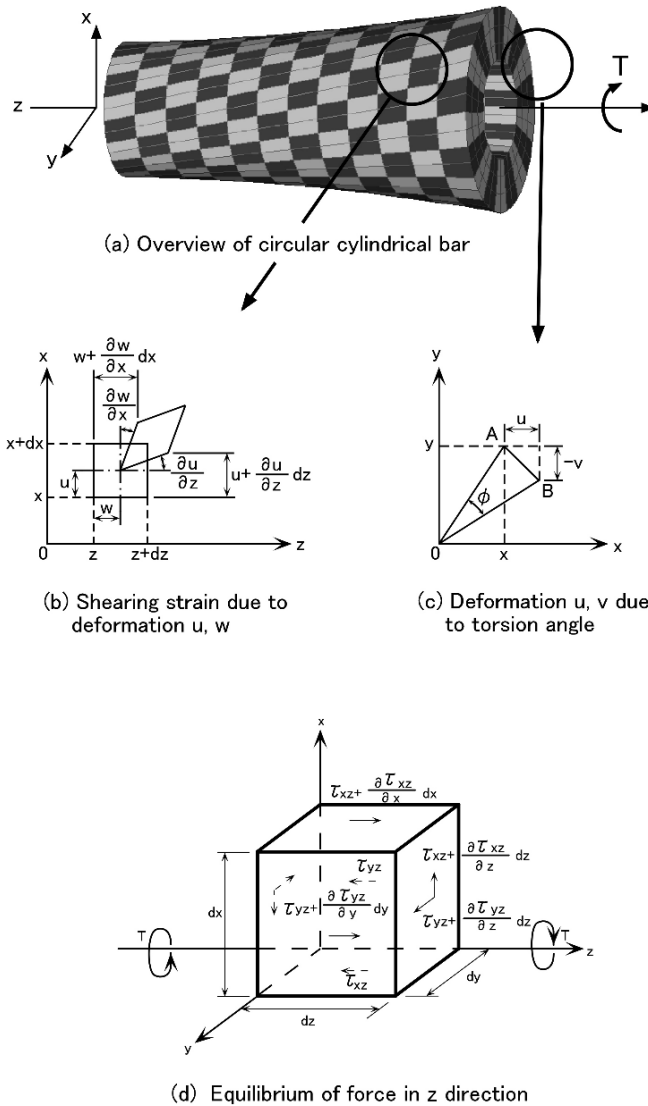


Fig. 7.2.2 Circular cylindrical bar under twisting

$$\frac{\partial \tau_{xz}}{\partial x} + \frac{\partial \tau_{yz}}{\partial y} = 0 \tag{7.2.7}$$

In Fig. 7.2.2(c), when Point A of coordinate  $(x, y)$  moves to Point B due to a twisting by angle  $\phi (= \theta z)$ , the displacement of Point A can be obtained by the following form:

$$\begin{aligned} u &= -y\phi = -y\theta z \\ v &= x\phi = x\theta z \end{aligned} \tag{7.2.8}$$

The shearing strain caused by deformation of  $u$  and  $w$  can be obtained in the following form as shown in Fig. 7.2.2(b):

$$\gamma_{xz} = \frac{\partial u}{\partial z} + \frac{\partial w}{\partial x} = -y\theta + \frac{\partial w}{\partial x} \quad (7.2.9)$$

In the same manner, the following equation can be derived:

$$\gamma_{yz} = \frac{\partial v}{\partial z} + \frac{\partial w}{\partial y} = x\theta + \frac{\partial w}{\partial y} \quad (7.2.10)$$

Therefore, from Eqs. (7.2.8), (7.2.9) and (7.2.10), the shearing stress is related to the displacement by the following equations:

$$\begin{aligned} \tau_{xz} &= G\gamma_{xz} = G \left( -y\theta + \frac{\partial w}{\partial x} \right) \\ \tau_{yz} &= G\gamma_{yz} = G \left( x\theta + \frac{\partial w}{\partial y} \right) \end{aligned} \quad (7.2.11)$$

Equations (7.2.7) and (7.2.11) are differential equations in terms of the two unknown parameters  $\tau_{xz}$ ,  $\tau_{yz}$  and they are solved for specified boundary conditions and applied torsional moments.

In order to put the equations in a more simple form, let us introduce a stress function  $\Psi$  as in the following formula, which automatically satisfies Eq. (7.2.7):

$$\tau_{xz} = \frac{\partial \Psi}{\partial y}, \quad \tau_{yz} = -\frac{\partial \Psi}{\partial x} \quad (7.2.12)$$

From Eqs. (7.2.11) and (7.2.12), the fundamental equation of torsion can be expressed as follows:

$$\frac{\partial^2 \Psi}{\partial x^2} + \frac{\partial^2 \Psi}{\partial y^2} = -2G\theta \quad (7.2.13)$$

Considering the equilibrium of the torsional moment created by  $\tau_{yz}$  and  $\tau_{xz}$ , the following equation is derived by considering that  $\Psi = 0$  at the outer surface:

$$\begin{aligned} T &= \iint (\tau_{yz}x - \tau_{xz}y) dx dy \\ &= - \iint \left( \frac{\partial \Psi}{\partial x} x + \frac{\partial \Psi}{\partial y} y \right) dx dy \\ &= 2 \iint \Psi dx dy \end{aligned} \quad (7.2.14)$$

This means that the torsional moment is equal to the twice the volume inside the closed surface indicated by the stress function  $\Psi$ . This equation is the governing equation of torsion, however, mathematical knowledge is necessary to handle this equation head-on.

Instead of solving the above torsional equation by mathematical analysis, membrane analogy suggested by Plandtl can be applied, because this approach is easier to understand than dealing with the above equation.

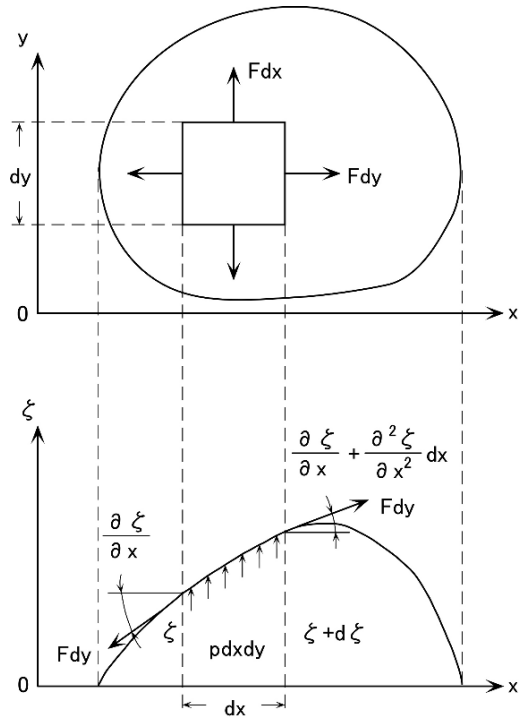
Plandtl has indicated that the behavior of a twisted bar is equivalent to that of a membrane under pressure, which has the same outline as that of the cross section of the bar. Let us imagine the membrane is deformed in the form of  $\zeta$  by the pressure  $p$  as shown in Fig. 7.2.3. Taking the tension of the membrane as  $F$ , we can obtain the equilibrium value for all normal forces:

$$Fdy \frac{\partial^2 \zeta}{\partial x^2} dx + Fdx \frac{\partial^2 \zeta}{\partial y^2} dy + p dxdy = 0 \tag{7.2.15}$$

$$\therefore \frac{\partial^2 \zeta}{\partial x^2} + \frac{\partial^2 \zeta}{\partial y^2} = -\frac{p}{F} \tag{7.2.16}$$

Comparing Eqs. (7.2.15) and (7.2.16) with Eqs. (7.2.13) and (7.2.14), we find the following relations between torsion and membrane analogy;

	Torsion	Membrane	
Function	$\Psi$	:	$\zeta$
	$2G\theta$	:	$p/F$
shearing stress	$\tau = \frac{\partial \Psi}{\partial x}, \frac{\partial \Psi}{\partial y}$	:	$\tau = \frac{\partial \zeta}{\partial x}, \frac{\partial \zeta}{\partial y}$
torsional moment	$T = 2 \iint \Psi dxdy$	:	$T = 2 \iint \zeta dxdy$

(7.2.17)


**Fig. 7.2.3** Equilibrium of deflected membrane under pressure

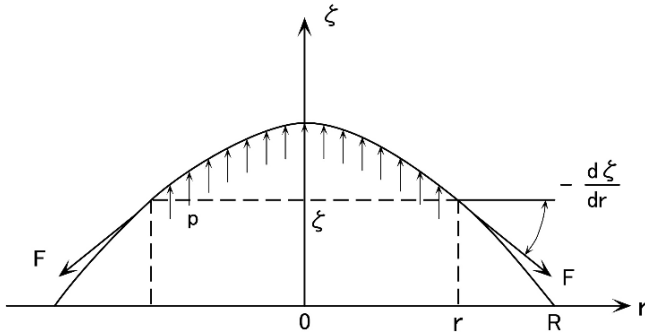


Fig. 7.2.4 Membrane analogy of cylindrical circular section

Therefore, twice the volume bounded by the expanded membrane equals the external torque  $T$ , and the shearing stress  $\tau$  is equal to the slope of the membrane's deflection. Consequently, instead of solving the torsional equation, the stress distribution by torsion can be obtained by investigating the deformation of a membrane.

For example, let us consider the case of a cylindrical section as we have already examined in Eqs. (7.2.5) and (7.2.6). Figure 7.2.4 shows the equilibrium of the upward force caused by the pressure and the downward membrane force. Hence we have the following differential equation:

$$\begin{aligned}
 p \cdot \pi r^2 &= -F \frac{d\xi}{dr} \cdot 2\pi r \\
 \therefore d\xi &= -\frac{rp}{2F} dr = -G\theta r dr \qquad (7.2.18)
 \end{aligned}$$

Solving the above differential equation by considering  $\xi = 0$  at  $r = R$ , we find the deformation of the membrane:

$$\therefore \xi = \frac{1}{2}(R^2 - r^2)G\theta \qquad (7.2.19)$$

Differentiating the above deformation, we obtain the shearing stress in the form

$$\tau = -\frac{d\xi}{dr} = Gr\theta \qquad (7.2.20)$$

As the torsional moment is twice the volume bounded by the deformed membrane,  $T$  can be obtained:

$$T = 2 \int_0^R \xi \cdot 2\pi r dr = \frac{1}{2} G\pi R^4 \theta \qquad (7.2.21)$$

The result of the above calculation agrees with Eqs. (7.2.4) and (7.2.5).



### 7.3 Torsional Rigidity of Various Sections

Let us calculate torsional rigidity of several cross sections by applying the membrane analogy.

(1) *Cylindrical thin plate section:* Let us imagine a thin cylindrical shell, where the inner radius is  $R_1$  and the outer radius  $R_2$  as shown in Fig. 7.3.1. The plate thickness is  $t = R_2 - R_1$ . With the aid of membrane analogy, the deformation of the membrane increases in the thin plate area and the deformation of the inside area of the inner circle becomes constant, because there is no shearing stress in this area. Let us assume the height of this plateau to be  $h$ . Then, according to the relation between torsion and membrane as explained in Eq. (7.2.17), we have the shearing stress expressed by the slope of the membrane in the same way as in Eq. (7.2.20). Hence,

$$\tau = \frac{h}{t} = Gr\theta \tag{7.3.1}$$

Since the torsional moment is twice that of the volume bounded by the deformed membrane, we have the following equation by putting  $R = (R_1 + R_2)/2$

$$T = 2\pi R^2 h = 2G\pi R^3 t\theta \tag{7.3.2}$$

Hence, the torsional rigidity will be

$$C = 2\pi GR^3 t \tag{7.3.3}$$

(2) *Closed section composed of thin plate:* Let us consider a bar having a closed cross section composed of thin plate as shown in Fig. 7.3.2. The membrane is deformed by pressure and it creates the height  $h$  of the membrane.  $A$  is the area surrounded by the centerline of plate thickness  $t$  and  $s$  is the local coordinate along that

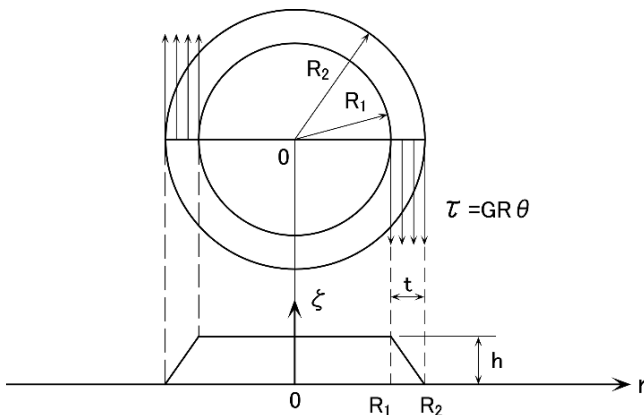


Fig. 7.3.1 Cylindrical thin plate section

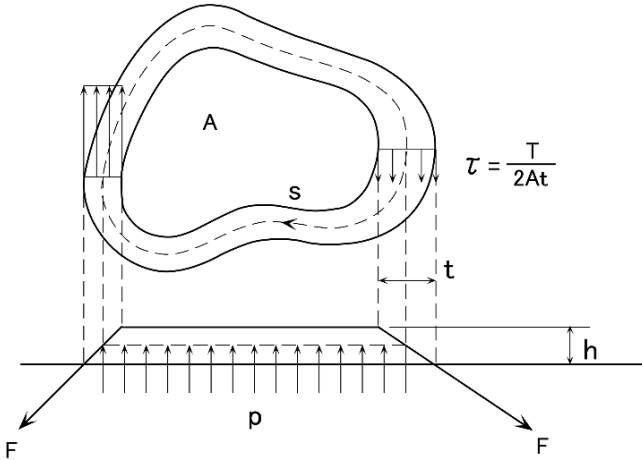


Fig. 7.3.2 Closed thin plate section

centerline. By considering the equilibrium of the upward force due to pressure  $p$  and the downward force induced by the membrane tension  $F$ , we have

$$p \cdot A = \oint F \frac{h}{t} ds \tag{7.3.4}$$

On the other hand, we have the following relation as expressed by Eq. (7.2.16):

$$\frac{p}{F} = 2G\theta \tag{7.3.5}$$

The torsional moment equals twice the volume of the membrane deformation, thus we find

$$T = 2Ah = C\theta \tag{7.3.6}$$

By eliminating  $h, p/F$  and  $\theta$  from Eqs. (7.3.4), (7.3.5) and (7.3.6), we find

$$C = \frac{4GA^2}{\oint \frac{ds}{t}} \tag{7.3.7}$$

The above equation is applicable to the general case of a closed section with one chamber inside the cross section. A typical application of Eq. (7.3.7) is indicated in Fig. 7.3.3. In this example, the area surrounded by the centerline of box plates is  $A = ab$ , therefore, we find the torsional rigidity:

$$C = \frac{4G(ab)^2}{2\left(\frac{a}{t} + \frac{b}{t}\right)} = \frac{2Ga^2b^2t}{a+b} \tag{7.3.8}$$

(3) *Rectangular section of thin plate:* Let us imagine a thin plate having a rectangular section of width  $l$  and thickness  $t$  as shown in Fig. 7.3.4. If we suppose the

**Fig. 7.3.3** Box shape section composed of thin plates

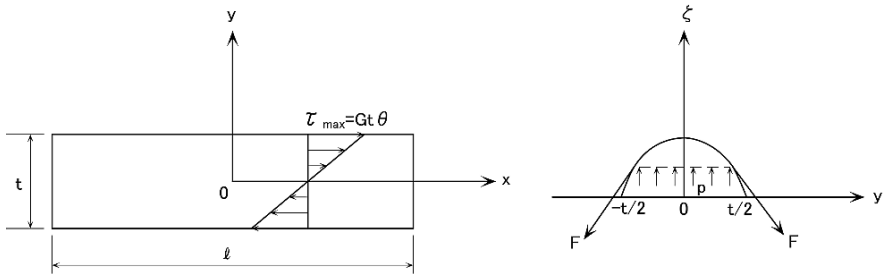
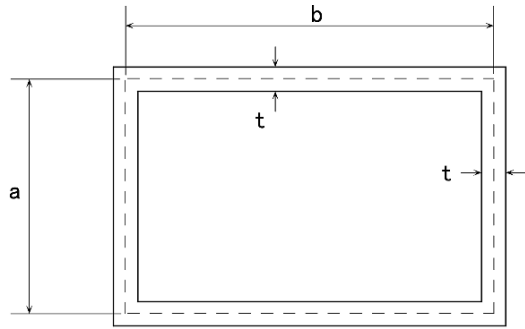


**Fig. 7.3.4** Rectangular section of thin plate

membrane deformation does not change along the plate width and neglecting any distortions near the short edge, from the equilibrium of forces we have:

$$p \cdot 2y = -2F \cdot \frac{d\zeta}{dy} \tag{7.3.9}$$

Hence, the following differential equation can be obtained

$$d\zeta = -\frac{p}{F} y dy = -2G\theta y dy \tag{7.3.10}$$

By integrating this differential equation, we have the deformation of the membrane

$$\zeta = \left( \frac{t^2}{4} - y^2 \right) G\theta \tag{7.3.11}$$

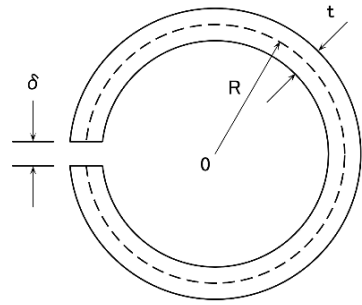
Using the above deformation, we have the torsional moment

$$T = 2l \int_{-t/2}^{t/2} \zeta dy = \frac{1}{3} Glt^3 \theta \tag{7.3.12}$$

Thus, the torsional rigidity of the rectangular plate section is

$$C = \frac{1}{3} Glt^3 \tag{7.3.13}$$

**Fig. 7.3.5** Thin cylindrical section with slit



(4) *Thin cylindrical section with slit:* Equation (7.3.13) gives the general solution to obtain the torsional rigidity of an open cross section composed of thin plates. An example is indicated for the case of a thin cylindrical section with a slit as shown in Fig. 7.3.5. In this case, the circumference of the cylinder is  $2\pi r$  and we have

$$C = \frac{1}{3}G(2\pi r)t^3 = \frac{2}{3}G\pi R t^3 \tag{7.3.14}$$

Comparing the above rigidity with Eq. (7.3.3), in which the cylindrical section has no slit, the rigidity is reduced to

$$\frac{C_{\text{with slit}}}{C_{\text{without slit}}} = \frac{1}{3} \left( \frac{t}{R} \right)^2 \tag{7.3.15}$$

In the case of  $t/R = 1/5$ , the rigidity of a cylinder with a slit becomes 1/75 of that of the cylinder without a slit.

## 7.4 Torsion Theory of I-Section

Let us consider an I-section bar which is fixed at one end and twisted as illustrated in Fig. 7.4.1. From Fig. 7.4.1(b), the plane composed of flanges and webs is distorted at the free end of the bar. Hence, the assumption (D) is not satisfied in this I-section bar. This distortion of the plane is called “warping”.

When the section rotates around the z-axis, the web of the section experiences only torsion, on the other hand, the two flanges will experience bending as well as torsion. If the section rotates by an angle  $\phi$ , the rotation will cause a horizontal displacement of the flanges of  $h\phi/2$ . These displacements induce shearing forces in the upper and lower flanges and each component is

$$V_1 = \frac{h}{2}EI_f \frac{d^3\phi}{dz^3} \tag{7.4.1}$$

Where  $h$  is the height of the web and  $I_f$  is the sectional moment of inertia of the flange around the x-axis.

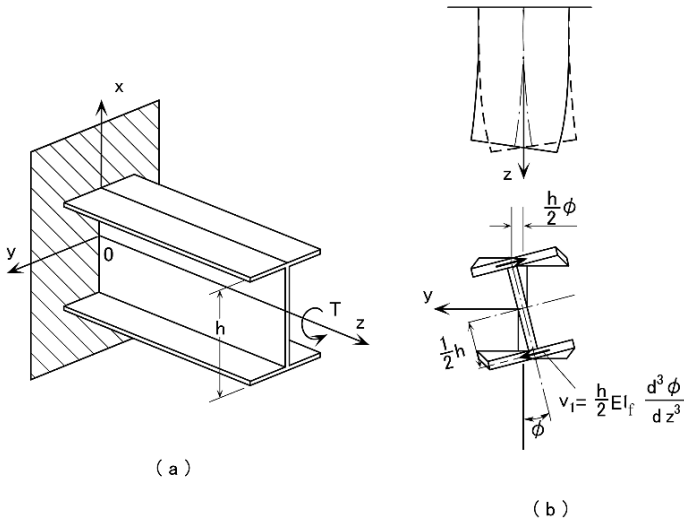


Fig. 7.4.1 Torsion with warping deformation of I section bar

These shearing forces in a flange make a twisting moment  $T_2$ :

$$T_2 = -EI_f \frac{h^2}{2} \frac{d^3 \phi}{dz^3} \tag{7.4.2}$$

In addition, pure torsion is induced due to twisting as follows:

$$T_1 = C \frac{d\phi}{dz} \tag{7.4.3}$$

Therefore, equilibrium of external torsional moment and internal torsional moment can be expressed as in the following form:

$$T = T_1 + T_2$$

$$\therefore T = C \frac{d\phi}{dz} - EI_f \frac{h^2}{2} \frac{d^3 \phi}{dz^3} \tag{7.4.4}$$

This is a fundamental equation of torsion with warping of an I-section bar. This equation is different from that of “pure torsion” in terms of the existence of  $EI_f h^2/2$ , which is called “warping rigidity” and expressed by  $\Gamma$ . Therefore, Eq. (7.4.4) can be rewritten in the form:

$$T = C \frac{d\phi}{dz} - \Gamma \frac{d^3 \phi}{dz^3} \tag{7.4.5}$$

This example of an I-section bar is an easy case to understand in that the flange creates an additional moment due to warping.

### 7.5 Torsion Theory of Open Section Bars

In the case of a twisted bar with an open section, the bar generates not only torsional deformation but also warping deformation as explained in Sect. 7.4. Since that warping is not constant at any point in a cross section, it induces normal stress as a result. The general theory of torsion with warping was established by Wagner.

Before discussing the torsion with warping, let us investigate the shear center. When a shearing force is applied at an arbitrary point on a bar having an open section, the force creates a torsional moment around the center of twisting and consequently it induces torsional deformation and bending deformation simultaneously. However, in the case where the force acts on the center of twisting, torsional deformation will never occur and only bending deformation will be induced. That twisting center point is called “shear center”.

In order to obtain the shear center, the shearing distribution of a cross section must first be considered. Figure 7.5.1 represents the mechanism where a change in normal stress induces shearing stress. Figure 7.5.1(a) illustrates the cross section. Let us consider the equilibrium force in the lower portion of the section; i.e. hatched area. In the longitudinal direction of this bar, the normal stress  $\sigma$  due to bending of the bar is distributed as shown in Fig. 7.5.1(b). By cutting out the lower portion from this section at  $y = y_1$  level, we can observe that the normal stress is acting on both sides of the portion and the shearing stress is working on the cut out surface in Fig. 7.5.1(c). The difference in the normal stress  $\Delta\sigma$  on both sides is caused by the change of moment  $V \cdot \Delta x$ , where  $V$  is a shearing force acting on the cross section, and the sum of the differences in the normal stresses must equal the shearing stress  $\tau_{yx}$

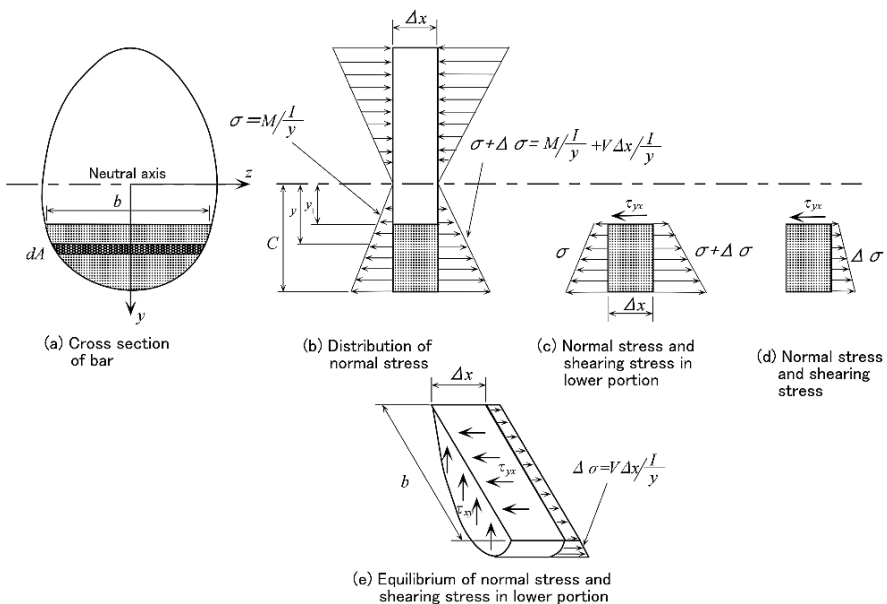


Fig. 7.5.1 Shearing stress distribution due to change of normal stress

as explained in Fig. 7.5.1(d). Hence from the equilibrium of the horizontal forces acting on the lower portion in Fig. 7.5.1(e), the following equation can be derived:

$$\tau_{yx} \cdot \Delta x \cdot b = \int_{y_1}^C V \cdot \Delta x \cdot \frac{I}{y} \cdot dA$$

$$\therefore \tau_{xy} = \tau_{yx} = \frac{V}{Ib} \int_{y_1}^C ydA \tag{7.5.1}$$

The derivation of this equation is already explained by Eq. (2.1.7) in Sect. 2.1. Equation (2.1.7) deals with the shearing stress in the web plate, whereas, the above Eq. (7.5.1) is more generalized.

By using this relation between shearing stress and bending stress, let us calculate the shear center of a channel section subjected to a vertical force of 7500 kgf in Fig. 7.5.2(a). The sectional moment of inertia  $I$  is obtained as follows:

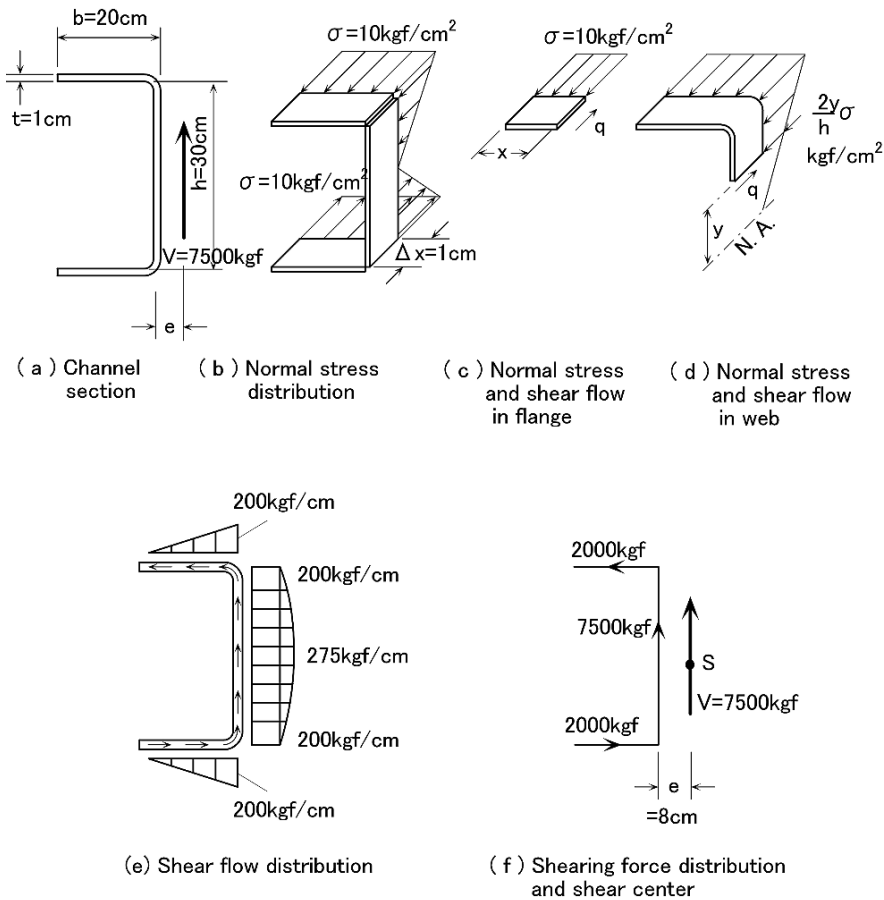


Fig. 7.5.2 Detail of shearing stress distribution

$$I = 2bt \left( \frac{h}{2} \right)^2 + \frac{th^3}{12} = 2 \times 20 \times 1 \times 15^2 + \frac{1 \times 30^3}{12} = 11,250 \text{ (cm}^4\text{)} \quad (7.5.2)$$

When a slice of length  $\Delta x = 1$  (cm) is cut from the channel, the bending moment created by a shearing force  $V$  becomes  $V\Delta x$ , then the difference in the normal stress of the flange  $\sigma$  due to this bending moment is calculated in the following form as shown in Fig. 7.5.2(b):

$$\sigma = V\Delta x \left/ \frac{I}{y} \right. = 7500 \times 1 \left/ \frac{11,250}{15} \right. = 10 \text{ (kgf/cm}^2\text{)} \quad (7.5.3)$$

If we define the shear flow  $q$  by multiplying shearing stress  $\tau$  and plate thickness  $t$ , then the shear flow of the flange at the point  $x$  from the free edge is obtained as follows by considering that the shearing stress must equal the sum of the normal stress as shown in Fig. 7.5.2(c):

$$q = \frac{\sigma x t}{t \Delta x} \cdot t = \frac{10x \times 1}{1} = 10x \text{ (kgf/cm)} \quad (7.5.4)$$

In the vicinity of the web plate of the channel, the shear flow at the point  $y$  from the neutral axis must support the sum of the normal stress of the flange and the normal stress in the upper part of web as shown in Fig. 7.5.2(d). Therefore, it becomes

$$q = \frac{t}{\Delta x} \left\{ \sigma b + \frac{1}{2} \left( \sigma + y \frac{2}{h} \sigma \right) \times \left( \frac{h}{2} - y \right) \right\} = 275 - \frac{1}{3} y^2 \text{ (kgf/cm)} \quad (7.5.5)$$

In the lower part of the web or in the lower flange, the shear flow can be calculated in the same manner, thus the shear flow distribution in this channel section is obtained as illustrated in Fig. 7.5.2(e). The total shearing force in the web plate is estimated by integrating the shear flow over the web plate height and this is

$$F = \int_{-h/2}^{h/2} q dy = 275h - \frac{h^3}{36} = 7,500 \text{ (kgf)} \quad (7.5.6)$$

This shearing force equals the applied shearing force  $V$ .

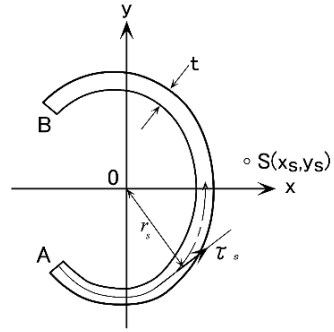
From Fig. 7.5.2(e), the shearing force in the flanges and web is calculated by integrating the shear flow and these forces are plotted in Fig. 7.5.2(f). The torsional moment around the shear center  $S$  in the flanges must be equivalent to that of the web plate, hence, the equilibrium of these torsional moments is expressed in the following form by taking from the distance of shear center to the web plate as  $e$ :

$$\begin{aligned} 2000h &= 7500e \\ \therefore e &= \frac{2000}{7500} \times 30 = 8 \text{ (cm)} \end{aligned}$$

In more general form, the shear center  $S$  of the open section as illustrated in Fig. 7.5.3 is proved by the following equation:



**Fig. 7.5.3** Shear center of channel section



$$\begin{aligned}
 x_s &= \frac{1}{I_x} \int_A^B r_s \left( \int_0^s y t ds \right) ds \\
 y_s &= \frac{1}{I_y} \int_A^B r_s \left( \int_0^s x t ds \right) ds
 \end{aligned}
 \tag{7.5.7}$$

where  $r_s$ : projection length between the origin of coordinate and the subject point  
 As explained in Sect. 7.4, the general form of the fundamental equation of torsion with warping is expressed by the following equation:

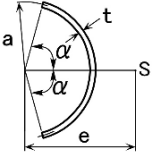
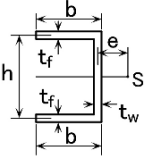
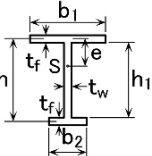
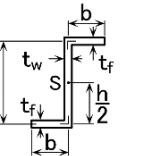
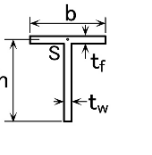
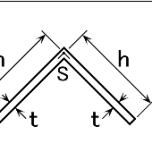
$$C \frac{d\varphi}{dz} - \Gamma \frac{d^3\varphi}{dz^3} = T
 \tag{7.5.8}$$

where the warping rigidity  $\Gamma = E \int_A^B w^2 \cdot t ds$  can be obtained by performing the following integration in terms of warping function  $w$ :

$$w = \frac{\int_A^B t \left( \int_0^s r ds \right) ds}{\int_A^B t ds} - \int_0^s r ds
 \tag{7.5.9}$$

As shown in the above equation, torsional moment  $T$  includes the pure torsional moment as well as moment due to warping. Typical examples of torsional rigidity and warping rigidity are listed in 7.5.1.

**Table 7.5.1** Shear center, torsional rigidity and warping rigidity

Cross section	e J $\Gamma$
	$e = \frac{2a(\sin \alpha - \alpha \cos \alpha)}{\alpha - \sin \alpha \cos \alpha}$ $J = \frac{2}{3} a \alpha t^3$ $\Gamma^* = \frac{2}{3} a^5 t \left\{ \alpha^3 - \frac{6(\sin \alpha - \alpha \cos \alpha)^2}{\alpha - \sin \alpha \cos \alpha} \right\}$
	$e = \frac{3b^2 t_f}{6bt_f + ht_w}$ $J = \frac{1}{3} (2bt_f^3 + ht_w^3)$ $\Gamma^* = \frac{b^3 h^2 t_f}{12} \frac{3bt_f + 2ht_w}{6bt_f + ht_w}$
	$e = \frac{I_2}{I_1 + I_2} h, \quad I_1 = \frac{1}{12} b_1^3 t_1, \quad I_2 = \frac{1}{12} b_2^3 t_2$ $J = \frac{1}{3} (h_1 t_w^3 + b_1 t_1^3 + b_2 t_2^3)$ $\Gamma^* = \frac{1}{12} \{ b_1^3 t_1 e^2 + b_2^3 t_2 (h - e)^2 \}$
	$J = \frac{1}{3} (2bt_f^3 + ht_w^3)$ $\Gamma^* = \frac{b^3 h^2}{12(2b+h)^2} \{ 2(b^2 + bh + h^2)t_f + 3bht_w \}$
	$J = \frac{1}{3} (bt_f^3 + ht_w^3)$ $\Gamma^* = \frac{b^3 t_f^3}{144} + \frac{h^3 t_w^3}{36}$
	$J = \frac{2}{3} ht^3$ $\Gamma^* = \frac{1}{18} h^3 t^3$

e : Location of shear center (S)

J : Torsional constant C=GJ

$\Gamma^*$  : Warping rigidity  $\Gamma^* = \frac{\Gamma}{E}$

# Chapter 8

## Deflection of Hull Structures

Generally, in designing a structure there are three important considerations: strength, deflection and vibration. Strength is the most important item because any structures can not hold its intended form without strength.

Deflection depends on the rigidity of the structure. Vibration causes trouble by resonance where the exciting frequency coincides with the natural frequency of the structure. From the failure viewpoint deflection and vibration are not so important as they cause only small additional stresses, but from the habitability and fitting viewpoints they are becoming more important.

For a bending member as a beam the strength is denoted by  $I/y$ , the rigidity for deflection is expressed by  $I$  and the vibration depends on  $I/a$ . It is important to note that in all cases  $I$ , the sectional moment of inertia, is involved which is a fundamental property of the structure.

Up to here, from Chapters 1 to 7, the following five items are explained about deflection.

(1) *Section 1.11 additional bending moment due to forced displacement:* A beam supported by a girder will have additional bending moment which causes additional stress due to displacement of the girder.

(2) *Section 2.3 bottom transverse supported by centerline longitudinal girder:* In a bottom transverse, additional bending moments and shearing forces will be generated by deflection of the centerline longitudinal girder.

(3) *Section 2.4 deflection of girders:* The deflection pattern caused by shearing and the ratio of bending and shearing deflections are explained.

(4) *Section 5.1 boundary conditions of plates:* Additional stresses will be induced in a plate by deformation of the boundary of the plate.

(5) *Section 6.3 optimum space of beams:* The conditions by which stiffened panels will not be resonant with exciting frequencies lower than 1000 cpm, is explained.

All items except Sect. 2.4 “Deflection of Girders” are concerned with the additional stress in a secondary member caused by the deflection of a primary supporting member.

In a design based on stress in the case of elastic design as well as plastic design, the deflection itself cannot be a main design condition but is a supplementary condition limiting additional stress due to deflection.

On the other hand classification society's rules, which have been established based on long years of experience, restrict the deflection to some extent. From the viewpoint of avoiding failure the restriction on deflection seems not to be necessary. The fact that the classification societies have some restriction on deflection means that some problems have been experienced in the past.

In this chapter the deflection of hull structure, hull girder deflection, deflection of beams, deflection of girders and webs, additional stress in secondary members caused by the deflection of a primary supporting member, and the limitation of deflection from viewpoints other than strength, are explained.

## 8.1 Deflection of Hull Girder

For the components in ships to limit the deflection of a hull girder, the following items are to be considered but no limitation exists from the strength viewpoint. A bigger hull girder deflection will be expected for a ship with bigger  $L/D$ , to which attention will be paid.

- (1) Expansion and contraction of pipes and rods fitted in longitudinal direction on the upper deck or bottom.
- (2) Increase of draft caused by deflection of hull girder.
- (3) Generation of secondary stress by the deflection of hull girder.
- (4) Flexural vibration of hull girder, "whipping".

For item (1) usually expansion joints are fitted where necessary. Generally hull girder bending stress is to be estimated at about 200 MPa which corresponds to a strain of  $\varepsilon = \sigma/E = 200 \text{ MPa}/205,800 \text{ MPa} = 1/1029 \approx 1/1000$ . Accordingly an expansion joint of  $\pm 1 \text{ cm}$  is enough for a 10 m long fitting. Actually a fitting designer designs long pipes with expansion joint of  $\pm 2 \text{ cm}$  per 10 m in length.

Item (2), the increase of draft will be a problem when a ship with a deep draft passes through some shallow straight. Another problem is the decrease of deadweight in the case of sagging deflection because the freeboard mark is at midship.

A welded ship usually has sagging deflection even with no load because the deck part is welded at the last stage and because of shrinkage of welded metal, the deck part contracts. Because of this sagging there will be a loss of deadweight as mentioned above. To avoid this loss of deadweight a ship will be constructed originally with a hogging deflection which is called initial hogging.

The amount of the initial hogging is expressed by the following equation depending on the  $L/D$  of the ship and the welding volume in the upper deck which is replaced by the number  $n$  representing the number of erection butts on upper deck [25].

$$\delta = 0.75 \frac{L}{D} n - 77 \text{ mm}$$

where

- $\delta$  : amount of initial hogging
- $L$  : length of ship
- $D$  : depth of ship
- $n$  : numbers of erection butts on upper deck

After launching, a ship deforms in the sagging condition and the amount of the initial hogging is equal to the sagging deformation after launching. In this condition there remains tensile residual stress in the upper deck and in other parts of the ship, such as bottom and side members, compressive residual stress will remain.

The main concern regarding (3) secondary stress generated by the deflection of the hull girders, is the compression in vertical members such as transverse bulkheads. In Fig. 8.1.1 the mechanism of how compressive stress is generated by hull girder deflection is shown. This is the same mechanism as explained in Fig. 4.5.3.

Here the compressive stress in a transverse bulkhead is studied. Assuming the area of the upper deck is  $A_l$ , the longitudinal bending stress in the upper deck is  $\sigma_l$ , the sectional area of the transverse bulkhead is  $A_t$  and the compressive stress in the transverse bulkhead is  $\sigma_t$  the following equation is derived.

$$2A_t \sigma_t = A_l \sigma_l \theta \tag{8.1.1}$$

$\theta$  is approximately expressed as follows where  $\delta$  is the deflection of the hull girder and  $L$  is length of the ship.

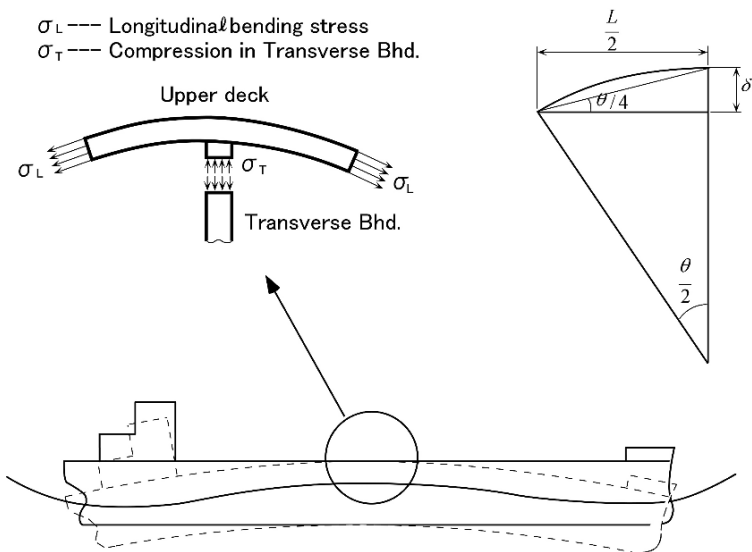


Fig. 8.1.1 Compression in vertical member due to hull girder bending

$$\begin{aligned}\delta &\approx \frac{L}{2} \cdot \frac{\theta}{4} \\ \therefore \frac{\delta}{L} &\approx \frac{\theta}{8}\end{aligned}\quad (8.1.2)$$

From Eqs. (8.1.1) and (8.1.2), the relation of (8.1.3) can be obtained.

$$\sigma_t = 4 \frac{A_l}{A_t} \cdot \sigma_l \cdot \frac{\delta}{L} \quad (8.1.3)$$

Assuming  $A_l/A_t = 2.0$  and  $\delta/L = 1/1000$ , then  $\sigma_t/\sigma_l = 1/125$  which is negligible.

The amplitude of the flexural vibration of a hull girder is proportional to the static deflection of the hull girder and inversely proportional to the sectional moment of inertia of the hull girder. However it is very difficult to establish a limit for the hull girder rigidity from the vibration viewpoint because in the vibration problem, resonant phenomena are very important. Recently the vibration response caused by whipping has established and it may be possible to have an allowable limit for whipping stress [26].

From the longitudinal strength viewpoint deflection of the hull girder cannot be limited. However the classification societies have a rule which limits the deflection of the hull girder based on their long experience. That is because hull girder deflection has a good correlation with  $L/D$  and the tensile strength of steel, such as HT32 and HT36.

The following relation is established where the longitudinal strength is evaluated keeping upper deck and bottom stresses lower than  $\sigma_a$ .

$$\delta = K \frac{WL^3}{EI} = \frac{K \cdot WL \cdot L^2}{E \cdot \frac{I}{y} \cdot y} = 2K \frac{\sigma_a}{E} \cdot \frac{L}{D} \cdot L \quad (8.1.4)$$

where

$\delta$  : deflection of hull girder at midship

$W$  : load applied on hull girder

$E$  : Young's modulus

$I$  : sectional moment of inertia of hull girder

$L$  : ship length

$D$  : ship depth

$y$  : distance between neutral axis and upper deck or bottom ( $y \approx D/2$ )

$K$  : constant

From the above analysis it is found that the ratio of deflection to ship length  $\delta/L$  is proportional to the ratio of ship length and ship depth  $L/D$ . Classification society rules provide for an upper limit of  $L/D$ . For example, the Lloyds Register of Shipping 1976 Rules give 17 as the maximum value of  $L/D$ . In cases where  $L/D$  is over 17, the allowable longitudinal stress has to be modified so that  $\sigma_a \times \frac{17}{L/D}$

which makes the hull girder deflection equivalent to the case of  $L/D = 17$ . In the case where high tensile steel HT32 or HT36 is applied on the deck and bottom, the reduction coefficient of section modulus has a limitation of 0.059 ( $L/D$ ) where 0.059 corresponds to  $1/17$ .

The latest classification rules, for example, the Nippon Kaiji Kyokai (NK) 1996 rules have the following regulation which follows the IACS unified rule:

$$I \geq 3ZL \quad (8.1.5)$$

where

$I$  : sectional moment of inertia at midship section in  $\text{cm}^4$

$Z$  : section modulus at midship section in  $\text{cm}^3$

$L$  : length of ship in m

Equation (8.1.5) can be rewritten using cm units as follows:

$$I \geq \frac{3ZL}{100} \quad (8.1.6)$$

Putting  $Z = I/y \approx 2I/D$  into Eq. (8.1.6), the following relationship is obtained:

$$I \geq \frac{6IL}{100D} \\ \therefore L/D \leq 16.7 \quad (8.1.7)$$

The above  $L/D \leq 16.7$  corresponds well to  $L/D = 17$  of the Lloyds Register of Shipping 1976 Rules.

Figure 8.1.2 shows the actual data for the hull girder deflection  $\delta$  in still water against ship length  $L$ . Recently  $\delta/L$  is getting bigger than  $1/1000$ .

Hull girder deflection used to be calculated by integrating the  $M/I$  curve twice. As an approximation it was estimated using the midship bending moment. The former requires time and labour, and the latter is preferred to the deflection in a wave where the bending moment distribution is quite similar to the actual conditions, but not good for still water because the bending moment distribution is changed by the loading condition.

Assuming the hull girder as a simply supported beam, the deflection for each load at midship can be calculated. By summing up these deflections the total deflection of the hull girder can be obtained easily and accurately [27].

Figure 8.1.3 shows a beam supported at both ends. The deflection  $\delta$  at midship from a load  $W$  is expressed by the following equation.

$$\delta = \frac{W}{12EI} (2l^3 - 3lx^2 + x^3) \quad (8.1.8)$$

where

$W$ : amount of load

$x$  : distance between midship and loaded point

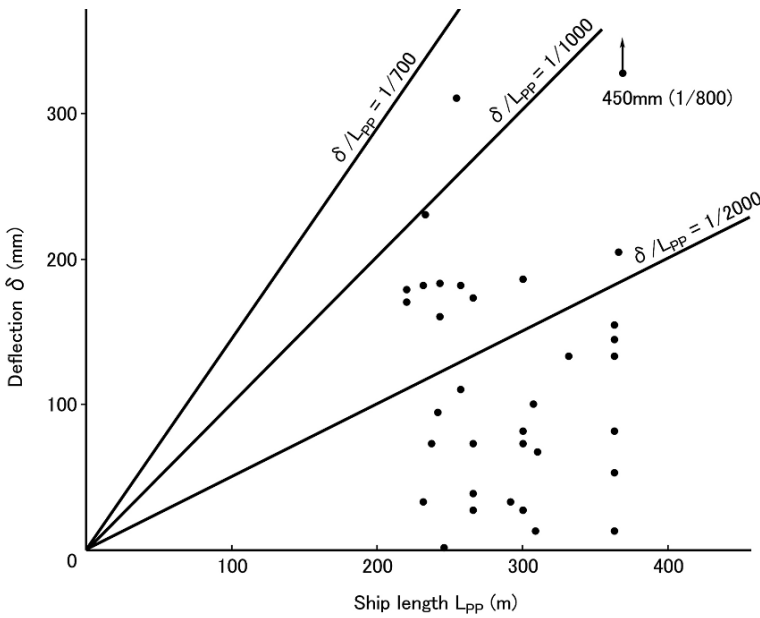


Fig. 8.1.2 Deflection of hull girder still water

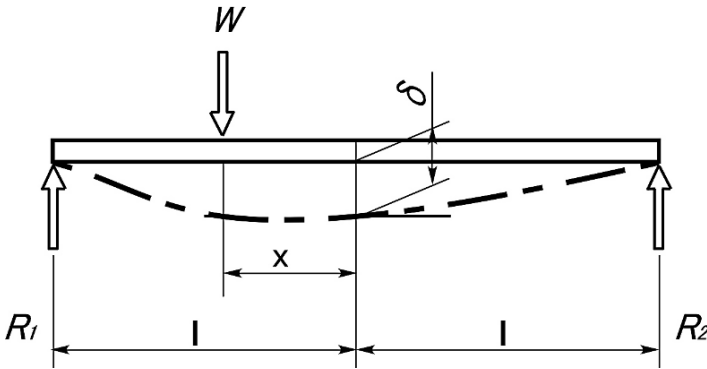


Fig. 8.1.3 Deflection of both ends supported beam

- $l$  : half length of ship
- $E$  : Young's modulus
- $I$  : sectional moment of inertia of midship section

Applying the above formula, the deflections at midship from each load and buoyancy are calculated and added.

For each load a reaction is generated at the supporting points, i.e., the fore and aft ends of the ship, but after summing up the total reaction will be zero which means that both ends are free, that is, a floating condition.



## 8.2 Deflection of Beams with Optimum Section

The deflection of the optimum beam explained in Sect. 1.8 is studied hereafter. Assuming the beam is fixed at both ends and has uniform load, the maximum bending moment  $M$  and the maximum deflection  $\delta$  are expressed by the following equations:

$$M = \frac{Wl}{12} \quad (8.2.1)$$

$$\delta = \frac{Wl^3}{384EI} \quad (8.2.2)$$

where

$W$ : total weight applied to the beam

$l$  : span of the beam

$E$  : Young's modulus

$I$  : sectional moment of inertia

Putting the allowable stress into  $\sigma$  and the section modulus into  $Z$ , the following equation can be obtained:

$$\sigma = \frac{M}{Z} = \frac{Wl}{12Z} \quad (8.2.3)$$

$$\therefore Wl = 12Z\sigma$$

Putting the above into Eq. (8.2.2) the following equation is obtained:

$$\frac{\delta}{l} = \frac{12Z\sigma l}{384EI} \quad (8.2.4)$$

Putting the equations for the optimum section of a beam, based on the elastic design shown in Table 1.8.1(a) into Eq. (8.2.4),  $\delta/l$  for the optimum section is obtained as follows.

$$d = \alpha \sqrt{Z/t_w}$$

$$I = \beta Z \sqrt{Z/t_w}$$

$$\therefore I = \frac{\beta}{\alpha} Z d \quad (8.2.5)$$

$$\frac{\delta}{l} = \frac{12Z\sigma l}{384EI} = \frac{12Z\sigma l}{384E \frac{\beta}{\alpha} Z d} = \frac{12\sigma}{384E} \cdot \frac{\alpha}{\beta} \cdot \frac{l}{d} \quad (8.2.6)$$

Equation (8.2.6) shows that the deflection per length of a beam  $\delta/l$  is proportional to the allowable stress  $\sigma$  and the slenderness ratio  $l/d$ .  $\alpha/\beta$  is 2.0 for a balanced girder, 1.0 for a girder with plate and 1.3 for an intermediate section. The deflection of a balanced girder is twice that of a girder with plate where  $\sigma$  and  $l/d$  are equal in both cases. For a given span and load, the bending moment is calculated irrespective of whether the balanced girder or not, and for an allowable stress

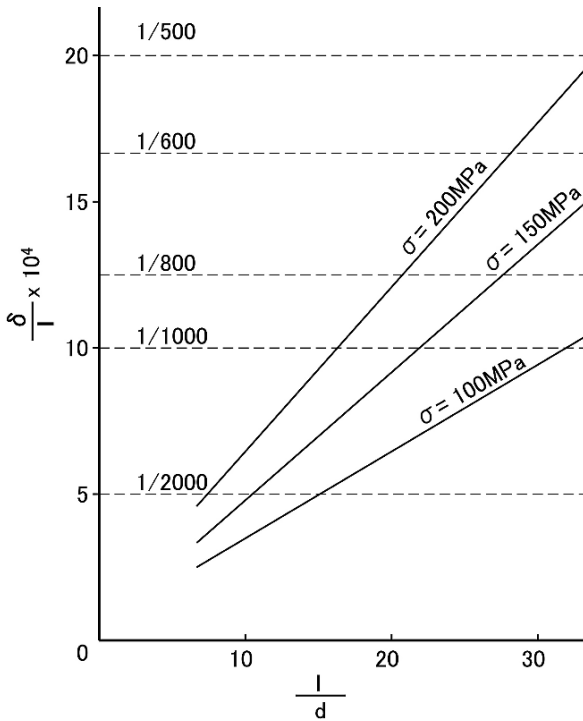


Fig. 8.2.1 Deflection of optimum beam

$\sigma$ , the necessary section modulus is derived. For a given section modulus the optimum depth of the balanced girder is  $1.10\sqrt{Z/t_w}$  and that of the girder with plate is  $1.23\sqrt{Z/t_w}$ . Accordingly in the optimum condition,  $l/d$  for a balanced girder is bigger than that for a girder with a plate by 12%.

Comparing  $\frac{\alpha}{\beta} \times \frac{l}{d}$  in Eq. (8.2.6) for the balanced girder and for the girder with a plate, the former is 2.24 times bigger than the latter. As seen from the above consideration, a balanced girder has a smaller sectional moment of inertia for a certain section modulus.

In Fig. 8.2.1 the relation between  $\delta/l$  and  $l/d$  is shown for the optimum section of a girder. For example, in the case that  $\delta/l$  is 1/800 and  $\sigma$  is 200 Mpa,  $l/d = 20$  is optimum.

### 8.3 Deflection of Girders and Web Frames

As known from Eqs. (8.1.4) and (8.2.6), the ratio of deflection and span  $\delta/l$  is proportional to the design stress  $\sigma$  and to the ratio between span and depth  $l/d$ . Hull structure designers have to pay particular attention so as to detect extraordinary cases where the deflection of a beam or a girder may cause troubles.

A hull girder acts like a free-free beam (both ends supported and no reaction at both ends), and the deflection is bigger than that for a both ends fixed beam. As shown in Fig. 8.1.2 the hull girder deflection in still water is in the order of  $L/1000$ . In waves, assuming the longitudinal bending stress in waves is twice that in still water, the deflection will be  $L/500$ . These values are for ordinary ships with  $L/D = 11 - 13$ , but for special ships with a  $L/D$  of over 14, special attention has to be paid to the deflection of the hull girder.

In the 1960s some troubles were experienced regarding the alignment of propeller shafts in ships with bigger  $L/D$  than ordinary ships. The deflection of the hull girder might badly affect the shaft alignment.

For secondary members such as beams, frames, and stiffeners  $l/d$  is usually 20–25, for deck girders 15–20, and for girders in a tank around 8.

Figure 8.2.1 shows that for a design stress of 150 MPa, deflection is 1/1000 of the span for the secondary member, 1/1200 for the deck girder, and 1/3000 for the girder in tank.

The hatch side girder and the hatch end strong beam of a cargo ship are designed to have a shallow depth to ease cargo handling. In this case the deflection will be big. A senior designer chose a value of  $\delta/l \leq 1/1000$  based on his/her know-how with both ends supported condition, which seems to be a little severe.

As stated in Eq. (2.4.7) in Sect. 2.4. in the case of a girder with small  $l/d$  i.e. less than 14, the shearing deflection is not negligible but sometimes bigger than the bending deflection. In this case both bending and shearing deflections are to be considered.

## 8.4 Additional Stress Caused by Deflection

In Sects. 1.11 and 2.3 the additional stresses in a beam and girder caused by the deflection are explained. The deflection at the supporting point causes an additional stress in the supported member.

In Sect. 1.11 Additional Bending Moment due to Forced Displacement, it is explained that the displacement  $\delta$  at the supporting point will cause an additional bending moment  $M_\delta$  in the supported member as follows.

$$M_\delta = \frac{6EI}{l^2} \delta \quad (8.4.1)$$

where

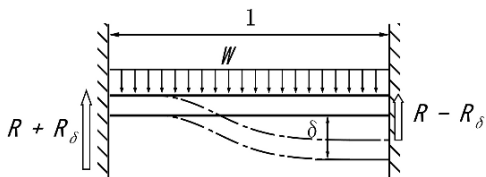
$l$  : span of beam

$I$  : sectional moment of inertia of beam

$E$  : Young's modulus

In this case the following reaction force  $R_\delta$  is generated at the supporting points at the same time.

**Fig. 8.4.1** Reaction due to deflection at support



$$R_{\delta} = \frac{12EI}{l^3} \delta \tag{8.4.2}$$

As shown in Fig. 8.4.1 the reaction force is added at the rigid supporting point and deducted from the deflected supporting point. This is a natural philosophy, that is, the stronger supports a bigger load and the weaker a less load.

Supposing that on the longitudinal stiffener supported by a transverse bulkhead and the adjacent vertical web, the deflection of the vertical web is bigger than that of the transverse bulkhead, when water pressure is applied. Accordingly a longitudinal stiffener has an additional bending stress and simultaneously a reaction is added to the supporting point of the transverse bulkhead. As an example shown in Fig. 8.4.2, the following calculation is carried out.

$$M = \frac{Wl}{12} = 52.2 \text{ kN-m}$$

The longitudinal stiffener is designed with allowable stress  $\sigma$  which is 150 MPa.

$$Z = \frac{M}{\sigma} = 348 \text{ cm}^3$$

The thickness of the web plate is 10 mm and the optimum section is adopted.

$$I = 1.23Z\sqrt{Z/t_w} = 8200 \text{ cm}^4$$

$$M_{\delta} = 63.2\delta \text{ kN-m}$$

$$R_{\delta} = 31.7\delta \text{ kN}$$

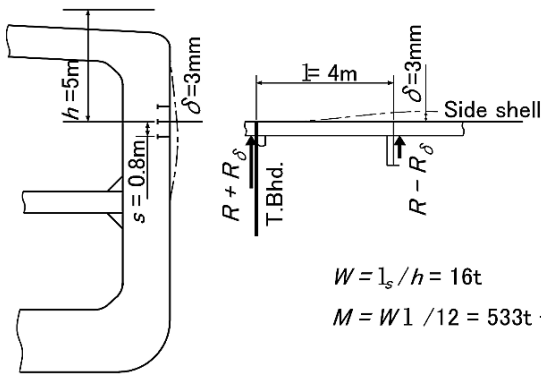


**Fig. 8.4.2** Additional stress on side longitudinal

Here, assuming  $\delta = 0.3$  cm, the following results are obtained:

$$M_\delta = 19.6 \text{ kN-m}$$

$$R_\delta = 9.8 \text{ kN}$$

$M_\delta/M = 0.375$ ,  $R_\delta/R = 0.125$  then the additional stress is 38% and the additional reaction is 13%.

## 8.5 Shearing Deflection

When the hull girder is in a sagging condition, the aft part including the aft engine room deforms in a convex upwards mode. This phenomenon has been known for a long time but not clearly understood. It can be explained by the shearing deflection stated in Fig. 2.4.1 (b) and is simple but very important for design [28].

Figure 8.5.1 shows the shearing deflection of a cantilever with uniform load. Common sense does not expect such deflection to be convex downwards because one is familiar with the bending deflection which is convex upwards.

When one of the authors calculated the hull girder shearing deflection in the vicinity of the aft part of a ship including the aft engine room, the result was not expected. The aft part of the ship was considered as a deep girder with dominant shearing deflection. The load was the buoyancy difference between fully loaded and ballast conditions, that is, a downwards load from the loss of the buoyancy. The results showed that the deflection mode was convex downwards. Repeated calculations showed the same results and finally it was understood that in this case the deflection by bending is convex upwards and the deflection by shearing is convex downwards.

These phenomena can be applied in the control of the deflection of a double bottom in an aft engine room in which shafting is installed.

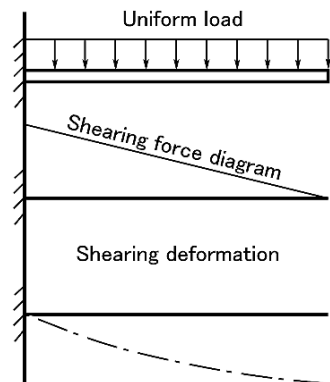


**Fig. 8.5.1** Shearing deformation of cantilever beam with uniform load

Recently with the use of computers, the deflection can be calculated quickly and easily but not by separating that by bending and that by shearing. The mode of the shearing deflection can be understood only by means of a manual calculation, and then the data are integrated from the end of the ship. Such considerations should be kept in a designer's mind even in the computer era.

## Chapter 9

# Welding

A hull structure is constructed by welding steel plates together. Before the use of welding methods in hull construction, the steel plates were joined by rivets. In the case of rivet jointing, because of the many drill holes for riveting in the plates, the strength of the plate decreases comparing that of a non-drill holed plate, i.e. the efficiency of a connection is reduced, and also drilling needs much man-power. In addition to that, from the view point of the structural designer, the design of a rivet connection needs much work, since it is required to determine the location of every rivet hole. On the contrary, in case of welding, the designer has only to draw a line to present a weld line, instead of every rivet hole, and to indicate the edge preparation and to decide the welding sequence, if necessary.

In applying a rivet joint to a connection, the adjacent connections were designed so as not to be in line with each other, because the efficiency of a rivet joint is reduced. Such a practice of joint arrangement remained long after welding was adopted.

In the 1950s, although rivet joints were still used for seams, welding was applied to the butts in the outer shell plate connections and deck plate connections. This joint arrangement means that there was no complicated joint connected by three plates at the cross point of a butt joint and a seam joint. Such connections were inconvenient for both the construction people and the design people, for it was difficult to arrange three plates accurately. Rivet joints were gradually replaced by welding one after another, and in the 1970s only the riveting of bilge keel and shell plating was left. The purpose of this rivet joining was to prevent crack propagation from the bilge keel to the shell plating, however, nowadays this joint has been changed to welding due to the development of reliable welding processes, and a rivet joint is utilized only for a special connection, such as between steel plate and aluminum plate, etc.

In recent ship design, the designer doesn't pay so much attention to welding. However, it is recommended that designers consider the importance of welding connections because the vessel will break into pieces if welding is destroyed.

In designing for welding, it is important to maintain welding strength as well as to maintain productivity, since the welding process takes the most man-hours in the hull construction process.

Several unexpected happenings have taken place during the transition from riveted construction to welded construction. One example occurred in tank testing

when a tank was filled with water to confirm the tightness of the tank boundary. There was no leakage of water around the tank, but the water flowed out at the far point of the tank. The reason of this happened was that water went through a gap in the fillet welding of the tank and it flowed out from pin holes at the far point. We usually regard a welded structure as a water and gas tight structure, however, it is not correct to consider that a welded structure is 100% tight against water and gas because welding contains a certain percentage of defects.

When welding was first introduced to the production of vessels, strength and toughness of the welding joint was thought to be less than that of the base metal because of welding defects. This thought was reflected in the welding practice that welding lines should be staggered. Another example was seen in the practice of a welding line not being designed to interfere with another welding line. It was because that the strength of the steel plate might be damaged by being heated twice.

Comparing butt welding and fillet welding, the latter is useful for the saving of man power in many cases. In joining an upper plate and lower plate by horizontal welding, butt welding can be replaced by fillet welding.

This chapter explains butt welding and fillet welding, which are the basis of welding, and then gives examples of welding design to achieve high productivity. Finally, detail design for welding is described in association with methods to prevent water leakage, scallops to prevent interference of welding lines, replacement of butt welding by fillet welding.

## 9.1 Butt Welding

The strength of a butt welding joint is considered to be satisfactory for static loads.

That is because

- (1) The ultimate strength of deposited metal is said to be more than that of the base metal.

For example, in the case of mild steel, the ultimate strength  $\sigma_B$  of base metal is 41–50 kgf/mm<sup>2</sup> and  $\sigma_B$  of deposited metal is 41–57 kgf/mm<sup>2</sup>.

- (2) Reinforcement of the weld is provided.
- (3) Small welding defects don't affect the static strength.

On the other hand, fatigue strength of a butt welded joint reduces from that of the base plate as shown in Fig. 9.1.1 [29, 30]. The reason for that fatigue strength reduction is explained as

- (1) There is a discontinuity of shape between the deposited metal and base plate which causes a stress concentration.
- (2) *Small defects inside welding affect the fatigue strength.* The fatigue strength of a welded joint can be evaluated in terms of the cumulative fatigue damage factor calculated by (1) the S–N curve obtained by fatigue tests of welded joints under repeated tension and (2) the distribution of encountered stress cycles. The failure of a welded joint due to fatigue usually occurs in the base plate, not in the deposited metal.



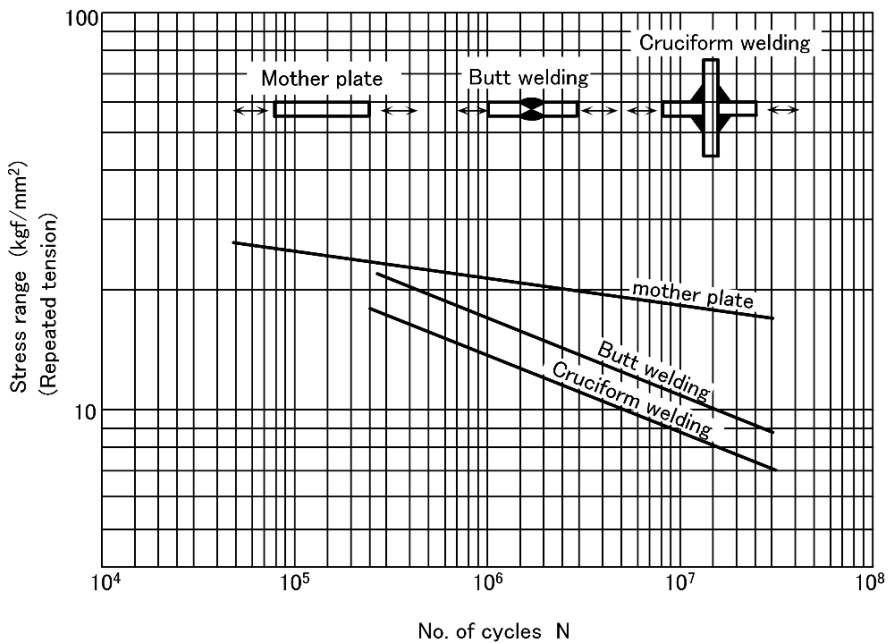


Fig. 9.1.1 Example of fatigue strength of mild steel welding

Regarding the butt welding method for connecting flat plates such as outer shell platings, deck platings etc., the submerge arc welding process is applied for downward welding and the electrogas arc welding process for upright welding. These welding processes are used in the workshop and in the building dock, which can contribute to efficient production. In contrast with this situation, manual welding or semi-automatic welding is normally applied to the connection of internal members.

Let us consider the relation between the edge preparation and the sectional area of deposited metal, as shown in Fig. 9.1.2. From this figure, we find that the sectional area of the X-shape groove is considerably smaller than that of the V-shape. For example, comparing the sectional area of the X-shape groove, which is vertically symmetric, with the area of the V-shape, the former is just half of the latter. Therefore, from the view point of productivity, a symmetric X-shape edge preparation is helpful to save welding man-power for upright and horizontal butt welding. In spite of that, a V-shape edge preparation, or X-shape of which the upper groove is larger than the lower, may be applicable to downward butt welding.

Another effective way to reduce the man-power for welding is to decrease welding length. In order to do this, the application of wider plates is the most simple and useful solution. If a large panel of uniform thickness is fabricated by several small panels, the use of wider plates doesn't cause an increase of steel weight. But in the case where the thickness of a large panel varies such as in a transverse bulkhead, the application of wider plates increases the steel weight.

As an example, let us calculate the increase of weight by applying wider plates based on the NK deep tank rule. The plate thickness  $t$  of deep tank bulkheads is given by the following Equation:

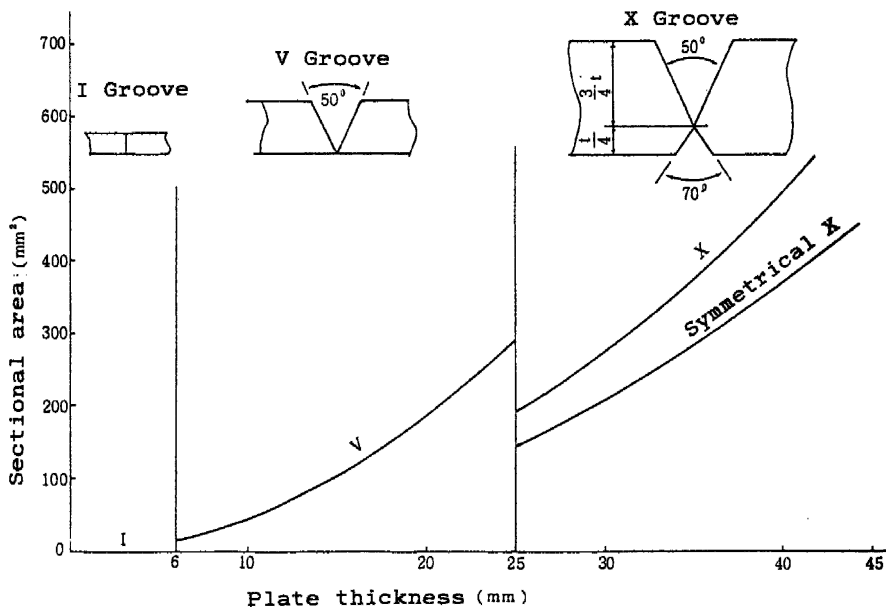


Fig. 9.1.2 Shape and sectional area of welding groove

$$t = 3.6s\sqrt{h} + 3.5 \text{ mm} \tag{9.1.1}$$

where

$s$  : stiffener space

$h$  : water head at the lowest point of plate

Assuming the transverse bulkhead of depth  $D$  is divided equally by  $n$  into narrow plates of width  $D/n$ , and the water head is taken as the distance from the top of the bulkhead to the bottom of the subject plate. Thus the plate thickness at each height is obtained as follows:

$$\left. \begin{aligned} t_1 &= 3.6s\sqrt{\frac{D}{n}} + 3.5 \\ t_2 &= 3.6s\sqrt{\frac{2D}{n}} + 3.5 \\ &\vdots \\ t_n &= 3.6s\sqrt{\frac{nD}{n}} + 3.5 \end{aligned} \right\} \tag{9.1.2}$$

Hence the total area of the bulkhead plate  $A$  is calculated by summing up the multiplication of plate thickness  $t_1, t_2, \dots, t_n$  and plate width  $D/n$  as follows:

$$\begin{aligned}
 A &= \frac{D}{n} \times 3.5 \times n + \frac{D}{n} \times 3.6s \sqrt{\frac{D}{n}} \{ \sqrt{1} + \sqrt{2} + \dots + \sqrt{n} \} \\
 &= 3.5D + 3.6s \sqrt{\frac{D^3}{n^3}} \{ \sqrt{1} + \sqrt{2} + \dots + \sqrt{n} \}
 \end{aligned}
 \tag{9.1.3}$$

Introducing area  $A_1$  is the total area of the bulkhead in the case of  $n = 1$ , i.e. bulkhead plate thickness is constant, the area ratio  $A/A_1$  represents the weight ratio and it becomes

$$A_1 = 3.5D + 3.6s\sqrt{D^3}
 \tag{9.1.4}$$

$$\begin{aligned}
 \therefore A/A_1 &= \frac{3.5D + 3.6s\sqrt{\frac{D^3}{n^3}} \{ \sqrt{1} + \sqrt{2} + \dots + \sqrt{n} \}}{3.5D + 3.6s\sqrt{D^3}} \\
 &= \frac{1}{\sqrt{n^3}} \{ \sqrt{1} + \sqrt{2} + \dots + \sqrt{n} \} + \frac{3.5D \left[ 1 - \frac{1}{\sqrt{n^3}} \{ \sqrt{1} + \sqrt{2} + \dots + \sqrt{n} \} \right]}{3.5D + 3.6s\sqrt{D^3}}
 \end{aligned}
 \tag{9.1.5}$$

$$\cong \frac{1}{\sqrt{n^3}} \{ \sqrt{1} + \sqrt{2} + \dots + \sqrt{n} \}
 \tag{9.1.6}$$

Figure 9.1.3 represents the calculated relation of area ratio  $A/A_1$  against the dividing number  $n$ . In Fig. 9.1.3, a realistic example is also shown in which  $D = 14.4\text{m}$

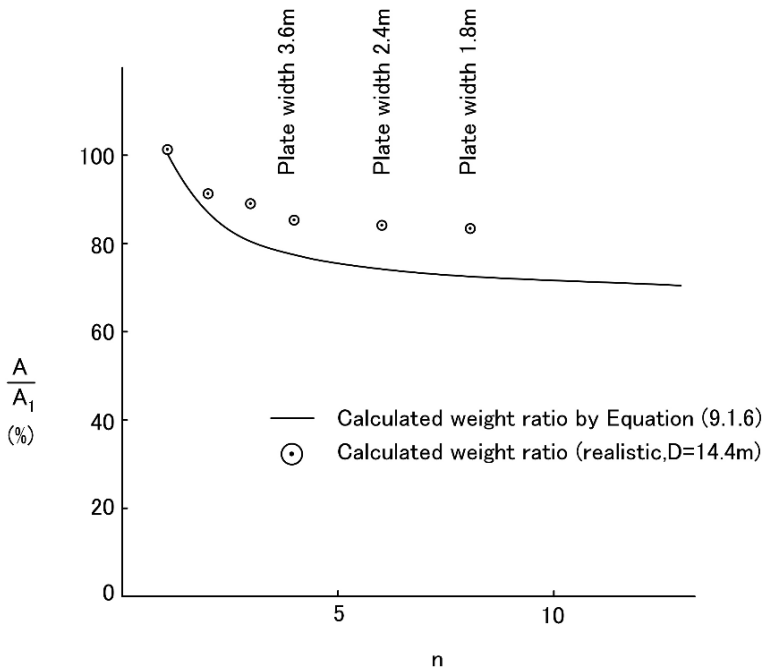


Fig. 9.1.3 Division number  $n$  of transverse bulkhead vs. weight ratio

is assumed, the top of water head is taken from 2.44 m above  $D$  and the plate thickness is expressed in round figures of 0.5 mm intervals. From the figure, we find that the total weight changes only slightly when the number of plates becomes more than 5 or 6 in both cases. In Fig. 9.1.3, the calculated weight ratio by Eq. (9.1.6) is always less than those of a realistic example. That is because Eq. (9.1.6) is derived by neglecting the second term of Eq. (9.1.5) in order to simplify the calculation.

## 9.2 Fillet Welding

A fillet welded joint is generally subjected to the following forces, as illustrated in Fig. 9.2.1:

- (1) tension, where the fillet welding acts as a cruciform joint against tension (Fig. 9.2.1(a))
- (2) bending moment (Fig. 9.2.1(b))
- (3) shearing force, where the fillet welding transmits the shearing force between the web plate and the face plate of a beam (Fig. 9.2.1(c))

The strength of a fillet welded joint was investigated in the report [31]. Referring to this report, let's explain its summary.

A fillet welded joint subjected to tension is generally called a cruciform joint in Fig. 9.2.1(a). In this case, the summation of throat thickness  $w$  of the both sides equals the plate thickness  $t$  under tension, therefore, leg length  $l$  of the fillet welding is given by the following Equation:

$$t = 2w \quad (9.2.1)$$

$$\therefore l = \frac{\sqrt{2}}{2}t = 0.7t \quad (9.2.2)$$

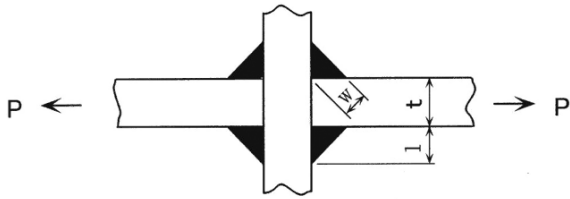
A typical example of the above joint is seen in the case where a transverse web is sandwiched between two longitudinal deck girders, where the longitudinal stress acting on one deck girder is transferred through to another deck girder via a fillet welding.

Figure 9.2.1(b) represents the fillet welding under a bending moment. From the view point of elastic design, the elastic section modulus  $Z_w$  of the deposited metal must equal the elastic section modulus  $Z_b$  of the plate, and in this condition:

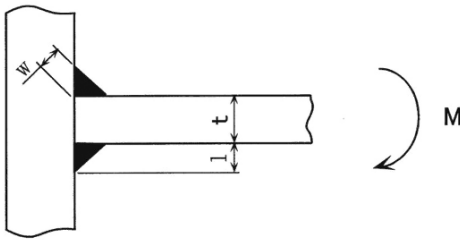
$$Z_b = \frac{bt^2}{6} \quad (9.2.3)$$

$$Z_w = \left\{ \frac{b(t+2w)^3}{12} - \frac{bt^3}{12} \right\} \frac{2}{t+2w} \quad (9.2.4)$$

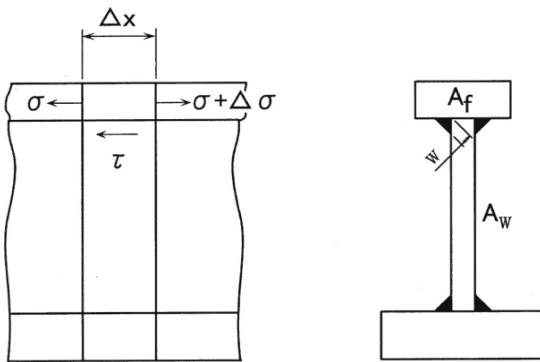
$$\therefore \frac{bt^2}{6} = \frac{b(t+2w)^2}{6} - \frac{bt^3}{b(t+2w)} \quad (9.2.5)$$



(a) In case of tension



(b) In case of bending



(c) In case of shearing

Fig. 9.2.1 Fillet weld joint

$$8 \left(\frac{w}{t}\right)^3 + 12 \left(\frac{w}{t}\right)^2 + 4 \left(\frac{w}{t}\right) = 1 \tag{9.2.6}$$

$$w = 0.165t$$

$$l = 0.233t \tag{9.2.7}$$

On the basis of plastic design, the plastic section modulus  $M_w$  of a fillet weld should be equal to the plastic section modulus  $M_b$  of the plate. Hence the requirement meets the Equation:

$$M_b = \frac{t^2}{4} \sigma_{yb} \quad (9.2.8)$$

$$M_w = w(w+t) \sigma_{yw} \quad (9.2.9)$$

where

$\sigma_{yb}$  : yield stress of plate

$\sigma_{yw}$  : yield stress of welding metal

In the case that the yield stress of weld metal is the lowest,  $\sigma_{yw}$  is equal to  $\sigma_{yb}$ , then we find

$$\begin{aligned} \frac{t^2}{4} &= w(w+t) \\ \left(\frac{w}{t}\right)^2 + \left(\frac{w}{t}\right) &= \frac{1}{4} \end{aligned} \quad (9.2.10)$$

$$w = 0.21t$$

$$l = 0.296t \quad (9.2.11)$$

From both points of view, i.e. elastic design and plastic design, we can say that half of the leg length of a fillet weld under tension is much enough for the required leg length against the bending moment.

Typical examples of fillet welding against bending stress are observed in the bulkhead structure of tank boundaries. On the other hand if fillet welding is used for connecting the web plate and face plate of a corrugated bulkhead structure, the stress distribution of the fillet welding is different from the above one. Because the face plate of a corrugated bulkhead plays a role of extreme fiber based on beam theory, the fillet welding is subjected to tension or compression.

As discussed previously, different types of stress occur when the same fillet welding is applied to different kinds of structure. Therefore, the designer has to imagine the type and direction of the stress induced in the structural member, and also think about possible failure modes of the structure due to the stress.

Figure 9.2.1(c) represents an example of a fillet welding under shearing force. In the case of a fillet weld against tension or in the case of a fillet weld against bending, the leg length can be rationally determined, since the plate stress directly flows through the fillet welding and is transmitted to the adjacent plate.

On the contrary, in the case of a fillet welding under shearing force, the discussion is slightly complicated. Cutting out a narrow slice, length  $\Delta x$ , of a beam under a shearing force including fillet welding in Fig. 9.2.1(c), we obtain the equilibrium of forces in the following form:

$$2w\tau\Delta x = \Delta\sigma A_f$$

$$\therefore w = \frac{A_f \Delta \sigma}{2T \Delta x} \tag{9.2.12}$$

where

$w$  : throat thickness of fillet welding

$T$  : shearing stress

$\Delta \sigma$  : change of nominal stress in face plate

$A_f$  : sectional area of face plate

Considering the following relationship between bending moment and shearing force:

$$\frac{dM}{dx} = F \tag{9.2.13}$$

Then we can rewrite Eq. (9.2.12) into Eq. (9.2.14) as in the form:

$$w = \frac{A_f}{2T} \cdot \frac{F}{Z} \tag{9.2.14}$$

where

$F$  : shearing force

$Z$  : section modulus of beam

Introducing the sectional area of the web plate as  $A_w$ , the shearing force of the web is expressed as  $F = A_w T$ , then we find

$$w = \frac{A_f \cdot A_w}{2Z} \tag{9.2.15}$$

From the above Eq. (9.2.15), the throat thickness is the function not only of sectional web area but of sectional area of face plate and section modulus of beam.

In order to simplify Eq. (9.2.15), let us take advantage of the optimum design of beam as described in Sect. 1.8. In Table 1.8.1, if the theory of the optimum section of a beam is applied, the sectional area of a web plate  $A_w$  and sectional area of a face plate  $A_f$  can be determined by the section modulus  $Z$ . For instance, in case of a balanced girder, the following equations are derived:

$$\left. \begin{aligned} A_w &= 1.10\sqrt{Zt} \\ A_f &= 0.73\sqrt{Zt} \end{aligned} \right\} \tag{9.2.16}$$

Substituting Eq. (9.2.16) into Eq. (9.2.15), we obtain the following equation:

$$w = \frac{1.10 \times 0.73}{2} t = 0.4t \tag{9.2.17}$$

$$l = 0.565t \tag{9.2.18}$$

Consequently the leg length of a fillet weld under shear can be simply decided by the plate thickness.

As mentioned earlier, the optimum design of a beam is able to uniquely provide the sectional shape, sectional moment of inertia and weight, once the required section modulus is given. In addition to that, the optimum design of a beam is helpful to treat several variables in terms of one parameter.

To summarize the above investigation, Fig. 9.2.2 illustrates the relation between the required leg length of a fillet weld and plate thickness in these three cases; fillet weld against tension Eq. (9.2.2), bending Eq. (9.2.7) or Eq. (9.2.11) and shearing Eq. (9.2.18). Requirement of NK's leg length, F1 and F2, for fillet welding are also plotted in the same figure. In order to compare directly the leg length requirement by the classification societies and the derived equations, the corrosion margin of a plate is assumed to be 2.5 mm and the corresponding leg length of a fillet weld as  $2.5 \text{ mm} \times \sqrt{2} = 3.5 \text{ mm}$ . For reference, the F1 requirement of leg length for a fillet weld by NK, is normally applied to the following weld connections; rudder frames and rudder horn, bracket beneath main engine and inner plate of double bottom, tank boundary of water/oil-tight bulkhead.

From Fig. 9.2.2, it can be said that the leg length of the fillet weld under tension is the biggest. The relation between the leg length of a fillet weld and deposit metal is indicated in Fig. 9.2.3, which shows that the quantity of deposit metal increases proportionally to the square of leg length. In order to decrease deposit metal and to save man-power for welding, the fillet weld with edge preparation is often used particularly for thicker plate more than 25 mm. In this case,  $50^\circ$  of groove is normally applied the same as for butt welding in Fig. 9.1.2.

Let us assume that the shape of deposit metal is an isosceles triangle having equal side length  $a$  as shown in Fig. 9.2.4, then the throat thickness must be half of the plate thickness  $t$  and it becomes

$$\left. \begin{aligned} x &= a \cos 50^\circ \\ w &= a \cos 25^\circ = \frac{t}{2} \end{aligned} \right\} \quad (9.2.19)$$

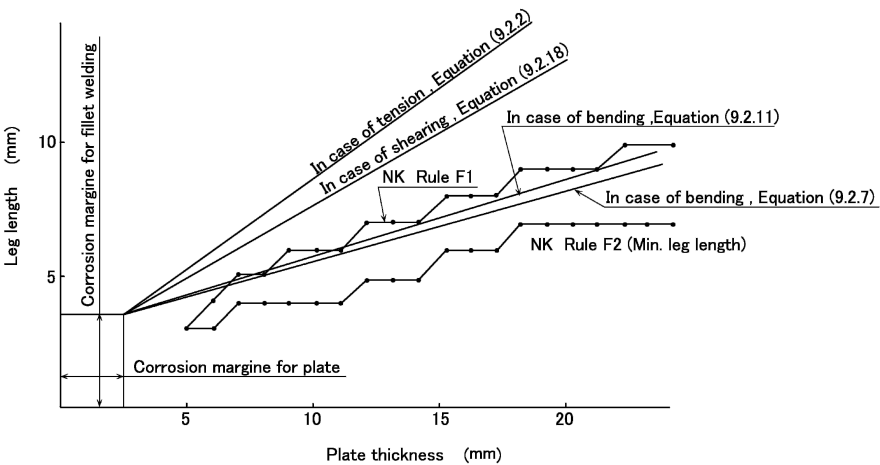
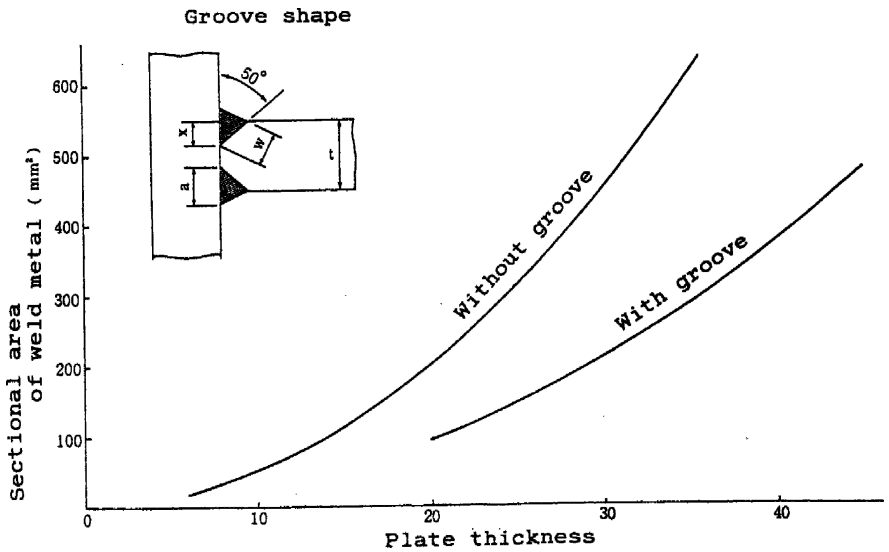
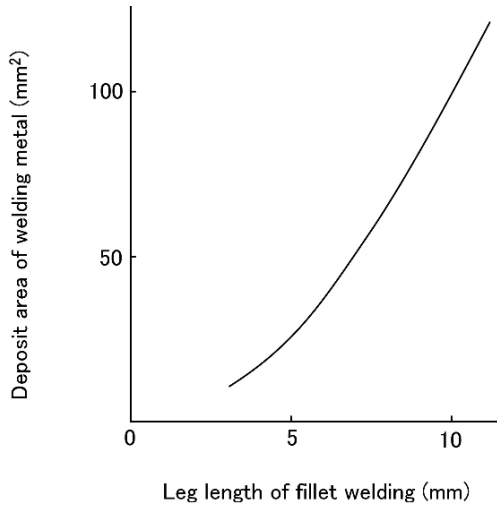


Fig. 9.2.2 Leg length of fillet weld



**Fig. 9.2.3** Deposit of welding metal vs. leg length of fillet weld



**Fig. 9.2.4** Sectional area of fillet weld with and without groove

$$\therefore x = \frac{\cos 50^\circ}{2 \cos 25^\circ} t = 0.35 t$$

Namely, both edges of the plate should be cut by a  $50^\circ$  of groove with  $0.35 t$  depth and the middle of the plate thickness must be left uncut for  $0.3 t$  thickness.

Figure 9.2.4 represents the area of deposit metal of a fillet weld in both cases; with and without edge preparation. If the plate edge is prepared with a groove, then the area of weld deposit is less than half compared to that without a groove. In addition to that, the edge preparation is beneficial to reduce stress concentration due to smooth flow of stress.

### 9.3 Fillet Welding with Higher Strength Electrode

There are two effective ways to decrease the deposit metal of fillet welding; one is to provide edge preparation and another is to carry out welding of mild steel plate by means of higher strength electrode. According to Fig. 9.2.3, we find that the weld deposit could be reduced to 77%, if the leg length of fillet welding decreases from 8 mm to 7 mm. Furthermore the leg length of 7 mm can be obtained by one pass welding, although the length of 8 mm is achieved by two passes. For the sake of leg length reduction, the use of the higher strength electrode than the base plate is effective. Taking  $\sigma_{BH}$  as the breaking stress of a higher strength electrode and  $\sigma_{BM}$  as that of a mild steel electrode,  $l_H$  and  $l_M$  are leg length of fillet welding, respectively, then the following equation can be obtained for the breaking condition:

$$\sigma_{BH} \cdot l_H = \sigma_{BM} \cdot l_M \quad (9.3.1)$$

Hence the leg length of fillet welding can be reduced to 80% by the use of a higher strength electrode of  $50\text{kgf/mm}^2$  class instead of a mild steel class of electrode.

Nevertheless, this equation gives an overestimated result, since the corrosion margin is neglected here. To take account of this margin, let us assume  $a$  is corrosion margin for both mild steel and higher strength steel of  $50\text{kgf/mm}^2$  class, then Eq. (9.3.1) can be interpreted in the following form:

$$(l_H - 1.4a) = \frac{\sigma_{BM}}{\sigma_{BH}} (l_M - 1.4a) \quad (9.3.2)$$

Figure 9.3.1 shows a relation between  $l_H$  and  $l_M$  calculated by substituting  $a = 2.5\text{ mm}$  into Eq. (9.3.2). It is found that 7 mm of leg length with a higher strength electrode in  $50\text{kgf/mm}^2$  class is enough to compensate 8 mm of length with mild steel electrode.

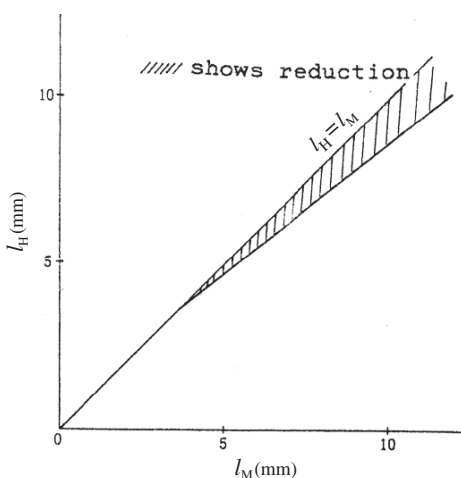


**Fig. 9.3.1** Leg length reduction by high tensile electrode

### 9.4 Water Stopping Welding

When a riveted joint was applied to connect the plates, water flow through the gap between the lapped part of plates was prevented by caulking the edge of the plate and the head of the rivets as illustrated in Fig. 9.4.1. In the same manner, the gap between the plate and stiffener still remains in the case of a fillet weld, therefore, it is necessary to provide water stopping welding to avoid the water flow in the gap.

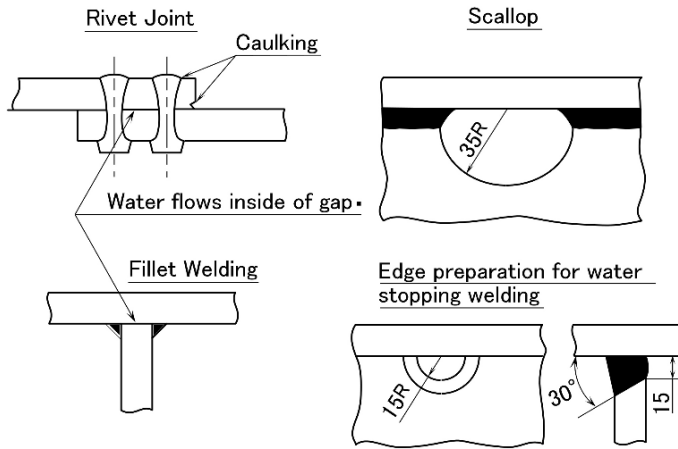


Fig. 9.4.1 Water stopping welding

Water stopping can be realized when this gap is separated into two portions welding. For this purpose, wrap round welding is carried out at the end of the scallops or short full penetration welding is performed in association with edge preparation of the stiffener.

In order to confirm the water tightness of a fillet weld, air pressure is often applied to the compartment where the connection gap between plate and stiffener is interrupted by several water stopping welds. This way of confirmation can be performed when a block has been constructed and before the whole tank test, therefore, the final water tightness test can be done with full confidence.

### 9.5 Scallop and Serration

Scallops are to be provided to prevent the interference of welding lines, as shown in Fig. 9.5.1(a). However, nowadays the designer is apt to eliminate scallops as much as possible for the following reasons:

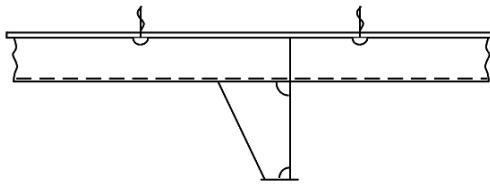
- (1) It was found that the interference of welding lines doesn't cause harmful damages neither to the strength or to the material deterioration.
- (2) Scallops cause high stress concentration due to abrupt change of structure.
- (3) Welding of scallops takes much time because of wrap round welding at both ends of a scallop.

When scallops are deleted, the designer must pay attention to the following two points:

- (1) Reinforcement of a butt weld joining two plates should be well ground off in way of stiffener to make a smooth surface, which enables stiffeners to be welded on this plate.
- (2) The corner of a web plate should be cut off in isosceles right angled triangle where the corner directly touches a fillet weld of a stiffener as in Fig. 9.5.1(b).

In the above two cases, the scallop works as an air hole or drain hole. If this scallop is eliminated, another air hole or drain hole must be provided to compensate for this scallop as illustrated in Fig. 9.5.1(b).

a) Scallop preventing interference of welding lines



b) Deletion of scallop

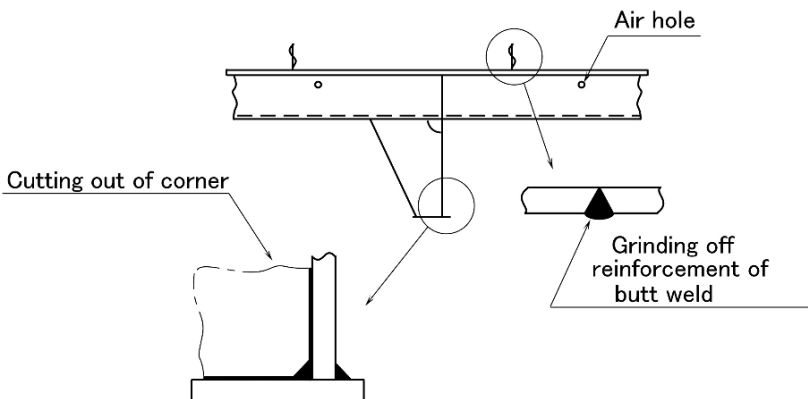
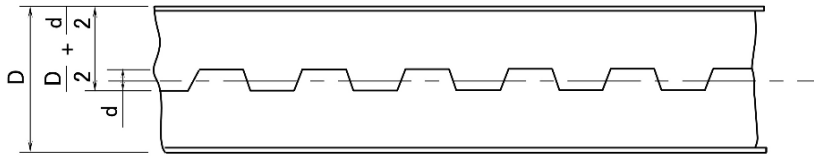


**Fig. 9.5.1** Scallop preventing interference of welding line and it's deletion

Cutting out two T-bars from one I-section bar



Stiffener with serrations

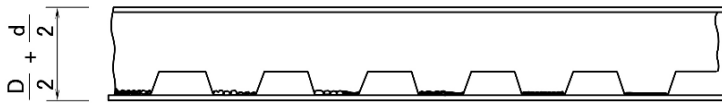


Fig. 9.5.2 Serration

Serration means an edge having a row of V-shapes like the teeth of a saw and it is applied to the edge of a stiffener with the intention of reducing weld length of the connection between stiffener and plate. In the case where two stiffeners are produced by cutting one channel bar or one I-section beam, the depth of the stiffener can be increased by providing serrations; i.e. the depth of a serrated stiffener becomes larger by a half depth of serration relative to that of non-serrated stiffener in Fig. 9.5.2. For this reason, serrated stiffeners were very popular until the 1950s. Nevertheless, serrated stiffeners have disappeared together with scallops these days because of cracks due to high stress concentration and the difficulty for gravity welding due to lap round welding.

## 9.6 Conversion of Butt Welding to Fillet Welding

Butt welding can be changed to fillet welding by inserting a plate in the athwart direction. Moreover, it is also converted to fillet welding by applying lap joint instead of butt joint.

The all welded ship *Shinwa-Marui*, which was constructed in Japan for the first time, was designed so as to be able to carry out all welding in the downward position or upright position. The purpose of this design is to maintain good welding quality by changing difficult butt welding to easy fillet welding in the downward position or upright position, even when welding technique was not well established. This system is now called “intercostal arrangement”. In the design of *Sinwa-Marui*, the intercostal arrangement is found in way of the connection between the bottom block and the side block, where the extension of the side longitudinal web is sandwiched

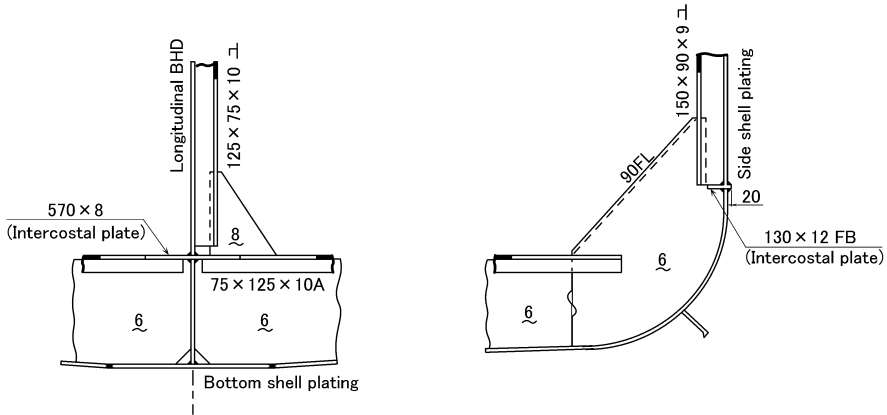


Fig. 9.6.1 Intercostal arrangement in “Sinwa-Maru”

by upper end of bilge shell plate and lower end of side shell plate as shown in Fig. 9.6.1. A similar arrangement is made for the joining between bottom block and bulkhead block [32].

Nevertheless, nowadays horizontal butt welding can be performed more efficiently than fillet welding in an intercostal arrangement. Because butt welding can be done without any qualitative problem by the progress of welding technology, and in addition butt welding is carried out by automatic welding machines. We tend to overestimate the advantage of the intercostal arrangement, since that arrangement is able to replace difficult butt welding with easy fillet welding. However, we had better not forget that the intercostal arrangement usually takes much more time for welding because we have to weld four lines of fillet weld instead of one butt weld.

Another important point in designing the intercostal arrangement is to prevent mis-alignment of sandwiching plates. It is easy to avoid mis-alignment, when the facing plates are welded near to the edge of sandwiched plate. But in cases where the two plates are joined in the middle of a wide sandwiched plate, it is not an easy task to arrange two plates to be in line with each other. To avoid mis-alignment in this case, it is recommended to provide drain holes to the sandwiched plate for the sake of easy adjustment in Fig. 9.6.2.

Another significant point in the design of the intercostal arrangement is the need to be careful in determining the leg length of the fillet welding connecting web plates and sandwiched plate. Although the leg length of fillet welding for shearing is applicable for the general case of a connection, a leg length  $0.7t$  for tension should be given for the fillet welding near a face plate.

A corrugated bulkhead, in general, is constructed in such a way that the flat plate is bent in a Z shape and then the edges of the two bent plates are connected by butt welding as shown in Fig. 9.6.3(a). This butt welding can be replaced with fillet welding by using two plates; i.e. flat plate and bent plate in a  $\pi$  shape. Let us compare the productivity of both types of corrugated bulkhead in Table 9.6.1, where the

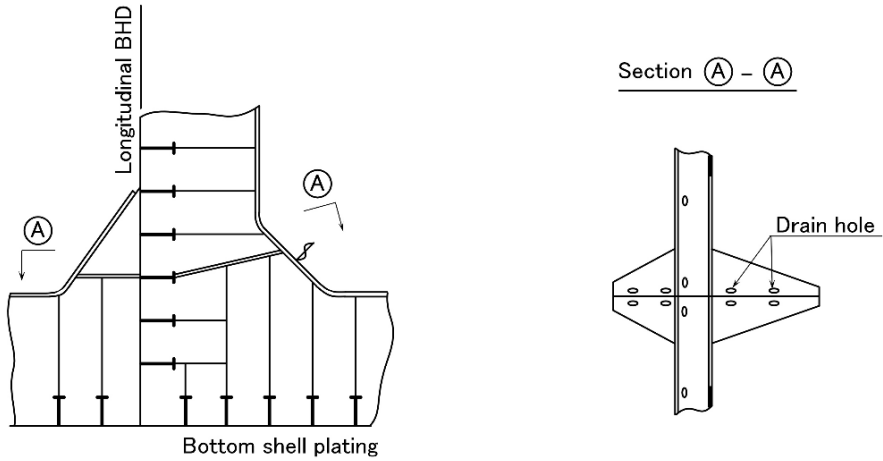


Fig. 9.6.2 Prevention of misalignment in intercostal arrangement

bulkhead consists of three corrugations. The corrugated bulkhead produced by fillet welding is more advantageous than the bulkhead by butt welding, from the view point of constructive efficiency. In addition to that, the corrugated bulkhead with fillet welding has such merit in designing that the designer can decide the spacing of corrugations freely because the width and thickness of the flat plates is independent of those of the bent plates in the  $\pi$  shape. On the contrary, in the case of a butt welded bulkhead, the spacing of corrugation has restrictions, for the plate thickness must be same in web plate and in face plate.

If the corrugated bulkhead is divided into lower and upper parts, then they are fabricated by inserting a horizontal girder between them, which creates an intercostal arrangement. It is difficult to avoid mis-alignment between lower and upper

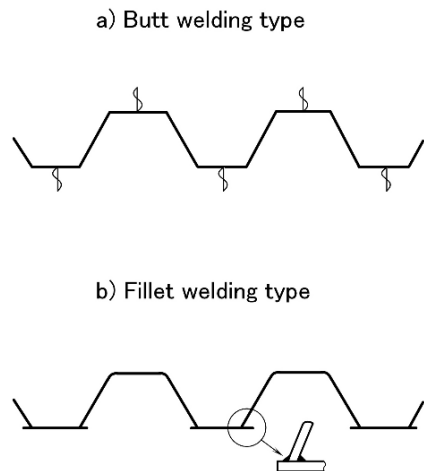


Fig. 9.6.3 Corrugated bulkhead

**Table 9.6.1** Comparison of productivity of corrugated bulkhead

	Butt welding type	Fillet welding type
Number of plates	6	7
Number of welding lines	10	12
Number of back gougings	5	0
Number of press bendings	12	6*

\* : 6 can be reduced to 3 by press bending with mould.

corrugated bulkhead, since the horizontal girder is wide. It is still more difficult in the case of a butt welded bulkhead, because two bends separately pressed in one corrugation piece may cause spacing error. In contrast, in the case of a fillet welded bulkhead, the corrugated bending is carried out by one press using a press mould in the  $\pi$  shape, which helps to keep good accuracy of corrugation piece. Furthermore, as explained previously, the designer needs to provide drain holes along the welded joint between horizontal girder and corrugated bulkhead.

An alternative idea to change butt welding to fillet welding is to make use of a lap joint. A lap joint is used to be frequently adopted when the accuracy of the constructed block was not well controlled, since the lap joint allowed disagreement of connected edges. The welding time of a lap joint is half of that of a butt joint, therefore, lap welding is preferable from the view point of productivity. However, the lap joint gradually disappeared in way of structural members due to of the following reasons:

- (1) Fatigue strength of lap joint is less than other joints.
- (2) Lap joint applied to the internal members of a tanker causes corrosion quickly.
- (3) Lapping of plates brings useless weight of steel.

This weight is in no ways negligible, in the case of a large tanker.

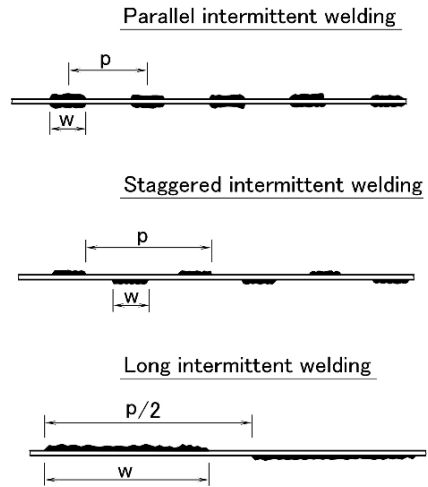
## 9.7 Long Intermittent Welding

There are two types of fillet welding; i.e. continuous welding and intermittent welding. Continuous fillet welding is applied to structural member in tanks or a member in exposed areas, since intermittent welding may causes rust in the gap between plate and stiffener. Hence intermittent welding is normally used for the welding of stiffeners in dry space such as accommodation spaces or the under deck space of cargo hold. Figure 9.7.1 represents an example of intermittent welding. Intermittent welding is carried out in the form of continuous welding of  $w = 75$  mm length arranged in a parallel row or in a staggered row, and that pitch  $p$  of the welding varies 150 mm, 200 mm, 300 mm and etc. according to the required strength.

After developing the gravity process welding, long intermittent welding is taken into the welding practice to reduce the number of short continuous welding (75 mm)



**Fig. 9.7.1** Variable intermittent welding



with the aid of long continuous welding (600 mm) of electrode used in gravity process welding, as shown in Fig. 9.7.1. Long intermittent welding seems to be curious, however, as fillet welding of continuous part transmits shearing force from web to plate and only one side of the welding is enough to support this shearing stress.

## 9.8 Shrinkage of Deposit Metal

At the beginning of welding, the deposit metal is melting in more than  $1000^{\circ}\text{C}$ , and then it starts coagulating at the transformation temperature from liquid to solid, finally it becomes solid steel at normal temperature. In this process, the deposit metal shrinks, which results in a tensile stress inside the deposit metal and tensile or compressive stress in the base metal around the deposit. These stresses are called “residual stress”, which affects detail structural strength [33].

Let us roughly estimate this residual stress by assuming that the thermal expansion coefficient of steel is  $10^{-5}$  and the change of temperature is  $1000^{\circ}\text{C}$ , then the order of strain becomes  $10^{-2}$  and it creates the stress  $210\text{kgf}/\text{mm}^2$  by multiplying the Young’s modulus. This simple calculation overestimates the stress because the effect of stress yielding is neglected. However, we can easily imagine by this rough example that stresses around the yield stress are induced in way of the deposit metal. A designer should not forget the shrinking of this deposit metal, when he is in charge of detail welding design.

This shrinkage of deposit metal causes structural damages, as shown in Fig. 9.8.1. In order to prevent such welding damage, it is effective to extend the end of the sandwiched plate between the upper and lower plates as indicated by the chain line in Fig. 9.8.1.

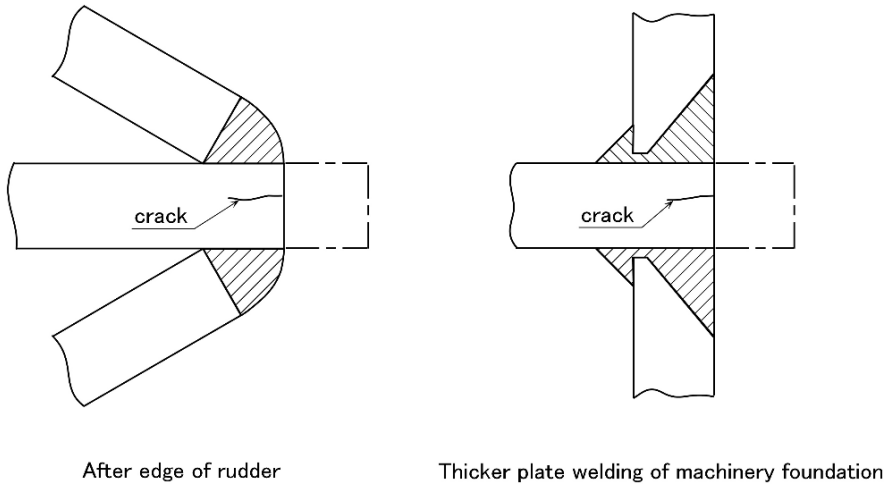


Fig. 9.8.1 Example of cracking due to welding metal shrinkage

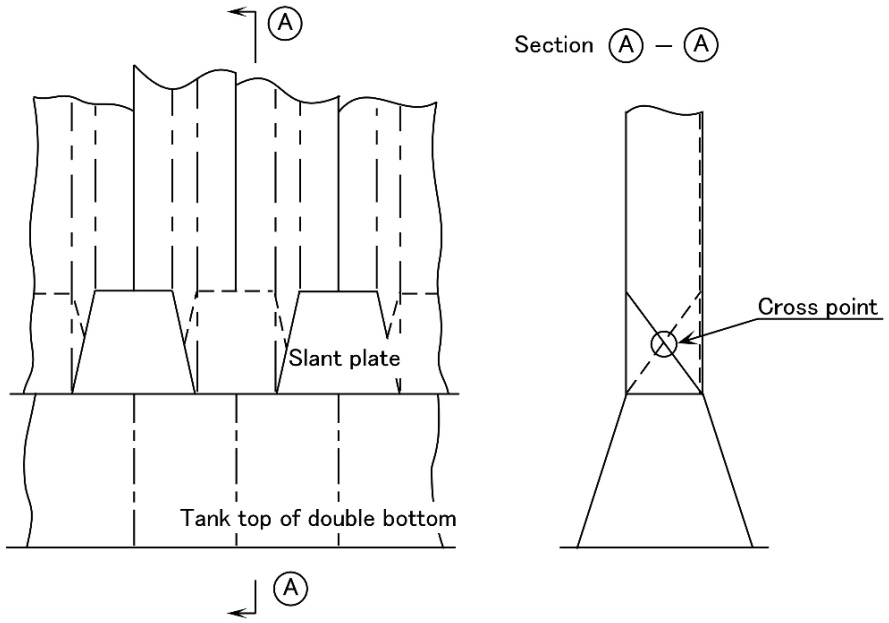


Fig. 9.9.1 Slant plate of lower corrugated bulkhead

## 9.9 One Side Welding

Both sides of a plate should be welded in butt welding as well as in fillet welding, in general. However, one side welding is inevitably accepted where the space behind a plate is insufficient to permit welding. In such cases, it is necessary to execute complete fusion welding by using a backing metal strip.

One of the worst cases of one side welding is the case where a cover plate should be welded in the corner of a dead space. In this case, the welding is carried out without backing and it fails to obtain good fusion. Figure 9.9.1 represents an example of this case where the slant plates are provided at the lower ends of a corrugated bulkhead of a bulk carrier for the purpose of preventing the accumulation of grain cargo in the corners. While the welding of this slant plate is not so important in an ordinary cargo hold, it must be performed with the greatest care in a hold where dry cargo or ballast water is loaded alternately, in particular, where dry cargo or cargo oil is loaded. If this slant plate is not perfectly tight, ballast water or cargo oil can seep into a space through imperfect welding, and then this liquid seeps out causing damage to any adjacent grain cargo.

These slant plates cause another structural damage; i.e. cracking, because adjacent slant plates cross, which creates stress concentration at a point. Therefore, it is especially important to avoid one side welding in this case.

# Chapter 10

## Fracture Control

### 10.1 Jack-Knifed Failure of Liberty Ships

During the World War II, USA was obliged to construct a large number of vessels urgently and the first all-welded ships, Liberty ships and T-2 Tankers, were produced according to an emergency ship building program. Some of these ships later broke completely in two, like a jack knife. Most of the failure occurred during the winter months. Failures occurred both when the ships were in rough sea condition and when they were anchored at dock as shown in Figs. 10.1.1 and 10.1.2 [34]. The failure of these vessels gave a driving force to the study of brittle fracture and fracture mechanics. Brittle fracture is the phenomena where normally ductile mild steel becomes brittle in low temperature and the crack propagates very rapidly. The study of brittle fracture resulted in both improvement of assessing steel strength, and development of the design method. Hereafter, the failure of Liberty ships due to brittle fracture is explained and the fracture managing technology based on fracture mechanics is addressed.

At 11 pm on 16 January 1943, a few days after completing sea trials, the 152 m long T2 tanker the “Schenectady” broke in two amidships while lying at the outfitting dock in the construction yard in Portland, Oregon, USA. The temperature of the harbor water was about 4°C and the conditions were still. The air temperature was approximately −3°C and the winds were light.

The failure was sudden and accompanied by a report that it was heard a mile away. The fracture extended through the deck, the sides of the hull, the longitudinal bulkheads and the bottom girders. The vessel jack-knifed, hinging on the bottom plate which had remained intact. The central part of the ship rose clear of the water, so no flooding of the hull through the fracture occurred.

The “Schenectady” was built by the Kaiser Company as part of the huge World War II emergency shipbuilding program. This program produced 2580 Liberty ships, 414 Victory ships and 530 T2 tankers over the years 1941–1946.

The failure of the “Schenectady” initiated on the deck between two bulkheads. A defective weld existed in a region of stress concentration arising at a design detail. The nominal tensile stress in the deck was calculated to be 68 N/mm<sup>2</sup>. Poor welding procedures caused the catastrophe also.



**Fig. 10.1.1** Jack-knifed failure of Liberty Ship

A broad research program was undertaken to find the causes of these failures and to prescribe the remedies for their future prevention. In addition to the above research, other research was aimed at gaining a better understanding of the mechanism of brittle fracture and fracture in general.



**Fig. 10.1.2** Collapse of Liberty Ship T2 tanker "Schenectady"

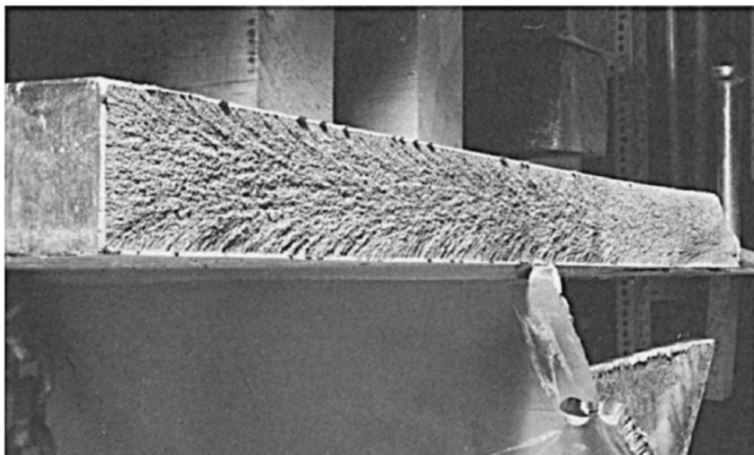


**Fig. 10.1.3** Photograph of typical brittle-fracture surface

Brittle fracture is quite dangerous, because normally ductile mild steel becomes brittle in low temperature and the crack propagates very rapidly at the rate of 1500–2000 m/s causing sudden fracture of the vessel as shown in Fig. 10.1.3 [35].

In order to avoid failure due to brittle fracture, the following measures are taken on the basis of much research;

- (1) The absorbed energy in the Charpy V notch test correlates well with the observed crack initiation, propagation and arrest behavior of the ship's steel. Hence the Charpy V notch test is standardized in such a way that the absorbed energy of the ship's steel is required according to the specified temperature.
- (2) High quality steels, more ductile steels, are developed by modifying alloy elements, grain size, deoxidation methods and normalizing heat treatments.
- (3) More proper ship design and welding methods are implemented to avoid sharp defect in welded part, because these defects often initiate the crack.

## 10.2 Fracture Mechanics

### 10.2.1 Principles

Although the traditional design criteria of hull structures are generally based on the tensile strength, yield strength, and buckling strength, they are insufficient when there is the likelihood of cracks; especially in the case of the wide application of high strength steels, weight savings by detail stress analysis using Finite Element Method, and the development of refrigerated cargo ships such as LPG and LNG carriers which are exposed to low temperatures.

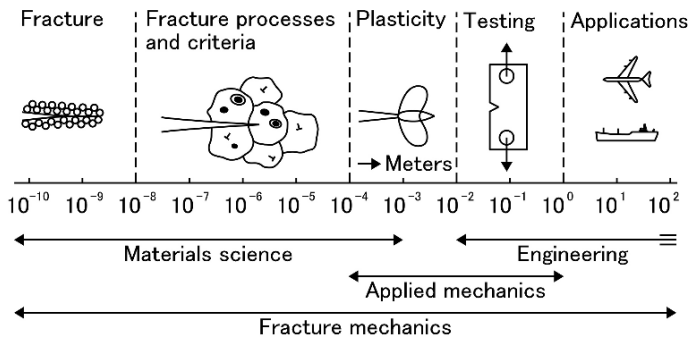


Fig. 10.2.1 Broad fields of fracture mechanics

If preexisting flaws or high stress concentrations are present, especially in the vicinity of welding beads, the structures have a low crack resistance, that is, low fracture toughness, and the residual strength will be low. In such cases, the fracture may be brittle, and the application of fracture mechanics has been used for the evaluation of hull strength recently.

Figure 10.2.1 [36] shows the overall disciplines of fracture mechanics from the transgranular/intergranular fractures to engineering applications. Recently, “fail-safe design” has been widely applied. The criteria allow for the occurrence of small cracks and crack growth, if they are under the allowable values, subject to manage the residual strength so as to keep the structural safety. Hence, the occurrence, propagation, and transition to the brittle fractures of fatigue cracks be well investigated, and the allowable stress, residual strength, allowable flaws, and material selection must be considered during the structural design.

### 10.2.2 Linear Fracture Mechanics

A crack in a solid is categorized in three modes as shown in Fig. 10.2.2. In these, mode, opening mode, in which the displacement of the cracked surfaces are perpen-

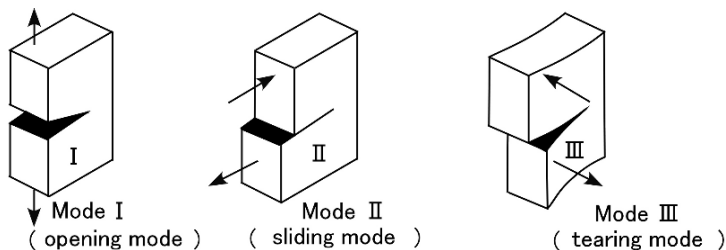
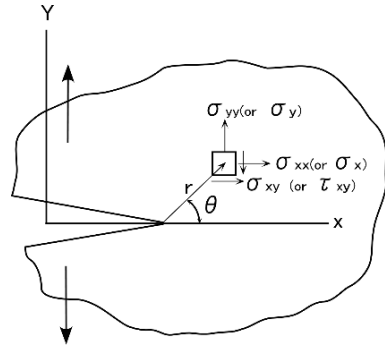


Fig. 10.2.2 Three modes of loading

**Fig. 10.2.3** Crack in arbitrary body



dicular to the plane of crack, is the most fundamental and important. In mode II, sliding mode, the displacement of the cracked surfaces is in the plane of the crack and perpendicular to the leading edge of the crack. Mode III, tearing mode, is caused by out-of-plane shear.

In model, in-plane crack tip stress is expressed as follows for an infinite plate subject to uniform tension (Fig. 10.2.3).

$$\sigma_{ij} = \frac{K_1}{\sqrt{2\pi r}} f_{ij}(\theta) \tag{10.2.1}$$

$\sigma_{ij}$ : stress acting on a plate element  $dxdy$  at a distance  $r$  from crack tip and at  $\theta$  from the crack plane.

$K_1$ : stress intensity factor for model

The stresses for an area close to the crack tip as shown in Fig. 10.2.4 are shown in these equations:

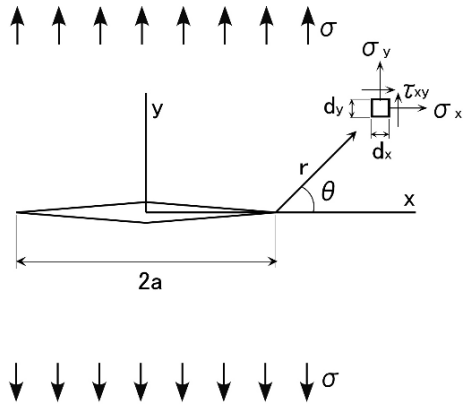


**Fig. 10.2.4** Crack in infinite plate



$$\begin{aligned}
 \sigma_x &= \sigma \sqrt{\frac{a}{2\pi r}} \cos \frac{\theta}{2} \left[ 1 - \sin \frac{\theta}{2} \sin \frac{3\theta}{2} \right] \\
 \sigma_y &= \sigma \sqrt{\frac{a}{2\pi r}} \cos \frac{\theta}{2} \left[ 1 + \sin \frac{\theta}{2} \sin \frac{3\theta}{2} \right] \\
 \tau_{xy} &= \sigma \sqrt{\frac{a}{2\pi r}} \sin \frac{\theta}{2} \cos \frac{\theta}{2} \cos \frac{3\theta}{2}
 \end{aligned}
 \tag{10.2.2}$$

When  $\theta = 0$ ,  $\sigma_y = \frac{\sigma \sqrt{a\pi}}{\sqrt{2\pi r}} \equiv \frac{K_I}{\sqrt{2\pi r}}$

Hence,

$$K_I = \sigma \sqrt{a\pi} \tag{10.2.3}$$

$K_I$  is called the “stress intensity factor”, which has the dimension of stress times the square root of the length, and is defined only by the remote stress  $\sigma$  and the crack length.

For mode I and II, stress intensity factors are defined similarly. These values are applied for fractures under lower stress conditions such that the plastic zone is small compared to the size of the crack.

On the other hand, crack growth per unit thickness is written as:

$$G = \frac{\pi \sigma^2 a}{E'} = \frac{K^2}{E'} \tag{10.2.4}$$

$U$ : elastic energy  
 $E' = E$  for plane stress condition  
 $E' = \frac{E}{1 - \nu^2}$  for plane strain condition  
 $E$ : Young’s modulus  
 $\nu$ : Poisson’s ratio

$G$  is called “elastic energy release rate” per crack tip, or crack driving force. When  $G$  exceeds a certain critical value  $G_c$ , crack growth occurs.

$$G \geq G_c \tag{10.2.5}$$

$G_c$  is called “critical energy released rate”, and is generally determined by measurements.

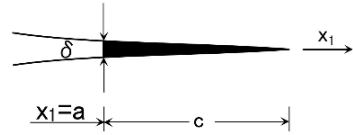
Correspondingly, brittle fracture will occur when the  $K$  value exceeds a certain critical value  $K_c$ , which is called critical fracture toughness.

$$K \geq K_c \tag{10.2.6}$$

### 10.2.3 Non-Linear Fracture Mechanics

When the plastic zone in the vicinity of a crack tip is not small, the crack opening displacement or crack-tip opening displacement (COD, CTOD) concept is applied;

**Fig. 10.2.5** COD  $\delta$  in a thin plate



when the material at the crack tip reaches a maximum permissible plastic strain, crack extension takes place. The crack tip strain is related to COD, hence, crack extension or fracture is assumed to occur when COD exceeds a critical value. COD is  $\delta$  as shown in Fig. 10.2.5. This criterion is equivalent to  $K_c$  and  $G_c$  in the case of a small plastic arrangement.

In the case of Fig. 10.2.4, COD is written as

$$\delta = \frac{8\sigma_y a}{\pi E} \ln \left[ \left( \cos \frac{\pi\sigma_\infty}{2\sigma_y} \right)^{-1} \right] \tag{10.2.7}$$

With decreasing  $\sigma_\infty/\sigma_y$  (and hence  $c/a$ ) this will asymptotically approach.

$$\delta = \frac{K_1^2}{E\sigma_y} \tag{10.2.8}$$

### 10.2.4 Fracture Toughness

For fractures involving small-scale yielding, the Charpy test is usually applied to evaluate fracture toughness. The notched test piece is hit by a hammer at each temperature, and the energy loss is measured by the differences in hammer elevation force and after breakthrough. The test piece has usually V-notch in the center and is supported at both ends. Results of the V-notch Charpy impact tests are shown in Fig. 10.2.6. Fracture surface of V-notch Charpy impact tests is shown in Fig. 10.2.7.

The temperature at a half of maximum energy is called mean energy transition temperature and also such the temperature that the brittle fracture appearance occupies a half is called 50% fracture transition temperature  ${}_vT_{rE}$ , while such temperature that the areas of fibrous fracture and crystal fracture are same is called fracture appearance transition temperature  ${}_vT_{rS}$ .  ${}_vT_{rE}$  and  ${}_vT_{rS}$  is approximately same. Furthermore, such temperature that the absorbed energy becomes 15 ft-lb (2.1 kgf-m) is called to be related to the occurrence of brittle fracture due to experience of Liberty ships during world war II in USA.

### 10.2.5 Grade of Steel

Grades of steel materials are regulated by IACS unified rules. Here, the background of the application is introduced based on the NK rules [37, 38]. The principle is

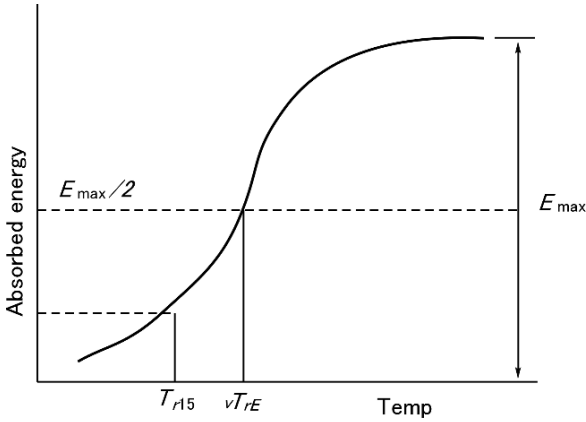
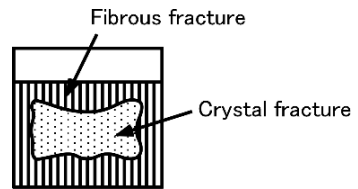


Fig. 10.2.6 Temperature curve of absorbed energy

Fig. 10.2.7 Fracture of V notch Charpy



Eq. (10.2.6); the toughness  $K$  is taken to be less than the critical fracture toughness. The model is shown in Fig. 10.2.8, in which a crack crosses at right angle to a weld bead. The length of the crack is estimated to be 240 mm at important places and 200 mm at others. The applied stresses are categorized as shown in Table 10.2.1. In addition the residual stress is taken as being half the yield stress, then applied stress and  $K$  value are

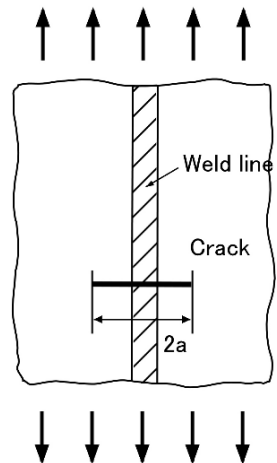


Fig. 10.2.8 Model with crack

**Table 10.2.1** Applied stresses and  $K$

Class	Mild steel			Higher tensile strength steel		
	$\sigma$ (kgf/mm <sup>2</sup> )	$a$ (mm)	$K$	$\sigma$ (kgf/mm <sup>2</sup> )	$a$ (mm)	$K$
I	16.8	100	298	22.2	100	393
II	24	100	425	31.4	100	557
III	26.4	100	468	34.5	100	611
IV	28.8	100	510	37.5	100	665
V	28.8	120	559	37.5	120	728

$$\sigma = \sigma_d + 0.5\sigma_y \tag{10.2.9}$$

$$K = (\sigma_d + 0.5\sigma_y) \sqrt{\pi a} \tag{10.2.10}$$

- $\sigma_d$ : applied stress (Table 10.2.1)
- $\sigma_y$ : yield stress
- $a$ : crack length

On the other hand,  $K_c$  is derived using the master curve of WES3003 using the V-notch Charpy impact test. The absorbed energy is expressed as follows as shown in Fig. 10.2.9.

$$vE_T = \frac{1}{\sqrt{2\pi}} \int_{-\infty}^{T-vT_{rE}} \exp \left\{ -\frac{1}{2} \left( \frac{T-vT_{rE}}{20} \right)^2 \right\} dT \tag{10.2.11}$$

- $T$ : temperature of impact test (°C)
- $vE_T$ : absorbed energy (kgf·m)
- $vT_{rE}$ : fracture transition temperature (°C)

The brittle fracture temperature is determined from deep notch impact tests, for applied stresses of  $\sigma_{y0}/2$  and crack lengths of 80 mm as follows:

$${}_IT_k = (0.00321\sigma_{y0} + 0.391) vT_{rS} + 2.74\sqrt{t} - 5.44 \tag{10.2.12}$$

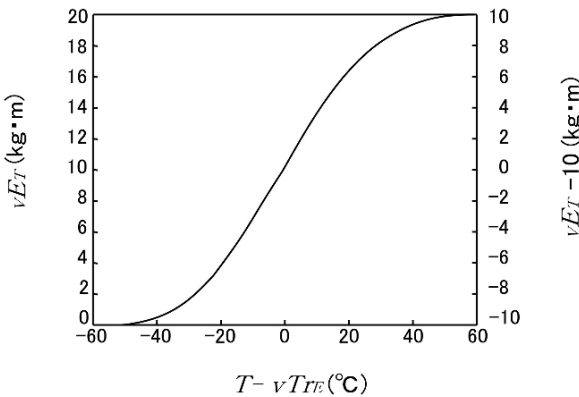


**Fig. 10.2.9** Master curve of absorbed energy

- ${}_I T_K$ : Temperature of brittle fracture ( $^{\circ}K$ )
- $\nu T_{rS}$ : transition temperature of 50% brittle fracture
- $\sigma_{y0}$ : nominal yield stress ( $kgf/mm^2$ )
- $t$ : plate thickness (mm)

Since  $\nu T_{rS}$  is almost same as  $\nu T_{rE}$ ,  ${}_I T_K$  can be calculated from the above equation using  $\nu T_{rE}$  instead of  $\nu T_{rS}$ , and  $K_c$  is obtained from the following equation for a given temperature  $T_K(^{\circ}K)$ .

$$K_c = 3.81 \sigma_{y0} \exp \left\{ 562 \left( \frac{1}{{}_I T_K} - \frac{1}{T_K} \right) \right\} \tag{10.2.13}$$

As a result, Table 10.2.2 is gained by Charpy impact test at  $0^{\circ}C$ . Comparing the  $K$  value of Table 10.2.1 and  $K_c$ , steel grades are applied for each plate thickness and each stress class. Table 10.2.3 shows the IACS unified rules.

**Table 10.2.2**  $K_C$  value

Grade	Plate thickness(mm)								
	10	15	20	25	30	35	40	45	50
KA	550	536	509	484	473	461	451	440	430
KB	630	597	580	550	536	522	509	484	473
KD	730	688	649	630	613	580	565	550	536
KE	1173	1089	1014	979	945	884	855	828	802
AH	715	679	646	630	601	587	573	560	548
DH	917	891	841	795	774	753	734	715	696
EH	1261	1178	1140	1059	1036	1004	974	945	917

### 10.3 Fatigue Strength Design

#### 10.3.1 Crack Propagation Calculation by Paris's Equation

In general, crack growth rate is considered to be governed by the  $K$ -value (stress intensity factor) range at the crack tip. The simplest application of fracture mechanics to fatigue strength design is the Paris's equation, expressed as follows:

$$\frac{da}{dN} = C(\Delta K)^m \tag{10.3.1}$$

- $da/dN$ : crack growth rate, or crack growth per cycle
- $C, m$ : material constant
- $\Delta K$ : stress intensity factor range

This equation is valid only within the region where crack growth is stable, and bounded at lower and upper extremes by  $\Delta K_{th}$  and  $K_c$ .  $\Delta K_{th}$  is the threshold stress

**Table 10.2.3** IACS unified rule

Class Thickness (mm)	I		II		III		IV		V	
	MS	HT	MS	HT	MS	HT	MS	HT	MS	HT
$t \leq 15$	A	AH	A	AH	A	AH	A	AH	D	DH
$15 < t \leq 20$	A	AH	A	AH	A	AH	B	AH	E	DH
$20 < t \leq 25$	A	AH	A	AH	B	AH	D	DH	E	EH
$25 < t \leq 30$	A	AH	A	AH	D	DH	E	DH	E	EH
$30 < t \leq 35$	A	AH	B	AH	D	DH	E	EH	E	EH
$35 < t \leq 40$	A	AH	B	AH	D	DH	E	EH	E	EH
$40 < t \leq 45$	B	AH	D	DH	E	EH	E	EH	E	EH

Structural member	Within 0.4 Lamidships	Outside 0.4 Lamidships
Lower strake in longitudinsl bulkhead Deck plating exposed to weather, in general Side plating	II	I
Bottom plating including keel plate Strength deck plating <sup>2</sup> Continuous longitudinal members above strength deck Upper strake in longitudinal bulkhead Upper strake in top wing tank	III	I
Sheer strake at strength deck <sup>4</sup> Stringer plate in strength deck <sup>4</sup> Deck strake at longitudinal bulkhead <sup>1</sup> Bilge strake <sup>3</sup>	IV	III ( II outside 0.6L)

NOTES

1. In ships with breadth exceeding 70 m at least three deck strakes to be class IV.
2. Plating at corners of large hatch openings to be specially considered. Class IV or V to be applied in positions where high local stress may occur.
3. May be of class III in ships with a double bottom over the full breadth and with length less than 150 m.
4. To be class V within 0.4L amidships in ships with length exceeding 250 m.

intensity factor range, and the crack growth rate can be combined with Paris’s equation as follows:

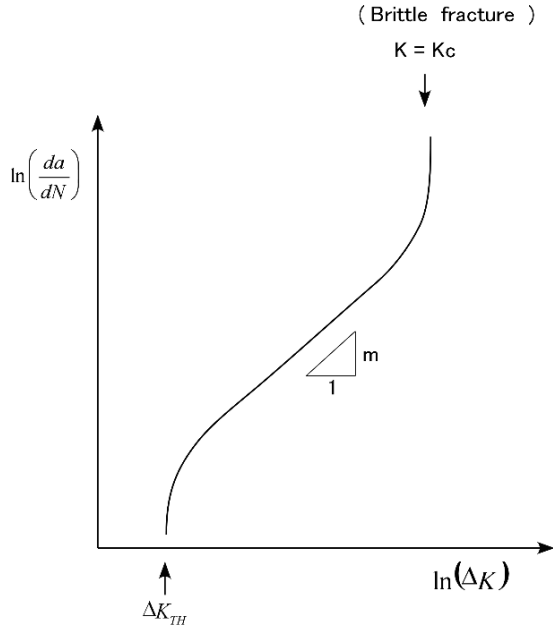
$$\frac{da}{dN} = C(\Delta K)^m \quad \Delta K > \Delta K_{th} \tag{10.3.2}$$

$$= 0 \text{ (no crack)} \quad \Delta K \leq \Delta K_{th}$$

Schematically, the crack growth rate curve is illustrated in Fig. 10.3.1.

Regarding the application of crack propagation analysis to a ship’s structure, the IGC code for liquefied gas carriers requires this analysis for the independent Type B tanks, and there are many actual applications. However, recently such applications are spreading into conventional ships such as container ships, bulk carriers, and tankers. This makes it possible to evaluate the tolerance limit of undercut of the welding and the allowable values of initial crack defects or initial scratches. This

**Fig. 10.3.1** Schematic crack growth rate curve



improves the quality of hull structures rationally by integrating the design, workmanship, and inspection.

**10.3.2 Fatigue Strength Design Taking into Account Construction Tolerances [39]**

Fatigue cracks are caused by variation in stresses at local points, and are influenced by structural stress concentration, construction tolerances, alignment, welding bead shape, as well as the exerted stress range and residual stress. In actual ship structure, some construction deviation such as thin horse distortion and misalignment to some extent is inevitable. Such construction deviations are controlled under construction standards such as JSQS, and it is considered that strength is warranted by the feedback from actual structural damage of ships in service.

Although a long history of shipbuilding proves that this system has functioned, simple standards such as JSQS do not accurately take into account the influence of design variations such as a wider application of higher tensile strength steel leading to increased nominal stress, or different structural configurations. By quantitatively evaluating the influence of construction tolerances, the quality in terms of fatigue strength can be enhanced.

- (1) Influence of construction tolerances to local stress

Table 10.3.1 shows equations of local stress at the weld toe of several types of welding joints, and the stress concentration factor to be taken into account. In the case of wrap-around welding and cruciform joints (non load transmitted), only the stress concentration factor at the weld toe ( $K_t$ ) suffices, but in the case of butt joints and cruciform joints (load transmitted), the stress concentration factor due to misalignment ( $K_m$ ) is also to be considered. In the case of fillet welding of skin plate or butt welding of skin plates, the stress range is to be divided into membrane stress and bending stress, and the stress concentration factor due to thin horse distortion ( $K_d$ ) and due to misalignment ( $K_m$ ) is applied only to the membrane stress portion.

Table 10.3.2 shows the equations to derive each stress concentration factor. By applying such factors, the construction department can rationally control construction tolerances quantitatively depending on the location and exerted stresses.

(2) Welding bead shape and  $K_t$  control

As shown in the equation of  $K_t$  in Table 10.3.2,  $K_t$  is affected by the flank angle ( $\theta$ ) and the toe radius ( $\rho$ ). It is readily understood that wide variation in the welding

**Table 10.3.1** Local stress at weld toe

Local stress at weld toe	
	$\sigma_L = K_t \sigma_N$
	$\sigma_L = K_t K_m \sigma_N$
	$\sigma_L = K_t (\sigma_B + K_d \sigma_N)$
	$\sigma_L = K_t [\sigma_B + (K_d + K_m - 1) \sigma_N]$

- $K_t$  : stress concentration factor at weld toe
- $K_m$  : stress concentration factor due to misalignment
- $K_d$  : stress concentration factor due to distortion
- $\sigma_L$  : local stress at weld toe
- $\sigma_N$  : nominal stress
- $\sigma_B$  : bending stress of tank plate



**Table 10.3.2** Stress concentration factor and construction tolerances

	$K_t = [1 + f(\theta)(g(\rho) - 1)] C \left(\frac{a}{t}\right)$ <p><math>\theta</math> : flank angle  <math>\rho</math> : toe radius</p>
	$K_m = 1 + 3 \frac{d}{t}$
	$K_m = 1 + 3 \frac{d}{t_1} \left[ \frac{1}{(l_1/l_2)(t_2/t_1)^2 + 1} \right]$
	$K_\sigma = 1 + 6(1 - \nu^2) \frac{d}{t} \frac{\tanh(m/2)}{m}$ $m = \sqrt{12(1 - \nu^2) \frac{\sigma_N}{E} \left(\frac{1}{t}\right)^2}$ <p><math>E</math> : Young's modulus  <math>\nu</math> : Poisson's ratio  <math>\sigma_N</math> : membrane stress</p>
	$K_d = 1 + 6(1 - \nu^2) \frac{d}{t} \times 2 \left[ \frac{m \sinh(m) \tanh(m/2) + m - \sinh(m)}{m^2 \sinh(m)} \right]$

bead shape, or of such parameters as the flank angle and the toe radius, leads to a large probability of non conformity. That is, if the variation in bead shape is large, the capability distribution as shown in Fig. 1.6.2 in Part I becomes lower and more spread out, and the probability of fracture increases.

From this point of view, we adopt the idea of the  $K_t$  control method to control the stress concentration factor of weld toes. This means carrying out special control on bead shape for important places of high stress, and inspect and record them quantitatively. Figure 10.3.2 [40] shows the probability distribution of the  $K_t$  values of the beads of wrap-around weld portions extracted at random. It is known that the welding quality is considerably enhanced through such special control.

Stress concentration factor at welding toe

Detail of A sec

Bracket toe

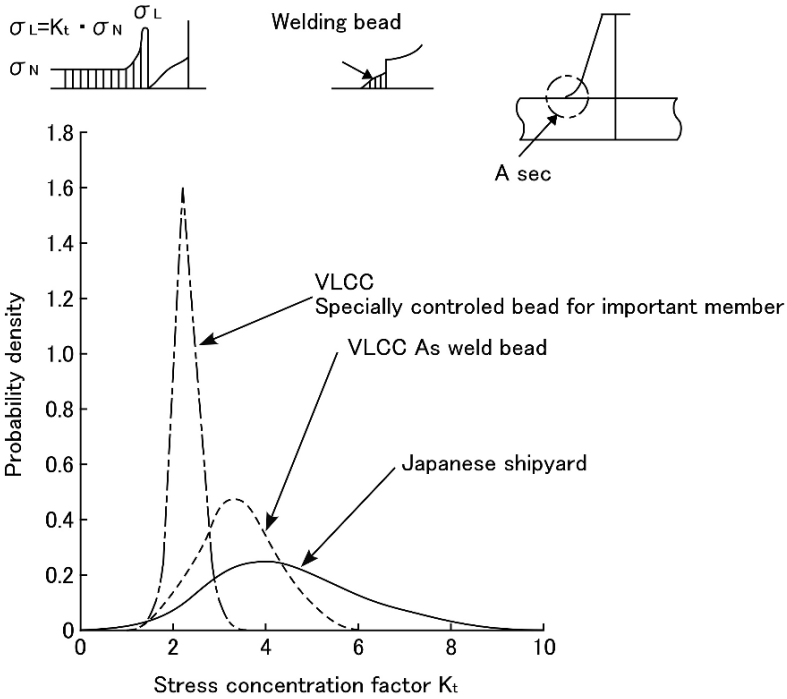


Fig. 10.3.2 Probability distribution of stress concentration factor  $K_t$

One important aspect of  $K_t$  control is the rational agreement between design conditions and fabrication deviations. To warrant fatigue strength, actual bead shape (flank angle and toe radius) is to be measured and the resulting  $K_t$  is to be assessed such that it's within the allowable limits given by the design conditions.

# Chapter 11

## Hull Structural Vibration

### 11.1 Introduction

“Hull structural vibration is an old but a new problem” is often said by many managers. That is because the vibration of the hull structures caused serious problems in old times and that it still now brings new kinds of problems.

In addition, it is also frequently said “When some area vibrates heavily, vibration can be decreased by providing reinforcements to that part. Nevertheless, these reinforcements are likely to cause vibration in another area.”

In order to explain these matters, the authors would like to propose the introduction of the concept of “the change of boundary conditions”. In the former case, for instance, the change of social and economical environments will bring different types of vibration problems. In the latter case, if reinforcements in the vibrating area are provided, they will change the boundary conditions of the surrounding areas. In other words, the reinforcements change the rigidity of bounded areas and the natural frequency of these ones as a result. This causes resonance between the exciting frequency and the natural frequency of the bounded areas, which did not resonate with the exciting force before adding reinforcement.

There are three important relationships between the exciting force and the vibration response of a structure as follows:

1. The structure always vibrates at the same frequency as the exciting frequency.
2. The structure almost always vibrates in the same direction as in the exciting force.
3. The vibration response of the structure is proportional to the magnitude of the exciting force.

In the following sections, we will explain two items; (a) basic features of hull structure vibration, (b) social, economical and physical changes of the environment affecting the boundary conditions of the hull structure vibration.

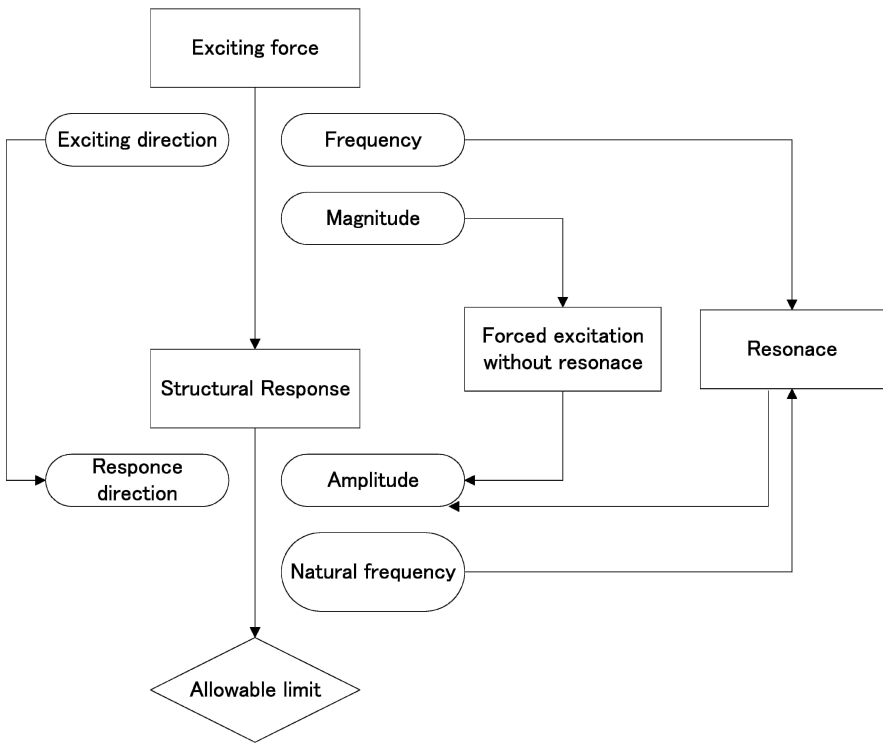
## 11.2 Basic Features of Hull Structure Vibration

Figure 11.2.1 illustrates the relationship between the basic vibration items. The figure shows that the basic vibration items are the exciting forces, responses and criteria. Such basic items have three important parameters for each, i.e. direction, frequency and amplitude. The vibration itself cannot be not clearly defined, unless these three parameters “direction, frequency and amplitude” are specified.

Let us explain the above matter by considering some examples.

### Example 1

Let’s suppose the following case, when we receive a report from a guarantee engineer on board a maiden voyage of a vessel saying that there is heavy vibration in the captain’s room and that the captain complains seriously. Can we make any



Concept to minimize hull vibration

- 1) Prevent resonance
- 2) Reduce exciting force

Fig. 11.2.1 Basic feature of hull structure vibration

effective decisions or useful comments? Because we know nothing about the basic parameters of the vibration.

On the contrary, when the report says that the deck plate of the captain's room vibrates vertically and that the frequency is 600 cpm (at the main engine shaft revolution 120 rpm) with single amplitude of 0.2 mm, what can we do? In such a case, we can easily investigate the reason for the vibration and also can take effective countermeasures.

Because

- we can deduce from by the report that the frequency of vibration is 5 times the shaft revolutions, hence, the vibration is probably caused by the exciting force of the propeller which has 5 blades.
- we can compare the vibration criteria, 9 mm/s for example, with the current vibration velocity of the deck 11 mm/s estimated from the frequency and the amplitude. Consequently, the result indicates some countermeasure is necessary.
- we can determine a suitable countermeasure, for the deck vibration occurs only in the captain's room and not over a more wide area, then this means we can solve the vibration trouble by providing reinforcements on the deck plate of the captain's room.
- we can ask the guarantee engineer on board to provide additional information; the distribution of vibration amplitude of deck plate, i.e. vibration level of deck girders and beams, the vibration level at the mid-point of panels surrounded by girders and beams. From these additional data, we can decide the most suitable countermeasure with confidence.

### *Example 2*

Let's suppose we have a vibration problem, such that heavy vibration has appeared in a fresh water tank in the after of a vessel. In the first stage of investigation, judging from the vibration frequency which matched the exciting frequency due to the propeller, we have planned to take the following two countermeasures to reduce the vibration force of the propeller; (a) replacement of the ordinary propeller by a highly skewed propeller, (b) installation of the damping tank to decrease propeller surface forces. Since the vibration response decreases proportionally to the reduction of the exciting force, the countermeasures to reduce the propeller exciting force are expected to be effective.

However, the situation was found to be slightly different in this occasion, by careful observation of the measured data. From the data, we found heavy vibration only in the panels of the tank, with the stiffeners of the tank scarcely vibrating. That is, in other words, the tank panels vibrate severely due to resonance with propeller excitation. Heavy vibration might be induced even by a small exciting force, as long as the tank panels resonate with the force. In such a case, it is a best to avoid resonance from a practical point of view. In order to avoid resonance, there are two approaches: change the exciting frequency, or change the natural frequency of the structure. We thought the latter way is applicable for this case.

If the frequency of the exciting force agrees with the natural frequency of a structure, the structure is in resonance and it will vibrate severely. That situation can be easily understood by considering that the structure absorbs the energy of the exciting force in resonance.

As discussed previously, the best way to prevent vibration is to avoid resonance. Thus in planning a new vessel, it is necessary for designers to estimate natural frequencies of structural members and then to confirm them to avoid resonance with the frequencies of the exciting forces due to the propeller and main engine. It is, therefore, important in the design stage to estimate accurately the natural frequencies of structural members.

On the other hand, in the case that resonance is inevitable, an alternative way has recently been applied in designing. In this design method, firstly the response of the structure to resonance is estimated, secondly the response is compared with the allowable limit, then the design is accepted if the calculated result is within the limit. However, that judgment requires high accuracy of calculation, such as the estimation of the natural frequency and estimation of the exciting force. Therefore, we consider the response calculation method is not as reliable as the resonance avoiding method, unless we accumulate much experience.

### 11.3 Overview of Ship Vibration

Ship structure vibration is mainly caused by the propeller and main engine. There are other vibration sources such as

- impact force due to slamming which causes hull girder vibration, called “whipping”.
- cyclic forces of machinery: pumps, generators, compressors, etc.

However, structural vibration due to the propeller or main engine is especially important, because the countermeasures for such vibration need a huge amount of expense and time compared to those of other vibration trouble. Therefore, we will focus on the vibration induced by the propeller and main engine.

Figure 11.3.1 illustrates the relationship between the exciting force and ship structural vibration, induced by the propeller and main engine. In the figure, an item boxed by a rectangle indicates an exciting force and an item circled by an ellipse shows a countermeasure suppressing the structural vibration which is induced by the exciting force.

Since the propeller is located at the aft part of a hull, the flow of the water is disturbed by the aft hull and the velocity of flow becomes non-uniform. As the propeller rotates in this non-uniform flow, the propeller creates fluctuating forces, which result in exciting forces acting in the ship structure. The exciting forces from propeller rotation in non-uniform flow can be called propeller shaft force. In addition, the propeller shaft force is usually considered as having two different components:

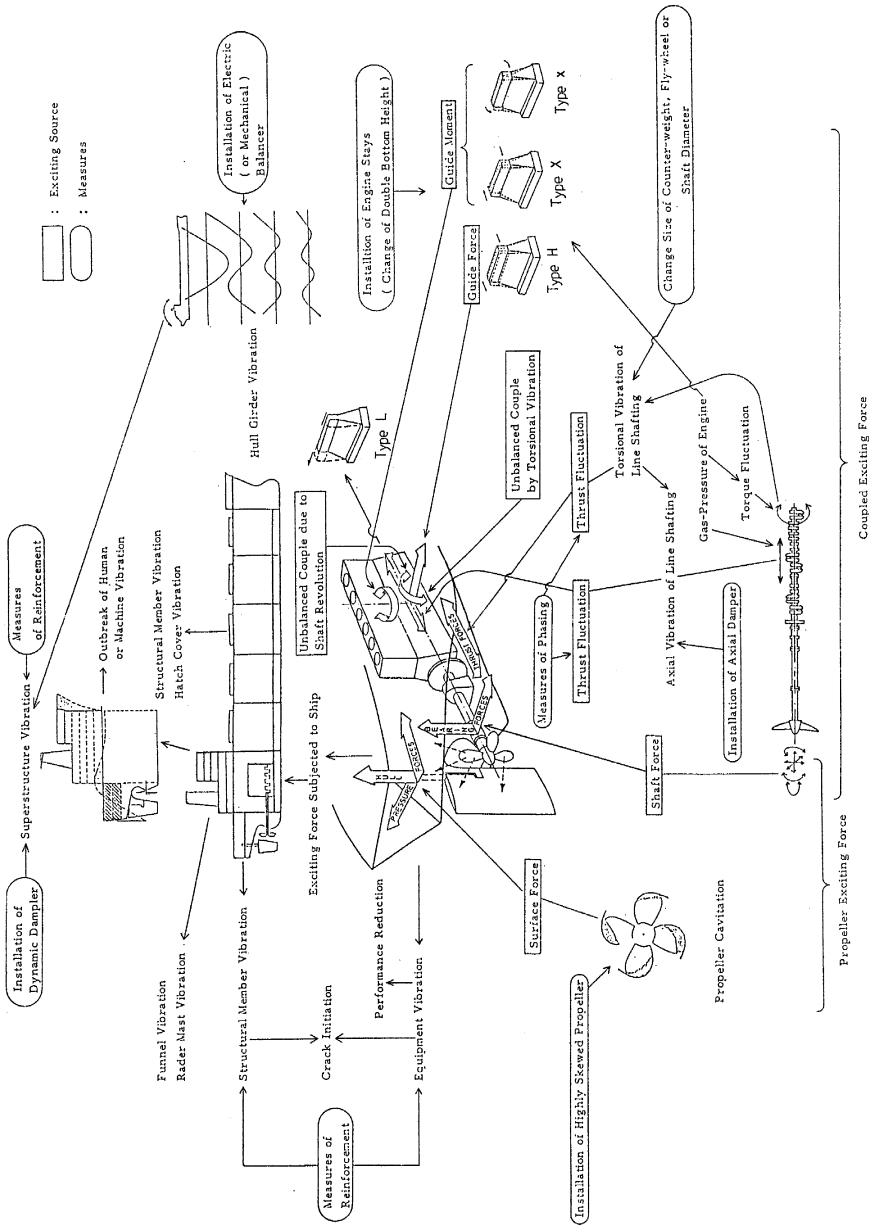


Fig. 11.3.1 Overview of ship vibration

one is bearing force which acts on the propeller shaft in an orthogonal direction, and the other is thrust force which works in the axial direction of the shaft.

On the other hand, the distance between the propeller blade and shell plating of a hull varies according to the propeller rotation. This leads to a change of pressure around the shell plating of the bottom structure. This kind of force is called a surface force and it is independent of the shaft forces. A surface force is induced even in uniform flow because of the change of distance between the propeller blade and shell plate, while the shaft force happens only in non-uniform flow. The magnitude of the surface force is amplified by the existence of cavitation on a propeller blade, therefore, it is particularly important not to generate propeller cavitation to prevent the vibration due to surface force. The first step to decrease the surface force is to increase the distance between the propeller blade and hull surface as much as possible. The second step is to install a highly skewed propeller, which has a large skew-back angle of the blades.

Since a merchant vessel is normally driven by a diesel engine to minimize fuel consumption, the exciting forces of a diesel engine can be categorized by the following components according to the mechanism by which they are produced:

- Unbalanced forces or unbalanced moments induced by inertia forces due to the movement of pistons, etc.
- Guide forces or guide moments which are generated by the explosive pressure of gas. These are transmitted to the cylinder of main engine.
- Longitudinal exciting force which is induced by the inertia force of longitudinal deflection of the crankshaft due to gas pressure.
- Fluctuation in thrust force which comes from torque variation in line shafting: Torque variation due to gas pressure causes torsional vibration of line shafting, including the propeller and propeller shaft, and torsional vibration of shafting causes cyclic fluctuation in flow velocity of propellers, which results in thrust fluctuation.

The magnitude of the unbalanced force and the unbalanced moment is so large, in general, that they can produce hull girder vibration if they resonate with the natural frequency of the hull girder vibration. Furthermore, hull girder vibration will bring longitudinal vibration to the superstructure. Therefore, it is normal in the design of the line shafting to provide appropriate counterweights or a fly-wheel to the crankshaft which reduces the magnitude of the unbalanced forces or moments. In spite of the above measures, for in cases where considerable amount of unbalanced forces or moments still remain, and cases where it is predicted to cause hull girder vibration, an electric balancer is often installed at the aft end of the hull. The electric balancer generates an exciting force which can cancel hull girder vibration due to the unbalance force or moment.

Guide forces and moments are the exciting forces which induce lateral vibration in the main engine structure. Guide forces cause lateral vibration of the main engine structure which is called "H" type vibration. Guide moments can cause torsional vibration, that is "X" type, and it can also cause horizontal bending vibration, that is  $x$  type. When the natural frequency of the main engine structure resonates with



the exciting frequency of the guide force or moment, the exciting force due to the guide force or moment is amplified extremely because the engine structure acts as a resonator. Such an increased exciting force is transmitted to the structural members in the engine room and these may cause severe vibration. In order to avoid the lateral vibration of main engine structure, it is a normal practice to provide engine stays at the top of the engine structure.

Once longitudinal vibration in a crankshaft happens, it causes a longitudinal exciting force on the crankshaft which is transmitted to the double bottom structure of the engine room via the thrust block of the main engine. This exciting force may cause a vibration problem in the superstructure or cause structural failures of panels, stiffeners, etc. in the area of the tanks. To prevent such vibration trouble, a longitudinal vibration damper is usually installed at the fore end of the main engine crankshaft. This damper, which is a kind of oil damper, can reduce the longitudinal vibration amplitude by absorbing the vibration energy.

The fluctuating thrust force due to torsional vibration of the line shafting will cause longitudinal vibration of the main engine structure. If the natural frequency of the longitudinal vibration of the engine structure agrees with the frequency of the thrust fluctuation, the fluctuating thrust is magnified by this resonance, and this vibration is transmitted to structural members through the thrust block. In such cases, the installation of a torsional damper is a quite effective countermeasure to suppress torsional vibration of the line shafting.

## 11.4 Boundary Conditions of Hull Structure Vibration

Whenever a new type of vibration problem arises, it is caused by a change of the basic vibration items; (a) exciting force, (b) response of structure, (c) allowable criteria.

One of the above examples is seen in the vertical vibration problem of hull girder, which became troublesome in the latter half of the 1940s. This trouble is produced by the introduction of a diesel engine as the main engine, instead of a steam turbine driven engine, because the unbalanced moment of a diesel engine resulted in a large vibration response in the hull girder. The steam turbine engine had no such unbalanced moment.

The second example is a problem induced by the change of response. This trouble was due to the construction of the after-bridge ship, in accordance with the rationalization of design philosophy in the 1960s. The above after-bridge ship results in an increase in the height of the navigation bridge, consequently the fore-aft vibration of bridge has been high-lighted.

Another example is a recent case where the requirements by the ship's crew for quiet habitability become more severe, in addition to that, the requirement of highly advanced electrical devices to keep reliable performance is also serious. These requirements generate more severe criteria for vibration assessment. This matter can

be considered as one of social and technical changes in the environment which bring a change of boundary conditions for vibration.

Hull structural vibration is induced by the propeller and main engine, and these exciting sources acting on the hull may generate responses in the steel structure. Nowadays, we are able to estimate the exciting forces, the natural frequencies of the structure and the structural responses, with the aid of the rapid progress of computers. In addition to this technical development, if we can predict what changes in the boundary conditions of hull vibration will be brought by changes in social and economical environments, we will be able to solve all vibration problems by providing suitable countermeasures in advance.

With regard to the physical boundary conditions, we will explain these by considering some more examples.

### *Example 1*

Figure 11.4.1 illustrates a deck beam model of a pure car carrier (PCC). Figure 11.4.1(a) shows a deck beam fixed to a rigid wall at both ends and the natural frequency is calculated as 670 cpm; also, the natural frequency of a simply supported beam in Fig. 11.4.1(b) is estimated to be 300 cpm. Nevertheless, the measured natural frequency of the beam is 595 cpm as shown in Fig. 11.4.1(d). Therefore, these estimated frequencies are very different from the measured ones. Considering the above matter, we have to establish more reasonable boundary conditions for the beam; more flexible than one with the fixed ends, but more stiff than simply supported ends. Hence, if we take into account the stiffness of the vertical frames supporting both ends of the beam, as shown in Fig. 11.4.1(c), then the calculated natural frequency becomes 608 cpm. The calculated results show very good agreement with the measured frequency 595 cpm.

This indicates that even a simple beam model can be useful for estimating the natural frequency, if the boundary condition is considered in a reasonable way.

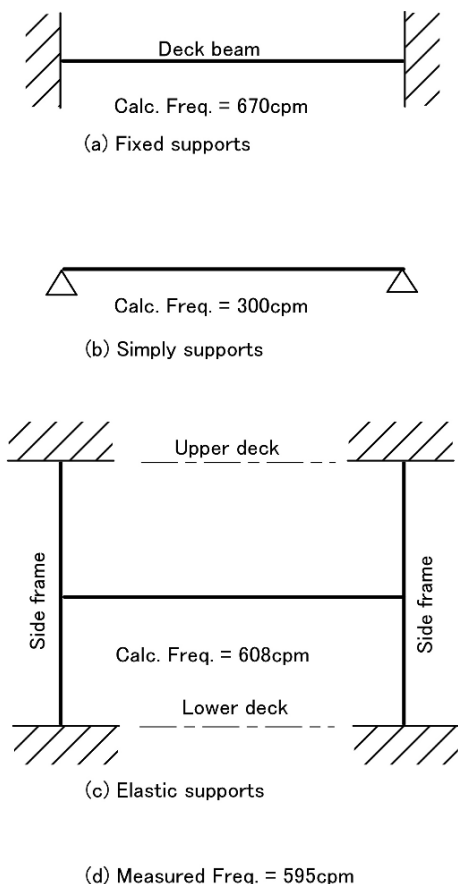
### *Example 2*

The next example is a hatch cover vibration in a 60,000 DWT bulk carrier as shown in Fig. 11.4.2. The bulk carrier was installed with a main engine of 5 cylinders and a propeller of 4 blades. The hatch covers of the vessel vibrated vertically at 110 rpm of main engine revolution, and the vibration amplitude was 0.4 mm at 550 cpm. We considered the vibration was caused by the resonance of hatch cover with the exciting force of main engine, because the order of vibration was 5 times the main engine revolutions, which coincides with the number of 5 cylinders.

By modeling the hatch cover as a uniform beam simply supported at both ends, the natural frequency of the hatch cover can be obtained by the following equation:

$$f_{hc} = C\sqrt{\frac{I}{A}} \quad (11.4.1)$$

**Fig. 11.4.1** Deck beam model of pure car carrier



where

- $C$  : constant
- $I$  : sectional moment of inertia of cross section
- $A$  : sectional area

The beam was reinforced by providing an additional web of 300 mm depth and a flange as indicated in Fig. 11.4.2(a). From this increase in rigidity, we expected to increase  $I/A$  to twice the original value, consequently the natural frequency of the hatch cover would become  $1.41 (= \sqrt{2})$  times that of the original one. In spite of our expectation, the natural frequency of about 550 cpm was found by measurements carried out after the reinforcement, which means the natural frequency was not increased by the reinforcement.

From this measured result, we found that the boundary condition of the hatch cover should be considered in a different way; the beam should be modeled not as a simply supported beam but as an elastic supported beam. Since the hatch cover is mounted on the hatch coaming on the top side tank, the outer edge of hatch cover

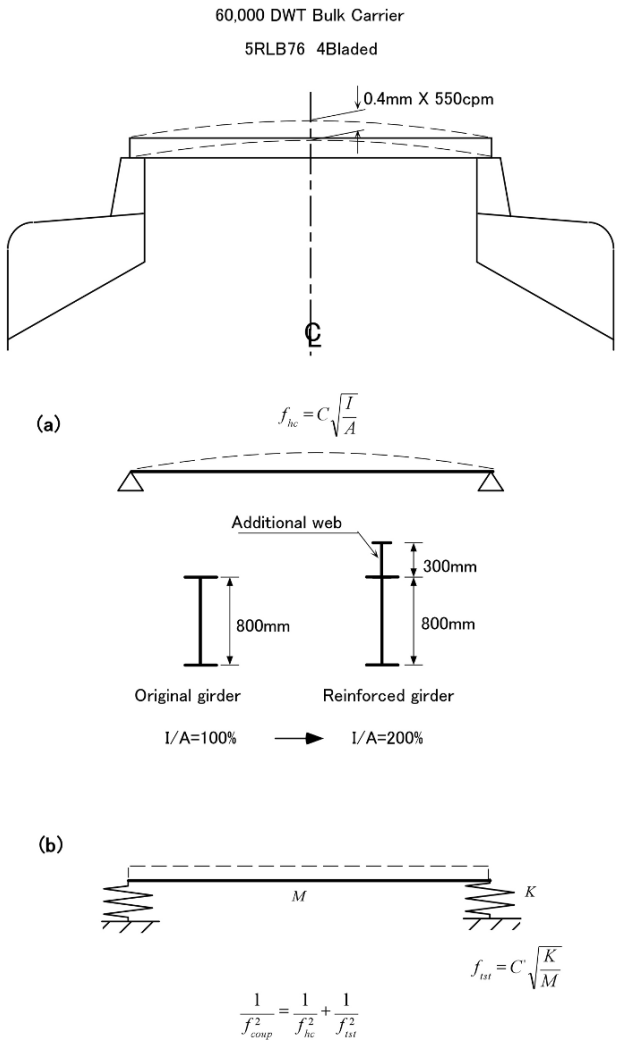


Fig. 11.4.2 Vertical vibration of hatch cover

may move vertically, if the top side tank vibrates as shown in Fig. 11.4.2(b). Hence, the natural frequency of an elastic supported beam is

$$\frac{1}{f_{coup}^2} = \frac{1}{f_{hc}^2} + \frac{1}{f_{st}^2} \tag{11.4.2}$$

where

- $f_{coup}$  : coupled natural freq. of between hatch cover and top side tank
- $f_{hc}$  : natural freq. of hatch cover itself

$f_{1st}$  : natural freq. of rigid hatch cover supported by equivalent spring of hatch coaming and top side tank

From the above equation, in the case where  $f_{1st}$  is much smaller than  $f_{hc}$ , an increment in  $f_{hc}$  can not increase the coupled frequency  $f_{coup}$ . In this case,  $f_{coup}$  was 550 cpm. Therefore, if we assume the natural frequency of the hatch cover itself is  $f_{hc} = 1,400$  cpm, then  $f_{1st}$  becomes 600 cpm. Based on the assumption, the natural frequency of the hatch cover increases from 1400 cpm to  $1400 \times 1.41$  cpm, but on the contrary, the natural frequency of the hatch cover foundation  $f_{1st}$  is reduced by the increase of the hatch cover weight due to the reinforcements. When we take 20% of the original weight of hatch cover as the weight of the reinforcement,  $f_{1st}$  reduces to 94% of the original and it becomes 564 cpm. Consequently, the coupled frequency becomes

$$\frac{1}{f_{coup}^2} = \frac{1}{(1400 \times 1.42)^2} + \frac{1}{564^2}$$

$\therefore f_{coup} = 543$  cpm

From the above calculation, we found that the coupled natural frequency decreases by 1.5% by providing the reinforcement to the hatch cover.

Example 2 shows that the boundary conditions of the hatch cover largely affects the natural frequency of the hatch cover.

### Example 3

This example shows the vibration problem due to hydro-elastic interaction. The natural frequency of the upper deck structure of a tanker will change drastically, when the ballast water in the wing tank is touching the upper deck plate of the tank as shown in Fig. 11.4.3. In the case shown in the figure, the upper deck plate resonates with the exciting force of the propeller of 4 blades at 112 rpm of shaft revolution, because the natural frequency of the upper deck was 448 cpm caused by the water contacting the the deck plate. In order to avoid the resonance, the volume of ballast water was reduced to 98% of the tank volume, which resulted in a diminishing of the contact of ballast water with deck plate. By taking this countermeasure, the natural frequency of the deck plate becomes larger than the exciting frequency, consequently the vibration due to resonance can be removed.

This example shows the ballast water changed the boundary conditions of the wing tank; the water acted to increase the weight of the deck plate, when it came into contact with the deck plate.

## 11.5 Current Boundary Conditions of Hull Structure Vibration

As we have mentioned in Sect. 11.4, hull structure vibration takes place in a different form when the boundary conditions are changed. In this section, we will explain the current situation of the boundary conditions together with the vibration problems induced by them.

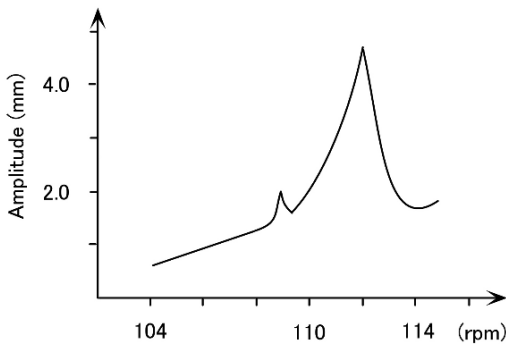
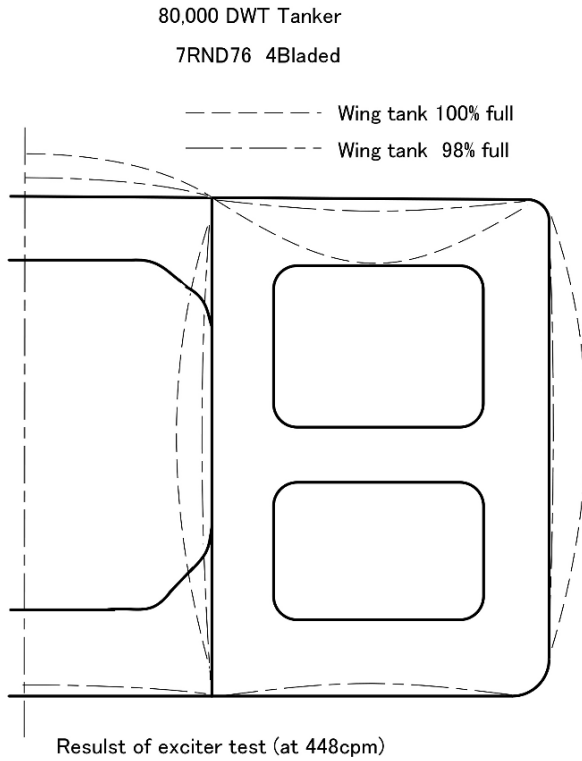


Fig. 11.4.3 Vertical vibration of upper deck of tanker

The oil crisis in 1973 and 1977 led to a sudden rise in crude oil prices. Since that situation increased the proportion of fuel oil cost in the total running cost of ships, necessary countermeasures were immediately taken in order to save energy. For the purpose of saving energy, ship owners, ship builders and main engine makers have undertaken research and development. These efforts have reduced the fuel oil consumption, nowadays, to about a half of that prior to the oil crisis.

The energy saving efforts were achieved in the following three fields:

- Improvement of propulsive efficiency by the change of hull form
- Reduction of fuel oil consumption of main engine
- Improvement of heat efficiency by recovering the exhausted gas energy

In addition to these, the application of higher strength steel to the hull structure helped with the energy saving, because this brought about a decrease in the total hull steel weight. Furthermore, the adoption of self-polishing paint on the outer shell was successful.

Among these changes of the environment, the change of hull form, the improvement of propulsive efficiency, the reduction of fuel oil consumption, and the application of higher tensile strength steel have considerably affected hull vibration.

This is because, the change of hull form reduced the horse power of the main engine which had been required for the older type of vessel in order to produce the same deadweight and the same speed. In addition to the above changes, the decrease of ship's service speed due to the rapid rise of fuel oil prices reduced the main engine power, which resulted in the decrease of engine exciting forces. For instance, although propeller revolution was 100 ~ 120 rpm in the case of a diesel driven vessel, and 80 ~ 90 rpm in the case of a turbine vessels, and it recently became 70 ~ 80 rpm in diesel driven vessel, in an extreme case it decreases down to 60 rpm.

The decrease of propeller revolutions contributes to the reduction of flow velocity of propeller, and this prevents propeller cavitation, which means the reduction of propeller exciting forces.

Improvement of propeller efficiency in the design of the after body of the vessel for a more uniform distribution of wake, have reduced propeller cavitation, which consequently has decreased the propeller exciting forces.

Considering the above situation, both the improved hull form and improved propulsive efficiency have positive effects in preventing vibration problems. On the contrary, efforts to reduce fuel oil consumption of a diesel engine have produced negative results from vibration viewpoint. Because the adoption of long stroke of main engines and the application of a small number of cylinders have caused a change in engine profile: larger height than length. Such a profile caused the longitudinal vibration of the main engine structure. And the latter causes bigger torque variation which induces thrust variation. In the latest boundary conditions, a propeller is no longer strong enough to provoke vibration of hull structures.

# **Part III**

## **Applications**



# Chapter 1

## Hull Structure Arrangement

As explained in Chap. 1 of Part I the general arrangement of a ship is defined by the strength of the ship and many kinds of socio-economic requirements. The performance of the ship is closely related to the general arrangement. It used to be said that a ship designed by a designer with no experience in hull structure design may have deficiencies.

Hereunder we refer to the general arrangement from the viewpoint of hull structure design. In this design there are two main items, one of which is the tank arrangement not having excess longitudinal hull girder bending moment, and the other is the bulkhead arrangement, that is, the number of tanks or holds.

The former is well known and will be explained in Chap. 2 “Design of Longitudinal Strength of Hull Girder”. The latter is not so widely known and is explained here under as the hull structure arrangement.

### 1.1 Hold Arrangement

It has been a common view in the case of bulk carriers that a 5 holds arrangement can be applied up to 70,000 DWT, 7 holds up to 150,000 DWT and 9 or 11 holds for ships bigger than 150,000 DWT. Also there exists an opinion that a double hull side construction will be applied for ships bigger than 150,000 DWT. The biggest bulk carrier ever built is 250,000 DWT which has 9 holds and a single side hull construction.

How to decide the bulkhead arrangement, that is, the number of holds is a very important factor at the initial design stage but not yet clearly reported. Nowadays the hull structure is designed by being analyzed as a whole structure by computer. In this way the problem of how to decide the number of holds is submerged in the computer calculation process.

The main loads applied on the hull structure are buoyancy and weight which are forces in the vertical direction. Against these vertical loads, the vertical members such as side shell plates, transverse bulkheads and longitudinal bulkheads form the strength of hull structure. In other words it can be said that the strength of the hull structure as a whole is maintained principally by the shearing strength of the side

shell plates, transverse bulkheads and longitudinal bulkheads. Accordingly, for the larger ships, to increase the number of transverse bulkheads as well as increasing the thickness of side shell plates, transverse and longitudinal bulkheads plates are desirable. Also to construct a double hull structure is considered to be very effective.

In 1960's much damage was reported on the transverse rings in the wing tanks of large tankers. This was caused by the relative displacement between the longitudinal bulkhead and side shell plating due to the increased wing tank length. The swash bulkhead in long wing tanks was designed only for reducing the sloshing motion of free water surface in a tank and not for rigidity of the wing tank structure.

Figure 1.1.1 shows areas of buckling damage on a center line girder of one such 100,000 DWT tanker. In this case the center line girder was designed with the

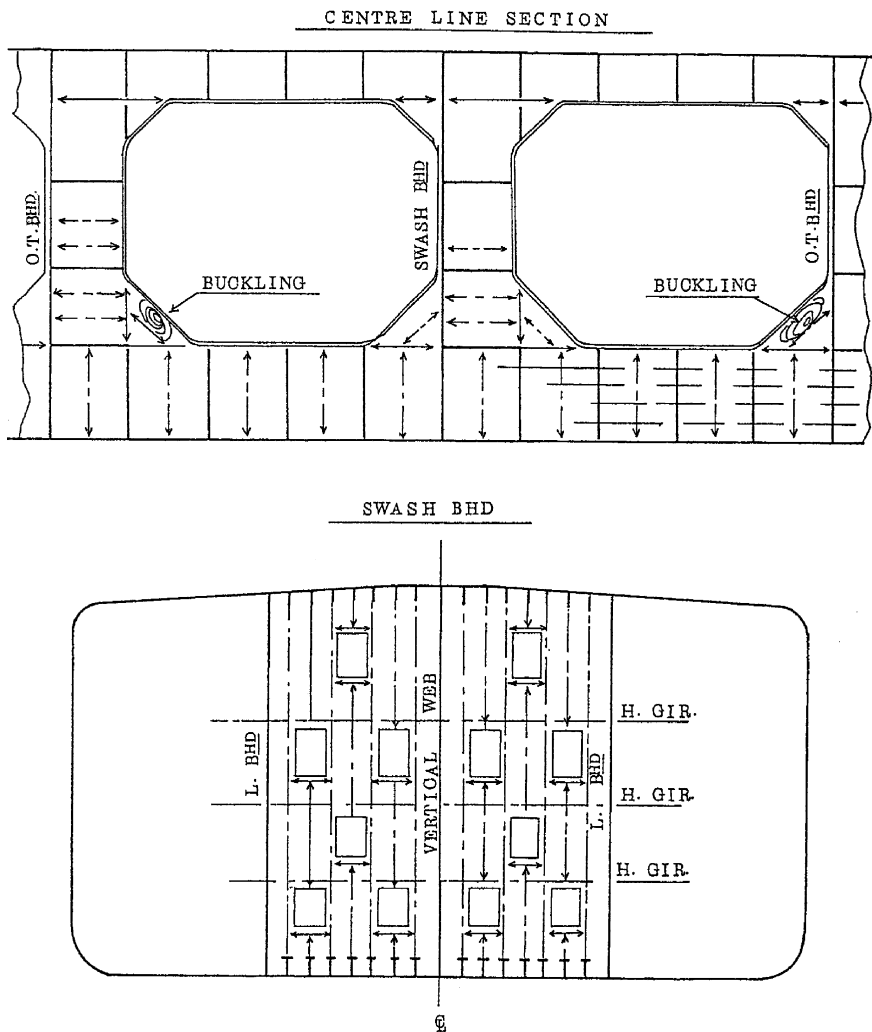


Fig. 1.1.1 Example of damage caused by lack of shear rigidity of swash bulkhead

condition of being fixed at both ends by transverse bulkheads, one of which was a watertight bulkhead and the other was a swash bulkhead which had insufficient shear rigidity due to openings.

In the wing tank as well as in the center tank the strength members resisting the vertical loads should have a rigid frame work, otherwise the design condition (both ends fixed) of the primary supporting members will be faulty. By relaxing the both-ends-fixed condition there arises additional stresses in the primary supporting members which causes damage such as cracks and buckling.

## 1.2 Criteria of Design of Hull Structure Arrangement

### 1.2.1 Wing Tanks of Tankers

In the rule book of Nippon Kaiji Kyokai there was a regulation to limit the relative displacement between longitudinal bulkhead and side shell plate as follows:

Special consideration is to be paid to wing tank construction when the  $S$ -value as calculated by Eq. (1.2.1) exceeds 0.15.

$$S = \frac{h - 0.32d}{n_b k_b + n_s \eta_s k_s + n_t \eta_t k_t} \cdot \frac{a}{b} \cdot l \quad (1.2.1)$$

where

$a$ : half breadth of center tank in m

$b$ : breadth of wing tank in m

$h$ : distance above top of keel to hatch opening top in center tank in m

$d$ : full load draft in m

$l$ : center tank length between tight bulkheads in m

$n_b$ ,  $n_s$  and  $n_t$ : numbers of transverse bulkheads, swash bulkheads and transverse rings in way of  $l$  respectively (in case of the ends of  $l$ , the number is 1/2)

$\eta_s$  and  $\eta_t$ : coefficients depending on the opening ratio of swash bulkheads as shown in Table 1.2.1, for intermediate opening ratio coefficients delivered by interpolation

$k_b$ ,  $k_s$  and  $k_t$ : values to be obtained by the following Eq. (1.2.2)

$$81.0 \frac{Dt}{\alpha b} \quad (t \text{ in mm}) \quad (1.2.2)$$

$t$ : in calculation of  $k_b$ , mean thickness of the trans. bulkhead in the wing tank

in calculation of  $k_s$ , mean thickness of the swash bulkhead in the wing tank

in calculation of  $k_t$ , mean thickness of the trans. ring in the wing tank in mm

$\alpha$ : 1.0 for flat bulkheads and for the corrugated bulkhead the values of following equations

$$\text{in case of vertical corrugation } \alpha = \frac{\text{girthinglength(breadthwise)}}{b}$$

$$\text{in case of horizontal corrugation } \alpha = \frac{\text{girthinglength(depthwise)}}{D}$$

**Table 1.2.1** Coefficient  $\eta_s, \eta_t$  due to opening ratio

Opening ratio (%)	0	5	10	20	30	40	50	60	70
$\eta_s, \eta_t$	1.00	0.95	0.80	0.55	0.35	0.23	0.15	0.10	0.06

The numerator of Eq. (1.2.1) represents load  $W$  on the longitudinal bulkhead in the center-tank side in the floating condition with a shallow draft of  $0.32d$  and with full ballast in the center tank. And the denominator represents shear rigidity of wing tank construction which can be understood by the following deduction: 81.0 represents the shear modulus of steel in tonf/m · mm

$$(n_b k_b + n_s \eta_s k_s + n_t \eta_t k_t) b = 81.0 D \left( n_b \frac{t_b}{\alpha} + n_s \eta_s \frac{t_s}{\alpha} + n_t \eta_t k_t \right) \tag{1.2.3}$$

$$\text{Putting } n_b \frac{t_b}{\alpha} + n_s \eta_s \frac{t_s}{\alpha} + n_t \eta_t k_t = \sum t \tag{1.2.4}$$

$\sum t$  represents shear effective plate thickness.

Collecting the details above from Eqs. (1.2.1), (1.2.2), (1.2.3) and (1.2.4), the following Eq. (1.2.5) can be obtained.

$$S = \frac{W}{81.0 \times D \sum t} \leq 0.15 \tag{1.2.5}$$

where  $W$  in tonf,  $D$  in m,  $t$  in mm and 81.0 in tonf/m·mm Accordingly  $S$  is non dimensional.

Because  $W$  is the load on the longitudinal bulkhead and  $81.0 D \sum t$  is the shear rigidity of the wing tank construction,  $S$  is the shearing strain of the wing tank as shown in Fig. 1.2.1.

Hereafter based on the above Nippon Kaiji Kyokai’s regulation, a criterion for bulkhead arrangements of tankers is investigated.

Equation (1.2.5) can be modified to the following Eq. (1.2.6) assuming that the shear rigidity of a transverse ring is 10% of the shear rigidity of an oil tight bulkhead.

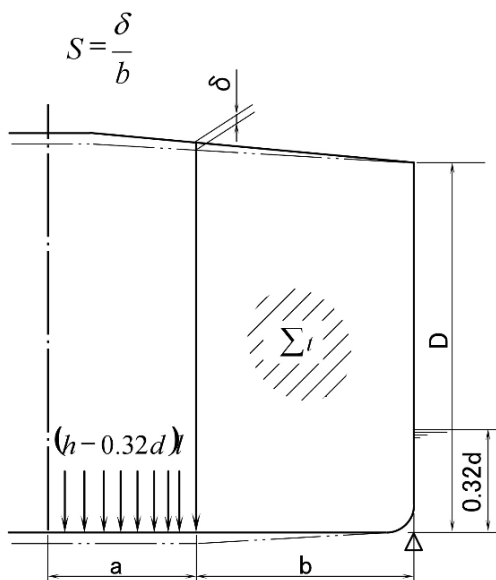
$$\frac{W}{D \{ t_b + 0.1 t_b \left( \frac{l}{s} - 1 \right) \}} \leq 12.15 \tag{1.2.6}$$

where  $s$  : spacing of transverse ring

Furthermore, assuming  $t_b \approx 0.7 (3\sqrt{D} + 3.5)$  and  $h \approx D$ , Eq. (1.2.6) can be simplified into (1.2.7) as follows.

$$\frac{(D - 0.32d) a l}{D \times 0.7 (3\sqrt{D} + 3.5) \times (0.9 + 0.1 \frac{l}{s})} \leq 12.15 \tag{1.2.7}$$

**Fig. 1.2.1** Shearing deformation of VLCCS wing tank



By applying (1.2.7), the limits of  $a$  and  $l$  which are the main factors in determining the bulkhead arrangement can be obtained based on the principal dimensions of  $D$  and  $d$ .

For an example in Fig. 1.2.2 the limitation of length of the center tank for its half breadth is shown for a 200,000 DWT tanker which has  $D = 26.3$  m,  $d = 20.32$  m and  $s = 4.8$  m. Actually this ship has a 48 m long center tank for a half breadth of 9.4 m, whereas (1.2.7) gives a 39 m center tank length for 9.4 m of center tank half breadth. From the viewpoint of shear deformation in the wing tank, the design of the hull structure arrangement of this ship will not be sufficiently strong.

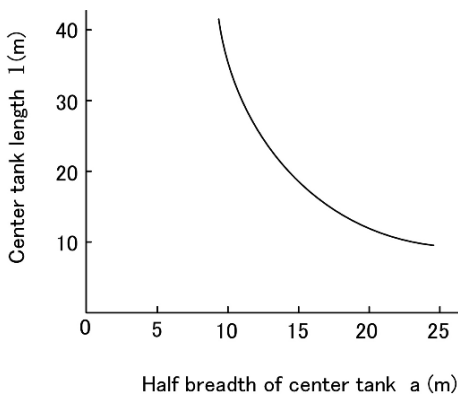


**Fig. 1.2.2** Limitation for center tank size of VLCC

## 1.2.2 Bulkhead Arrangement of Bulk Carriers

Let's apply the same principle of Sect. 1.2.1 to a bulk carrier. In the case of a bulk carrier the holds have the same breadth as the ship's breadth hence the hold length provides the problem. Shear deformation on the transverse bulkhead is caused by the vertical load on the transverse bulkhead. For the loading condition in question, though the fully ballasted tank was considered in the ballast condition of tankers, there are two severe conditions in the case of the bulk carriers. One is an empty hold in the ballast condition and the other is a loaded hold in the fully loaded condition. Here the former case is investigated, that is, an empty hold in the ballast condition.

Assuming a transverse bulkhead supports  $b/(b+l)$  of total load applied on the double bottom, the vertical load on a transverse bulkhead  $W$  is expressed by Eq. (1.2.8) as follows.

$$W = \frac{b}{b+l} \times 0.32d \times b \times l \quad (1.2.8)$$

where

$b$ : breadth of double bottom in m

$l$ : length of hold in m

$d$ : full load draft in m

Assuming the shear rigidity of a double bottom floor is 1% that of the transverse bulkhead, total shear rigidity  $G$  of a transverse bulkhead and floors is expressed by the following Eq. (1.2.9).

$$G = 81.0D \left\{ \frac{t_b}{\alpha} + 0.01 \times t_b \left( \frac{l}{s} - 1 \right) \right\} \quad (1.2.9)$$

where

$D$ : depth of ship in m

$t_b$ : mean thickness of bulkhead in mm

$\alpha$ : correction factor for corrugated bulkhead see 1.2.1

$l$ : length of hold in m

$s$ : floor space in m

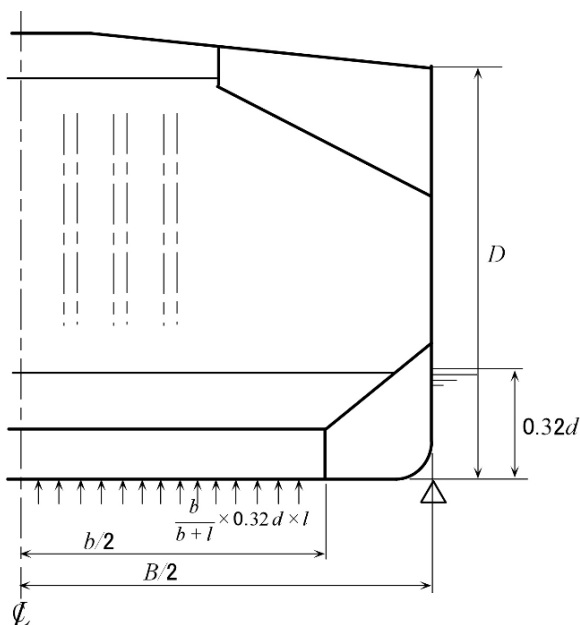
Modeling these as shown in Fig. 1.2.3, the shearing strain  $S$  in the transverse bulkhead is expressed by Eq. (1.2.10).

$$S = \frac{W}{2G} \quad (1.2.10)$$

Furthermore assuming  $b = 0.7B$ ,  $\alpha = 1.8$  and  $t_b = 0.7(3\sqrt{D} + 3.5)$ , Eq. (1.2.11) can be derived from Eqs. (1.2.8), (1.2.9) and (1.2.10) as follows.

$$S = \frac{B^2 dl}{722D(0.7B+l)(3\sqrt{D}+3.5)(0.55+0.01\frac{l}{s})} \quad (1.2.11)$$

**Fig. 1.2.3** Shearing deformation model of bulk carrier transverse bulkhead



In the case of a wing tank of a tanker, we imposed the limitation of  $S \leq 0.15$  referring to Nippon Kaiji Kyokai’s regulation, but in the case of bulk carriers we have no such reference. In such cases it is reasonable to refer to data of ships in service.

We calculated  $S$  values for two ships in service without any trouble. One is a 30,000 DWT ship with 5 holds and another is a 130,000 DWT with 9 holds. The  $S$  values are 0.051 and 0.064 respectively, and we selected  $S = 0.07$  as a criterion.

In the case of a 250,000 DWT bulk carrier,  $S$  values are 0.104 with 9 holds and 0.096 with 11 holds. It is recommended to have a stiffened flat plate or double hull transverse bulkhead instead of the current corrugated bulkhead.

### 1.3 Bulkhead Arrangement Beyond Cargo Hold

For large ships not only the structural arrangement in the vicinity of the cargo hold or tank but also the structure arrangement beyond cargo holds or tanks, such as bow and engine room construction, is important. In the vicinity of cargo tanks of a tanker, the side shell, longitudinal and transverse bulkheads provide the strength of the ship as a whole. However at both ends of the tank part, to keep the strength continuity is difficult due to the absence of longitudinal bulkheads, hence a special attention should be paid.

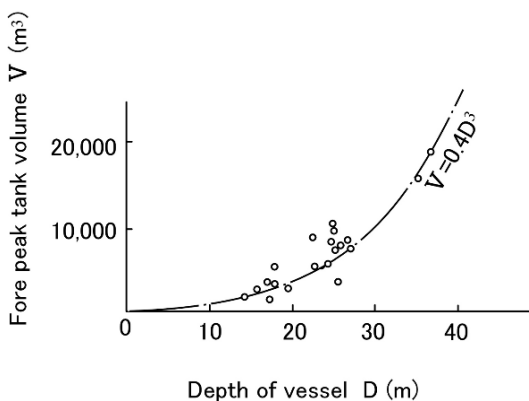
### 1.3.1 Bow Construction Without Extended Longitudinal Bulkheads

There are usually two rows of longitudinal bulkheads in way of the cargo tanks of a tanker. Also forward of the collision bulkhead is usually the fore peak tank where no longitudinal bulkhead is necessary. In the case of a wide fore peak tank a center line swash bulkhead will be installed to avoid sloshing motion of the ballast water.

The volume of the fore peak tank will be quite considerable for large ships especially for a broad beam ship with a bulbous bow. The big volume of the fore peak tank causes great buoyancy in the fully loaded condition and a big load in the ballasted condition, while the fore peak tank is supported by the shear area of the side shell plate and the transverse bulkhead plate. In Fig. 1.3.1 volumes of fore peak tanks are plotted for the ship's depth. Assuming the volume  $V$  of the fore peak tank is proportional to the cube of the ship's depth  $D$ , Eq. (1.3.12) can be obtained as follows.

$$V = 0.4D^3 \quad (1.3.12)$$

**Fig. 1.3.1** Fore peak tank volume vs. depth of vessel



The shearing force caused by the volume  $V$  of the fore peak tank is supported easily in the aft part of the collision bulkhead by side shell plates and longitudinal bulkhead plates. However in the vicinity of the fore peak tank in some case it is hard for side shell plates to support the shearing force. In such cases a center line longitudinal bulkhead is to be fitted.

### 1.3.2 Engine Room Construction Without Extended Longitudinal Bulkheads

Usually the two rows of longitudinal bulkheads in the cargo tank space are to be extended into the engine room as fuel oil tank bulkheads. But in the case of three rows



of longitudinal bulkheads in the cargo tank the center line longitudinal bulkhead is not able to be extended into the engine room. The shearing force supported by the center line longitudinal bulkhead is transmitted to side shell and side longitudinal bulkhead plates in the vicinity of engine room via the transverse bulkhead at the aft end of the cargo tank space.

To investigate the transmission of the shearing force a FEM calculation was carried out with a model as shown in Fig. 1.3.2. The results are shown in Fig. 1.3.3. The ship was a 600,000 DWT tanker of a trial design and has three rows of longitudinal bulkheads in the cargo tank space. The center line longitudinal bulkhead is extended aft to Fr.66 and two side longitudinal bulkheads are extended into the engine room. The model in Fig. 1.3.2 is fixed at Fr.71 and a uniform load of 10,000 tf is applied on half the breadth of the upper deck at Fr.28. The shearing stresses in the side shell, side and center line longitudinal bulkheads plates are calculated, then shearing forces are obtained by multiplying plate thickness by the calculated stresses. In Fig. 1.3.3 the supporting ratio of each member is shown.

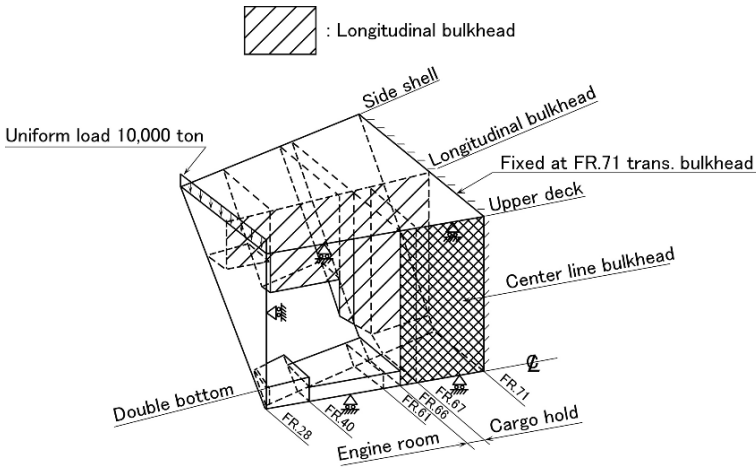


Fig. 1.3.2 Structural model of engine room fore part and cargo hold aft part

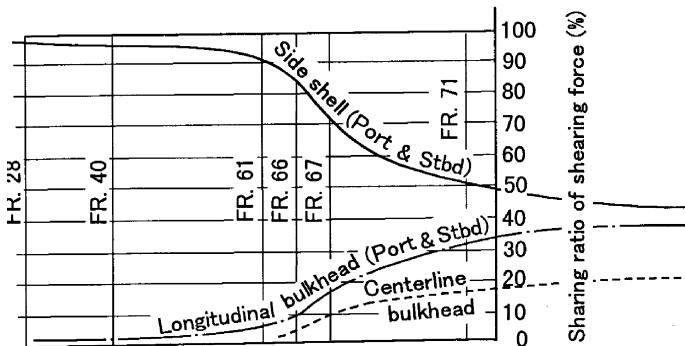


Fig. 1.3.3 Share of shearing force for each member

From considerably forward of Fr.67, i.e. the aft end bulkhead of the aftermost tank, the shearing force supporting ratio of the longitudinal bulkheads decreases, on the contrary the shearing force supporting ratio of the side shell plates increases. The shearing force supporting ratio of the side longitudinal bulkheads also decreases from considerably forward of Fr.67, i.e. the aft end bulkhead of the tank part, which may be caused by reduced sectional area due to hull form.

Careful attention should be paid to avoid having troublesome deformation in the engine room structure caused by large buoyancy forces in the fully loaded condition, because there are many items such as main engine and main shafting for which alignment is very important. To avoid such troublesome deformation in the engine room structure, an effective bulkhead arrangement will be necessary.

## Chapter 2

# Longitudinal Strength of Hull Girder

The longitudinal strength of the hull girder is one of the most important strength considerations in a ship, because lack of longitudinal strength may be a direct cause of the sinking of a ship. Damage such as jack knife deformation and breaking of the hull girder at midship are caused by the lack of longitudinal strength.

One example is shown in Fig. 2.1 [1]. Generally speaking, damage due to the lack of longitudinal strength occurs mainly in older ships. Here the lack of longitudinal strength is caused by corroded deck plates and hence reduced thickness, and by reduced connections between deck plates and deck longitudinals because of corroded fillet weld beads.

Brittle fracture may happen in non notch tough steel because of defects caused by poor welding. Such damage to the longitudinal strength of hull girder can be avoided by anti-corrosion devices, good selection of materials, and good welding. It can be said that these are not design problems but workmanship and maintenance problems.

In the design of hull structure arrangement, the vertical members such as side shells and bulkheads play a major role. On the other hand, in the design of the longitudinal strength of hull girders, the horizontal members at a greater distance from the neutral axis such as deck and bottom structures, will play the major role.

The authors consider that no problem will happen with regard to the longitudinal strength of a ship provided that the longitudinal strength is designed according to the classification societies' rules which are based on past experiences. Anti-corrosion methods such as epoxy paint under the upper deck, notch tough materials, workmanship and maintenance should also be well controlled.

Hereunder some items are introduced on which the authors paid attention in the design of the longitudinal strength of hull girders.

### 2.1 Allowable Stress for Longitudinal Strength

In the design of the longitudinal strength of hull girders, a total system for longitudinal strength design and direct calculation is becoming popular. These methods used to be applied in the designs of special ships such as super size ships, high speed

**Fig. 2.1** Example of damage on longitudinal members



ships, unusual proportion ships, and ship with large deck opening. These methods were based on the response calculations in regular waves by strip theory, short term response predictions in irregular waves with sea spectrum, and long term response prediction with statistic sea conditions as shown in Sect. 2.4 of Part I.

In the design of the longitudinal strength of hull girders, classification societies' rules have simple calculation methods, which give the required section modulus of the hull girder based on the bending moments in still water and in waves obtained from simple formula for the standard loading condition of the ship. There are two required section modulus, one is for wave bending moment  $M_w$  and the other is for sum of still water bending moment  $M_s$  and wave bending moment  $M_w$ . The former can be obtained from the ship length  $L$ , breadth  $B$  and block coefficient  $C_b$  irrespective of tank arrangement.

Here as an example, where the rule of the Lloyds Register of Shipping 1970 edition is applied. The wave bending moment is given by the following Eq. (2.1.1).

$$M_w = \sigma_w C_1 L^2 B (C_b + 0.7) \times 10^{-3} \quad \text{in tonf} \cdot \text{m} \quad (2.1.1)$$

where  $C_1$  depends on ship length  $L$

The section modulus  $Z$  is taken as the bigger value obtained in the following Eqs. (2.1.2) and (2.1.3).

$$(a) Z = C_1 L^2 B (C_b + 0.7) \quad \text{cm}^3 \quad (2.1.2)$$

$$(b) Z = \frac{M_s + M_w}{\sigma_c} \times 10^3 \quad \text{cm}^3 \quad (2.1.3)$$

$\sigma_w$  in (2.1.1) means an allowable stress against the wave bending moment, and  $\sigma_c$  in (2.1.3) means an allowable stress against the total bending moment in still water  $M_s$  and in wave  $M_w$  which are shown in Table 2.1.1.  $\sigma_s$  in Table 2.1.1 means the allowable stress against the still water bending moment.

**Table 2.1.1** Example of allowable stress for longitudinal strength (Unit in kgf/mm<sup>2</sup>)

Ship	$\sigma_c$	Seagoing Service		Sheltered Water		Short Voyages	
		$\sigma_s$	$\sigma_w$	$\sigma_s$	$\sigma_w$	$\sigma_s$	$\sigma_w$
Tanker Ore oil carrier Ore carrier	16.40	6.4	10.0	11.4	5.0	8.4	8.0
Bulk carrier	18.15	8.15	10.0	13.15	5.0	10.15	8.0

The required  $Z$  by Eq. (2.1.2) is for the wave bending moment and is the minimum requirement based on the principal dimensions, and the required  $Z$  by Eq. (2.1.3) is for the total bending moment in still water  $M_s$  and in waves  $M_w$ , which can be reduced by reducing the bending moment in still water  $M_s$ .

In this case it is usual to decide the required  $Z$  from (2.1.3) for the total bending moment in still water  $M_s$  and in waves  $M_w$  so as not to exceed the required value given from by Eq. (2.1.2) for the wave bending moment by adjusting the tank arrangement and the loading condition.

In Fig. 2.1.1 the maximum still water bending moments for each tank arrangement of a 600,000 DWT tanker (trial design) are shown. These are the values for

Ballast tank arrangement	B <sup>hd</sup> Arr. at aft.	Max. still water bending moment(KN-m)
	A	SAG. $1.44 \times 10^7$
	B	SAG. $1.27 \times 10^7$
	C	SAG. $1.20 \times 10^7$
	A	SAG. $1.44 \times 10^7$
	B	SAG. $1.27 \times 10^7$
	C	SAG. $1.20 \times 10^7$
	A	SAG. $1.85 \times 10^7$
	B	SAG. $1.61 \times 10^7$
	C	SAG. $1.56 \times 10^7$

$\triangle$  denotes the position where max. bending moment occurs

**Fig. 2.1.1** Still water bending moment in full load condition according to ballast tank arrangement

fully the loaded condition. In the case of the ballast condition there is more flexibility than in the fully loaded condition in arranging the ballast water to produce a smaller bending moment.

In Fig. 2.1.1 three cases of the ballast tank arrangement are investigated:

- case (1) No. 7 wing tanks
- case (2) No. 6 and .9 wing tanks
- case (3) No. 5 and .10 wing tanks.

**Table 2.1.2** Longitudinal bending moment of existing vessels

$\sigma_{s.w}$ .....stress in still water(kgf/mm<sup>2</sup>),  $\sigma_{wave}$ .....stress in wave(kgf/mm<sup>2</sup>)

Ship No.	Kind of ship	Class society	L <sub>bp</sub>	Full load		Nor. ballast		Heavy ballast		Wave height(m)	Note
				$\sigma_{s.w}$	$\sigma_{wave}$	$\sigma_{s.w}$	$\sigma_{wave}$	$\sigma_{s.w}$	$\sigma_{wave}$		
1	TANKER	NK	230.0	4.1	15.8	4.5	15.0			10.657	
2	"	"	228.0	3.8	15.7	1.2	10.8	1.0	11.1	10.59	
3	"	BV	215.0	1.6	11.7	2.2	11.3			8.07	
4	"	"	220.0	1.7	12.3	2.1	10.4	1.1	10.6	8.45	
5	"	NK	245.0	3.1	17.3	2.5	12.2	0.1	12.5	11.8	△
6	"	AB	240.0	4.5	13.7	2.7	13.7			11.01	
7	"	"	240.0	4.7		3.3		1.4			
8	"	AB,NK	290.0	5.2	13.3	3.4	12.1			9.162	
9	"	"	326.0	2.5	13.6	2.8	12.8	3.8	12.3	9.24	△
10	"	LR	310.0	5.2	19.1	6.9	15.4	4.4	16.3	10.692	
11	"	AB	240.0	3.8	13.7	2.8	14.1			11.01	
12	"	NK	260.0	4.6	14.7	8.8	19.7	8.9	15.3	8.96	
13	"	"	290.0	5.4	17.5	5.9		8.3	16.2	9.2	△
14	"	AB	254.0	4.0	13.3	3.4	13.3	0.9	11.9	9.34	
15	"	"	330.0	6.8	15.0	5.4	11.5	5.1	12.7	9.23	
16	"	NK	260.0	4.6	14.7	2.9	11.3	1.4	10.1	8.9	△
17	"	AB,CR	240.0	5.5		2.1		4.5			
18	"	NK	300.0	5.9	15.6	3.8	5.4	3.3	5.0	9.23	
19	"	NK,AB	330.0	6.4	16.5		12.7		11.8	9.28	
20	"	AB	360.0	5.7	17.1	6.2	17.4	4.5	15.6	10.806	
21	"	"	360.0	5.7	15.3	6.2	15.8	5.4	13.9	9.28	
22	ORE/OIL	"	236.8	5.6	16.9	5.4	15.6	0.8	10.8	9.246	
23	"	NK	223.26	1.3	11.8	3.1	12.7	0.2	10.3	8.358	△
24	"	AB	243.8	4.1	15.0	5.2	15.1	3.9	13.9	9.246	
25	"	NK	235.0	5.4	18.2	4.5	17.9	0.9	12.0	8.64	△
26	"	"	240.0	6.4	18.8	4.3	15.8	2.5	14.2	8.2	△
27	ORE	"	247.0	4.7		4.5		4.1			△
28	ORE/OIL	"	240.0	7.2		7.5		6.1			△
29	ORE	"	220.0	0.9	10.8	3.1	11.3	4.9	12.7	8.078	△
30	ORE/OIL	"	290.0	7.4	19.8	5.1	12.9	5.0	12.7	9.2	△
31	B/C	AB	180.0	4.5	14.8	4.3	13.3			8.671	
32	"	NV	241.0	4.5	16.7	1.0	11.0	4.2	14.9	9.25	
33	"	NK	213.0	0.8	13.7			1.8	12.8	10.02	△
34	"	"	182.0	4.7	14.1	2.9	11.4	0.7	9.3	7.934	△
35	"	"	213.0	2.1	12.3	2.7	11.9			8.358	△
36	"	AB	184.0	3.1	12.4	4.3	13.0	2.7	11.7	8.05	
37	"	"	190.14	3.8	15.3	4.4	13.7	1.9	12.2	8.266	
38	"	LR	236.4	2.4	15.0	5.7	17.9	1.9	14.8	9.165	
39	"	"	175.0	2.8	11.8	5.9	14.9	1.0	10.6	8.03	
40	"	NK	197.0	2.7	12.8	1.0	10.2	3.5	13.1	8.20	△
41	"	AB	200.0	4.6		5.4					
42	BULK/LUMB	"	144.0	6.7		3.8					
43	B/C	NK	137.0	2.5		4.2		4.4			△
44	"	"	197.0	4.6		3.1		5.0			△
45	CARGO	LR	156.97	4.6	9.9	6.8	11.5			7.725	
46	CONTAINER	NK	175.0	7.9	14.3					7.89	△
47	CARGO	AB,CR	147.0	6.1		5.5					

NK.....Nippon Kaiji Kyokai  
 BV.....Bureau Veritas  
 AB.....American Bureau of Shipping  
 LR.....Lloyd's Register of Shipping  
 NV.....Det Norske Veritas  
 CR.....Chinese Register  
 △.....without corrosion margin of 3mm

For each arrangement the maximum still water bending moment is calculated in these three cases where the aft end bulkhead of the tank part is arranged at the A, B and C position as shown in Fig. 2.1.1. The maximum bending moments are all sagging moments. In case (3) where the ballast tanks are No. 5 and .10 wing tanks, bigger bending moment than in case (1) and case (2) is shown for all cases where the aft end bulkhead of the tank part is arranged at the A, B and C position. In case (1) and case (2) the maximum bending moments are equal for all cases where the aft end bulkhead of tank part is arranged at the A, B and the C position. The smallest bending moment is obtained in cases where the aft end bulkhead of tank part is arranged at the C position. And the biggest moment is obtained in case where the aft end bulkhead of tank part is arranged in the A position. This is a general rule and very important. To have a smaller still water bending moment, an arrangement with a shorter engine room and longer tank part is very effective.

The authors suggest that in the design of a new ship the designer should have his/her own allowable stress values for the longitudinal bending moment independent of the classification society rules. There is an owner who makes it a rule to have 10% bigger section modulus than the requirement of classification society rule for easy maintenance and longer life of the ship.

To establish the designer's own allowable stress, it is a sure and practical way to refer to the data of previous ships in service. In line with this aim, Table 2.1.2 is prepared. The longitudinal bending stresses are obtained by dividing the still water and wave bending moments calculated by the section modulus of the hull girder. The wave applied is assumed to be the same length as the ship, and the wave height is the value according to each classification society's instructions which are described in the table.

## 2.2 Position of Maximum Longitudinal Bending Moment

In Fig. 2.1.1 the positions of the maximum longitudinal bending moment are shown. It can be shown that the position of the maximum longitudinal bending moment in still water lies in some cases far from midship. Generally the position of the maximum longitudinal bending moment in a wave lies at midship because the moment calculation is to be carried out in the condition where the crest or the hollow of the wave is at midship. However, in other conditions where the crest or hollow of the wave does not coincide with midship the maximum longitudinal bending moment may not exceed that at midship.

The value and the position of the maximum longitudinal bending moment in a wave are investigated for the case where the crest or hollow of the wave does not coincide with midship. This investigation was carried out for a 600,000 DWT trial design tanker and the results are shown in Fig. 2.2.1. It can be shown from the Fig. 2.2.1 that in this ship in the heavily ballasted condition the hogging moment is bigger than the sagging moment and the maximum longitudinal bending moment arises around S.S.6(1/2) and the value is about 85% of that in the fully ballasted condition. On the other hand in the fully loaded condition the sagging moment is bigger than the hogging moment and the maximum longitudinal bending moment rises to around S.S.4.

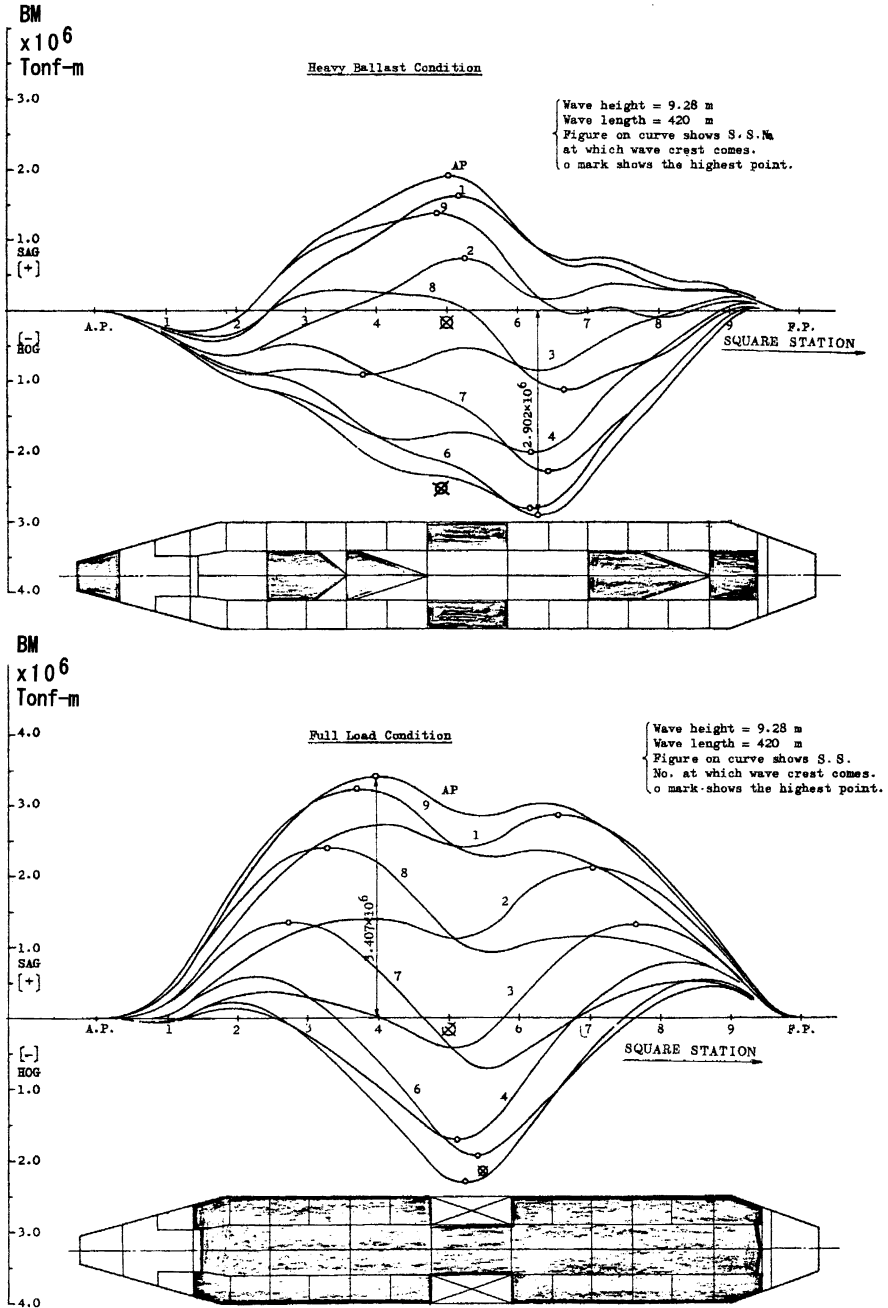


Fig. 2.2.1 Longitudinal bending moment in wave of which crest comes at each square station



In this ship the above maximum bending moments arise within  $0.4L$  of midship part, where the midship section modulus is kept constant and no problem is expected. However, it is recommended to check the longitudinal bending moment for cases where the crest or the hollow of the wave does not coincide with midship.

### 2.3 Calculation of Section Modulus of Hull Girder

One of the calculations of hull girder section modulus is shown in Fig. 2.3.1. In this figure, the required section modulus for deck and bottom are specified at first.

1) Required section modulus

$$Z_{DK} = 6,749,200 \text{ cm}^3$$

$$Z_{BM} = 6,749,200 \text{ cm}^3$$

2) Assumed neutral axis

$$Y'_{DK} = 9.8 \text{ m}$$

$$Y'_{BM} = 8.0 \text{ m}$$

3) Summation of scantlings

Item	B (m)	T (mm)	A =BxT (mxmm)	L (m)	M =AxL (m <sup>2</sup> xmm)	I =AxL <sup>2</sup> (m <sup>3</sup> xmm)	H (m)	Self I (m <sup>3</sup> xmm)
KLPLT1	1.095	13.0	14.235	-8.007	-113.97	912.5	0.00	0.00
BMPLT1	7.916	12.5	98.952	-7.796	-771.45	6014.4	0.42	1.45
BILGE1	4.712	12.5	58.905	-6.490	-382.28	2481.0	3.198	50.21
SSPLT1	5.38	12.5	67.25	-1.890	-127.10	240.2	5.380	162.21
:	:	:	:	:	:	:	:	:
DKLONG17F	0.141	9.0	1.267	9.730	12.33	120	0.141	0.00
DKLONG17W	0.09	9.19	0.827	9.655	7.990	77.1	0.00	0.00
Total			990.966		-492.4	41744.7		316.99

$$E = \sum M / \sum A - 0.497 \text{ (m)}$$

$$\sum (I + \text{self } I) = 42061.7$$

$$\sum A \times E^2 = -244.7$$

$$I^* = 41817.0$$

4) Distance from true neutral axis to top and bottom

$$Y_{DK} = 9.8 + 0.497 = 10.297 \text{ m}$$

$$Y_{BM} = 8.0 - 0.497 = 7.503 \text{ m}$$

5) Comparison with required section modulus

$$\text{For deck } 2I^*/Y_{DK} = 83634.0 / 10.297 * 1000 = 8122245.2 \text{ (cm}^3\text{)}$$

$$120.344(\%)$$

$$\text{For bottom } 2I^*/Y_{BM} = 83634.0 / 7.503 * 1000 = 11146591.2 \text{ (cm}^3\text{)}$$

$$165.154(\%)$$

Fig. 2.3.1 An example of section modulus calculation

The position of an initial neutral axis is assumed tentatively by putting the distance from the neutral axis to deck and to bottom as  $Y'_{DK}$  and  $Y'_{BM}$ , respectively. Then following the procedure already explained in Sect. 1.3.1(3) of Part II, the sectional moment of inertia can be obtained by summing up the sectional moment of inertia for each member. In the summary table,  $B$  is the breadth of a member,  $t$  is the thickness,  $L$  is the vertical distance between the assumed neutral axis and the center of gravity of the member and  $H$  is the height of projecting length of the member. The distance from the true neutral axis to top or bottom can be derived by modifying the position of the neutral axis. Eventually, the obtained section modulus of the hull girder is compared with the required one and judgment is carried out as to whether the actual section modulus satisfies the requirement.

## 2.4 Longitudinal Strength and Hull Steel Weight

In Fig. 2.4.1 the weight ratio of the longitudinal strength members relative to the total hull steel weight is shown. The ratio is about 70–80% even though the value fluctuates depending on the ship's size and the type of ship. And in Fig. 2.4.2 fluctuation in the weight of the longitudinal strength members for 1% change in the section modulus of the hull girder is shown. The absolute value of the increase or decrease of the weight of the longitudinal strength members for 1% change of the section modulus of the hull girder is considerable. Whereas the same 1% change of the section modulus of the hull girder will change the longitudinal bending stress by 1%, for example 200 MPa of the longitudinal bending stress comes to 202 or 198 MPa, which seems to be negligible.

To design a midship section which has exactly 100% of the required section modulus, adjusting the scantlings of many longitudinal members is a very important job at the initial design stage. The section modulus is obtained by dividing the moment of inertia by the distance from the neutral axis to the farthest member. It has been impossible to obtain exactly 100% of the required section modulus by adjusting the scantlings of a member in one action. Because the adjustment of the scantling of a member brings not only a change of moment of inertia but also a change of the position of the neutral axis. Thus it has to be done by a trial and error method. Practically it is done as follows:

The midship section modulus  $Z_0$  is calculated from the longitudinal strength members using scantlings which are decided from a local strength viewpoint. Expressing the required section modulus by  $Z_r$ , in the case where  $Z_0 \geq Z_r$  the scantling of these members can be applied as they are, but in the case where  $Z_0 < Z_r$  the scantling of some member should be increased so as to have the condition of  $Z_0 = Z_r$ . In this case to increase the upper deck plate thickness which lies farthest from the neutral axis is most simple and effective.

The above story can be understood easily but actually some difficulties exist. For example, if the calculation result shows that the deck plate thickness should

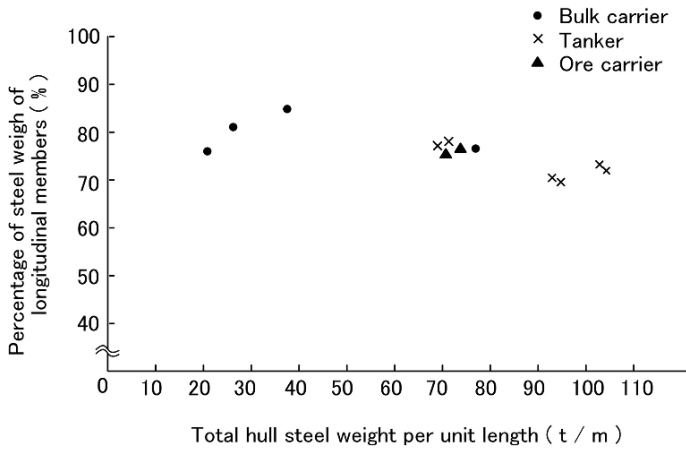


Fig. 2.4.1 Hull steel weight of longitudinal members

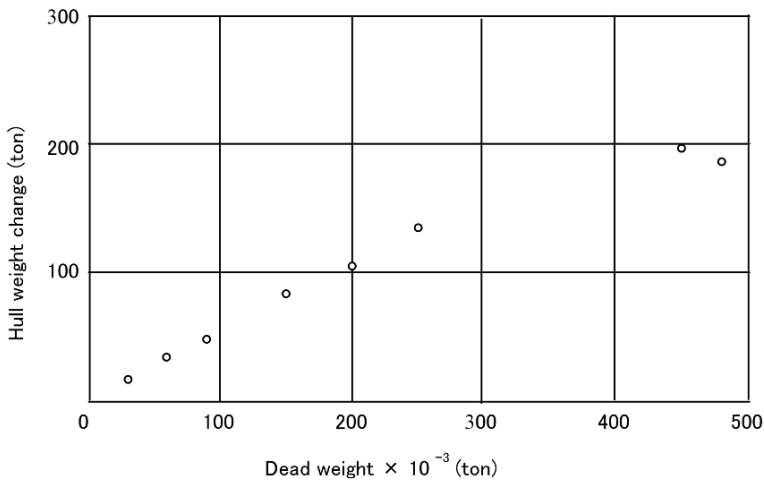


Fig. 2.4.2 Hull steel weight change due to 1% longitudinal I/y change

be 20.32 mm to have just the required section modulus, we can not have the plate of 20.32 mm. We can have 20 or 20.5 mm thickness plate actually. The former gives insufficient section modulus and the latter gives excess section modulus. In such a case the 20.5 mm thickness plate will be used, giving 0.18 mm in excess thickness.

One solution to this problem is to apply a wider longitudinal spacing keeping the thickness of the deck plate as 20.5 mm. By applying wider longitudinal spacing, the number of longitudinal stiffeners can be reduced, and accordingly the sectional

areas of the longitudinal stiffeners may be reduced. The thickness of the upper deck plate can be actually increased step by step by 0.5 mm, causing then the section modulus to also increase in a step function. By adjusting the number and the size of the deck longitudinal stiffeners, the effect of the step function may be relieved [2].

Another solution is to apply different thickness plates to the upper deck. In this case to apply a thicker plate to the center line strake keeping the same thickness for other plates, because the center line strake is further from the neutral axis than the other plates.

Comparing the above two solutions, the latter is more effective than the former from hull steel weight viewpoint and changing the spacing of the longitudinal stiffeners will cause many other modifications. However in the case where view point different thickness plates for deck plating can not be accepted from material handling, the former solution will be applied.

As shown in Fig. 2.4.2 a very small difference in the midship section modulus causes a big hull steel weight difference, and hence ship's cost difference. The section modulus should be just 100% (practically 99.95% is acceptable). A designer should take one of the above two ways with his own clear design philosophy.

## 2.5 Application of High Tensile Steel

Recently thanks to the development of steel mill technology TMCP (Thermo-Mechanical Controlled Process) high tensile steel with good weldability has been widely applied in hull structure. The usage percent of high tensile steel is now 70–80% of total hull steel weight. High tensile steel has been applied in hull structures in the following two cases:

- a. Cost reduction can be achieved.
- b. Instead of heavy mild steel thicker than previously 38 mm (1.5 in.), now 50 mm (2 in.) thanks to the improved material and welding technology.

The cost reduction is evaluated in the following way. Hereafter HT means high tensile steel and MS means mild steel. And each item is described as follows.

Total weight of HT applied	$W$	ton
Reduction in weight due to HT application	$\Delta W$	ton
Price of HT	$P_{HT}$	Yen/ton
Manufacturing cost of HT	$L_{HT}$	Yen/ton
Price of MS	$P_{MS}$	Yen/ton
Manufacturing cost of MS	$L_{MS}$	Yen/ton
Ship's price per dead weight	$P$	Yen/ton

Using the above symbols the following Eq. (2.5.1) means that the HT is more beneficial than MS.

$$W\{(P_{HT} + L_{HT}) - (P_{MS} + L_{MS})\} - \Delta W \cdot P_{MS} - \Delta W \cdot P < 0 \quad (2.5.1)$$

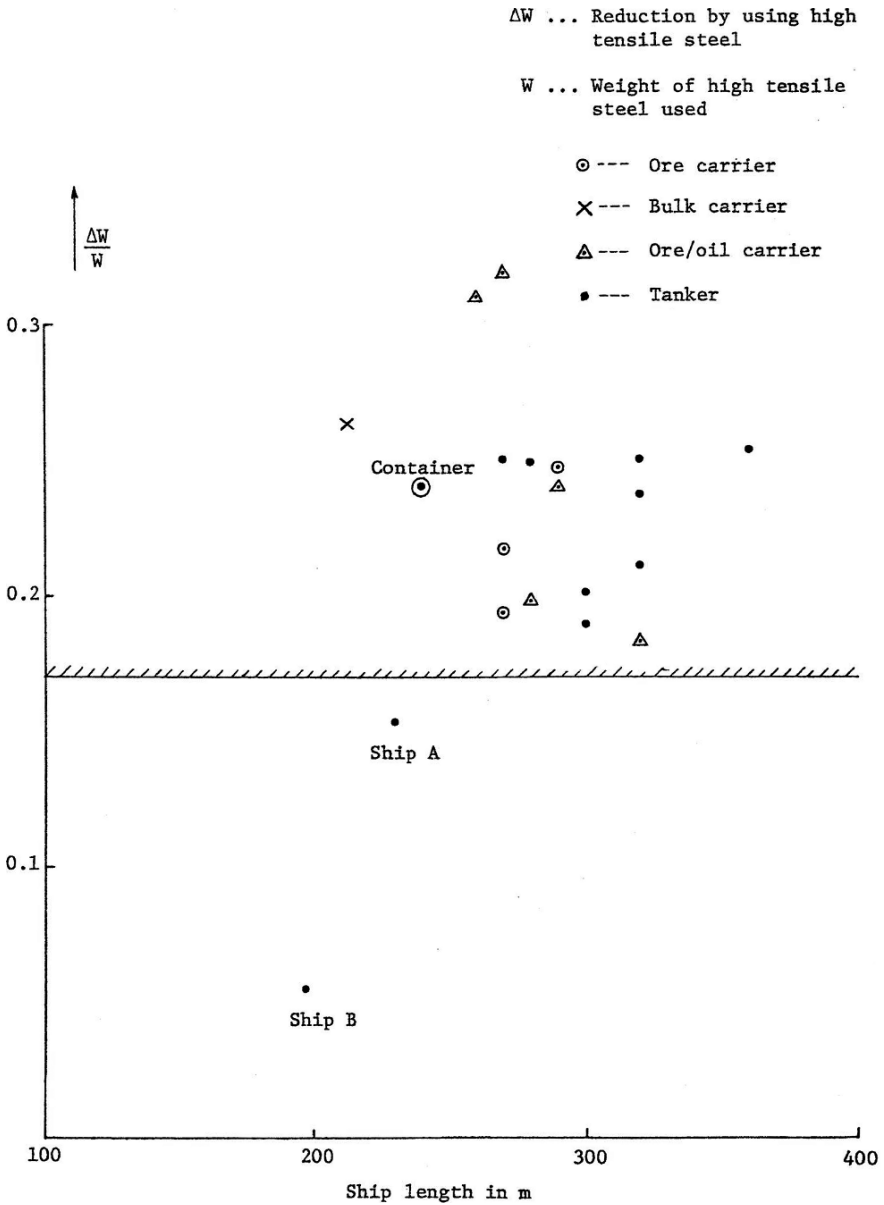


Fig. 2.5.1 Hull steel weight reduction due to use of high tensile steel

In the case of TMCP steel  $L_{HT}$  is nearly equal to  $L_{MS}$ , then (2.5.1) can be simplified as follows.

$$W(P_{HT} - P_{MS}) - \Delta W(P_{MS} + P) < 0 \quad (2.5.2)$$

$$\therefore \frac{\Delta W}{W} > \frac{P_{HT} - P_{MS}}{P_{MS} + P} \quad (2.5.3)$$

$\Delta W/W$  depends on the yield strength of high tensile steel, and also each ship has a different value. In Fig. 2.5.1 the actual examples of  $\Delta W/W$ , where 315 MPa high tensile steel is applied to highly stress parts of longitudinal strength members, are shown. In the case where the value of the right side of (2.5.3), which depends on the steel price and ship's price, is smaller than  $\Delta W/W$ , high tensile steel can be applied economically.

For Ship A and Ship B in Fig. 2.5.1,  $\Delta W/W$  is smaller than those of other ships, because these ships have greater depth than ordinary ships, and have excess section modulus for longitudinal strength with longitudinal members decided by local strength. In these ships the application of high tensile steel is not economical.

## 2.6 Longitudinal Strength Analysis in Waves

In addition to the static strength design method based on the longitudinal bending moment on the standard wave, the longitudinal strength analysis in waves, so called total system, is now available. In the total system the vertical bending moment, the horizontal bending moment and the torsion of a hull girder are analyzed simultaneously considering the ship motion in waves.

This total system of longitudinal strength analysis is to be applied in the design of new types of ships such as particular large ships, higher speed ships, and ships with abnormal principal dimensions.

In applying the new design method it is very important to decide the allowable stresses applying the new design method, subject to confirm its reliability by calculating again for many previous ships in service using new design method.

In the design of hull structures there are three important items, estimation of load, response calculation, and allowable limit, and the designer should keep in mind that these three items should be connected together. A change in load estimation must be followed by modified allowable limit which is to be decided based on the data of the ships in service with loads estimated by the new method. This is experimental technology and in this way the reliability of ships can be maintained.

Here, as an example, the above method, as applied to a 600,000 DWT tanker trial design, is explained. The "total system for hull girder longitudinal strength analysis by Nippon Kaiji Kyokai" [3] is applied in this analysis. The analysis was carried out by following Nippon Kaiji Kyokai's requirements previously, because the analyzed results are to be compared with the results for other ships analyzed by Nippon Kaiji Kyokai. It would be inappropriate to compare these with the results

obtained by different calculation conditions even with the same computer program. The calculation conditions are as follows.

- (1) ship speed 15.2 knots (normal speed)
- (2) encounter angle with wave 0, 45, 90, 135, 180 (in degree) where 0° is following wave
- (3) wave height wave length 2 m (double amplitude) with 0.1 intervals between 0.5 and 2.0 of  $\sqrt{L/\lambda}$  where  $L$  is ship length,  $\lambda$  is wave length

The response of the ship’s motion in regular waves for combinations of the above conditions was calculated.

The hull girder is divided equally into 20 portions and the variation in the load is calculated on each section. Analyzing the hull girder strength, the response function of stress variation at S.S.2(1/2), S.S.5 and S.S.7(1/2) is obtained. Then based on the wave frequency data in winter in the North Atlantic Ocean, the long term peak value is obtained for the probability of  $10^{-8}$ .

In Fig. 2.6.1 the expected values of loads acting on each section are shown. In the vertical axis, single amplitudes for each variation are shown. In Fig. 2.6.2 the stress variation in regular waves at the gunwale and bilge parts is shown. In the figure,  $\sigma_n$  is the total stress in the longitudinal direction which is the sum of axial stress  $\sigma_a$ , vertical bending stress  $\sigma_{bx}$ , horizontal bending stress  $\sigma_{by}$  and warping stress  $\sigma_w$ , with consideration of their phases. In the transverse section of the hull six points are selected as main points, they are; center of keel  $P_1$ , bottom of longitudinal bulkhead  $P_2$ , bilge part  $P_3$ , center of upper deck  $P_4$ , top of longitudinal bulkhead  $P_5$ , and gunwale part  $P_6$ . In Table 2.6.1 the maximum expected values of each stress component at the above six points are shown.

The analyzed results for a 600,000 DWT tanker obtained in this way are to be compared with the data of ships in service obtained in the same way, and the longitudinal strength of this ship can then be evaluated. In Table 2.6.2 the principal dimensions of the analyzed ships in service are shown.

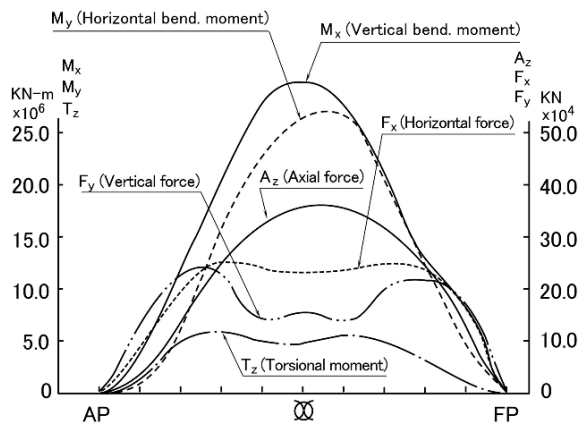


**Fig. 2.6.1** Max. moment and force distribution acting on hull girder

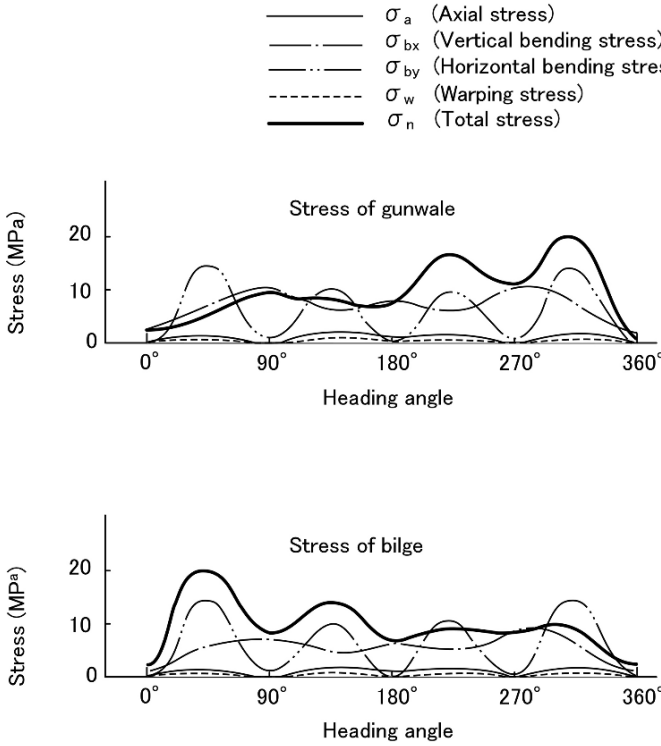


Fig. 2.6.2 Longitudinal stress component in regular wave

Table 2.6.1 Max. longitudinal stresses in waves of  $10^8$  cycles

Unit : kgf/mm<sup>2</sup>

POSITION		STRESS	Axial stress $\sigma_a$	Bending stress $\sigma_{bx}$	Horizontal bending stress $\sigma_{by}$	Warping stress $\sigma_w$	Total stress $\sigma_n$	Still water bending stress $\sigma_{bx(s)}$	$\sigma_n +  \sigma_{bx(s)} $
S.S. 2-4	P-1 Bottom $\sigma$		1.5	9.1	0.0	0.0	9.0	4.0	13.0
	P-2 Bottom OF L.BHD		1.5	9.1	2.4	0.3	9.9	4.0	13.9
	P-3 Bilge		1.5	7.6	4.4	0.4	9.7	3.3	13.0
	P-4 Gunwale		1.5	9.8	0.0	0.0	11.2	-4.3	15.5
	P-5 Top of L.BHD.		1.5	9.8	2.4	0.3	11.2	-4.3	15.5
	P-6 Upper Deck $\sigma$		1.5	9.3	5.0	0.4	11.4	-4.1	15.5
S.S. 5	P-1 Bottom $\sigma$		2.3	15.2	0.0	0.0	13.5	-1.2	14.7
	P-2 Bottom of L.BHD		2.3	15.2	7.1	0.3	15.1	-1.2	16.3
	P-3 Bilge		2.3	13.5	10.8	0.4	17.7	-1.1	18.8
	P-4 Gunwale		2.3	17.1	0.0	0.0	19.0	1.4	20.4
	P-5 Top of L.BHD.		2.3	17.0	7.1	0.3	19.5	1.4	20.9
	P-6 Upper Deck $\sigma$		2.3	16.3	10.8	0.4	22.3	1.3	23.6
S.S. 7-4	P-1 Bottom $\sigma$		1.9	9.3	0.0	0.0	8.1	3.8	11.9
	P-2 Bottom of L.BHD		1.9	9.3	3.4	0.2	9.2	3.8	13.0
	P-3 Bilge		1.9	8.3	7.0	0.3	12.5	3.4	15.9
	P-4 Gunwale		1.9	10.5	0.0	0.0	11.9	-4.3	16.2
	P-5 Top of L.BHD.		1.9	10.5	3.4	0.2	12.0	-4.3	16.3
	P-6 Upper Deck $\sigma$		1.9	10.0	7.0	0.3	12.8	-4.1	16.9

[Higher tensile steel is applied at deck and bottom]

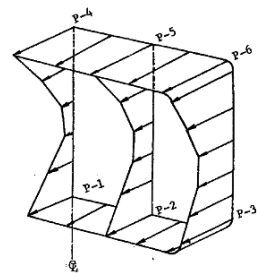




Table 2.6.2 Principal dimensions

Ship	L (m) x B (m) x D (m) x d (m)	(ton) DW	(ton) Δ	Cb	Vs (kt)	L/B	L/D	B/D	Longitudinal Bending Stresses in Shell Plating (Midship) (Kg/mm <sup>2</sup> )	
									Bm	Dk
A	205.06 x 30.50 x 15.80 x 12.237	50,831	62,747	0.797	16.5	6.72	12.98	1.93	3.4	-3.9
B	213.00 x 32.00 x 16.90 x 12.993	60,584	73,023	0.804	15.5	6.66	12.60	1.89	6.9	-7.9
C	230.00 x 35.30 x 18.00 x 12.487	70,871	85,919	0.814	15.3	6.52	12.78	1.96	1.6	-1.9
D	246.00 x 40.20 x 21.80 x 15.101	103,670	121,110	0.799	15.6	6.12	11.28	1.84	5.2	-5.9
E	260.00 x 43.50 x 22.80 x 17.032	138,539	160,771	0.815	15.4	5.98	11.40	1.91	0.8	-1.0
F	270.00 x 44.00 x 25.00 x 17.833	155,755	179,749	0.829	14.8	6.14	10.80	1.76	4.3	-5.1
G	281.00 x 46.20 x 25.00 x 17.034	157,825	183,138	0.840	16.1	6.08	11.24	1.85	-1.2	1.4
H	302.00 x 50.40 x 24.30 x 18.436	204,540	236,250	0.814	16.1	5.99	12.43	2.07	0.3	-0.3
I	326.00 x 49.80 x 23.20 x 17.685	209,413	241,881	4.830	16.5	6.55	14.05	2.15	5.3	-6.4
J	314.00 x 54.80 x 26.40 x 20.530	261,354	297,960	0.825	15.8	5.73	11.87	2.08	1.1	-1.3
K	330.00 x 54.50 x 35.00 x 27.074	372,698	425,674	0.853	15.0	6.06	9.43	1.56	3.9	-4.6
L	360.00 x 62.00 x 36.00 x 28.000	477,000	547,301	0.852	14.7	5.81	10.00	1.72	2.2	-2.5
U	420.00 x 74.00 x 38.30 x 30.000	683,000	793,980	0.836	15.2	5.68	10.98	1.93	-1.2	1.4

Principal Dimensions of Ships Analyzed

In Fig. 2.6.3 stresses at the above points  $P_1, P_3, P_4,$  and  $P_6$  in the midship section are compared with each other for the analyzed ships, and the following results are found.

1. Generally the axial stress  $\sigma_a$  is small but it increases slightly with an increase in the ship's size.
2. The vertical bending stress  $\sigma_{bx}$  is the biggest among these stresses. It seems not to depend on ship's size. Usually the stress at the upper deck center line is the biggest.
3. The horizontal bending stress  $\sigma_{by}$  increases with an increase in ship's size. It may depend on  $B/D$  of the ship.
4. The warping stress  $\sigma_w$  is very small for tanker which has a closed section. That will cause no problem at all.
5. The total stress in the longitudinal direction  $\sigma_n$  is high at the gunwale and bilge parts where high vertical and horizontal bending stresses exist, and it increases with an increase of ship's size. The maximum value at the gunwale part is  $18 \text{ kgf/mm}^2$ .

The stress distribution at S.S.2(1/2) and S.S.7(1/2) is similar to that at the midship section shown in Fig. 2.6.3 but the stress level is considerably lower.

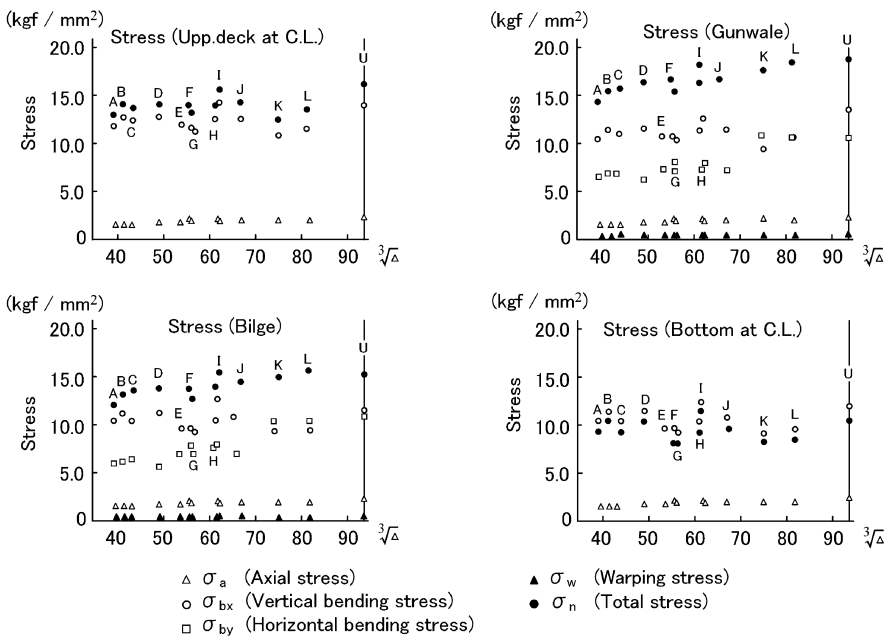


Fig. 2.6.3 Max. longitudinal bending stress occurring at midship section

## 2.7 Arrangement of Longitudinal Strength Members

At the beginning of Chap. 2, it is explained that almost all of the damage caused by the lack of longitudinal strength happen on older ships, and this can be avoided by anti-corrosion methods, selection of materials, and good welding. However this damage can happen even on not so old ships.

The over-sizing of ships during the period 1960–1980 was achieved by means of three important technical innovations; rationalization of longitudinal strength, wider spacing of frames and transverses, and increased tank length. The first of these was achieved by huge and energy requiring research on the generation of sea waves and ship motion in waves. By this research the hull girder bending moment could be estimated more accurately than the traditional calculation using  $L/20$  wave height. As shown in Fig. 1.5.1 in Part I the required section modulus has decreased since 1950 down to 75% of the maximum [4].

The longitudinal strength is designed rationally, but actually the reduced section modulus is applied which means that higher longitudinal bending stress is generated than before. In addition to the above, by applying high tensile steel it is considered that practically little reserve remains in hull girder longitudinal strength. This is proved by the crack on the deck girder of a container ship shown in Fig. 2.7.1.

Before adoption of computerized method for longitudinal strength, actually it had the biggest reserve among all the hull structure members because it is most important. As explained in Sect. 2.4 small differences in longitudinal strength greatly affect the hull steel weight and hence ship's cost. Therefore every effort to reduce the scantling of the longitudinal members was done with reasonable excuse. Examples are shown in Fig. 2.7.2, one is a trunk section, and the other is a large camber section. In the calculation of the section modulus of the midship section, the sectional moment of inertia which includes all longitudinal members is divided by the distance from the neutral axis to the upper deck at the side. In this method it is beneficial to arrange longitudinal members as far from the neutral axis as possible.

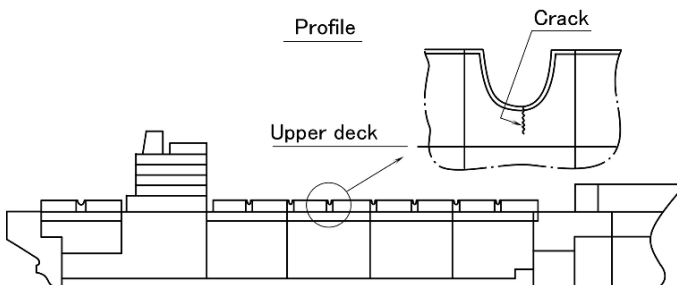
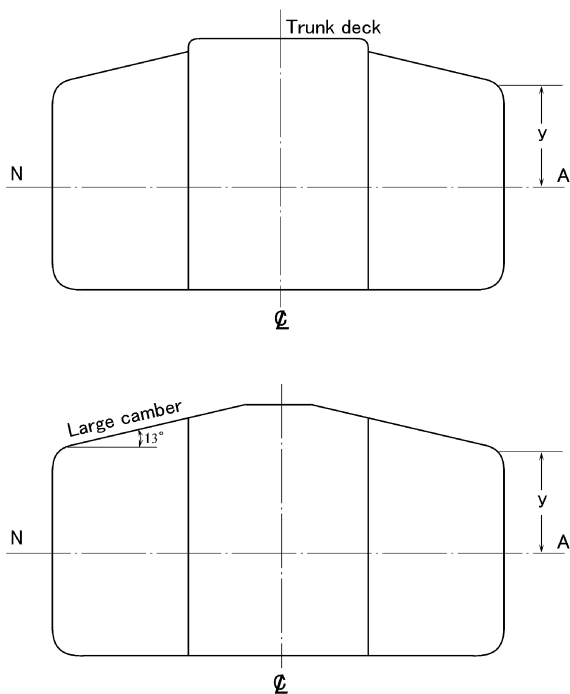


Fig. 2.7.1 Cracking of hatch side coaming of container vessel

**Fig. 2.7.2** Midship section of trunk deck type and large camber type



In the case where the section modulus is calculated by dividing the sectional moment of inertia by the distance from the neutral axis to the farthest members, continuous members above upper deck, such as continuous hatch side coamings and bulwarks are effective in contributing to longitudinal strength as well as in saving hull steel. An example is reported in which a continuous heavy bulwark reduced the longitudinal bending stress by 7–11% [5].

In the case of ordinary camber, the center line strake lies farther than other strakes from the neutral axis, and a thicker center line strake is preferable to keep the thickness of other strakes to a minimum.

It is current practice not to apply any reinforcement around the upper deck openings provided the shape of the opening is ellipse with the longer axis in the longitudinal direction, more than twice the length of the shorter axis, and the length of shorter axis should not so big. However if reinforcement is necessary around the upper deck opening, keeping the strake which has the opening as thin as possible, and increasing the thickness of the center line strake is preferable.

In general, by adding some sectional area to the midship section, the section modulus of the midship section can be increased but with some exceptions which are explained as follows.

By putting sectional area  $A_2$  at “a” distance from the neutral axis, the increment of the section modulus  $\Delta Z$  can be expressed by Eq. (2.7.1) as follows.

$$\Delta Z = \frac{A_2 a (A_1 a - Z_1) + (A_1 + A_2) I_2}{(A_1 + A_2) y_1 + A_2 a} \quad (2.7.1)$$

where  $I_2$  is the sectional moment of inertia of  $A_2$  around its neutral axis which is negligibly small. Accordingly putting  $A_2$  in the vicinity of  $(A_1 a - Z_1) < 0$ , namely  $a < Z_1/A_1$ , causes  $(-\Delta Z)$  which means that the added material causes a reduction of the section modulus. On the contrary by reducing material in the vicinity of  $a < Z_1/A_1$ , an increase in the section modulus can be obtained. The above phenomena can be explained by the fact that putting material in that region brings bigger neutral axis movement than the increase in the sectional moment of inertia.

In an actual design the above phenomena can be put into effect by reducing the total sectional area of the plate and longitudinal stiffener below the neutral axis with narrower longitudinal stiffener spacing.

## 2.8 Stress Concentration on Longitudinal Strength Members

The crack shown in Fig. 2.7.1 is caused by cyclic high stress at a region of stress concentration. Although there are many discontinuous points in the hull structure and stress concentrations can not be avoided, effort should be made to avoid high stress concentration.

The actual stress caused by the stress concentration is described by the following Eq. (2.8.1) [6].

$$S_a = f(S_n, K_d, K_w) \quad (2.8.1)$$

where

- $S_a$  : actual stress
- $S_n$  : nominal stress due to scantling of member
- $K_d$  : stress concentration factor for member's shape
- $K_w$  : stress concentration factor for workmanship such as shape of weld bead, welding defects, misalignment of members, etc.

To avoid cracks it is important to have low  $S_a$  which can be obtained by reducing  $S_n$ ,  $K_d$  and  $K_w$ .

To reduce the nominal stress  $S_n$ , increasing the scantlings of the members is necessary. For a given tension or bending moment, a bigger sectional area or section modulus can result in a smaller nominal stress  $S_n$ . However, an increase in the scantlings means an increase in hull steel weight.

The stress concentration factor for workmanship  $K_w$  depends on the fabrication process and the welding techniques which are peculiar to the shipyard. The stress concentration factor for a member's shape  $K_d$  can be reduced by improving the member's shape without increasing the hull steel weight. For the improvement of the member's shape, the photo-elasticity technique has been applied, and nowadays the FEM calculation is applied effectively.

Equation (2.8.1) indicates how important the design of the shapes of the structural members is in the detail design of the hull structure.

To avoid the crack shown in Fig. 2.7.1, an investigation of the shape of the deck girder in the vicinity of the hatch end coamings was carried out [7]. In this girder cut outs are necessary to pass pipes and to provide a passage. Accordingly a continuous structure is not available. For several shapes of the cut-out, the stress concentration factor is calculated, then the best one was selected.

In Fig. 2.8.1 the FEM models and results are shown. The type “O” is the original shape which suffered from a crack. The types “A” and “D” have the same sill height as the type “O”, and the types “B” and “E” have smaller sill heights than the type “O”. The type “C” has highest sill height.

The calculations show the following facts.

1. Type “E” has a higher stress concentration because of smaller sill height.
2. Type “B” which has a smaller sill height than type “E” has a slight improvement because of smaller curvature.
3. Type “A” which has the original sill height and smaller curvature has stress concentration factor 7.5% less than the original type “O”.
4. Type “C” shows a 15% improvement thanks to the higher sill height and smaller curvature.

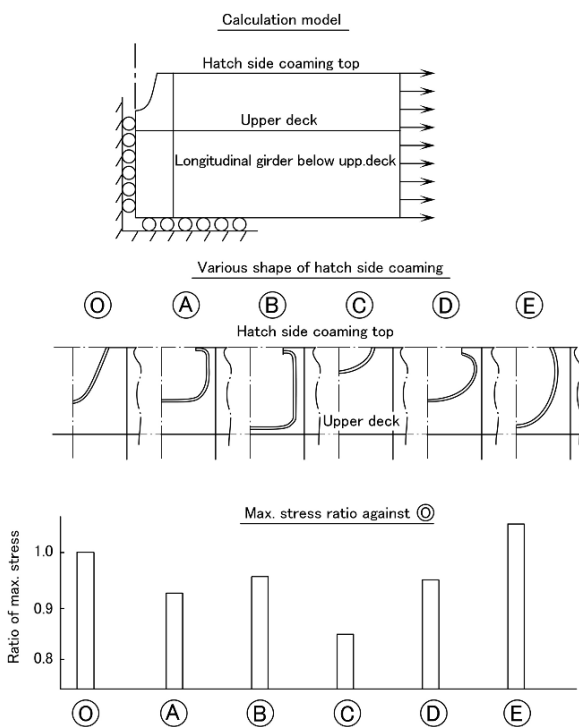


**Fig. 2.8.1** Stress concentration due to hatch side coaming

The above investigation shows that a higher sill height and smaller curvature are effective in reducing the stress concentration in this case.

The crack shown in Fig. 2.7.1 happened only on the deck girder between three rows of hatches and not on the side coaming above the longitudinal bulkhead which has the same cut out as on the deck girder between the three rows of hatches. From this fact it can be said that the reduction of a girder's sectional area due to a cu-out can be a cause of cracking and the deck girders between the three rows of hatches support the longitudinal hull girder strength.

## 2.9 Additional Bending of Local Members Due to Hull Girder Bending

When deep girders and small longitudinal beams are longitudinally connected, an additional bending moment is exerted at the connection. Figure 2.9.1 shows an example of such an arrangement, where a crack was found at the toe end of a bracket at the end of a partial deck girder under a crane post in a single hull tanker.

This structure consists of deck longitudinal beams, additional girders, and brackets. An additional girder is provided against the load of the on-deck crane. In this case, it is usual to arrange the brackets at both ends of additional girder to avoid an abrupt change of rigidity. However, the crack was found at the toe end of these brackets.

The mechanism of this failure was studied and a new structural arrangement was proposed [8]. We assumed that this crack was caused by the longitudinal bending moment of the hull girder, and we carried out a comparison of the original structure and the modified structure using finite element analysis. The original structure, which has brackets, is shown in Fig. 2.9.1, and the modified structure, which has no brackets, is shown in Fig. 2.9.2. The axial force to induce a nominal stress of  $98 \text{ N/mm}^2$  is loaded. The results of this analysis are shown in Figs. 2.9.3 and 2.9.4, respectively.

From the observation of Fig. 2.9.3, it is found that:

1. The deck longitudinal is forced to deflect downward by 2.7 mm at the toe end of the bracket, due to rotation of the bracket caused by a shift in the position of the neutral axis between the deck longitudinal and the partial deck girder.

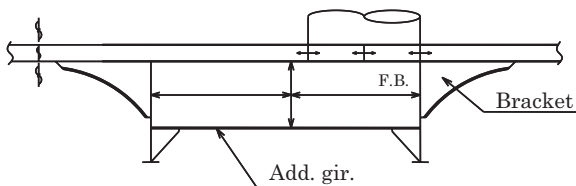


Fig. 2.9.1 Partial deck girder (with brackets)

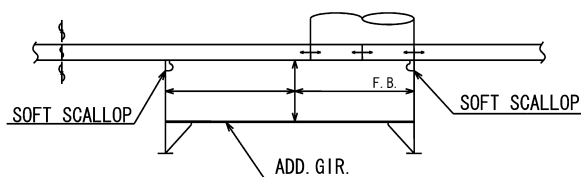


Fig. 2.9.2 Partial deck girder (without brackets)

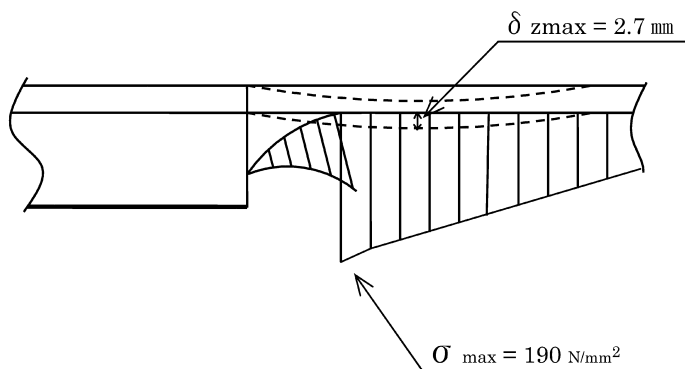


Fig. 2.9.3 Stress distribution of longitudinal with brackets

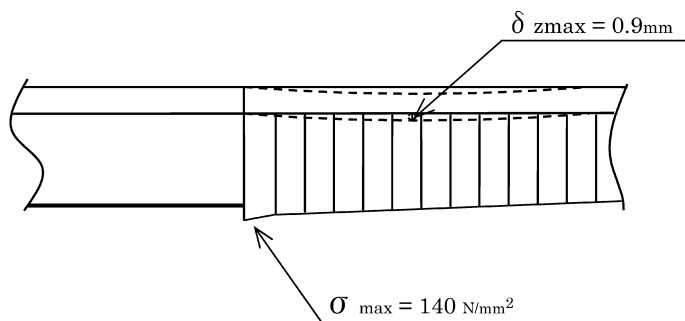


Fig. 2.9.4 Stress distribution of longitudinal without brackets

2. The maximum boundary stress on the face plate of the deck longitudinal is  $190 \text{ N/mm}^2$ , and the stress magnitude varies gradually along the length of the deck longitudinal. This fact indicates that the stress concentration at the toe end of the bracket is not big thanks to the very soft shape of the bracket, but that the large stress is mainly caused by the additional bending moment exerted on the deck longitudinal due to the rotation of the bracket.

Based on this study, it was concluded that the cause of the damage was the additional bending moment exerted on the deck longitudinal due to the rotation of the bracket caused by the change in the position of the neutral axis between the deck longitudinal and the partial deck girder. Modification of the bracket to a softer



shape cannot reduce the stress much, because the stress concentration at the toe end is already sufficiently small, as described above. To avoid the excessive additional bending stress by the rotation of the bracket, the following two countermeasures are considered to be effective:

1. Decrease the additional bending moment acting on the longitudinal beam, by adding slightly less-deep girders at the fore and aft locations of the existing deep girder
2. To create a structural arrangement to make the additional bending moment not to flow into the deck longitudinal

The former countermeasure should actually work, but this solution requires much cost and weight. Then we studied the latter one and reached the bracket-less arrangement. From Fig. 2.9.4, we can observe that:

1. By dispensing with the brackets, the downward deflection of the deck longitudinal was much improved (from 2.7 to 0.9 mm).
2. Maximum stress on the face plate of the deck longitudinal was reduced to  $140 \text{ N/mm}^2$ . A local stress concentration is also avoided by making the corner scallop of the partial deck girder softly rounded.

From this study, we can conclude that by dispensing with the brackets, the part of the downward force on the deck longitudinal due to the additional bending moment was moved to the position of the transverse web, thus additional bending stress was considerably reduced because the acting point of the force is the same as the supported point.

This structural arrangement seems very strange at the beginning because common sense of structural designers is that an abrupt change of rigidity is to be avoided as far as practicable. Honestly speaking, some Classification Society's surveyors and ship owners commented about this bracket-less structure to add a bracket. However, by investigation about the stress flow, we can find some cases where adding reinforcing members sometimes deteriorates strength.

## 2.10 Longitudinal Bending Stress in Fore & Aft Parts of Ship

In designing longitudinal strength members, firstly the scantlings of the members at midship, which are to be maintained in the vicinity of  $0.4L$  midship, are decided so as to maintain the necessary section modulus and resist the midship bending moment, then the midship scantlings are tapered down to the scantlings at  $0.1L$  from the ship's ends.

The above practice has been applied for a long time without any trouble. However the situation changed with the appearance of high speed ships and energy saving ships which have different hull forms from traditional ships. Damage was caused by the bending moment outside of the midship part. An example is that of a 10,000 DWT high speed cargo ship bent convex upwards at  $(1/4)L$  from F.P. She

suffered damage off South Africa in heavy weather. The damage looked like a folding jack knife and people called it “jack knife damage”. This kind of damage has put into question the above traditional design practice, that is, the midship scantlings are to be tapered down to the scantlings at  $0.1L$  ship’s ends; this practice has been revised so as to keep the necessary section modulus at each section [9].

Actually a high speed container ship has a very fine bow form (refer Fig. 5.3.1 in Part I), and it is necessary for the fore part of the  $0.4L$  midship to have thicker plate than the midship part in order to have enough section modulus. In the case of a high speed ship with large bow flare, the slamming impact causes a big bending moment at the forward part in the sagging condition, which was proved by recent research using the strip method with consideration of elastic deformation of the hull structure [10].

The stern shape of the energy saving ships recently designed is quite different from the traditional ship. As shown in Fig. 5.3.1 in Part I the so called “open bulbous stern” is so fine that the boss part has little connection to the main hull. In such a stern form, to keep the necessary section modulus requires heavy shell plates to be applied.

In a container ship, the semi-aft engine room arrangement used to be applied with many containers loaded on the upper deck aft of the engine room which caused a big hogging moment to occur in the vicinity of the open bulbous stern part. Attention should be paid to the buckling strength of the bottom shell plate in this area.

## 2.11 Hull Steel Weight Reduce to Ultimate Strength

In Fig. 2.4.1 it is indicated that the weight of the longitudinal strength members is about 70–80% of the total hull steel weight. On the other hand recent research proves that the ultimate strength of existing hull girders is about 70% of the total plastic moment [11]. In other words an existing hull girder collapses by buckling before a plastic hinge appears at the section where the maximum bending moment happens.

From the above, it can be said that the non-buckling design with existing scantling will bring better ultimate strength by 43% ( $100/70 = 1.43$ ), which means a 30% area reduction of the longitudinal members while keeping existing strength. Then the total hull steel weight can be reduced by 21–24% ( $0.7 \times 0.3 = 0.21$ ,  $0.8 \times 0.3 = 0.24$ ).

# Chapter 3

## Transverse Strength of Ship

The longitudinal strength of a hull girder explained in Chap. 2 is the most important aspect of the ship strength, and its deficiency may cause the total loss of the ship. Accordingly it has been designed so carefully that very little trouble has been reported. In the design of the longitudinal strength, the hull structure can be simply assumed to be a hull girder, and a sophisticated total system of the longitudinal strength calculation was developed. And now reliable design methods for the longitudinal strength are available.

On the other hand the transverse strength of a ship is also important. Deficiency in the transverse strength will cause fatal damage as shown in Fig. 3.1. Both cases shown are damage to a tanker. One is an indent of a side shell caused by the buckling of a cross tie, and the other is bulging of the side shell construction caused by the loss of the connection between the shell plate and the transverse ring. Even in cases of big deformation, no crack in the shell plate was detected, except a small crack of a so called “flying bird” happened in the latter case.

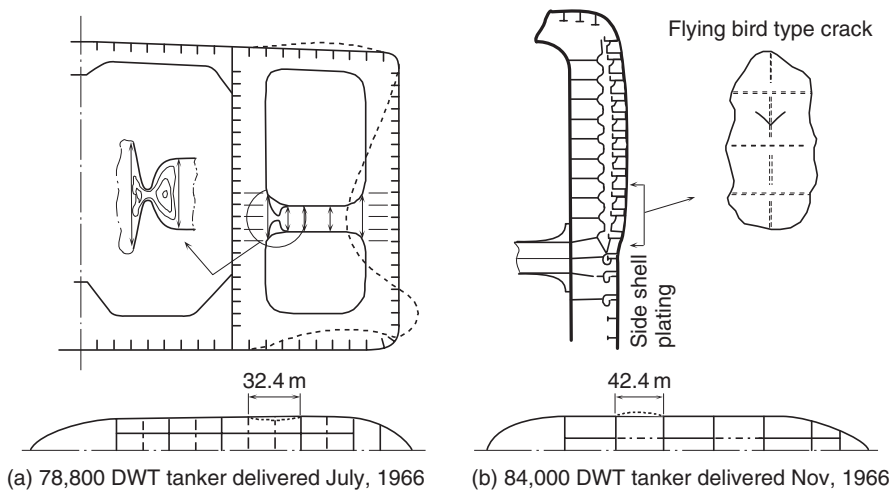


**Fig. 3.1** Examples of failure due to lack of transverse strength

The transverse strength members are statically indeterminate, being connected and affecting each other, therefore it is not easy like in the case of the longitudinal strength members to find the response to the applied load. This is a reason why a total system for transverse strength has not been developed yet.

The design of the hull structure arrangement explained in Chap. 1 very much affects the transverse strength. The shear deformation of a wing tank structure of a tanker causes secondary stress due to forced displacement on the structural members inside. The design criteria for the hull structure arrangement stated in Chap. 1 is to avoid an excess secondary stress on the transverse strength members.

In this chapter the allowable stress in the transverse members and some other considerations regarding in their design will be explained.

### 3.1 Allowable Stress for Transverse Strength

The allowable stress for transverse strength is given by each classification society together with a stress calculation method. As explained in Sect. 2.6 the load estimation, the response calculation, and the allowable limit are always to be connected together. For example an allowable stress of a classification society can be applied only on the response calculated by the method specified by the classification society [12].

In hereunder the following example of load estimation, the response calculation and the allowable limit is introduced which was established in the 1970's by the authors when the increase in ship-size was so fast that the classification society's rules were not so effective.

The load is divided into two kinds, the long term and the short term. The former is for full loaded and ballast conditions in still water, and the latter is full loaded and ballast conditions in waves and the tank test condition.

The response is calculated by means of a three dimensional frame model and a two dimensional FEM model. The mesh division is shown in Fig. 3.1.1(b) which is better for the determination of the stress distribution along the face plate than that in Fig. 3.1.1(a). Firstly the cargo tank part of the tanker is modeled into a three dimensional frame work and the shear deformation of the wing tanks is calculated with a draft corresponding to the trough of the wave. The model is supported at both ends of the side shell plates and longitudinal bulkheads. The wave height is that given by Nippon Kaiji Kyokai. Secondly a two dimensional FEM calculation is carried out at the transverse ring where the shear deformation of the wing tank is a maximum with the draft at that transverse ring position.

The six tankers shown in Table 3.1.1 are analyzed by the above method. These have a transverse main and no center girder construction system. Referring to the analyzed data, the allowable stress is decided as shown in Table 3.1.2 for each part shown in Fig. 3.1.2. The allowable stress is the maximum value analyzed on a ship in service without any structural trouble.

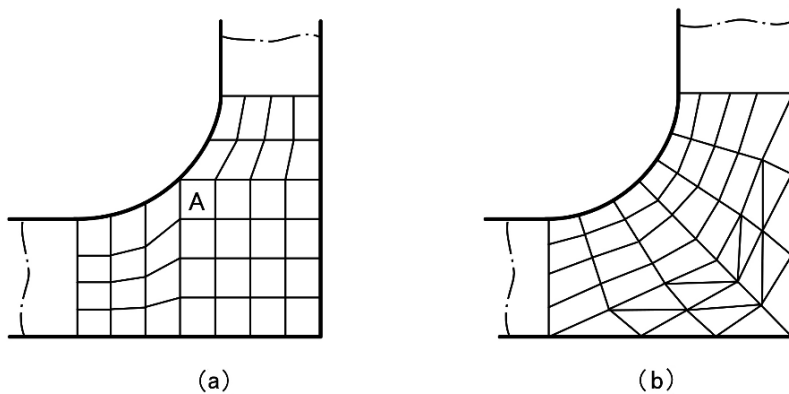


Fig. 3.1.1 Examples of FEM mesh subdivision

Table 3.1.1 Existing vessels analyzed for transverse strength

Vessel	Deadweight (t)	Principal dimensions (m)				Delivered year
		L	B	D	d	
A	80,352	230	33.0	21.7	15.0	1965
B	150,000	290	47.5	24.0	16.0	1966
C	372,400	330	54.5	35.0	27.0	1971
D	210,000	300	50.0	25.5	19.0	1971
E	251,978	320	54.5	26.0	19.1	1971
F	477,000	360	62.0	36.0	28.0	1973

High stress zones as shown in Table 3.1.2 are to be designed carefully, because there are high or low stress concentrations in this zone. In Fig. 3.1.3 examples of cracks are also shown.

In Table 3.1.2 the allowable stress in the vicinity of the parallel part is lower than that of the corner part which seems unreasonable because the parallel part has no discontinuity, no stress concentration, and no reduction of effective breadth of the

Table 3.1.2 Allowable stress of transverse ring

		Unit in MPa			
		Long term	Short term	Location indicated by F	
Web (combined stress)	High stress part	186	225	C, F, G, H, I, L, M, N, O	
	Corner part	147	186	① ~ ⑩, A, B, D, E, J, K, P	
	Uniform part	118	147	1 ~ 12	
Face (normal stress)	High stress part	186	225	A, B, C	
	Corner part	127	157	D, E, F, G, H, I, J, K, L, M, N	
	Uniform part	118	137	1 ~ 12	

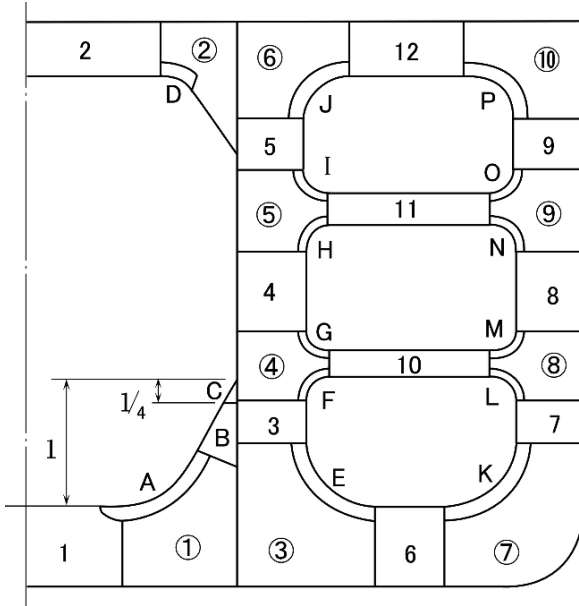


Fig. 3.1.2 Category of transverse strength member due to location

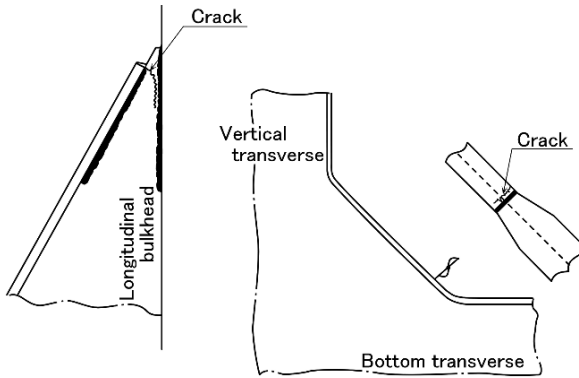


Fig. 3.1.3 Examples of crack in high stressed part

face plate. This is caused by the analytical method, namely the allowable stress was based on the data of previous ships in service and not theoretically. Theoretically the allowable stress in the vicinity of the parallel part can be higher than the corner part. In this matter, however, one important point should be kept in mind; the high stress in the vicinity of the parallel part of a transverse ring will cause a big deflection which causes additional stress in the secondary members supported by the transverse ring. The maximum deflection in this analysis occurred on the longitudinal bulkhead during tank testing with a fully loaded center tank and its value

was about  $1/1500$  of the ship's depth. A deflection bigger than this value may cause problems for the secondary supporting members.

### 3.2 Long Taper & Snake Head

In Sect. 3.1 it is mentioned that the allowable stress at the bracket toe of the bottom transverse is 225 MPa as a high stress zone, and a low stress concentration shape is necessary. For this purpose a long taper and "snake head" are proposed [7].

In Fig. 3.2.1 a bottom transverse in the center tank of a tanker is shown. The bottom transverse has brackets at both ends where high shear stress and a large bending moment occur. In the face plate which lies farthest from the neutral axis high bending stress is generated. The face plate has a taper at its end at usually  $15^\circ$  on one side to allow for smooth stress flow at the end of the bracket. On this point an idea came to the mind of one of the authors, that is, a taper with a smaller angle than  $15^\circ$  will have a more smooth stress flow, and it will require less material also.

In Fig. 3.2.1 a comparison is made of the stress distribution in the case of an ordinary taper and a long taper. The stress is calculated with the condition that both ends of the bottom transverse are fixed and have uniform bottom pressure. The difference between the ordinary taper and the long taper is not so big, except at the bracket toe where the long taper shows about half the stress of the ordinary taper.

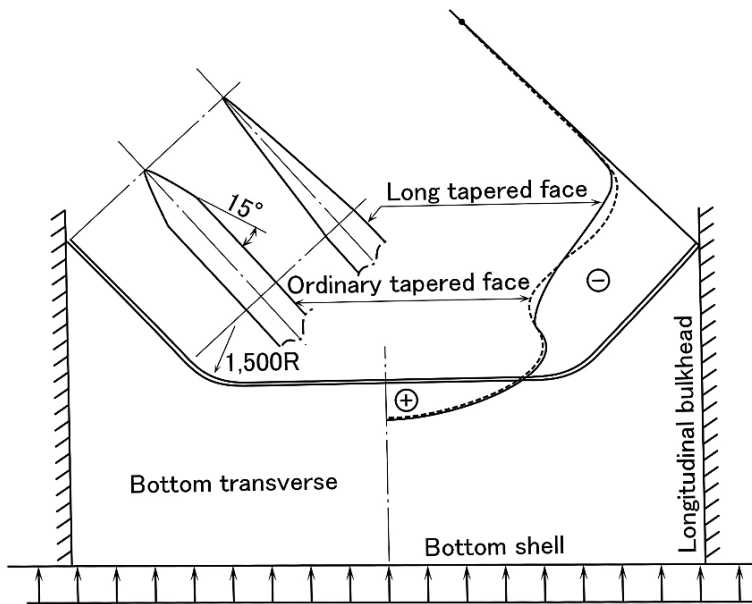


Fig. 3.2.1 Long tapered face plate of bottom transverse

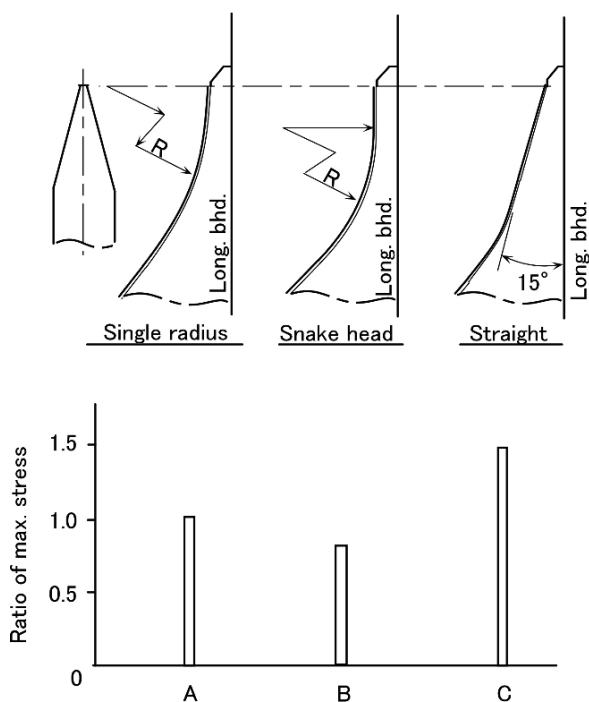


Fig. 3.2.2 Max. stress ratio against shape of bracket toe

The weight saving by the long taper is estimated to be about 4 tons in the case of a 480,000 DWT tanker which has  $500 \times 35$  mm face plates.

Even with the long tapered face plate, a high stress remains at the end of the bracket. To reduce this high stress a snake head bracket toe has been found effective; this was proposed and named by Dr. Ken-ichi Hattori. As shown in Fig. 3.2.2 the stress at the “snake head” is about 80% that of a circular bracket end, which used to be adopted.

By combining a long taper and a snake head, the crack as shown in Fig. 3.1.3 can be avoided with an allowable stress of 186 MPa for long term loads and 225 MPa for short term load.

### 3.3 Shape of Bottom Transverse in Center Tank

In Sect. 3.2 a long taper and snake head is discussed, keeping the section of the bottom transverse uniform except for the bracket part. In this section the stress distribution in the face plate of a bottom transverse with a non-uniform section is explained [13].



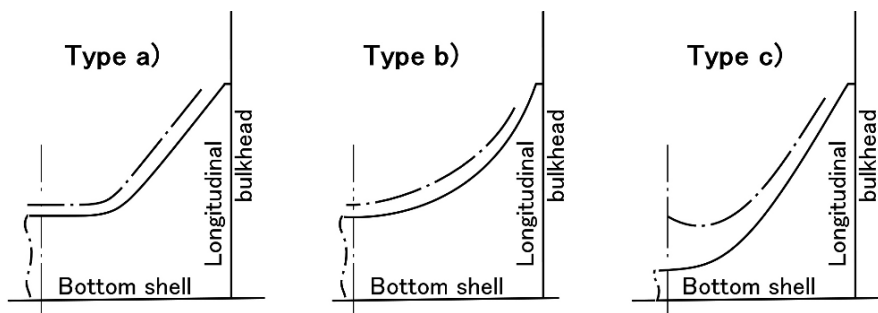


Fig. 3.3.1 Face plate stress due to shape of bottom transverse in center tank

As shown in Fig. 3.3.1 three shapes were investigated (a) an ordinary shape (b) a large circle in way of bracket and (c) no uniform section with small depth at the center line. Type (c) is reasonable from a shearing force viewpoint which is zero at the center line and beneficial in the arrangement of low cargo pipes on the bottom transverse. The stress distribution in the face plate at a light draft condition with a fully loaded center tank is shown also in Fig. 3.3.1 from which it can be said that the stress distribution is quite similar for these three types except at the center line of Type (c).

### 3.4 Shape of Bottom Transverse in Wing Tank

At the connecting bracket of a bottom transverse in a wing tank and the vertical web on a longitudinal bulkhead, high bending stress in the face plate is often generated and cracks occur as shown in Fig. 3.1.3. The stress distribution was investigated for four types of bracket as shown in Fig. 3.4.1. Type (a) and (c) are circular types and Type (c) has a larger radius, and Type (b) and (d) are combination of circles and straight line, which are called “tray type”, and Type (d) has a larger area [13].

The calculated stress distribution in each face plate is shown in Fig. 3.4.1. It is natural that the stress will be lower in the case of a larger radius of the circular

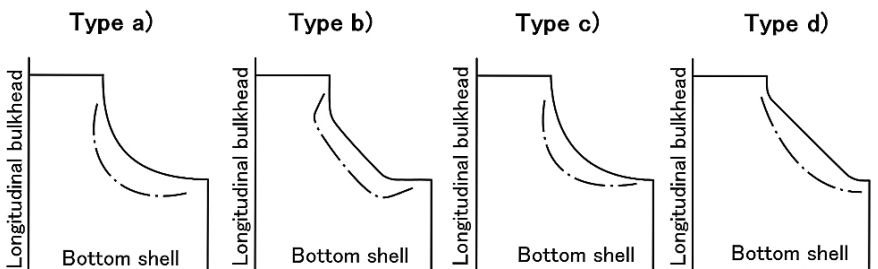


Fig. 3.4.1 Face plate stress due to shape of bottom transverse corner in wing tank

face plate than that in the case of a smaller radius. Additionally the tray type is better than the circular type.

The hull structure detail designer should keep in mind how important shape is.

“Good appearance has good performance.” and “good appearance conceals seven deficiencies.” are old Japanese proverbs.

## 3.5 Transverse Strength of Tanker

The transverse strength of a tanker is maintained by the transverse bulkheads and transverse rings. As explained in Chap. 1 “Design of Hull Structure Arrangement”, the transverse bulkheads form a grillage structure with the longitudinal bulkheads and side shells, and form the basic strength of a ship. The transverse rings are supported by the grillage structure and prevent out-of-plane deflection of the grillage.

Hereunder the design of a transverse ring is explained.

### 3.5.1 Cross Ties

At the beginning of the design of a transverse ring, the number of cross ties is to be decided, one cross tie, two cross ties, three cross ties or no cross ties. In the 1960's when a rapid increase in tanker size occurred, it was the common sense that the more cross ties the more safety, and the three cross ties arrangement was applied. The background of this common sense is that in the case of three cross ties, after one cross tie is broken, there remains still two cross ties which will maintain the transverse strength. However this is not correct because the remaining ties cannot support the load which was taken by the three cross ties.

Then the two cross ties arrangement for big tankers and the one cross tie for small ships have been common practice. A 380,000 DWT tanker built in 1971 and a 480,000 DWT tanker in Fig. 3.5.1 built in 1973 have two cross ties. And a 78,800 DWT tanker built in 1966 has one cross tie as shown in Fig. 3.1.

The K type cross tie as shown in Fig. 3.5.2 was proposed and some European shipyards adopted it, but not the Japanese shipyards because of difficulty of erection work. From the strength and stiffness viewpoints, K type cross tie is effective in the avoidance of shear deformation of the wing tank and also in increasing the strength of the vertical webs on the side shell and longitudinal bulkhead.

From the steel weight viewpoint there is little difference between one cross tie and two cross ties. One cross tie for a big ship means a longer unsupported span of vertical webs on the side shell and longitudinal bulkhead. This is a reason why the two cross tie arrangement is applied in big ships. No cross tie with deep bottom transverse is another arrangement, but it is inferior in term of steel weight. The idea to connect the vertical webs on the side shell and longitudinal bulkhead is effective in increasing the strength and stiffness of these members.

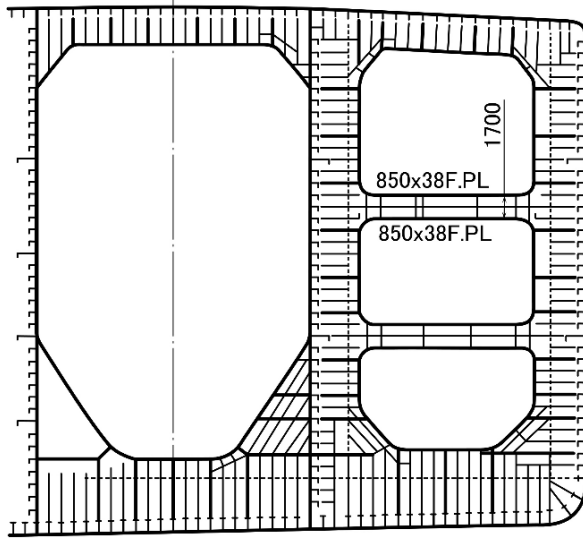
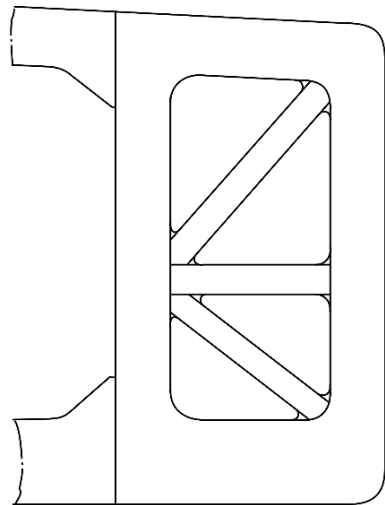


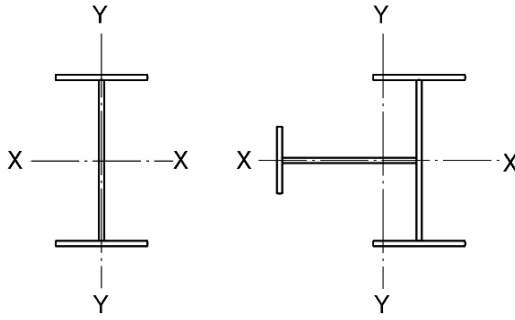
Fig. 3.5.1 Midship section of 480,000 DWT tanker

Fig. 3.5.2 Wing tank with K type of cross tie



The cross tie supports tension and compression as a pillar, and in addition to this it supports bending moments as a member of the transverse ring. The section of a cross tie has been “I” or “J” shape, but these shapes have unbalanced sectional moment of inertia around the x-axis and y-axis which is not suitable as pillars. Recently a well balanced section shown in Fig. 3.5.3(b) has been applied.

In the case of an “I” section, the sectional moment of inertia around the y-axis seems far less than that around the x-axis, accordingly the buckling strength around the y-axis is supposed to be far less than that around the x-axis. To confirm



(a) I type section

(b) Well balanced section

Fig. 3.5.3 Sectional shape of cross tie

this, the actual buckling strength of the upper cross tie shown in Fig. 3.5.1 for a 480,000 DWT tanker was calculated. The sectional moment of inertia around the x-axis  $I_x$  and around the y-axis  $I_y$  are expressed by the following equations respectively.

$$I_x = \frac{1.4 \times 170^3}{12} + 2 \times \left( \frac{170 + 3.8}{2} \right)^2 \times 85 \times 3.8 = 5,451,523 \text{ cm}^4$$

$$I_y = \frac{1}{12} \times (170 \times 1.4^3 + 2 \times 3.8 \times 85^3) = 388,985 \text{ cm}^4$$

Then the radii of gyration,  $k_x$  and  $k_y$ , are obtained as follows.  $A$  is the cross-sectional area.

$$A = 170 \times 1.4 + 2 \times 85 \times 3.8 = 884 \text{ cm}^2$$

$$k_x = \sqrt{\frac{I_x}{A}} = \sqrt{\frac{5,451,523}{884}} = 78.5 \text{ cm}$$

$$k_y = \sqrt{\frac{I_y}{A}} = \sqrt{\frac{388,985}{884}} = 21.0 \text{ cm}$$

The buckling critical stress  $\sigma_{cr}$  is obtained by Tetmajer's formula as follows.

$$\sigma_{cr} = 31 \left( 1 - 0.00368 \frac{l}{k} \right) = \begin{cases} 285 \text{ MPa for } k_x \\ 234 \text{ MPa for } k_y \end{cases} \quad (3.5.1)$$

From the above it can be seen that the sectional moment of inertia around the y-axis is only 7% of that around the x-axis, but the buckling strength around the y-axis is 82% of that around the x-axis. This fact is proved by the cross tie buckling shown in Fig. 3.1 which buckled locally in the x-direction, not in the y-direction.

### 3.5.2 Load Applied on Transverse Strength Members

The load applied on the transverse strength members is given by the rules of the classification societies such as 2.45 m above the upper deck for the tank inside pressure fully loaded, 1/3 of the fully loaded draft for the tank outside pressure of at tank test condition, etc. The wave load is also given corresponding to the ship's size.

Hereunder the cross tie's strength is investigated based on a design standard established applying the above load and noting the buckling damage shown in Fig. 3.1.

Using long-term probability data due to variable pressure from the ship motion in waves prepared by Nippon Kaiji Kyokai [14] shows that the maximum variable pressure around the water line is 11.4 m at a probability level of  $Q = 10^{-5}$  for ships over 200 m length. That around the bilge part is 5.1 m, therefore the maximum variable pressure around the bilge part is (5.1 m + draft d). The above applied load is shown in Fig. 3.5.4, whose original formula is indicated in Fig. 2.3.1 of Sect. 2.3 "Transverse Strength Load" in Part I.

The axial force on a cross tie is given by Eq. (3.5.2).

$$P = h_c \times S \times l_i \tag{3.5.2}$$

where

$h_c$ : load at the level of cross tie

$S$ : spacing of side transverse

$l_i$ : distance from the cross tie to the midpoint between the cross tie and adjacent cross tie or deck transverse and or bottom transverse

The design standard for a cross tie panel is given by Eqs. (3.5.3) and (3.5.4).

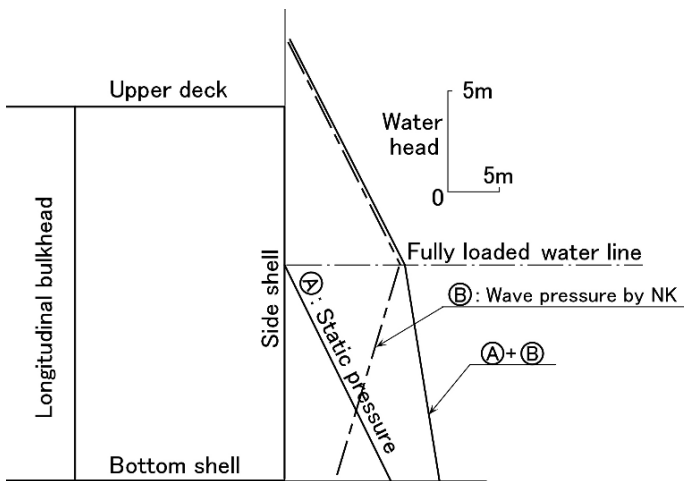


Fig. 3.5.4 Water pressure acting on side shell

$$\frac{\sigma_{cr}}{\sigma_A} \geq 2.0 \tag{3.5.3}$$

$$\sigma_A = \frac{P}{A_C} \tag{3.5.4}$$

where

$A_C$  : sectional area of cross tie

$\sigma_{cr}$  : critical buckling stress by compression of panel surrounded by stiffeners in a boundary supported condition

The design standard for a cross tie as a pillar is given by Eqs. (3.5.5) and (3.5.6). The critical buckling stress  $\sigma_{cr}$  of a cross tie as a pillar is calculated by means of Tetmajer’s formula.

$$\sigma_{cr} = 31 \left( 1 - 0.00368 \frac{l}{k} \right) \tag{3.5.5}$$

$$\frac{\sigma_{cr}}{\sigma_A} \geq 2.0 \tag{3.5.6}$$

where

$l$  : length of cross tie

$k$  : minimum radius of gyration of cross tie

The analysis is shown in Table 3.5.1. Ship B had buckling damage as shown in Fig. 3.1 and it can be seen that the safety factor for the panel of ship B is lower than 1.0. According to the above analysis a reinforcement was applied on the end panel of ship G which has a safety factor of 1.1.

**Table 3.5.1** Safety factor of cross tie buckling

Vessel	Principal dimensions (m)					Safety factor		
	L	B	D	d	S	for pillar buckling	for panel buckling at middle of cross tie	for panel buckling at cross tie end
A	240	37.8	17.5	13.17	5.5	2.5	2.5	
B	232	38.0	17.8	13.01	5.4	2.1	0.8	0.8
C	290	47.5	24.0	16.00	4.5		3.1	2.0
D	230	33.3	19.5	13.29	4.6	2.5	2.2	
E	230	35.3	18.0	11.55	4.45	3.0	1.9	
F	245	39.0	23.0	16.33	4.05	3.2	1.8	
G	260	43.5	22.8	17.80	5.1	2.4	1.6	1.1
H	360	62.0	36.0	28.15	5.3		2.8	
I	360	62.0	36.0	28.15	5.3		2.1	
J	270	44.5	22.0	16.80	4.8	3.3	4.4	2.9
K	320	54.5	27.0	21.00	5.3	2.8	2.9	1.8

The above load is applied not only on the cross tie but also on the side shell vertical web. In Fig. 3.5.4 the variable pressure in waves as regulated by Nippon Kaiji Kyokai is also shown.

### 3.5.3 Inside Pressure in Wide Tanks

It is clear that the bulging damage in the side shell in the 84,000 DWT tanker shown in Fig. 3.1 was caused by inside pressure of the tank which was designed as a stabilizer tank where the longitudinal bulkheads had openings. The liquid in a tank moves, for example to the port side when the ship is going to roll to starboard and at the maximum roll angle to starboard, it hits the upper part of the port side shell. Moreover in the fully loaded condition unexpected pressure will be caused on the upper part of the side shell by the ship's heel, as shown in Fig. 3.5.5.

From Fig. 3.5.5 the following relation can be derived:

$$B \times U = \frac{1}{2} a \times a \cot \theta \tag{3.5.7}$$

$$\therefore a = \sqrt{2BU \tan \theta} \tag{3.5.8}$$

$$c = B \tan \theta \tag{3.5.9}$$

where

$B$  : breadth of tank

$U$  : ullage

$\theta$  : heel angle

Accordingly the increase of water head  $H$  above the upper deck at side is given by the following Eq. (3.5.10).

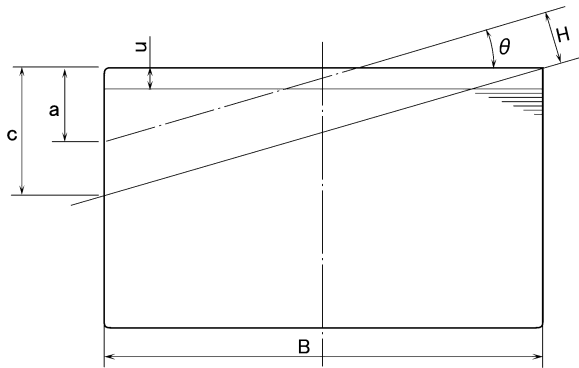


Fig. 3.5.5 Water head increase due to rolling

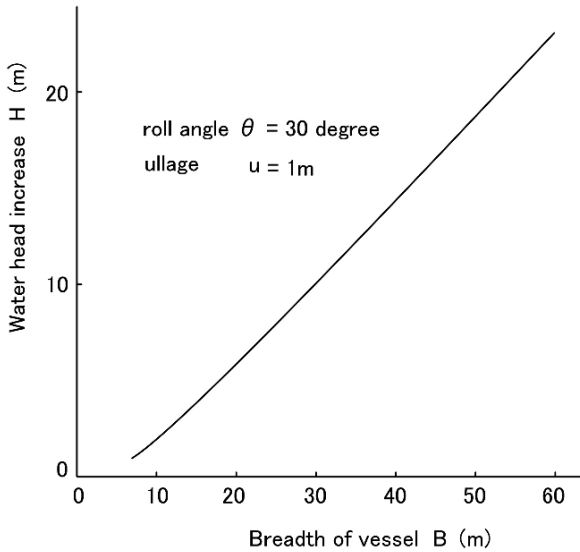


Fig. 3.5.6 Estimated water pressure head increase according to ship's breadth

$$H = (c - a) \cos \theta = (B \tan \theta - \sqrt{2BU \tan \theta}) \cos \theta \quad (3.5.10)$$

In Fig. 3.5.6 the relation between  $B$  and  $H$  is shown in the case of  $\theta = 30^\circ$  and  $U = 1$  m. In the case of an ordinary tank,  $H$  is more or less 2 or 3 m for about 15 m of  $B$ ; however, for a wider tank,  $H$  will be about 10 m.

The ballast hold of a bulk carrier is in a similar condition and indent damage to a shoulder tank bottom will be caused by the above behavior.

### 3.5.4 Connection Between Transverse Ring and Side Shell

The bulging damage of the side shell in the 84,000 DWT tanker shown in Fig. 3.1 was caused by disconnection between the transverse ring and the side shell longitudinal. As shown in Fig. 3.5.7 the connection consists of two parts, one is welding "A" between the transverse web and side longitudinal, and the other is welding "B" between the web stiffener on the transverse web and side shell longitudinal. Stronger connections for the collar plate "C" and bracket "D" are necessary. The damage to this connection is called "crack around slot" and much damage had been experienced during the era of the increase in ship size. This problem was solved in the 1970's by cooperative research in the shipbuilding industry [15, 16].

Let's consider the reason why the increase in the size of ships caused damage at this connection. The connection is to transmit the load applied on the side shell to the transverse ring. In spite of the load transmitted through this connection becoming



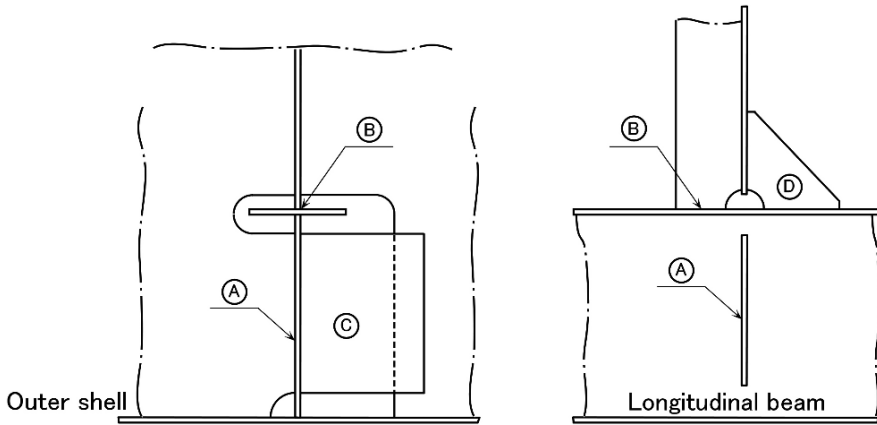


Fig. 3.5.7 Connecting part of transverse ring and outer shell

bigger with the increase in  $f$  ship size, the scantlings of this connection were not increased.

The load  $W$  transmitted from the side shell longitudinal to the transverse web through this connection is expressed by Eq. (3.5.11).

$$W = h \times s \times S \quad (3.5.11)$$

where

- $h$  : pressure head
- $s$  : spacing of side longitudinals
- $S$  : spacing of transverse web

With the increase in the size of ships,  $s$  increased up to 850–900 mm from previous 760 mm, and  $S$  increased to 5.5 m from 3.0 m, as shown in Table 3.5.1. In this case  $W$  increases by 2.05 times ( $850 \times 5.5 / 760 \times 3.0 = 2.05$ ). On the other hand the web thickness of a transverse ring has remained at 11–12.5 mm and the depth and thickness of a web stiffener on the transverse web remained at 100–150 mm and 11–12.5 mm respectively. The load doubled and the scantlings remained the same, therefore the damage appeared.

### 3.5.5 Buckling on Web of Transverse Rings

Nowadays with computers well developed, buckling on the web of a transverse ring is checked by computer, however the authors consider a paper model to be more suitable to assess buckling. Around the end of the 1960's buckling damage often appeared on the web of a transverse ring, as well as cracks, explained in Sect. 3.5.4. To establish suitable countermeasures, after finishing the detailed design of the midship

section of a 150,000 DWT tanker, a paper model (1/50) of the midship section was prepared. Buckling was investigated by applying possible loads by finger pressure and applying reinforcement against the observed buckling pattern. In this way the designer can apply any load he/she wants and observe the buckling pattern for that load.

Paper models were prepared for the study of buckling as shown in Fig. 3.5.8. This is a bottom transverse in a wing tank of a 110,000 DWT tanker completed in November 1966. Corrosion control was applied in the ship and structures in the tank were coated by epoxy paint. In this case it is important to make clear that any buckling was caused by shearing force or bottom pressure. In the former case reinforcement was applied only to the high shearing stress area, but in the latter case it had to be applied to all of the bottom area. Reinforcement by means of welding will cause damage to the epoxy paint and it will take much work and expense to recover the paint damage.

Paper models were prepared as shown in Fig. 3.5.9 and a shearing force and bottom pressure were applied by finger pressure. The buckling patterns were clearly different. Figure 3.5.9(a) shows the buckling pattern by a shearing force which runs in a diagonal direction. Figure 3.5.9(b) shows the buckling pattern caused by bottom pressure which happened locally close to the bottom. By this confirmation, the actual buckling pattern is quite similar to that caused by shearing force, and reinforcement was applied only to the high shearing stress area, saving much labor and much expense.

Figure 3.5.9(c) shows no buckling was caused by a shearing force which was opposite to the shearing force shown in Fig. 3.5.9(a). In this case a tensile stress was generated at the free edge of the slot which cannot cause any buckling.

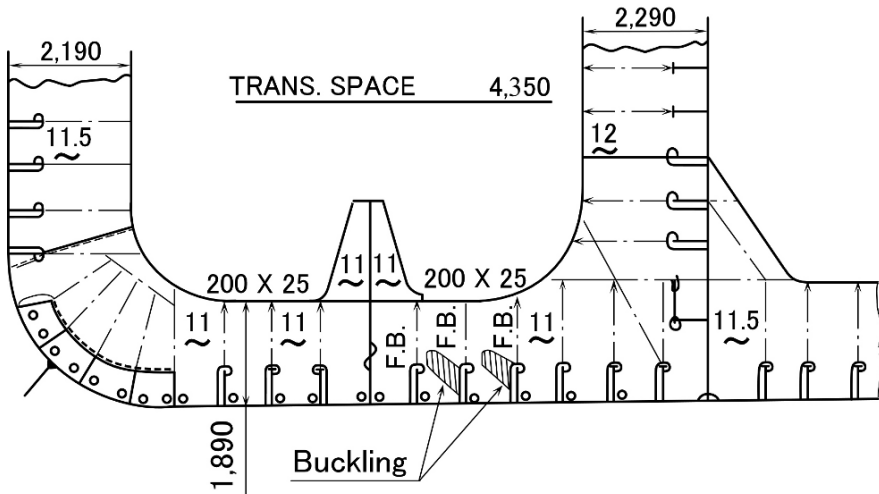


Fig. 3.5.8 Example of transverse ring buckling

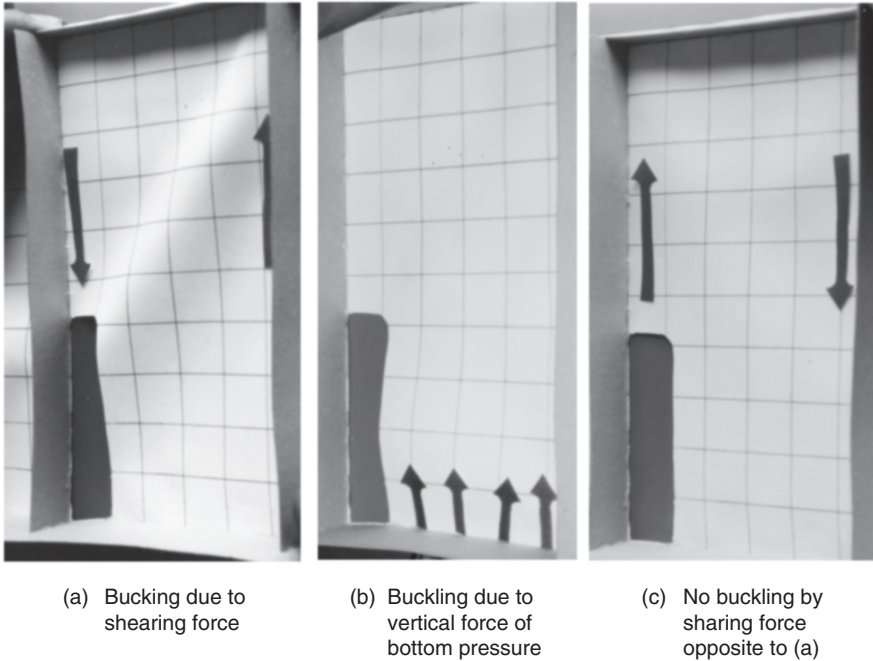


Fig. 3.5.9 Paper craft model of transverse web buckling

Figure 3.5.10 shows the shear buckling critical stress  $\tau_{cr}$  of a plate with a slot compared with the shear buckling critical stress  $\tau_0$  of a plate without a slot.  $\tau_0$  is obtained for the boundary supported condition [17].

### 3.5.6 *Straight Type and Circular Type Construction*

From the fabrication viewpoint, much discussion has been held on which is better, straight type or circular type construction. Eventually in Japanese shipyards the circular type was adopted, on the other hand in European shipyards, the straight type is widely adopted. The straight type construction is better for labor saving and the circular type is better for weight saving and strength. New fabrication techniques such as NC cutting and automatic welding support the circular type construction.

A cross tie mainly plays the role of a pillar and the straight type cross tie seems to be reasonable in supporting the axial force. However, the circular type cross tie is lighter, because as shown in Fig. 3.5.11 the heavy face plate of the “A” part can be omitted.

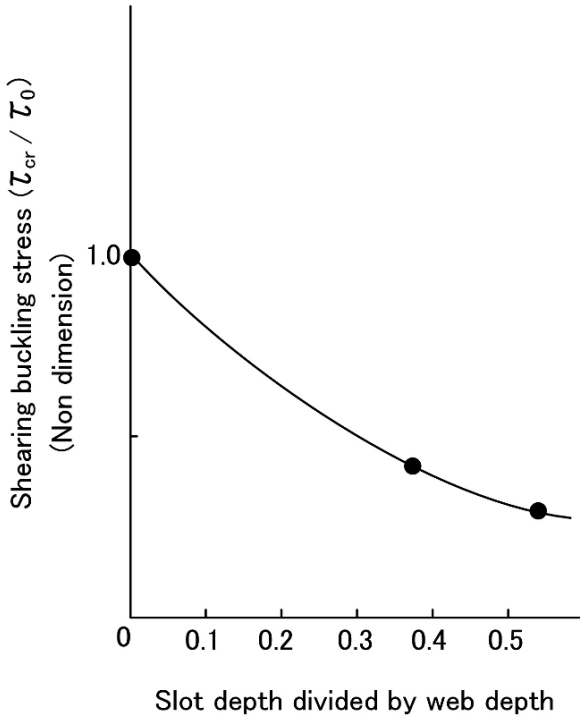


Fig. 3.5.10 Decrease of shearing buckling stress due to slot opening

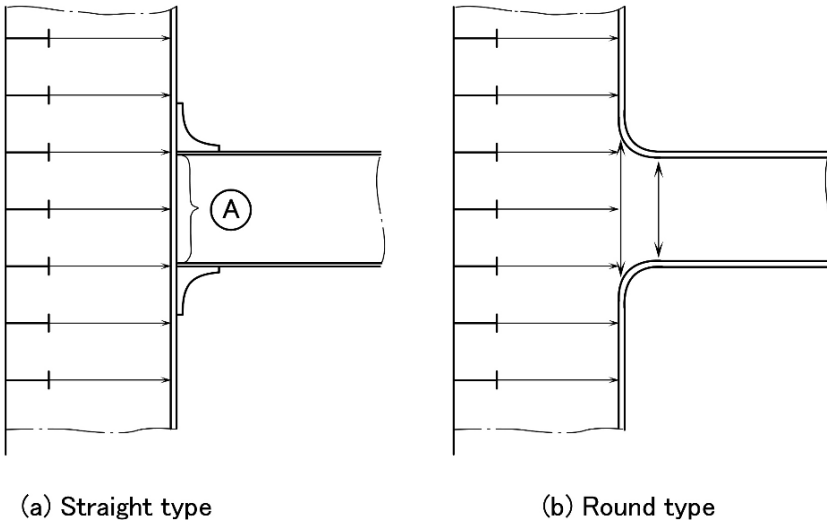


Fig. 3.5.11 Straight type and round type of cross tie

### 3.5.7 *Transverse Rings at Fore & Aft Parts of Tank*

In the design of the transverse strength of the tank part of a tanker, the scantlings of each member are decided based on the midship shape and the same scantling is applied to the fore and aft parts of a tank where the shape is different from the midship part. In Fig. 3.5.12 the shapes of transverse rings at the fore and aft parts of a 250,000 DWT and a 150,000 DWT tanker are shown respectively. It seems that a remarkable material saving can be achieved if the proper design to meet the shapes is carried out.

## 3.6 Transverse Strength of Ore Carrier

As stated in Sect. 5.2 of Part I, the ore carrier has a long and big ore hold in the middle of the ship which is sandwiched by ballast tanks. To achieve more efficient ore handling, no transverse bulkhead is fitted in the cargo hold and the hatch opening is bigger than that of an ordinary cargo ship. The transverse bulkhead is an important member in maintaining the transverse strength of a ship, and special care must be taken when designing a hull structure without a transverse bulkhead. In such a case, the double bottom and decks between hatches play a major role in maintaining transverse strength. In this Section the transverse strength members in the wing tank, knuckled part of longitudinal bulkhead, double bottom floor and deck between hatches are explained.

As shown in Fig. 3.6.1 the transverse bulkhead and the transverse ring in a wing tank suffer from compression in the fully loaded condition, and tension in the ballasted condition. This is also true for a transverse ring in a ballast wing tank of a tanker. However for a transverse bulkhead the condition is a little different. As shown in Fig. 3.6.2 for the fully loaded condition the transverse bulkhead supports about twice the compression than in the case of a tanker. This is why a horizontal girder on a transverse bulkhead of an ore carrier suffers from buckling damage.

A knuckle is, in some cases, provided at the mid-level between the upper deck and double bottom on the longitudinal bulkheads of an ore carrier. In the design of the knuckle part and the radius part, attention should be paid to the vertical force on the plate caused by in-plane force. Designers of land structures always provide reinforcement against the vertical force on the plate caused by an in-plane force but the hull structure designers are so optimistic that they pay little attention to this point. Buckling damage happens at the radius part of a cross tie shown in Fig. 3.1, and this is caused by the vertical force on the plate due to an in-plane force. An example of a crack caused by the vertical force on the plate due to an in-plane force is shown in Fig. 3.6.3. A countermeasure against this crack is to provide a longitudinal stiffener at the knuckled part to prevent the vertical movement of the plate.

In the design of an ore carrier, the height of the double bottom can be increased taken because of the small volume of the cargo hold due to the high specific gravity of ore. In this regard the design of transverse strength of an ore carrier is easier than that of a bulk carrier.

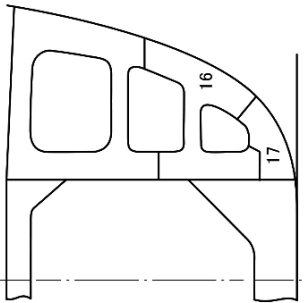
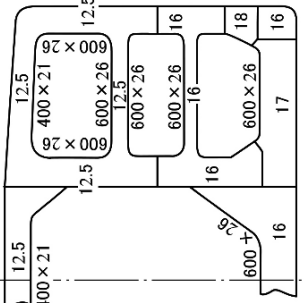
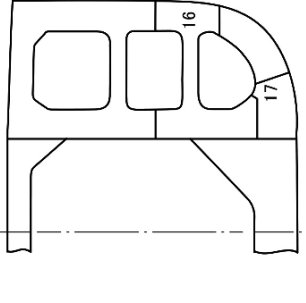
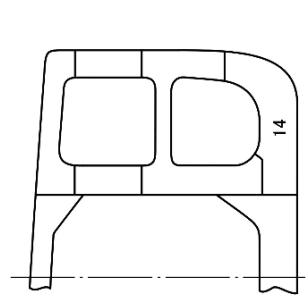
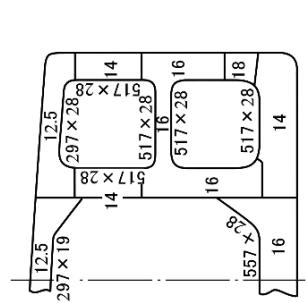
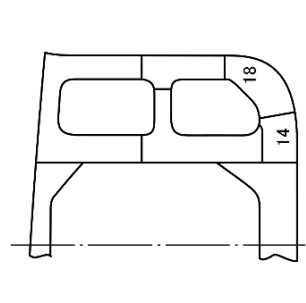
Class	Item	Aft part	Midship	Fore part
250,000 DWT Tanker				
150,000 DWT Tanker				

Fig. 3.5.12 Shape of transverse ring at fore, midship and aft

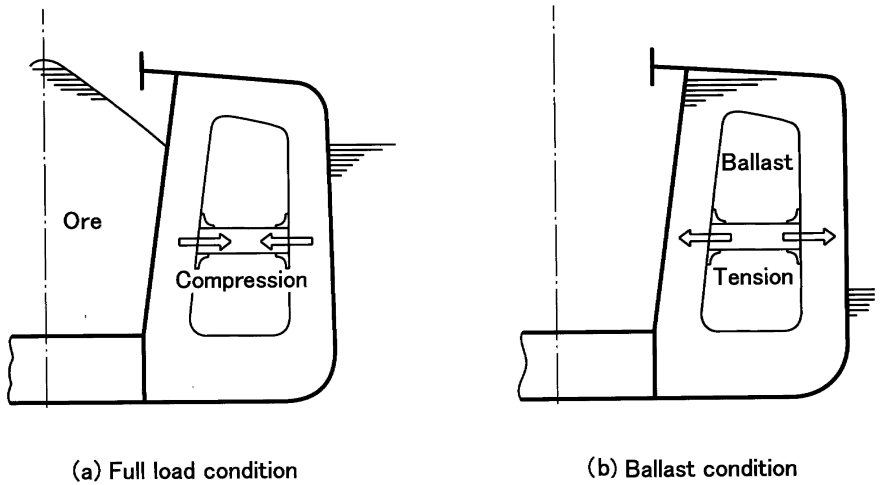


Fig. 3.6.1 Load on wing tank of ore carrier

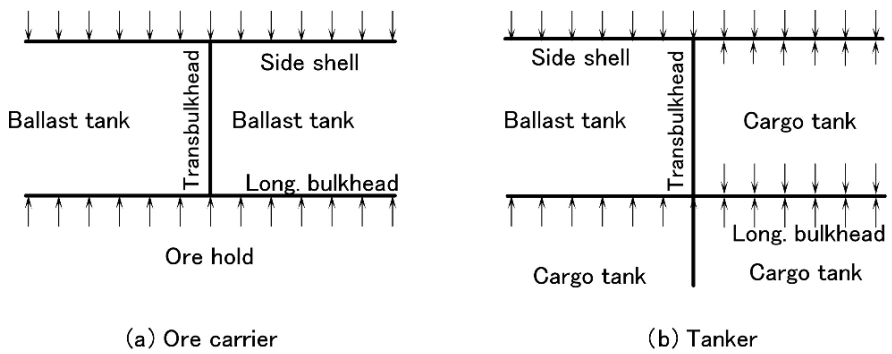


Fig. 3.6.2 Horizontal load acting on transverse bulkhead in full load condition

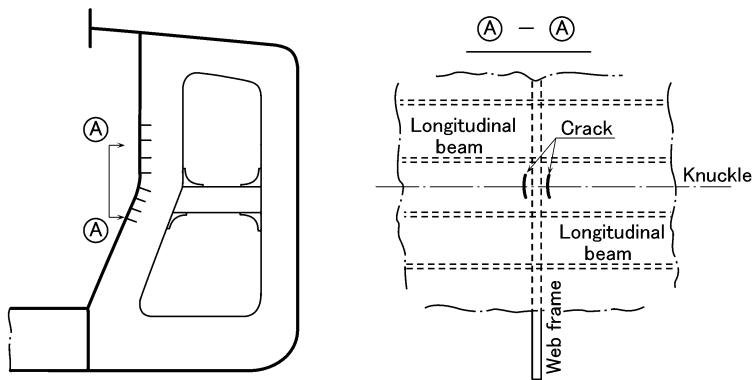


Fig. 3.6.3 Crack occurring at knuckled part in longitudinal bulkhead of ore carrier

In the floor in a double bottom, slots are provided for the longitudinal stiffeners as well as in a transverse ring of a tanker or an ore carrier's wing tank. Around the slots in a transverse ring of a tanker or an ore carrier's wing tank, many cracks occurred. However no cracks were reported around the slots in the double bottom floors of ore carriers, bulk carriers, and cargo ships. This is an important phenomenon, and we need to make clear the reason why such cracks happened around the slots. As shown in Fig. 3.6.4 the stress distribution at the connection between a web stiffener and a longitudinal stiffener is uniform in the case of the double bottom floor because there is no out-of-plane displacement of the floor. On the other hand, the stress concentration due to out-of-plane displacement of a transverse ring exists at the connection between a web stiffener and a longitudinal stiffener in a transverse ring of a tanker or an ore carrier's wing tank. For this reason no countermeasure will be necessary against cracks around the slots in the case of a double bottom floor.

In ore carriers a transverse force is generated in the deck between hatches. The force is compression in the case of a fully loaded condition, and tension in the case of a ballasted condition.

The forces can be estimated easily as follows. In a fully loaded condition a section of an ore carrier can be modeled as shown in Fig. 3.6.5. Applying bottom pressure, side pressure and weight of ore on the model the following equation can be obtained by the equilibrium of moments. Here the double bottom is more rigid than on upper deck between hatches.

$$l \left( \frac{dB}{2} \times \frac{B}{4} - W \times \frac{b}{2} \right) - F_m \times D = 0 \quad (3.6.1)$$

where

$d$  : full load draft

$l$  : distance between centers of upper decks between hatches

$B$  : breadth of ship

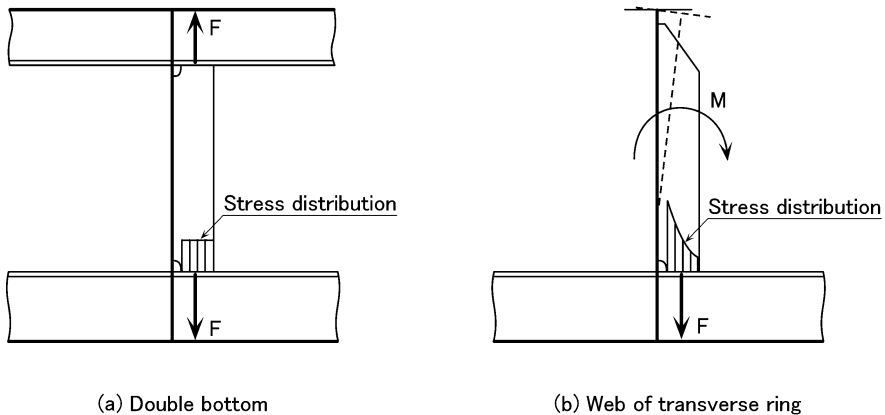


Fig. 3.6.4 Stress distribution in lower end of web stiffener



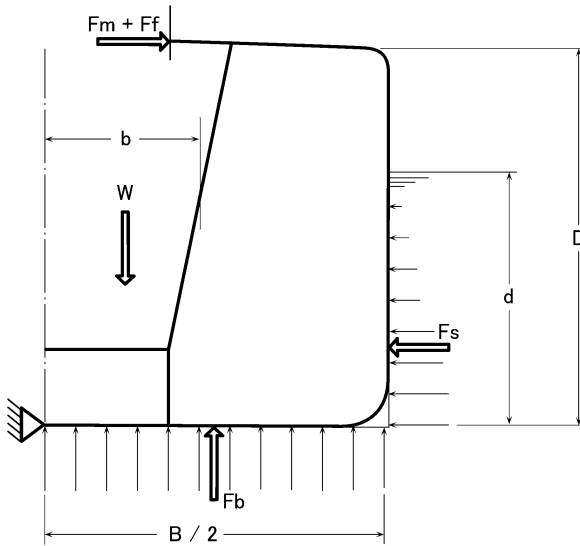


Fig. 3.6.5 Equilibrium of forces acting to transverse members of ore carrier

$W$  : half of ore weight per unit length of ship

$b$ : half the breadth of the ore hold

$D$ : depth of ship

$F_m$ : force on upper deck between hatches due to bottom pressure and ore weight

Expressing the force on the upper deck between hatches due to side pressure by  $F_f$ , Eq. (3.6.2) can be derived.

$$F_f \times D - l \times \frac{d^2}{2} \times \frac{d}{3} = 0 \tag{3.6.2}$$

From Eqs. (3.6.1) and (3.6.2) the total force in the upper deck between hatches ( $F_m + F_f$ ) can be obtained as shown by Eq. (3.6.3).

$$(F_m + F_f) = \frac{l}{2D} \left( \frac{dB^2}{4} - Wb + \frac{d^3}{3} \right) \tag{3.6.3}$$

The estimated compressive stresses in the upper decks between hatches, for large ore carriers, are shown in Table 3.6.1, and these were obtained assuming that the upper deck plate is 12 mm thick and the transverse beams of  $300 \times 90 \times 11/16$  inverted angle are fitted with 800 mm spaces. The critical buckling stress of the  $800 \times 4,000 \times 12$  rectangular plate with compressive force on the shorter edges is 152 MPa. Accordingly the safety factor for Ship A is 1.34, for Ship B is 1.17, and for Ship C is 2.54. In this case the design criteria of safety factor is taken to be the minimum value among the analyzed values for ships in service without any buckling, or the maximum value among the analyzed values for ships in service with buckling, if any.

**Table 3.6.1** Compressive stress of upper deck between hatch openings of ore carrier

Vessel	Deadweight DW(ton)	Breadth B(m)	Depth D(m)	Draft d(m)	1/2 Breadth of cargo hold b(m)	Longitudinal distance between cargo hold centers <i>l</i> (m)	Ore weight (tonf/m)	Compressive stress (kgf/mm <sup>2</sup> )	Delivered year
A	226,300	52.0	23.45	18.1	13.6	41.6	907	11.5	1988
B	196,800	50.0	23.90	17.5	12.9	48.4	813	13.3	1985
C	197,100	50.0	23.30	17.8	14.3	39.6	830	6.1	1984

### 3.7 Transverse Strength of Bulk Carrier

As explained in Sect. 5.2 in Part I, a bulk carrier has hopper tanks at both sides of the double bottom and shoulder tanks below the upper deck, the torsional rigidity of which supports the double bottom and side frame. From this view point the distance between transverse bulkheads, that is the length of a hold, is important.

The shoulder tank and the hopper tank are connected by the side shell construction and have a strong resistance against the vertical force. Against the horizontal force the hopper tanks connected to the double bottom also have a strong resistance. The vertical force on the double bottom, such as water pressure on the bottom and the cargo weight, and the vertical force on the side shell, causes torsional moments in the fixed parts of the hopper and shoulder tanks. The torsional rigidity of these parts is important in resisting the torsional moments. The torsional rigidity of a cylinder is proportional to the square of the sectional area of the cylinder, so the structural arrangement of small hopper and shoulder tanks, and of long cargo hold may have a transverse strength deficiency.

The torsional angle  $\theta$  of a thin hollow tube is expressed by the following equation:

$$\theta = \frac{sTl}{4A^2Gt} \quad (3.7.1)$$

where

$s$  : round length passing through mid-points of plate thickness

$T$  : torsional moment

$A$  : area surrounded by  $s$

$G$  : shear rigidity of material

$t$  : thickness of  $s$

$l$  : length of tube

In the application of (3.7.1) to the hopper tank,  $l$  is to be half the length of a hold and  $T$  is to be a function of the ship breadth  $B$ , draft  $d$  and  $l$ . Here  $T$  is represented in (3.7.2) and  $\theta$  is expressed by Eq. (3.7.3).

$$T \propto B^2dl \quad (3.7.2)$$

$$\theta \propto \frac{sB^2dl^2}{4A^2Gt} \quad (3.7.3)$$

The structural arrangement of a bulk carrier is to be based on the standard  $\theta$  which is derived by the analysis of  $\theta$  in (3.7.3) for many ships in service.

The side shell construction connecting the hopper tank and the shoulder tank originally consisted of ordinary frames and web frames which were arranged in line with the transverse webs in the hopper tank and the shoulder tank. However, in the new design it is common to omit the web frames, but the ordinary frames are retained. This is because as explained above the transverse strength of a bulk carrier is maintained by the torsional rigidity of the hopper and shoulder tanks. The upper and the lower ends of the side shell construction suffer from a forced torsional moment; in a deeper frame higher bending stress is generated and in a more shallow frame a lower bending stress is generated.

At the upper and the lower ends of the side frame, brackets should be fitted inside the shoulder tank and the hopper tank. There is no instruction to decide the scantling of these brackets in classification rules. Hereunder a suggestion to design these brackets is explained. As shown in Fig. 3.7.1(a) the bracket inside the hopper tank is supported by the side longitudinal A and the longitudinal stiffener B on the hopper plate; this resists the bending moment  $M$  at the lower end of the side frame. In this condition the equilibrium of the forces is expressed by Eq. (3.7.4).

$$M = l_1 F_1 + l_2 F_2 \tag{3.7.4}$$

$M$  can be expressed by  $M = Z\sigma$  where  $Z$  is the section modulus of the side frame and  $\sigma$  is the design stress of the frame.  $F_1$  and  $F_2$  are the reactions from the longitudinal frame A and B, and can be obtained by limiting the stresses  $\sigma$  in the longitudinal frame A and B as shown in Fig. 3.7.1(b). On the other hand there exists a relation of (3.7.5) between  $F_1, F_2, l_1$  and  $l_2$  as shown in Fig. 3.7.1(c), assuming the bracket is rigid.

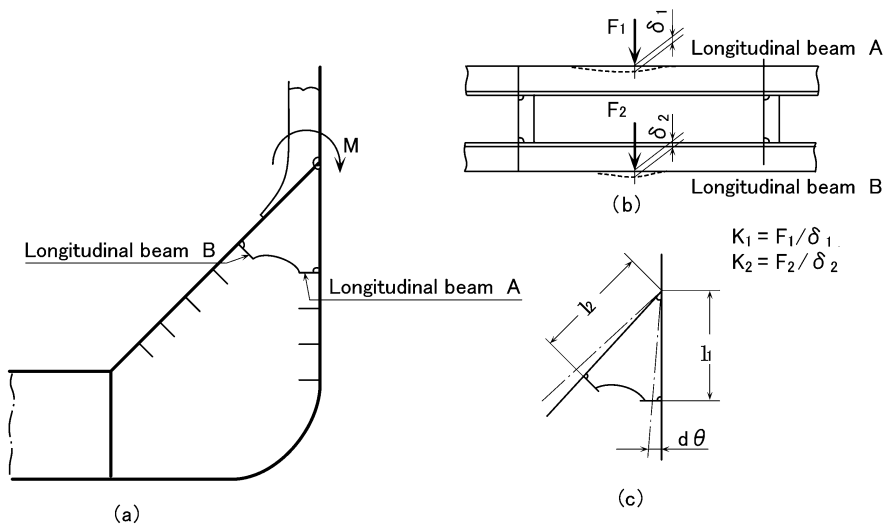


Fig. 3.7.1 Bracket supporting lower end of side frame

$$d\theta = \frac{k_1}{l_1} F_1 = \frac{k_2}{l_2} F_2 \quad (3.7.5)$$

where  $k_1$  and  $k_2$  are spring constants of longitudinal frames.

According to the above consideration a reasonable design of the brackets at the lower and the upper ends of the side frames can be obtained and this depends on the size of the side frame.

An important point in designing the transverse strength of a bulk carrier is the connection of the double bottom to the hopper tank. Many cracks shown in Fig. 3.7.2 where reported during the era of the increasing size of bulk carriers. There are two ways of construction in this part, a straight welded type and a curved bending type, on which many discussions have been held from design and fabrication view points.

It is easily understood that the crack shown in Fig. 3.7.2 is caused by the tensile stress due to the cargo weight on the double bottom. However in the smaller bulk carrier which has a narrow floor space in the double bottom no such crack has been reported even with a scallop in this part. From experience with such cracking, closing the scallop with a collar plate has been a common practice but for a narrow floor space up to about 2 m no collar plate arrangement is required.

At the connection of the double bottom to the hopper tank, either a straight welded type or a curved bending type has to be chosen from a fabrication view point as well as a strength view point. The latter requires a plate bending process but the fillet welding is half of the former. As shown in Fig. 3.7.3 a side girder

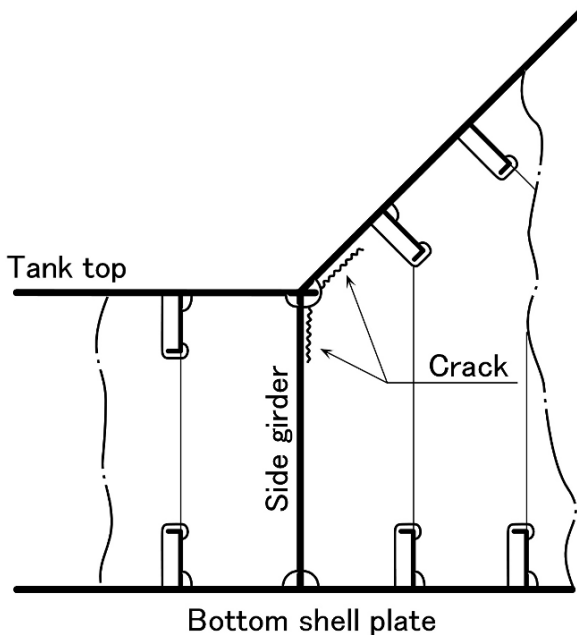
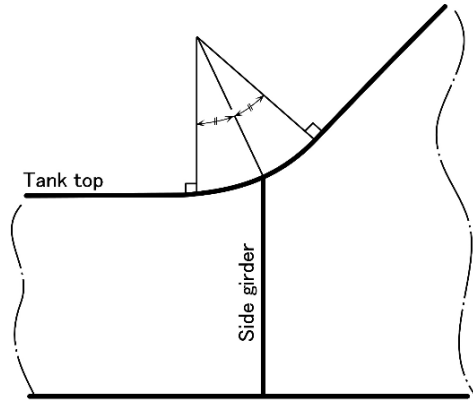


Fig. 3.7.2 Example of crack in double bottom end of bulk carrier

**Fig. 3.7.3** Rounded inner bottom plate construction



is to be fitted around the midpart of the curve to avoid movement perpendicular to the plate. Such movement caused cracks at the knuckled part of the longitudinal bulkhead of an ore carrier, as shown in Fig. 3.6.3. This alignment of the side girder is important to prevent structural damage from view point of strength, but it takes many labor hours to provide accurate alignment from the fabrication view point.

In the case of the curved bending type, the effective breadth of the curved part relative to the bending moment at the end of the double bottom is reduced, for which some reinforcement to avoid out of plane displacement is necessary. Summing up the above discussion, the authors consider the curved type seems to have an advantage due to strength, in spite of the curved type not being so easily fabricated.

At the time when designers discuss the strength of a structure, the load on the structure should be kept in the designer's mind. In the case of heavy cargo, alternate holds are loaded. This is called alternate loading or jumping loading, because uniform loading will bring the center of gravity lower causing a shorter rolling period. Alternate loading is most important in bulk carriers.

Here as an example, uniform loading and alternate loading are compared with for a 33,000 DWT bulk carrier. The loads on the double bottom are shown in Table 3.7.1. The load for the alternate loading is 6–7 times of that for the uniform loading. The load for the ballast condition is obtained assuming the draft is 32% of that of the fully loaded condition which is bigger than that for uniform loading. As explained above the load for the alternate loading is important for a bulk carrier double bottom which is supported by the torsional rigidity of the hopper tank.

Next, the in-plane load in the transverse bulkhead is to be considered. As shown in Fig. 3.7.4 the load on the double bottom is transmitted to the transverse bulkhead as an in-plane load, as well as to the side shell plates. The in-plane load in the transverse bulkhead  $W$  is expressed by the following Eq. (3.7.6):

$$W = \frac{a_1 w_1}{2} \alpha + \frac{a_2 w_2}{2} \alpha = \frac{a_1 \alpha}{2} (w_1 + w_2) \quad (3.7.6)$$

**Table 3.7.1** Applied load to double bottom of bulk carrier

Condition			Cargo load tonf / m <sup>2</sup>	Bottom pressure tonf / m <sup>2</sup>	Total load tonf / m <sup>2</sup>
Full load	Homogeneous loading		12.56	10.90	+ 1.66
	Alternate loading	Empty hold	0	10.90	- 10.90
		Loaded hold	23.36	10.90	+ 12.46
Ballast			0	3.49	- 3.49

+: downward      -: upward

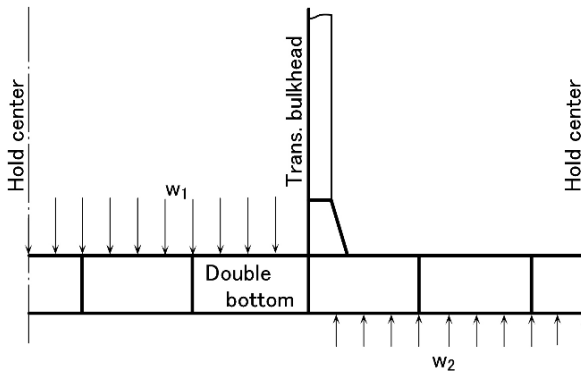


**Fig. 3.7.4** Applied load to transverse bulkhead

where

- $\alpha$  : double bottom load supporting ratio of transverse bulkhead
- $a$  : area of double bottom
- $w$  : load on double bottom shown in Table 3.7.1

The suffix 1 and 2 indicate the values for the adjacent holds. Generally in the midship part  $a_1 = a_2$  and with uniform loading and the ballast condition  $w_1 = w_2$ .  $(w_1 + w_2)$  is called the load factor for the transverse bulkhead and is shown in Table 3.7.2 which is obtained using the values in Table 3.7.1. It can be seen that the load factor for alternate loading is low because the load in the empty hold and the loaded hold cancel each other at the transverse bulkhead. According to the result shown in Table 3.7.2 for the ballasted condition, the value for an empty hold is

**Table 3.7.2** Load coefficient of transverse bulkhead of bulk carrier

		Load factor. tonf/m <sup>2</sup>
Full load condition	Homogeneous load	+ 3.32
	Alternate load	+ 1.56
Ballast condition		- 6.98

applied in the calculation of the shear deformation of a transverse bulkhead, when considering the total strength evaluation of a bulk carrier as shown in Sect. 1.2.2.

### **3.8 Transverse Strength of Container Ships**

In the design and the construction of the first generation of container ships, many wide and detailed assessments were made, especially on the torsional strength due to large hatch openings and on engine room construction due to high engine output. Regarding the transverse strength of a container ship, the hull structure designers seem to be optimistic because a container ship has many transverse bulkheads with intermediate partial bulkheads; also the breadth of a container ship is limited up to 32.2 m, to be able to pass through the Panama Canal, which is called Panamax. In addition to these the load on a double bottom is smaller than that of other kinds of ship. As a result, very little damage on the transverse strength of container ships is reported.

However to increase the efficiency of transportation, longer holds with less transverse bulkheads and the deletion of the partial bulkhead will be required; sizes above Panamax also appeared recently. For these matters more attention should be paid.

# Chapter 4

## Torsional Strength

Following Chap. 2 “Longitudinal Strength of Hull Girder” and Chap. 3 “Transverse Strength of Ship”, in this chapter torsional strength is explained referring the actual damages.

A ship, which has smaller large openings in its upper deck like a tanker, has enough torsional strength, and no damage caused by torsion has been reported. A bulk carrier and a container ship have large openings in the upper deck and a hull structure designer has to pay attention to the torsional strength.

As in the case of buckling, the torsional strength can be understood easily and clearly by means of a paper model. In Photo 4.1 and 4.2, two paper models are shown. One is with a slit throughout the upper deck in a longitudinal direction, which has very low torsional rigidity, as shown in Photo 4.1. And the other is with large openings in the upper deck which shows tension and compression at the hatch corners as shown in Photo 4.2. Actually damage such as buckling and cracking at the hatch corner are caused by torsion as explained in the following sections.

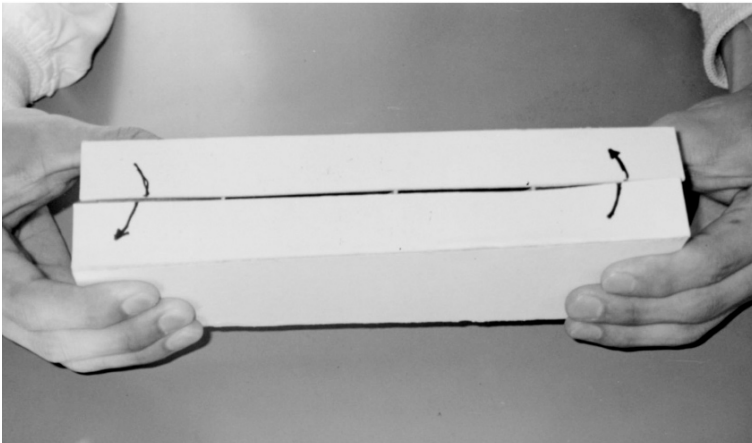


Photo 4.1



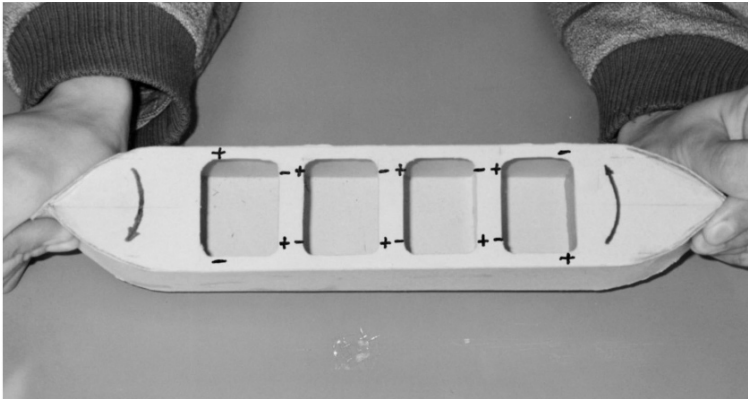


Photo 4.2

### 4.1 Structural Damage Due to Torsion (Example No. 1)

A 750 TEU container vessel (175.0 × 25.2 × 15.3 × 9.724 m, 28,000 HP) was sailing in the north pacific ocean from Oakland in North America to Kobe in Japan in the winter season, when she suffered heavy weather damage in the area of the bow structure. The damage was cracks in the starboard shell plate and buckling in the region of the upper deck, forecastle deck and shell plating on the port and starboard side. After investigations, the reason for the damage was concluded to be that the bow structure was twisted counter-clockwise around the longitudinal axis of ship due to a large impact wave load on the large bow flare.

Figure 4.1.1 shows the port side shell plate where buckling occurred. The buckling was induced by a shearing force, judging from the fact that the direction of buckling is not straight upwards but inclined aft-wards. Accordingly the damage

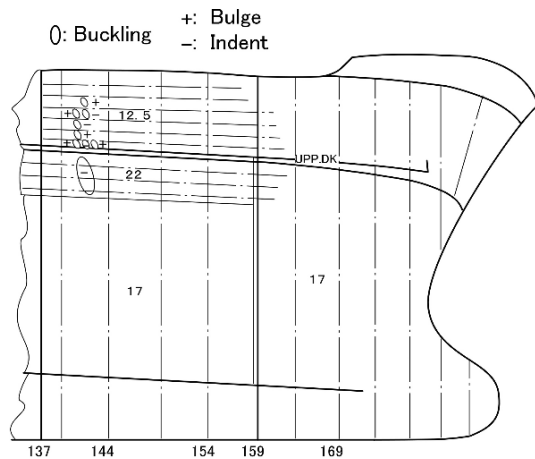
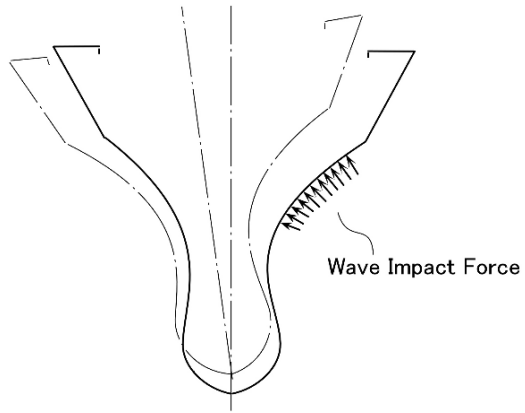


Fig. 4.1.1 Buckling of port side shell plating

**Fig. 4.1.2** Deformation of FR.154 Cross Section



was caused not by an upward force due to a wave impact load but by a counter-clockwise torsional moment around the longitudinal axis which was induced by a wave impact load acting on the starboard bow flare.

Figure 4.1.2 shows the deformed shape of the bow structure by FEM analysis at frame 154, in the forward-looking direction. The result shows that the cross section was twisted counter-clockwise due to the wave impact load acting on the starboard bow flare.

Figure 4.1.3 illustrates the buckling of the forecastle deck plate of the subject vessel. A counter-clockwise torsional moment resulted in the buckling of the port side fore corner of the hatch opening and the starboard aft. We have to pay attention that the buckling of the forecastle deck might have been induced not only by torsional moments but also by horizontal bending moments which bent the bow structure in the port direction due to a starboard side wave impact load.

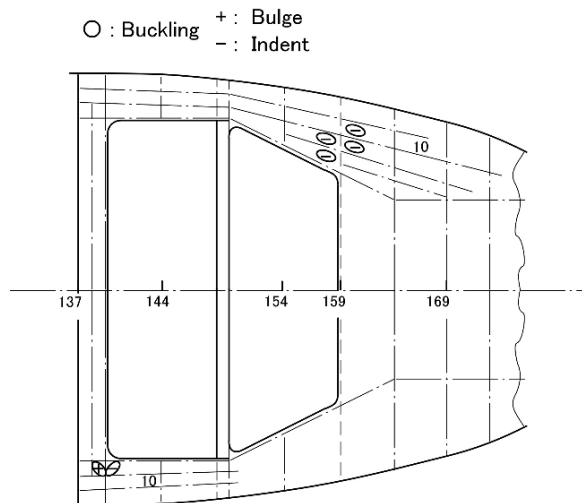


**Fig. 4.1.3** Buckling of forecastle deck plating

## 4.2 Structural Damage Due to Torsion (Example No. 2)

When a fully-loaded bulk carrier of 250,000 DWT, with ore cargo was sailing from Brazil to Korea via the Cape of Good Hope, she encountered rough seas in the Indian Ocean and she suffered structural damage to the deck area between hatch openings. According to the log data, the wind was force 8 grade on the Beaufort scale and the significant wave height was 7 m. The ship's speed was 7–8 knots and she proceeded with a rolling motion of 12–15°. The waves and winds were coming from ahead at 65° to starboard. Such heavy weather continued for 7 days and after the bad weather the above damage was found [18].

It happened in the return voyage of her maiden voyage and the wind class was around 3 Beaufort everyday during the maiden voyage except for the damage period. The distribution of damage is shown in Figure 4.2.1. There is no damage fore and aft of the No.6 hold, because No.6 is an empty hold and because the deck plate thickness fore and aft of the No.6 hold is thicker than that at the other holds. Figure 4.2.2 shows the scantlings of the deck plates where buckling occurred. Buckling took place in the transition area of 13–25 mm thick plate. From the distribution of buckling, it was deduced that the damage was caused by a torsional moment which created a clockwise twisting at the bow and a counter-clockwise twisting at stern. This deduction can be justified by the fact that the vessel encountered the winds and waves from 65° starboard ahead, and such winds and waves generate a torsional moment of a clockwise twisting at the bow and a counter-clockwise twisting at the stern.

This structural damage was investigated in detail and stress measurements on the vessel were carried out. Based on the analysis, the reinforcement of the deck structure was performed as shown in Figure 4.2.3 and the following 4 recommendations were made:

- 1) Since a bulk carrier is thought to have sufficient torsional strength, stress due to torsional deformation of the ship had been neglected. However, in cases where she carries ore in holds and in cases where large hatch openings whose breadth exceeds 50% of ship breadth are provided, special reinforcement is to be considered for deck structures against torsional deformation of the ship.
- 2) In investigating the strength of the deck structure between the hatches, additional consideration is needed where the deck structure is subjected to bending due to a lateral load in the transverse bulkhead.

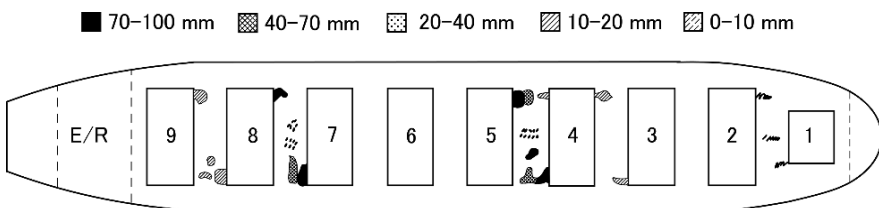
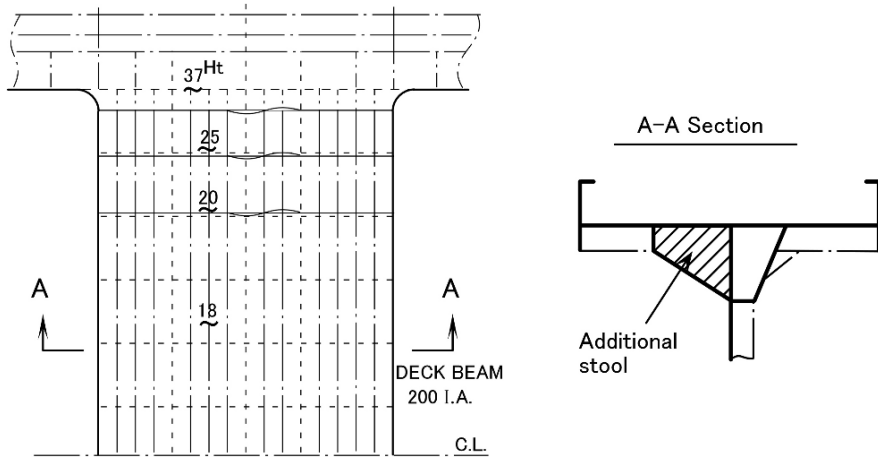
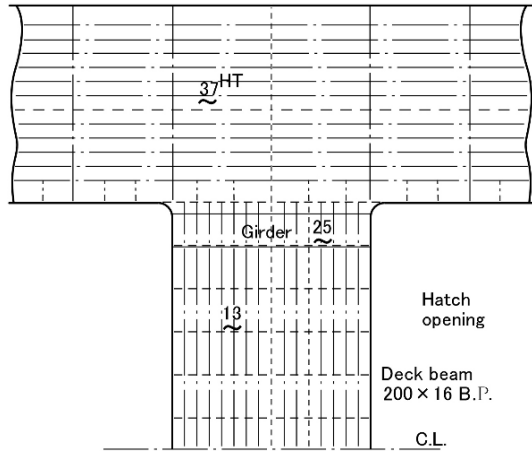


Fig. 4.2.1 Buckling of deck plating between hatches of 25,000 DWT bulk carrier

**Fig. 4.2.2** Scantling of deck plating of between hatches



**Fig. 4.2.3** Reinforcement for buckled deck plating between hatches

- 3) The number of transverse bulkheads, that is the number of cargo holds, is to be carefully investigated, because this directly affects the compressive strength of the deck between hatches as well as the torsional strength of the ship.
- 4) From the view point of the strength of the deck between hatches, homogeneous loading of ore cargo in holds is to be avoided. In spite of this, alternate loading of ore is not preferable because it induces high stress in the double bottom.

# Chapter 5

## Shell Structure

In Chaps. 1–4, the structural design of a ship hull as a whole body is presented. Now let's explain the design for each part of the hull structure. The aim of the shell structure is to prevent water coming inside a hull, keeping the hull form. The shell structure supports generally a lateral pressure to the shell, and in some places it supports in-plane forces such as tension and compression due to hull girder bending.

The thickness of the shell plate is very thin considering the huge structure of a ship. It can be said that the shell plate is not a plate but a membrane. The side shell plate of a VLCC of 300 m length is about 25 mm. This corresponds to 0.4 mm shell plate of a car of 5 m length, and 0.06 mm plate of a can of 10 cm diameter. Considering the scale effect the ship's shell plate is very thin compared with other structures.

In the 1960's when ship size was increased, the shell plate thickness was not so increased. Hull structure designers were afraid of the shell plate thickness, and established a reasonable design method for the shell plate.

In this chapter a reasonable design method for the shell plate and examples of shell damage are explained.

### 5.1 Thickness of Shell Plates

The side shell plate endures lateral outer forces caused by the water pressure, as well as in-plane loads caused by hull girder bending. Since the stiffening system of the shell plate is usually longitudinal, except for small-size cargo ships; the in-plane load due to local bending of the side longitudinals is added in shell plate. The stresses acting in the shell plate are categorized as follows (See Fig. 5.1.1):

- (1) longitudinal stress due to the hull girder bending:  $\sigma_1$
- (2) shearing stress due to the hull girder bending:  $\tau$
- (3) longitudinal stress due to the bending of the longitudinal frame:  $\sigma_2$
- (4) stress due to the lateral water pressure:  $\sigma_3, \sigma_4$

Considering a rectangular plate supported by longitudinal stiffeners longitudinally and the transverse webs transversely,  $\sigma_1$  and  $\sigma_2$  act longitudinally and  $\sigma_3$

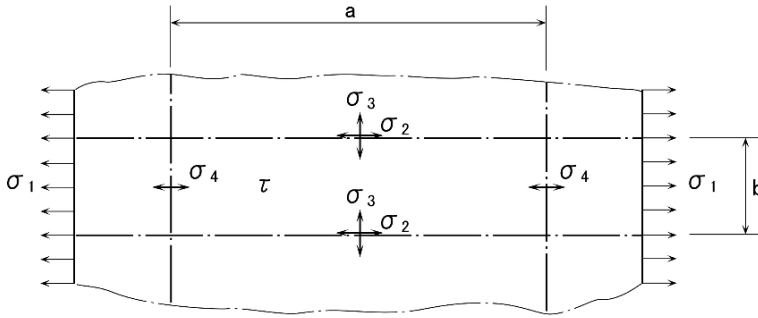


Fig. 5.1.1 Kind of stress component in shell plate

transversely in the mid-part along the longitudinal stiffeners, while  $\sigma_4$  acts in the mid-part along the transverse webs. Of these stresses,  $\sigma_3$  is generally the greatest because  $a > b$ . Hence, the stress in the mid-part along the longitudinal stiffeners should be considered.

The shearing stress  $\tau$  mentioned above is negligible in the bottom shell plate, while  $\tau$  in the side shell plate is calculated from the hull girder shearing force allowing for the share taken by the longitudinal bulkheads and the side shells. In this case, the combined stress at the mid-point along the longitudinal stiffeners is calculated for the plane stress condition, using the Von Mises theory as follows:

$$\sigma_e = \sqrt{(\sigma_1 + \sigma_2)^2 - (\sigma_1 + \sigma_2)\sigma_3 + \sigma_3^2 + 3\tau^2} \tag{5.1.1}$$

$\sigma_e$ : equivalent stress

The design criterion is that this equivalent stress is less than the yield stress of the material.

$$\sigma_e \leq \sigma_y \tag{5.1.2}$$

$\sigma_y$ : yield stress

(1) *Fully loaded condition*: In the fully loaded condition, the large water pressure in the empty tanks acts on the shell structure. Since the side longitudinals are bent inwards,  $\sigma_2$  is a compressive stress. Hence  $\sigma_2$  and the compressive hull girder bending stress  $\sigma_1$  are combined in the bottom shell plate in the hogging wave condition, and in the upper side shell plate in the sagging condition.

$\sigma_2$  or  $\sigma_3$  are combined at the section where the hull girder bending moment or the shearing force becomes a maximum. It is noted that the shearing stress becomes zero where the bending moment becomes maximum, while the bending moment is not zero where the shearing force becomes maximum.

(2) *Ballast condition*: In the ballast condition, a large water pressure in the ballast tanks acts on the shell structure from inside. Since the shell longitudinal is bent outwards,  $\sigma_2$  is a tensile stress. Hence  $\sigma_2$  and the tensile hull girder bending stress  $\sigma_1$  are superposed in the bottom shell plate in the sagging condition and in the upper side shell plate in the hogging condition.

The thickness of the shell plate in the above mentioned calculations is applied usually in the 0.4L (L: ship scantling length) midship region. However, it should be

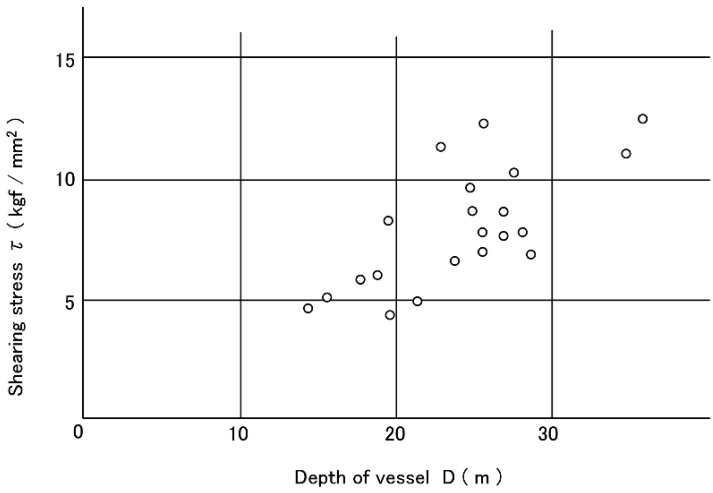


Fig. 5.1.2 Shearing stress of side shell plate around collision bulkhead

considered that a large shearing stress due to hull girder bending may occur at the front part of the engine room and at the aft part of the fore peak tank. Examples of the shearing stresses calculated in the side shell of oil tankers at the aft part of the fore peak tank are shown in Fig. 5.1.2.

### 5.2 Shell at Bottom Forward

Due to the large increase in size of ships, dents of the shell plate in the bottom forward have arisen, because the distance from the pitching center to the forward shell is greater, and also the shape of the bottom forward region becomes flat. Figure 5.2.1 shows an example of the damage.

Where the draft is insufficient in rough seas, reinforcements are carried out in accordance with the classification rules. Since no reinforcement is usually carried out where there is sufficient draft, the ship operator should know this condition and operate carefully in rough seas.

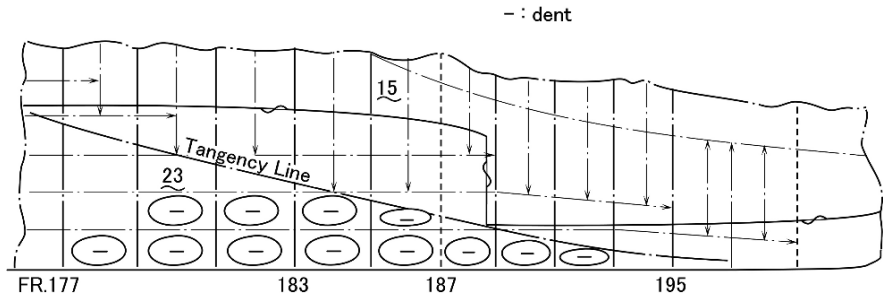


Fig. 5.2.1 Example of slamming damage

### 5.3 Shell at Bow Flare

Since most ships now have large bulbous bows, the bow flare in the vicinity of the bell mouth is made larger in order to avoid contact of the anchor with the shell. High speed ships also have a large bow flare for good seaworthiness. However when the bow flare is large, the pressure due to wave impact becomes large, and cracking and buckling will easily happen.

Figure 5.3.1 shows an example of a crack on the shell plate at the bow flare in a high-speed container ship. The crack started at Fr.151a and extended about 6.6 m horizontally and 3.5 m vertically. The ship had navigated in rough seas for 6 days before the accident; the scale of the wind force was over 10 for 11 h, and over 8 for 82 hours; 69% of 6 days. It was reported that the ship had sailed at 9–12 knots in the center of a low atmospheric pressure region of 980 hPa with a 10–12 scale wind force for 7 hours continuously.

The impact pressure due to the waves on the shell plate of the starboard side was calculated, based on ship motions in regular waves. The length of the waves was assumed to be  $0.8 \times$  ship length with an encounter angle of  $45^\circ$  against the center line. The maximum value is shown in Fig. 5.3.2, which includes two wave heights of 12 and 20 m. This shows that the pressure is proportional to the ship speed and that reducing speed is important to avoid damage due to wave impact.

Figure 5.3.3 shows also an example of bow damage. In this case, the water pressure seems to be equivalent to 100 m static head.

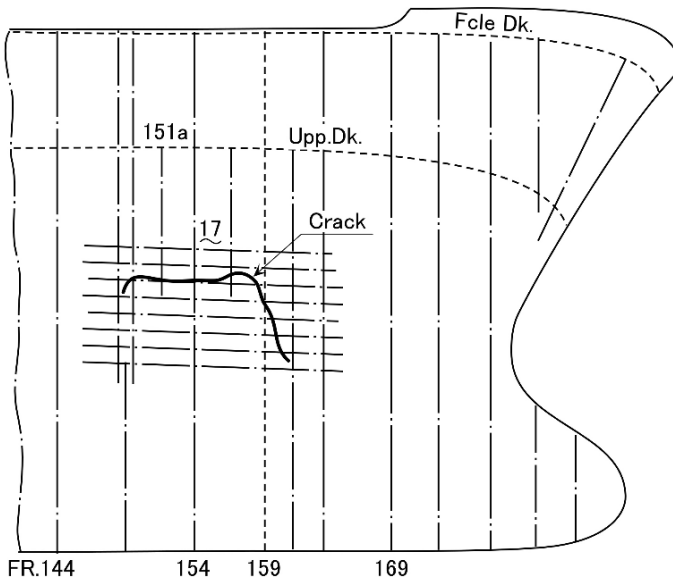
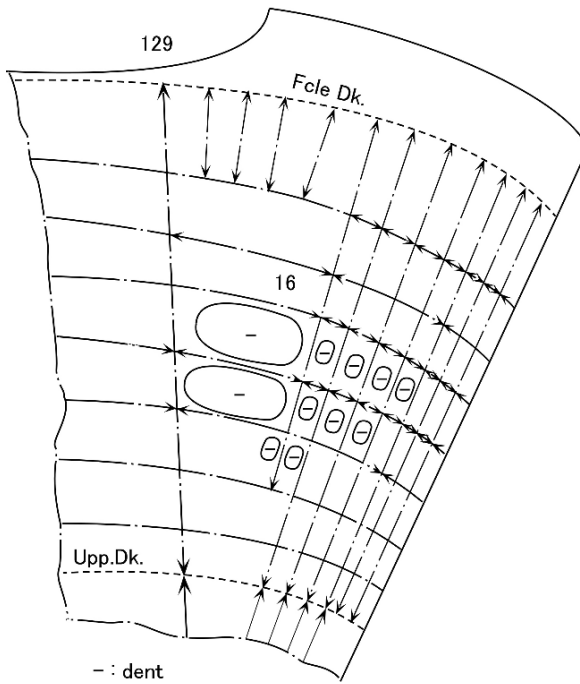
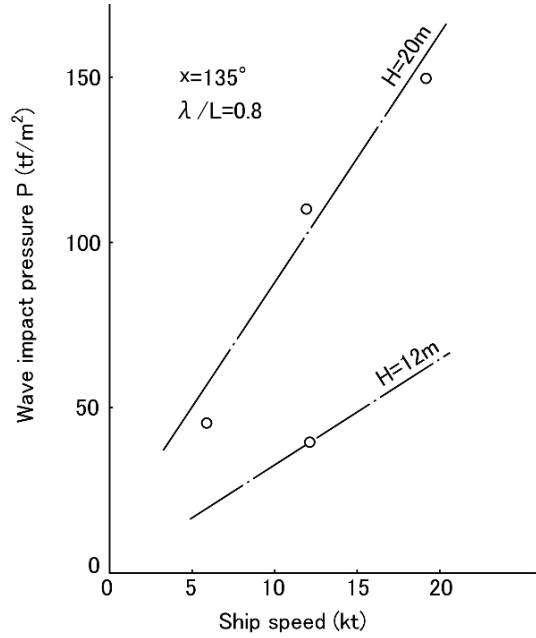


Fig. 5.3.1 Example of crack in bow flare



**Fig. 5.3.2** Wave impact pressure of bow flare against ship speed



**Fig. 5.3.3** Example of bow dent

## 5.4 Bilge Shell

It is preferable to have a large radius of bilge and a large rise-of-floor from the propulsion/resistance point of view, while smaller dimensions of both are desirable from the construction point of view. In calculating the hold capacity using Simpson's law, the breadth of the start point should be the smallest value. Hence, the half breadth of the keel plate was originally adopted as the breadth, and the rise-of-floor was taken as 10 mm for the large ships. By bending the steel plate of 2,600 mm breadth, 1,600 mm can be adopted as the bilge radius.

It was thought that reinforcement seemed to be unnecessary for a part of a cylinder having a small radius like this, and therefore bilge-longitudinal-less structures (without the longitudinal framing) appeared after structural analysis using FEM. At first it was of concern, but now this structure has been adopted in many ships, and no damage in this structure seems to have occurred.

Though such a cylindrical surface is only seen on the bilge part and the rounded gunnel in the midship area, there are many cylindrical shell areas in the fore and aft structures. Since such a cylindrical shell is stronger than a flat plate under lateral force, in some areas the plate thickness can be reduced or the stiffener space can be wider, in accordance with each curvature. Further studies of the strength and vibration for such curved surfaces are now necessary for the hull designer in order to rationalize the hull structure design.

## 5.5 Shell near Stern Frame

For the shell in the vicinity of the stern frame, thicker plates are used in comparison with other shell plates. The stern frame with a G type rudder is an important structure in supporting the propeller, propulsive shaft, and rudder. The lower part comes in contact with a keel block first during docking and transmits the force from the block to the hull.

Recent ship structures with a bulbous stern or open bulbous stern, associated with energy-saving, do not support the hull weight at docking, do not support the rudder as shown in Fig. 5.5.1, and only support the propeller shaft.

In the case of a structure with an open bulbous stern, increasing the thickness of the side shell in the vicinity of the casting is not desirable from the strength/vibration point of view, because it increases the weight at the end of a cantilever beam. If it is necessary to increase the rigidity, increasing the plate thickness around Part B not Part A in Fig. 5.5.1 is effective. However, the ship breadth at B with a bulbous stern is already wide, hence the transverse rigidity seems to be strong enough.

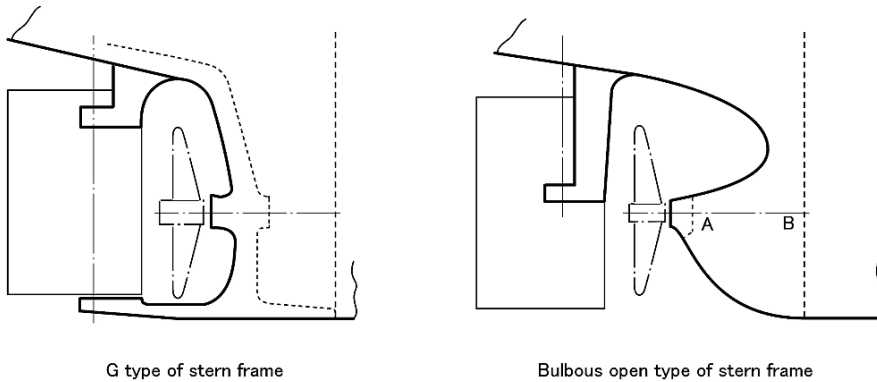


**Fig. 5.5.1** Stern frame structure

## 5.6 Shell Damage

Since the shell structure protects a ship from exterior forces, it suffers easily from damage by waves, and also collides with floating objects. From the viewpoint of preventing the flooding by seawater as a purpose of the shell, the damage is classified into 2 cases; with cracks and without cracks. When there are no cracks even if damage occurs on the shell, the shell structure will be allowable and safe actually. The outflow of oil from a large tanker becomes a social problem from the environmental protection point of view, hence cracks in the shell cannot be allowed.

An example in Fig. 3.1(a) shows that the shell plate was dented in more than 3 m inside the hold by the buckling of a cross tie. But cracking of the shell plate did not occur in this case fortunately. In the damage example shown in Fig. 3.1(b), the shell plate was bent severely together with damage of the transverse webs. In this case the shell plate deformed 300 mm outside convexly, and then a flying bird type crack occurred in the shell plate. This was to the propagation of the crack which was generated in the web plate of the transverse web.

Figure 5.6.1 shows an example of damage to the bottom shell plate of a VLCC, which occurred by contact with the seabed when she navigated through the Malacca Strait in the fully loaded condition. Cracking did not occur. Such damages at grounding are shown in the reference [19]

It is said that a crack will not occur in the case of a local dent in the shell plate, even though damage was suffered from wave impact as shown in Figs. 5.2.1 and 5.3.3. On the other hand, cracking of the shell will occur when hoop stress acts on the shell plate over a wide area caused by wave pressure, as shown in Fig. 5.3.1, and this cracking will start at a point having a welding defect.

Figure 5.6.2 shows damage with cracking which occurred due to lateral shearing forces by contact with a floating object. In addition, damage to the shell occurs often when the pushing force of a tug boat is excessive, or when the ship hits a pier at high speed.



**Fig. 5.6.1** Dent of bottom shell by grounding

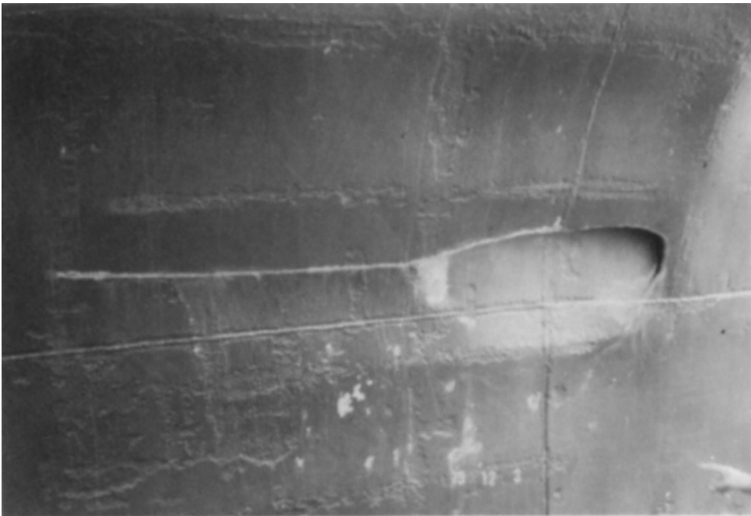


**Fig. 5.6.2** Cracks of shell plate by floating object

# Chapter 6

## Bulkheads

Bulkheads which are installed to form the boundary of a compartment in which liquid cargo is to be loaded support a normal perpendicular force on the bulkhead plate, in addition to this they support an in-plane force when they are installed as part of the frame work of the ship's whole structure, as explained in Chap. 1. Also the longitudinal bulkheads of a tanker support the tensile and compressive forces as well as the side shell plating, due to the longitudinal hull girder bending.

Especially in the case of a large ship, the in-plane force is important, and special attention is to be paid to the design of the swash bulkhead, in a long tank which is non-watertight and perforated.

A corrugated bulkhead is lighter than a stiffened plane bulkhead because it has no stiffeners but the plate itself plays the role of the stiffeners.

### 6.1 Strength of Bulkhead Plates

As well as for the side shell plating, the stress generated in a bulkhead plate is divided into the following four kinds. For a longitudinal bulkhead a similar consideration will be applied and hereafter the consideration on a transverse bulkhead is explained.

1. in-plane shearing stress for the frame work of the ship's whole structure  $\tau$
2. bending stress as the extreme fiber of a bulkhead stiffener  $\sigma_1$
3. max. bending stress at the midpoint of the longer edge of a bulkhead plate caused by the lateral water pressure  $\sigma_2$
4. max. bending stress at the midpoint of the shorter edge of a bulkhead plate caused by the lateral water pressure  $\sigma_3$

Among the above  $\sigma_2$  is the most important, and the magnitude is estimated as follows.

The plate thickness  $t$  of a transverse bulkhead is given by the following equation (Nippon Kaiji Kyokai's rule).

$$t = 3.6s\sqrt{h} + 3.5 \quad (6.1.1)$$

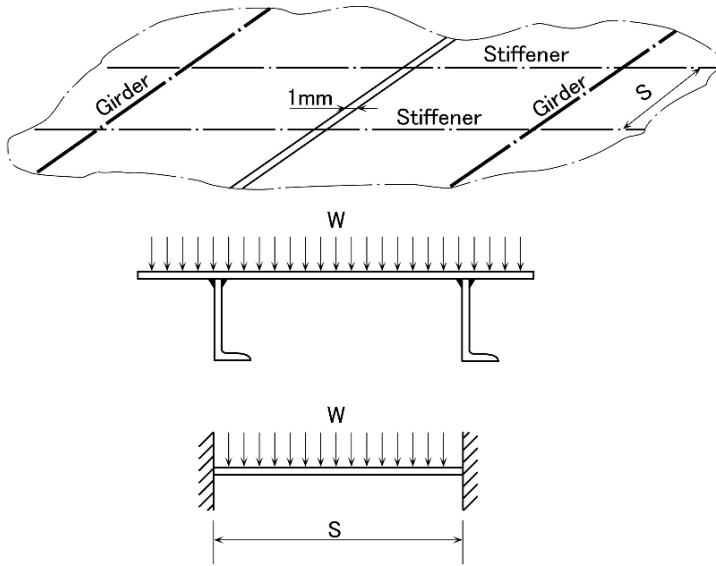


**Fig. 6.1.1** Structural model of plate subjected to lateral pressure

where

- $s$  : space of stiffeners in m
- $h$  : water head to the plate in m
- 3.5 : corrosion margin which is not a stress consideration

As the aspect ratio of a bulkhead plate is generally bigger than 2.0,  $\sigma_2$  is obtained by modeling a bulkhead plate as a both-ends-fixed beam with span  $s$  and a unit breadth of 1 mm, as shown in Fig. 6.1.1. The bending moment at a fixed end and the section modulus of the beam are given by the following equations.

$$M = \frac{h \cdot s^2}{12} \times 9.8 \quad (\text{kN} \cdot \text{mm}) \tag{6.1.2}$$

$$Z = \frac{t^2}{6} = \frac{3.6^2 \times s^2 h}{6} (\text{mm}^3) \tag{6.1.3}$$

$$\therefore \sigma_2 = \frac{M}{Z} = \frac{9.8hs^2}{12} \times \frac{6}{3.6^2 \times s^2 h} = 373 \text{ MPa} \tag{6.1.4}$$

Equation (6.1.4) shows that the bending stress in a bulkhead plate caused by the water pressure is quite high, however, the stress  $\sigma_2$  exists alone and not together with  $\sigma_1$  or  $\sigma_3$ .

The bending stress in a bulkhead plate caused by the water pressure exceeds the yield stress of mild steel, but actually the bulkhead plate has a higher strength than the calculated strength based on the simple elastic bending theory, because

the membrane force that is generated by the lateral water pressure supports higher pressure. In this situation at the beginning the plate is considered as an elastic beam, then plastic hinges are generated at both the fixed ends and at the midpoint of the beam, and finally the plate acts as a membrane; the plate supports higher water pressure than an elastic beam [20].

## 6.2 Horizontal Girders on Transverse Bulkheads (in Center Tank)

Here the measured behavior of a horizontal girder in a center tank with a vertical stiffener arrangement is explained. Nowadays, thanks to the development of computer calculations such as matrix methods of structural analysis for frame and shell, on-board measurements have scarcely been carried out. However, such calculated results depend on the boundary conditions which can be understood only by on-board measurements. It is important for a designer to confirm the accuracy of a calculation by measurement.

At around the end of the 1960's, the horizontal girder on a transverse bulkhead was designed as a girder with both ends fixed, assuming the span points where the girder was fixed. With the increase in size of ships the span of the horizontal girder was getting bigger and accordingly the question was raised whether span points for a smaller ship can be similarly applied to larger ships. Then measurements were carried out on board a 70,000 DWT tanker. The outline and the result of the measurements are shown in Fig. 6.2.1.

Assuming the horizontal girder has both ends elastically supported at the longitudinal bulkheads, the bending moment  $M$  at a point  $x$  m from a longitudinal bulkhead is presented by the following equation.

$$M = \mu \frac{wl^2}{12} - \frac{wl}{2}x + \frac{w}{2}x^2 \quad (6.2.1)$$

where

- $\mu$  : coefficient of degree of rigidity at ends
- $l$  : distance between longitudinal bulkheads
- $w$  : magnitude of applied uniform load

From the measurements, the distance  $x$  where  $M = 0$  and the moment at midspan  $x = l/2$  can be obtained. Then  $\mu$  and  $w$  are derived using (6.2.1) as follows:

$$\begin{aligned} \mu = 1.07, \quad w = 1.54w_0 & \text{ for No.2 horizontal girder} \\ \mu = 1.07, \quad w = 1.03w_0 & \text{ for No.3 horizontal girder} \end{aligned}$$

where  $w_0$  is the nominal applied load, that is, the product  $hb$  of the water head  $h$  and the breadth of the applied load  $b$  on the horizontal girder, as shown in Fig. 6.2.1.

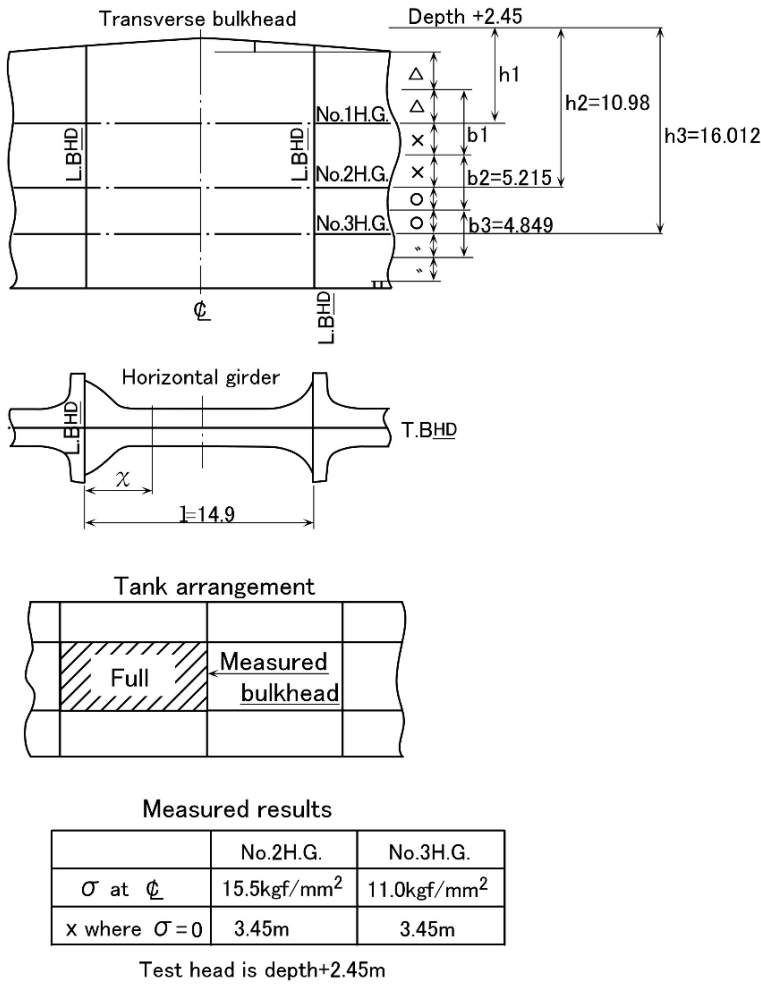


**Fig. 6.2.1** Example of stress measurement in horizontal girder of transverse bulkhead

Theoretically  $\mu = 1.0$  in the case where a girder is fixed at the longitudinal bulkhead, and  $\mu = 0$  in the case where a girder is supported at the longitudinal bulkhead with a value varying between 0 and 1.0 corresponding to the elasticity of the end condition. However the measured result shows that  $\mu = 1.07$  which is out of the above range. This means that the span point (fixed point) lies a little inside of the center tank from the longitudinal bulkhead as shown in Fig. 6.2.2.

The span point can be obtained by solving the following Eq. (6.2.2).



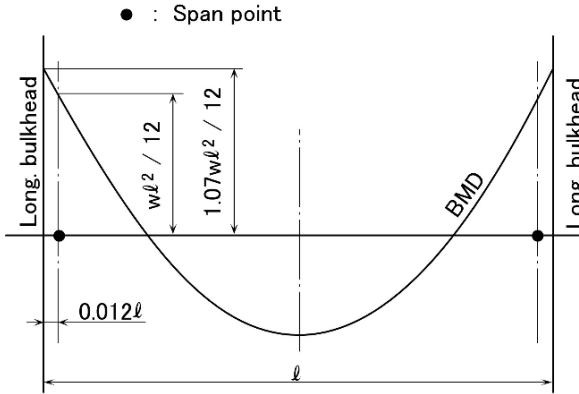


Fig. 6.2.2 Span point of horizontal girder of transverse bulkhead (Measured result)

$$M = 1.07 \frac{wl^2}{12} - \frac{wl}{2}x + \frac{w}{2}x^2 = \frac{wl^2}{12} \tag{6.2.2}$$

$$\therefore \frac{x}{l} = 0.0118$$

From the above results it was found that the span point lies at a point 1.2% of span inside of the center tank from the longitudinal bulkhead. It was made clear from the measurements that in spite of the big brackets at both ends of the horizontal girder, the span points are quite close to the longitudinal bulkheads.

One more important item made clear by the measurement relates to the load supporting ratio of each horizontal girder. Putting  $\mu = 1.0$ ,  $\alpha = w/w_0$  is calculated for each horizontal girder. Then  $\alpha = 1.32$  for the No.2 horizontal girder, and  $\alpha = 0.89$  for the No.3 horizontal girder are obtained. It can be understood that the load supporting ratio of the No.2 horizontal girder (at the mid-depth of the tank) is bigger than that of the No.1 and No.3 horizontal girders, which are connected to the rigid deck or bottom structures by vertical bulkhead stiffeners. However an  $\alpha = 1.32$  for the No.2 horizontal girder is more than common sense suggests.

Based on the above measured results, the following design criteria for the horizontal girder in a center tank are established.

1. The span is to be equal to the distance between the longitudinal bulkheads.
2. The ratio  $\alpha$  between the design load and the nominal load is to be:
  - 1.35 for the middle girder in the case of a one or three horizontal girder arrangement.
  - 1.15 for the uppermost horizontal girder in the case of a two or more horizontal girder arrangement.
  - 1.0 for other horizontal girders.

Applying the above criteria on ships in service, the data shown in Table 6.2.1 were obtained. The data show the differences between classification societies.

**Table 6.2.1** Calculated bending stress and shearing stress of horizontal girder of transverse bulkhead

Ship	Class	$\sigma$ ( kgf / mm <sup>2</sup> )			$\tau$ ( kgf / mm <sup>2</sup> )			$\tau_{cr} / \tau$			Note
		Upper	Middle	Lower	Upper	Middle	Lower	Upper	Middle	Lower	
A	NK	13.5	18.3	14.0							
B	NK	16.8	23.0	17.4							
C	AB	8.2	10.2	7.2							
D	NK	15.1	20.1	14.6							
E	NK	18.8	24.0	15.6							
F	NK	17.2	25.7	16.2							
G	AB NK	6.2	5.8	4.6	6.2	8.7	9.1	3.0	2.2	2.1	
H	NK	7.3	10.1	8.1	4.6	7.5	6.8	4.9	3.0	3.4	
I	NV				/	11.6	/		0.8		
J	AB				/	9.5	/		1.8		
K	NK				/	11.0	/		1.6		
L	NK				9.0	/	7.7	2.3		3.4	
M	AB				/	10.6	/		1.8		
N	AB				/	10.4	/		1.9		
O	AB				/	12.2	/		1.3		
P	LR				/	10.2	/		1.9		
Q	AB				/	12.6	/		1.8		
R	LR				7.1	11.0	11.7	2.4	1.6	1.5	
S	AB				6.1	8.1	6.3	3.9	2.9	3.8	

NK – Nippon Kaiji Kyokai

AB – American Bureau of Shipping

NV – Det Norske Veritas

LR – Lloyd's Register of Shipping

### 6.3 Horizontal Girder Arrangement on Bulkheads

The water pressure on a bulkhead of a tank increases with water depth. In the case of a vertical stiffener system, the vertical stiffeners with a uniform section are to be arranged so as to be supported by horizontal girders, deck and bottom. In this condition the horizontal girders are best arranged so as to have an equal bending moment in each vertical stiffener supported by the horizontal girders, deck and bottom.

The bending moment in each vertical stiffener supported by the horizontal girders, deck and bottom is proportional to the product  $hl^2$  of the water head  $h$  at the midspan of the vertical stiffener, and the square of the span  $l^2$ . The condition for

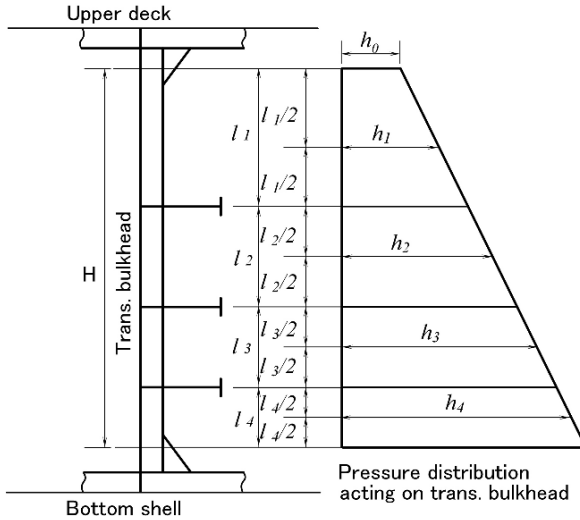


**Fig. 6.3.1** Optimum arrangement of horizontal girders on transverse bulkhead for lateral pressure equal bending moment in each vertical stiffener is the following:

$$h_i l_i^2 = \text{constant} \quad (i = 1, 2, 3, \dots) \tag{6.3.1}$$

For example, in the case of a three horizontal girders arrangement, as shown in Fig. 6.3.1, the following equation can be obtained:

$$h_1 l_1^2 = h_2 l_2^2 = h_3 l_3^2 = h_4 l_4^2 \tag{6.3.2}$$

The water head for each stiffener  $h_1, h_2, h_3$  and  $h_4$  can be expressed using the water head  $h_0$  at the top span point of the uppermost stiffener, and the span of each stiffener expressed as  $l_1, l_2, l_3$  and  $l_4$ , then the following equations are derived:

$$\left(h_0 + \frac{l_1}{2}\right) l_1^2 = \left(h_0 + l_1 + \frac{l_2}{2}\right) l_2^2 \tag{6.3.3}$$

$$= \left(h_0 + l_1 + l_2 + \frac{l_3}{2}\right) l_3^2 \tag{6.3.4}$$

$$= \left(h_0 + l_1 + l_2 + l_3 + \frac{l_4}{2}\right) l_4^2 \tag{6.3.5}$$

Equation (6.3.3) can be written as follows and the relation between  $l_1/l_2$  and  $h_0/l_1$  can be obtained:

$$\frac{l_1}{l_2} = \sqrt{\frac{\frac{h_0}{l_1} + 1 + \frac{l_2}{2l_1}}{\frac{h_0}{l_1} + \frac{1}{2}}} \tag{6.3.6}$$

In a similar way, Eq. (6.3.4) will become

$$\frac{l_1}{l_3} = \sqrt{\frac{\frac{h_0}{l_1} + 1 + \frac{l_2}{l_1} + \frac{l_3}{l_1}}{\frac{h_0}{l_1} + \frac{1}{2}}} \tag{6.3.7}$$

And (6.3.5) will become

$$\frac{l_1}{l_4} = \sqrt{\frac{\frac{h_0}{l_1} + 1 + \frac{l_2}{l_1} + \frac{l_3}{l_1} + \frac{l_4}{2l_1}}{\frac{h_0}{l_1} + \frac{1}{2}}} \tag{6.3.8}$$

From Eqs. (6.3.6), (6.3.7) and (6.3.8), the span ratios of  $l_2/l_1, l_3/l_1$  and  $l_4/l_1$  are expressed as the function of the water head  $h_0/l_1$ .

Accordingly the optimum girder arrangement is obtained as shown in Fig. 6.3.2 in which the span of each stiffener is given as the ratio against the total length of stiffeners  $H$ . In Fig. 6.3.2 the optimum girder arrangements in the cases of one horizontal girder and two horizontal girders are also indicated. Figure 6.3.2 shows

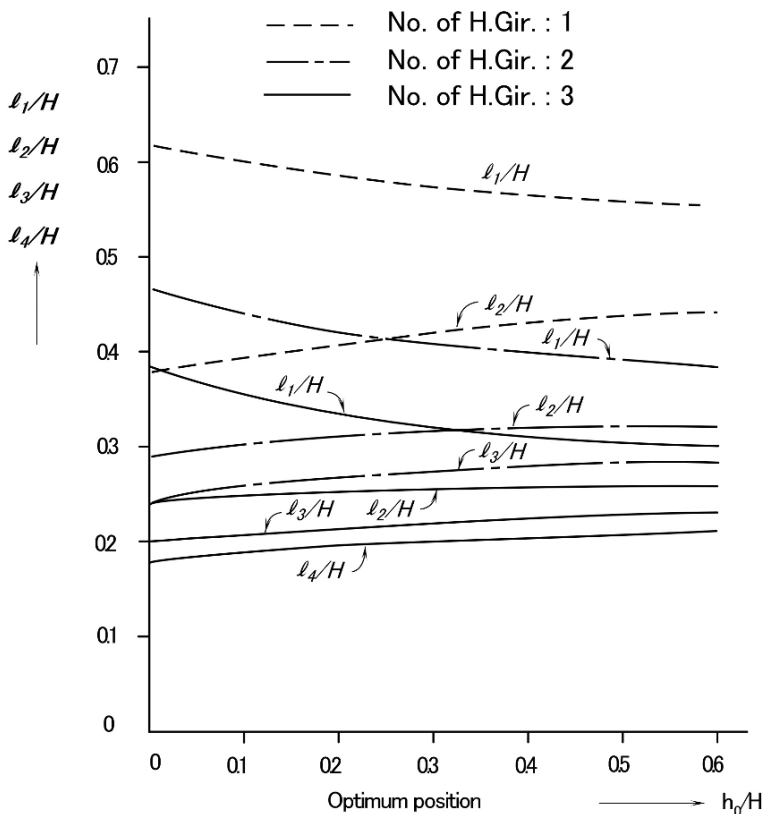
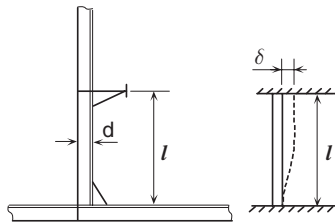


Fig. 6.3.2 Optimum position of horizontal girders subjected to lateral pressure

that the span of the uppermost stiffener is 1.5 or 2.0 times longer than the span of the lower stiffener; a bigger  $h_0$  will reduce the difference between the spans of the stiffeners.

### 6.4 Vertical Stiffeners on Transverse Bulkheads

In the design of a vertical stiffener on a transverse bulkhead which is supported at one side or both sides by horizontal girders, not only the water pressure but also the displacement of the horizontal girders needs to be considered. The lowest stiffener



$$\sigma = 6E \frac{y}{l} \cdot \frac{\delta}{l}$$

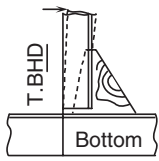
Where

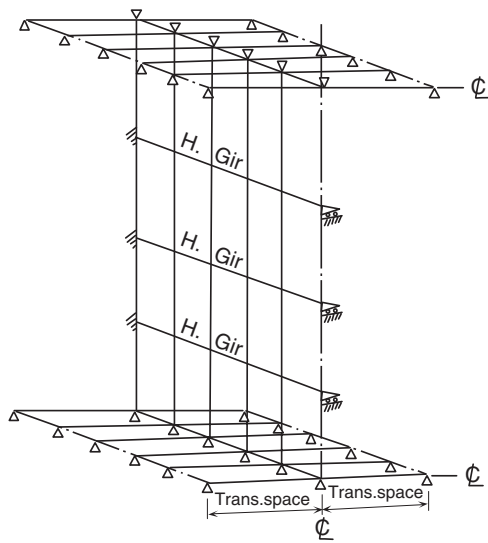
- E ... Young's modulus
- y ... Distance between center of gravity and extreme fibre of stiffener section

Assume  $y \approx d$

$$\sigma = 6E \frac{d}{l} \cdot \frac{\delta}{l}$$

(A) Additional stress on stiffener caused by deflection of horizontal girder





(B) Example of damage

(C) Modelization of T. BHD

**Fig. 6.4.1** Additional stress of stiffener due to deflection of horizontal girder and example of damage

especially suffers from the effect of displacement of the lowest horizontal girder because of the smaller span, no displacement at the bottom, and the large depth of the stiffener. Figure 6.4.1(A) shows the additional stress in the vertical stiffener caused by the displacement of the horizontal girder, and Fig. 6.4.1(B) shows an example of the damage caused by the additional stress.

In the design of a vertical stiffener on a transverse bulkhead of a large ship, the displacement of the horizontal girders is first calculated, including the effect of the stiffness of the vertical stiffeners, and the scantling of the vertical stiffener is then decided considering the displacement of the horizontal girders. The model of the calculation is shown in Fig. 6.4.1(C).

In the case of a large displacement of the lowest horizontal girder, a large bracket connecting the horizontal girder to the adjacent bottom transverse is to be fitted to reduce the displacement, as shown in Fig. 6.4.2. Attention needs to be given to the design of the vertical stiffener between the lowest horizontal girder and the second one from the bottom, because the relative displacement between them is considerable.

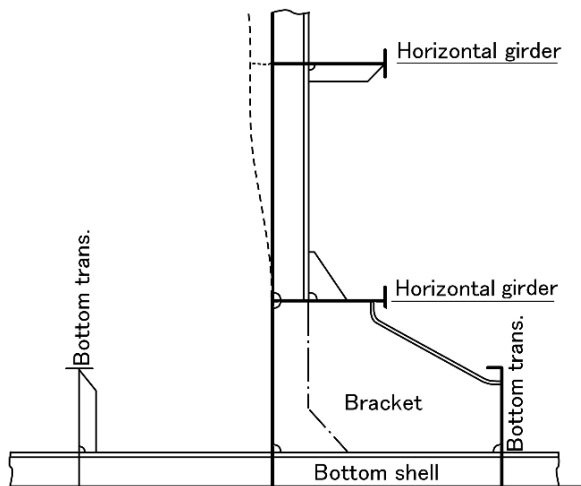


Fig. 6.4.2 Large bracket reducing deformation of horizontal girder

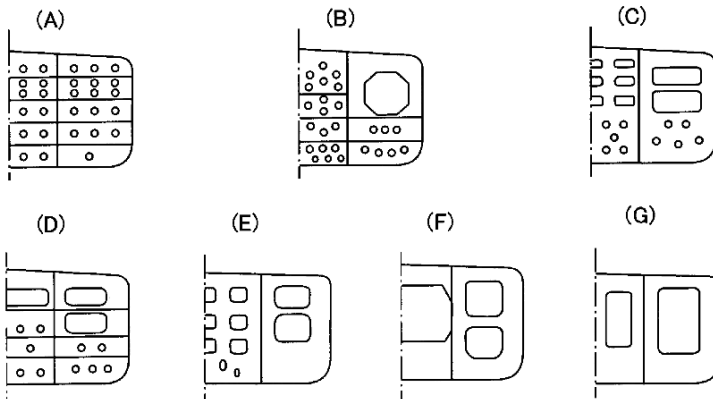
## 6.5 Swash Bulkheads

At the beginning of the era in large increase in ship size much research was carried out and rationalization was achieved with the fruits of the research. One special fruit was the increase of the tank length. For a 30,000 DWT tanker the cargo oil tank length was 9 m or 12 m. With the increase in size of tankers a longer tank length was applied, for example from 15 m up to 45 m. In such long tanks one or two swash bulkheads were provided to avoid high dynamic water pressure on the transverse

**Table 6.5.1** opening shape of swash bulkhead, opening area ratio and weight ratio

Ship	Principal dimensions (m)			Class	Type of swash bhd	Opening area ratio		Swash bulkhead weight ① (T/m <sup>2</sup> )		Tight bulkhead weight ② (T/m <sup>2</sup> )		Weight ratio ①/②	
	L	B	D			Center tank	Wing tank	Center tank	Wing tank	Center tank	Wing tank	Center tank	Wing tank
	A	320.0	54.5			27.0	NK	F	0.52	0.35	0.10	0.13	0.37
B	190.0	28.2	17.0	NK	F	0.66	0.34	0.06	0.09	0.21	0.21	0.28	0.43
C	250.4	41.6	23.3	AB	E	0.17	0.38	0.17	0.13	0.34	0.28	0.50	0.46
D	320.0	54.5	27.0	AB	E	0.16	0.35	0.21	0.13	0.38	0.33	0.55	0.39
E	300.0	50.5	27.0	AB	E	0.14		0.21		0.35		0.60	
F	320.0	54.5	26.0	AB	E	0.17	0.30	0.21	0.16	0.36	0.33	0.58	0.48
G	360.0	62.0	36.0	AB	E	0.19		0.25		0.51		0.49	
H	260.0	43.5	22.8	AB	G	0.30	0.30	0.20	0.13	0.31	0.28	0.65	0.47
I	300.0	50.0	27.0	NK	C	0.14	0.28	0.22	0.19	0.36	0.35	0.61	0.54
J	300.0	50.0	27.0	NK	D	0.29	0.28	0.17	0.19	0.36	0.35	0.47	0.55
K	320.0	54.5	27.0	AB	B	0.13	0.27	0.22	0.16	0.36	0.33	0.61	0.49
L	307.0	48.2	25.5	AB	D	0.49	0.32	0.11	0.14	0.34	0.31	0.32	0.45
M	330.0	54.5	35.0	AB	D	0.27	0.28	0.19	0.16	0.40	0.35	0.48	0.46
N	330.0	54.5	35.0	AB	A	0.11	0.08	0.24	0.22	0.40	0.35	0.60	0.63
O	260.0	43.5	22.8	NK	A	0.14	0.12	0.22	0.18	0.30	0.25	0.73	0.72
P	230.0	32.2	10.7	AB	G		0.29		0.12		0.24		0.50

Type of swash bulkhead



bulkhead due to cargo oil movement. The swash bulkhead is non-tight and has uniform thickness of 10 mm or 12 mm with openings as shown in Table 6.5.1. Such an arrangement is good for avoiding cargo oil movement but has low shear rigidity to assist the frame work of the hull structure or to support the primary supporting members. Figure 1.1.1 shows damage caused by the lack of rigidity of a swash bulkhead.

In a swash bulkhead, openings of many kinds of shape are cut out. However the shape of the cut-out does not affect the shear rigidity too much. The shear rigidity depends mainly upon the area ratio of the opening. Figure 6.5.1 shows the relation

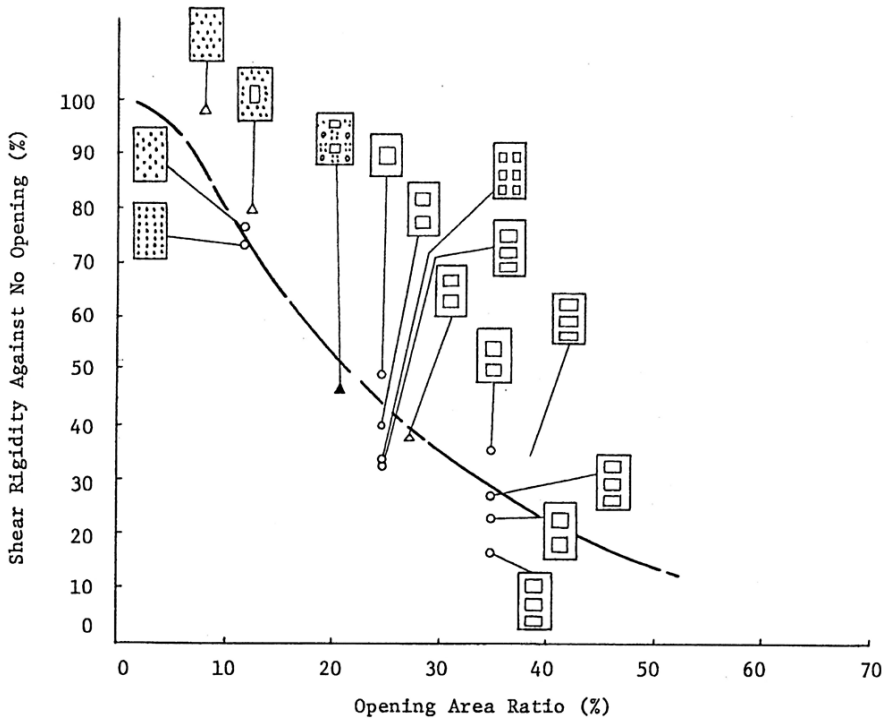


Fig. 6.5.1 Shear rigidity and opening area ratio of swash bulkhead

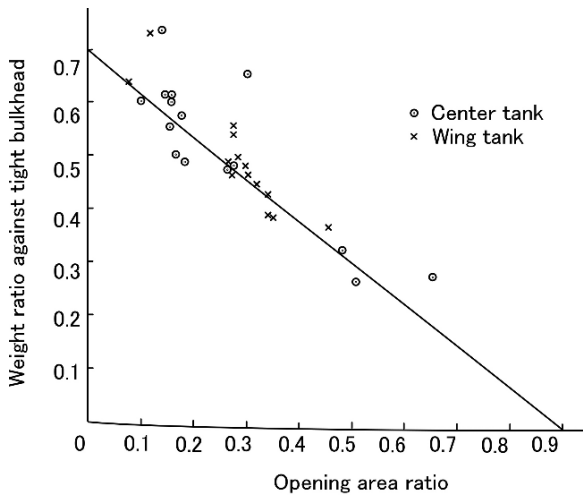


Fig. 6.5.2 Weight ratio of swash bulkhead vs. opening area



between the shear rigidity and the area ratio of the opening [21], and Fig. 6.5.2 shows the relation between the opening area ratio and the weight ratio of a swash bulkhead relative to a tight bulkhead. From Fig. 6.5.2 it can be seen that the swash bulkhead without opening has 70% of the weight of the tight bulkhead which means the shear rigidity of the swash bulkhead will be about 70% of that of a tight bulkhead, even in the case of no opening. Some times an ore carrier or an ore/oil carrier is designed with an arrangement that has a swash bulkhead only in a wing tank and no bulkhead in the center tank at the same frame line. In this case the horizontal girders on the swash bulkhead support compressive force in the same way as the cross ties of an ordinary transverse ring, as explained in Sect. 3.5. Attention should be given not to cause any buckling.

### 6.6 Horizontal Stiffeners on Transverse Bulkheads

Nowadays a transverse bulkhead is constructed with vertical stiffeners, but previously horizontal stiffeners were used. In the case of a horizontal stiffener system, the horizontal stiffeners were not arranged at the same level as the longitudinal stiffeners on the longitudinal bulkhead, or on the side shell and no connection was provided between them. The ends of the horizontal stiffeners were snipped. The horizontal stiffeners were supported by vertical webs which were arranged so as to have an equal bending moment on the horizontal stiffener at the supporting points.

The horizontal stiffener can be modeled as shown in Fig. 6.6.1. And the following equation is derived by the three moment theory:

$$\frac{M_B}{3}(\alpha l + l) + \frac{M_c l}{6} = \frac{w\alpha^3 l^3}{24} + \frac{wl^3}{24} \tag{6.6.1}$$

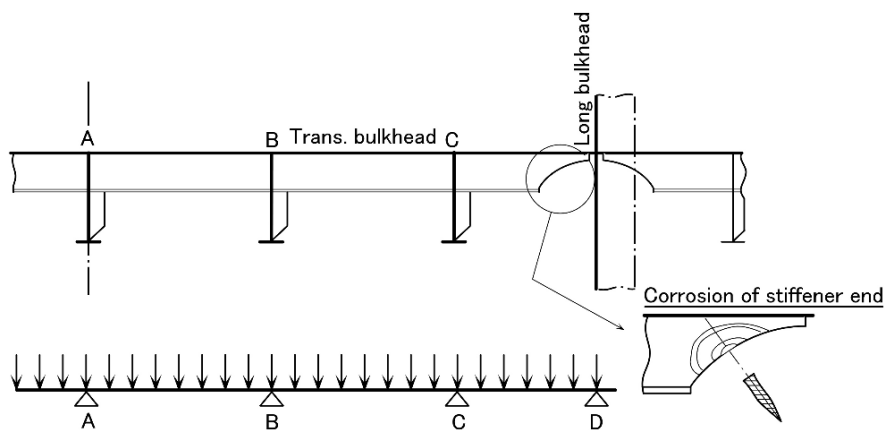


Fig. 6.6.1 Horizontal stiffener of trans. bulkhead

where

- $l$  : span of horizontal stiffener at midpart
- $\alpha l$  : span of horizontal stiffener at end
- $M_B$  and  $M_C$  : bending moments at point B and point C respectively

In (6.6.1) assuming  $M_B = M_C = wl^2/12$ ,  $\alpha = 0.816$  can be obtained, that is, where the end span is 81.6% of the midspan, the bending moments at the supporting points by the vertical webs will be equal.

The horizontal stiffener system was applied on 40,000 or 50,000 DWT tankers at the beginning of the era of the large increase in size of ships. The problem was corrosion at the snip end as shown in Fig. 6.6.1.

A transverse bulkhead supports the water pressure corresponding to the water head, accordingly the lower part is designed to be stronger than the upper part. As shown in Fig. 6.6.2 where the horizontal stiffeners are arranged to have equal spacing, the lower stiffener has the bigger scantling corresponding the water head. In addition to this the lower bulkhead plate is thicker than the upper one but in a plate, the thickness is uniform. In Fig. 6.6.2 the A and B parts have the same thickness so the B part which supports less water pressure than the A part, has excess strength. The excess strength is caused by the equal thickness of the plate and the equal space arrangement of the horizontal stiffeners, and can be avoided by applying non-uniform thickness or unequal spacing.

The thickness  $t$  of the bulkhead plate is given by Nippon Kaiji Kyokai's rule as the followings.

$$t = 3.6s\sqrt{h} + 3.5 \tag{6.6.2}$$

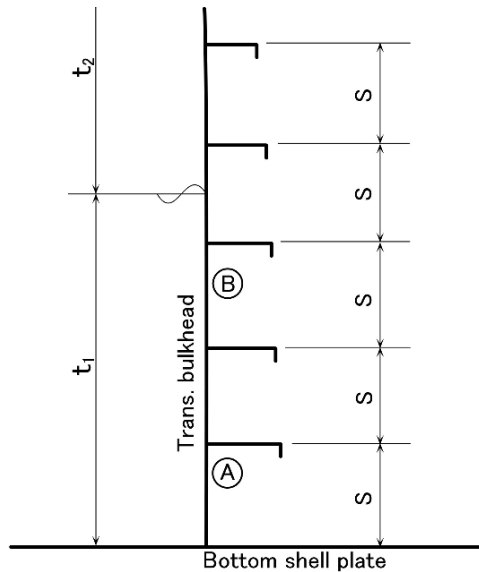


**Fig. 6.6.2** Horizontal stiffener arrangement of trans. bulkhead

And the section modulus  $Z$  of the horizontal stiffener is given as follows.

$$Z = 7cshl^2 \tag{6.6.3}$$

where

- $h$  : water head
- $s$  : stiffener space
- $l$  : span of stiffener
- $c$  : coefficient (in case of bracket connection  $c = 0.7$ )

In the case of an equal space arrangement of the stiffeners, the thickness of the bulkhead plate is to be proportional to  $\sqrt{h}$ . Existing steel mill technology is able to roll such a non-uniform thickness plate, however in a shipyard some difficulty in the material control will appear. Another possibility is unequal spacing of stiffeners with uniform plate thickness, which is practical. Equation (6.6.2) can be modified as follows.

$$s = \frac{t - 3.5}{3.6\sqrt{h}} \tag{6.6.4}$$

Putting the lowest stiffener space as  $s_1$ , the next space as  $s_2$  and so on, and putting the corresponding water head as  $h_1, h_2$  and so on, the following equation can be obtained.

$$s_i = \frac{t - 3.5}{3.6\sqrt{h_{i-1} - s_{i-1}}} \tag{6.6.5}$$

where

$$s_1 = \frac{t - 3.5}{3.6\sqrt{h_1}}$$

$$i = 2, 3, 4, \dots$$

As an example,  $s_i$  is calculated putting  $t = 15$  mm and  $h = 16$  m, and the result is shown in Table 6.6.1. In this stiffener arrangement the required section modulus of the stiffener is given by the following equation.

**Table 6.6.1** Required stiffening space keeping constant panel thickness—Equation (6.6.4)

i	$S_i$ (mm)	$S_i / S_1$
1	799	1.000
2	819	1.025
3	842	1.054
4	868	1.086
5	897	1.123
6	931	1.165
	total	
	5,156	

**Table 6.6.2** Required section modulus of stiffener keeping constant panel thickness—Equation (6.6.6)

i	Z <sub>i</sub> ( cm <sup>3</sup> )	W ( kg/m )	Z <sub>i</sub> / Z <sub>1</sub>
1	1,220	52.0	1.000
2	1,186	51.3	0.972
3	1,149	50.5	0.942
4	1,110	49.6	0.910
5	1,068	48.7	0.875
6	1,023	47.7	0.839
		total	
		299.7	

$$Z_i = 7cl^2 \cdot \frac{1}{2}(s_i + s_{i+1})(h_{i-1} - s_i) \tag{6.6.6}$$

In the case of  $c = 0.7$ ,  $l = 4.5$  m and  $h_0 = 16$  m,  $Z_i$  is calculated and shown in Table 6.6.2 in which the weight of the stiffener per unit length (kg/m) is also shown. The stiffener is assumed to have the optimum section shape.

The total length of  $s_1$  to  $s_6$  is 5,156 mm which corresponds to an equal spacing of 859.3 mm multiplied by 6. In this case the bulkhead plate thickness is 15.87 mm according to (6.6.2), and the required section modulus  $Z_i$  is calculated for each water head according to (6.6.3); this is shown in Table 6.6.3.

Comparing Table 6.6.2 with Table 6.6.3 it can be found that in the case of the unequal space arrangement the difference between the required section modulus of the adjacent stiffeners is smaller than that in the equal space situation, which is good for material management. In addition to the above, the total weight of plate and stiffeners of the 5,156 mm breadth and 1 m length panel is 906.8 kg/m for the unequal space arrangement, and 939.59 kg/m for the equal space arrangement.

The above suggests that a profit can be produced by applying a non-uniform instead of a uniform structure [22].

**Table 6.6.3** Required section modulus of stiffener keeping constant stiffening space

i	Z <sub>i</sub> ( cm <sup>3</sup> )	W ( kg/m )	Z <sub>i</sub> / Z <sub>1</sub>
1	1,291	53.5	1.000
2	1,218	52.0	0.943
3	1,144	50.4	0.886
4	1,071	48.8	0.830
5	998	47.1	0.773
6	925	45.3	0.716
		total	
		297.1	

### 6.7 Minimum Thickness of Longitudinal Bulkhead Plates

The main role of a longitudinal bulkhead is to support the water pressure as well as a transverse bulkhead. However in large ships some examples of buckling caused by an in-plane shearing force have occurred. The longitudinal bulkhead is one of the longitudinal strength members and supports the longitudinal bending moment which causes a tensile or compressive stress in the top and the bottom strakes of the longitudinal bulkhead. However, buckling damage caused by compressive stress has been scarcely reported because of the thicker top and bottom strakes where high compressive stress is generated. On the other hand, for plates around the neutral axis of the hull girder, where the shearing force is maximum, the minimum thickness for the water pressure is usually applied. This is a reason why the buckling is caused by a shearing force and not by a bending moment. An example of the buckling is shown in Fig. 6.7.1. In this case the thickness at the neutral axis is 14 mm and above the neutral axis it is 13 mm and 12 mm, below the neutral axis 15 mm and 16 mm. The buckling occurred on the 14 mm thick plate around the neutral axis and on the 13 mm and the 12 mm thick plates above the neutral axis. No buckling occurred on the 15 mm and the 16 mm thick plates below the neutral axis. The buckling pattern has an oblique axis which means the buckling is caused by the shearing force.

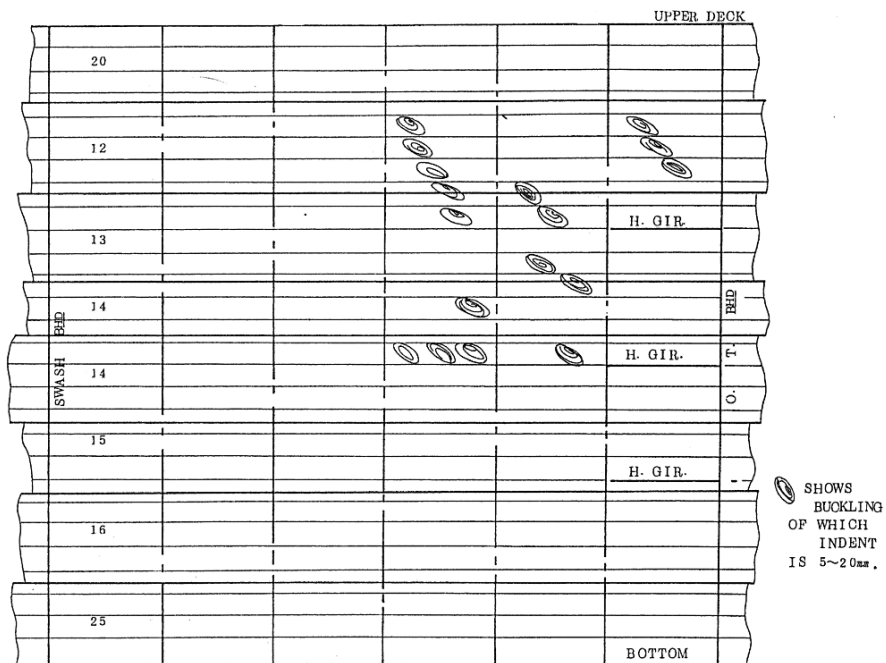


Fig. 6.7.1 Example of buckling on longitudinal bulkhead

To avoid such buckling damage, the minimum thickness of a longitudinal bulkhead is to be decided based on the shearing force. The shearing force at a transverse section of a tanker is supported by the longitudinal bulkheads and the side shells. Disregarding the relative displacement between the longitudinal bulkhead and the side shell, the supporting ratio is given by the following equation.

$$F = 2(\alpha_L F + \alpha_S F) \tag{6.7.1}$$

where  $F$  is shearing force,  $\alpha_L$  and  $\alpha_S$  are supporting ratio coefficients for the longitudinal bulkhead and the side shell respectively. According to the above expression the shearing force  $F_L$  to be supported by the longitudinal bulkhead is given by the following equation.

$$F_L = \alpha_L F \tag{6.7.2}$$

The maximum shearing stress in the longitudinal bulkhead  $\tau_{\max}$  appears in the thinnest plate and is expressed by the following equation.

$$\tau_{\max} = \frac{F_L}{D \cdot t_L} = \frac{\alpha_L F}{D \cdot t_L} \propto \frac{\alpha_L \Delta}{D \cdot t_L} \tag{6.7.3}$$

where

- $D$ : depth of ship.
- $t_L$ : thinnest plate thickness of longitudinal bulkhead.
- $\Delta$ : full load displacement.

Table 6.7.1 and Fig. 6.7.2 show the relationship between  $\tau_{\max}$ , which is represents by  $(\alpha_L \Delta / D \cdot t_L)$ , and the ship length in service.

Figure 6.7.2 shows that a bigger  $\tau_{\max}$  exists for bigger ships. This comes from the assumption that the maximum shearing force is proportional to the full load displacement.

**Table 6.7.1** Max. shearing stress of logitudinal bulkhead

Ship	$L$	$B$	$D$	$d$	$\Delta$	$a$	$b$	$\frac{b}{a+b}$	$t_L$	$t_s$	$\alpha_0^L$	$\frac{\alpha^L}{\alpha_0^L}$	$\alpha^L$	$\frac{\Delta \cdot \alpha^L}{D \cdot t_L}$
A	360.0	62.0	36.0	28.00	547,300	10.34	20.66	0.666	14.0	26.0	0.175	1.213	0.212	230.0
B	330.0	54.5	35.0	27.00	424,890	9.40	17.85	0.655	14.0	26.0	0.175	1.215	0.213	185.0
C	320.0	54.5	27.0	21.00	312,435	9.40	17.85	0.655	14.0	23.0	0.189	1.215	0.230	190.0
D	300.0	50.0	27.0	20.70	266,469	8.46	16.54	0.661	14.0	24.0	0.184	1.210	0.223	157.0
E	279.6	44.5	24.7	18.88	201,063	8.10	14.15	0.635	14.0	23.5	0.187	1.220	0.228	133.0
F	230.0	40.0	18.0	13.50	102,154	7.20	12.80	0.640	12.5	22.0	0.181	1.218	0.218	99.0
G	230.0	33.0	21.7	15.15	94,560	7.45	9.05	0.548	9.5	20.0	0.161	1.220	0.196	89.8
H	230.0	35.5	18.0	12.46	84,551	7.65	10.00	0.566	10.0	20.0	0.167	1.222	0.204	95.8
I	236.0	38.0	17.2	12.05	90,356	8.50	10.50	0.552	10.5	21.0	0.167	1.220	0.204	102.0
J	340.0	68.0	29.0	22.60	426,234	11.28	22.72	0.668	15.0	22.0	0.203	1.210	0.246	241.0
K	320.0	54.5	28.0	21.00	312,360	11.75	15.50	0.569	14.0	24.5	0.182	1.220	0.222	177.0
L	278.8	44.5	24.5	17.90	191,412	9.00	13.25	0.600	14.0	23.0	0.189	1.220	0.230	128.0
M	190.0	28.2	17.0	12.60	55,183	4.80	9.30	0.660	11.5	18.5	0.203	1.220	0.248	70.0

Note :  $L$  : length of ship  
 $B$  : breadth of ship  
 $D$  : depth of ship  
 $b$  : draft of ship  
 $\Delta$  : full load displacement  
 $a, b$  : See Figure 6.8.1  
 $t_L$  : min. thickness of longitudinal bulkhead  
 $t_s$  : thickness of side shell

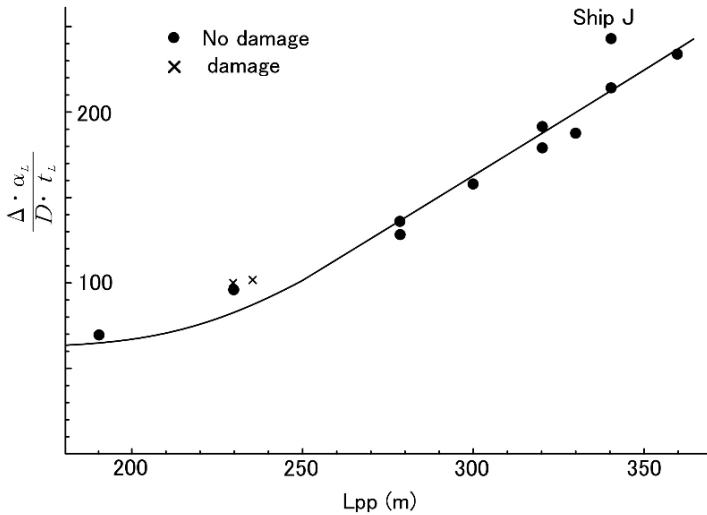


Fig. 6.7.2 Max. shearing stress of longitudinal bulkhead vs. ship length

Ship J, which is in the design stage, are considered not to be sufficient, while the designed thickness of 15 mm for the longitudinal bulkhead and 22 mm for the side shell, To have a similar value of  $(\alpha_L \Delta / D \cdot t_L)$  as that for ships in service without any damage, the designed thickness of 15 mm for the longitudinal bulkhead is to be increased up to 19 mm keeping 22 mm for the side shell thickness. In another way the value of  $(\alpha_L \Delta / D \cdot t_L)$  can be reduced by increasing the side shell plate. In this case the designed thickness of 22 mm for the side shell will be increased up to 30 mm, keeping 15 mm for the longitudinal bulkhead.

For reinforcement against the shearing force due to the longitudinal hull girder bending, it is usual to increase the side shell plate thickness. However as explained above the longitudinal bulkhead also supports the shearing force, so it is recommended to apply an efficient countermeasure, considering the supporting ratio coefficients for the longitudinal bulkhead and the side shell.

Actually the side shell plate is more important than the longitudinal bulkhead, and the ratio of the longitudinal bulkhead thickness  $t_L$  to the side shell thickness  $t_S$  will realistically fall between 0.55 and 0.80 ( $0.55 \leq t_L/t_S \leq 0.80$ ).

## 6.8 Sharing Ratio of Shearing Force

The sharing ratio of the shearing force by the longitudinal bulkhead  $\alpha_L$  and the side shell  $\alpha_S$  can be obtained by the following equations [23].

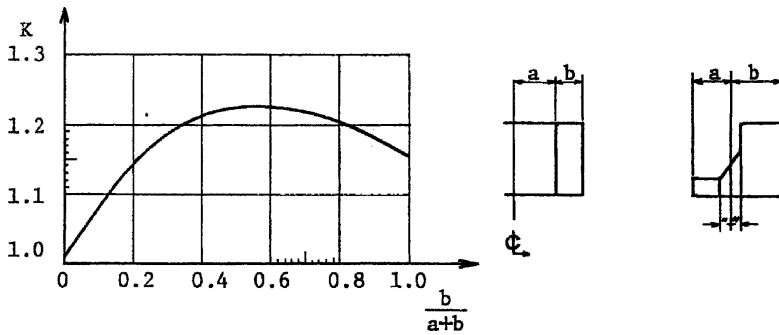


Fig. 6.8.1 Sharing coefficient of shear force on longitudinal bulkhead

$$\alpha_L + \alpha_S = \frac{1}{2} \quad (6.8.1)$$

$$\alpha_L = K\alpha_{L0} \quad (6.8.2)$$

$$\alpha_{L0} = \frac{t_L}{2(t_L + t_S)} \quad (6.8.3)$$

$K$  depends upon the distance between the longitudinal bulkhead and the center line and is given in Fig. 6.8.1. Figure 6.8.1 is effective in the case of a two-longitudinal bulkhead arrangement.

The sharing ratio of the shearing force by the longitudinal bulkhead is decided by the distance between the longitudinal bulkhead and the center line, and the minimum thickness of the longitudinal bulkhead.  $K$  has a maximum value of 1.23 where  $b/(a+b)$  is 0.5, where the longitudinal bulkhead lies at a quarter of the ship breadth from the side shell. And  $K$  decreases corresponding to the distance between the longitudinal bulkhead and the center line down to 1.15 where the longitudinal bulkhead lies at the center line. On the other hand,  $K$  decreases also in cases of a closer position of the longitudinal bulkhead to the side shell, down to 1.0 where the longitudinal bulkhead comes to the side shell position. And the value 1.0 means that the effect of the longitudinal bulkhead becomes the same as the side shell.

$\alpha_{L0}$  increases incrementally in the minimum thickness of the longitudinal bulkhead. This will be the natural providence that the stronger one supports more load. And the rate of increase can be reduced by arranging closer for the longitudinal bulkhead to be closer to the side shell. From this viewpoint, a criterion of  $0.55 \leq t_L/t_S \leq 0.80$  stated in the previous section can be said to be practical.

In the case of a three longitudinal bulkheads arrangement, an example of the sharing ratio is shown in Figs. 6.8.2 and 1.3.3. This was calculated for a 600,000 DWT tanker which was not built actually. Figure 6.8.2 shows that the center line longitudinal bulkhead supports more than one of the longitudinal bulkheads. The longitudinal bulkheads of a two-longitudinal bulkhead arrangement, and even the side longitudinal bulkheads in the case of a three-longitudinal bulkhead arrangement can be extended into the engine room to maintain the structural continuity. However the center line longitudinal bulkhead cannot be extended into the engine room. On the



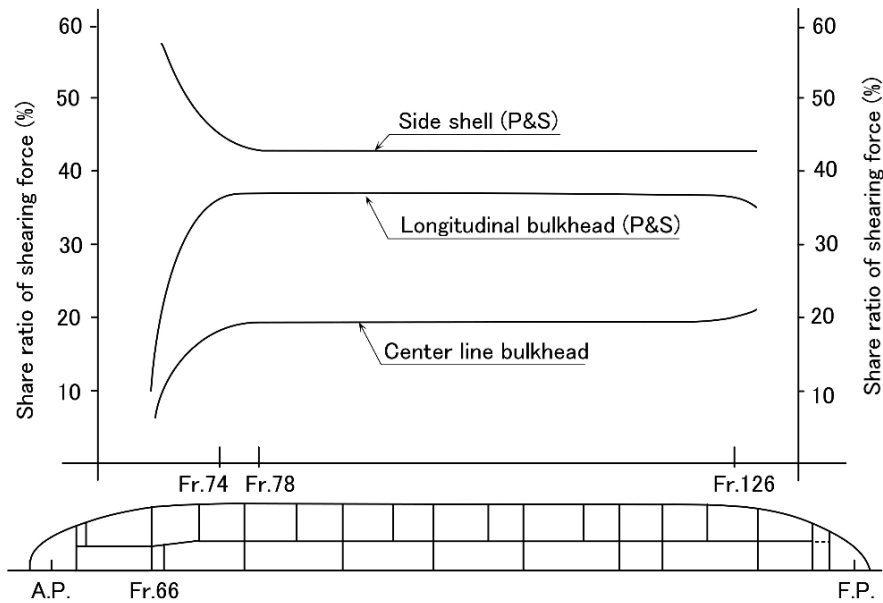


Fig. 6.8.2 Share ratio of shearing force of a tanker with three longitudinal bulkheads

other hand in the forward part the side longitudinal bulkheads are not extended into the fore peak tank but the centerline longitudinal bulkhead is. In such cases some countermeasures are necessary to maintain the structural continuity.

In Sect. 1.3 “Bulkhead Arrangement out of Cargo Hold” some attention to maintain the structural continuity at the ends of the cargo hold were introduced. And here special attention should be paid to the fact that the shearing force supporting ratio of the longitudinal bulkhead reduces at some distance from the ends of the longitudinal bulkhead.

## 6.9 Corrugated Bulkheads

In a corrugated bulkhead the bulkhead plate itself resists the lateral load, such as water pressure, with a wave shaped section as shown in Fig. 6.9.1. Here, how to decide the shape and the scantlings is explained.

A corrugated bulkhead consists of parallel plates, and sloping plates which connect the parallel plates. Both of them support the water pressure equally and can have the same plate thickness provided the breadth is equal. In such a case the corrugated bulkhead can be made from one plate by bending. The strength calculation is to be carried out using the half breadth  $S$  of a wave as shown in Fig. 6.9.1. Assuming the breadth of the parallel plate and the sloping plate are both  $a$  and the distance between the parallel plates is  $H$ , the following equations are obtained:

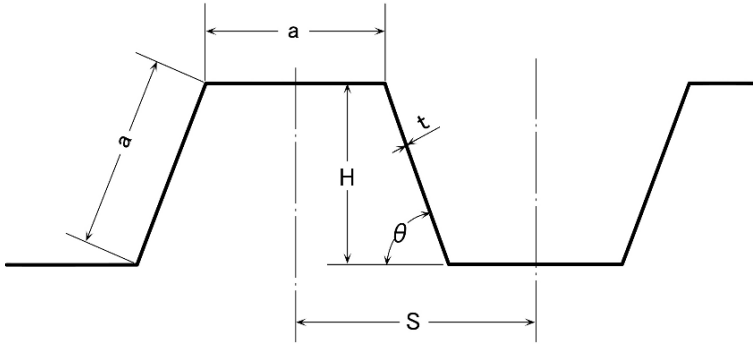


Fig. 6.9.1 Plan of corrugated bulkhead

$$a \sin \theta = H \quad (6.9.1)$$

$$a \cos \theta = S - a \quad (6.9.2)$$

$$Z = \frac{2atH}{3} \quad (6.9.3)$$

where

$Z$ : section modulus of corrugated section

$t$ : thickness of corrugated plate

$t$  and  $Z$  are given by Nippon Kaiji Kyokai's rule shown in Eqs. (6.6.2) and (6.6.3) and they are to be modified by the following equations.

$$t = 3.6a\sqrt{h} + 3.5 \Rightarrow ka \quad (6.9.4)$$

$$Z = 7cSh'l^2 \Rightarrow mS \quad (6.9.5)$$

where

$h'$ : water head at midspan of corrugated bulkhead

$h$ : water head at bottom of corrugated bulkhead

Now five Eqs. from (6.9.1), (6.9.2), (6.9.3), (6.9.4) and (6.9.5) have six unknowns of  $a$ ,  $\theta$ ,  $H$ ,  $S$ ,  $Z$  and  $t$ .  $h'$ ,  $h$  and  $c$  are given. So they can be solved by adding one more condition for which it is suitable that the sectional area per unit breadth ( $2at/S$ ) is a minimum.

From Eqs. (6.9.3), (6.9.4) and (6.9.5) the following equation is derived:

$$mS = \frac{2akaH}{3}$$

$$\therefore S = \frac{2ka^2}{3m}H \quad (6.9.6)$$

And from Eqs. (6.9.6), (6.9.1) and (6.9.2) the following equation is derived.

$$S = \frac{2ka^2}{3m} a \sin \theta = a(1 + \cos \theta)$$

$$\therefore a^2 = \frac{3m(1 + \cos \theta)}{2k \sin \theta} \tag{6.9.7}$$

From (6.9.7) a value of  $a$  can be decided corresponding to  $\theta$ , and  $H$  and  $S$  can be decided accordingly. Finally the optimum  $\theta$  to have the minimum sectional area per unit breadth  $(2at/S)_{\min}$  can be obtained.

The sectional shapes of the corrugated bulkheads are shown in Fig. 6.9.2 for  $\theta$  equals 30, 45, 60, 75 and 90°. In this calculation an assumption of  $l = 4.5$  m,  $h' = 13.75$  m and  $h = 16$  m is applied. In Fig. 6.9.2 the relation between  $\theta$  and the sectional area per unit breadth  $(2at/S)$  is also shown. In the case of  $\theta = 65^\circ$  the sectional area per unit breadth  $(2at/S)$  becomes to a minimum. The sectional shape of the corrugated bulkhead for  $\theta = 65^\circ$  is also shown in Fig. 6.9.2. It seems well balanced. The calculated values for  $\theta$  equals 30, 45, 60, 65, 75 and 90° are shown in Table 6.9.1.

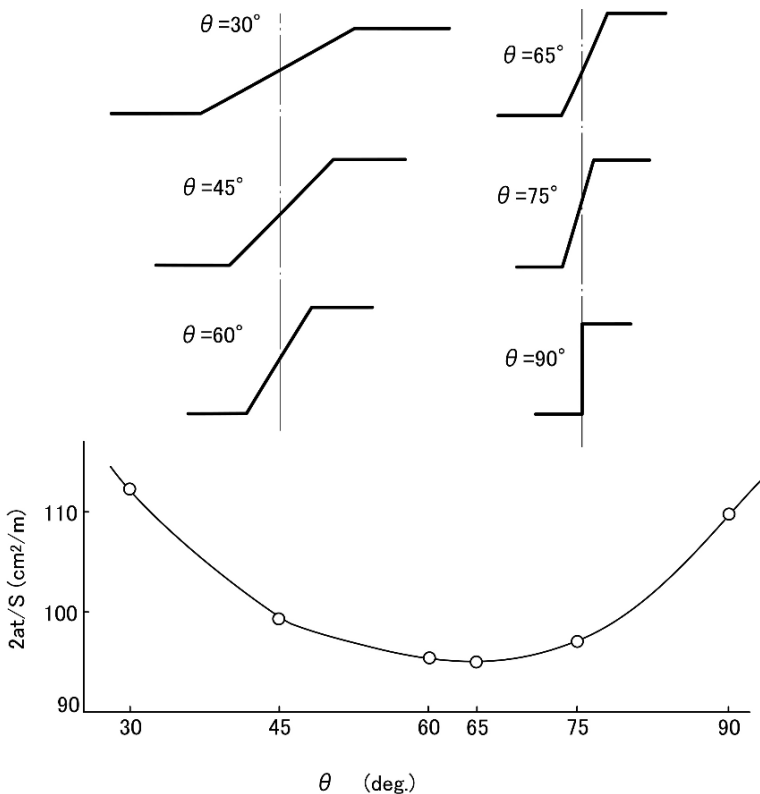


Fig. 6.9.2 Sectional area per unit length of corrugated bulkhead vs. inclination of web plate

**Table 6.9.1** Principal dimensions of corrugated bulkheads

$\theta$ (deg)	30	45	60	65	75	90
$a$ (cm)	73	59	50	47	43	38
$H$ (cm)	37	42	43	43	42	38
$t$ (cm)	1.05	0.85	0.72	0.68	0.61	0.55
$S$ (m)	1.36	1.01	0.75	0.67	0.54	0.38
$\frac{2at}{S} \left( \frac{\text{cm}^2}{\text{m}} \right)$	112.7	99.3	96.0	95.4	97.1	110.0

To compare the weight of a corrugated bulkhead with that of a flat plate bulkhead, the scantlings are calculated. Assuming  $S$  the stiffener spacing in the case of the flat plate bulkhead is 0.67 m, the plate thickness and the section modulus of the stiffener are obtained as follows.

$$t = 3.6S\sqrt{h} = 3.6 \times 0.67\sqrt{16} = 9.6\text{mm}$$

$$Z = 7cSh'l^2 = 7 \times 0.7 \times 0.67 \times 13.75 \times 4.5^2 = 914\text{cm}^3$$

The sectional area  $A$  of the optimum stiffener of  $914\text{cm}^3$  section modulus is  $54.78\text{cm}^2$ , so the total sectional area of the plate and the stiffener is as follows.

$$\frac{S_t + A}{S} = \frac{67 \times 0.96 + 54.78}{0.67} = 177.8\text{cm}^2/\text{m}$$

In the case of a corrugated bulkhead of  $\theta = 65^\circ$ , the weight per unit length is  $95.4\text{cm}^2/\text{m}$  which is 54% of the weight of the flat plate bulkhead. In this comparison no horizontal girder is included. The big weight difference is caused by the plate thickness which is decided by  $S$ , which is 9.6 mm in the case of the flat plate bulkhead. On the other hand, in the case of the corrugated bulkhead it is decided by  $a$ , giving a thickness of 6.8 mm.

## 6.10 Horizontal Girders on Corrugated Bulkheads

One important item in the design of a horizontal girder on a corrugated bulkhead is the fact that the corrugated plate has little rigidity in the wave direction and does not play a role in the extreme fiber of the girder. In the early days of the corrugated

bulkhead, without paying attention to this fact, horizontal girders were provided on one side of the corrugated bulkhead as shown in Fig. 6.10.1. As a result, cracks occurred at the discontinuous points as shown in Fig. 6.10.1. In these cases the scallops at the knuckled points helped the occurrence of the cracks.

To compensate for such a deficiency, a horizontal girder is provided on both sides of the corrugated bulkhead. In the era of the large increase in size of tankers, the horizontal girder was fitted to one side of the corrugated bulkhead for a 20,000 DWT or a 30,000 DWT tanker, on both sides for a 50,000 DWT or a 60,000 DWT tanker, and for bigger tankers than these no corrugated bulkhead was fitted.

In the case where a horizontal girder is fitted on both sides of the corrugated bulkhead, the corrugated plate has to be divided into upper and lower parts, and welded to the girder, because it is difficult to cut the horizontal girder accurately into the wave shape. In such a case, attention should be paid to avoid misalignment between upper and lower parts of the corrugated plate. Especially for the parallel part of the corrugated bulkhead the alignment is more important than that for sloping plate, because the parallel part acts as part of the extreme fiber of the bulkhead stiffener and supports high tensile and compressive stress. To avoid misalignment of the corrugated plates, the drain hole arrangement shown in Fig. 6.10.2 is effective. In addition to the above the horizontal girder on the corrugated bulkhead is to be designed to support the axial force without a bulkhead plate because the corrugated plate has little rigidity in the wave direction.

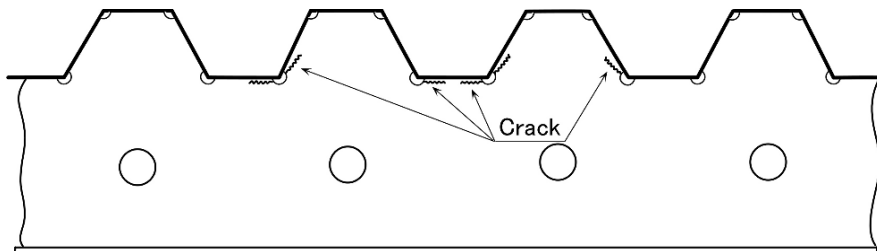


Fig. 6.10.1 Example of damage occurred in horizontal girder of corrugated bulkhead

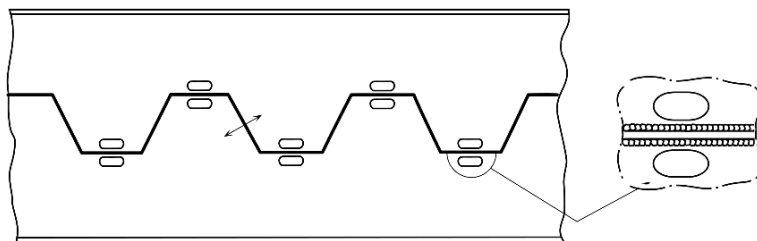


Fig. 6.10.2 Prevention of misalignment between upper and lower corrugated plates

## 6.11 Stiffness of Corrugated Bulkheads Against In-Plane Loads

During the era of the large increase in size of tankers, corrugated bulkheads were not fitted but plane ones were used for tankers bigger than about 60,000 DWT. This might be due to the designer's feeling that it may be dangerous to apply it in a big ship where such corrugated bulkheads would have little in-plane rigidity.

However, the economical pressure to improve transportation efficiency forced hull structure designers to apply the corrugated bulkhead even for 200,000 DWT bulk carriers. For a bulk carrier or an ore carrier no horizontal girder is fitted on the transverse bulkhead to allow for good cargo handling. For big bulk carriers or big ore carriers, double plated transverse bulkheads have been fitted because the deep vertical stiffeners interfere with the cargo handling. A double-plated bulkhead has a disadvantage from the view point of not only weight but also hold capacity. From this view point the corrugated bulkhead has big advantages, and its application in big ships has been getting progressively popular.

Here, apart from a designer's feeling, some engineering analysis has been carried out on the in-plane rigidity of corrugated bulkheads. In-plane loads are divided into two types, the shearing load and the direct load. The shearing rigidity of the bulkhead is important in supporting the hull structure frame work as explained in Sect. 1.1. And the shearing rigidity of a corrugated bulkhead is estimated roughly as  $1/\alpha$  of a plane bulkhead, as explained in Sect. 1.2. Here  $\alpha$  is the ratio of the girth length of a corrugated bulkhead and the length of a plane bulkhead.

More reasonably the shearing rigidity of a corrugated bulkhead can be calculated by FEM [24]. This calculation was carried out on the corrugated bulkhead of a bulk carrier which had a depth of 10 m and a breadth of 31 m as shown in Fig. 6.11.1. Fixing the bulkhead at the side shell and putting a concentrated load at each corrugated corner, the deflection at the center line of the bulkhead is calculated. The total load was 900 t and a both sides symmetrical condition at the center line was applied. The calculated deflection at the center line was 17.1 mm.

According to the above rough estimation  $\alpha = 2$  which means that the deflection of the corrugated bulkhead is 1/2 of that of the plane bulkhead. In the case of a plane plate of breadth 15.5 m, depth 10.0 m, thickness 12 mm with a total 900 t uniform load, the shearing force diagram is a triangle shape and the deflection is calculated as follows.

$$F = F_0 - \frac{F_0}{l}x = 900 - \frac{900}{15.5}x \quad (6.11.1)$$

$$\frac{dy}{dx} = \frac{F}{GA} = \frac{F}{810 \times 1.2 \times 1000} \quad (6.11.2)$$

Putting (6.11.1) into (6.11.2) and integrating from the side shell to the centerline, that is, from  $x = 0$  to  $x = 15.5$ , then the deflection  $y$  at the center line can be obtained.

$$y = \int_0^{15.5} \frac{F}{GA} dx = \frac{2F_0 l}{2GA} = \frac{900 \times 15.5}{2 \times 810 \times 1.2 \times 1000} = 0.0072 \text{ m} \quad (6.11.3)$$

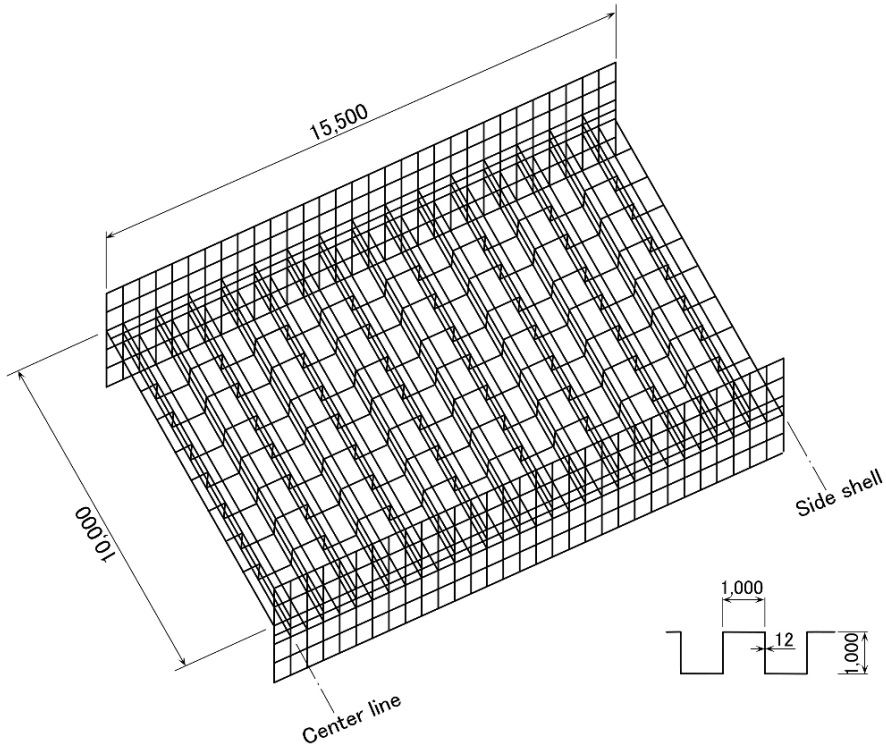


Fig. 6.11.1 FEM model of corrugated bulkhead

The deflection at the centerline for the plane bulkhead is 7.2 mm, and by applying the  $\alpha$  correction, that for the corrugated bulkhead will be 14.4 mm. This is a little smaller than that by the FEM calculation but it can be accepted for practical use.

It seems that the rigidity of a corrugated bulkhead against the direct load, tension, and compression is very small. How small is calculated by taking out a unit breadth of the corrugated bulkhead and modeling it as shown in Fig. 6.11.2.

Assuming that the sloping plate is deformed by bending, the deformation  $\delta_c$  is calculated as follows.

$$P = \frac{12EI}{H^3} \delta_c = \frac{12Ebt_c^3}{12H^3} \delta_c \tag{6.11.4}$$

where

- $P$ : load applied
- $t_c$ : thickness of the corrugated bulkhead
- $b$ : breadth of the corrugated bulkhead taken out for calculation
- $E$ : Young's modulus

On the other hand in the case of the plane bulkhead, as shown in Fig. 6.11.2, assuming that the plate of the S part is contracted by compression, the deformation  $\delta_p$  is calculated as follows:

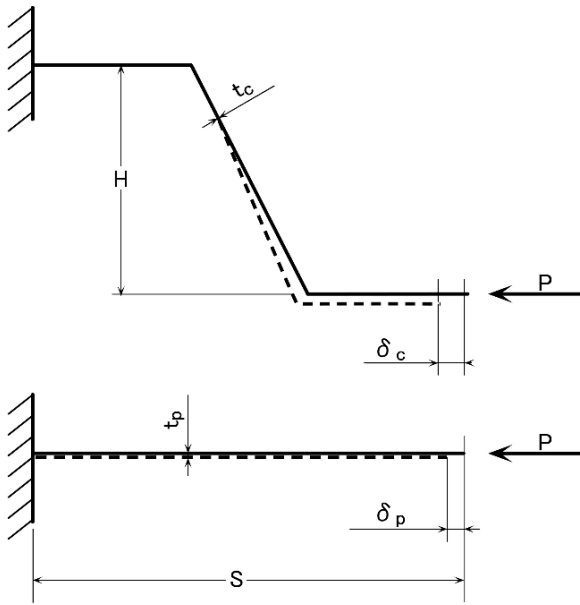


Fig. 6.11.2 Analysis model of corrugated and plane bulkheads subjected to horizontal force

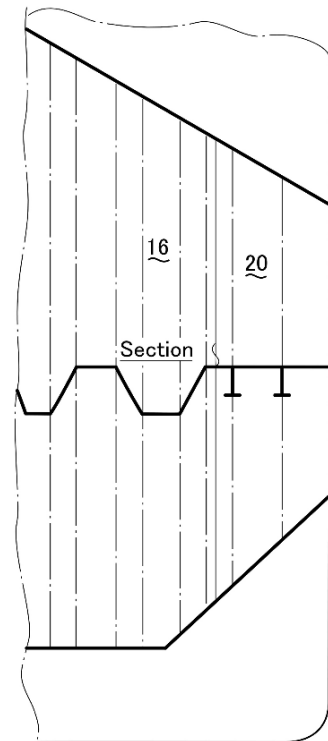


Fig. 6.11.3 Side structure of corrugated bulkhead



$$P = \frac{t_p b E}{S} \delta_p \quad (6.11.5)$$

Putting Eqs. (6.11.4) and (6.11.5) equal, the ratio of  $\delta_c$  and  $\delta_p$  for the equal load  $P$  can be obtained as follows:

$$\frac{\delta_c}{\delta_p} = \frac{H^3 t_p}{S t_c^3} \quad (6.11.6)$$

For a slope angle  $\theta = 65^\circ$  corrugated bulkhead, as explained in Sect. 6.9, the ratio  $\delta_c/\delta_p$  is calculated as:

$$\frac{\delta_c}{\delta_p} = \frac{H^3 t_p}{S t_c^3} = \frac{43^3 \times 0.96}{67 \times 0.68^3} = 3623 \quad (6.11.7)$$

Compared with a plane bulkhead, a corrugated bulkhead deforms more than 3,000 times under an in-plane load, that is, the rigidity of a corrugated bulkhead against an in-plane load is negligibly small. So the transverse corrugated bulkhead of a bulk carrier has the flat part adjacent to the side shell as shown in Fig. 6.11.3.

In the case of a chip carrier the ends of a horizontal girder, which support the side frames, are to be connected to the transverse corrugated bulkhead. In this construction the end moment of the horizontal girder is an out-of-plane load which is supported by the vertical stiffeners fitted on the end flat part of the transverse corrugated bulkhead. Also the end reaction force of the horizontal girder is an in-plane load which is supported by the flat end-part of the transverse corrugated bulkhead.

# Chapter 7

## Deck Structure

The deck receives a lateral external force as well as an in-plane force in relation to the longitudinal strength and the transverse strength; same as the shell and the bulkhead. Tensile and compressive stresses occur longitudinally on the upper deck due to bending of the hull girder and, for cargo ships, and container ships, tensile and compressive stresses also occur transversely on the cross deck between the hatch openings regarding transverse strength and torsional strength.

The strength characteristics are different between an upper deck having a full width, such as in a tanker, and a narrow upper side deck such as in a container ship. They are also different for the upper deck, the 2nd deck and the 3rd deck.

Though the lateral loads on the shell and the bulkhead are assumed to be uniformly distributed, the deck loads aren't always uniform depending on the cargo, and are often concentrated or locally distributed loads.

### 7.1 Stress Concentration at Hatch Corners

#### 7.1.1 General

A stress concentration occurs near the hatch corners in the upper deck of a container ship, bulk carrier, and general cargo ship due to the hull girder bending and torsion. The maximum value of the stress is located at a point of 15–20° inside the circle from the end of the radius in the case of longitudinal bending, and the stress concentration factor depends on the ratio of (corner radius)/(hatch width).

Since the stress concentration factor is 3 for a circle and 2 for an ellipse (when the long axis is in the longitudinal direction) in the case of a hole in an infinitely wide plate, the latter is preferable for a hatch corner where longitudinal bending dominates. The stress distribution around the corner is obtained from the photo-elasticity tests, measurements using strain gauges, and also FEM analysis. Figure 7.1.1 shows these results [25]. The stress concentration factors are

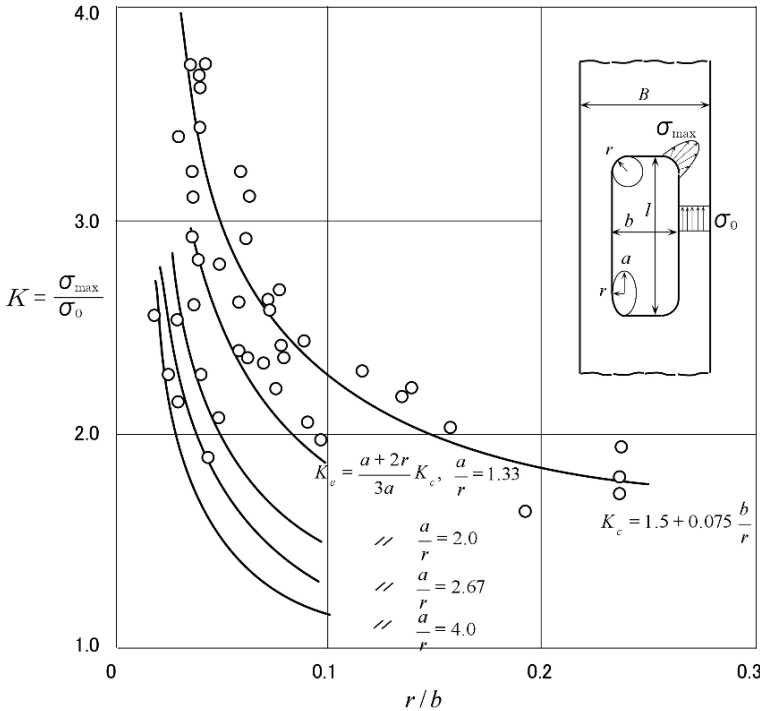


Fig. 7.1.1 Stress concentration factor around hatch corner

$$K_c = 1.5 + 0.075 \frac{b}{r} \quad (0.025 \leq \frac{b}{r} \leq 0.25) \tag{7.1.1}$$

$$K_e = \frac{a+2r}{3a} K_c \quad (0.025 \leq \frac{b}{r} \leq 0.10, \frac{a}{r} < 4)$$

$r$  : radius of circle or half length of shorter axis of ellipse  
 $b$  : hatch breadth  
 $a$  : half length of longer axis of ellipse

It is desirable to adopt a large radius of the circle, the double curvature, the elliptic shape, or the parabolic shape as shown in Fig. 7.1.2.

For the hatch corner of a container ship, the cell guide angle which holds containers is located near the corner, therefore a small radius is preferable to keep the hold space wider. On the other hand, the container ship has less torsional strength in the hull girder, because the ship has a smaller deck area, including both the side deck and the cross deck, due to the wide hatch. The stress concentration due to torsion is added.

The stress concentration at the hatch corner due to torsion is shown in Fig. 7.1.3. Since angular deformation between the side deck and the cross deck occurs, higher stress arises at the hatch corner. The position of maximum stress will be  $45^\circ$  to the side deck, while in the case of the longitudinal bending the position of maximum stress is  $15\text{--}20^\circ$  away from  $45^\circ$  inside the side deck as shown in Fig. 7.1.4.

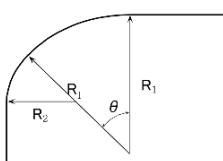
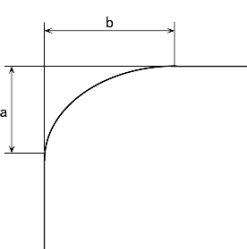
NK	LRS
<p>1. Circle  <math>r \geq 600\text{mm}</math></p> <p>2. Double curvature  <math>R_1 \geq 900\text{mm}</math>  <math>R_2 \geq 300\text{mm}</math>  <math>\theta \geq 45 \text{ deg.}</math></p> 	<p>1. Ellipse or Parabola  <math>a \geq \frac{b_l}{20}</math>  <math>(305\text{mm} \leq a \leq 610\text{mm})</math>  <math>b \geq a</math></p> 

Fig. 7.1.2 Shape of hatch corner

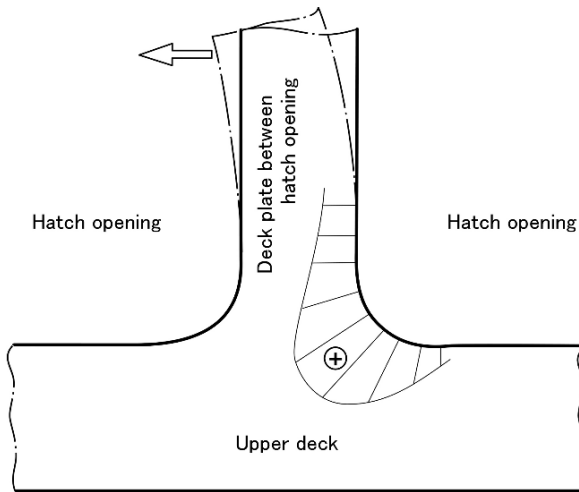


Fig. 7.1.3 Stress concentration around hatch opening corner due to torsion

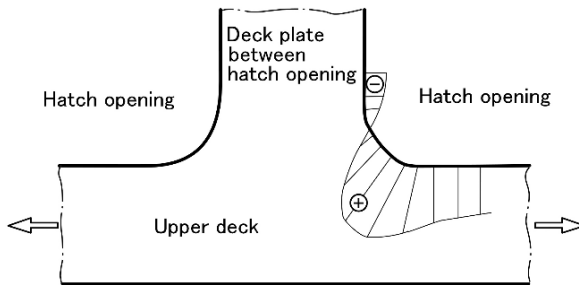


Fig. 7.1.4 Stress concentration around hatch opening corner due to tension

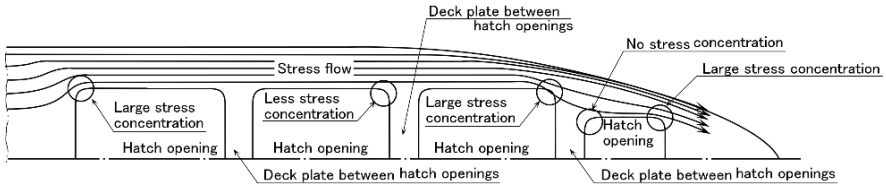


Fig. 7.1.5 Stress flow of upper deck due to longitudinal bending

The shape of the hatch corner should be carefully designed at the forward and aft hatches, because the stress levels are larger there as shown in Fig. 7.1.5.

### 7.1.2 Contour Shape Optimization of Container Ship Hatch Corners

Because the stress of a hatch corner of a container ship is influenced by several factors as explained in the previous section, the optimum shape that minimizes the stress level or stress variation is not necessarily similar to that shown in Fig. 7.1.2. In this section, we describe an example of contour shape optimization of a container ship hatch corner [26].

Figure 7.1.6 shows a bird's eye view of the finite element mesh configuration for the container ship concerned, which is one of the PANAMAX container ships of 4,000TEU class. Because this container ship has longitudinally continuous hatch side coaming, hatch corners on the coaming top level as well as on the upper deck level are studied.

(1) *Hatch corners on upper deck level:* Table 7.1.1 shows combination of design parameters (independent variables) and constraints. Under the constraint that the clearance between the hatch corner contour and the cell guide is to be not less than

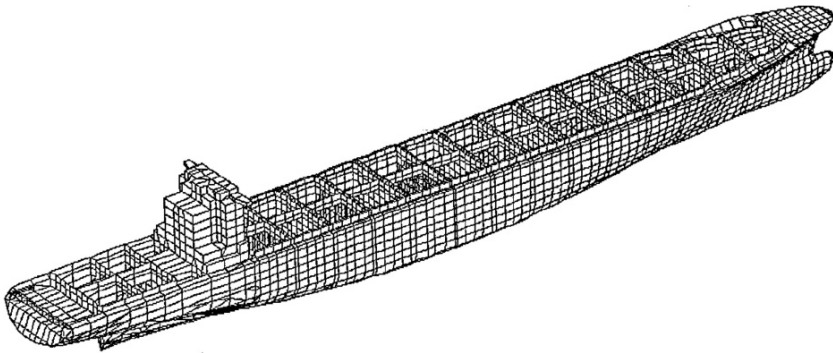
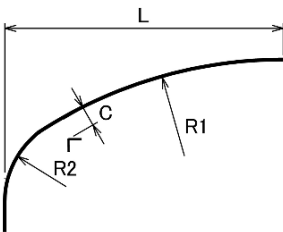
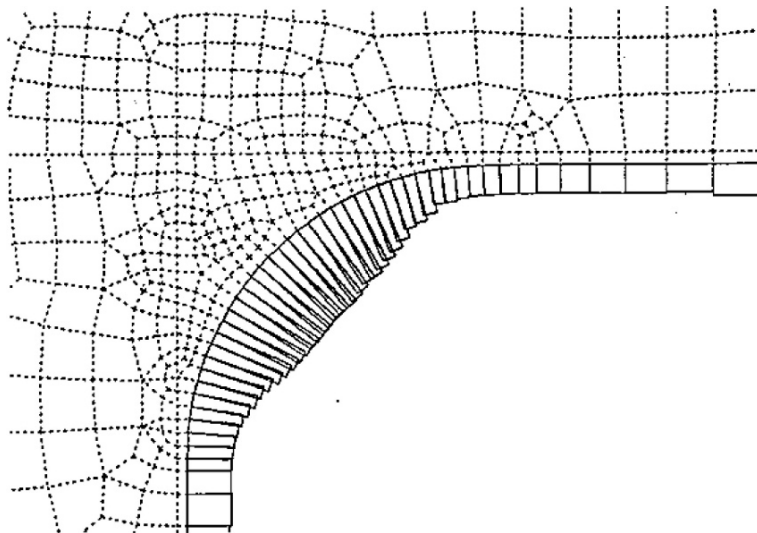


Fig. 7.1.6 Bird's eye view of finite element model of container ship

**Table 7.1.1** Results of hatch corner optimization at upper deck level

 <p style="text-align: right;">C : Clearance to cell guide (<math>\geq 20</math>) (unit : mm)</p>					
	Design parameters			Maximum stress range (N/mm <sup>2</sup> )	
	L	R1	R2	Longitudinal bending	Torsion
900R + 300R	580	900	300	447	654
Optimum shape for longitudinal bending	660	1020	180	379	710
Optimum shape for torsion	510	1140	450	453	521

20 mm, L, R1 and R2 were optimized. The results are also shown in Table 7.1.1. Figure 7.1.7 shows the shape optimized for torsion and boundary stress distribution under torsional loads in oblique seas.



**Fig. 7.1.7** Boundary stress distribution of hatch corner at upper deck level – shape optimized for torsion; torsional load applied –

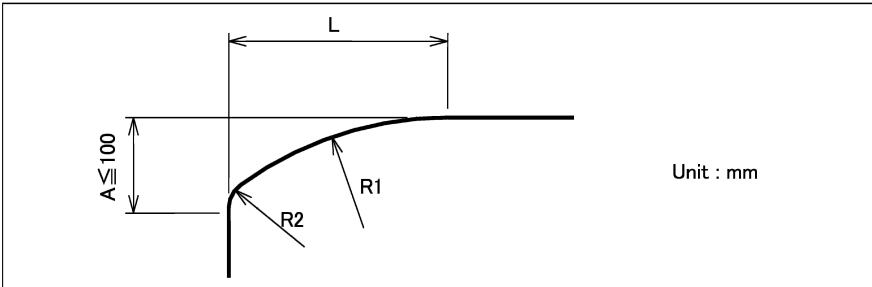
It is observed that we could obtain 15% less stress by optimization for vertical bending, and 20% less stress by optimization for torsion, compared with the double radius shape. The optimized shape for vertical bending is quite good for vertical bending, but does not have good performance for torsion. On the other hand, the optimized shape for torsion has become similar to a single radius contour shape, and has quite good performance for both vertical bending and torsion. We can say that in this position, torsion is dominant and the optimized shape for torsion is to be selected.

In recent years, to enhance container stowage efficiency, large container ships that dispense with the between-hatch deck girders are becoming popular. In the case of such structural configuration, the inertia force of loaded containers in the longitudinal (fore-aft) direction acts directly on the cross deck structure. We can easily imagine that the maximum stress around the hatch corner due to this load would be rather closer to the centerline, than 45°. The designers should always be free from any fixed idea, and should endeavor to seek optimum structure under changing circumstances.

(2) *Hatch corners on hatch coaming top*: Table 7.1.2 shows combination of design parameters (independent variables) and constraints on the coaming top level. Under the constraint that the athwartship distance between the inside end of radius R2 and the outside end of radius R1 is to be not greater than 100 mm, L, R1 and R2 were optimized. The results are also shown in Table 7.1.2. Figure 7.1.8 shows the shape optimized for vertical bending and boundary stress distribution under vertical bending load in head seas.

It is observed that we could obtain 30% less stress by optimization for vertical bending, and 21% less stress by optimization for torsion, compared with the single radius of 100 mm. In this case, the optimized shape for vertical bending has quite

**Table 7.1.2** Results of hatch corner optimization at coaming top level



	Design parameters			Maximum stress range (N/mm <sup>2</sup> )	
	L	R1	R2	Longitudinal bending	Torsion
Single radius (100R)	100	100	100	754	474
Optimum shape for longitudinal bending	230	370	30	526	457
Optimum shape for torsion	190	250	30	580	373

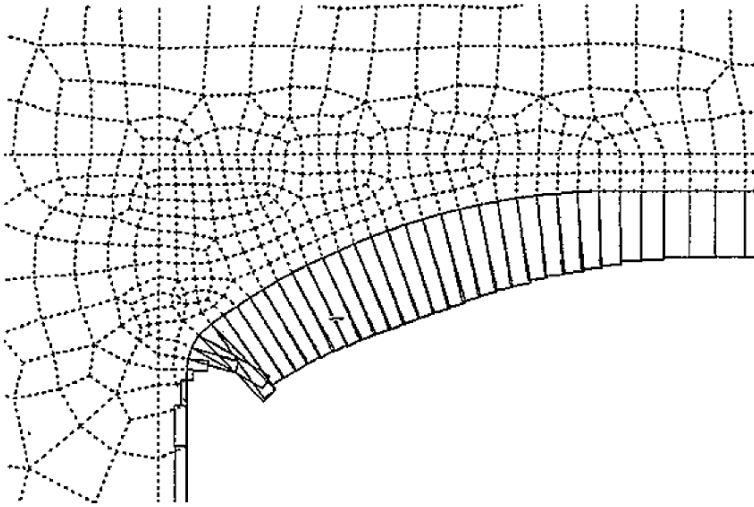


**Fig. 7.1.8** Boundary stress distribution of hatch corner at coaming top level – shape optimized for vertical bending; vertical bending load applied –

good performance for both vertical bending and torsion, and the optimized shape is characterized by very large  $R_1$  and small  $R_2$ . It is interesting that under the exactly same loading conditions, the optimum shape on the upper deck nearly becomes a single radius, and the optimum shape on the coaming top became very biased double radius.

This is considered to be due to the relation of rigidity between the cross deck strip and side structure. On the upper deck level, the side structure is wider than the cross deck strip, and on the coaming top level, the side structure is narrower than the cross deck strip. Longitudinal bending stress is larger on the coaming top, whereas the bending moment of the cross deck strip due to torsion is supported mainly on upper deck level due to the strong rigidity of side structures by the upper deck level. These facts contributed to the optimized shape of each level.

## 7.2 Deck Strength for Locally Distributed Loads

The car deck or the inner bottom which supports the wheel loads of vehicles or fork lift tracks and steel coils is treated as a calculation of panels with locally distributed lateral load, not uniformly distributed loads as for water pressure. In this case, plastic theory is usually applied.

The steel coil is a product of thin steel plates, reeled as a cylindrical shape, which is produced by the roll process using a hot strip mill. The steel coils are loaded on the deck and the double bottom of a liner, a general cargo ship, or a bulk carrier, using the wooden dunnage as shown in Fig. 7.2.1. Though the arrangement of the



Fig. 7.2.1 Loading of hot coil

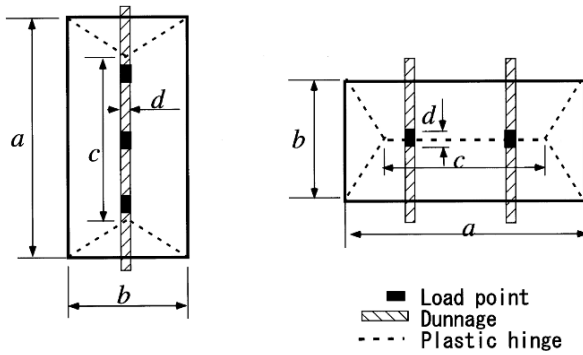
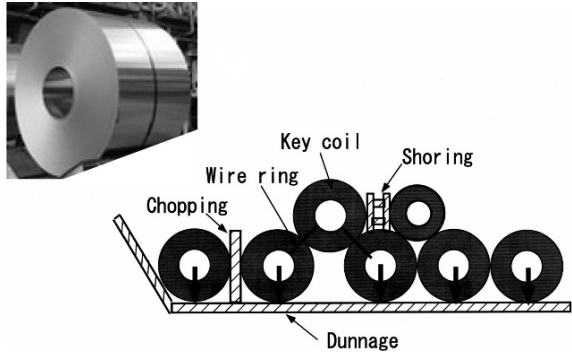


Fig. 7.2.2 Deck strength for hot coil loading

wooden dunnage varies, the severest case for the plate strength seems to be the case where the load acts in the panel center as shown in Fig. 7.2.2. In order to simplify the calculation, intermittent loads on the center line of the panel are assumed to be distributed uniformly on the centerline as illustrated in Fig. 7.2.3, and roof

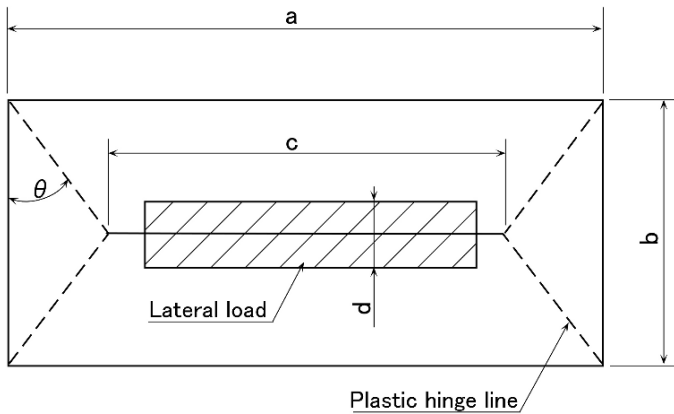


Fig. 7.2.3 Rectangular plate subjected to band width lateral load

**Table 7.2.1** Internal work and external work due to applied load

$U$ Internal work	4 Edges simply supported	$4 \left( \tan \theta + \frac{1}{\tan \theta} + \frac{c}{b} \right) M_p \delta$
	4 Edges clamped	$4 \left( \tan \theta + \frac{2}{\tan \theta} + \frac{a+c}{b} \right) M_p \delta$
$W$ External work		$\left( 1 - \frac{d}{2b} \right) P \delta$
Symbols :	$\tan \theta = \frac{a-c}{b}$ $M_p = \frac{4\sigma_y}{t^2}$ $\delta$ : deflection of plastic hinge line c	$P$ : total load $\sigma_y$ : yield stress

shape collapse of a deck panel is considered on the basis of plastic theory. The work done by the external load and the work done by the plastic collapse are shown in Table 7.2.1 respectively [27]. As both values are the same,

$$P = \frac{8M_p \{a + b^2 / (a - c)\}}{2b - d} \quad \text{for simply supported panel} \quad (7.2.1)$$

$$P = \frac{16M_p \{a + b^2 / (a - c)\}}{2b - d} \quad \text{for fully clamped panel} \quad (7.2.2)$$

$$M_p = t^2 \sigma_y / 4$$

$t$ : plate thickness

$\sigma_y$ : yield stress

Then, the collapse load is estimated for the panel according to the panel size and the print area of the local load.

Next, let's consider a car deck sustaining a wheel load as shown in Fig. 7.2.4. A wheel load of 25 tons is acting in the center of the panel through two tires whose print areas are 350 × 420 mm each. The FEM calculation model is shown in Fig. 7.2.5, and the load distribution is assumed to have one of three types, as shown in Fig. 7.2.6. Figure 7.2.7 shows the results of the deflection, which are similar for the three types of loads. Case c, for the uniformly distributed load including the clearance between two print areas, is practical in evaluating the strength.

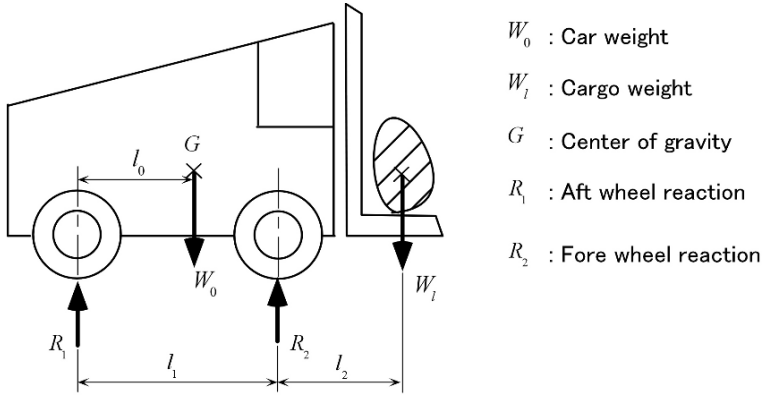


Fig. 7.2.4 Wheel load by fork lift

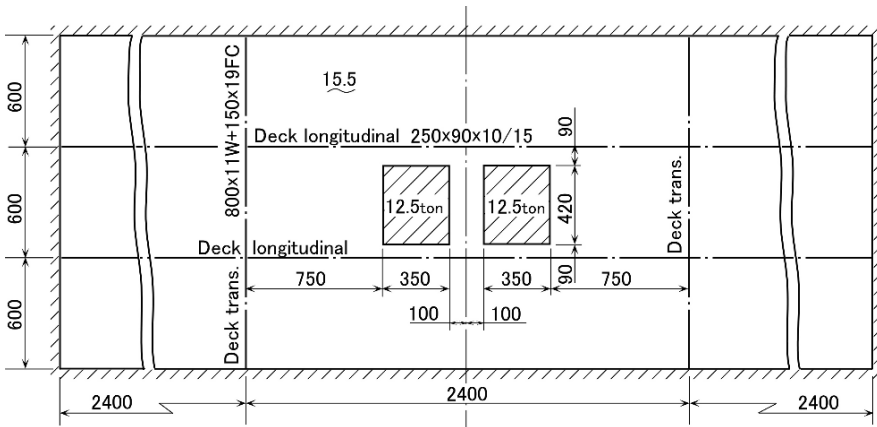


Fig. 7.2.5 Strength calculation model of deck plate subjected to wheel loads

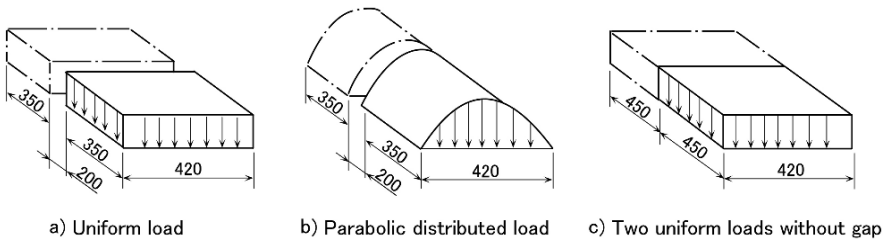


Fig. 7.2.6 Type of wheel load

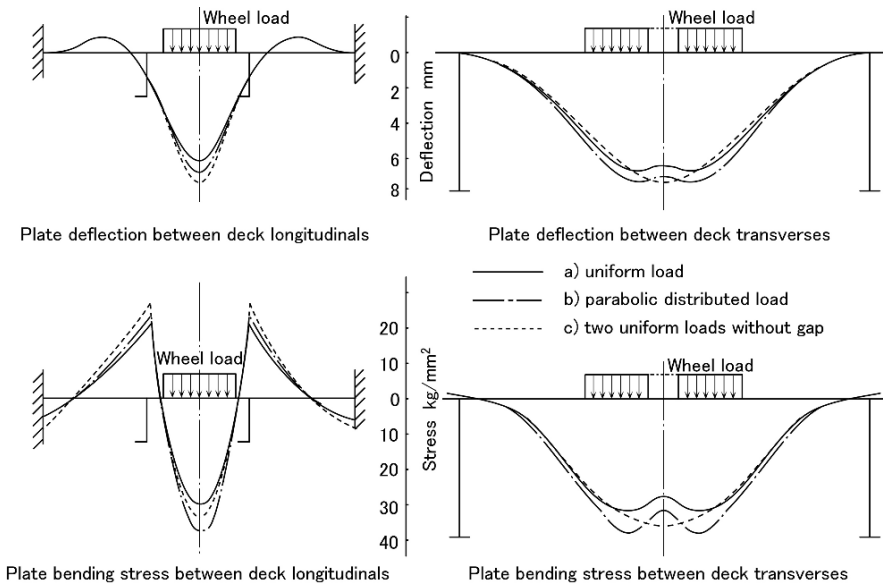


Fig. 7.2.7 Calculated results of deck plate deflection and bending moment under wheel loads

### 7.3 Deck Sustaining Upward Loads

Though the deck structure is usually loaded downward, an upward loading happens in some cases. When liquid is filled in a tank and there is an over flow pipe, the upward load of the water head of the over flow pipe acts on the deck.

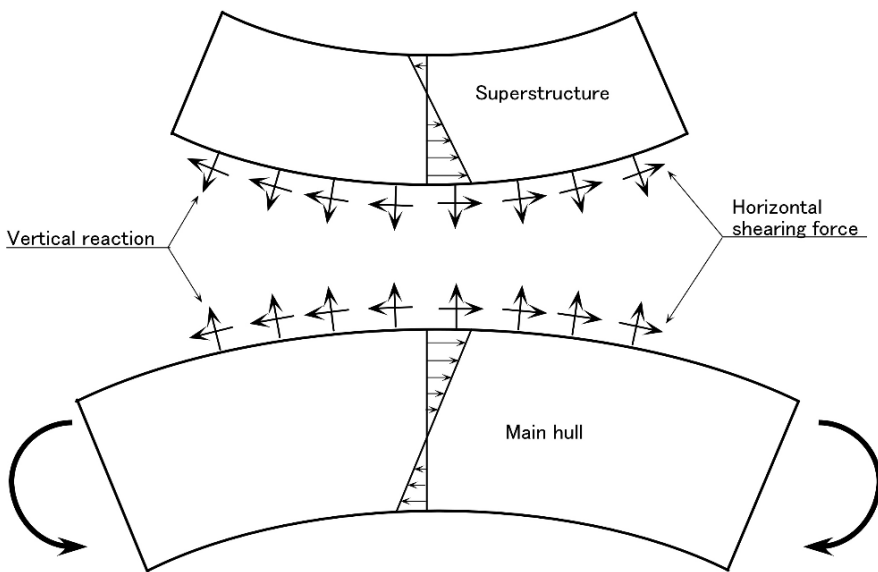


Fig. 7.3.1 Forces between main hull and superstructure

The plate, beam and girder, which comprise the deck structure, are to be designed both for under load and upper load, and the structure has to work safely even with an upward load. Attention needs to be paid to the pillar that supports a deck structure.

Though the pillar is designed for the compression force generally, it also receives a tensile force. However, careful attention is needed regarding the detailed structure at the upper and lower ends of a pillar, because cracks will occur in these connecting parts from a tensile force. The welding bead in these areas should have enough leg length to prevent such cracks.

A tensile force is experienced in a pillar arranged under the front and end walls of a superstructure and a deck house. When the hull is in a hogging condition, the deformation is as shown in Fig. 7.3.1, then the pillar under the deck is pulled.

## 7.4 Damage to Deck Structure

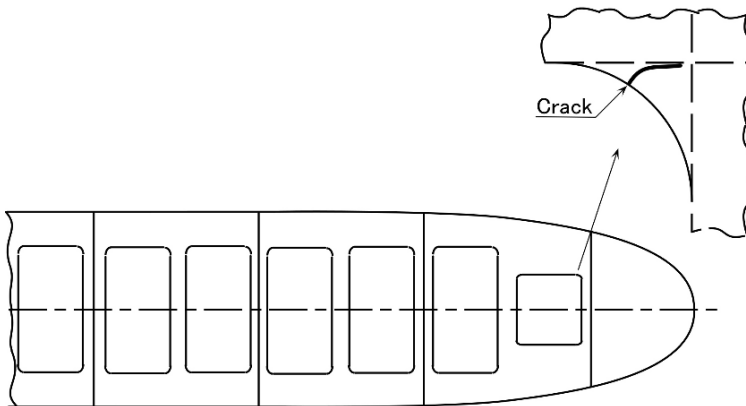


**Fig. 7.4.1** Cracks around hatch corner

A crack near a hatch corner will be seen often, especially at No.1 hold and the last hold. Such cracks are caused by stress concentration by the hull girder bending and torsion. Figures 7.4.1 and 7.4.2 show examples of such a crack at the hatch corner of No.1 hold of a bulk carrier and the aftermost hatch before the engine room of a container ship respectively. Cracks also occur at the ends of hatch side coamings, because of the stress concentration due to the longitudinal force.

The collapse of the whole ship body often occurs in old ships, because of a lack of buckling strength due to the reduced thickness of plate suffering from corrosion. Painting maintenance is extremely important to maintain strength and for long life.

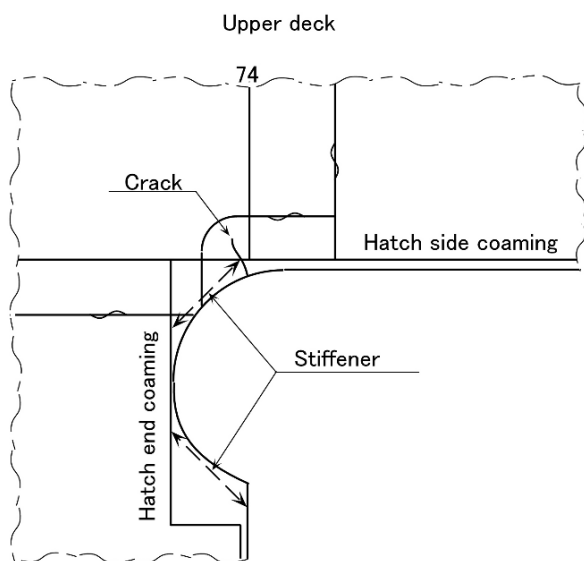


**Fig. 7.4.2** Crack around aftermost hatch corner

# Chapter 8

## Double Hull Structure

The double hull structure has popularly been applied to the bottom of cargo ships, and also to the newer types of ship such as container ships and LNG carriers. Furthermore, it has been recently regulated that for a large tanker the double hull structure has to be applied to the bottom and the side shell. The double hull structure of a cargo ship can prevent the water coming into the hold when the outer shell is wrecked by grounding and collision. For a container ship the double side hull structure is to be applied to maintain torsional strength which is reduced by the large hatch openings. A small container ship is designed with a single hull structure. These double hull compartments are used as ballast tanks.

The double side hull structure of a LNG carrier was originally for ballast tanks but it is hardly effective in protecting the LNG tank from damage due to collision. The double side hull structure of a nuclear powered ship is designed to protect the nuclear reactor from damage due to a collision. The double side hull structure of a large bulk carrier is designed to support the shearing force. A famous 54,000 DWT bulk carrier, “*Bolivar Maru*” had a double side hull structure with 5 long-holds arrangement. Usually a ship of her size has 7 holds.

An OBO (Ore/Bulk /Oil) ship also has a double side hull structure without stiffeners inside the hold, for easy cleaning. Double side hull and bottom structures in large tankers are for the prevention of oil outflow during collision or grounding.

As explained above, there are many aims in applying the double hull structure, and the double hull structure has to be designed to meet these aims. In this chapter, the following are explained; the structural system of a double hull s, a comparison with the single hull structure, and how to design the double hull structure to meet the aims.

### 8.1 Structural System of Double Hull Structure

The ideas explained in Part II, Chap. 6 “Stiffened Panel” can be applied to the double hull structure. As shown in Fig. 8.1.1 in the case of the single hull structure a plate and a stiffener always act together as one beam. On the other hand in the case of the double hull structure, the top and the bottom parts act together, or separately

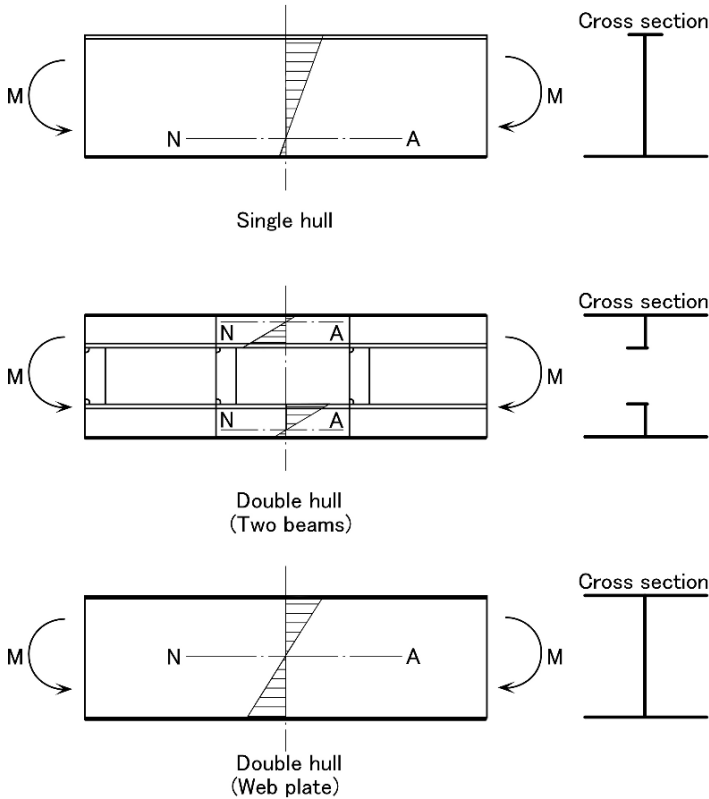


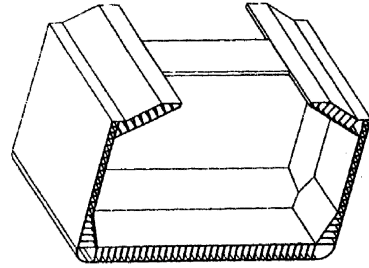
**Fig. 8.1.1** Bending stress distribution of single hull and double hull structures

depending on the boundary conditions. In the former case the merits of the double hull can be enjoyed, but in the latter case the structure is that of two beams and only has twice the strength of one side. Therefore for the top and the bottom parts to act together, shearing members are to be provided between the top and the bottom plates instead of stiffeners. Hitachi Zosen Co. Ltd. in Japan applied such a structure system to a product carrier named Epoch Mark II as shown in Fig. 8.1.2, and Burmeister & Wain shipyard in Denmark also applied it to a 70,000 DWT OBO ship named BCT70 [28].

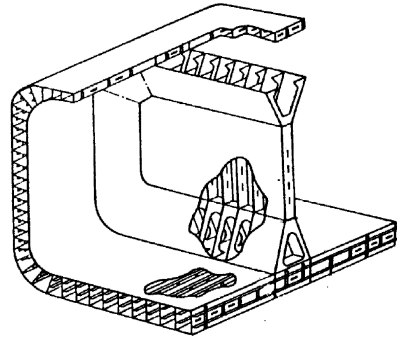
This web structure system has no structural member perpendicular to the web (usually girders are provided, but no floors) and therefore it has little rigidity in that direction. Accordingly special attention is necessary to avoid any deformation of the blocks during construction and transportation. Because of the longitudinal web arrangement, it is efficient to have shorter distances between the transverse bulkheads. A wider and shorter tank arrangement is better for the application of the web structure system. In this system the structural members are arranged in one direction and there is no cross member, which brings a big advantage during production. Fabrication can be done by running automatic welders in one direction only.



**Fig. 8.1.2** Example of web structure system



a) Double hull structure in BCT70



b) Double hull structure in EPOCH MARK II

## 8.2 Double Hull Structure and Single Hull Structure

Many hull structural members support bending moment. Here the comparison of a double and single hull structure from the viewpoint of bending is explained. As shown in Fig. 8.1.1 the double hull structure is divided into two kinds; the double-beam system and the web structure system. In the case of the double-beam system, the plate has low bending stress similar to that of single hull structure. In the case of the web structure system the plate becomes a part of the extreme fiber of the structure and has high bending stress. In Sect. 5.1 the method of how to decide the shell plate thickness is explained. In this method the stress  $\sigma_2$  in the face plate of the longitudinal stiffener is bigger in the case of a web structure system than in a single hull structure or double beams system.

In addition to the above, the welding throat thickness is to be equal to the plate thickness as similar to that for the corrugated bulkhead.

The web structure system is more rigid than the double beams system for equal depth. In other words the web structure system is more effective than the double beams system with higher bending stress in the top and bottom plates.

In the 1960's with the increase in size of single hull tankers many cracks occurred at the cross points of the longitudinal stiffeners and the transverse rings, which were called cracks around the slot. These were caused because the transverse ring and the connecting flat bar between the longitudinal stiffener and the transverse ring, did not increase as the original size, even though the load transmitted through this connection became greater because of the wider spacing and the greater draft of the larger ships. However such cracking around slot has never been observed in the double bottom of a cargo ship even in the double bottom of a large bulk carrier.

The reason is, as explained in Fig. 3.6.4(b), the effect of the lateral movement of the face plate. The lateral movement of the face plate causes a bending stress at the connection of the flat bar. In the case of the double hull structure no such lateral movement of the face plate appears and the countermeasures against a crack around the slot are less important than for a the single hull structure.

### 8.3 Examples of Double Hull Structures

As already explained, there are many aims in applying the double hull structure, and the double hull structure is to be designed to meet these aims. Here the structural system of the double hull for each kind of ship is explained. In Fig. 5.2.1 in Part I examples of double hull structures are shown.

#### 8.3.1 *Cargo Ships*

The double bottom of a cargo ship including a bulk carrier has to have water tightness of the inner bottom plate even in the case of damage to the outer shell plate caused by grounding or collision. To reduce the effect of a damaged outer shell plate to the inner bottom plate, it is more efficient to have a weak connection between them. From this view point it may be reasonable for the thickness of the double bottom floors to have reduced scantlings.

A structural system which has a strut connecting the inner and bottom longitudinals at the midpoint between the floors has been applied popularly in the double bottom of cargo ships. This system is good from the structural viewpoint, because by connecting the inner and bottom longitudinals both of them can carry load cooperatively. However, from the emergency viewpoint it is a little dangerous; the strut may pierce the inner bottom plate in the case of grounding.

A large bulk carrier once broke at the starboard side bilge in the area of the hold. It was important to note that the web ring in the hopper tank had little damage because the thickness of the web was heavy and the big stiffeners were fitted nearly perpendicular to the shell and the sloped hopper plates. The applied force on the bilge shell plate by the grounding was transmitted directly to the sloped hopper plate which was badly broken. This is a bad example of the double bottom structure of a cargo ship.

### 8.3.2 Tankers

The double hull of a tanker, in a similar way to that of a cargo ship, has to be provided with oil tightness in the inner hull plate, particularly in the case of damage caused by grounding or collision to the outer shell plate. In the case of the double bottom of a cargo ship, a weak connection between the outer shell and the inner hull plate is preferable so that the inner hull plate is not directly affected by a load applied to the outer shell plate. This principle can be applied to the double bottom of a tanker.

Due to the application of the double hull side structure on a tanker, there are two problems which are different from a single hull side structure; one is the rigidity unbalance between the vertical webs on the side shell and the longitudinal bulkhead, and the other is the sharing ratio of the shearing force supported by the longitudinal bulkhead.

In the case of a single hull side structure, the rigidities of the vertical webs on the side and the longitudinal bulkhead are well balanced and they are effectively connected by cross tie. However, in the case of a double hull side structure (Fig. 8.3.1) the rigidity of the vertical web on the side shell is far bigger than the rigidity of the vertical web on the longitudinal bulkhead. A trial calculation for a 300,000 DWT tanker indicates that the sectional moment of inertia of the vertical web on the longitudinal bulkhead is 28% of that of the vertical web on the side shell. It is not so efficient to connect two members with different rigidities by a cross tie. A new arrangement with the cross tie in the center tank appeared as shown in Fig. 8.3.1(b). In this arrangement a cross tie effectively connects the vertical webs of the same scantling on the longitudinal bulkheads. Similar discussions can be carried out based on the principle explained in Sect. 1.10 in Part II.

The sharing ratio of the shearing force supported by the longitudinal bulkhead is estimated by the method explained in Sect. 6.8. A trial calculation for a 300,000 DWT tanker indicates that in the case of the double hull side structure the sharing ratio of the shearing force supported by the longitudinal bulkhead is 69% of that for the single hull structure. This reduction can be utilized in design improvement.

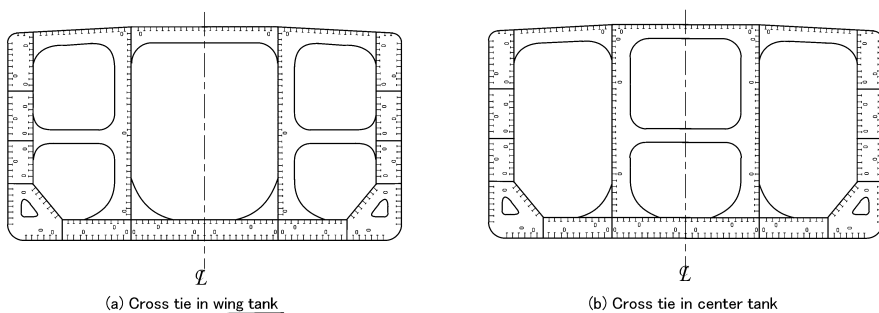


Fig. 8.3.1 Example of cross tie arrangement

### 8.3.3 Container Ships

A container ship has large openings in the upper deck and a high warping stress is expected at the corners of the openings due to the lack of torsional rigidity. To keep the necessary torsional rigidity, the double hull side structure is usually applied as a torsion box in the upper part of a large container ship.

The torsional strength depends on the enclosed cross-sectional area of such plates, as shown in Fig. 8.3.2 by hatching. However due to design limitation, a container ship cannot usually have enough cross-sectional area, and the designer has no other way but to increase the surrounding plate thickness.

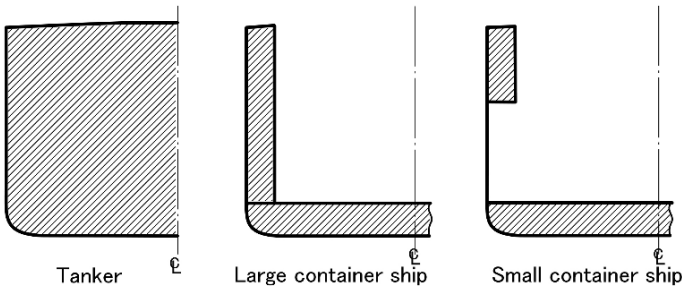


Fig. 8.3.2 Closed section of ships causing torsional rigidity

### 8.3.4 Nuclear Ships

The aim of the double hull side structure of a nuclear ship is to protect the nuclear reactor and to prevent damage caused by collision with the other ships. Accordingly enough strength against the collision is necessary. In this case, water tightness of the inner hull after the collision is not always required. Therefore a strong connection between the outer and inner hull structures is preferable.

The collision is usually caused by bow impact of the other ship. To prevent the bow from entering into the reactor room heavy horizontal plates are fitted wherever possible. Also an adequate distance between the outer and inner hull plates is necessary.

The nuclear ship “*Mutsu*” built in Japan ( $L \times B \times D = 116 \times 19 \times 13.2\text{m}$ ) has a 4 m wide double side hull structure at both sides of the reactor room, and five horizontal heavy plates are fitted as shown in Fig. 8.3.3.

In the case of a tanker, to prevent the oil outflow is of prime importance, and the oil tightness of the inner hull plate is most important. The design principles of double hull side structures of a tanker and a nuclear ship are similar but a little different.

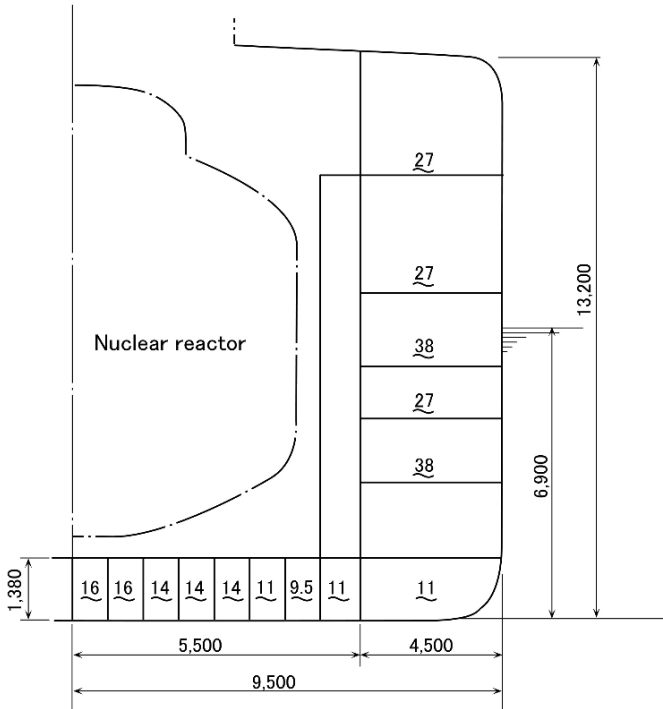


Fig. 8.3.3 Cross section of nuclear reactor room of nuclear vessel “MUTSU”

### 8.3.5 Large Bulk Carriers

As explained in Chap. 1 “Hull Structure Arrangement”, at an early stage in the large increase in ship size, there was an idea that a large bulk carrier over 150,000 DWT should have a double hull side structure. The 130,000 DWT tanker the “*Nissho Maru*” built in the early 1960’s has double hull side structures in the engine room. The design principle at that time is not clear now. It is supposed that the hull structure designer felt at that time that it was necessary based on his experience. Nowadays the double or single hull side structure can be decided based on the shear rigidity and the shearing strength of the side shell.

The OBO ship has a double hull side structure so as to have a flat surface inside the hold. The vertical stiffeners are fitted inside the double hull structure and the inner side plate is not so heavy.

# Chapter 9

## Fore Construction

The fore construction is defined generally as the region from the collision bulkhead to the forefront of the ship. There are four important concepts in designing the fore construction. The first of them is that this portion collides with floating objects or other ships, and also suffers from wave impact. The second is that the vertical acceleration depending on the pitching motion is large due to a long distance from the pitching center. The third is that a structural discontinuity area exists at the hold portion behind it. The last one is that the structural arrangement varies according to the ship body form.

### 9.1 Structural Arrangement

The transverse framing system has been generally adopted for the structure of a fore construction so far. The side stringer supports the frames at the ends. Since the ship side inclines toward the ship centerline, the transverse frames are fitted inclined to the shell plate, not perpendicular. Therefore, the effectiveness of the shell plate as an attached plate of the frame is less. If the frame is fitted perpendicularly to the shell, it is more effective from a strength point of view, but it is not preferable for assembly because the fabrication of the frame is quite complex, especially in the area of a bulbous bow. As a result, a longitudinal framing system is now widely adopted, with the side longitudinals, the web frames, and the panting stringers as shown in Fig. 9.1.1.

The structural arrangement of the fore construction depends mainly on the bow shape. The main strength is maintained by the shell, the collision bulkhead, and the center line bulkhead.

Since the structure of the fore construction can be considered to be a cantilever beam fixed at the collision bulkhead to the main hull, the global strength such as bending, shearing, and torsional strength against the wave load should be considered as well as the local strength.

These points are considered relative to the strength evaluation of the members inside the fore construction, for example, secondary stress due to the forced displacement at the fore end should be studied for the center bottom girder, as shown in Fig. 9.1.2.

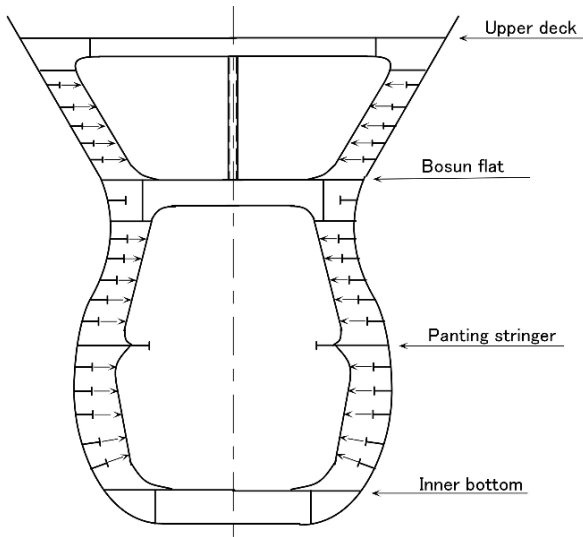


Fig. 9.1.1 Fore construction (Longitudinal framing system)

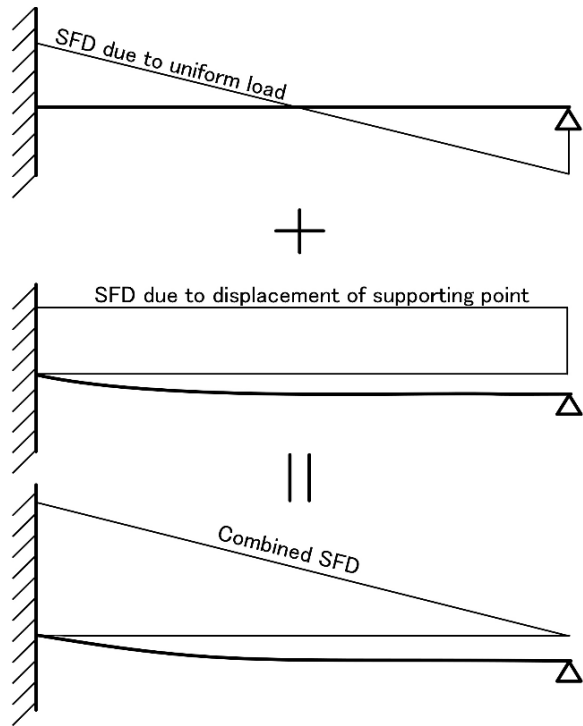


Fig. 9.1.2 Shearing forces on bottom center line

Usually a swash bulkhead is fitted at the center line for a wide forepeak tank. It is thought that the thickness of this plate is sufficient at 12 mm even for large ships, from the viewpoint of its purpose as a swash bulkhead. However, from the viewpoint of the whole structural design of the bow construction, the bulkhead is most important in maintaining the strength of the fore construction as a cantilever beam, especially for the shearing force, since a large shearing stress acts on the bulkhead and therefore buckling can easily occur.

## 9.2 Structure of Shell Construction

It is a common concept of current hull structure design that damage from a wave impact is not allowed though damage by collision against a floating object or another ship is permissible. Here, damage to the longitudinal frames and the web frames as a result of wave forces is introduced.

Figure 9.2.1 shows cracking and buckling of the web frame on a container ship as shown in Fig. 5.3.1. Plate buckling occurred at the upper and lower parts of the web frame, and the web plate was cut in its mid-part, due to external water

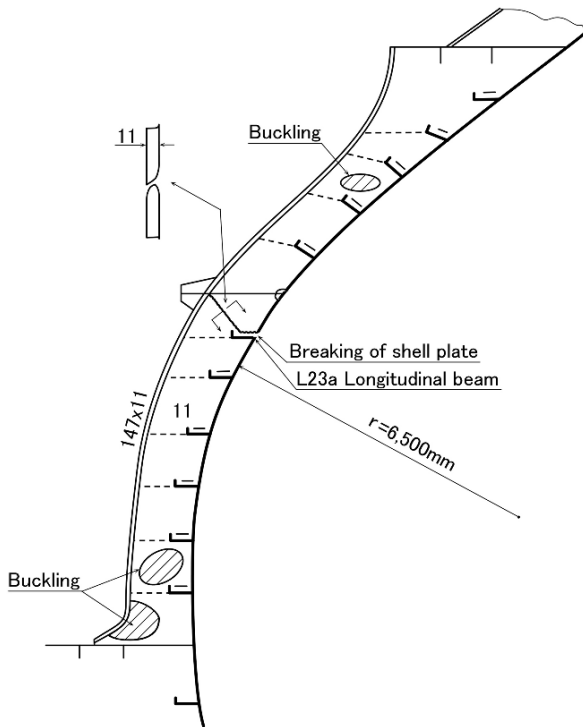
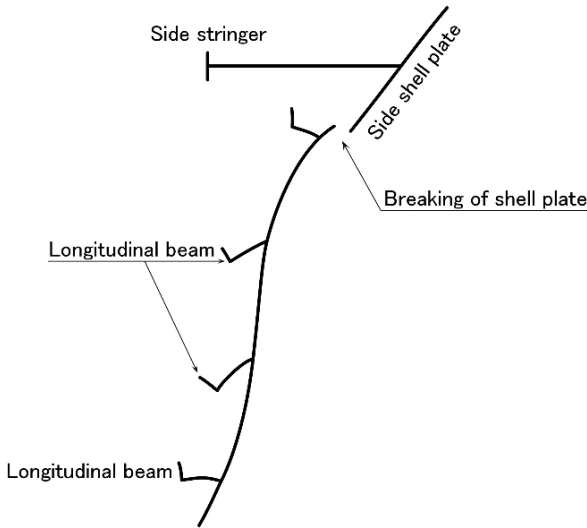


Fig. 9.2.1 Damages of web frame





**Fig. 9.2.2** Lateral buckling of longitudinals

impact. The side shell plate was also cut at the upper part of L-23a. In this case, the shell plate seems to have a cylindrical form of approximately 6.5 m radius, which sustains the water pressure, and therefore a hoop stress of uniform distribution will be acting in the shell plate. The static water head, for which the hoop stress reaches to its rupture value, is estimated as 100 m in this case, as a result of detail calculation.

Figure 9.2.2 shows lateral buckling in the longitudinals at Fr.154-1/2. The flanges of the L-shaped angle have rotated backwards. The mechanism has already been stated in Chap. 1, Part II.

### 9.3 Vertical Acceleration Depending on Pitching

The 2nd characteristic of the fore construction is that it is far away from amidship. Therefore, the influence of the pitching is large. For a ship length of 300 m, a pitching angle of  $1^\circ$  corresponds to vertical amplitude of 2.6 m at the fore end.

The larger the pitching angle becomes, the bigger the vertical acceleration becomes. Hence, the water pressure on the bulkheads and the shell becomes larger when the fore peak tank is filled with ballast water. Such an additional water head due to the acceleration by pitching, as well as heaving, should be considered in the structural design of the fore construction.

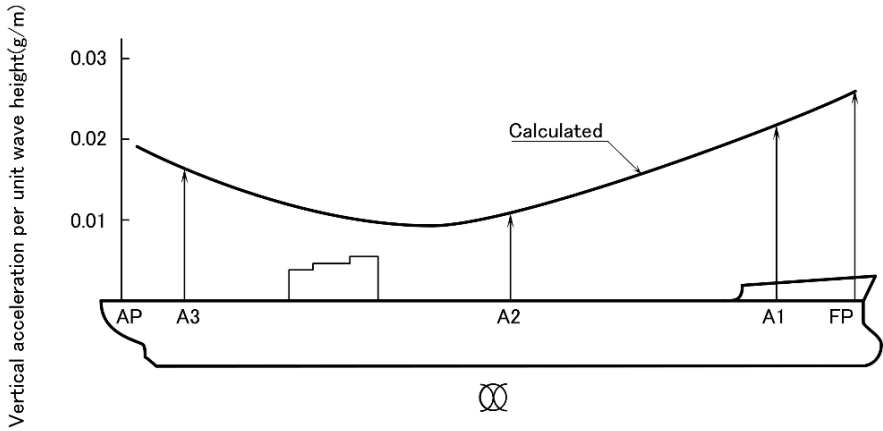


Fig. 9.3.1 Vertical acceleration due to ship motion

Figure 9.3.1 shows the distribution of the vertical acceleration due to pitching and heaving along the ship length, from calculations using strip theory, for a container ship of 175 m length.

### 9.4 Deck Structure

The exposed deck located at the fore construction suffers from heavy wave loads, compared with other decks; it is said that the equivalent water head is 20 m.

There are three kinds of wave load; the wave impact on the ship bottom (bottom slamming), on the bow (bow flare slamming) and on the exposed deck (green water). They are related to each other, that is, a ship suffering from heavy bottom slamming and bow flare slamming has less green water, because the bottom slamming and bow flare slamming resist the pitching motion, and also a large flare diverts waves away from the deck, as already seen in Fig. 2.2.4, Part I.

Recently, statistical analysis of ship motion and wave load can be done by using computer programs for each type of ship. Applying these may be an optimal design method for the fore construction.

The chain lockers are located in the fore construction. Although it is difficult to install them in high-speed ships because of their slender shape, a cylindrical type instead of a square type has been adopted for e large ships because there is enough space, as illustrated in Fig. 9.4.1. In this type, the anchor chains are stored easily, and the stiffeners around the wall are not necessary. The standardization of the shape is also easy because it is an independent structural object. What is more, they act as a pillar between the upper deck and the lower deck.

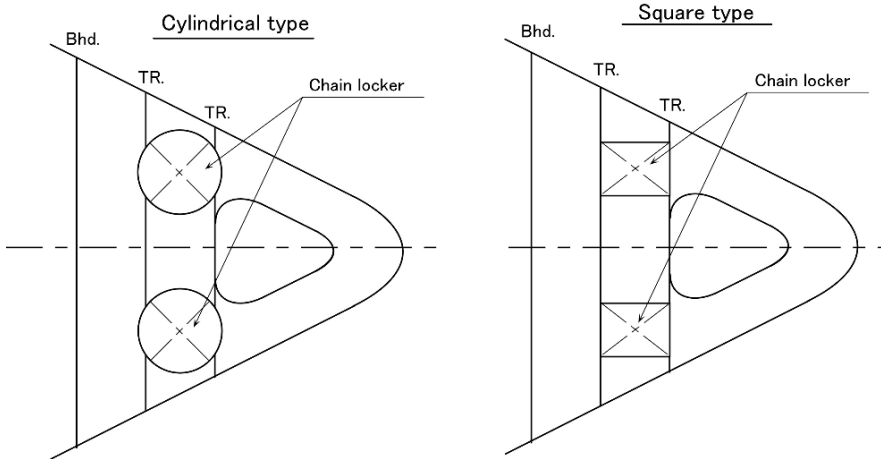


Fig. 9.4.1 Type of chain locker

## 9.5 Structural Continuity

The fore construction is a rather strong structure but the hold part following it is not so strong, hence structural continuity is very important.

For the transverse framing system in the hold of a cargo ship, the depth of the frames is ruled to be less than  $1/22$  of the span in the region from the collision bulkhead to  $0.15L$  from FP, in order to prevent sudden structural change.

In the case where a horizontal girder is fitted inside the fore peak tank, a bracket is usually fitted in the hold part behind it. The shape should be rounded to prevent stress concentration and fatigue cracks, especially the aft end toe of the bracket.

Usually, the steel weight becomes less and the production costs rise when the space between the longitudinal frames is narrow. The space is likely to be smaller in the fore peak tank from the strength viewpoint and to be larger in the hold from the production viewpoint. However the continuity of the structure between the two regions needs to be considered.

## 9.6 Large Damage in Fore Construction

In September 26, 1935, a Japanese fleet encountered a violent typhoon during an exercise in the east of Aomori Prefecture Shiriyazaki-cape. A destroyer the “*Hatsuyuki*” and the “*Yugiri*” were cut in two in front of the bridge and then the fore part sunk. The Japanese navy set up a committee and investigated the accident as the 4th fleet incident in those days [29].

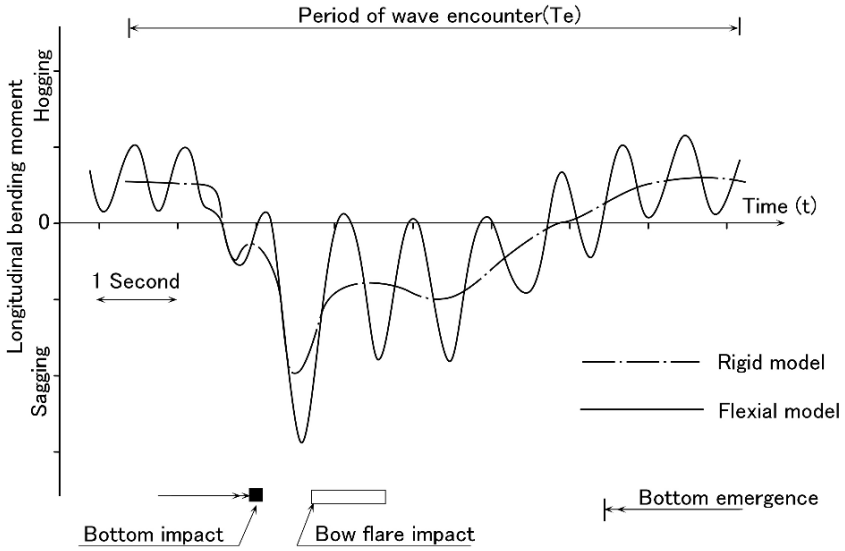


Fig. 9.6.1 Longitudinal bending moment due to wave impact

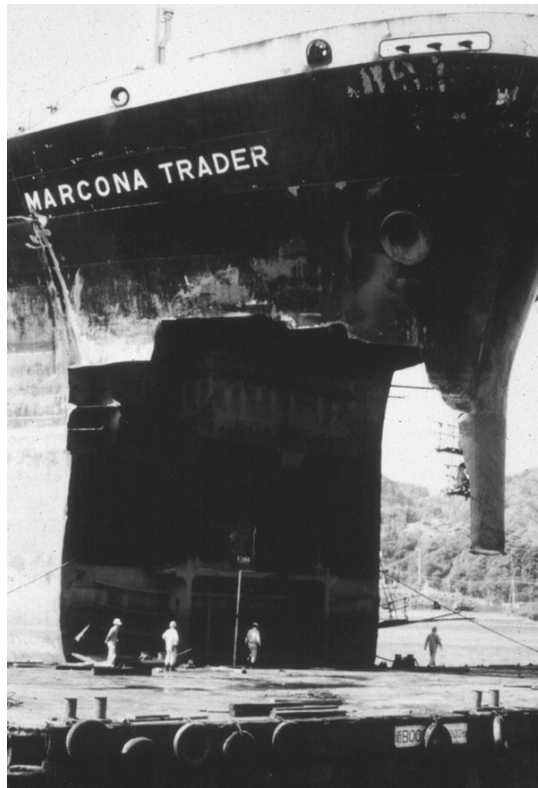


Fig. 9.6.2 Failure at fore part of "Marcona Trader"

The loss of the “*Bolivar Maru*” in January 5, 1969, and the “*California Maru*” in February 9, 1970 were caused by the collapse of the fore part due to wave impact. Furthermore, the “*Onomichi Maru*” collapsed at the No.1 hold in December 30, 1980, and the remaining main hull sank after drifting.

Such collapse of the fore part resulted from buckling of the upper deck after wave impact. Figure 9.6.1 shows the time history of the vertical wave bending moment obtained from a tank test of a container ship. It is clearly shown that additional vibration stress induced by wave shock and the bending stress in the sagging mode becomes large, when bow impact has occurred on the flare part.

The “*Marcona Trader*” encountered such crucial accidents that the bottom and side shell of the fore region were torn off. Figure 9.6.2 shows the photograph at repair dock [30].

# Chapter 10

## Engine Room Construction

The most important item in the design of an engine room construction or a pump room construction of a tanker is to pay attention to the machinery installed there. Usually the hull structure is to be designed based on the stress not on the deflection. In the case of a small ship the deflection is too small to cause any trouble to the machinery. However in the case of a large ship the deflection of the hull structure causes some troubles.

Deformation in the turbine flat on which the turbines for the cargo oil pumps are installed, causes a shaft misalignment between turbine and cargo oil pump. The deflection of a double bottom in the engine room badly affects the crank shaft of the main Diesel engine and the shafting. It also badly affects, in a turbine ship, the alignment of the reduction gear and the shafting which causes non-uniform teeth contact between the bull gear and the pinion, as shown in Fig. 10.5.2. Excess bearing load on a shaft bearing sometimes causes damage to the bearing white metal.

Another important item concerning engine room construction is that the structure is also the foundation of the superstructure, especially in the case of an aft engine and an aft bridge arrangement. Inadequate foundation may cause some vibration problems. Usually the engine room and the superstructure arrangement is decided from the viewpoints of operation, handling and habitability. With these considerations a poor foundation will result. A proverb says “a ship designed by a designer who has no experience in the hull structure design will be malformed.” This proverb will be true in the hull structure design of an engine room.

In the hull structure design of an engine room, the machinery arrangement is, of course, important, and besides this a hull structure designer should pay attention to the hull form in the area of the engine room. In the energy saving era after the oil crisis a hull form designers created very narrow forms in the area of the engine room to improve the propulsion efficiency. A bow structure has been affected by the new hull form of a bulbous bow, and the engine room structure has been also affected by a bulbous stern and an open bulbous stern. In these hull forms a big propeller is fitted at the end of a slender and weak cantilever.

In the hull structure design of an aft engine room which has a big main engine at the center and which is situated near the propeller with an exciting force, more attention should be paid to anti-vibration design than in the case of a semi-aft or a midship engine room. A container ship built before the oil crisis had two diesel

main engines of 34,800 BHP each and had a high speed of 25 knots. It is understood she had very little vibration during her sea trial, because of the semi-aft engine and the semi-aft bridge arrangement.

In this chapter the arrangement and the deformation of the engine and pump rooms are mainly explained.

### 10.1 Engine and Pump Rooms Arrangement

Here mainly the aft engine room arrangement is explained. The pump room arrangement is affected by the type of the pump, vertical or horizontal. As explained above in the case of a vertical shaft pump, the turbine flat is not to be connected to the pump room front bulkhead.

Figure 10.1.1 shows the pump room arrangement of a 100,000 DWT tanker [31]. The turbine flat in the engine room is connected to the No.3 horizontal girder on

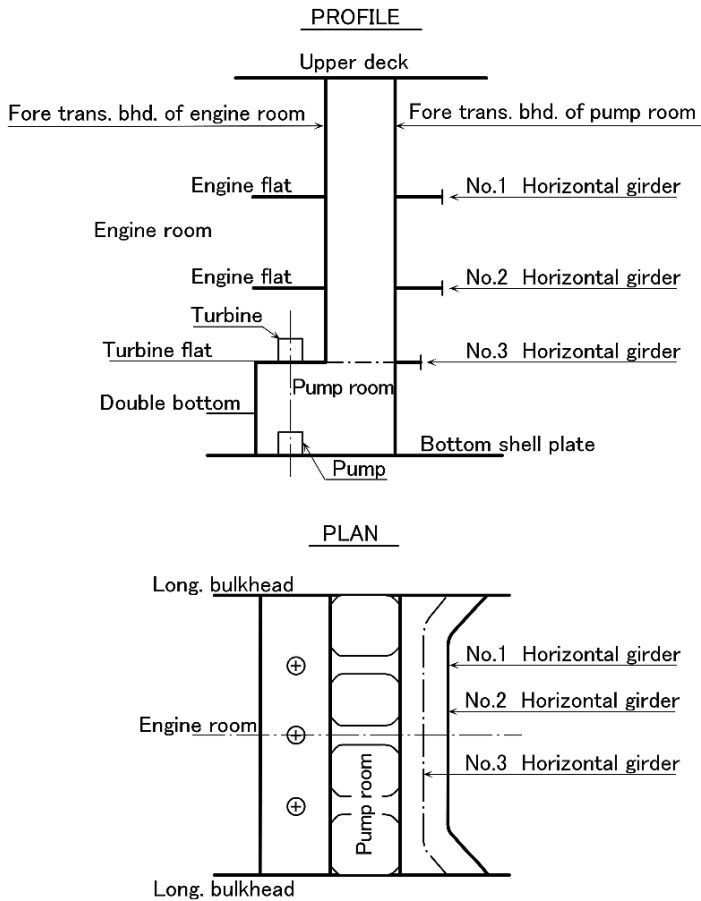


Fig. 10.1.1 Pump room arrangement of 100,000DWT tanker

the pump room front bulkhead to reduce the scantling of the No.3 horizontal girder. From the strength viewpoint this design will be OK. However the water pressure in the aftermost center tank causes deflection in the turbine flat. Accordingly the alignment of the shaft connecting the pump and the turbine was destroyed.

Generally a horizontal girder on a bulkhead is designed based on the stress and no consideration will be paid to the deflection. It is important for not only a hull structure designer but also a naval architect to know the amount of deflection of a girder. The deflection of a girder is around  $1/2,500$  of the span. In this case the span of the No.3 horizontal girder, that is the breadth of the center tank, is 15 m, accordingly the deflection will be about 6 mm which is big enough to cause the misalignment of the shaft.

In the machinery arrangement, the position of the boilers is important, i.e. whether to install them fore or aft. Originally they were installed in the fore part of the engine room because the boiler tubes may crack due to vibration. The vibration level at the fore part of the engine room is less than that in the aft part. Now the improved wall-tube type boiler is tough enough to resist vibration and they can be installed in any place in the engine room. It is common knowledge for a hull structure designer to install any machinery which may have trouble due to vibration at the fore part of the engine room.

Machinery which generates the exciting force is best installed at the aft part of the engine room, because on aft part is narrow and the shorter span of the girder gives high local rigidity. In this view point a diesel generator is usually installed at the aft part of the engine room.

The main engine is to be installed as far aft as possible to make the engine room length shorter. This is good for a rigid engine bed because the span of the double bottom floor is shorter at the aft part of the engine room. The container ship with two 34,800 BHP engines, referred to above, has a semi-aft engine room arrangement which has a wider span of the double bottom floor in the engine room. In this case a center line longitudinal bulkhead is provided to support the wider span of the double bottom floor. In addition to the longitudinal center line bulkhead, the double bottom in the engine room is designed to be as high as possible to accommodate the raked propeller shaft. Then the rigidity of the double bottom, that is, the foundation of the main engines, seemed to be sufficient for the two Sulzer 12RND90 engines which were the most powerful in the world at that time.

In the design of the engine room, it will be the right road to firstly decide the height of the double bottom and the arrangement of the longitudinal and transverse bulkheads. Then the machinery, including the main engine, is to be arranged. At that stage the walls such as the front and the side walls of the superstructure are to be arranged over the bulkheads in the engine room. In this way vibration problems in the engine room, as well as in the superstructure, will be avoided.

The steel wall arrangement shown in Fig. 10.1.2 is for an 84,000 DWT tanker which suffered from a heavy vibration problem in the superstructure as well as in the engine room. The side walls of the superstructure are in step style and not on the longitudinal bulkhead in the engine room. The bridge front wall, the boat deck front wall and the poop deck front wall are not in a plane. The fore and aft ends



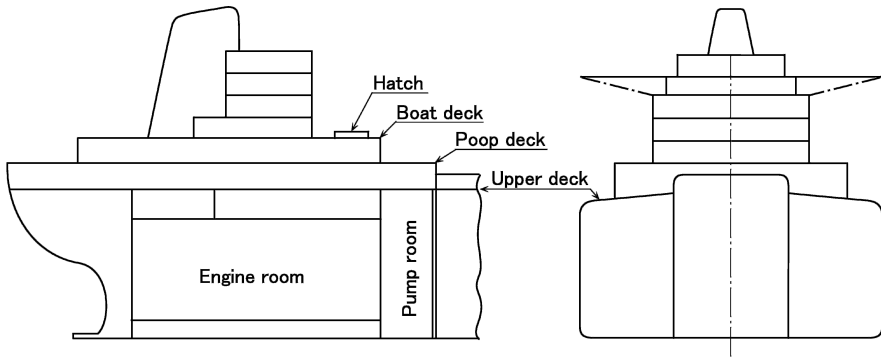


Fig. 10.1.2 Steel wall arrangement in engine room and in super structure

of the big superstructure, including the funnel, are not supported by the transverse bulkhead in the engine room. This arrangement was decided from the view point of operation and habitability. For example, the replacement of a crankshaft can be performed through the hatch on the boat deck easily and not through the skylight as is usual, which is a little complicated. This is the reason why the front wall of the boat deck comes far forward from the bridge front wall. To separate the captain's and the owner's rooms from the crew space, a wider area under the boat deck is required which causes the step style side wall arrangement.

As explained above, the steel wall arrangement in the engine room as well as in the superstructure should be decided not from the view points of the operation and the habitability but from the view point of the structure.

## 10.2 Rigidity Criteria in Engine Room Structure Design

Generally the rigidity of a structure is expressed by the deflection of the structure. However, for a structure which may have a vibration problem such as an engine room, it is better to express its rigidity in terms of the natural frequency.

For a both-ends-fixed uniform beam, the deflection  $\delta$  caused by its own weight is expressed by the following equation:

$$\delta = \frac{Wl^3}{384EI} \quad (10.2.1)$$

where

- $W$ : weight of beam
- $l$ : span of beam
- $E$ : Young's modulus
- $I$ : sectional moment of inertia of beam

The natural frequency  $f$  of the beam is expressed by the following equation:

$$f = \frac{60 \times 4.73^2}{2\pi} \sqrt{\frac{EIg}{l^3W}} \quad (10.2.2)$$

where  $g$ : gravity acceleration

From Eqs. (10.2.1) and (10.2.2), the relation between  $\delta$  and  $f$  can be derived as follows:

$$f = \frac{116488}{\delta} \quad (10.2.3)$$

where

$f$ : lowest natural frequency of beam in cpm

$\delta$ : deflection of beam due to its own weight in cm

The rigidity of a structure is usually shown in the form of the deflection or the natural frequency, and their relation can be expressed by Eq. (10.2.3)

The calculation method of the natural frequency of the double bottom, flat, etc. has been often described [32], however the criteria for rigidity have been scarcely introduced. The authors consider it should be decided based on the designer's experience and his/her design philosophy.

For reference, here are some suggestions on how to decide the rigidity, that is, the natural frequency of the engine room structure.

### 10.2.1 Double Bottom in Engine Room

The vibration of the double bottom in an engine room is of fundamental one in the engine room. The main vibration modes in the double bottom in the engine room are shown in Fig. 10.2.1. The diesel main engine has several kinds of excitation which cause resonant vibration in the double bottom in the engine room when the vibration mode, natural frequency and the exciting mode and frequency coincide. For example the exciting mode of the vertical unbalance force of the main engine corresponds to the fundamental vibration mode, and the exciting mode of the H-type lateral movement of the main engine corresponds to the transversely-unsymmetrical vibration mode. These relations are also shown in Fig. 10.2.1.

As explained above each exciting force of the main engine corresponds to a vibration mode of the double bottom in the engine room. So it is a rigidity criterion that the natural frequency  $f_n$  of each mode of the double bottom vibration does not come close to the exciting frequency  $f_{ex}$  of the corresponding exciting mode. Assuming that the estimation allowance of the natural frequency of the structure is  $\pm 10\%$  and the resonance interval is also  $\pm 10\%$ , the following relation can be obtained.

$$\frac{f_n}{f_{ex}} \leq 0.85, \quad \frac{f_n}{f_{ex}} \geq 1.15 \quad (10.2.4)$$

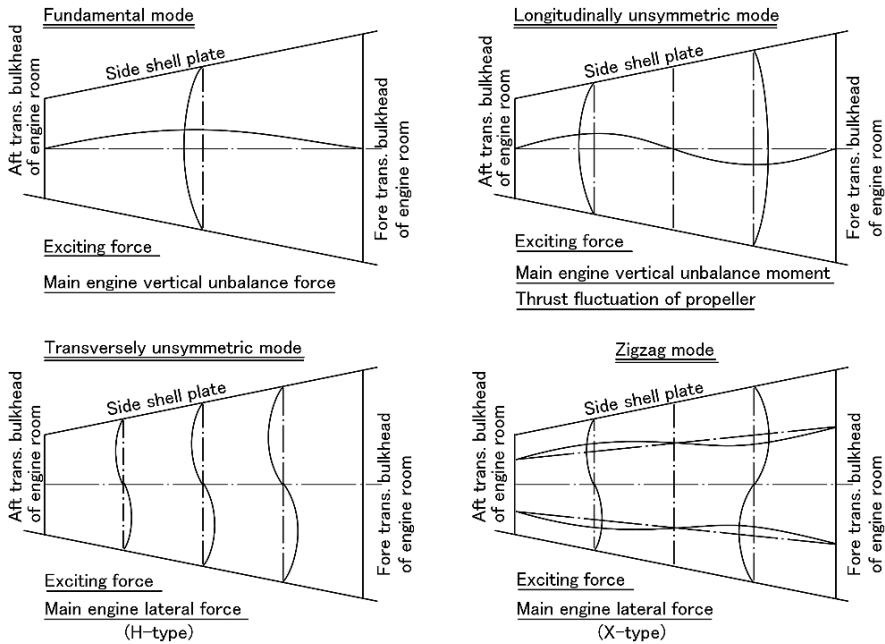


Fig. 10.2.1 Vibration mode of engine room (Aft engine room)

The above is for excitation of the main engine. The thrust variation among the propeller excitations causes a moment on the double bottom in the engine room through the thrust block, giving a similar effect to that of the main engine vertical unbalance moment. In this case (10.2.4) is also effective by putting the propeller blade frequency as  $f_{ex}$  and the natural frequency of the double bottom longitudinal unsymmetrical mode vibration into  $f_n$ .

Equation (10.2.4) is derived based on the assumption that the estimation allowance of the natural frequency of the structure is  $\pm 10\%$ . The figures of 0.85 and 1.15 depend on the estimation accuracy of the natural frequency of the structure. With improvement in the estimation accuracy, they can be modified.

### 10.2.2 Panel, Web, Stiffener Etc.

For these members it is troublesome to apply the method explained in Sect. 10.2.1. To keep the natural frequency above some level is the practical way. These members are excited by the vibration displacement of the adjacent structures. As explained before the vibration level in the aft part of the engine room is higher than that in the fore part. And it is reasonable to have more severe criteria in the aft part than in the fore part.

One example is that these members are to have a natural frequency of 1,500 cpm and over, in the aft part of the engine room, and 1,000 cpm and over in the fore part of the engine room. In this case the natural frequency is calculated with the fixed boundary condition with its own weight and added water if any.

### 10.3 Design of Structural Members in Engine Room

It is explained in Sect. 10.1 that in the design of the engine room, it is important to decide the height of the double bottom and the arrangement of the longitudinal and transverse bulkheads prior to the machinery arrangement. After fixing the bulkhead arrangement, i.e. the main frame work of the engine room, the structural members such as the engine flat and the web frame are designed.

The side shell in the engine room always supports the water pressure from the outside, especially in the fully loaded condition as it will be quite high. The water pressure is supported by the longitudinal frames and the load is transmitted to the web frames which are finally supported by the engine flats. From this viewpoint the engine flat is not only the foundation of the machinery but also an important strength member. In order to reduce the hull steel weight as a consequence of the water pressure, the thickness of the engine flat reduced and finally the engine flat is constructed by a frame work without a plate. Even in such a situation the hull structure designer should keep in mind that the engine flat is an important strength member to support the web frames in the engine room. Moreover, in the case of a narrow hull form at the aft part of the engine room, attention is to be paid to have enough breadth for the engine flat as shown in Fig. 10.3.1.

The engine flat is better arranged with an equal distance between the upper deck and the double bottom top so that the span of the web frame is equal; this will be a well balanced structure.

The web frame is to support the water pressure from the side shell as a beam as well as supporting the water pressure from the bottom as a pillar. The web frame

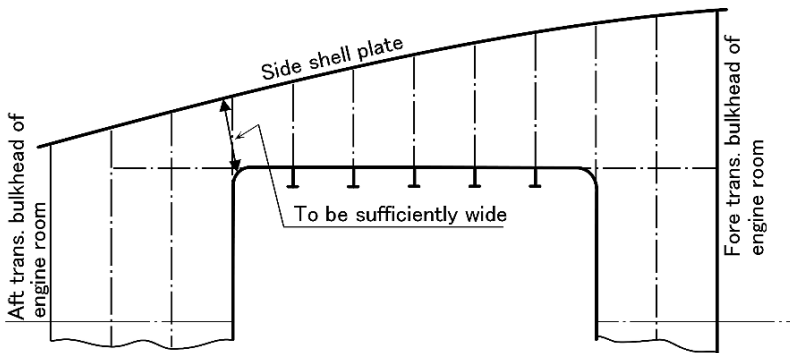


Fig. 10.3.1 Engine flat

is compressed by water pressure from the bottom. Because of this contraction of the web frame in the engine room, the double bottom in the engine room which is supported by the web frame moves parallel upwards, and accordingly a deformation of the double bottom is caused. The deformation of the double bottom in the engine room badly affects the main engine and the shaft alignment. However, the designer can control such deformation by adjusting the thickness of the web frame [33].

The pillar is also an important structural member in the engine room. It is popular to install H-section pillars below the engine casing at the web frame sections. These pillars which are installed apart from the center line, can be extended down to the double bottom in the engine room. However in the aft part of the engine room the center line pillar can not be extended down to the double bottom because of the propeller shaft. In this case the pillar is to be supported by a strong beam under the engine flat, as shown in Fig. 10.3.2. Such a structural arrangement is a kind of a misalignment and the pillar does not work well. One example is shown hereunder.

Assuming  $I$  is the sectional moment of inertia of the strong beam under the engine flat,  $l$  is the span of the strong beam and  $W$  is the concentrated load applied at the midspan of the strong beam, then the deflection  $\delta$  of the strong beam is given by the following equation.

$$\delta = \frac{Wl^3}{192EI} + \frac{Wl}{2GA_w} \quad (10.3.1)$$

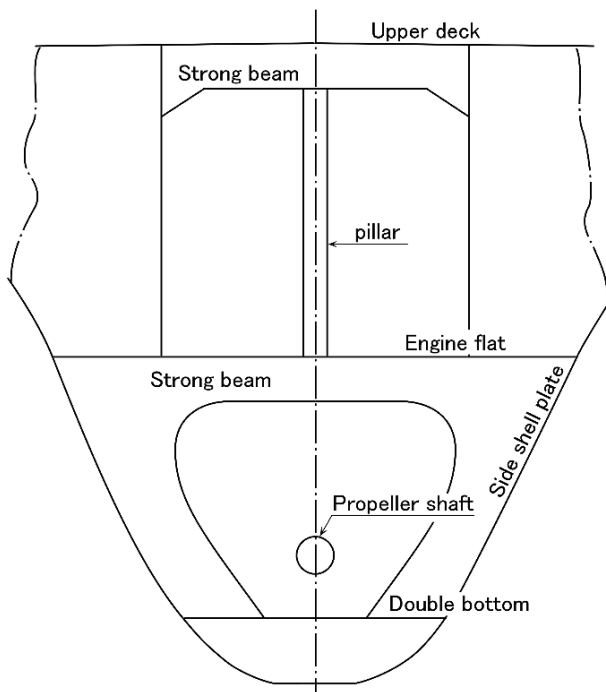


Fig. 10.3.2 Pillar installed on strong beam

where

- $E$ : Young's modulus  
 $G$ : shear rigidity  
 $A_w$ : sectional area of web plate

The first term of (10.3.1) shows the bending deflection and the second term shows the shear deflection.

The strong beam shown in Fig. 10.3.2 consists of a web of  $1,000 \times 11$  mm and a face plate of  $300 \times 22$  mm, and the span  $l$  is 8 m. The deflection  $\delta$  can be calculated as follows.

$$\begin{aligned}\delta &= \frac{800^3 \text{cm}^3 \times W^{\text{tonf}}}{192 \times 2,100^{\text{tonf/cm}^2} \times 421,667 \text{cm}^4} + \frac{800 \text{cm} \times W^{\text{tonf}}}{2 \times 800^{\text{tonf/cm}^2} \times 110 \text{cm}^2} \\ &= (0.003 + 0.0045)W^{\text{cm}} \\ &= 0.0075W^{\text{cm}}\end{aligned}$$

The shear deflection is bigger than the bending deflection because the strong beam is deep relative to the span and the web thickness is quite thin. Such a strong beam seems to have been designed paying more attention to the bending than to the shearing.

On the other hand, assuming the load  $W$  is supported by a pillar under the engine flat and on the double bottom, the shrinkage of the pillar  $\Delta h$  will be as follows.

$$\Delta h = \frac{hW}{EA} \quad (10.3.2)$$

where

- $A$ : sectional area of pillar  
 $h$ : length of pillar

Assuming an H-type pillar of  $400 \times 400 \times 13/21$  between the engine flat and the double bottom shown in Fig. 10.3.2, the sectional area of the pillar is  $200 \text{cm}^2$ , length  $h$  is 6 m, and the shrinkage  $\Delta h$  is as follows:

$$\Delta h = \frac{600 \text{cm} \times W^{\text{tonf}}}{2,100^{\text{tonf/cm}^2} \times 220 \text{cm}^2} = 0.0013W^{\text{cm}}$$

Accordingly  $\delta$  is 5.8 times that of  $\Delta h$  which means the strong beam can not support the pillar as rigidly as the pillar on the double bottom.

## 10.4 Girders and Floors in Engine Room Double Bottom

It is common practice to fit heavy engine girders just under the side plates of the main diesel engine structure. These heavy engine girders are usually provided only

in the region of the main diesel engine. In a similar way to a strong beam which supports a pillar at its midspan as explained in Sect. 10.3, the double bottom is a kind of a deep girder and its shear rigidity is important. So the plate thickness of the girder as well as the thickness of the floor is more important than the plate thickness of the tank top plate and the bottom shell plate.

It would be regrettable to fit heavy engine girders only in the area of the main Diesel engine. They are to be extended to the engine room front bulkhead to support the main engine effectively.

In designing the girder and the floor arrangement in an engine room double bottom, the design philosophy of how to support the main engine is to be established, in addition to the engine maker's instructions and the classification society's rules.

Figure 10.4.1 shows a plan of an engine room double bottom of an aft engine ship. For the case where the distance between the fore end of the engine and the engine room front bulkhead is shorter than the distance between the fore end of the engine and the side shell, it is reasonable to extend the heavy engine girders to the engine room front bulkhead. On the other hand, for the case where the distance between the fore end of the engine and the engine room front bulkhead is bigger, the floors supporting the fore part of the engine are to be thicker.

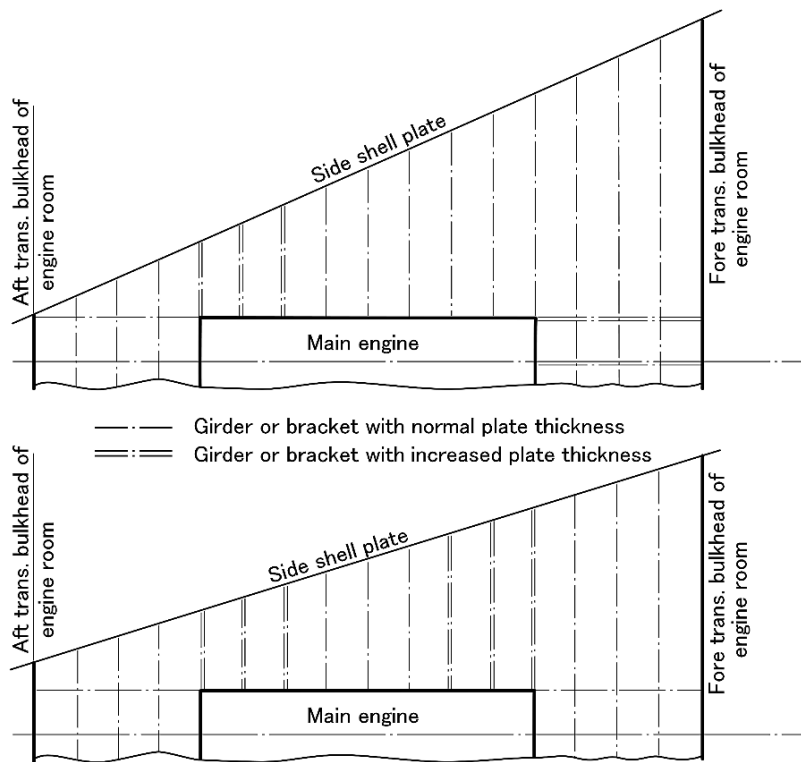


Fig. 10.4.1 Floor and girder arrangement of engine room double bottom

In both cases the shorter member is to be stiff which is understood in terms of the natural engineering philosophy.

There are many holes for access and easy fluid flow in the girders and floors, which destroy the shear rigidity of the double bottom. The number of holes is to be limited and the holes should be cut in the areas where the shearing stress is low.

### 10.5 Problems Caused by Deflection of Engine Room Double Bottom

The large increase in size of a ship and their horse power in the era from 1950's to 1970's, brought many important problems. One of them was the deflection of the engine room double bottom on which a high power main engine was installed. The profiles of such ships are shown in Fig. 10.5.1 [34].

According to the reference [34] the large increase in size is realized by increasing the length and the breadth of the ship. The depth of the ship was not increased so much. An increase in the breadth of the engine room double bottom followed an increase in ship breadth. The breadth of a 500,000 DWT tanker is about twice of that of a 36,000 DWT tanker. Supposing that the floor in the engine room double bottom is fixed at both ends by the side shell and the load does not change much, twice the breadth will bring 16 times the deflection of the double bottom.

On the other hand, the diameter of the propeller shaft increased following the horse power increase. The shaft was designed for constant shearing stress, and the shaft revolution was reduced to have higher propulsion efficiency. Accordingly the torque became very big. The increase of horse power from 8,000 HP to 60,000 HP required a shaft with twice the diameter which had 16 times the bending rigidity.

The problems were caused by the deflection of the engine room double bottom which changed depending on the loading condition, i.e. full load or ballast, the thrust variation at sailing, the wave load, and the thermal condition of the main engine. The rigid shaft is installed on a flexible hull structure, and this incompatibility has caused trouble at the connection parts between them, i.e. the shaft bearings.

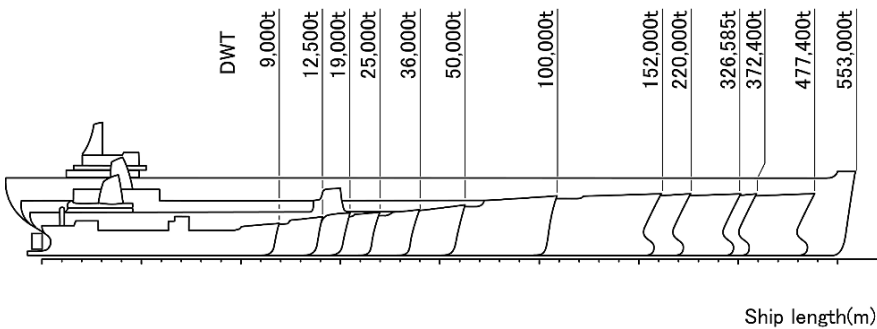


Fig. 10.5.1 Time history of increasing ship size



The large increase in size of ships and their horse power caused much trouble at the shaft bearings and the reduction gear. This was because the propulsion machinery and the shafting were installed without paying any attention to the increased deflection of the engine room double bottom, which is the foundation for the propulsion machinery and the shafting. Recently high tensile steel has been applied widely in the hull structure which makes ships more flexible. The hull structure is mainly designed based on strength considerations. However, for some structural members, rigidity design or vibration design considerations are to be applied in addition to strength.

The trouble caused by the incompatibility between the rigidities of the hull and the machinery is divided into two: the damage to the shaft bearings and the damage to the reduction gear. The damage to the shaft bearings is caused by excess bearing load. Because of hull structure deformation an unbalance bearing load will appear, that is, some bearings support less load than the design load consequently the other bearings should support more load which destroys the bearings. In the case of a bearing which has no load, the unsupported span of the shaft will be nearly twice as long and the long span of the shaft may cause shaft lateral vibration which will destroy the bearing.

Damage to the reduction gear is caused by the non-uniform contact between the bull gear and the pinion which is caused by the deflection of the hull structure in the vicinity of the shafting, as shown in Fig. 10.5.2. The damage to the reduction gear shown is for a turbine ship and in the case of a diesel ship, the bigger crank shaft deflection, due to the engine room double bottom deflection, causes trouble such as an increase in the fillet stress in the crank shaft and damage to the bearing white metal.

One solution to this problem is to reduce the rigidity of the shafting by removing some shaft bearings, making the unsupported span longer.

Another solution is the rational alignment of the shafting. In this method shaft alignment is carried out so as to not have excess bearing load, and to settle the teeth contact in the reduction gears within the allowable limits, taking into account the hull structure deformation.

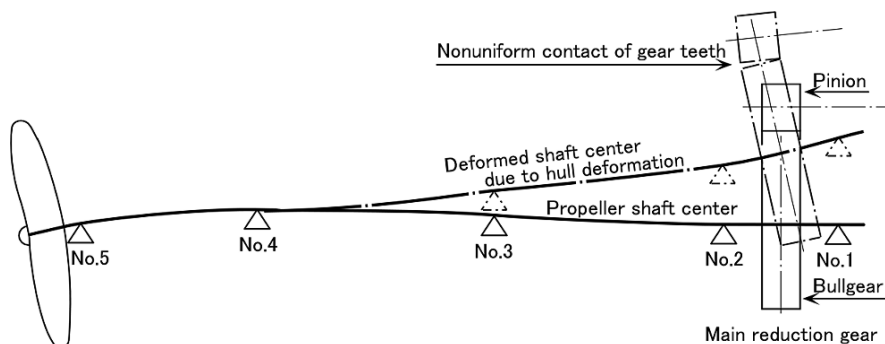


Fig. 10.5.2 Non-uniform contact of teeth of main reduction gear due to hull deformation

## 10.6 Deflection of Engine Room Double Bottom

For the rational alignment of the shafting, taking into account the hull structure deformation, the hull structure deformation should be established by calculation. These days the final deflection mode can be accurately calculated by computer. However, to control the deflection it is better to estimate the deflection analytically.

The deflection of the engine room double bottom consists of the following three terms [33].

- (1) Hull girder bending and shearing deflections in the vicinity of the engine room
- (2) Deformation of the web frame which supports the engine room double bottom
- (3) Bending and shearing deflection of the engine room double bottom itself

By obtaining the deflection of the engine room double bottom in this way, we can find which is the biggest component and how can we reduce the deflection effectively.

Moreover by this analytical consideration the following question was clearly solved. It has been a well known phenomena that the deformation of the engine room double bottom of an aft engine tanker is convex upwards (hogging) in the fully loaded condition while the midship cargo tank part shows sagging, and in the ballast condition it is convex downwards (sagging) while the midship cargo tank part shows hogging as shown in Fig. 10.6.1. But no body has explained this phenomenon clearly. In the above analytical consideration it was found that shear deflection is dominant and its deflection is in the opposite direction to the bending deflection. Thus this long-continued question was clearly solved.

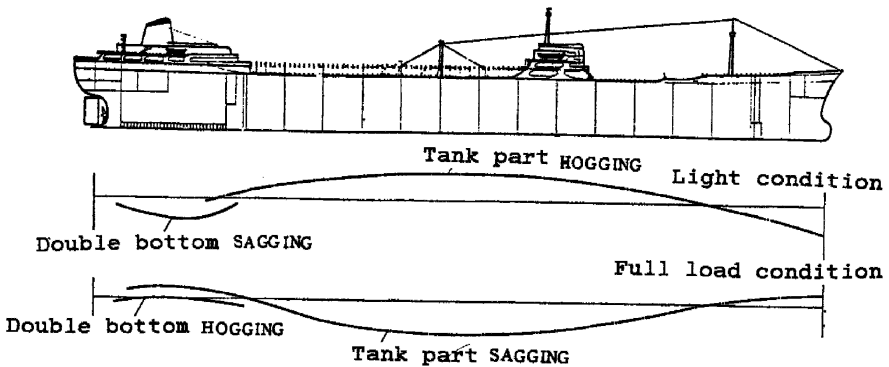


Fig. 10.6.1 Deflection of hull girder and double bottom in engine room

### 10.6.1 Bending and Shearing Deflection of Hull Girder in the Vicinity of Engine Room

Deflection in the engine room double bottom which affects the shaft alignment is the deviation from the straight line connecting the engine room fore and aft bulkheads.

In the discussion of the deflection of the engine room double bottom, we can treat the hull girder in the vicinity of the engine room as a cantilever fixed at the forward section of the engine room front bulkhead, because the structure forward of the engine room front bulkhead does not affect the deflection of the engine room double bottom at all. Here the deflection is analyzed on the hull girder fixed at the midship section as shown in Fig. 10.6.2.

The deflection which causes trouble in the shafting, the reduction gear or the crank shaft is not that of the absolute value in the fully loaded or the ballast conditions, but rather the difference in the deflection caused by the load differences when in service, that is, the difference between the fully loaded and the ballast conditions. Based on this understanding, the load difference between the fully loaded and the ballast conditions is used in hull structure modeling the above cantilever.

Assuming the ballast condition is the original condition, at the fully loaded condition upwards buoyancy caused by the draft increase is applied in the vicinity of the engine room; in contrast a downwards force caused by the cargo weight is applied in the vicinity of the cargo tank. Based on the above consideration, the load curve, the bending moment diagram, and the shearing force diagram were prepared as shown in Fig. 10.6.2. In Fig. 10.6.2 the deflections caused by the bending moment and the shearing force are also shown.

In Fig. 10.6.2 it is shown that the deviation from the straight line connecting the engine room fore and aft bulkheads is downwards for the bending deflection and it is upwards for the shearing deflection. And the deviation caused by shearing is bigger than that by bending, because the hull girder cantilever is a deep girder in the engine room. Then the total deviation comes upwards. This is the answer to the question raised in the previous discussion.

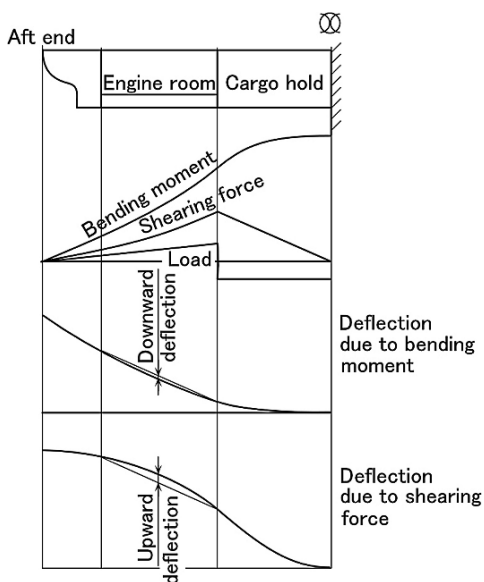


**Fig. 10.6.2** Vertical deflection of hull girder

### 10.6.2 Deformation of Web Frame Which Supports Engine Room Double Bottom

The web Frame which supports the engine room double bottom is simplified and modeled as shown in Fig. 10.6.3. The deformed shape in the fully-loaded condition is shown in the broken line and the full line shows the original ballast condition.

As shown in Fig. 10.6.3 the web frame and the pillar are in compression because of the bottom water pressure and the double bottom moves upwards accordingly, also the center of the double bottom moves downwards as a result of side water pressure.

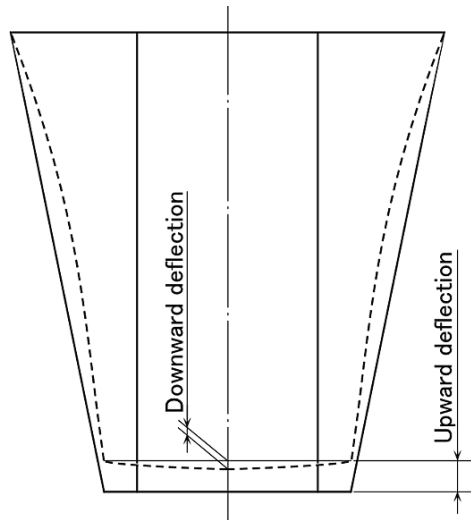


**Fig. 10.6.3** Simplified deformation model of transverse ring of engine room

### 10.6.3 Bending and Shearing Deflections of Engine Room Double Bottom Itself

The engine room double bottom is a grillage structure consisting of floors and girders, and deforms upwards by the bottom pressure caused by the increased draft in the fully loaded condition.

The above deflection of the engine room double bottom is calculated for each component and the results are shown in Fig. 10.6.4. The ship is a 200,000 DWT turbine tanker of which the principal particulars are as follows:

$$L_{pp} = 300.0 \text{ m}$$

$$B_{mld} = 50.0 \text{ m}$$

$$D_{mld} = 25.5 \text{ m}$$

$$d = 19.0 \text{ m}$$

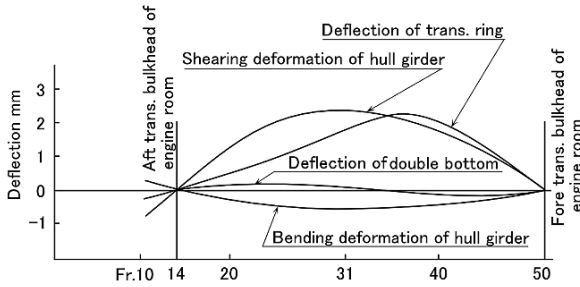


**Fig. 10.6.4** Calculated example of deflection components of engine room double bottom

Main engine: 33,000 SHP at 80 rpm  
Speed: 16.4 knots

From Fig. 10.6.4 it can be found that the bending and the shearing deflections of the engine room double bottom itself are smaller than expected, and the main parts of the deflection come from deformation of the web frame, which supports the double bottom and the hull girder bending and shearing deflections. Accordingly increasing the double bottom height is not so effective in reducing the deflection of the engine room double bottom. On the other hand, as deflection by the hull girder shearing is dominant for a ship of shallow draft and for the sloped side shell plate in way of the engine room, special attention will be paid to the deflection of the engine room double bottom.

Measured data for the engine room double bottom deflection at the reduction gear are shown in Fig. 10.6.5. It can be seen that the deflection is proportional to the draft increase.

## 10.7 Allowable Limit of Deflection of Engine Room Double Bottom

The ship for the model is a 200,000 DWT turbine tanker, and its shaft arrangement is shown in Fig. 10.7.1. In this shaft arrangement, the operating condition of each shaft bearing is as follows.

- (1) The bearing load on the No.1 and 2 bearings is less than 46 tonf each and is positive (surface pressure is less than  $10 \text{ kgf/cm}^2$ ).
- (2) The load difference between the No.1 and 2 bearings is less than 9.5 tonf (less than 20% of the total load).
- (3) The bearing load of the No.3, 4 and 5 bearings is less than 29, 27 and 89 tonf respectively (surface pressure is less than  $5 \text{ kgf/cm}^2$ ) and is positive.

Assuming the bearing load on each bearing at the setting of the shaft with a light draft is  $R_1, R_2, R_3, R_4$  and  $R_5$  respectively and the bearing load on each bearing at

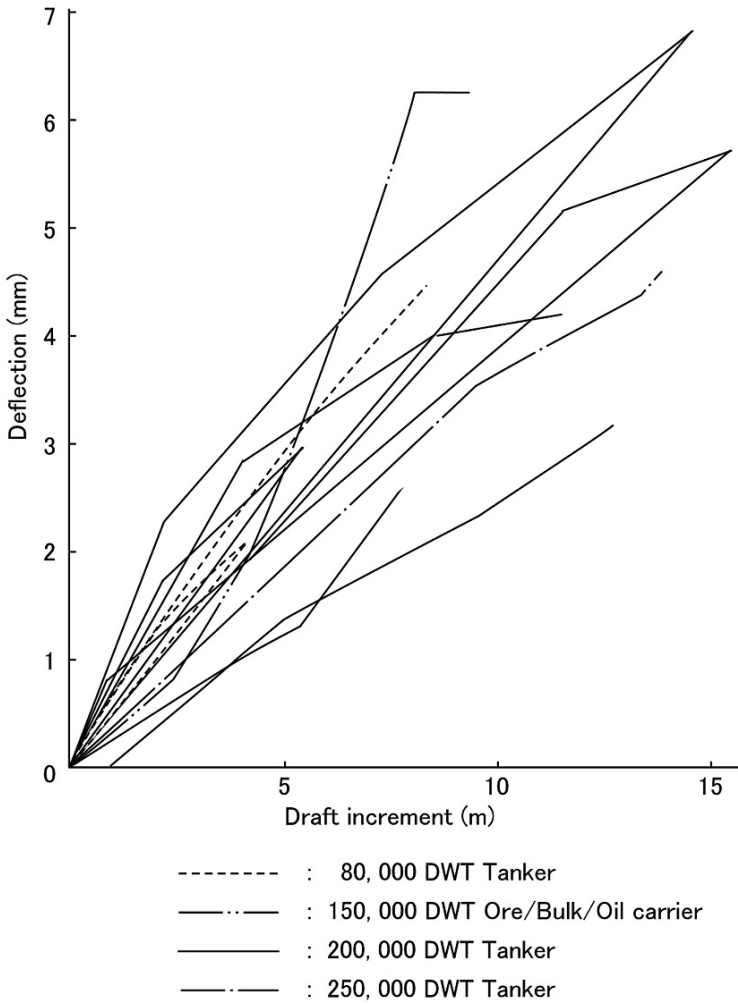


Fig. 10.6.5 Measured deflection of engine room double bottom at reduction gear

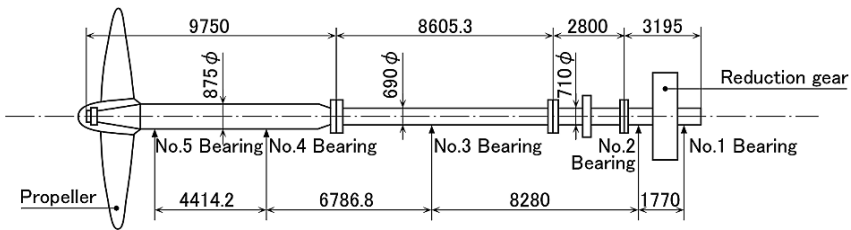


Fig. 10.7.1 Shaft arrangement of 200,000DWT turbine tanker

the fully loaded condition is  $R'_1, R'_2, R'_3, R'_4$  and  $R'_5$  respectively, the above conditions are represented by the following equations.

$$\begin{aligned}
 0 < R'_1 &= R_1 + I_{11}\Delta_1 + I_{12}\Delta_2 + I_{13}\Delta_3 \leq 46 \text{ tonf} \\
 0 < R'_2 &= R_2 + I_{21}\Delta_1 + I_{22}\Delta_2 + I_{23}\Delta_3 \leq 46 \text{ tonf} \\
 0 < R'_3 &= R_3 + I_{31}\Delta_1 + I_{32}\Delta_2 + I_{33}\Delta_3 \leq 29 \text{ tonf} \\
 0 < R'_4 &= R_4 + I_{41}\Delta_1 + I_{42}\Delta_2 + I_{43}\Delta_3 \leq 27 \text{ tonf} \\
 0 < R'_5 &= R_5 + I_{51}\Delta_1 + I_{52}\Delta_2 + I_{53}\Delta_3 \leq 89 \text{ tonf} \\
 -9.5 \text{ tonf} &\leq R'_1 - R'_2 \leq 9.5 \text{ tonf}
 \end{aligned}
 \tag{10.7.1}$$

where

$I_{ij}$  : influence coefficient

$\Delta_i$  : deviation of each bearing from straight line connecting No.4 and 5 bearing

The influence coefficient  $I_{ij}$  is the variation in the bearing load (kgf) at the bearing  $i$  when the bearing  $j$  is moved in a vertical direction by the unit length (mm), and it depends on the rigidity of the shaft and the arrangement of the bearings. In the case of a 200,000 DWT turbine tanker, the influence coefficient is given in Table 10.7.1, and the bearing load on each bearing at the setting of the shaft, with a light draft, is given in Table 10.7.2.

By putting these values in Tables 10.7.1 and 10.7.2 into (10.7.1), the allowable limits of,  $\Delta_1, \Delta_2$  and  $\Delta_3$  can be obtained. The allowable limits of  $\Delta_1$  and  $\Delta_2$  in the

**Table 10.7.1** Coefficient  $I_{ij}$

No.j \ No.i	1	2	3	4	5
1	39,450	-50,130	14,700	-6,010	1,980
2	-50,130	64,480	-20,880	9,740	-3,210
3	14,700	-20,880	14,480	-15,390	7,080
4	-6,010	9,740	-15,390	25,000	-13,340
5	1,980	-3,210	7,080	-13,340	7,490

No.i : Supporting point where supporting force of bearing changes

No.j : Supporting point where 1mm of vertical displacement is applied

**Table 10.7.2** Supporting force for bearing and surface pressure

Supporting point \ Item	Supporting force for bearing (kgf)	Surface pressure (kgf/cm <sup>2</sup> )
1	23,520	5.1
2	23,880	5.1
3	23,580	4.0
4	16,680	3.0
5	68,020	3.8

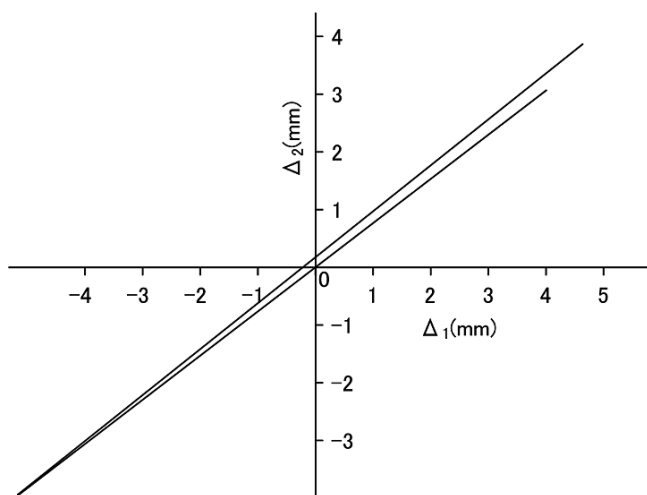


Fig. 10.7.2 Allowable deflection of engine room double bottom from shaft arrangement view point

case of  $\Delta_3 = -0.25$  mm is shown in Fig. 10.7.2. It can be said that the allowable limits of  $\Delta_1$  and  $\Delta_2$  in absolute values are moderately large, provided they have the relationship given in Fig. 10.7.2.

## 10.8 Control of Deflection of Engine Room Double Bottom

The phenomena of and the allowable limit of the deflection of the engine room double bottom have been made clear. So now how the deflection of the engine room double bottom is controlled, is explained. The 200,000 DWT turbine tanker previously introduced is taken as a model ship again.

In this case there are five bearings, so the deviations of the No.1, 2 and 3 bearings from the straight line connecting the No.4 and 5 bearings are important. As shown in Fig. 10.7.2 the allowable limits of the deviation of the No.1 and 2 bearings are to be given for the given value of the deviation of the No.3 bearing. For example in the case of  $\Delta_3$  is  $-0.25$  mm, the combination of  $\Delta_1 = -1.6$  mm and  $\Delta_2 = -1.2$  mm is within the allowable limit, but the combination of  $\Delta_1 = -1.6$  mm and  $\Delta_2 = -0.8$  mm is outside of the allowable limit, even though the absolute value of the deviation is small. In this case having more deflection of the engine room double bottom at the No.1 bearing and less deflection at the No.2 bearing is satisfactory. For example  $\Delta_1 = -1.4$  mm and  $\Delta_2 = -1.0$  mm is satisfactory.

For the above control, adjustment of the thickness of the web plate which supports the engine room double bottom seems to be effective and practical.

Generally in the case of trouble with the shafting and the reduction gear, it is recommended, and this has been applied, to increase the double bottom height in



the vicinity of the shaft bearings and the reduction gear. As shown in Fig. 10.6.4 in an ordinary aft engine ship, the deflection of the engine room double bottom itself is very small and the increase of double bottom height will not solve the problem. A fine adjustment, giving a bigger deflection at the No.1 bearing and smaller one at the No.2 bearing as explained above, cannot be achieved by a uniform increase of the double bottom height.

Another way to control the deflection of the engine room double bottom is through adjustment of the hull girder deflection. As explained in Sect. 10.6.1 hull girder deflections by bending and by shearing have opposite direction. So there is a possibility to cancel them. Usually deflection by shearing is bigger than that by bending. How to increase the bending deflection of the hull girder in the engine room without increasing the shearing deflection, will be the correct solution.

Natural phenomena are so well organized that a concentrated load at the end of a cantilever causes bending deflection only, and no shearing deflection is caused. In the case of a concentrated load applied at the end of a cantilever, the shearing force is equal at any section of the cantilever and it is not possible to cause the shearing deflection defined here (deviation from the base line). In an actual ship the ballast water in the aft peak tank can play the role of this concentrated load. The above case is outlined in Fig. 10.8.1.

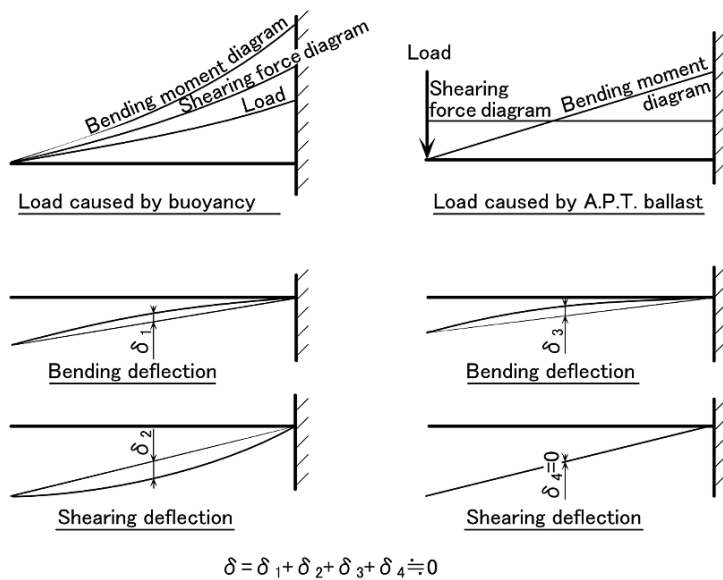


Fig. 10.8.1 Reduction of hull girder deflection

## 10.9 Sea Chest in Engine Room Double Bottom

Cracks were found just after the sea trial of the newly built ship. As instructed in the design standard of Fig. 10.1, a stiffening continuous-tie-band was to be fitted round the sea chest. However in this case it was omitted.

The trouble which was experienced by a company senior more than 30 years ago, appeared again. However this time a young designer did not follow the instructions prepared by a senior. The senior, who instructed to fit a stiffening continuous-tie-band around the sea chest, by considering that the crack was caused by the vibration of the sea chest panel, was excellent. And the young designer was excellent too because he wanted to make clear the phenomena applying the latest technology. He solved the problem clearly by means of measurements on board the actual ship, the model test in a cavitation tunnel, and theoretical calculations.

The crack was caused by the vibration of the sea chest panel induced by the vortex of the incoming water flow. The resonance of the frequency of the induced vortex and the natural frequency of the sea chest panel, caused the heavy vibration. Accordingly the problem was solved by the accurate estimation of the frequency of the induced vortex and the natural frequency of the sea chest panel.

The measurements of the frequency of the induced vortex for several shapes of sea chest opening, and of the natural frequency of a steel box filling with water, using an exciter were carried out, and a design standard was established [35].

# Chapter 11

## Stern Construction and Stern Frame

The stern structure has the following special features not found in other structures:

- It is located near the propeller which is a vibration source.
- It supports the propeller and rudder.

That is, the stern must be designed so as not to allow excessive deflection which would disturb the smooth rotation of propeller and rudder, as well as keeping the stress in the stern within allowable limits. In general, design criteria based on allowable deflection requires much heavier scantlings for structural members, relative to that based on allowable stress.

Stern structure and engine room structure have several rotating machines inside them, therefore, they must be designed from the view point of allowable stress and also from allowable deflection. It was already mentioned that it is important in the design of an engine room that the structure is designed so as not to cause misalignment of machines or pumps, due to large deflection in the structure. In the same manner, much attention must be paid to restrict excessive deflection in the stern structure.

If we calculate the stress of the stern or stern frame by assuming proper external load, we find that the stress level of these members is almost one tenth those of the other structures. That is because the scantlings of these members are decided not by allowable stress criteria but by allowable deflection.

As explained in Sect. 10.7, in order to progress a design based on allowable deflection, allowable limits must be clarified first, and then the stiffness of structural members is determined so that the deflection of the member is lower than the critical limit. However, for the stern, stern frame and rudder, it is regretted that the allowable criteria of deflection has not been completely established at this stage.

Establishment of the following criteria is essential in designing more reasonable and more sophisticated structures:

- allowable stress to prevent cracking or buckling
- allowable amplitude to prevent vibration
- allowable deflection to prevent machinery damage

## 11.1 Aft Peak Tank Construction

We normally call the after part of a vessel back from the aft peak bulkhead the stern structure, whose lower part is often utilized as an aft peak tank and upper part is for the steering gear room.

In the design of the stern structure, it is an important matter to choose whether a longitudinal framing system or a transverse framing system should be provided. Furthermore, when a transverse framing system has been selected, we should then decide which is best, a transverse system constituted by solid floors or transverse system by built-up frames?

Although it is a recent tendency to apply the longitudinal system in a stern structure, several years ago the transverse framing system was used, in particular, the transverse system by built-up frames.

For example, soon after the time when one of the authors joined IHI, that is the middle of the 1950's, a 32,000 DWT tanker was planned to be built by IHI, which was a size larger than the 20,000 DWT tanker that we usually designed in those days. The owner gave us several structural drawings drawn by ISHERWOOD, a British company, which indicated that the aft peak tank was fabricated by a solid floor system. Considering that a fluctuating pressure induced by the propeller acts on the outer shell plating of the aft peak tank, it is reasonable to provide solid floors to the tank structure because they support the outer shell very rigidly. We were deeply impressed that such a rigid structure was used in the aft peak tank even for the larger size of vessel. Nevertheless, we had also some pity on the worker who had to perform tasks in the narrow space surrounded by solid floors; the floor space was 610 mm.

On the other hand, these solid floors are effective in preventing the vibration of the outer shell plating, but they may cause another vibration problem: vibration of the solid floor plate itself. Once the aft peak is filled with ballast water, the natural frequency of the floor plate will decrease due to the increase of water weight, that is the effect of added mass of water. As a result, the possibility of vibration of the solid floor exists. Hence, we thought it would be helpful to arrange several lightning holes in the floor plating to reduce the weight of added mass.

In the case of the longitudinal framing system, longitudinal stiffeners are supported by transverse web frames, which means that slot openings are inevitable at the intersection between longitudinals and web frames. Such slots were recognized as starting points for cracks, because they create a stress concentration at the intersection. For this reason, we hesitated to apply a longitudinal framing system to the stern structure before the design of the 32,000 DWT tanker. Of course, regarding the application of a longitudinal system to the aft peak tank, we were well aware of the advantage of easy construction and of steel weight saving, while we knew the disadvantage of high stress concentration.

At the beginning of the stern structure design of the vessel, one young designer proposed to take the longitudinal framing system. "All slot openings had better be covered by collar plates, as long as there are problems because of high stress concentration caused by openings." It was a great idea to apply the longitudinal system to the stern structure, like Columbus' egg.

## 11.2 Vibration of Stern Structure

The magnitude of the hull girder vibration is largest at the aft end of the stern part, in general. If we stand near the flag pole of the aft end during sea trials, we can experience the largest vibration amplitude. In other words, even when the vibration amplitude of other structures is greater than that of the stern, we will be able to reduce it to less than the stern by providing suitable reinforcement.

### 11.2.1 Vibration of Stern Overhang

Figure 11.2.1 shows a profile of the stern structure. As the length  $l$  of the overhang and its breadth  $b$  become larger, the natural frequency of the overhang decreases and it may cause a vibration problem.

The estimation method of the natural frequency of a stern overhang is explained hereafter. In this method, firstly the stern overhang is regarded as a uniform cantilever beam, secondly the natural frequency is obtained for the shearing deformation of the beam and finally it is modified by taking account the effect of bending deformation and of non-uniformity of the cross section of the beam. In addition to that, the weight of rudder and added mass is considered. The natural frequency is expressed by the following equations:

$$f = f_0 \times K_b \times K_v \tag{11.2.1}$$

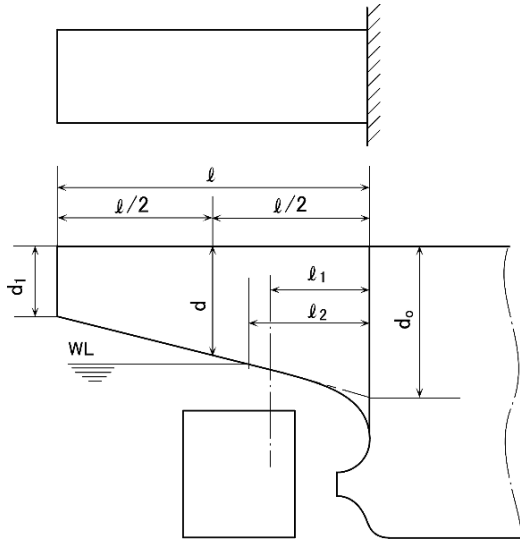


**Fig. 11.2.1** Definition of stern overhang

where

$$f_0 = \frac{15}{l} \sqrt{\frac{g \times G \times A_s}{w}} \tag{11.2.2}$$

$$w = w_H + w_R + w_W$$

- $w_H$ : average hull steel weight per unit length
- $w_R$ : equivalent weight of rudder per unit length

$$w_R = \frac{W_R}{l} \times C_R$$

- $W_R$ : weight of rudder
- $C_R$ : equivalent coefficient of rudder as indicated in Fig. 11.2.2
- $w_W$ : equivalent weight of added mass per unit length

$$w_W = \bar{w}_W \times C_W$$

$$\bar{w}_W = \frac{1}{2} \times \gamma_W \times \pi \times b^2$$

- $C_W$ : equivalent coefficient of added mass as indicated in Fig. 11.2.3
- $\gamma_W$ : weight of sea water per unit volume
- $l_2$ : length of overhang attaching to sea water
- $b$ : breadth of water plane at the mid-point of  $l_2$
- $G$ : shear rigidity
- $A_s$ : effective shear area at the middle point of  $l$
- $K_b$ : modification factor to include bending deformation as indicated in Fig. 11.2.4
- $I$ : sectional moment of inertia at the mid-point of  $l$
- $K_v$ : modification factor to include the change of cross section as indicated in Fig. 11.2.5

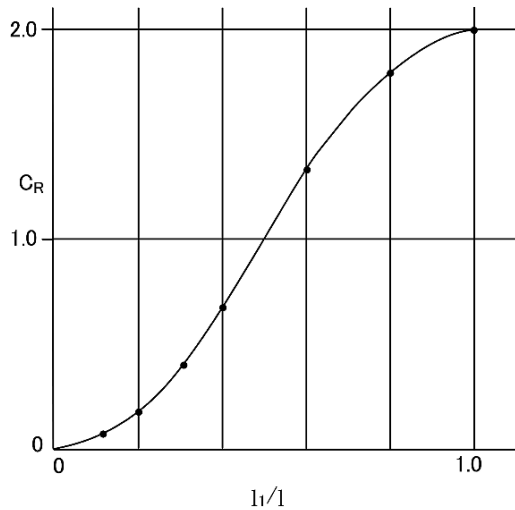
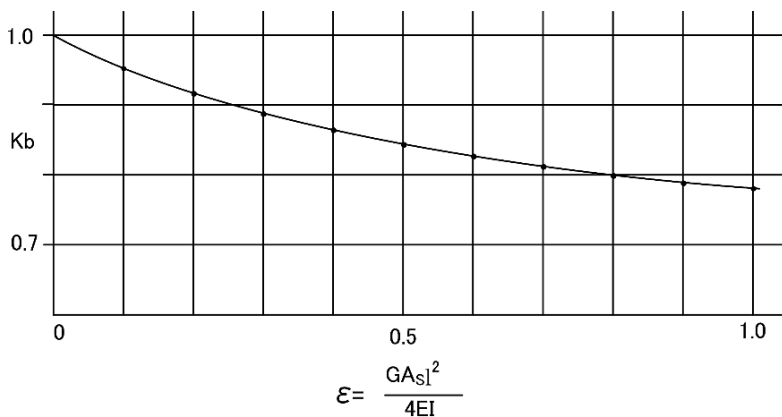
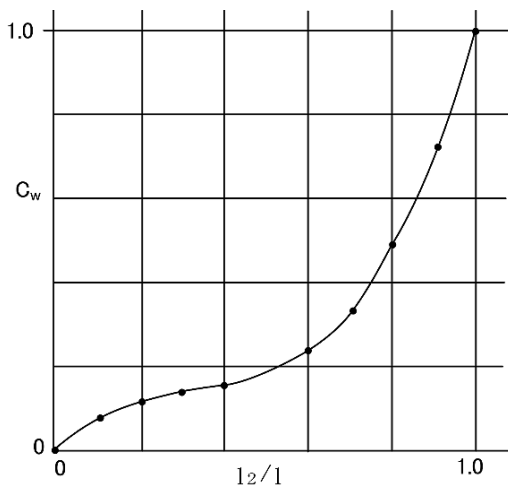
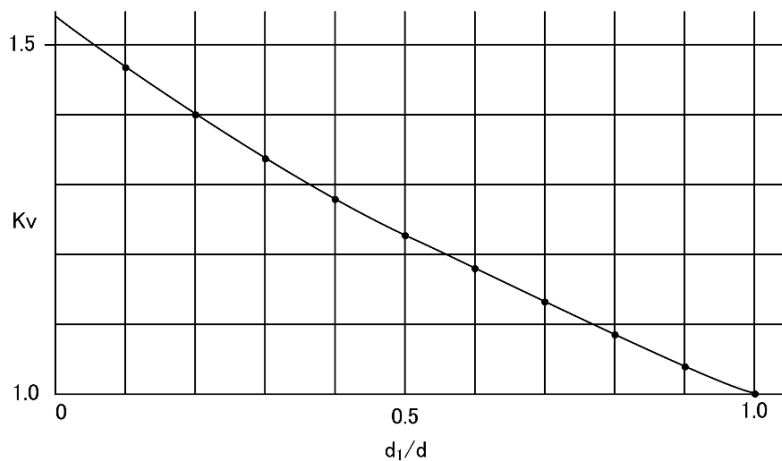


Fig. 11.2.2 Equivalent coefficient of rudder weight

**Fig. 11.2.3** Equivalent Coefficient of added water mass



**Fig. 11.2.4** Modification factor of bending



**Fig. 11.2.5** Modification factor of cross section change

In the case that the natural frequency obtained by Eq. (11.2.1) is close to the exciting frequency due to the propeller, resonance should be avoided by the following measures:

- Provide additional longitudinal bulkheads
- Increase plate thickness of the outer shell plating

### ***11.2.2 Transverse Vibration of Stern Bossing of a Single Screw Vessel***

Vibration of the bossing is induced by the vibration of the hull structure around bossing and of the propeller including the propulsive shaft. The vibration of the hull structure is affected by the movement of shaft and propeller through the spring effect of the lubricating oil film in the stern tube bearing and intermediate bearing. Hence the natural frequency of the bossing is usually calculated by means of FEM. We will explain the correlation between the exact result from the FEM calculations and the result obtained by simplified three-dimensional frame analysis. The model of the FEM calculations is illustrated in Fig. 11.2.6. An accurate natural frequency for the bossing can be obtained by the FEM model, however, making such FEM models takes much cost and time.

Therefore, a simplified calculation method is proposed with the aid of a three dimensional frame model as shown in Fig. 11.2.7. The stern bossing is modeled as co-supported beams connected to the propeller and propulsive shaft by an oil film spring bearing. The co-supported beams are composed of two groups of beams: the vertical cantilever beams, whose upper ends are fixed and which represent the transverse members of the hull structure and stern frame, and the longitudinal cantilever beams with fixed fore ends represents the longitudinal members of the hull structure.

Table 11.2.1 demonstrates the calculated results obtained by each structural model. The simplified three-dimensional frame model can give only the natural frequencies in air, therefore, it must be calibrated by correlation between the frequency in air and in water obtained by FEM analysis. The reduction factor of the natural frequency due to water becomes  $309/363 = 0.85$ .

Consequently, when the natural frequency of the bossing in air is obtained by a simplified three dimensional frame model, multiplying it by 0.85 gives the natural frequency in water.

### ***11.2.3 Vertical Vibration of Twin Bossing in Twin Screw Vessel***

In a vessel with twin screws, the vertical vibration of bossing may appear in two different vibration modes. One is a symmetrical mode, that is, portside and starboardside bossings vibrate simultaneously in a vertical direction, and the other is an unsymmetrical mode where the portside bossing moves downward when the starboardside moves upward, and vice versa. Strictly speaking, each bossing moves in



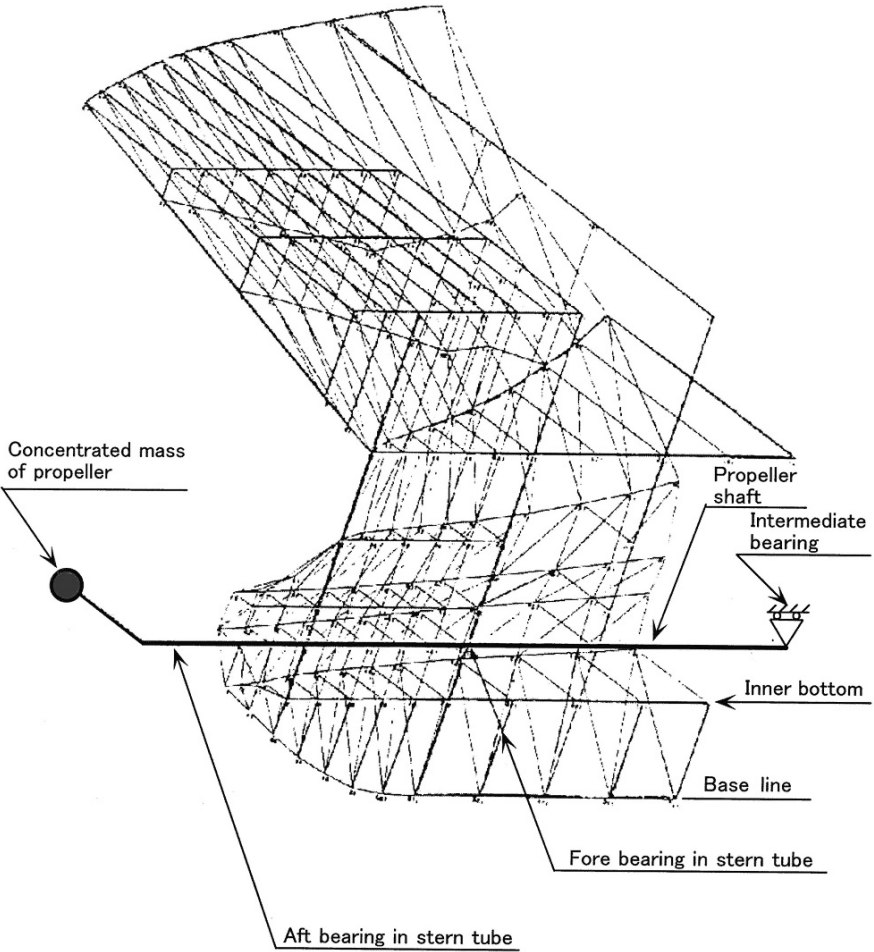


Fig. 11.2.6 3 Dimensional FEM model of bossig

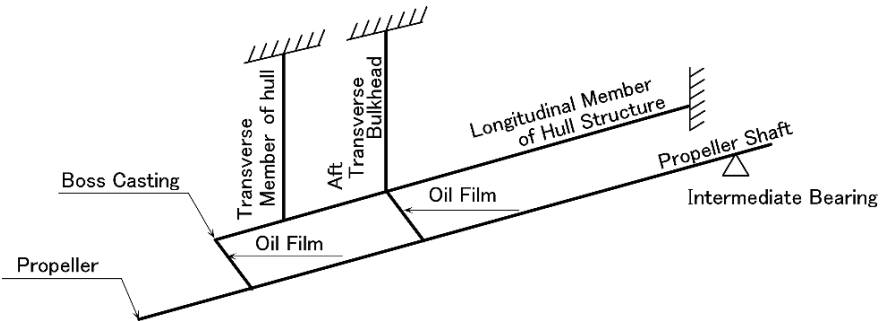


Fig. 11.2.7 Simplified frame analysis model of stern bossing

**Table 11.2.1** Natural frequency of vertical vibration of bossing (single screw)

	Natural frequency		Note
	In air	In water	
3D FEM model with plate elements	330 cpm	309 cpm	Including propeller shaft
	530 cpm	487 cpm	Omitting propeller shaft
3D frame analysis model	363 cpm	309 cpm	Assuming natural freq. in water to be 0.85 times of natural freq. in air
Measurement		295 cpm	

a circular shape in the latter case. The symmetrical mode is caused by the vertical exciting force, while the unsymmetrical mode responds to transverse forces.

As for the calculation for vertical vibration of twin bossings, the method suggested by Ayling is well known and is still utilized for design purposes [36]. He assumed the bossings to be cantilever beams fixed to the main hull structure and derived the natural frequency of the symmetrical mode  $N$  as follows;

$$N = \phi_2 \cdot \frac{60}{2\pi} \sqrt{\frac{3E(I_1 + I_2)g}{(W_1 + W_2)l^3}} \quad (\text{cpm}) \tag{11.2.3}$$

where

- $\phi_2$ : experimental modification factor of inclined angle of bossing as indicated in Fig. 11.2.8
- $I_1, I_2$ : sectional moment of inertia of cast steel section and fabricated steel plate respectively at the base of the bossing. (detail is explained in Fig. 11.2.9)

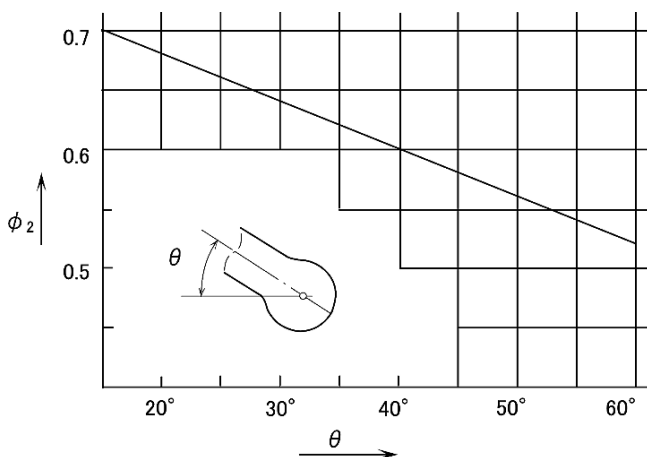


**Fig. 11.2.8** Modification factor of raised angle of stern bossing

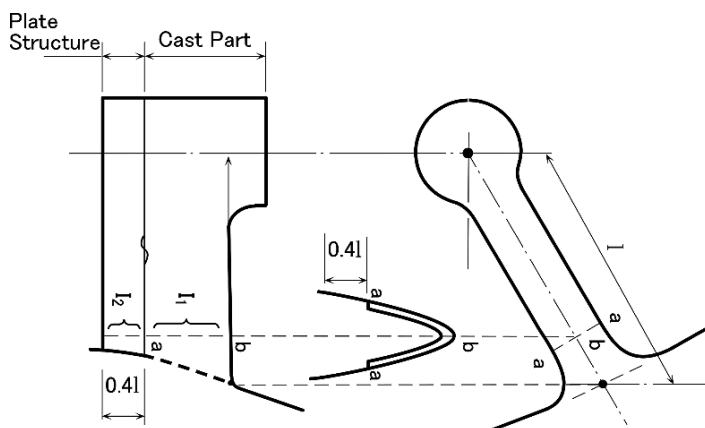


Fig. 11.2.9 Definition of stern bossing

- $W_1$ : propeller weight
- $W_2$ : weight of bossing and propeller shaft
- $l$ : distance between propeller shaft center and hull structure as shown in Fig. 11.2.9
- $E$ : Young's modulus
- $g$ : acceleration of gravity

Moreover, the natural frequency of the unsymmetrical mode is reported to be approximately 85% of that of the symmetrical one. In order to confirm the above report, an excitation test was carried on a 1,800 TEU container carrier which was designed to have two diesel driven main engines and twin bossings to realize 34,800 HP. According to the measured results, the natural frequency of the symmetrical mode was 505 cpm and that for the unsymmetrical mode was 437 cpm, therefore, the ratio of the unsymmetrical frequency against the symmetrical one was proved to be 86.5%.

### 11.3 Stern Frame

The structure of the stern frame has changed drastically in response to the variation of rudder type and the change of stern shape.

In the case of a G type stern frame, not only the weight of the propeller and rudder but also the reaction force induced by keel blocks in dry dock must be supported, because the vessel touches the keel blocks firstly at the stern frame. In the design of a G type stern frame, the cast steel part around the propeller, called the propeller post, is easily designed for it acts as a pillar for the compressive load due to the reaction force from the keel blocks. On the contrary, it is difficult to maintain sufficient strength in the shoe piece, because it works as a long cantilever beam if it

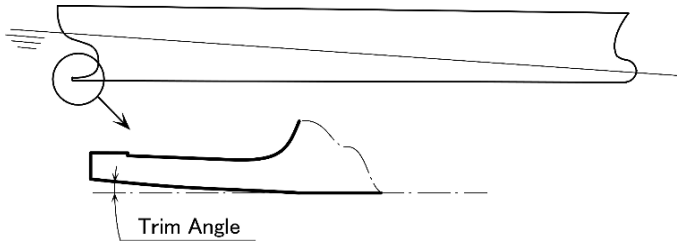


Fig. 11.3.1 Inclination of shoe piece bottom

is subjected to a reaction force at its aft end. To avoid this, the shoe piece must be designed so as to have a slight inclination which is greater than the maximum trim angle as illustrated in Fig. 11.3.1.

As previously discussed in Sect. 5.5, in the case where the vessel has an open type of bulbous stern as indicated in Fig. 5.5.1, no reaction force is transmitted to the propeller post at dry docking. Consequently, the thickness of the lower part of the propeller post is considered to be sufficient as long as it has the same thickness as the side shell plate. If the plate thickness of this part is increased, it results in an increase of bossing weight, which acts as additional weight at the aft end of the cantilever beam. Therefore, such a design is not preferable in order to prevent any vibration problems.

By providing inclination to the shoe piece bottom, the reaction force can be avoided. Hence, the shoe piece is subjected to only a horizontal force due to the rudder. To investigate the strength of the shoe piece under such loading conditions, it is modeled as a cantilever beam subjected to a concentrated load at its end, and in this case the deflection at the end becomes of great concern.

Let us compare the deflection of a beam in the following two cases:

- Case A : shoe piece is modeled as a cantilever beam which has a triangular plan
- Case B : shoe piece is modeled as an uniform cantilever beam which has a straight form

Provided that the depth of the shoe piece  $b$  is the same in both cases, the total weight is also the same as shown in Fig. 11.3.2. In Case A, if the breadth at the fixed end is  $d_0$ , the breadth at the position whose distance is  $x$  from the fixed end is given by  $(l-x)d_0/l$  and the bending moment at that section is  $W(l-x)$ . Thus, the deflection can be obtained by integrating the curvature according to the following process;

$$\begin{aligned}
 \frac{d^2y}{dx^2} &= \frac{M}{EI} \\
 &= \frac{W(l-x)12I^3}{Ebd_0^3(l-x)^3} \\
 &= \frac{12Wl^3}{Ebd_0^3(l-x)^2}
 \end{aligned} \tag{11.3.1}$$

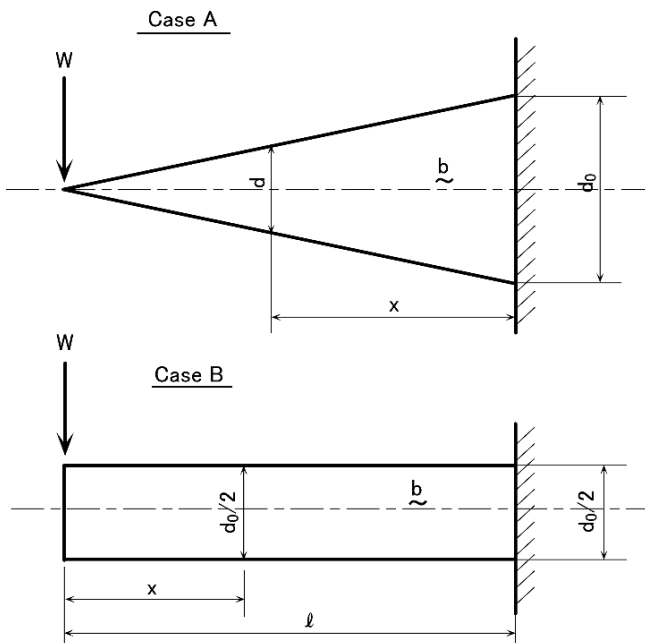


Fig. 11.3.2 Canti-lever beams with triangular plane and with uniform plane

Integrating the above curvature, we find the slope of the beam

$$\begin{aligned} \frac{dy}{dx} &= \frac{12Wl^3}{Ebd_0^3} \int (l-x)^{-2} dx \\ &= \frac{12Wl^3}{Ebd_0^3} (l-x)^{-1} + C \end{aligned} \tag{11.3.2}$$

At the fixed end  $x = 0$ , the slope of deflection must become zero, that is  $\frac{dy}{dx} = 0$ , therefore, the arbitrary constant  $C$  must satisfy

$$C = -\frac{12Wl^3}{Ebd_0^3} \times \frac{1}{l}$$

Then the deflection can be expressed by introducing an arbitrary constant  $C_1$

$$\begin{aligned} y &= \frac{12Wl^3}{Ebd_0^3} \left[ \int (l-x)^{-1} dx - \int \frac{dx}{l} \right] \\ &= \frac{12Wl^3}{Ebd_0^3} \left[ -\log(l-x) - \frac{x}{l} \right] + C_1 \end{aligned}$$

An arbitrary constant  $C_1$  can be determined by the boundary condition that the deflection must be zero, i.e.  $y = 0$ , at the fixed end, i.e.  $x = 0$ .

$$C_1 = \frac{12Wl^3}{Ebd_0^3} \log l$$

Thus, we obtain the deformation form

$$\begin{aligned} \therefore y &= \frac{12Wl^3}{Ebd_0^3} \left[ -\log(l-x) - \frac{x}{l} + \log l \right] \\ &= \frac{12Wl^3}{Ebd_0^3} \left[ -\frac{x}{l} - \log \left( 1 - \frac{x}{l} \right) \right] \end{aligned} \tag{11.3.3}$$

In Case B, the deflection of the uniform beam is expressed by Eq. (11.3.4)

$$y = \frac{12Wl^3}{Ebd_0^3} \times \frac{8}{3} \left( 1 - \frac{3x}{2l} - \frac{x^3}{2l^3} \right) \tag{11.3.4}$$

The deformed shape of the beam is shown in Fig. 11.3.3 for both cases where the triangle beam and the uniform beam are loaded by the same magnitude of force. According to the figure, the triangular shape of the cantilever beam creates a large deflection around the tip of the beam. Considering the above, the rational design of the shoe piece is to have a triangular shape from the fixed end to 0.7l distance, and a uniform shape from 0.7l to the tip end.

Although the shape of the tip end of the shoe piece used to be designed in such a way that it had a teardrop section similar to the horizontal section of the rudder, it has been changed to a blunt shape. This is because it is unreasonable to provide such a sophisticated form to the tip of the shoe piece while it is in the turbulent flow induced by the propeller. The changes in the shoe piece tip are illustrated in Fig. 11.3.4. In spite of the above discussion, the forward part of the shoe piece rather than the propeller position should be rounded at the corners, because rectangular corners will generate vortices which may damage the propeller.

A fabricated type of shoe piece which consists of a few steel plates was widely used, since it is neither heavier nor as expensive as a steel casting. However, even in

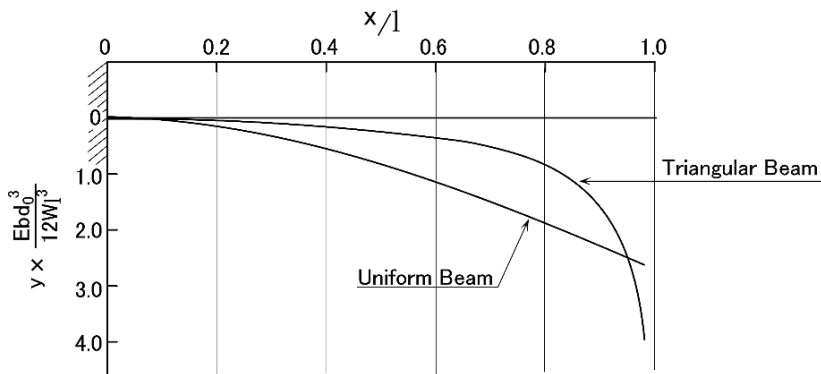
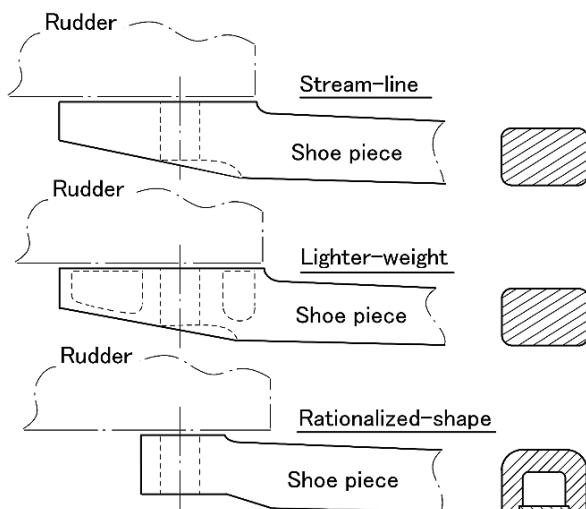


Fig. 11.3.3 Deformation of triangular beam and uniform beam



**Fig. 11.3.4** Change of shoe piece tip

the case of applying a steel casting to the shoe piece, the steel weight can become approximately the same as a fabricated type by providing a  $\square$  shape in cross section in which the steel around the neutral axis of the horizontal bending is reduced. In addition to the above fact, a casting is more convenient than fabricated steel for the forming of a large corner radius to prevent the vortex problem.

In the case of the stern frame without a shoe piece, the upper part of the stern frame, that is called the rudder horn, is important, because it must support every kind of the force induced by the rudder without the help of a shoe piece. As the rudder horn becomes larger, the bending moment created at the base of the rudder horn increases. On the contrary, the force acting on the lower end of rudder horn decreases because the rudder bearings can share the load acting on the upper part of the rudder.

The bending moment of the rudder horn is so big at the base of the horn that the rudder horn is usually designed to penetrate the outer shell plating and to extend to the upper flat or deck.

There are two types of rudder horn: welded type of rudder horn fabricated from steel plates, and forged-steel type. In case of the forged-steel type, the rudder horn is like a cylinder whose horizontal cross section has a D shape.

The stern frame is very important not only from the view point of strength but also from that of the construction schedule, for it takes a longer time to produce cast steel than ordinary steel parts. Therefore, the designer must pay careful attention to the production schedule of cast steel so as not to disturb the construction schedule.

In spite of these points, the authors suffered from serious trouble relating to the stern frame. Let us explain the valuable lessons learned from our experiences, which may benefit other structural designers:

The stern frame must be annealed by heating up to  $650 \pm 25^\circ\text{C}$ , for both fabricated type and casting type. The designer has to check if the size of the stern frame is within the capacity of the heating furnace. If the whole stern frame cannot be stored in the furnace, it must be divided into a few parts which are annealed individually and then connected to each other; being annealed by local heating. The designer has to take it for granted that he/she describes the above procedure of annealing very clearly in the drawing so as not to cause confusion in production.

Non-destructive tests of a stern frame are sometimes troublesome, in particular for radiographic tests utilizing X-rays. In some cases, it needs a special instrument for inspection due to the large thickness of cast steel. Therefore prior to the examination process, the designer must investigate the capability of the X-ray equipment.

The designer needs to prepare a repair plan for structural defects. For example, in almost all cases cast steel has internal defects. Cracks sometimes appear on the surface of the thicker steel plates during the bending process of the plate. This is often treated as a matter for the production engineer, but we think that the designer must go and see the defects himself to make a proper judgement to see if it is possible to repair the defects or not, and to determine a suitable repair method. The designer is apt to stay in his design office and to make decisions without going out to see the defects. However, we have to emphasize that the structural designer must go and see them himself in order to gather exact information to make correct decisions.



## Chapter 12

# Vibration Prevention

When we consider the structural strength, first we calculate the structural responses to the external forces and then we judge whether the result is within the allowable limits which are determined according to the data from existing vessels. In the same manner, when we design a structure from a vibration aspect, we first calculate the structural response to the exciting force and then we judge the result considering the allowable limits which are determined from comfort considerations for crew, or the lifetime of the machinery.

Considering structural strength, an external force is predominantly induced by the sea conditions, which vary widely according to the change of sea state. Therefore, it is quite difficult to obtain the external forces correctly. For this reason, judgement must be carried out on the basis of calculations by assuming the external force appropriately.

In contrast with the above strength design, in the design of structural vibration, the exciting force can be estimated correctly. In spite of this advantage, the calculated structural response is not so accurate in many cases. This is because the estimation of damping contains many unknown factors and consequently they mislead the calculated response.

In the structural strength, it is impossible for the designer to decrease the external force. As a result, the purpose of the structural design is to reduce the structural response to the constant external force.

On the contrary, in vibration design there is no vibration of the structure as long as the exciting forces do not exist. Hence the designer must aim to reduce the exciting forces as low as possible in order to achieve a good vessel which has low vibration. Consequently, it is more important to pay attention to decreasing the exciting force than to calculating exactly the vibration response.

In this section, we are not willing to explain exact calculation methods for estimating damping etc. but we introduce experimental methods to allow the right decisions for vibration. The development of this method [37] was based on the vibration measurements on many actual vessels together with experience of heavy vibrations of superstructures and vibrations of in-tank structure.

### 12.1 Exciting Forces

For the exciting forces, the frequency and magnitude are important. And in a situation where there are two exciting forces of the same frequency, the phase difference between them is an important factor. The exciting forces on ship vibration come from the propeller and diesel engine. It is important to recognize that these exciting forces are magnified in the ship structure by resonator. For example, where there is resonance of axial vibration of the diesel engine crankshaft, the exciting force which comes from the diesel engine is transmitted to the hull and superstructure after being magnified by the resonator of the crankshaft, with the result that the superstructure then vibrates heavily [38, 39].

From the resonance viewpoint, the frequency of the exciting force is important, and in Fig. 12.1.1 the range of frequencies of exciting forces on a ship structure are

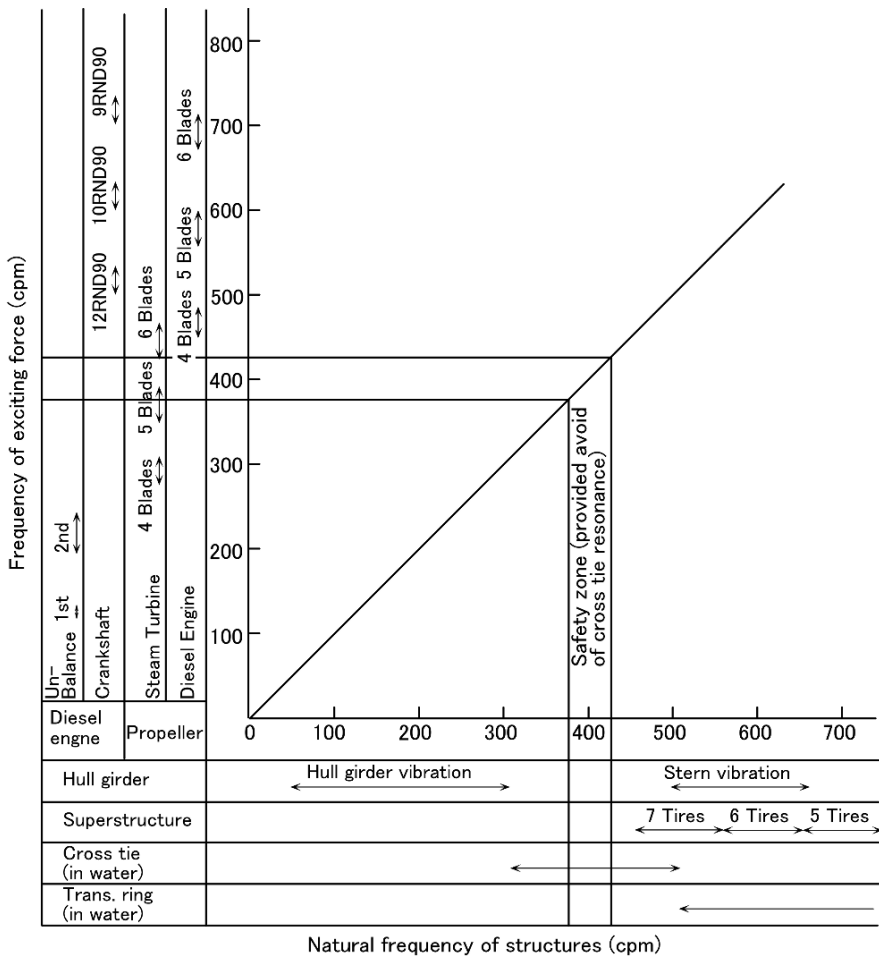


Fig. 12.1.1 Natural frequency of hull structure and frequency of exciting force

shown. The frequency of propeller exciting force is mainly blade frequency (revolutions of propeller shaft multiplied by number of propeller blades) and sometimes twice that. The frequencies of diesel engine exciting forces are 1st, 2nd, 3rd orders, etc. ( $N$ th order means  $N$  times propeller shaft revolutions). First and second order unbalanced forces or moments which sometime cause hull girder flexural vibration are well known. Higher order exciting forces are transmitted to the hull structure after being magnified by resonators, such as crankshaft or engine structure. The magnitude of the higher order exciting force is usually too small to cause heavy vibration on a ship structure by itself. In spite of that, where the natural frequency of the crankshaft or engine structure vibration coincides with a certain order of the exciting force, it becomes a resonator and causes heavy vibration in the ship structure. In Fig. 12.1.1 the ranges of natural frequencies of ship structures are shown. Countermeasures are necessary where both the ranges of excitation and response overlap.

Usually the propeller exciting force is treated as two forces: surface force and bearing force. The former depends very much on propeller aperture; recent research has discovered that a cavitating propeller generates far bigger surface force than a non cavitating propeller. The latter depends on the wake field,  $jN$ th,  $j(N - 1)$ th, and  $j(N + 1)$ th order components of wake distribution ( $N$  is number of propeller blades). Recommended sizes of the propeller aperture have been proposed by many researchers, and these recommended values seem to be practical in avoiding excess surface force. From the authors' experience it can be said that with these recommended propeller aperture sizes the exciting force of the propeller is not a problem.

As already stated, where there are two exciting forces of the same frequency the phase difference between them is important. The cases are, for example.

- (a) 6-bladed propeller and Sulzer 9RTA
- (b) 5-bladed propeller and Sulzer 10RTA
- (c) 4-bladed propeller and Sulzer 12RTA

In these cases, the optimum propeller fitting angle must be investigated to cancel the exciting forces.

### ***12.1.1 Magnitude of Propeller Excitation***

The relation between the size of the propeller aperture and the vertical propeller exciting force has been studied by many researchers. A sample of their results is shown in Fig. 12.1.2. The results shown in Fig. 12.1.2 are obtained by comparing the ship's aft end vertical vibration amplitude when sailing and during exciter tests with the exciter installed just above the propeller. From Fig. 12.1.2 it can be seen that the magnitude of the exciting force is about 4–5% that of the total thrust in the case of a large aperture. The frequency of the propeller exciting force is equal to the blade frequency. The thrust of a 250,000 DWT tanker is 200 tonf, so the exciting force of the propeller will be about 10 tonf in this case [38].

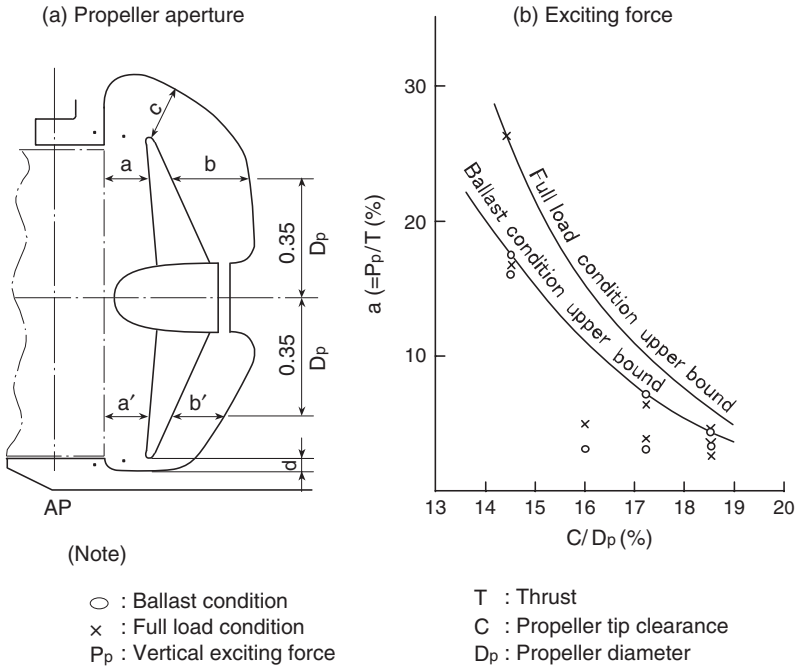


Fig. 12.1.2 Propeller aperture and exciting force

Figure 12.1.3 shows the results of an exciter test on a 250,000 DWT tanker in which the exciter was fitted at the aft end of the ship. The lower figure represents the fore and aft vibration in the superstructure, and the upper is for the vertical vibration at the aft end of the ship. An exciting force of 10 tonf cannot cause significant

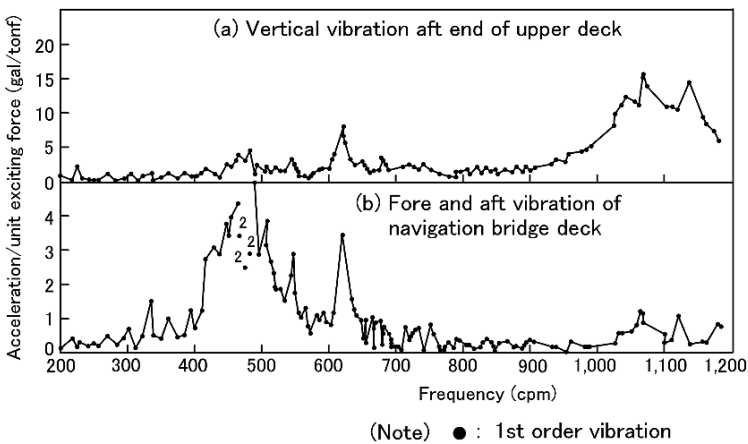


Fig. 12.1.3 Response of hull girder vertical vibration and bridge fore & aft vibration (250,000 DWT tanker) (resonance curve)

vibration except in cases of resonance. It is important to avoid resonance in connection with the exciting force of the propeller to prevent ship vibration.

Many studies have been made to estimate the magnitude of the propeller exciting force [40]. Here the authors introduce Fujino's method developed for the initial design stage [41]. The important component of the exciting force is the vertical one, and Fujino's method uses this. Propeller excitation is divided into bearing force  $F_B$  and surface force  $F_S$  and expressed by the following.

$$F_B = K_B \times \frac{SHP}{10 \times N \times D_P} \tag{12.1.1}$$

$$F_S = 0.0212 \times \frac{K_{CAV}}{Z - 1} \times \frac{SHP}{N \times D_P} \times \frac{0.1 + C/D_P}{(C/D_P)^{\frac{3}{2}}} \tag{12.1.2}$$

where

- $SHP$ : shaft horsepower (PS)
- $N$ : revolution of propeller shaft (rpm)
- $D_P$ : propeller diameter (m)
- $Z$ : number of propeller blades
- $C$ : tip clearance (m) 0.6 for 4-bladed propeller
- $K_B$ : 0.8 for 5-bladed propeller 1.0 for 6-bladed propeller
- $K_{CAV}$ : correction factor by cavitation (See Fig. 12.1.4)

In Fig. 12.1.4, parameters  $\sigma_0, k_T$  are as follows.

$$\sigma_0 = 19.6 \times \frac{d - h_0 + 9.707}{\left(\frac{N}{60} \times D_P \times J\right)} \tag{12.1.3}$$

where

- $k_T$ : thrust coefficient
- $d$ : draft (m)

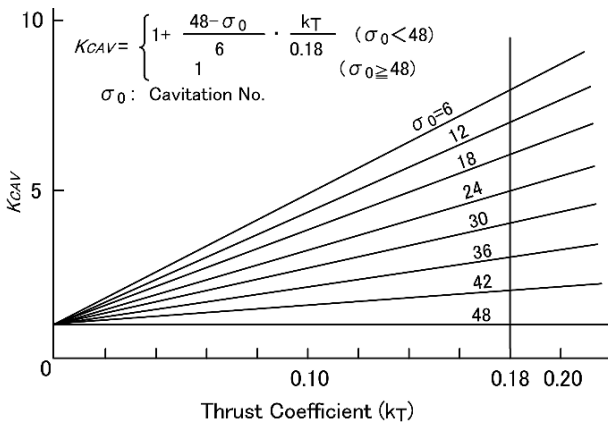


Fig. 12.1.4 Correction factor  $K_{cav}$  for cavitation

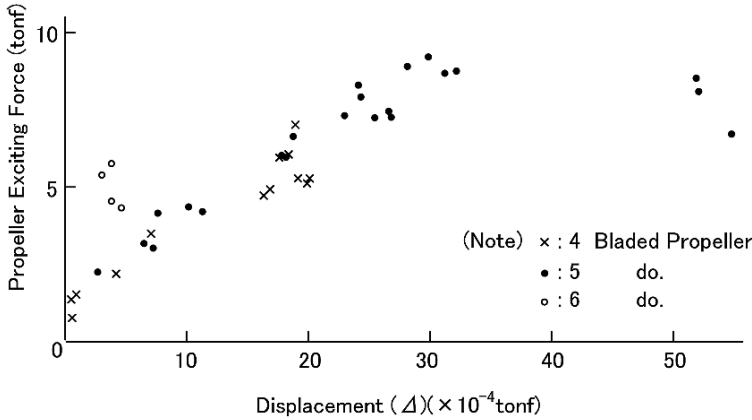


Fig. 12.1.5 Propeller exciting force and displacement

$h_0$ : height of shaft center above base line (m)  
 $J$ : advance coefficient

Finally, the vertical exciting force of the propeller is expressed as the sum of  $F_B$  and  $F_S$ . The response of the ship structure depends basically on the displacement, and the relation between displacement and the sum of  $F_B$  and  $F_S$ . For actual ships this is shown in Fig. 12.1.5. In the case of a new design, the designer should check the propeller exciting force using Fujino’s method. Regarding the propeller exciting force, it is important for the designer to keep in mind that the effect of cavitation on the surface force will be far bigger than expected. By applying a skew propeller, the propeller exciting force can be reduced remarkably.

### 12.1.2 Magnitude of Diesel Engine Excitation

In Table 12.1.1 the magnitude of the first and second order exciting forces caused by the unbalanced inertia force of the moving parts of a Sulzer diesel engine are shown. In any case, the vertical and horizontal unbalanced force is zero because of equal crank angle and equal moving mass of each cylinder. In Fig. 12.1.1 it can be seen that the first and second order exciting forces can provoke resonance with the hull girder flexural vibration. The natural frequency of hull girder flexural vibration can be estimated with reasonable accuracy and if resonance is anticipated, the following countermeasures are to be applied. The natural frequency of the hull girder flexural vibration depends on hull girder stiffness, displacement and weight distribution. To increase the hull girder stiffness much steel is required but displacement or weight distribution can be changed in some cases without any expense. One way to prevent resonance is to settle the critical displacements or critical weight distributions where hull girder flexural resonant vibration happens in a similar way to the critical rpm of propeller shaft revolution from the viewpoint of propeller shaft torsional resonant vibration.

**Table 12.1.1** Unbalanced moment of SULZER engine

Engine type		Revolution at MCR (rpm)	Unbalanced moment (kN-m)		
Cylinder No.			Vertical		Horizontal
			1st order	2nd order	1st order
5	RTA48T	124	71	1,034	88
6			0	719	0
7			43	209	53
8			142	0	177
4	RTA52	130	330	860	330
5			110	1,070	110
6			0	740	0
7			60	220	60
8	210	0	210		
5	RTA58T	103	141	1,878	149
6			0	1,306	0
7			84	379	88
8			282	0	297
4	RTA62	109	540	1,460	590
5			170	1,820	190
6			0	1,270	0
7			100	370	110
8	340	0	380		
4	RTA72	94	910	2,330	910
5			290	2,900	290
6			0	2,020	0
7			170	590	170
8	100	0	100		
5	RTA84T	74	328	4,186	482
6			0	2,981	0
7			195	865	287
8			128	0	188
9	350	1,498	514		
4	RTA84C	102	1,405	3,719	2,374
5			453	4,613	747
6			0	3,221	0
7			276	935	439
8			230	0	358
9			516	1,581	799
10			242	1,112	370
11			284	1,559	306
12	0	0	0		
4	RTA84M	81	825	3,392	2,051
5			268	4,223	645
6			0	2,937	0
7			122	853	422
8			137	0	310
9			312	1,442	689
10			146	1,014	321
12	0	0	0		
6	RTA96C	100	0	6,495	0
7			541	1,885	557
8			605	0	671
9			1,868	2,120	1,919
10			366	2,311	375
11			1,296	1,701	1,334
12	0	0	0		

However, the owners usually do not want to have such limitations. And for unbalanced moments of the first order it is usual practice to put a counterweight on the flywheel to adjust any vertical or horizontal unbalanced moments keeping the sum of them almost unchanged. For example where vertical resonant vibration is anticipated the vertical unbalanced moment is to be decreased by the use of a counterweight to increase the horizontal unbalanced moment. And in this case it is important to confirm that no horizontal resonance exists. For a second order unbalance, it is usual practice to install a balancer to cancel the engine unbalance. The balancer consists of two unbalanced counterweights and a rotating mechanism which rotates twice as fast as the shaft. The rotation is regulated mechanically (chain or gear) or electrically (synchro-motor or pulse-motor). Usually a 6 cylinder diesel engine has a large unbalanced moment of the second order vertically, and often it causes resonance on Panamax type ships. In Fig. 12.1.6, one example of the effect of a balancer installed on a Panamax type ship is shown.

The balancer is a kind of vibration exciter so attention must be paid to prevent overbalance; an adjustable balancer is desirable.

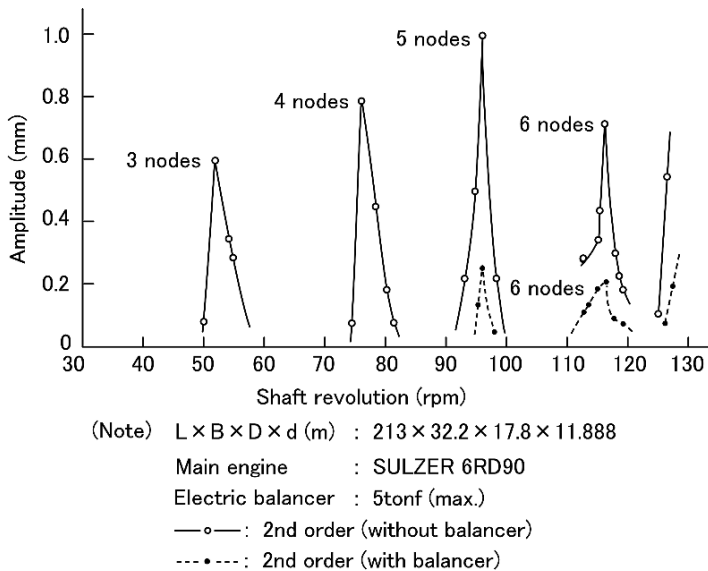


Fig. 12.1.6 Effect of balancer (vertical vibration at aft end in ballast condition)

### 12.1.3 Magnification of Exciting Force by Resonator

Where there is a resonator, exciting energy is accumulated and magnified on the way through the hull structure, largely affecting ship vibration. For example, resonances of the propeller shaft, crankshaft and diesel engine structure very often cause heavy

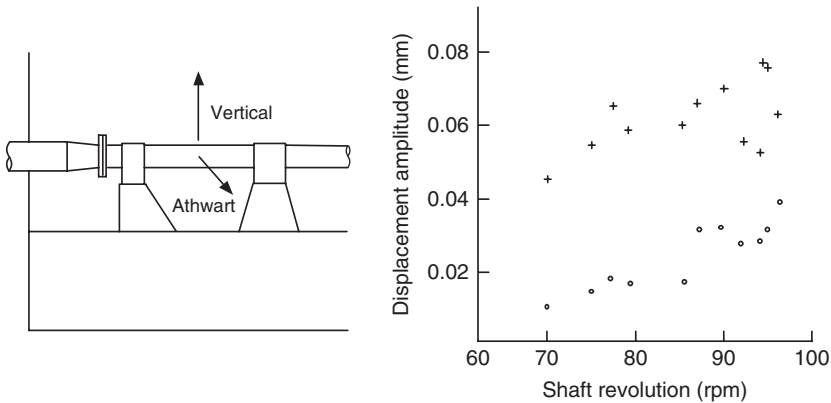


vibration of the hull structure and superstructure; even resonances of the funnel or radar mast affect superstructure vibration.

(a) *Lateral vibration of the propeller shaft:* It is reported that the resonant lateral vibration of the propeller shaft with a propeller exciting force affects hull structure vibration. In the case of a big tanker recently built, the authors seldom observed resonant vibration of the propeller shaft in the lateral direction, because the natural frequency of lateral vibration of the propeller shaft is far higher than the propeller blade frequency. One example is shown in Fig. 12.1.7. In the case of a container ship which has a narrow structure around the stern bossing, the natural frequency of the lateral vibration of the propeller shaft is low enough to cause resonance with the propeller exciting force.

In the case of nontraditional alignment of shafting, for example, on the occasion of straight alignment, shaft bearings do not work correctly in some cases because of the hull structure deformation caused by draft change. In such cases the span of the shaft becomes longer, and sometimes the natural frequency of the shafting becomes low enough to cause resonant vibration with the propeller blade frequency. To prevent resonant lateral vibration of the shafting, rational shaft alignment taking account of hull structure deformation caused by draft change is most important.

(b) *Axial vibration of diesel engine crankshaft:* The natural frequency of axial vibration of the shafting system including crankshaft, propeller shaft and propeller lies between 500–800 cpm, There is a possibility of resonant vibration with a 5–7th order component of cylinder pressure variation of the diesel engine in the normal revolution range of 110–120 rpm. In Fig. 12.1.8 natural frequencies of axial vibration of shafting systems of Sulzer RND engines are shown.



(Note) Ship : O/B/O  
 Dead weight capacity : 156,000 DWT  
 Main engine : Steam turbine (27,500 PS × 98 rpm)  
 Propeller : 5-bladed propeller  
 + : Athwart vibration (5th Order)  
 o : Vertical vibration (5th Order)

Fig. 12.1.7 Lateral vibration of propeller shaft

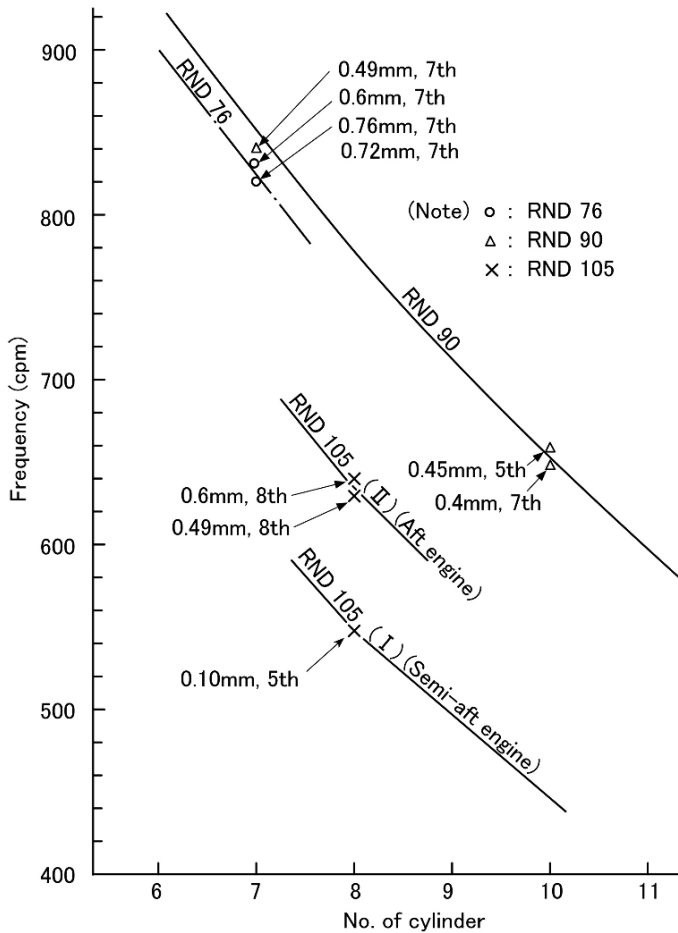


Fig. 12.1.8 Natural frequency of crankshaft axial vibration (at sea trial)

Where there is resonance of the axial vibration of the shafting system, fore and aft exciting force is transmitted to the hull structure and superstructure after being magnified by the resonator of the shafting system; this sometimes causes heavy vibration of the superstructure. In Fig. 12.1.9 fore and aft vibration of the superstructure is shown together with axial vibration of the crankshaft; the superstructure vibration increases as the shafting vibration increases. The authors estimated the magnified exciting force by resonance to be about several 10 tonf, which is considerably bigger than the propeller exciting force explained in Sect. 12.1.

To prevent resonant axial vibration of the shafting system, including diesel engine crankshaft, a detuner or damper is usually installed at the fore end of the crankshaft. In Fig. 12.1.10 the damper is illustrated. In Fig. 12.1.11 the effect of the damper on the axial vibration of the crankshaft and fore and aft vibration of the superstructure are shown. It can be seen that the effect of the damper is remarkable.

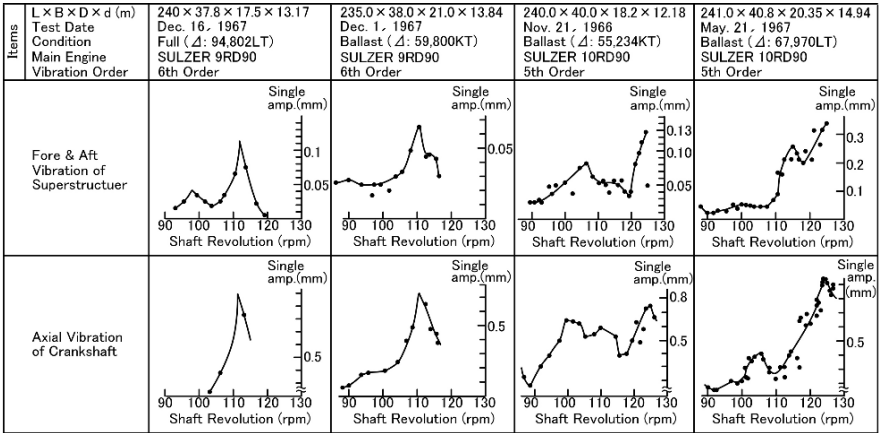


Fig. 12.1.9 Fore & aft vibration of superstructure and axial vibration of crankshaft

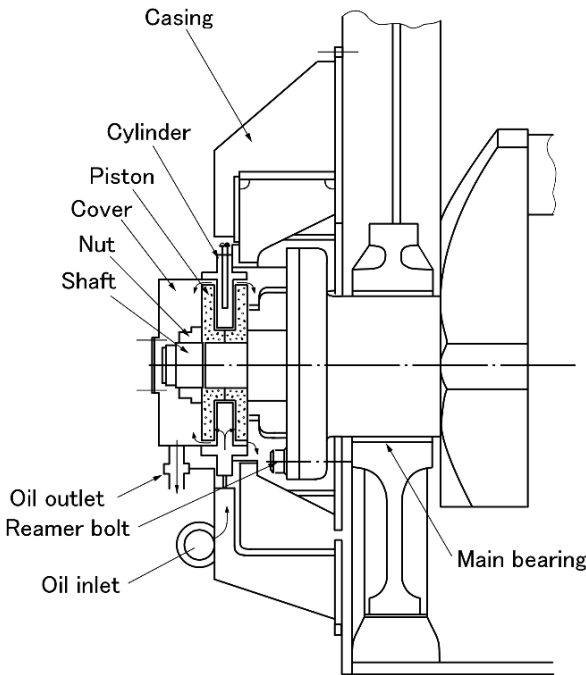


Fig. 12.1.10 Detail of damper

To decrease the axial vibration of the crankshaft of a diesel engine, improvement of the firing order was studied. In case of the Sulzer 10RND90 engine, the 5th order fore and aft vibration of the crankshaft at normal revolutions can be eliminated by changing the firing order from P-7 (1, 9, 5, 6, 2, 10, 4, 3, 8, 7) to N-8 (1, 8, 7, 3, 5, 9, 4, 2, 10, 6).

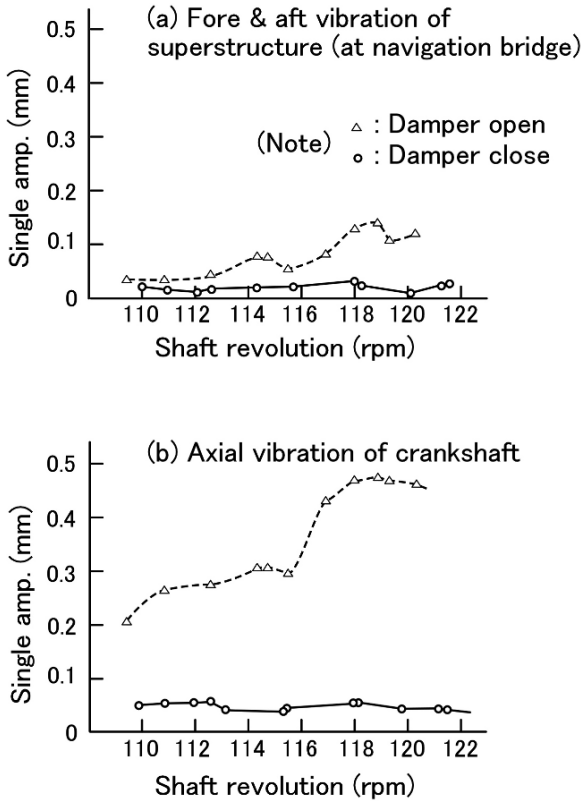


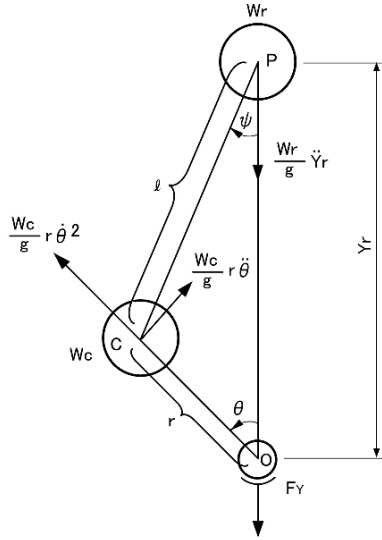
Fig. 12.1.11 Effect of damper

In the case where resonance of the crankshaft axial vibration is foreseen, the best way to prevent crankshaft axial vibration is to install a damper at the fore end of the crankshaft.

(c) *Torsional vibration of diesel engine crankshaft*: Torsional vibration of the crankshaft causes both a fore and aft exciting force and a vertical and horizontal exciting force. The fore and aft exciting force is generated by contraction and elongation of the shaft due to torsion, and the effect is similar to the axial vibration of the crankshaft explained above in (b). In records of fore and aft vibration of the crankshaft measured at the fore end of the crankshaft, the resonant points of torsional vibration of the crankshaft appear clearly.

The mechanism by which a vertical exciting force is generated by torsional vibration is shown in Fig. 12.1.12. Because of torsional vibration, the moving parts vibrate; the vertical component of that vibration is the vertical exciting force. The order of vibration is  $\pm$  one of the order of the torsional vibration, because the moving parts vibrate while rotating. This is an important phenomenon when considering the frequency of the exciting force.

**Fig. 12.1.12** Mechanism of vertical vibration force caused by torsional vibration of crankshaft



$$\begin{cases} F_Y = \frac{Wr}{g} \ddot{Y}_r - \frac{Wc}{g} \ddot{\theta}^2 \cos \theta - \frac{Wc}{g} r \ddot{\theta} \sin \theta \\ Y_r = r \cdot \cos \theta + l \cdot \cos \psi \\ \sin \psi = \frac{r}{l} \sin \theta \end{cases}$$

By torsional vibration,  $\theta$  oscillates

$$\theta = \omega_0 t + \beta \sin (n \omega_0 t + \alpha_n)$$

$$\therefore F_Y = - \frac{Wr+Wc}{g} r \omega_0^2$$

$$\begin{aligned} & \times \left[ \cos \omega_0 t + \beta_n \left( 1 + \frac{n}{2} \right) \cos \{(n+1) \omega_0 t + \alpha_n\} \right. \\ & \left. + \beta_n \left( 1 - \frac{n}{2} \right) \cos \{(n-1) \omega_0 t + \alpha_n\} \right] \end{aligned}$$

In a similar way, a horizontal force is generated by torsional vibration. In Fig. 12.1.13 some examples of vibration caused by torsional vibration are shown. The records show that the double bottom is excited by 10 and 12th order frequency excitation generated by 11th order crankshaft torsional vibration. To prevent torsional resonant vibration, it is usual practice to install additional weight to shift the natural frequency away from the frequency of the exciting force.

(d) *Lateral vibration of diesel engine structure:* The exciting force, magnified by lateral vibration of the diesel engine structure, is transmitted to the ship structure as vertical vibration of the engine room double bottom, and also through rolling stays if fitted. The most well known modes of lateral vibration of diesel engine structure are H, X, and x type vibrations, and each mode of vibration has a natural frequency corresponding to the particular engine. Some countermeasures are necessary when installing an engine which is expected to have resonance around the normal

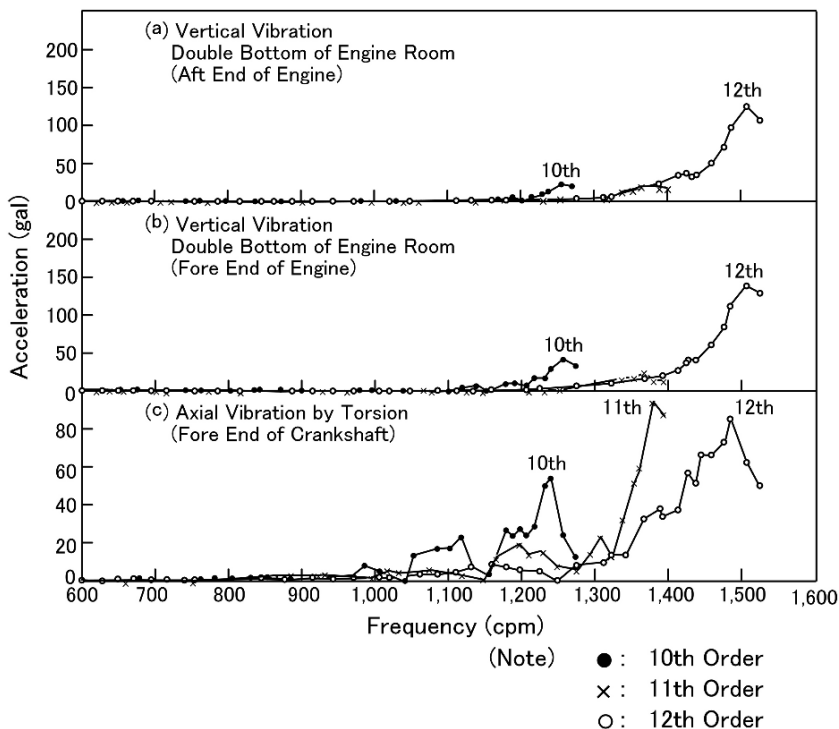


Fig. 12.1.13 Engine room double bottom vibration caused by torsional vibration of crankshaft (90,000 DWT tanker) (resonance curve)

operating revolutions. In Fig. 12.1.14 the relationship between the number of cylinders and the natural frequency of lateral vibration of the engine structure is shown.

To prevent lateral vibration of the engine structure, it is usual practice to install stays. In Fig. 12.1.15 the effect of stays is shown. Oil cylinder dampers must be provided to absorb deflection in the engine room side shell structures where the amount of deflection is considerable. By changing the firing order, the exciting force of the lateral vibration of the engine structure can be reduced. On the Sulzer 10RND90 engine, changing the firing order from P-7 (1, 9, 5, 6, 2, 10, 4, 3, 8, 7) to N-8 (1, 8, 7, 3, 5, 9, 4, 2, 10, 6) caused the vanishing of the resonant point of the 5th order X mode vibration around normal operating revolutions.

(e) *Fore and aft vibration of diesel engine structure:* The exciting force magnified by the fore and aft vibration of the diesel engine structure is transmitted to the ship structure through the engine room double bottom. The natural frequency of the fore and aft vibration of the engine structure lies in the range of 400–600 cpm for the Sulzer RND type engine, and where it has resonance with propeller thrust variation, the vibration becomes substantial. In Fig. 12.1.16 the resonance curve of this vibration for the Sulzer 8RND105 type engine is shown.

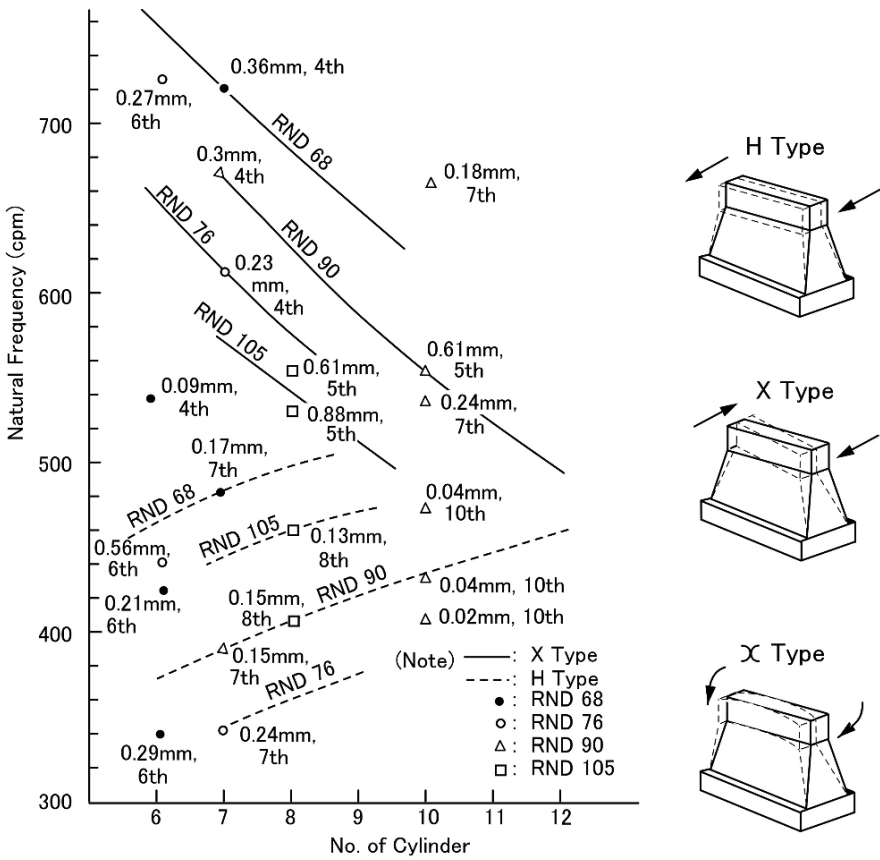


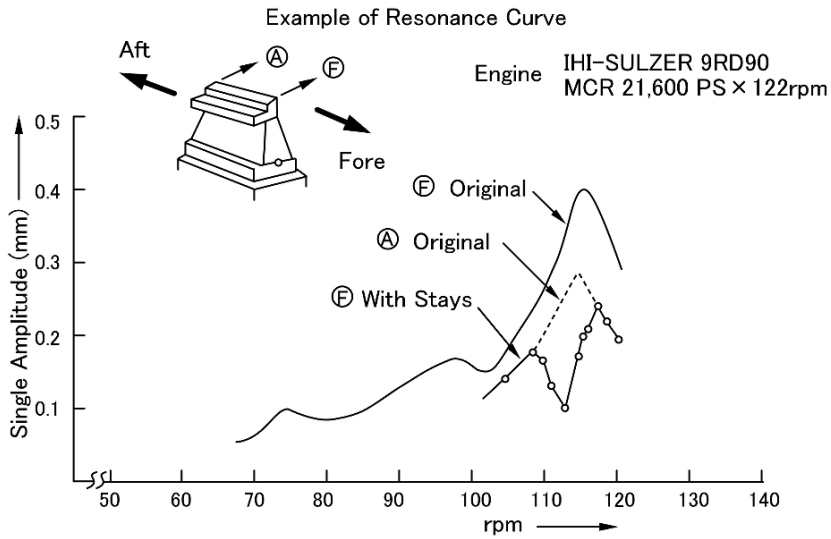
Fig. 12.1.14 Natural frequency of lateral vibration of SULZER engine

To prevent fore and aft vibration of the engine structure, stays must be installed just as for lateral vibration. Furthermore, it is possible to increase the stiffness of the engine structure to change the natural frequency of the fore and aft vibration of the engine structure.

### 12.1.4 Cancellation of Exciting Force

Exciting forces can be cancelled by selecting a propeller fitting phase angle where two or more exciting forces of the same frequency exist. A typical example of cancellation is cancellation of the propeller thrust variation and axial vibration of the diesel engine crankshaft.

In the case of the Sulzer engine, axial vibrations of the crankshaft of the 6th order for the 9RND90 and 5th order for the 10RND90 have resonance around normal



Ship	Main Engine	① Original Amplitude	② Amplitude with Stays	② / ①	Effects on Hull Vibration
105,000 LT Tanker	B & W 984-VT2BF-180	(Single) 0.18 mm	0.08	44 %	No
128,000 LT Tanker	B & W 1284-VT2BF-180	0.14	0.06	43	Engine room double bottom vertical vibration reduced
74,100 LT O/B/O	B & W 984-VT2BF-180	0.10	0.10	100	No
63,000 LT Tanker	SULZER 9RND90	0.22	0.09	40	No
750 TEU Container Ship	SULZER 8RND105	1.00	0.50	50	Trans. vibration of upper engine flat and navigation deck reduced

Fig. 12.1.15 Effect of stays for lateral vibration of main engine

operating revolutions. By this rationale, the exciting forces magnified by these resonances can be cancelled by the 6th order thrust variation of a 6-bladed propeller, or 5th order thrust variation of a 5-bladed propeller, if the optimum fitting angle of the propeller is selected. This technique is called “phasing”. In Fig. 12.1.17 an example of phasing for a Sulzer 9RND90 engine and a 6-bladed propeller is shown.



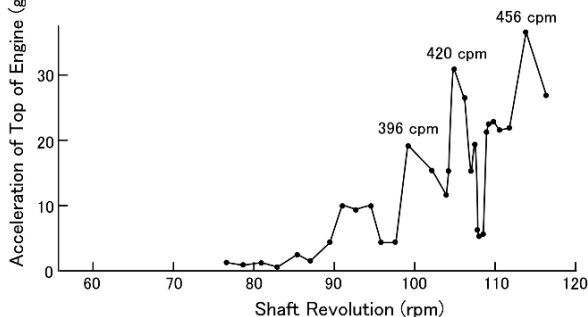


**Fig. 12.1.16** Fore & aft vibration of diesel engine (SULZER 8RND 105 type engine) (resonance curve)

### 12.1.5 Reduction of Main Engine Exciting Force by Elastic Mounting

It is important to reduce vibration and maintain comfortable habitability in vessels and this is particularly serious for passengers in luxury cruise ships. Although there are several forces inducing vibration problems in ships, one of the predominant vibration sources is its main engines. If the vibration forces due to the main engine are decreased considerably, this can contribute to a reduction in vibration trouble.

A luxury cruise ship of 660 passengers was built by IHI in 1990. The vessel was installed with two main engines, which were elastically mounted [42] on engine beds by elastic components such as rubber pieces sandwiched by steel plates as illustrated in Fig. 12.1.18. Furthermore, a flexible coupling system was applied to the line shafting of the main engine in order to permit large movement of the engine. That elastic mounting system was designed to isolate the transmission of vibration forces from the main engine to the engine bed, and it was the first time for us to provide the system to a large cruise ship.

The system has proved to be effective according to the measurements carried out on sea trials. In the measurements, the elastic mounting system was effective in allowing the elastic components to function and, after that, it was turned off by using rigid components. The results showed that the system is able to suppress the vibration level in the hull structure to a satisfactory lower level, as shown in Fig. 12.1.19. The system was especially effective for the higher-order exciting forces. In the case of the 4.5th order of vibration, the structural response can be reduced to one fourth of the original level by installing the elastic mounting system.

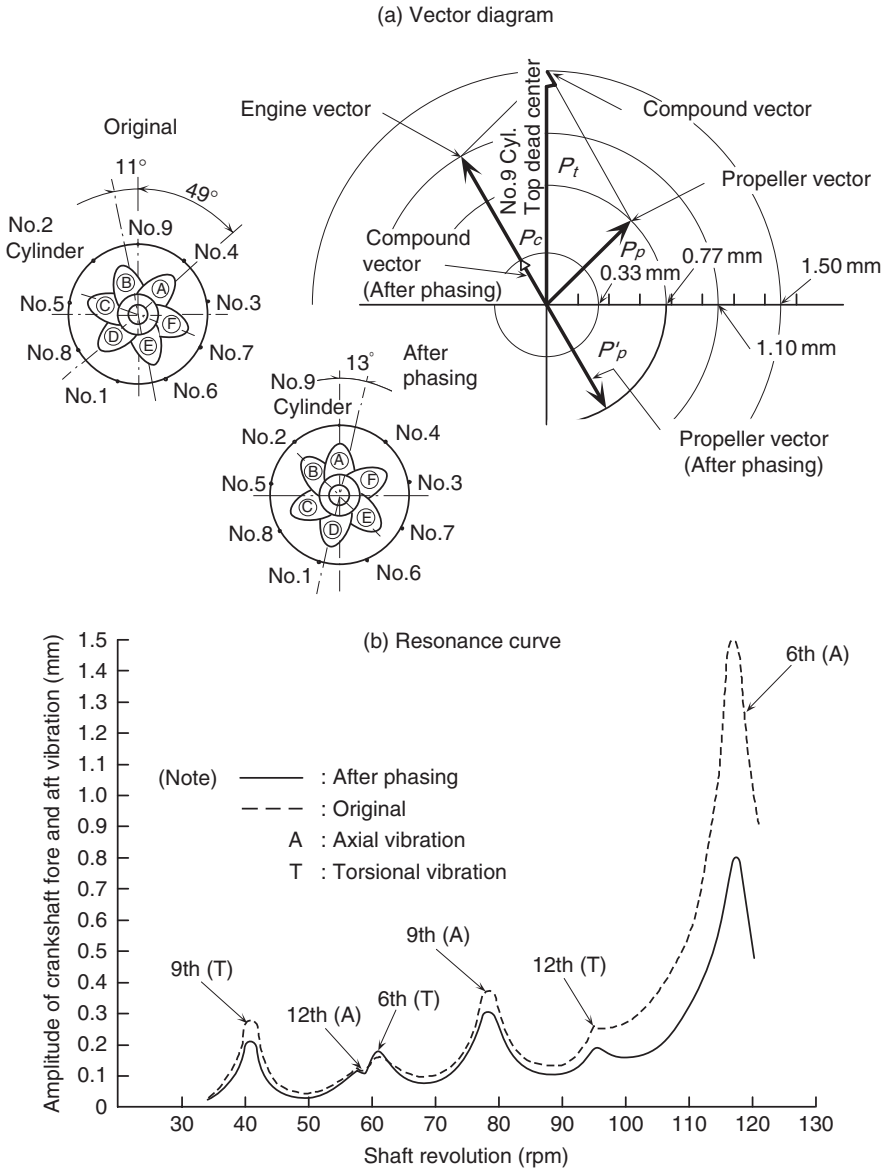


Fig. 12.1.17 Example of phasing

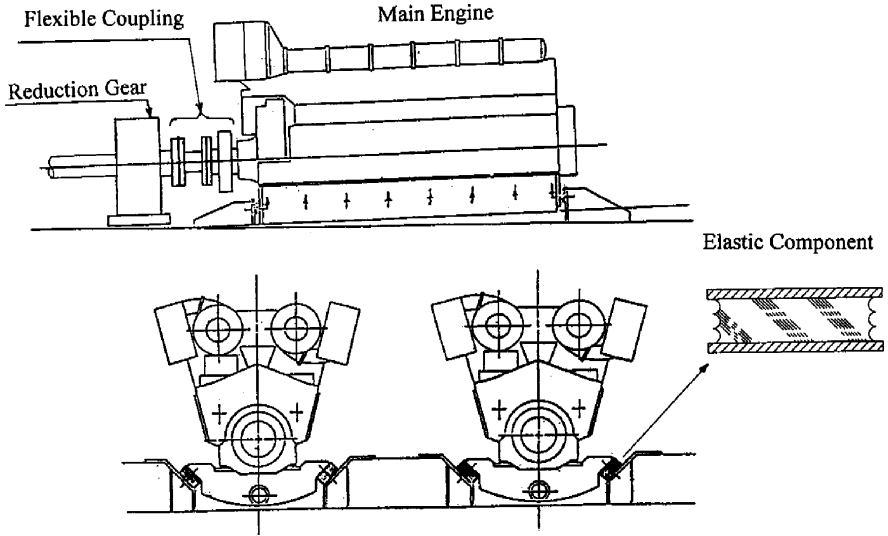


Fig. 12.1.18 Arrangement of elastic mounted main engine

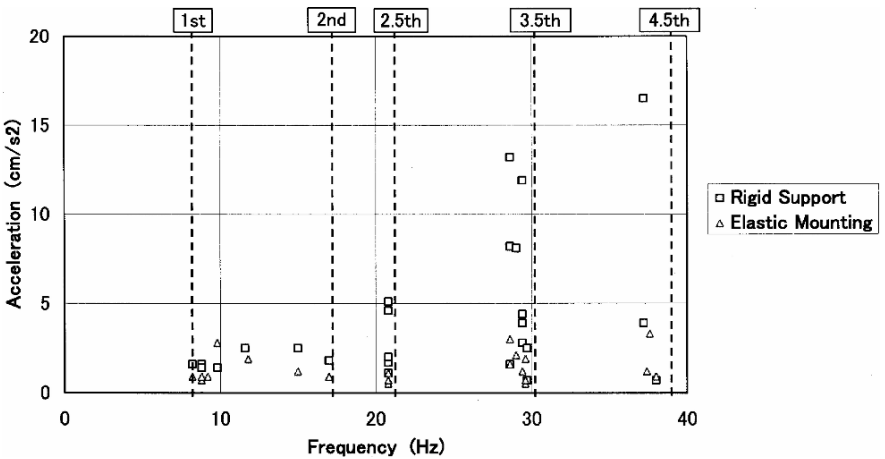


Fig. 12.1.19 Result of vibration measurement of No.5 deck (Elastic component on/off test)

## 12.2 Prevention of Ship Vibration

In Sect. 12.1, the authors explained the frequency of exciting force and how to reduce the magnitude of the exciting force. To reduce the magnitude of the exciting force is an important part of the prevention of ship vibration and to avoid resonance is the most important element in the prevention of ship vibration. In this section the authors explain how to avoid resonance. The crucial procedure in avoiding resonance is to estimate the natural frequency of the ship structure correctly.

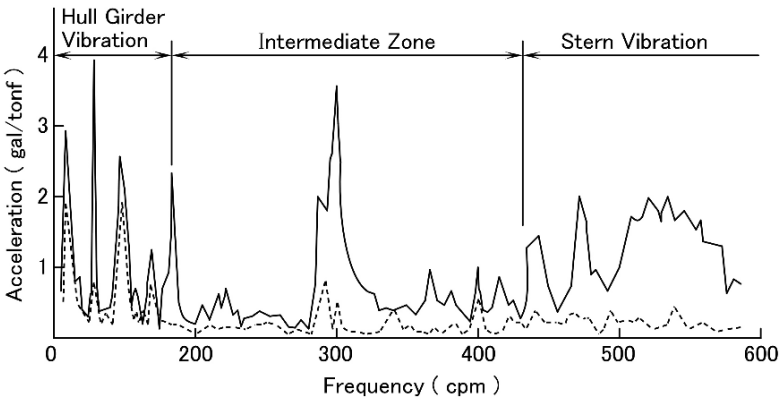
### 12.2.1 *Flexural Vibration of Hull Girder*

The calculation of the natural frequency of flexural vibration of the hull girder is done by using experimental formulae based on bending theory for 2–3 nodes of vibration, and on shear theory for 3 nodes and higher vibration. The experimental coefficients are determined from the analysis of measurements on actual ships. The results of calculations of the natural frequency of flexural vibration of the hull girder are accurate enough for practical design of up to 4–5 nodes of vibration vertically and horizontally. The exciting force, which can produce resonance with flexural vibration of the hull girder, is the diesel engine 1st order and 2nd order unbalanced moments.

Where it is foreseen that the flexural vibration of a hull girder at ballast condition may be resonant with the diesel engine 1st or 2nd order unbalance, it is usual practice to avoid resonance by adjusting the volume of the ballast, in the case of tankers, and adjusting the volume of the ballast in the aft peak tank in the case of cargo ships. It is reported that by filling the aft peak tank of a 40,000 DWT bulk carrier, the natural frequency of a 5-node vertical vibration comes down to 220 cpm from 230 cpm, and this 10 cpm of change is big enough to avoid resonance with a diesel engine unbalanced moment at normal operating revolutions. However, where the resonance is foreseen in the full load condition, and even at the ballast condition in cases where the owners do not want to have any operating limit, there is no way to avoid resonance. To increase the stiffness of the hull girders requires a large amount of steel, and to change the normal operating revolutions of a diesel engine results in a decrease of engine efficiency. In this case, a countermeasure to decrease the unbalanced moment of the diesel engine, as stated in Sect. 12.1.2 should be applied instead of attempting to avoid resonance.

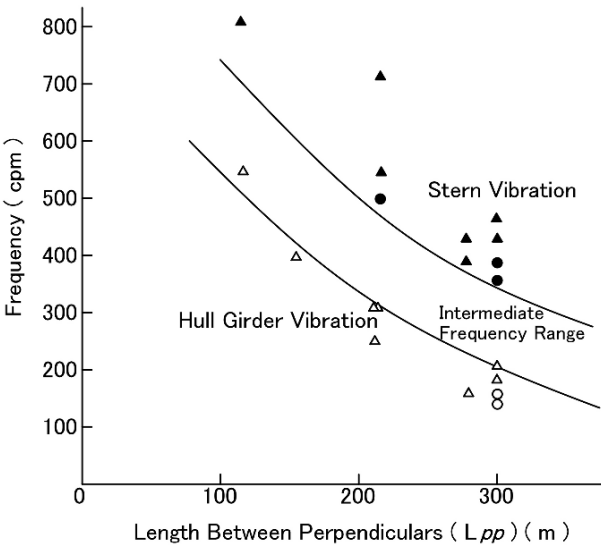
The above explanation is for lower frequency vibration which may cause resonance with diesel engine 1st and 2nd order unbalanced moments. Let's proceed to higher frequency vibration which may cause resonance with propeller excitation. In Fig. 12.2.1 an example of a resonance curve of flexural vibration of a hull girder is shown. It can be seen that resonances of 2, 3, 4 nodes – vibration clearly appears at 190 cpm, and above 430 cpm the response is large even though no remarkable resonance exists. The authors call the former the frequency zone of hull girder vibration and the latter the frequency zone of stern vibration. Between the hull girder vibration zone and stern vibration zone there is an intermediate zone where the response of the hull girder vibration is small. This fact was confirmed on many ships by the exciter test and by simulation calculations of hull girder flexural vibration using a computer.

To prevent resonance of hull girder flexural vibration with propeller exciting force, it is important to decide the number of propeller blades so as to have the blade frequency come into this intermediate zone. In Fig. 12.2.2 the relationship between ship size and the intermediate zone is shown. For example, the intermediate zone is  $300 \pm 60$  cpm for a ship  $L_{pp} = 300$  m, and  $500 \pm 60$  cpm for  $L_{pp} = 150$  m. In the case of a VLCC which has 300 m length and 80 rpm propeller shaft revolution,



( Note )      Test : Exciter Test  
                   Ship : 200,000 DWT Tanker  
                   Condition : Ballast ( Displacement = 121,500 ton )  
                   ———— : Aft End Vibration  
                   ----- : Fore End Vibration

Fig. 12.2.1 Hull girder vibration



( Note )    ● : Full Load Condition ( Stern Vibration )  
               ▲ : Ballast Condition ( Stern Vibration )  
               ○ : Full Load Condition ( Hull Girder Vibration )  
               △ : Ballast Condition ( Hull Girder Vibration )

Fig. 12.2.2 Ship size and intermediate frequency range

a 4 bladed propeller is recommended to prevent resonance of hull girder flexural vibration with propeller exciting force.

### ***12.2.2 Vibration of Superstructure***

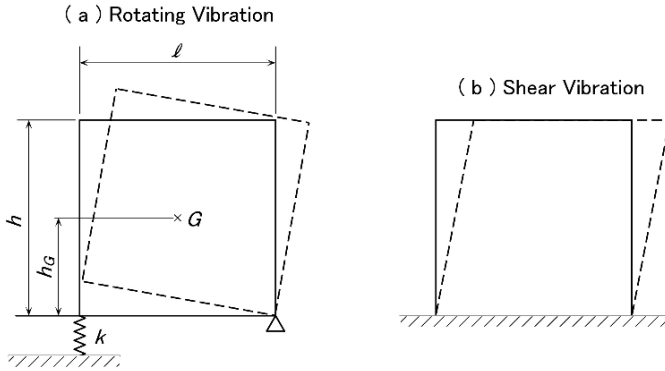
Since the aft bridge and aft engine arrangement was first applied in ship design, superstructure vibration has been one of the important problems in ship structure research. The aft part of the ship is close to the propeller which generates exciting forces, and has less stiffness than the midship part. Also diesel engines of large horse power are installed in the aft part of ships where the hull girder stiffness decreases and the aft bridge is higher to provide a better view [39].

None of these trends help to improve the superstructure vibration but only make matters worse. With a higher superstructure the natural frequency of the fore and aft vibration reduces so that there is the possibility of resonance from the exciting forces of the propeller or the diesel engine. Among the vibrations of a superstructure, the most important one is fore and aft vibration, and the authors explain below the calculation method to determine the natural frequency of this fore and aft vibration and countermeasures to prevent resonance.

The calculation method to determine the natural frequency of the superstructure fore and aft vibration has been studied for the past ten years by means of a computer. The accuracy of the results is not yet adequate and they require more labor and expense than simplified methods; designers nowadays apply a simplified method for correcting measured data. In Fig. 12.2.3 it is explained that the fore and aft vibration of the superstructure consists of rotational vibration and shear vibration; the natural frequency of superstructure fore and aft vibration depends on the height of each type of superstructure. Based on this principle in Fig. 12.2.4, the relationship between the natural frequency and the height of the superstructure for A-C type arrangements is shown.

The exciting force, which can cause resonance with this fore and aft vibration, is propeller exciting force and diesel engine crankshaft axial vibration. Propeller excitation has a blade frequency, and the Sulzer RTA diesel engine has a 7th order frequency for a 7 cylinder, 6th order for 12 cylinder, 5th order for 11 cylinder and 4th order for a 12 cylinder engine. Where it is foreseen that resonance from a propeller exciting force may happen, the easiest and most effective method is to change the number of propeller blades. But in the case where a the change of propeller blade number is impossible for some reason, the natural frequency of the superstructure fore and aft vibration must be changed to prevent resonance. And where resonance is foreseen with diesel engine crankshaft axial vibration, an axial damper must be installed at the fore end of the crankshaft, as stated in Sect. 12.1.3(b), or the natural frequency of the superstructure fore and aft vibration must be changed.

There are some cases where the natural frequency of the superstructure fore and aft vibration must be changed to prevent resonance. As shown in Fig. 12.2.5 the natural frequency of superstructure fore and aft vibration  $N$  is affected by the natural



( Note ) Natural Frequency of Rotating Vibration :  $N_R$

$$N_R = \frac{60}{2\pi} \sqrt{\frac{k\ell^2 g}{Wh^2 G}} \dots\dots\dots(1)$$

Natural Frequency of Shear Vibration :  $N_S$

$$N_S = \frac{\pi}{2} \frac{60}{2\pi} \sqrt{\frac{kGA_g}{hW}} \dots\dots\dots(2)$$

Weight of Superstructure :  $W \propto \ell \times h \times b$

Spring Constant :  $k \propto b$

Shear Rigidity :  $kGA_g \propto t \propto \ell$

$b$  : Breadth of Superstructure

$t$  : Thickness of Longitudinal Wall ( Const. )

$$\therefore N_R \propto \frac{\ell}{h} \sqrt{\frac{\ell}{h}} \dots\dots\dots(3)$$

$$N_S \propto \frac{\ell}{h} \sqrt{\frac{\ell}{b}} \dots\dots\dots(4)$$

Natural Frequency of Superstructure :  $N$

$$\frac{1}{N^2} = \frac{1}{N_R^2} + \frac{1}{N_S^2} \dots\dots\dots(5)$$

Fig. 12.2.3 Natural frequency of superstructure fore and aft vibration

frequency of rotational vibration  $N_R$  and the natural frequency of shear vibration  $N_S$ . The Eq. (5) in Fig. 12.2.3 shows that where either  $N_R$  or  $N_S$  is far greater than the other, to increase the greater value is not effective for increasing  $N$ . In Fig. 12.2.5 the above condition is shown. Where  $N_R$  is low, that is, the rigidity of the foundation is weak, to increase  $N_S$ , the increase of the shear rigidity of the superstructure, does not bring higher natural frequency  $N$ . With a reasonable value of  $N_R$ , an increase in shear rigidity becomes effective in increasing the natural frequency  $N$ .

Calculated values of  $N_R$  and  $N_S$  of typical ships are shown in Table 12.2.1. Table 12.2.1 shows that in general  $N_R$  is lower than  $N_S$ , so to increase the natural frequency of a superstructure fore and aft vibration,  $N_R$  must be increased, which means increasing the spring constant  $k$  in the Eq. (1) of Fig. 12.2.3.

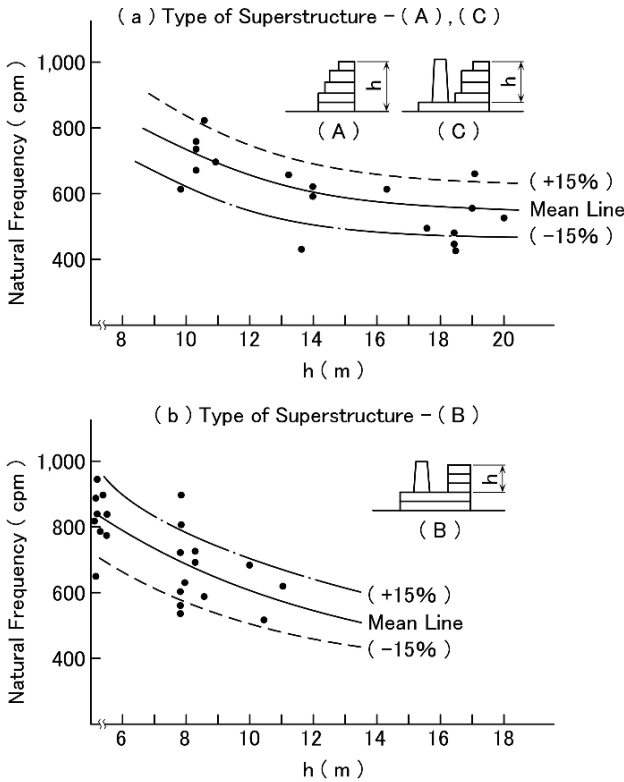


Fig. 12.2.4 Estimated natural frequency of superstructure fore and aft vibration

### 12.2.3 Active Mass Damper for Superstructure Vibration

The vibration amplitude of a superstructure has a large scatter, as much of the vibration is induced by the propeller, because propeller exciting forces fluctuate according to the change of flow velocity into the propeller. Moreover, the vibration frequency of a superstructure does not always have a single frequency but may have several frequencies because there are several exciting sources in a vessel. Therefore, the vibration of a superstructure cannot be cancelled by installing a balancer. A more sophisticated instrument is required.

In order to suppress such vibration, an active mass damper has been developed [43] as shown in Fig. 12.2.6. An active mass damper can effectively reduce the vibration of fluctuating amplitude and frequency induced by several vibration sources such as the main engine and the propeller. These vibration characteristics were confirmed by measurements on a 150,000 DWT tanker. Figure 12.2.7 shows the results of experiments on the active mass damper installed on the top of a superstructure. From the figure, the active mass damper reduced the vibration of the superstructure especially in the resonance peak area. The vibration due to an unbalanced moment



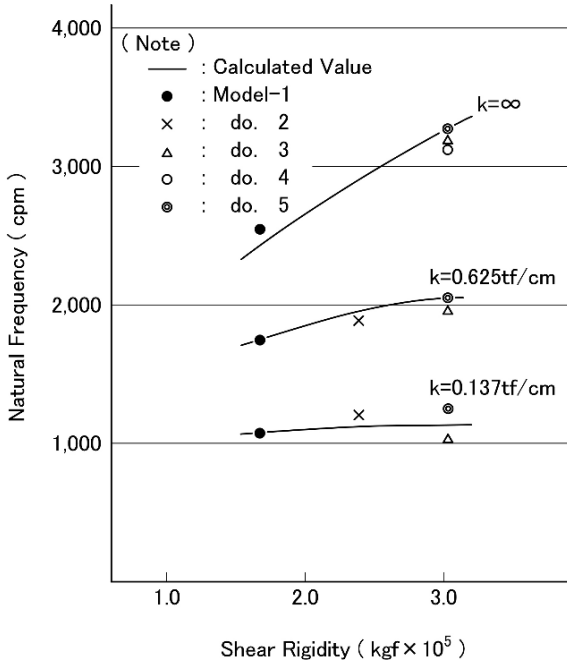
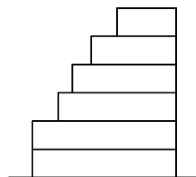


Fig. 12.2.5 Shear rigidity and natural frequency of superstructure

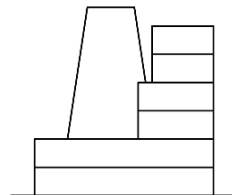
Table 12.2.1 Calculated value of  $N_R$  &  $N_S$

Ship	Calculated Value (cpm)			Measured Value (cpm)	Type of Superstructure
	$N_R$	$N_S$	$N$		
A	466	881	441	570	A
B	452	1,115	448	610	A
C	337	791	331	535	A
D	570	1,340	561	560	D
E	815	1,129	707	658	D
F	853	1,142	731	740	D

(a) Type of Superstructure-A



(b) Type of Superstructure-D



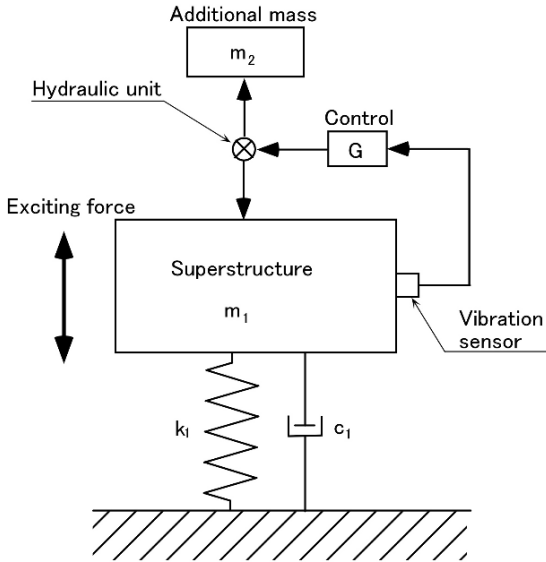


Fig. 12.2.6 Model of active mass damper on superstructure

(2nd order) decreased to one sixth of its original level, the vibration derived from the propeller (5th order) exciting force decreased to one half, and the vibration induced by the main engine exciting force (6th order) reduced to one fifth, by an active mass damper.

#### 12.2.4 Vibration of In-Tank Structures

The natural frequency of the in-tank structure of a tanker lies in the range of the propeller blade frequency and the frequency of the diesel engine exciting force, and therefore there is a possibility of resonant vibration. Moreover in case resonance happens, cracks may be generated throughout the tank structure by heavy vibration because the structure is similar throughout the tank. Therefore, it is important to calculate the natural frequency of the in-tank structure to prevent resonance.

Recently the methods for calculating the natural frequency of in-tank structures have been improved, providing accurate values for practical design.

#### 12.2.5 Calculation Methods of Natural Frequency of In-Tank Structures

(1) *Simple formula:* As shown in Fig. 12.2.8, the vibration of the web frame can be assumed to consist of panel vibration surrounded by stiffeners for which the natural

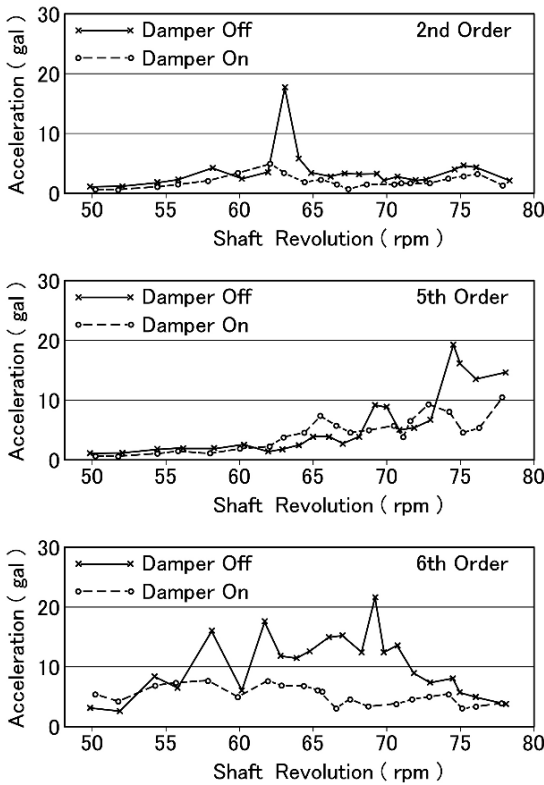
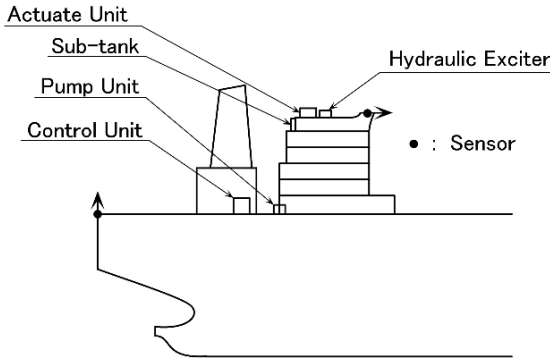


Fig. 12.2.7 Effect of active mass damper for longitudinal vibration of superstructure

frequency is  $f_P$ , the vibration of stiffeners for which the natural frequency is  $f_S$ , and the vibration of face plate for which natural frequency is  $f_{FB}$ . The calculation method for the natural frequency of a web frame is derived using  $f_P$ ,  $f_S$  and  $f_{FB}$ .

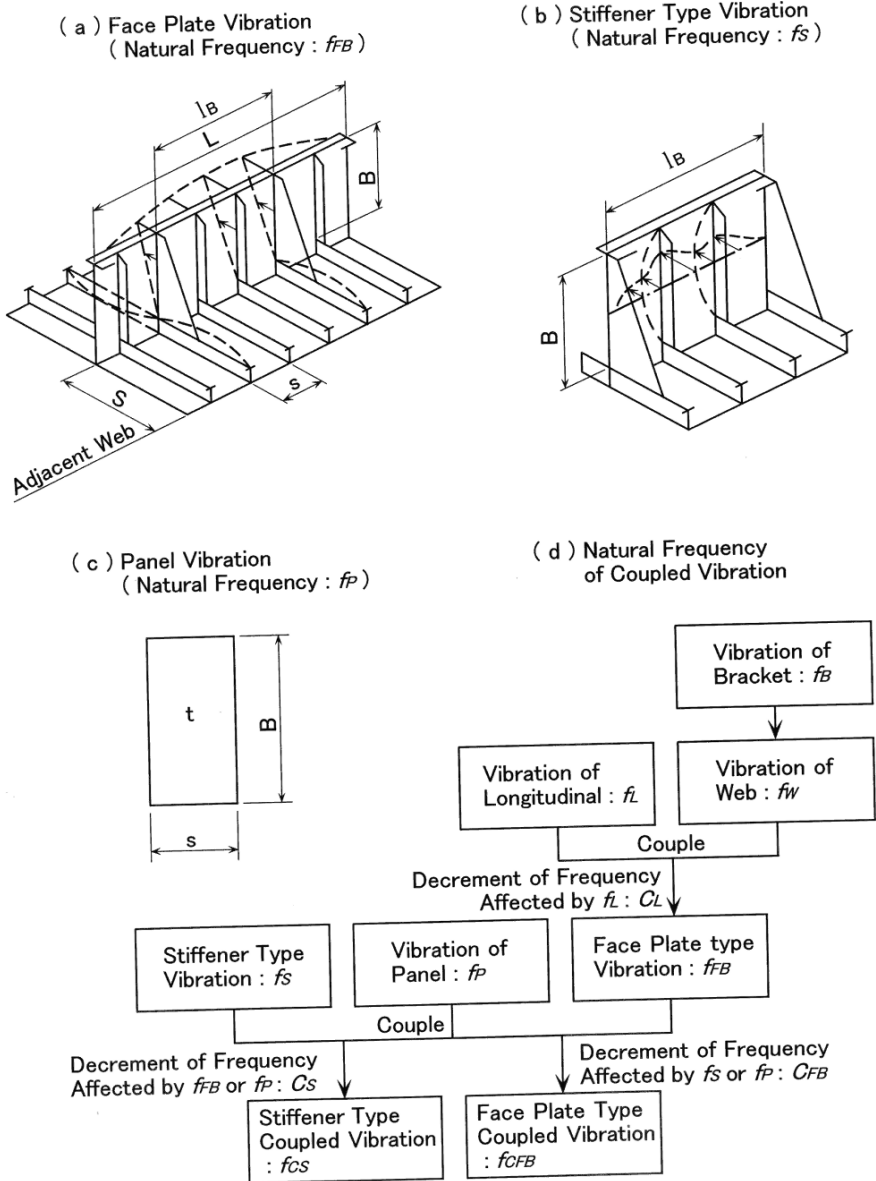


Fig. 12.2.8 Natural frequency of web frame

The natural frequency of face plate vibration which is affected by the existence of panel vibration or stiffener vibration  $f_{CFB}$  is described as follows.

$$f_{CFB} = C_{FB} \cdot C_L \cdot K_{LF} \cdot K_W \cdot \frac{428}{B^2} \cdot 10^5 \sqrt{\frac{1.2}{0.2 + \rho} \cdot \frac{I_B^*}{B I_B}} \quad (12.2.1)$$

where

- $C_{FB}$ : decrement of frequency affected by  $f_S$  or  $f_P$   
 $C_L$ : decrement of frequency affected by longitudinal stiffener vibration  
 $K_{LF}$ : correction factor for stiffness between longitudinal stiffener and face plate  
 $K_W$ : correction factor for span (L) of web frame  
 $f_W$ : natural Frequency of web frame (cpm)  
 $f_B$ : natural Frequency of bracket (cpm)  
 $\rho$ : specific gravity of liquid (1.0 for seawater or oil, 0 for air)  
 $l_B$ : space between brackets (cm)  
 $I_B^*$ : equivalent sectional moment of inertia of bracket including stiffener (cm<sup>4</sup>)  
 $B$ : depth of web frame (cm)

The natural frequency of stiffener vibration, which is affected by the existence of face plate vibration or panel vibration  $f_{CS}$ , is described as follows:

$$f_{CS} = C_S \cdot C_{HS} \cdot \frac{483}{B^2} \cdot 10^5 \sqrt{\frac{KI_S}{A_S + (t_W + \rho C_S'' B) S}} \quad (12.2.2)$$

where

- $C_S$ : decrement of frequency affected by  $f_{FB}$  or  $f_P$   
 $C_{HS}$ : increment of frequency affected by horizontal stiffener  
 $K$ : 1.0 for symmetrical stiffener 0.85 for asymmetrical stiffener  
 $I_S$ : sectional moment of inertia of stiffener (cm<sup>4</sup>)  
 $s$ : spacing of longitudinal stiffeners (cm)  
 $t_W$ : plate thickness of web frame (cm)  
 $A_S$ : sectional area of stiffener (cm<sup>2</sup>)  
 $C_S''$ : coefficient corresponding to the aspect ratio of the panel

$$\left( = \frac{0.08}{\sqrt{1 + (B/l_B)^2}} \right)$$

The natural frequency of a panel surrounded by stiffeners is described as follows.

$$f_P = \frac{934}{(C_P'' S)^2} \cdot 10^2 \cdot \frac{t_W}{\sqrt{1 + (\rho C_P'' S / t_W)}} \quad (12.2.3)$$

where:  $C_P''$ : Coefficient corresponds to the aspect ratio of a panel

$$\left( = \frac{0.08}{\sqrt{1 + (s/B)^2}} \right)$$

The ratio between the natural frequencies calculated in the above formulae and frequencies of exciting forces coming from propeller or diesel engine  $N_{CAL}/N_{EX}$  is an important parameter in any attempt to avoid the resonant vibration of in-tank

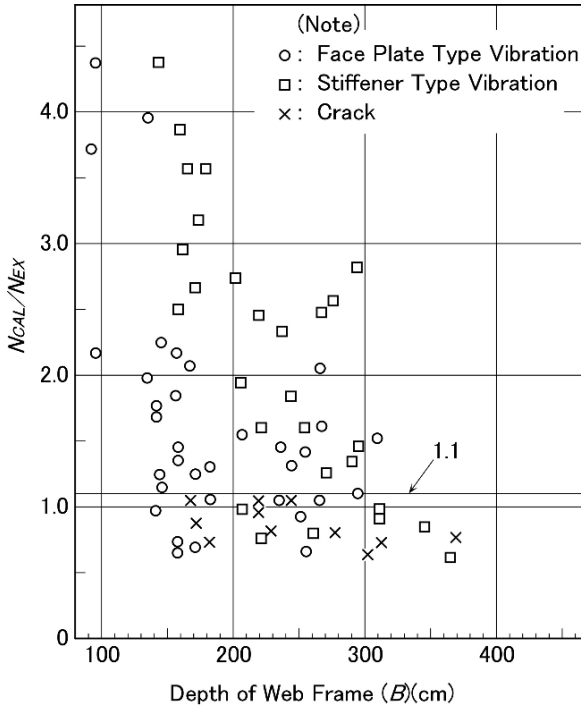


Fig. 12.2.9 Resonance of web and cracking

structure. In Fig. 12.2.9 the relationship between  $N_{CAL}/N_{EX}$  and the cracks caused by vibration are shown. No cracks occurred in the range where  $N_{CAL}/N_{EX}$  is over 1.1. According to this experience it can be stated that to prevent the cracks caused by vibration, the natural frequencies calculated by the above method must be higher than the natural frequencies of the exciting forces by 10% and more.

(2) *Computer analysis:* The calculated value of the natural frequency of a structure depends very much on the boundary conditions, which are difficult to assume correctly. To overcome this difficulty, the calculation for the whole structure has been done by means of a computer. In the case of an in-tank structure, the whole transverse ring or half of it which takes symmetrical condition into consideration, is analyzed by computer.

In Fig. 12.2.10 an example of this type of calculation is shown. In this case, the lowest natural frequency is for torsional vibration of the cross tie, the next is bending vibration of the tie, deck transverse vibration, vertical web vibration etc. Between the cross tie bending vibration, for which the natural frequency is 440 cpm, and the deck transverse vibration of 680 cpm, there is no resonant frequency, and above 680 cpm resonance appears to be closed. Accordingly it can be stated that the range of 440–680 cpm is a safety zone and it is better to have a frequency of exciting force in this range.

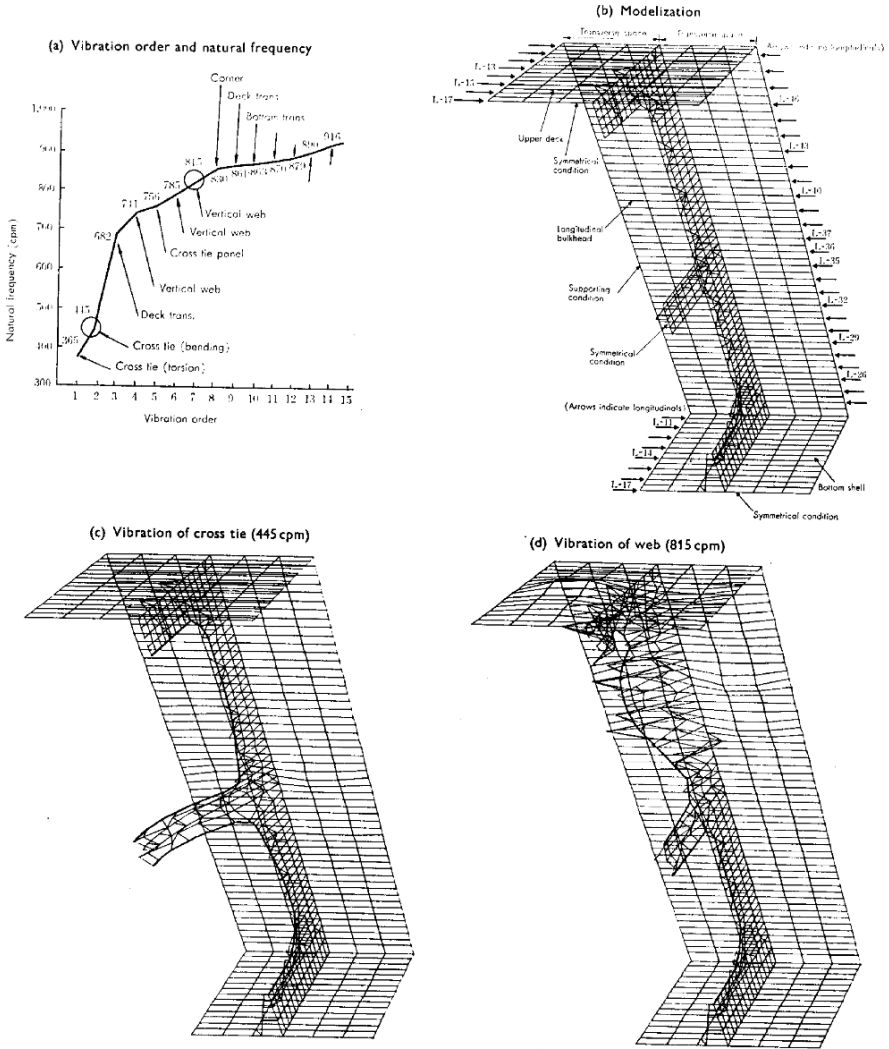


Fig. 12.2.10 Frequency and mode of transverse ring vibration

Generally it is difficult to keep the natural frequency of a cross tie higher than the frequency of the propeller and engine exciting forces. Therefore, designers used to design cross tie scantlings to have a natural frequency lower than and the natural frequency of the web frame higher, but than the propeller blade frequency and frequency of diesel engine forces.

# Chapter 13

## Superstructure

The superstructure, which is not so long in comparison with the main hull structure, does not deflect in the same way as the main hull does, since the longitudinal stress of the main hull is not completely transmitted to the superstructure. On the contrary, when the length of the superstructure is large enough, the longitudinal stress is fully transferred from the main hull to the superstructure, since the superstructure will act as part of the hull girder in absorbing hull girder bending.

The latter case has significance in for the strength of a superstructure, because the longitudinal bending stress flowing into the superstructure may cause structural damages in it. Therefore, the strength of a vessel with a long superstructure is mainly discussed in this chapter.

### 13.1 Example of Damage to Long Superstructures

Figure 13.1.1 represents an example of structural damages in a car ferry with a long superstructure. Structural damage is found (a) in the corner of door opening, (b) in the connecting part between the slant end wall of the upper-most deck and the lower deck and (c) in the connection area of the pillar and deck. The damage (a) shows the cracks initiating from the free edge of a door opening corner in the diagonal direction, (b) the crack extending along the welding bead joining the lower deck plate and the slant plate of the upper deck, and (c) the crack in deck plate beneath the doubling plate of a pillar.

### 13.2 Interaction of Superstructures and Main Hull

Longitudinal bending stress is not completely transmitted from the main hull to the superstructure, in cases where the superstructure is comparatively short, such as a short deckhouse. In this case, the superstructure deforms in a different way from the main hull as shown in Fig. 13.2.1. From this figure, when the main hull is subjected to a longitudinal bending moment  $M$ , a shearing force  $T$  in the longitudinal



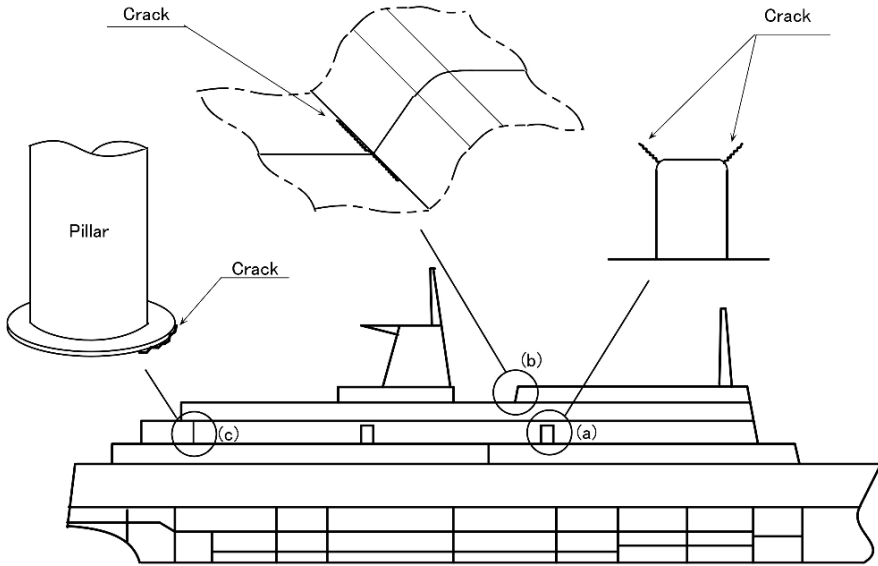


Fig. 13.1.1 Example of damage in car ferry with long superstructure

direction is induced in the interface between the upper surface of the main hull and the lower surface of the superstructure. Reaction forces  $q$  also exist in the vertical direction. The shearing force  $T$  acting on a superstructure is likely to generate a bending deformation with a curvature in the opposite direction to the main hull bending. Therefore, the reaction of vertical force  $q$  results in a separating force at

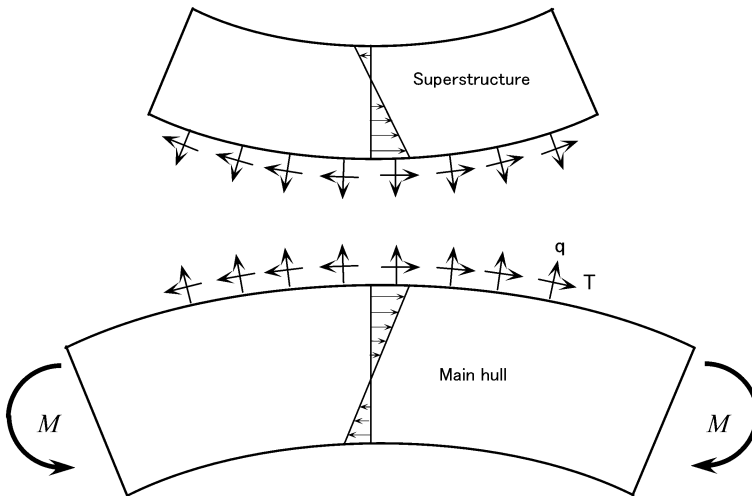


Fig. 13.2.1 Connecting force between main hull and superstructure due to longitudinal bending

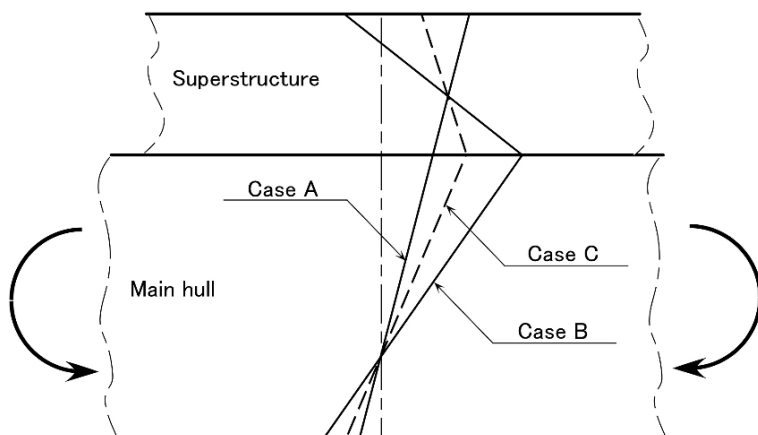


Fig. 13.2.2 Image of longitudinal bending stress distribution

the end of the superstructure, if a hogging moment is applied to the main hull. For this reason, the end of a superstructure may suffer from cracks due to a separation force, when the length of the superstructure is short. In order to prevent such structural failures by the separation force, it is important to provide transverse bulkheads in the main hull in line with the end wall of the superstructure.

On the other hand, in the case of a vessel with a long superstructure, the superstructure and the main hull deflect in one united beam against a longitudinal bending moment. Hence the separation force does not appear but longitudinal bending stress is induced in the superstructure.

The distribution of longitudinal bending stress in the superstructure and the main hull is described in Fig. 13.2.2, depending on the length of the superstructure versus that of the main hull. In case A, where the superstructure is relatively long compared to the main hull, the longitudinal bending varies in a linear form, because both structures act as one beam and are bent simultaneously by the bending moment. In contrast with this Case B, where the superstructure is short, shows the bending stress distribution has a sharp change at the interface of the main hull and superstructure, because the sign of curvature in the superstructure is opposite to that in the main hull. Case C is an intermediate case of Case A and Case B. Based on several investigations, whether the superstructure is long or short can be defined by the length ratio of the superstructure against the main hull exceeding 15 ~ 25% or not.

### 13.3 Magnitude of Longitudinal Bending Stress

In order to demonstrate what magnitude of longitudinal bending stress flows into a long superstructure, the results of one investigation are shown in Fig. 13.3.1. Figure 13.3.1(a) represents the outside view of the portside of a whole FEM model

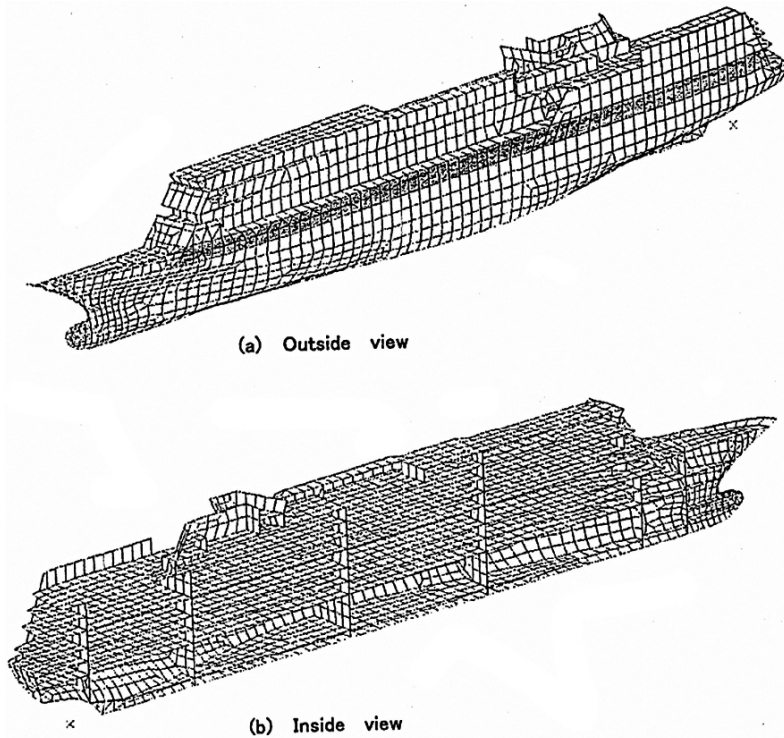


Fig. 13.3.1 Finite element model of cruise ship

looking forward from a cruise ship, 22,600GT, and Fig. 13.3.1(b) is the inside view from afterward. The length of this vessel is  $L_{pp} = 155$  m and the length of the superstructure is 140 m, hence, the length ratio of the superstructure is approximately 90%. This vessel has 7 decks as illustrated in Fig. 13.3.2, in which No.4 deck is a strength deck running through from fore to aft end. The superstructure consists of No.5–7 decks. Cross-hatching area in Fig. 13.3.1(a) means public space between No.3 and 4 deck where a series of large windows are provided in the side shell to obtain a fine view for passengers. From the view point of strength, these large openings may affect the distribution of longitudinal bending stress, because shearing rigidity is reduced largely in this area. Therefore, to confirm this effect of large openings on the longitudinal bending stress distribution, two FEM models were prepared; i.e. a model with window openings and a model without windows. A loading case was selected so as to give maximum still water bending moment, and then concentrated forces were applied to the grids on the side shell at the No.2 deck level in such a way that the difference in the shearing forces corresponds to the concentrated force.

The calculated longitudinal stress distribution in each deck at the side was obtained as shown in Fig. 13.3.2. In Fig. 13.3.2, the broken line denotes the bending stress when the window openings are included in the model, the dotted line

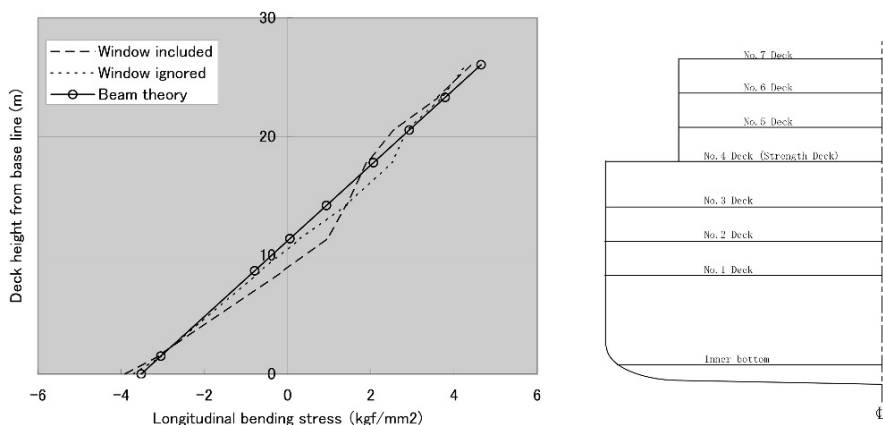


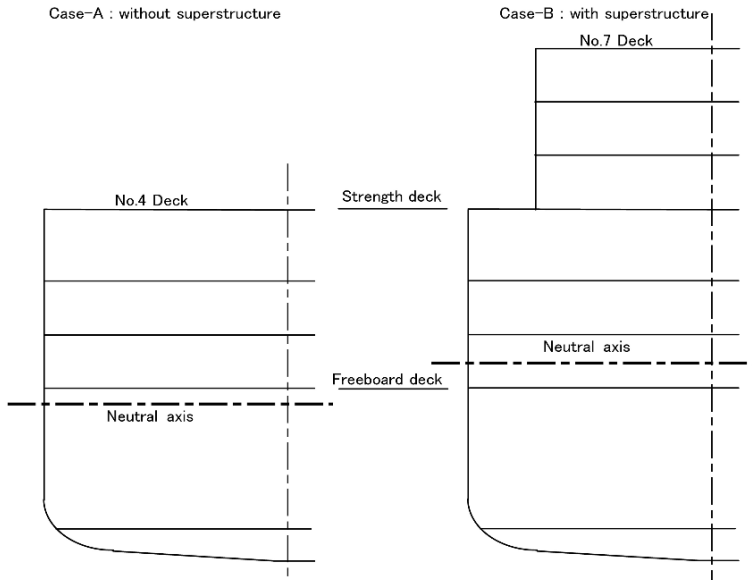
Fig. 13.3.2 Longitudinal bending stress distribution of cruise ship

represents that when windows are ignored, and the straight line is obtained by beam theory by assuming the superstructure and the main hull work together as one beam against the bending moment. From this figure, we find that the bending stress distribution in the case of no windows is almost linear. Although the bending stress increases around No.3 deck when the window openings are considered, the stress distribution can be regarded as straight in the superstructure. This stress increase at No.3 deck is caused by the reduction of shear rigidity to 20% due to window openings. As explained previously, the critical length of the superstructure is 15 ~ 25% of the main hull length. According to the above investigation, the superstructure of this vessel is long enough to transmit the longitudinal bending stress effectively, even though several large openings are provided in the side shell.

That brings us back to the question of what magnitude of longitudinal bending stress will flow into the superstructure. On the basis of the regulations specified by the Classification Society, only longitudinal strength members below the strength deck are taken into account in the section modulus of the hull girder; it is assumed other members in the superstructure, above the strength deck, are non-effective for longitudinal strength. However, as mentioned earlier, structural members in a superstructure contribute to a strength member for longitudinal bending together with the members in the main hull, where the superstructure is comparatively long. Therefore, the section modulus of the main hull is expected to increase by considering that members in the superstructure are also effective.

Let us take up this point by calculating the section modulus of the vessel in Fig. 13.3.1 in two cases: section modulus of main hull (a) with superstructure and (b) without superstructure. Table 13.3.1 indicates the comparison of section modulus: Case-A is the section modulus of the main hull only and Case-B is the section modulus of hull girder with superstructure. From this table, although the moment of inertia increases by 1.83 times by including the superstructure, the distance from the neutral axis to the upper most deck increases by 1.62 times simultaneously; consequently the section modulus becomes only 1.13 times larger. Therefore, the designer

**Table 13.3.1** Section modulus of hull girder with or without superstructure



		Case-B / Case-A
Moment of inertia	$I$	1.83
Distance from N.A. to upper most deck	$y_{DK}$	1.62
Section modulus	$I/y_{DK}$	1.13

should be careful about the strength of the superstructure, when it is a long superstructure, because the No.7 deck stress reaches approximately the same level as that of No.4 strength deck stress, required by the rules.

### 13.4 Prevention of Structural Failures

In this section, several countermeasures are explained to prevent structural failures due to longitudinal stress in a superstructure.

#### 13.4.1 Structural Discontinuity

As has been investigated above, longitudinal stress may be induced in the superstructure which is as large as the maximum stress in the main hull. For this reason,

structural failures such as cracks may be easily caused by structural discontinuities due to stress concentrations as shown in Fig. 13.1.1.

Since a relative displacement of the upper and lower decks occurs in the vicinity of the connection between the lower deck plate and the end wall of the upper deck, as illustrated in Fig. 13.4.1, a flexible connection is sometimes applied to prevent cracks so as to absorb this relative displacement. This figure shows a flexible type of connection and it is one of the available countermeasures to avoid structural failures at the discontinuous parts of a superstructure. Another solution is to apply a sufficiently strong structure to the discontinuous connection in order to reduce the stress induced by relative displacement. Which type of solution should be taken depends on the design philosophy and the situation.

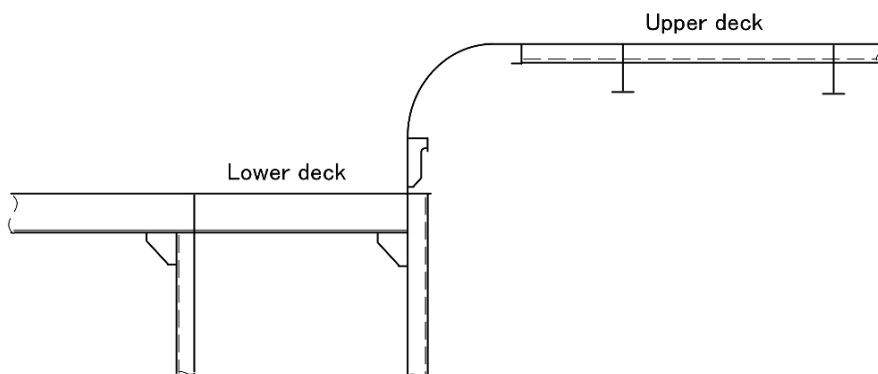


Fig. 13.4.1 Flexible connection at discontinuous part in long superstructure

### 13.4.2 Round Shape of Side Wall Opening Corner

Access openings are usually provided in steel walls in a superstructure and in some cases a negative rounded shape is applied to opening corners to overcome the interference between a corner edge and door frame, as indicated in Fig. 13.4.2. In these cases, cracks are apt to initiate from the free edge of the negative corner in the diagonal direction due to a combination of stress concentration at the round corner and the high longitudinal bending stress.

Cracks were found in a car ferry at the corners of these openings, and a FEM calculation was conducted to investigate the stress concentration around the corner. The structural model was a plane model as indicated by the cross-hatching area in Fig. 13.4.2 and was subjected to uniform tension, because longitudinal bending brings uniform tension in a longitudinal side wall. In order to confirm the stress concentration according to the corner shape, 4 types of door opening corner were modeled as illustrated in Fig. 13.4.3. Model CR1 is a damaged opening corner with a negative radius of  $20R$ . Model CR2 indicates a normal corner with positive  $200R$  and there is no damage in this type, however, the radius is so large that it is expensive to form such a door frame by bending work. Model CR3 is a negative radius corner

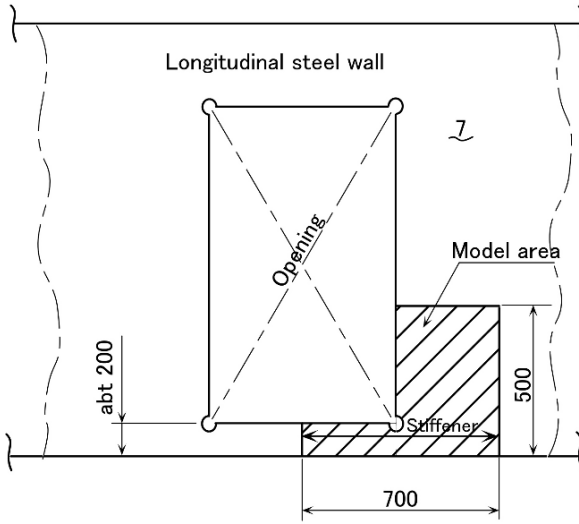


Fig. 13.4.2 Model area for stress concentration of door opening corner

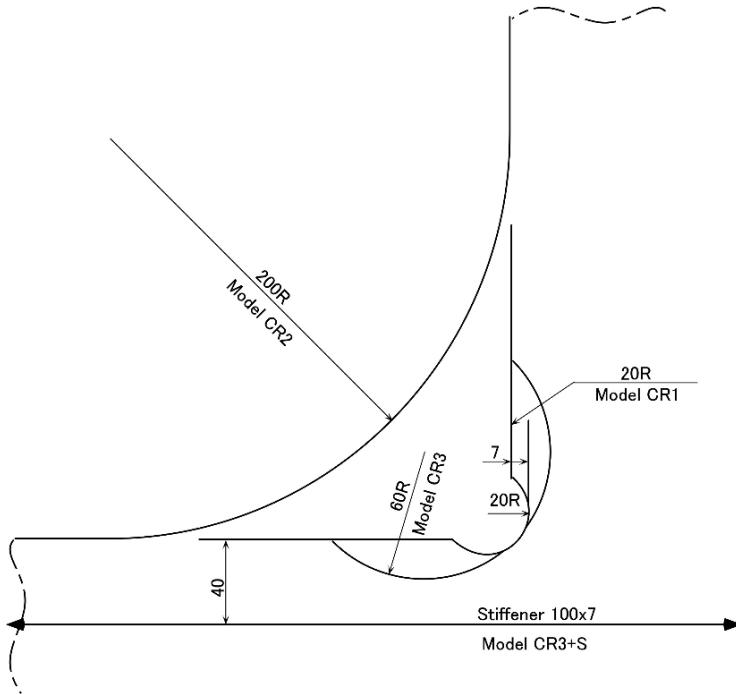


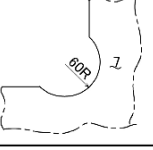
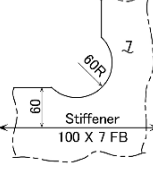
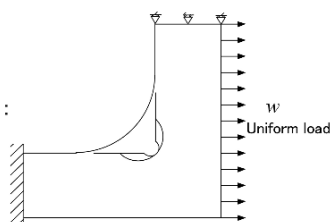


Fig. 13.4.3 Profiles of door opening corner

**Table 13.4.1** Stress concentrations around door opening corner

Model	Corner shape	Stress concentration factor	Note
CR1		4.9	Damage
CR2		2.4	No damage
CR3		3.9	
CR3+S		2.8	

Calculation model :



with 60R and Model CR3+S is an improved CR3 model by adding a horizontal stiffener.

The results are summarized in Table 13.4.1. From this table, the stress concentration factor of Model CR1, damaged, is 4.9, whereas the factor of Model CR2, with no damage, is 2.4. In Model CR3 it is 3.9. On the other hand, in Model CR3+S the stress concentration factor is 2.8, which is almost similar to that of Model CR2.

As a result of this investigation, adopting the shape of Model CR3+S can prevent cracks.



### 13.4.3 Buckling

Regarding vessels with large superstructures such as a car ferry and a cruise ship, the superstructure is designed so as to minimize steel weight because of severe stability restrictions. To satisfy this requirement, the deck plate thickness is thin in comparison with other merchant vessels, which may result in buckling of deck plates under a sagging moment. Hence a longitudinal framing system is preferable to transverse framing in view of the buckling strength.

However, even when longitudinal stiffening is applied to the deck plating, the buckling strength of a deck plate should be investigated thoroughly, since the critical buckling strength differs depending on the calculation method for thin plates. For example, let us estimate the critical buckling stress of the deck plate in Fig. 13.4.4 by an analytical method first. Using (3.5.21) of Chap. 3 of Part I, we obtain the critical buckling stress as follows under the boundary conditions:

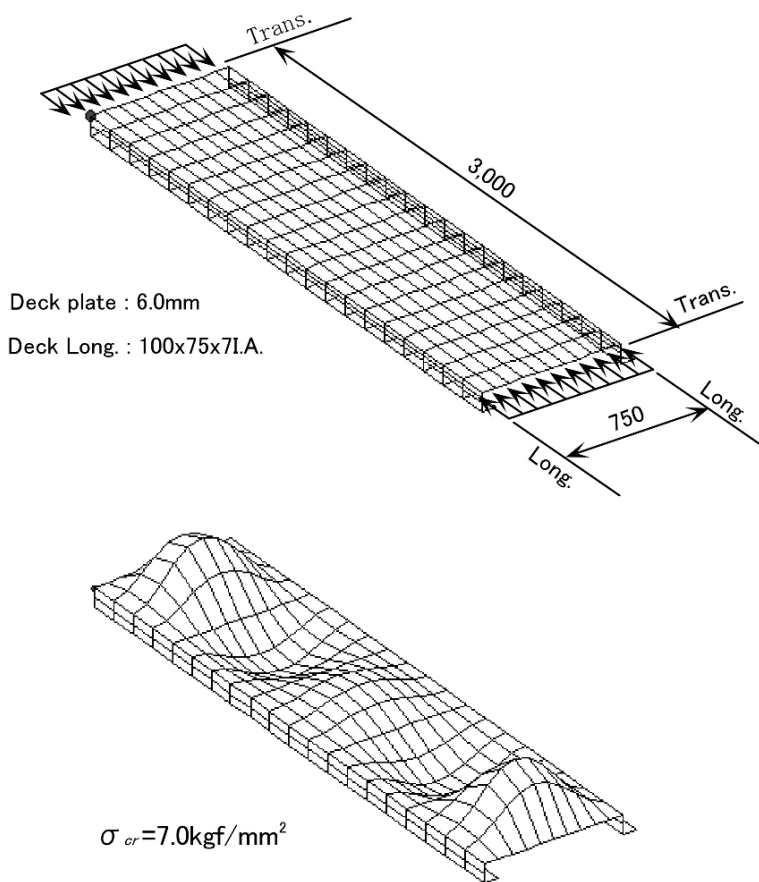


Fig. 13.4.4 Buckling strength of deck plate due to longitudinal bending stress

$$\sigma_{cr} = \frac{\pi^2 E}{12(1 - \nu^2)} \left(\frac{t}{b}\right)^2 K \eta$$

where

$$a = 3000$$

$$b = 750$$

$$\alpha = 3000/750 = 4$$

$$K = 4$$

$$E = 21,000 \text{ kgf/mm}^2$$

$$t = 6$$

$$\nu = 0.3$$

$$\eta = 1 \text{ for } \sigma_e = 4.85 < \sigma_y/2$$

$$\therefore \sigma_{cr} = 4.85 \text{ kgf/mm}^2$$

On the other hand, the critical buckling stress calculated by FEM analysis is  $\sigma_{cr} = 7.0 \text{ kgf/mm}^2$ , which is 1.4 times greater than the analytical result. This difference is derived from the torsional rigidity of the deck longitudinals modeled in the FEM, affecting the increase of buckling stress. The difference becomes large in cases where the rigidity of plate bending is less than the torsional rigidity of the stiffener.

As discussed above, it is important to evaluate the buckling strength accurately in particular for thin deck plate structures.

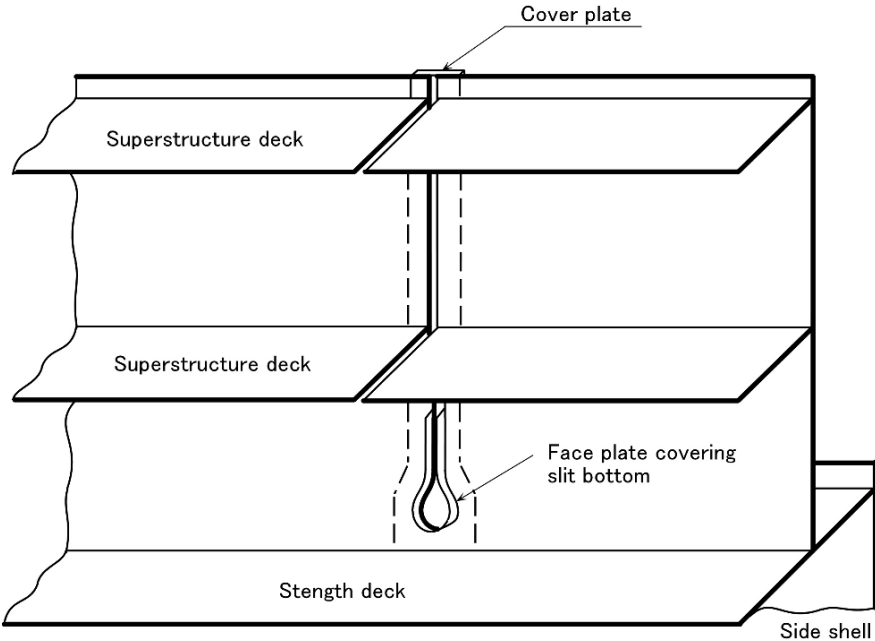


Fig. 13.4.5 Expansion joint applied to superstructure

### ***13.4.4 Expansion Joints***

For the purpose of reducing the longitudinal bending stress flowing into a superstructure, expansion joints are sometimes applied to the superstructure. An expansion joint is a slit provided in the side wall and decks of a superstructure to permit relative movement between adjacent superstructures as illustrated in Fig. 13.4.5 [44]. This slit is protected by a cover plate from the weather and has one edge welded to the side wall vertically with the other side free for sliding. Also the bottom of the slit is covered with a face plate to reduce the stress concentration around the free edge.

The expansion joint is effective in reducing longitudinal bending stress flowing into a superstructure. However, from the fatigue-strength view point, it behaves like a notch cut in a hull girder. Special attention should be paid regarding the shape of the bottom of the expansion joint [45].

# Index

## A

ABAQUS, 131  
Active mass damper, 550–552, 553  
Aft peak bulkhead, 514  
Allowable stress, 7, 14, 47–49, 60, 63, 149,  
163, 173, 203, 206, 208, 254, 257,  
258, 291–292, 294, 322, 363–367,  
374, 388–391, 392, 513  
Aluminum alloy, 117  
Annealing, 117, 526  
ANSYS, 131  
Approval drawing, 84, 90, 95  
Area ratio of opening, 441, 442, 443  
Attached plate, 143, 145, 150, 152, 163, 483  
Automatic nesting, 91, 92  
Ayling, 520

## B

Balanced girder, 150, 163, 164, 165, 166, 173,  
180, 291–292, 305  
Basic design, 81, 84–87, 88  
BCT70, 476  
Bearing force, 74, 340, 529, 531  
Bearing load, 491, 502, 506, 508  
Bilge-longitudinal-less structure, 428  
Blade frequency, 105, 496, 529, 535, 546, 548,  
552, 557  
*Bolivar Maru*, 475, 490  
Bottom slamming, 23, 487  
Boundary element method, 78  
Bow flare slamming, 23, 487  
Brittle fracture, 12, 112, 121, 123, 319, 320,  
321, 322, 324, 325, 327, 328, 363  
Buckling damage, 191, 194, 240, 241, 354,  
397, 398, 401, 405, 447, 448  
Buckling load, 55, 56  
Buckling pattern, 195, 201, 202, 402, 447  
Built-up section, 116, 151, 152, 178

Bulbous bow, 104, 105, 360, 426, 483, 491  
Bulkhead arrangement, 353, 356, 357, 358,  
359, 362, 450, 451, 497  
Butt welding, 123, 298, 299, 306, 311, 312,  
313, 314, 317, 331

## C

CAD/CAM, 82, 84  
*California Maru*, 490  
Capacity, 11, 12, 13, 428, 456, 526, 535  
Car  
deck, 467, 469  
ferry, 100, 559, 560, 565, 568  
Carbon equivalent, 114  
Cargo oil movement (in tank), 10, 24, 97, 441  
Cast steel, 117, 520, 521, 525, 526  
Cavitation, 340, 347, 511, 531, 532  
Chain locker, 95, 487, 488  
Charpy V notch test, 321  
Chip carrier, 459  
CIM, 84  
Closed section, 267, 268, 269, 274, 275,  
378, 480  
COD, 324–325  
Collapse, 8, 12, 60, 65–67, 68–69, 110, 154,  
232, 234, 235, 236, 237, 320, 386,  
469, 472, 490  
Collar plate, 206, 207–208, 210, 400, 412, 514  
Collision, 108, 360, 425, 475, 478, 479, 480,  
483, 485, 488  
bulkhead, 360, 425, 483, 488  
Column buckling, 55–57, 60  
Concurrent engineering, 82, 84  
Construction tolerance, 330–333  
Container ship, 3, 49, 100, 103, 104, 105, 108,  
329, 379, 386, 415, 417, 426, 461,  
462, 464–467, 472, 475, 480, 485,  
487, 490, 491, 493, 535

- Continuous beam, 154–155, 156, 157, 167–170, 227  
 Continuous hatch side coaming, 380, 464  
 Corrosion margin, 48, 116, 233, 235, 306, 308, 432  
 Corrugated bulkhead, 304, 312–313, 314, 317, 355, 358, 359, 431, 451–455, 456–459, 477  
 COSMOS, 84, 86  
 Crack around slot, 203, 400  
 Crack propagation, 44, 112, 297, 328–330  
 Crack-tip opening displacement, 324  
 Criteria of failure, 45–46  
 Critical energy release rate, 324  
 Critical load, 55, 56  
 Cross deck, 461, 462, 466, 467  
 Cross tie, 108, 194, 211, 221–224, 252, 387, 394–396, 397, 398, 399, 403, 404, 405, 429, 443, 479, 556, 557  
 CR steel, 249, 250  
 Cruciform joint, 302, 331  
 Cruise ship, 543, 562, 563, 568  
 CTOD, 324  
 Cumulative fatigue damage factor, 53, 298
- D**
- Damage factor, 52–53, 298  
 Damper, 341, 536, 537, 538, 540, 548, 550, 552, 553  
 Damping, 71, 72, 73, 76, 337, 527  
 Damping tank, 337  
 Dead load, 23  
 Deck wetness, 23, 28  
 Degrees of freedom, 80, 128, 136–137  
 Demand, 3, 5, 11, 12, 13, 14, 85  
 Design  
   procedure, 5–7, 33, 83, 92–93  
   spiral, 36, 84, 85, 88  
 Detail design, 81, 84, 92, 298, 382, 394  
 Detail drawing, 90–91  
 Detailed cutting plan, 91  
 Detuner, 536
- E**
- Effective breadth, 143, 144, 174, 175, 254, 257, 260, 389, 413  
 Effective width, 143, 144–145  
 Elastic buckling, 58, 60  
 Elastic energy release rate, 324  
 Elastic mounting, 543–545  
 Elastic-perfectly plastic body, 61  
 Electric balancer, 87, 340  
 Electrogas welding, 299  
 Elliptic opening, 244, 245, 246, 247  
 Endurance limit, 51  
 Energy saving, 5, 105, 107, 347, 385, 386, 428, 491  
 Epoch Mark II, 476  
 Equivalent stress, 42–43, 44, 131, 424  
 Euler's buckling, 56, 57  
 Euler's formula, 56  
 Exciter test, 529, 530, 546  
 Exciting force, 5, 74, 76, 87, 88, 107, 259, 335, 336, 337, 338, 340, 341, 342, 345, 347, 491, 493, 495, 520, 527, 528–529, 530, 531, 532, 534–545, 546, 548, 550, 552, 555, 556, 557  
 Exciting frequency, 73, 75, 76, 105, 107, 259, 285, 335, 337, 341, 345, 495, 518  
 Expansion joint, 286, 569, 570
- F**
- Failure  
   mode, 6, 7, 11, 33, 34, 36, 304  
   probability, 10, 11, 12, 13, 14  
 Fatigue  
   damage, 31, 52–54, 53, 298  
   failure, 49, 51, 53, 54  
   limit, 51  
 Faulkner, 145  
 Feedback system, 93  
 Fillet welding, 298, 302–307, 308, 311–314, 315, 317, 331, 412  
 FINEST, 91, 92  
 Finite element method, 10, 77, 78, 125–137, 247, 321  
 Firing order, 537, 540  
 Flank angle, 331, 332, 333  
 Fluctuating pressure, 23, 24, 74, 514  
 Flying bird (crack), 202, 387, 429  
 Forced displacement, 167, 172–174, 184, 228, 229, 285, 293, 388, 483  
 Forced vibration, 71, 72–73  
 Forged steel, 117, 525  
 Fork lift track, 467  
 4th fleet incident, 488  
 Fracture mechanics, 10, 319, 321–328  
 Free surface, 25  
 Free vibration, 70, 71, 72
- G**
- General arrangement, 5, 87, 88, 353  
 Genetic algorithm, 88, 89  
 Grade of steel, 248, 325–328  
 Green water, 23, 487

Grillage structure, 253, 254–256,  
394, 505  
Groove, 92, 299, 300, 306, 307  
Grounding, 108, 429, 430, 475, 478, 479  
G type (rudder), 428  
Guide force, 74, 340, 341  
Guide moment, 74, 340

## H

Hatch coaming, 244, 343–344, 345, 466  
Hatch corner, 417, 461–467, 472, 473  
Hatch cover, 342, 343–344, 345  
*Hatsuyuki*, 488  
High cycle fatigue, 51  
Higher-strength steel, 45, 95, 111, 116, 117, 123  
High(er) tensile steel, 7, 109, 167, 209, 210,  
289, 372–374, 379, 502  
Highly skew(ed) propeller, 337, 340  
Hogging (moment), 20, 21, 98, 367, 386, 561  
Hopper tank, 103, 410, 411, 412, 413, 478  
Hull (flexural) vibration, 74  
Hull girder deflection, 286, 287, 288, 289,  
293, 510  
Hydrodynamic load, 23  
Hydro-elastic interaction, 345  
Hydrostatic load, 23

## I

IACS, 20, 21, 22, 112, 289, 325, 328, 329  
I-DEAS, 131  
IMCO (=IMO), 108  
Impact load, 23, 24, 419  
Intermittent welding, 314–315  
Irregular wave, 27, 28, 29, 30, 364  
ISO 6954, 95  
ISSC's wave spectrum, 29

## J

Jack knife (damage), 105, 319–321, 363, 386  
Johnson, 57, 60  
JSQS, 95, 330

## K

Key plan, 90  
K type cross tie, 394

## L

Lamellar tear, 119, 120  
Large-sizing of ships, 379

Leg length, 302, 304, 305, 306, 307, 308,  
312, 472  
Liberty, 319–321, 325  
Linear fracture mechanics, 322–324  
LNG, 103, 321, 475  
Local strength load, 17, 19  
Longitudinally framed system, 242, 243  
Longitudinal strength load, 17, 20–23, 24, 28  
Long superstructure, 217–218, 559, 560, 561,  
564, 565  
Long taper, 183, 184, 391–392  
Long term prediction, 21, 22, 24, 27, 30–32  
Low cycle fatigue, 51  
Lower collapse load, 232  
LPG, 103, 321

## M

Magnification factor, 73  
MARC, 131  
Marcona Trader, 489, 490  
Maximum stress  
principal, 41, 43, 44, 45, 46  
shearing, 41, 45, 46, 178, 180, 269, 448  
Mechanism method, 67  
Membrane  
analogy, 268, 271, 272, 273, 274  
stress, 235, 236, 237, 331  
Mesh division, 133–134, 388  
0.4 L midship, 105  
Midship section modulus, 9, 87, 105, 161, 369,  
370, 372  
Million tonner, 3, 5, 7  
Miner-Palmgren, 52  
Minimum principal stress, 41, 43  
Minimum thickness, 262, 263, 265,  
447–449, 450  
Mis-alignment, 312, 313  
Mises, 42, 46, 424  
*Mutsu*, 480, 481  
Mutually support, 253, 254, 255, 256

## N

NASTRAN, 131, 133  
Natural frequency, 25, 70, 71, 73, 74, 75, 76,  
105, 107, 202, 259, 285, 335, 337,  
338, 340, 341, 342, 343, 344, 345,  
494, 495, 496, 497, 511, 514, 515,  
518, 520, 521, 528, 529, 532, 535,  
536, 539, 540, 541, 545, 546, 548,  
549, 550, 551, 552, 553, 554, 555,  
556, 557  
NBC Kure, 97  
NC, 81, 91, 92, 403

Nesting, 91, 92  
 No cross tie, 394  
 Non destructive examination, 526  
 Non-linear fracture mechanics, 324–325  
 Non-uniform thickness plate, 445  
 Nuclear ship, 108, 480

## O

Oil crisis, 3, 97, 346, 491–492  
*Onomichi Maru*, 490  
 Open bulbous stern, 105, 386, 428, 491  
 Opening (area) ratio of swash bulkhead, 355, 442  
 Open section, 267, 268, 279–283  
 Optimization, 88, 165, 464–467  
 Optimum  
   beam space, 253, 260–265  
   girder arrangement, 438  
   section, 163, 164, 165, 166, 167, 291–292, 294, 305, 446  
   space of girder, 257–258

## P

Panamax, 415, 464, 534  
 Paris's equation, 328–330  
 PATRAN, 131  
 Phasing, 542, 544  
 Piece drawing, 90, 91  
 Piece table, 92  
 Pierson-Moskowitz wave spectrum, 29  
 Plandtl, 271, 272  
 Plastic  
   hinge, 65, 66, 67, 68, 236, 237, 386, 433  
   moment, 47, 61, 62, 65, 67, 154, 242, 243, 386  
   section modulus, 64–65, 66, 67, 165, 166, 304  
 Plate buckling, 45, 57–60, 144–145, 227, 485–486  
 Post-processor, 131  
 Power spectra, 29  
 Pre-processor, 131  
 Principal shearing stress, 40–42  
 Principal stress, 38, 40–42, 43, 44, 45, 46, 131  
 Principle of virtual work, 67, 68  
 Probabilistic finite element analysis, 7  
 Probability density function, 11, 32  
 Production  
   design, 81, 84  
   drawing, 90  
 Product model, 82, 84

Propeller  
   aperture, 87, 88, 529, 530  
   exciting force, 74, 87, 88, 337, 347, 529, 531, 532, 535, 536, 546, 548, 550  
 Pump room arrangement, 492  
 Pure torsion, 268, 269, 278, 282

## R

Radius of gyration, 56, 211, 213, 224–225, 398  
 Rankine, 45, 57, 213  
 Rational design, 8, 181–184, 253, 524  
 Rayleigh's distribution, 30  
 Regular wave, 17, 27, 28, 29, 364, 375, 376, 426  
 Relative displacement, 100, 173, 184, 198, 221, 222, 354, 355, 440, 448, 565  
 Reliable design, 6, 7, 8, 10–15, 191, 207, 387  
 Required section modulus, 9, 48, 149, 161, 163, 165, 166, 182, 184, 254, 257, 306, 364, 369, 370, 371, 379, 445, 446  
 Residual stress, 112, 117, 121, 122–123, 287, 315, 326, 330  
 Resonance, 25, 70, 73, 74, 75–76, 87, 107, 259, 285, 335, 337, 338, 341, 342, 345, 495, 511, 518, 528, 530, 531, 532, 534, 535, 536, 538, 539–540, 541, 542, 543, 544, 545, 546, 548, 550, 552, 556  
 Resonator, 341, 528, 529, 534–541  
 Response function, 28, 29, 375  
 Rivet joint, 297  
 Roll direction, 114, 119, 248–250  
 Rough cutting plan, 91  
 Rudder, 95, 117, 306, 428, 513, 515, 516, 521, 522, 524, 525  
   horn, 306, 525

## S

Sagging (bending) moment, 20, 21, 98, 367, 568  
 Saint-Venant, 268, 269  
 SBT, 108  
 Scaling-up of ship, 3  
 Scallop, 84, 92, 298, 309–311, 385, 412, 455  
 Schenectady, 319, 320  
 Sea chest, 95, 511  
*Seawise Giant*, 3  
 Secondary stress, 225, 286, 287, 388, 483  
 Section modulus, 9, 48, 63, 64–65, 66, 67, 87, 105, 116, 149, 150–152, 161, 162, 163, 165, 166, 172, 173, 177, 182, 184, 254, 255, 256, 257, 258, 289,

- 291, 292, 302, 304, 305, 306, 364, 367, 369–370, 371, 372, 374, 379, 380, 381, 385, 386, 411, 432, 445, 446, 452, 454, 563, 564
  - Semi-automatic welding, 299
  - Semi-elliptic opening, 245, 246, 247
  - Serration, 309–311
  - Shear
    - center, 175, 279, 280, 281, 282, 283
    - rigidity, 354, 355, 356, 358, 410, 441, 442, 443, 481, 499, 500, 501, 516, 549, 551, 563
  - Shearing
    - deflection, 177, 178, 187, 188, 189, 198, 285, 293, 295–296, 503–504, 505–506, 510
    - strain energy theory, 46
  - Shinto hull form, 104
  - Shinwa-Maru*, 311
  - Shoe piece, 521–522, 524, 525
  - Short crested wave, 30
  - Short-term prediction, 27, 28–30, 31
  - Shoulder tank, 103, 400, 410, 411
  - Significant wave height, 28, 29, 30, 32, 420
  - Slamming, 22, 23, 24–25, 28, 74, 338, 386, 425, 487
  - Slant plate, 316, 317, 559
  - Slenderness ratio, 56, 57, 173, 189, 211–213, 219, 291
  - Sloshing, 10, 24, 25, 26, 60, 104, 354, 360
  - Slot, 84, 92, 99, 100, 191, 195, 197, 198, 199, 202, 203, 204, 205, 206, 207, 208, 210, 251, 400, 402, 403, 404, 408, 478, 514
  - Snake head, 391–392
  - S-N curve, 49–51, 52, 298
  - Social welfare, 14
  - Solid floor, 514
  - Span point, 146–149, 433, 434, 435, 437
  - Specialization of ship, 3, 5, 100–104
  - Specification, 84, 95, 117
  - Springing, 74
  - Spring-mass system, 70
  - Standardization, 12, 92–95, 487
  - Statically indeterminate beam, 154–156
  - Steel
    - cast steel, 117, 520, 521, 525, 526
    - coil, 467
    - CR steel, 249, 250
    - grade of, 248, 325–328
    - higher-strength, 45, 95, 111, 116, 117, 123
    - high(er) tensile, 7, 109, 167, 209, 210, 289, 372–374, 379, 502
    - section, 90, 116–117, 520
    - SUF steel, 110
    - TMCP steel, 109, 123, 374
  - Stern frame, 95, 117, 428–429, 513–526
  - Stiffened panel, 143, 144, 239, 253–265, 285, 475
  - Stiffness
    - equation, 127, 130, 131
    - matrix, 126–127, 130
  - Still water bending moment, 364, 365, 367, 562
  - Strain energy, 42, 46
  - Stress
    - concentration, 36, 51, 116, 133, 206, 207, 244–248, 298, 307, 310, 311, 317, 319, 322, 330, 331, 332, 333, 381–383, 384, 385, 389, 391, 408, 461–467, 472, 488, 514, 565, 566, 567, 570
    - factor, 207, 244, 246, 331, 332, 333, 381, 382, 461, 462, 567
    - intensity factor, 323, 324, 328
  - Stress-strain curve, 61, 111, 112
  - Strip theory, strip method, 21, 22, 27–28, 364, 386, 487
  - Strut, 57, 170–172, 191, 478
  - SUF steel, 110
  - Superstructure vibration, 74, 535, 536, 548, 550–552
  - Supporting ratio, 254, 256, 361, 362, 414, 435, 448, 449, 451
  - Surface force, 74, 337, 340, 529, 531, 532
  - Swash bulkhead, 97, 196, 354, 355, 360, 431, 440–443, 485
- ## T
- 600,000DWT tanker, 375, 450
  - T-2 Tanker, 319
  - Techno-Super-Liner, 100
  - Tetmajer, 213, 396, 398
  - Thin horse distortion, 330, 331
  - Thin shell theory, 34
  - Threshold stress intensity factor range, 328–329
  - Throat thickness, 302, 305, 306, 477
  - Thrust
    - fluctuation (=variation), 74, 340, 341
    - force, 74, 340, 341
  - TMCP steel, 109, 123, 374
  - Toe radius, 331, 332, 333
  - Torque variation, 340, 347
  - Torsional moment, 17, 20, 137, 174, 175, 269, 271, 272, 273, 274, 275, 276, 278, 279, 281, 282, 410, 411, 419, 420



Torsional rigidity, 103, 268, 269, 274–277, 282, 283, 410, 411, 413, 417, 480, 569

Torsional vibration of line shafting  
(=crankshaft), 340

Total system for long. strength, 363, 374, 387

Total system of trans. strength, 388

Transversely framed system, 240, 242, 243

Transverse strength load, 17, 18, 19, 23–27, 397

Tray type, 393, 394

Trunk section, 379

## U

ULCC, 97, 105, 107

Ultimate load, 60, 66, 67, 68

Ultimate strength, 51, 145, 298, 386

Unbalanced force, 340, 529, 532

Unbalanced moment, 74, 340, 341, 533, 534, 546, 550–551

Universe Apollo, 97, 108

Upper collapse load, 232

## V

Vertical acceleration due to pitching, 487

VLCC, 10, 97, 105, 107, 108, 208, 357, 423, 429, 546

V-notch Charpy, 250, 325, 327

## W

Wagner, 268, 279

Warping, 268, 277, 278, 279, 282, 283, 375, 378, 480

rigidity, 268, 278, 282, 283

Water stopping welding, 309

Wave

bending moment, 9, 20, 21, 28, 32, 364, 365, 367, 490

load, 5, 17, 22, 27, 207, 397, 418, 483, 487, 501

Weldability, 7, 112, 114, 116, 117, 372

Wheel load, 60, 169, 467, 469, 470, 471

Whipping, 74, 286, 288, 338

Work hardening, 111

## Y

Yard plan, 90

Yielding, 33, 34, 51, 69, 111, 315, 325

*Yugiri*, 488